Geology of the Northeastern Adirondack Mountains and Champlain–St. Lawrence Lowlands of New York, Vermont and Québec

Dix Mountain
Adirondack High Peaks

New York State Geological Association, 87th Annual Meeting
State University of New York at Plattsburgh,
Plattsburgh, NY
12–13 September 2015

2015 NYSGA Organizing Committee

David Valentino (*NYGSA Executive Secretary*)

Mary K. Roden-Tice (*2015 Meeting Coordinator*)

David Franzi (*2015 Guidebook Editor*)

Contributing Authors

John Aleinikoff
(U.S. Geological Survey)

David Bailey
(Hamilton College)

Graham Baird
(University Northern Colorado)

David Barclay
(SUNY–Cortland)

Ryan Brink
(University of Vermont)

Jeff Chiarenzelli
(St. Lawrence University)

James Dawson
(SUNY–Plattsburgh)

Nelson Eby
(UMASS–Lowell)

David Franzi
(SUNY–Plattsburgh)

Kimberly French
(Castleton University)

Robert Fuller
(SUNY–Plattsburgh)

Phillip Geer
(U.S. Geological Survey)

Kelly Gilson
(SUNY–Plattsburgh)

Tim Grover
(Castleton University)

Michael Jercinovic
(UMASS–Amherst)

Jonathon Kim
(Vermont Geological Survey)

Keith Klepeis
(University of Vermont)

Stephen Kramer
(Wm. H. Miner Agr. Res. Inst.)

Rebecca Kranitz
(SUNY–Plattsburgh)

David Lowe
(University of Ottawa)

Marian Lupulescu
(New York State Museum)

James McLelland
(Colgate University)

Charlotte Mehrtens
(University of Vermont)

Claire Pless
(UMASS–Amherst)

Douglas Reed
(Cambridge, NY)

Sean Regan
(UMASS–Amherst)

Edwin Romanowicz
(SUNY–Plattsburgh)

Peter Ryan
(Middlebury College)

Bruce Selleck
(Colgate University)

Rachel Schultz
(SUNY–Plattsburgh)

George Springston
(Norwich University)

Jacob Straub
(SUNY–Plattsburgh)

Alain Tremblay
(Univ. du Québec à Montréal)

David Valentino
(SUNY–Oswego)

John Van Hoesen
(Green Mountain College)

Gregory Walsh
(U.S.Geological Survey)

Michael Williams
(UMASS–Amherst)

Stephen Wright
(University of Vermont)

Eric Young
(Wm. H. Miner Agr. Res. Inst.)

Overview of Events

Friday, September 11th:

On-site Registration	4:00 to 8:00 PM
NYSGA Opening Reception	5:00 to 7:00 PM

Saturday, September 12th:

On-site Registration	7:00 AM to 8:00 AM
Saturday Field Trips (Check for assembly time and place)	8:00 AM to 5:00 PM
Informal Cocktail Hour (Comfort Inn, Brew Pub)	6:00 to 7:00 PM
NYSGA Banquet (Comfort Inn, Brew Pub)	7:00 to 8:00 PM
Keynote Address and Discussion: Dr. Michael Rygel (SUNY Potsdam) *"Impact of Geological Licensure in New York State"*	8:30 to 10:00 PM

Sunday, September 13th:

On-site Registration	7:00 AM to 8:00 AM
Sunday Field Trips (Check for assembly time and place)	8:00 AM to 3:00 PM

Table of Contents

Organizing Committee and Contributing Authors ii

Overview of Events iii

Table of Contents iv–vi

Saturday 12, September 2015

The Bennie's Brook Slide: A Window into the Igneous Core of the Marcy Anorthosite – Jeff Chiarenzelli, Marian Lupulescu, and Sean Reagan 1–29

Departure Point: Garden of the Gods Parking Lot Keene Valley, New York. The parking lot is at the end of Johns Brook Lane.

Meeting Point: Attendees will meet at the cairn where Bennies Brook meets the Southside Trail.

Meeting Time: 10:00 AM

Precambrian Geology of the Eagle Lake Quadrangle, Essex County, New York – Regan, S.P., Geer, P., Walsh, G.J, Aleinikoff, J.N., Baird, G.B., Williams, M.L., Valley, P.M., and Jercinovic, M.J. 30–59

Meeting Point: McDonalds Parking Lot, Ticonderoga, NY

Meeting Time: 08:30 AM

Current Research in Structure, Stratigraphy, and Hydrogeology in the Champlain Valley Belt of West-Central Vermont – Jon Kim, Keith Klepeis, Peter Ryan and Ed Romanowicz 60–97

Meeting Point: Park and Ride Lot, Colchester, VT

Meeting Time: 08:30 AM

Anatomy of Ordovician Volcanic arc and forearc basin in the Sherbrooke area, Southern Québec Appalachians – Alain Tremblay 98–119

Meeting Point: The meeting point for departure is the parking lot of the *Bureau en Gros* store, at the intersection between Jean-Paul-Perrault Street and Portland Blvd (in front of the Portland Mall).

Meeting Time: TBA

Sedimentology and Stratigraphy of the Cambrian Potsdam Group (Altona, Ausable and Keeseville Formations), Northeastern New York – David Lowe, Charlotte Mehrtens and Ryan Brink 120–161

Meeting Point: Southeastern parking lot of Hudson Hall on the SUNY Plattsburgh campus. The lot is located at the corner of Beekman and Broad streets.

Meeting Time: 8:30 AM

Table of Contents

Saturday 12, September 2015 (continued)

Quaternary Deglaciation of the Champlain Valley with Specific Examples from the Ausable River Valley – David Franzi, David Barclay, Rebecca Kranitz and Kelly Gilson 162–190

Meeting Point: Comfort Inn and Suites, 411 West Cornelia St. (NY 3), Plattsburgh, NY.
Alternate Meeting Point: Intersection of US Route 9 and NY Route 73 in New Russia, NY (west of Exit 30 on Interstate 87). Please inform the field trip leaders if you plan to meet the group at this location.
Meeting Time: 8:00 AM

Non-point Source Pollution in the Little Chazy River of New York – Robert Fuller, David Franzi, Stephen Kramer and Eric Young 191–208

Meeting Point: Southeastern parking lot of Hudson Hall on the SUNY Plattsburgh campus. The lot is located at the corner of Beekman and Broad streets.
Meeting Time: 9:00 AM

Geobotany of Globally Rare Sandstone Pavement Barrens, Clinton County, New York – Jacob N. Straub and Rachel Schultz 209–225

Meeting Point: Southeastern parking lot of Hudson Hall on the SUNY Plattsburgh campus. The lot is located at the corner of Beekman and Broad streets.
Meeting Time: 8:30 AM

Sunday 13, September 2015

An Igneous Origin for the Magnetite-Fluorapatite Ores from the Eastern Adirondacks, New York – Marian V. Lupulescu, Jeffrey R. Chiarenzelli, Sean Regan and David G. Bailey 226–238

Meeting Point: The field trip starts at the Port Henry Boat Launch Site. The site is at the intersection of Dock and Velez lanes in Port Henry, Essex County.
Meeting Time: 8:30 AM

Deciphering the Geological Evolution of the Eastern Adirondacks: New Field Petrologic and Geochronological Data – Grover, T.W., Williams, M.L., Regan, S.P., Baird, G.B., French, K.A., and Pless, C.R. 239–264

Meeting Point: Hwy 22 south of Ticonderoga in a parking area on the west side of the road immediately after entering the town of Putnam. If you are driving south from Ticonderoga there is a "Welcome to Putnam" sign just before the entrance to the parking area. The meeting point is about a 90 minute drive from Plattsburgh.
Meeting Time: 9:00 AM

Table of Contents

Sunday 13, September 2015 (continued)

Geology and Petrology of the Mont Royal Pluton – Nelson Eby 265–285

Meeting Point: Southeastern parking lot of Hudson Hall on the SUNY Plattsburgh campus. The lot is located at the corner of Beekman and Broad streets.
Meeting Time: 7:30 AM

The Middle Ordovician Section at Crown Point Peninsula, NY – Charlotte Mehrtens and Bruce Selleck 286–306

Meeting Point: Crown Point Reservation Historical Site
Meeting Time: 8:30 AM

An Overview of the Early Paleozoic Stratigraphy of the Champlain Valley of New York State – James Dawson 307–326

Meeting Point: The trip begins in the parking lot of the Comfort Inn and Suites/Perkins Restaurant, 411 Route 3, Plattsburgh, NY.
Meeting Time: 8:30 AM

Ice Retreat and Readvance across the Green Mountain Foothills: Bolton and Jericho, Vermont – Stephen Wright, George Springston, John Van Hoesen 327–352

Meeting Point: Southeastern parking lot of Hudson Hall on the SUNY Plattsburgh campus. The lot is located at the corner of Beekman and Broad streets.
Meeting Time: 8:00 AM

Borehole Geophysical Demonstration at Altona Flat Rock – Edwin A. Romanowicz 353–359

Meeting Point: Southeastern parking lot of Hudson Hall on the SUNY Plattsburgh campus. The lot is located at the corner of Beekman and Broad streets.
Meeting Time: 8:30 AM

THE BENNIES BROOK SLIDE:
A WINDOW INTO THE CORE OF THE MARCY ANORTHOSITE

JEFF CHIARENZELLI
Department of Geology, St. Lawrence University, Canton, New York 13617

MARIAN LUPULESCU
New York State Museum, Research and Collections, 3140 CEC, Albany, New York 12230

SEAN REGAN
Department of Geosciences, University of Massachusetts, Amherst, MA 01003

DAVE VALENTINO
Department of Atmospheric and Geological Sciences, SUNY Oswego, Oswego, NY 13126

DOUG REED
238 Little Colfax Rd., Cambridge, NY 12816

INTRODUCTION

The Marcy anorthosite massif forms the core of the Adirondack High Peaks region and is the geographic center of the associated topographic dome. On the State Geological Map (Adirondack Sheet, 1:250,000) it is depicted as a single rock type consisting of meta-anorthosite. However, this is a simplification and, in detail, numerous lithologies occur within the massif and display complex relations. This trip is designed to introduce participants to a 1.5 km, near continuous, linear landslide exposure which follows the course of Bennies Brook on the northern flank of Lower Wolf Jaw Mountain. Saturated conditions associated with Hurricane Irene in August of 2011 resulted in the most recent of landslide events along the course of Bennies Brook and additional exposure. The features unearthed here provide an unprecedented view into the interior of the massif and demonstrate its geological complexity.

GEOLOGICAL SETTING

The Marcy Massif is one of a number of variably sized anorthosite massifs in the Grenville Province (Figure 1). These enigmatic rocks, largely restricted to the Proterozoic, vary in age but are nowhere near as volumetrically significant as in the Grenville Province. Long collectively regarded as anorogenic, recent geochronological constraints demonstrate a close temporal relationship with orogenic activity in some cases. For example, the Marcy Massif was intruded at ca. 1160 Ma at a time corresponding to the close of the Shawinigan Orogeny. Observations made on this trip will demonstrate deformation at granulite grade, generally along lithologic discontinuities, in spite of exceptionally well preserved igneous features in adjacent rocks.

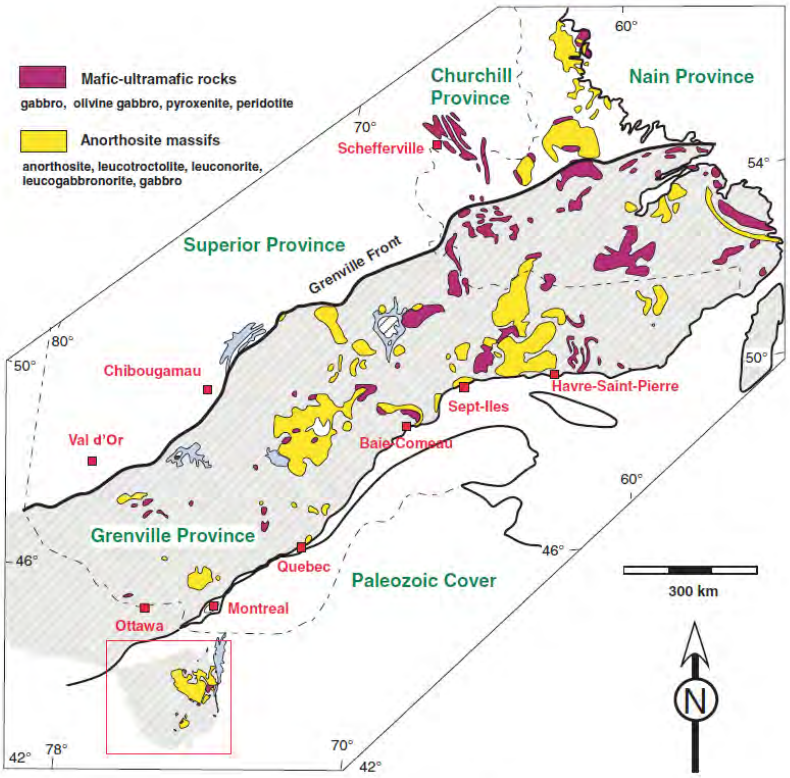

Figure 1. Map of the Grenville Province showing the distribution of anorthosite (yellow) and gabbroic (red) bodies throughout the region (modified from Corriveau et al., 2007).

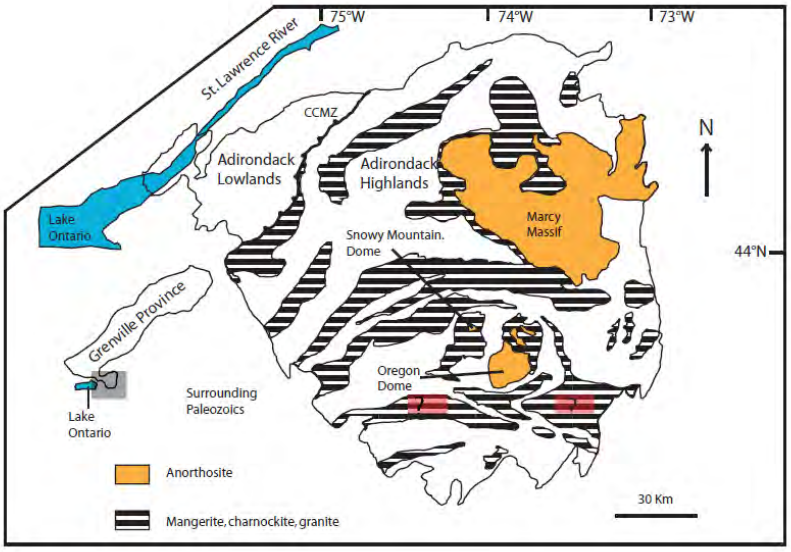

Figure 2. Simplified geologic map displaying the distribution of anorthosite-mangerite-charnockite-granite (AMCG) rocks within the Adirondack Highlands (modified from McLelland et al., 2004). Question marks represent the Piseco Lake shear zone; this granitic gneiss has been previously interpreted as a member of the AMCG suite, but this association is currently under review (Chiarenzelli and Valentino, 2008). CCMZ—Carthage-Colton mylonite zone.

Massif anorthosites are also geographically associated with a variety of other coeval igneous rocks including granitic and orthopyroxene-bearing granitoids (Figure 2). Collectively known as the AMCG Suite (Anorthosite-Mangerite-Charnockite-Granite Suite) these rocks are not considered comagmatic with the anorthosite but rather to represent the thermal effects of voluminous gabbroic melts at, or within, the base of the lower crust. Crustal melting of the deep crust and subsequent rise of coeval granitic melts is envisioned to explain the spatial association. Massif anorthosites are also associated with, and grade into, a variety of gabbroic

rocks, ilmenite-rich ores, and hybrid rocks known as ferrodiorites or jotunites with andesine megacrysts, presumably derived from the anorthosite itself.

Metamorphism to granulite facies is shown by the development of garnet coronas on pyroxenes and oxides. These minerals are concentrated in shear zones and often shown evidence of intense ductile deformation while the anorthosite wall rocks often show little or no sign of deformation. In fact, igneous features such as xenoliths, chill margins, ophitic texture, flow alignment of plagioclase, cumulate layering, block structure, and multiple intrusions are readily observed where exposures permit and these are plentiful and readily observed on the Bennies Brook slide. These features suggest the interior of the large anorthosite bodies, including the Marcy Massif, show repeat intrusions of varied composition and behaved as large rigid blocks during subsequent tectonism. Preservation of such features occur despite the profound deformation in the surrounding granitoid and metasedimentary country rocks exposed primarily as east-west trending belts crossing the Highlands (Figure 2).

AGE OF THE ROCKS

Several studies have addressed the age of the Marcy Massif, smaller Adirondack Massifs, and spatially related rocks (Figure 3). The most recent of these using the sensitive high-resolution ion microprobe (McLelland et al., 2004) suggests that the bulk of the anorthosite crystallized at ca. 1154 Ma, while associated granitoids are slightly older (ca. 1158 Ma). Perhaps a more accurate way of summarizing the data, including the errors reported, would be to state there are a range of overlapping ages within a relatively limited timeframe; basically they are more or less coeval.

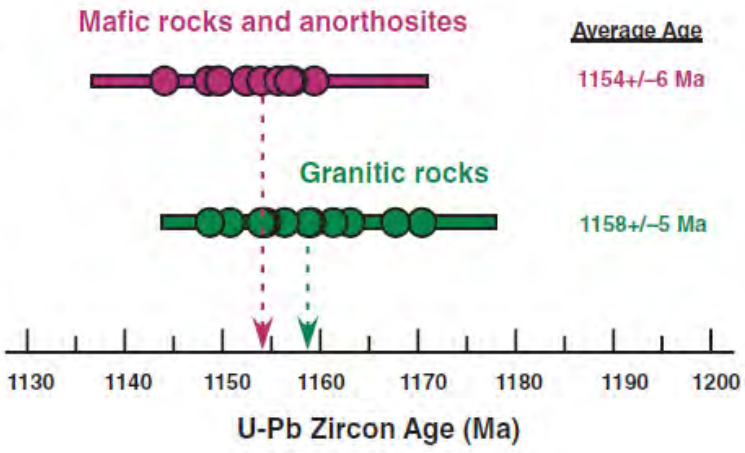

Figure 3. U-Pb zircon ages from dated rocks of the anorthosite-mangerite-charnockite-granite (AMCG) suite throughout the Adirondacks. Note the overlapping age range of anorthositic and quartz-bearing members, suggesting a coeval, but not comagmatic origin (after McLelland et al., 2004).

Abundant field evidence also confirms that the lithologies were intruded more or less synchronously. Within the boundary of the massifs themselves, however, a general sequence of extremely coarse "Marcy" type anorthosite (Kemp, 1920), followed by slightly more mafic anorthositic rocks of more moderate grain-size, gabbroic, and andesine-bearing, ferrodioritic rocks is observed. Granitoids including mangerites, syenites, aplites, and granitic pegmatites of lesser abundance and dike-like geometry are commonly observed but are not volumetrically significant. The total elapsed time represented by all of these events is unknown but is thought relatively limited. However, it is observed that ferrodioritic lithologies are chilled against anorthosite and undeformed along their margins on the Bennies Brook slide.

COMPOSITION AND ORIGIN

While the Marcy anorthosite massif does show a wide range of rock-types of variable composition, by far, it is composed of coarse-grained anorthosite *sensu stricto*. Gradation into, inclusion of, and or intrusion by rocks with slightly more mafic minerals such as anorthositic gabbro or gabbroic anorthosite, or in some cases, gabbronorite, is common. Distinctive gabbroic pegmatites, coronitic metagabbros, oxide-rich gabbros with or without apatite, pyroxenites, and ilmenite-rich, sometimes with apatite (i. e. nelsonite), ores also occur but in much lesser volume. Many workers regard these rocks as natural variants of gabbro fractionation, residual fluids or cumulates, parental magmas, and/or a variety of ore formation processes. Most or all of these rocks are thought to have a dominant mantle component with variable amounts of crustal contamination. Among these rocks coronitic metagabbros have the most primitive Nd-systematics, crystallized olivine, and are interpreted to be the parental magma from which the bulk of the anorthosite and gabbro rocks crystallized in the Adirondack region (Regan et al., 2012).

Distinct from these rocks are those of granitic composition with variable ratios of hornblende to orthopyroxene including mangerites, charnockites, and granites. As presented elsewhere, opx-bearing rocks include charnockites and mangerites and pyroxene syenites. They are generally thought of as dominantly crustally derived via melting of the lower crust during intrusion and staging of the parental magma of anorthosite at the base of the crust. Often they contain zircon xenocrysts and have neodymium whole rock systematics and hafnium-zircon signatures compatible with derivation from an arc terrane of similar age (1300-1400 Ma) and composition to that exposed in the southern Adirondacks. Thus, although not comagmatic, the anorthositic and gabbroic rocks and spatially associated felsic magmatic rocks are coeval and likely genetically linked. This association is seen throughout the Grenville Province and beyond and may represent thermal conditions on Earth restricted largely to the Mesoproterozoic.

Ferrodioritic rocks, also called jotunites, appear to have large components derived from both mantle and crustal sources and have been invoked as the parental magma for both anorthosite and granitic members of the suite. Their mineral assemblage often includes two pyroxenes, quartz, k-spar, plagioclase, apatite, and zircon, although many variants exist and provide strong arguments for a hybrid origin. There is clear field evidence, well exposed at Bennies Brook, supporting the contention that the megacrystic andesines found in them are derived from intrusion into the anorthosite. The andesines can vary from as much as half the rock volume to sparse or rare. The ferrodiorites often show chill margins against the anorthosite suggesting intrusion relatively late in the sequence.

On the slide, granitoid rocks are relatively rare but ubiquitously exposed as thin (1-10 cm) dikes cross-cutting anorthositic and gabbroic lithologies. They have remarkably straight-walled, vertical boundaries and include sugary aplites, granitic pegmatites, and syenitic variants. Most show extreme ductile strain parallel to the walls of the dike itself and trend 110°. In a few examples, deformation can be traced into the surrounding anorthosite but generally not for any considerably distance, with most anorthosite remaining undeformed right up to the contact. The intruding lithologies, particularly gabbroic pegmatites, have taken up the strain preferentially and show the bulk of metamorphic mineral growth.

OTHER FEATURES

The exposures on Bennie Brook document several other events in the geologic history of the region. The anorthosite and associated rocks are cut by a variety of basaltic dikes up to 2 m wide. Rarely the dikes are compound with felsic, largely trachytic, parallel intrusions within the basalt. While the age of these dikes is not known at this locality, similar dike swarms throughout extensive parts of the Grenville basement elsewhere yield Neoproterozoic ages. Nearby at Dannemora a trachytic dike, included in a swarm of basaltic dikes, yielded a U-Pb zircon age of 643±4 Ma. Although found elsewhere, Cretaceous-aged intrusions thought synchronous related to opening of the Atlantic Ocean were not noted here.

While the vast bulk of rocks exposed on the slide are undeformed, despite high-grade metamorphism and deformation, thin shear zones are common. The development of these shear zones occurred at high-grade conditions and where they cross-cut gabbroic and anorthositic rocks there is extensive development of garnet and pyroxene, which are also highly strained. Most shear zones occur along near vertical, lithologic discontinuities such as granitic dikes and gabbroic pegmatites. The vast major of shear zones record left-lateral shear. Displacement is moderate on small shears but collectively, based on the number of shear zones, considerable left-lateral displacement appears to have been accommodated. Where lineation is visible and well developed, it plunges shallowly at 100-120^{o}. Dextral shear is recorded in cross-cutting ductile shear zones which warp/fold pre-existing sinistral shears. In this slide, as well as others nearby, brittle deformation occurs in narrow zones up to several meters wide. Most often it consists of sets of closely spaced fractures, some of which intersect and brecciate the rock. Often these areas are highly altered to lower greenschist facies assemblages, bleached, and/or weathered.

SUGGESTIONS FOR THE TRIP

What follows is a number of waypoints along the slide starting at the intersection of Bennies Brook with the South Side trail just above confluence with Johns Brook. Because this area is within the Adirondack Park and highly traveled, and it is illegal to do so, we did not mark specific points of interest. A GPS is essential to retrace our route up the slide and stop at key locations. However, rest assured that the exposure is good enough that whatever route you take you will see all of the key features and likely many we haven't mentioned here.

Each of the waypoints was selected to point out specific features that occur in abundance or are particularly well developed in that area of the slide. You will note some progressive changes as you proceed upward in the proportions of lithologies and the structural features you observe. On a warm fall day the slide is very inviting and generally fairly dry. On a wet, overcast day it can be treacherous with red-brown algal films that virtually eliminate friction. It requires only moderate climbing to reach the ~2900' elevation just before where the slide forks, past this point, it steepens considerably to the head wall. Those without experience on steep slides may wish to return from here and avoid the steepest portions. Please remember it is illegal to collect rocks from the Adirondack Park without a permit and day use groups in the High Peaks are limited to 15. **The trip is weather dependent.**

ACKNOWLEDGMENTS

The senior author would like to thank Mr. Kevin MacKenzie for introducing him to Adirondack slides and the wonderful features they expose. He would also like to thank students Sam Hecklau and Paxton Rountree-Jabin for participating in the study of Adirondack slides. They were supported by the James S. Street Fund at St. Lawrence University. Last, but not least, he would like to thank Dr. James McLelland for his mentorship and tireless efforts to understand how the Adirondack Region was formed and evolved over time.

SLIDE GUIDE

Departure Point: Other than Saturday of the 2015 NYSGA meeting this is a self-guided field trip. Access to Bennie's Brook Slide can be had via the Garden of the Gods Parking Lot Keene Valley, New York. The parking lot is at the end of Johns Brook Lane. Note: This lot tends to be full on the weekends; however, there are shuttles and parking lots in town during the busy season. Drive time to Keene Valley from Plattsburgh is one hour; please factor this into your dinner (banquet) plans.

Departure Point Coordinates: Parking Lot - N44° 11' 20.6" W73° 48' 59.0" (Figure 4)

Meeting Point Coordinates: I will meet trip attendees at the cairn where Bennies Brook meets the Southside Trail at 10 am. N44° 09' 56.4" W73° 50' 43.4"

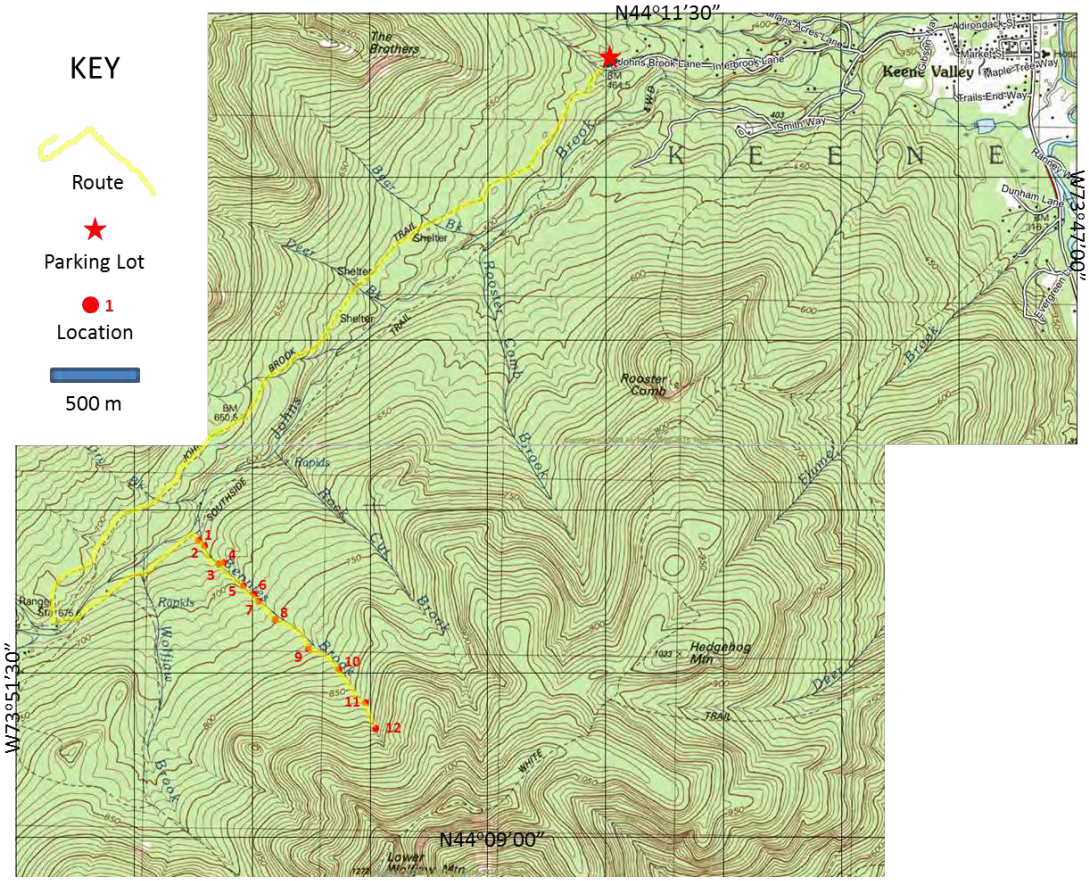

Figure 4. Topographic map showing route from Garden of the Gods parking lot to the Bennies Brook Slide.

Trip Length: The hike to the base of the slide is ~3.5 miles (6 km). The trip up the slide is approximately 1 mile (1.6 km) to the recommended turn around point. The total round trip distance is ~9.0 miles (14 km) of moderately strenuous walking and climbing. Allow at least eight hours of day light to complete your trip. Wet conditions will likely extend the time required.

Figure 5. Google Earth imagery showing the location of the Bennies Brook Slide on the northern slope of lower Wolf Jaw Mountain. Note the older, grown over forks of the bennies Brook slide and the new more southerly extension due to Hurricane Irene. Starting and finishing points shown by red circles.

Directions:

0.00 miles (0.00 km) Garden of the Gods Parking Lot (N44° 11' 20.6" W73° 48' 59.0"). Follow the Johns Brook Trail southwest to the Ranger Station (~4.6 km).

2.85 miles (4.6 km) Johns Brook Ranger Station (N44° 09' 38.9" W73° 51' 19.5"). From the Ranger Station follow the trail east over Johns Brook for approximately 150 m to its intersection with the South Side Trail. Follow the South Side Trail to the northeast. Pass the first major creek (~440 m), Wolf Jaw Brook until you reach the intersection of Bennies Brook and the South Side Trail (~410 m). The slide is to your right, proceed uphill towards the south up the north side of Lower Wolf Jaw Mountain.

3.46 miles (5.6 km) Bennies Brook Slide and start of trip (N44° 09' 56.4" W73° 50' 43.4")

4.43 miles (7.1 km) Turn-around point at base of steep head wall (N44° 19' 18.4" W73° 49' 57.7"). See Figure 5 below.

BB-1 Intersection of Bennies Brook Slide and South Side Trail. (N44° 09' 56.4" W73° 50' 43.4" – 633 m)

→ Features: 1) typical Marcy-type anorthosite; 2) garnet coronas; 3) small ductile shear zones; 4) sub-meter scale north-trending joints

The South Side trail follows John's Brook and was severely damaged during the flooding associated with Hurricane Irene. The trail crosses the slide a few hundred meters above the confluence of Bennies Brook with Johns Brook. A stone cairn marks the intersection (Figure 6). *If you don't see the stone cairn you are at one of the other nearby slides in drainages on the north side of the range and this guidebook won't be of much use.* If you look to the north towards Johns Brook you can see a variety of woody debris and boulders from the slide (Figure 7).

Exposed in the bed and banks of Bennies Brook is typical Marcy type anorthosite (Figure 8). Here it consists mostly of 90% or more of darker andesine, some reaching lengths of 5 cm or more; mere pikers compared to what is to come. The lighter colored matrix is also plagioclase, much of which shows bent twins and other features indicative of some type of strain (recrystallization or auto brecciation?) during or just after final emplacement. Other minerals include pyroxene (often of both persuasions), oxides (magnetite and/or ilmenite), and trace minerals including biotite, hornblende, and garnet. Close examination reveals that much of the garnet rims mafic minerals and provides evidence of high-grade metamorphism. Throughout the outcrop proportions of minerals and grain-size vary.

Here cm-wide shear zones are developed. Some concentrate and deform garnets and pyroxenes and this will be much more evident and convincing as you proceed upwards. They are generally subvertical and trend about 340° here. A set of parallel joints are developed slightly oblique to the ductile shear zones and trend 352° 90°.

Figure 6. Co-author Marian Lupulescu at stone cairn where the Bennies Brook Slide intersection the South Side trail.

Figure 7. Looking north towards debris from Hurricane Irene landslide in the bed of Bennies Brook just below its intersection with the South Side trail.

Figure 8. Typical features of the Marcy type anorthosite. Notice large bluish andesine crystals set in a finer-grained matrix of plagioclase. Pyroxene-rich gabbroic rock cross-cuts anorthosite filling in an angular interstice to the left of blue pen.

BB-2 Heavy Minerals in Bennies Brook and Garnet Coronas (N44° 09' 53.4" W73° 50' 41.8" – 638 m)

→ Features: 1) garnet and heavy mineral-rich sand in brook; 2) garnet coronas

There are deposits of reddish and black sand exposed in the bed of Bennies Brook, often forming layers or ripples or other bed forms (Figure 9). These are derived primarily from within the drainage basin and show the relative abundance, and density, of garnet, pyroxene, and oxides. A sample of this sand has been collected and will be characterized by SEM and detrital zircon studies.

Figure 9. Heavy mineral bands in sand in the bed of Bennies Brook. The heavy mineral population of the sand is dominated by garnet, pyroxene, and magnetite and has a distinctive red color.

Wandering up from this location for the next 50 m or so will show some excellent examples of garnet coronas. Coronas are developed upon mafic minerals such as pyroxene and olivine, as well as, on oxide minerals (Figure 10). Some form delicate single grain necklaces or chains. In many cases they may represent the only metamorphic reaction visible in the rock. Davidson and Van Breeman (1988) showed similar zircon coronas on baddeleyite in Grenville mafic dikes. The zircon gave ages 100 million years younger than the baddeleyite cores documenting both igneous crystallization (1150 Ma) and Metamorphism (1050 Ma). In shear zones garnets are deformed and particularly abundant indicative of deformation and high-grade conditions and the abundance of the residual components needed for it to form (i.e. Fe, Al, Si).

Figure 10. Thin garnet coronas developed around large pyroxenes and oxides (in circle) in gabbro pegmatite. Note the sheared boundary between the gabbro and anorthosite at the top of the photograph. Photograph compliments of Doug Reed.

BB-3 Altered Anorthosite and Brittle Structures (N44° 09' 50.0" W73° 50' 38.1" – 659 m)

→ Features: 1) alteration zones in anorthosite; 2) closely spaced fractures and brittle faults; 3) tiny carbonate veins

While typically fresh, and well preserved, some anorthositic rocks have experienced numerous lower grade alteration events. While the exact nature and timing of events is currently unknown many appear to be associated with low-temperature hydrothermal alteration associated with areas of high fracture density and brittle faults. Typically bluish grey when fresh, anorthosite often appears chalky white to pale green where altered and rusty where also weathered (Figures 11 and 12). In these zones andesine is nearly completely altered to epidote, pumpellyite, clinozoisite, chlorite, carbonate, and other secondary minerals.

At this locality there are composite alteration zones and veins that range in color from white to pink to pale green (Figure 11). They appear to be in close proximity and best developed where brittle faults occur (Figure 12). In addition, to these features the rock is heavily laced with thin (mm-scale) white calcite veins. Secondary calcite in microfractures is ubiquitous within the anorthosite (Morrison and Valley, 1988). A similar mineralized alteration zone up to several meters wide, cutting anorthosite, has been studied by the senior author and colleagues at SUNY Potsdam.

Figure 11. Example of extreme hydrothermal alteration in anorthosite; note the distinctive pale green color of the host rock.

Figure 12. Brecciated fault zone with closely spaced fractures and alteration cutting anorthosite. Note sharp boundary between altered anorthosite and fracture rock near center of photograph. The zone trends 255°90°.

BB-4 Xenoliths in Anorthosite (N44° 09' 50.3" W73° 50' 37.0" – 666 m)

→ Features: 1) xenoliths; 2) white, finer-grained anorthosite

In this stretch of the slide there are a number of xenoliths. This is not uncommon for the anorthositic rocks to include well documented metasedimentary country rock lithologies (Valley and Essene, 1980) and also igneous xenoliths (McLelland). Here their origin is debatable, although some display a deep green clinopyroxene, possibly diopside (Figure 13). Many of the xenoliths are highly disrupted and partially assimilated into the anorthosite. In some areas the anorthosite appears to be chilled against larger xenoliths resulting in white, fine-grained regions in the anorthosite where in contact with the xenoliths. However, white finer-grained anorthosite also appears to have intrusive relationship with fresh anorthosite as well.

Figure 13. Clinopyroxene-rich layer with white, finer-grained anorthosite. The whitish anorthosite may be a consequence of assimilation of xenoliths and/or chilling against them or intrusion by another magma batch.

BB-5 Dikes and Shear Zones (N44° 09' 46.1" W73° 50' 32.1" - 695m)

→ Features: 1) intrusive granitic dikes; 2) narrow ductile shear zones

In this section of the slide, as elsewhere, you will note a number of straight-walled and narrow 5-10 cm granite and pegmatite dike-like intrusions into the anorthosite. On closer inspection, shearing and mylonitic fabrics parallel to the boundaries of dikes are noted (Figure 14). Quite often the surrounding anorthosite is completely unaffected by the strain. Most of these shear zones trend nearly 110°, coincident with the major east-west trending Shawinigan-aged Piseco Lake Shear Zone in the southern Adirondacks. Where observable the shear zones display left-lateral kinematics. Many such dikes can be traced for 10's of meters across the slide.

Figure 14. Co-author Sean Regan investigating the mylonitic fabric in an aplitic dike cutting the anorthosite.

BB-6 Complex Shear Zone (N44° 09' 44.6" W73° 50' 29.2" – 715 m)

→ Features: 1) gabbroic pegmatite; 2) sinistral shear zone modified by late dextral motion; 3) relative age relations

At this stop a spectacular example of complex shearing, lithologic variation, and relative age relationships can be seen. Shown in Figure 15 there is a contact between Marcy-type anorthosite (left-hand side) and gabbro (right hand side). This contact was intruded by a gabbroic pegmatite with crystals approaching 10 centimeters in length. All three of these rocks were intruded by a thin aplitic granite trending 110°. After intrusion both the gabbroic pegmatite and aplite show strong left-lateral displacement parallel to the aplite margins. After cessation of left-lateral motion the rocks were affected by right -lateral shear (200°), deflecting the contact and the previously developed left-lateral shear fabric. Where observed elsewhere dextral shear also follows earlier sinistral shearing at 110° but also appears to have operated at high-grade metamorphic conditions.

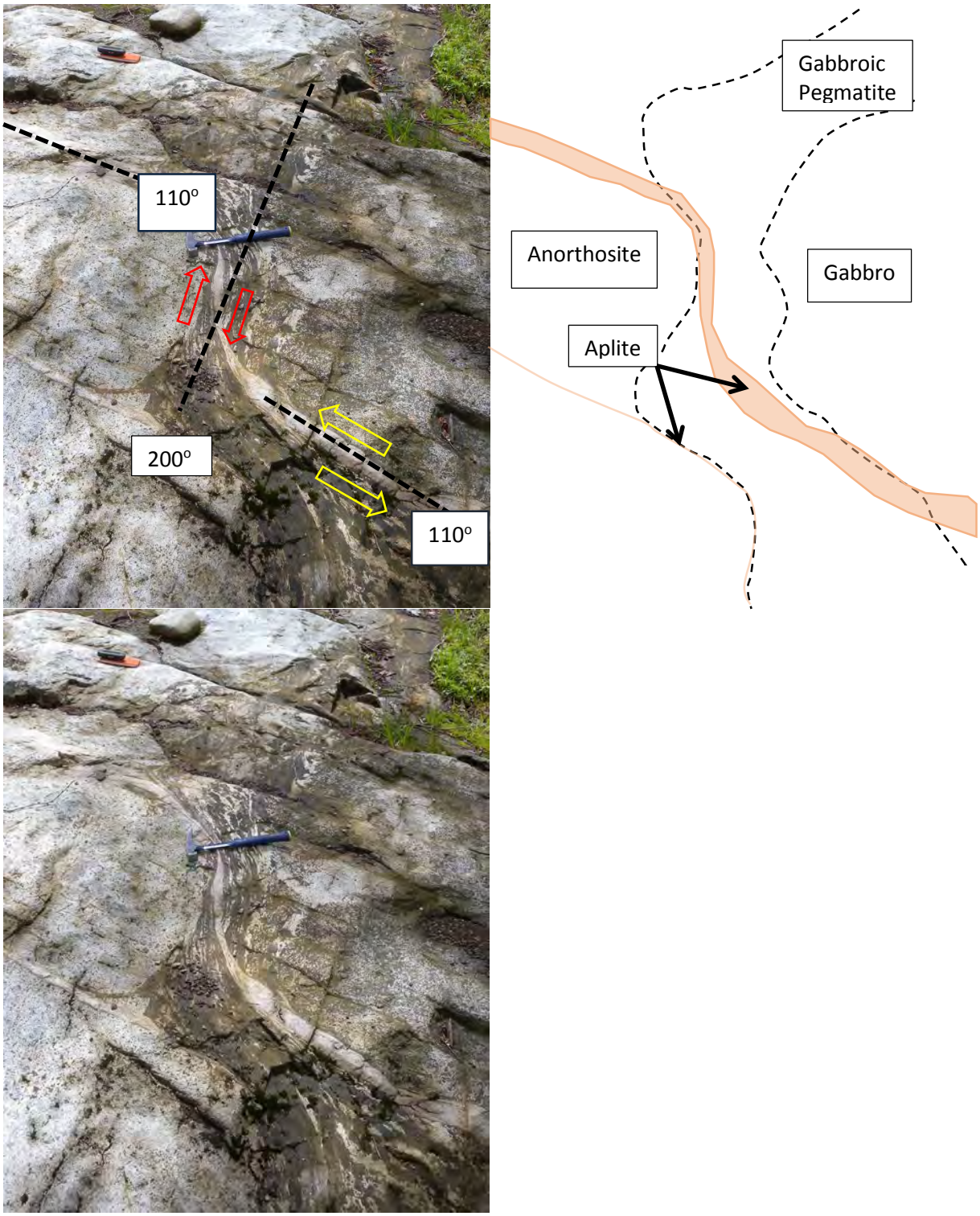

Figure 15. Diagram showing offset direction and trace of lithologic contacts of complex shear zone. Right had photograph: Left lateral shear shown by yellow arrows; right-lateral by red arrows. Left hand photograph: margins of gabbroic pegmatite shown by black dashed lines; margins of aplites shown by pink transparent overlay.

BB-7 High-grade Sinistral Shearing in Anorthositic Rocks (N44° 09' 43.4" W73° 50' 28.0" – 721 m)

→ Features: 1) large sinistral shear in anorthosite; 2) pyroxene kinematic indicator; 3) shear in granitic pegmatite

As observed at the previous location and elsewhere on the Bennies Brook slide a large number of small sinistral shear zones developed along lithologic discontinuities occur. In most cases the strain is taken up in the dike or pegmatite and is parallel to the dike walls and often is completely absent in the anorthositic wall rocks. At this location you will see a ~2m shear in anorthositic rocks indicating deformation of sufficient magnitude to affect a relatively rigid lithology (Figure 16). Also in the same shear zone you will see evidence of the high-grade nature of the shear zone in the form of sinistral pyroxene "fish-shaped" kinematic indicators (Figure 17). Finally, you will see evidence for opening of fractures approximately perpendicular to dike margins, followed by shearing parallel to the contact (Figure 18). This appears to indicate a nearly 90° change in stress direction after anorthosite intrusion.

These features provide clues to the overall kinematic history of the High Peaks region, when deformation occurred, and the relative age of events. Here they are clearly exposed without ambiguity. The trend of the shear zone is 114°82° and a brittle fault is developed parallel to its margin. A well- developed lineation in the ductile shear zone has the orientation of 115° 16°.

Figure 16. Approximately 2m wide shear zone developed in anorthosite.

Figure 17. Dolphin-shaped, pyroxene kinematic indicator just to the right of the dime. Note sinistral sense of off-set.

Figure 18. Zoned pegmatite dike with internal sinistral shear zone.

BB-8 Neoproterozoic dikes (N44° 09' 40.0" W73° 50' 24.0" – 744 m)

→ Features: 1) Neoproterozoic Dikes; 2) Magmatic layering in anorthosite

Straight walled Neoproterozoic dikes are common in the Adirondack Region but rarely exceed a meter or two in thickness. They are believed to be part of the extension and mafic magmatism associated with the opening of the Iapetus Ocean. The dikes cut Grenville rocks over a large area from the Appalachian inliers to Newfoundland, with ages ranging between ~570-640 Ma. Here a variety of dikes ranging in size from a few cm's to a few meters are found. Most are vertical and northeast (~40°). Some appear to be composite (Figure 19) and higher up in the slide relatively rare felsic trachytic dikes intrude the basalts, allowing the possibility of U-Pb dating.

In many areas anorthositic rocks subtle but regular changes in grain-size and mineral proportions are readily observable with the naked eye. Some are so subtle that only a vague meter-scale alteration of color demarks them (Figure 20). Others have finer layering and contain considerably more mafic minerals. While these layers are nowhere nearly as well developed as in mafic-ultramafic intrusions, they are believed to represent original magmatic, perhaps cumulate, layering with the anorthosite.

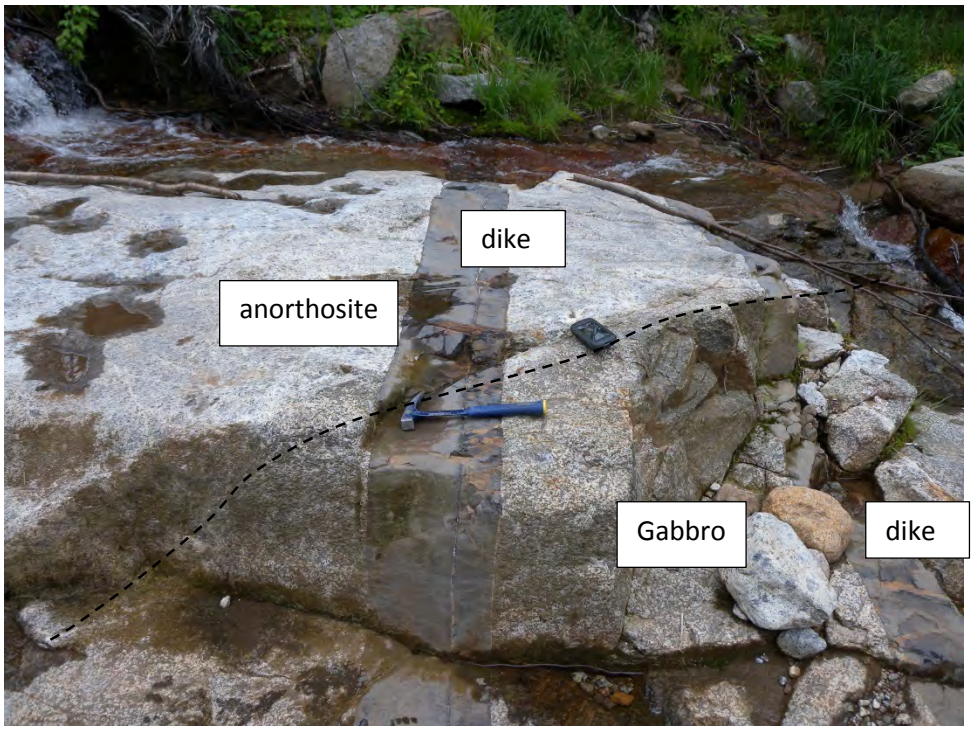

Figure 19. Possible composite Neoproterozoic dike cutting contact between anorthosite and gabbro (contact dashed). The trend of the dike is 40°90°.

Figure 20. Subtle, meter-scale, compositional layering in anorthosite. The trend of the contacts between the layers is 57°62°.

BB-9 Ferrodiorite Contact (N44° 09' 34.7" W73° 50' 15.5" – 782 m)

→ Features: 1) giant andesines; 2) raft of coarse Marcy type anorthosite; 3) ferrodiorite contact with anorthosite

The anorthosite within the massif is often a true pegmatite in terms of its grain-size and exceptionally large andesines can be found as xenoliths and rafts in other lithologies. At this locality large andesines up to 20cm or more can be found included in anorthosite of more moderate grain-size (Figure 21). In addition, a large raft of exceptional coarse anorthosite can also be seen (Figure 22). The raft has minimum dimension of 2 x 3 meters and consists of large andesine crystals with few other minerals. In an upcoming stop we will see exceptionally large pyroxenes as well.

On the upper portions of the Bennies Brook slide ferrodiorite or jotunite becomes a dominant rock type intruding the anorthosite and related rocks (Figure 23). Travelling up the slide another 20 meters or so reveals ferrodiorite as a network of thin, box-like dikes around anorthosite blocks and as large intrusive sheets. It is invariably chilled against the anorthosite and has scalloped or complex margins. In some cases andesine megacrysts can be seen increasing in abundance towards the contact and are often aligned along their long axis. The ferrodiorite is demonstratively one of the last intrusive phases as it cuts gabbroic pegmatites which have been previously deformed (Figure 24), indicating intrusion after ductile deformation.

Figure 21. Large andesine (30cm) xenocryst in anorthosite. The xenocryst is crossed by numerous alteration veinlets. Note gabbroic pegmatite and minor shear zone to right of hammer.

Figure 22. Co-author Doug Reed explores a large raft of exceptionally coarse Marcy-type anorthosite.

Figure 23. Irregular contact between ferrodiorite and anorthosite. Note fining of grain-size towards anorthosite indicating chilling of the ferrodiorite against the anorthosite and the lack deformation along the contact.

Figure 24. Crunch, the handsome geology dog, sniffs out an outcrop displaying a dike of ferrodiorite along a shear zone in a previously deformed gabbroic pegmatite. Relationships such as these establish the ferrodiorite as one of the last intrusive phases seen along Bennies Brook.

BB-10 Pyroxenite Block (N44^{o} 09’ 30.5” W73^{o} 50’ 7.8” – 822 m)

→ Features: 1) numerous xenoliths; 2) pyroxenite block; 3) composite shear zone

As previously noted a wide variety of xenoliths can be found in the anorthositic rocks including metasedimentary country rocks of the Grenville Supergroup (Valley and Essene, 1980) and those of igneous parentage. Those of igneous origin are generally assumed to be related to the anorthosite and related rocks. At this locality a large meter-scale block of coarse-grained pyroxenite can be observed (Figure 25). If the anorthosite did develop by fractional crystallization from gabbroic magma, then it is lacking in requisite mafic minerals. One way to explain this dearth of Fe and Mg-bearing silicates, is to separate the anorthosite by density differences. Perhaps this pyroxenite was entrained as a rising mass of anorthosite made its way higher into the crust?

Also at this locality is a second photogenic example of a composite shear zone with sinistral movement modified by a later dextral shear (Figure 26). This example is developed in a gabbroic pegmatite cutting anorthosite. The sinistral shear trends ~110^{o}, while the dextral shear, larger of the two in this case, trends ~350^{o}. This confirms the sequence of deformation described previously and suggests both sinistral and dextral components of late deformation affected the rocks exposed in the High Peaks.

Figure 25. A large pyroxenite block (xenolith) included in anorthosite. Individual pyroxene grains range from 2-3 cm in diameter.

Figure 26. Composite shear zone developed in gabbroic pegmatite showing initial sinistral motion modified by later dextral deformation. Hammer head points to the north.

BB-11 More Ferrodiorite (N44° 09' 24.6" W73° 50' 1.1" – 868 m)

→ Features: 1) ferrodiorite defining block structure in anorthosite; 2) giant pyroxenes; 3) off-set of chill margin

At this point on the slide ferrodiorite is a major rock type and it occurs on all scales from small dikes (2-3 cm across) to large sheets intruding anorthosite. At several locations irregular dikes of various orientations and sizes and shapes define anorthosite blocks in a jig-saw fashion (Figure 27). Also exposed is a meter-scale xenolith with giant pyroxenes up to 20 cm or more in diameter (Figure 28). It is engulfed in anorthosite, and both are cut by ferrodiorite. An offset contact between anorthosite and an andesine xenocryst-rich ferrodiorite or ferrogabbro is also exposed. The offset appears to be brittle and right lateral (Figure 29). However, the origin of the rock at the contact can be debated. Is it a contact chill margin or a layered dike that intruded along the contact or the wall of a magma chamber? We will let your group argue over how best to interpret and test the origin of this enigmatic exposure.

Figure 27. Ferodiorite intrusive dikes defining block structure in anorthosite. Note the seemingly random orientation, irregular shape of dikes, and connections. All of these features appear to argue for intrusion into a jig-saw pattern of anorthosite blocks. Did the anorthosite fracture first allowing rise of the magma or did the intrusion of the ferrodiorite cause the fracturing?

Figure 28. Pyroxenite xenolith with individual pyroxenes up to 20 cm in diameter. Note the contact with the andesine-rich darker rock on the right hand side of the photograph.

Figure 29. Dextral off-set of contact between anorthosite and ferrodioritic to gabbroic rock. What is the the origin of the layered rock at the contact?

BB-12 The End (N44° 09' 19.8" W73° 49' 58.5" – 913 m)

→ Features: 1) magmatic layering in xenolith; 2) composite bimodal Neoproterozoic dike

This is the final stop just before the splitting of the slide into three individual forks of different ages. Here the route steepens as you approach the head wall and it is an excellent place to turn around and descend. Two unique features are exposed in this section of the slide and include a layered mafic intrusion and a composite dike.

The layered mafic intrusion shows rhythmically cm-scale alteration in the proportion of mafic minerals (Figure 30). Its overall composition suggests it may be a variety of ferrodiorite; however, further work is needed to confirm this. Nonetheless it is striking in its difference from the bulk of the ferrodiorite and other rocks and testifies to the variety of igneous textures possible in this situation.

A number of small basaltic dikes occur at this elevation on the slide. One reaches a width of 2m and has an orientation of 50°90°. What is unique here, though, is a few small felsic dikes (Figure 31) that appear to concordantly intrude the basaltic dikes. This suggests that they are broadly coeval. A similar trachytic dike intruding in a swarm of Neoproterozoic basaltic dikes near Dannemora yielded zircon. This zircon gave a concordant U-Pb zircon age of 643±4 Ma. Work is in progress to date this dike as well.

Figure 30. Possible magmatic layering in mafic dike intruding anorthosite. Note alteration of layers on the cm-scale.

Figure 31. Composite Neoproterozoic dike cutting anorthosite. Note the upper felsic portion which appears to intrude the basalt.

Figure 32. Co-author Sean Regan, caught in geologic action pose, contemplates which way is up near where the slide steepens and forks beneath the summit of Lower Wolf Jaw Mountain.

REFERENCES

Chiarenzelli, J., and Valentino, D., 2008, Igneous protoliths of the Piseco Lake shear zone, southern Adirondacks: Geological Association of Canada, v. 33, p. 34.

Corriveau, L., Perreault, S., and Davidson, A., 2007, Prospective metallogenic settings of the Grenville Province, *in* Goodfellow,W.D., ed., Mineral Deposits of Canada: A Synthesis of Major Deposit Types, District Metallogeny, the Evolution of Geological Provinces, and Exploration Methods: Geological Association of Canada, Mineral Deposits Division, Special Publication No. 5, p. 819–847.

Davidson, A., and van Breeman, O., 1988, Baddeleyite zircon relationships in coronitic metagabbros, Grenville province, Ontario: Implications for geochronology: Contributions to Mineralogy and Petrology, v. 100, p. 291–299.

Kemp, J. F., 1920. Geology of the Mount Marcy Quadrangle, Essex County, *New York State* Museum Bulletin *229-230*, p. 5–86.

McLelland, J.M., Bickford, M.E., Hill, B.M., Clechenko, C.C., Valley, J.C., and Hamilton, M.A., 2004. Direct dating of Adirondack massif anorthosite by U-Pb SHRIMP analysis of igneous zircon: Implications for AMCG complexes: Geological Society of America Bulletin, v. 116, p. 1299–1317.

Morrison, J., and Valley, J.W., 1988, Post-granulite-facies fluid infiltration in the Adirondack Mountains: Geology, v. 16, p. 513–516.

Regan, S. P., Chiarenzelli, J. R., McLelland, J. M., and Cousens, B. L., 2011. Evidence for an enriched asthenospheric source for coronitic metagabbros in the Adirondack Highlands: Geosphere, v. 7, p. 694-709.

Valley, J. W. and Essene, E. J., 1980. Akermanite in the Cascade Slide xenolith and its significance for regional metamorphism in the Adirondacks: Contributions to Mineralogy and Petrology v. 74, p. 143-152.

PRECAMBRIAN GEOLOGY OF THE EAGLE LAKE QUADRANGLE, ESSEX COUNTY, NEW YORK

SEAN P. REGAN, PHILLIP S. GEER, GREGORY J. WALSH, AND JOHN N. ALEINIKOFF
United States Geological Survey

GRAHAM B. BAIRD
Department of Earth and Atmospheric Sciences,
University of Northern Colorado,
Greeley, CO 80639

PETER M. VALLEY
Weatherford Labs, Houston, TX 77086

MICHAEL L. WILLIAMS AND MICHAEL J. JERCINOVIC
Department of Geosciences, University of Massachusetts, Amherst, MA 01003

TIMOTHY W. GROVER
Castleton State College, Castleton, VT 05735

INTRODUCTION AND REGIONAL BACKGROUND

The Grenville Province of eastern North America has long been interpreted as the roots of an ancient orogenic system that formed approximately 1.0 billion years ago (Hoffman, 1988; McLelland et al., 2010). The entire region formed and evolved during punctuated phases of crustal growth during the Mesoproterozoic involving a variety of tectonic processes including accretion, arc magmatism, back-arc development and collapse, and unique to the Grenville, anorthosite-mangerite-charnockite-granite (AMCG) plutonism. These processes occurred over > 300 my and are collectively referred to as the Grenville Orogenic cycle (Fig. 1; McLelland et al., 1996; Rivers, 2008). The northeast Grenville Province has been shown to have a long history, extending back to ca. 1.35 Ga (McLelland et al., 1993), and contains evidence of long-lived active margin processes (Dickin and McNutt, 2007; Chiarenzelli et al., 2010a). However, the most extensive regional deformation has been interpreted as having formed during a culminating collision at ca. 1.07 Ga (Ottawan orogeny), which resulted in the final assembly of the supercontinent Rodinia (McLelland et al., 1992; 1996; 2001a; 2010; 2011; Rivers et al., 2008). The Grenville Province offers an excellent opportunity to study the growth and modification of mid to lower continental crust during these tectonic processes within the context of a long-lived active margin (Mezger, 1992).

The Adirondack Mountains of northern New York are a large domical uplift and are subdivided into the northwest Adirondack Lowlands and southeast Adirondack highlands separated by the Carthage- Colten shear zone (Streepey et al., 2001; Selleck et al., 2005). The Adirondack Highlands are dominated by granulite facies (meta)igneous rocks in contrast to the Lowlands, which are dominated by supracrustal rocks metamorphosed to amphibolite facies. Another important difference is the timing of deformation in each region. In the Lowlands the majority

of deformation was the result of Shawinigan orogenesis (ca.1.17 Ga; Fig. 1b; Wasteneys et al., 1999; Heumann et al.,2006; Chiarenzelli et al., 2010b; Wong et al., 2011a), and evidence for Ottawan deformation (ca. 1.07 Ga; McLelland et al., 2001a) is lacking (Baird and Shrady, 2011). In contrast, the Adirondack Highlands are known to have experienced both Shawinigan and Ottawan phases of the Grenville Cycle. Here, differentiating the effects of these two phases remains a major challenge that is critical for understanding the role and importance of the Ottawan orogeny in the Grenville Province as a whole (Rivers, 2011).

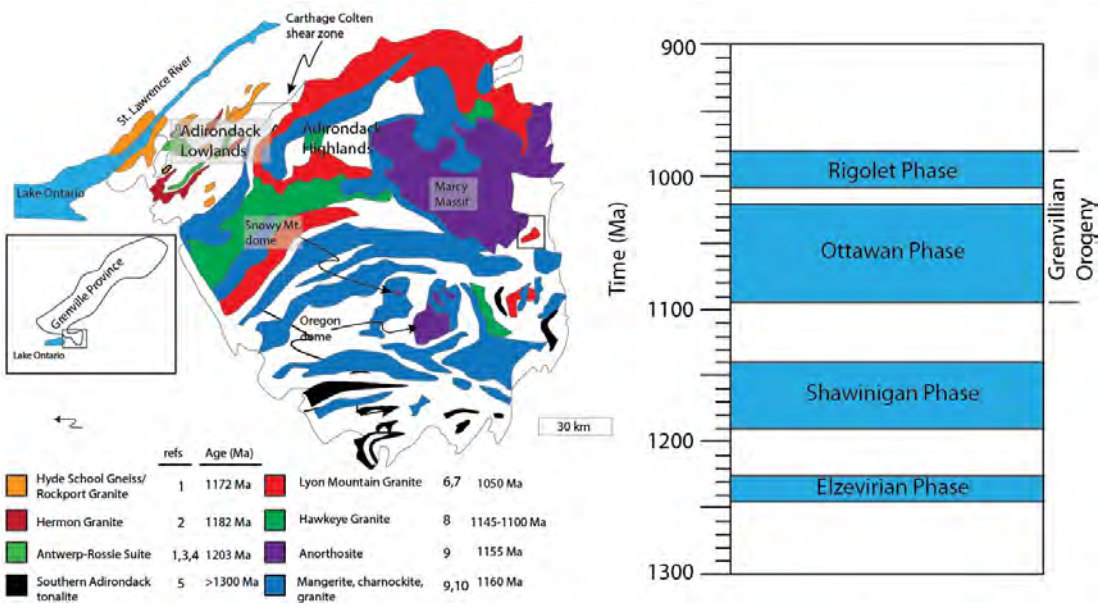

Figure 1: A) A simplified map of the Adirondacks divided into the northwestern lowlands and southeastern highlands. The map displays the distribution of (meta)igneous lithologies (modified from McLelland et al., 2004). Note the Eagle Lake quadrangle is outlined as a black rectangle along the southeastern margin of the Marcy Massif. U-Pb ages listed map below with references: 1. Wasteneys et al., (19999), 2. Heumann et al. (2006), 3. McLelland et al. (1992), 4. Chiarenzelli et al. (2011a), 5. Daly and McLelland (1991), 6. McLelland et al. (2001), 7. Valley et al. (2009), 8. Personal communication (Peter Valley, John Aleinikoff), 9. McLelland et al. (2004), Hamilton et al. (2004). B) A schematic displaying the traditional orogenic phases of the Grenville Province (after Rivers, 2008).

This field trip focuses on the general Precambrian geology of the Eagle Lake quadrangle (ELq) in the eastern Adirondack Highlands. We will discuss recent 1:24,000 scale mapping of the ELq and the historical mining area Hammondville (Geer et al., 2015). The new mapping represents work by Regan, Geer, and Walsh. Provisional mapping by Walton (1960) has proven quite helpful, and provided a foundation for the new work. We will present a new structural nomenclature established during mapping that is regionally transformative and will hopefully be a useful guide for future analytical work. New forward petrologic modeling of the metamorphic assemblages that define a major structural fabric, geochronologic data that constrain the timing of both granite petrogenisis and anatexis of metasedimentary lithologies, and geochemical data from the historical mining district of Hammondville.

The Adirondack Highlands are predominately underlain by granulite facies (meta) igneous lithologies (McLelland et al., 1996). The most voluminous plutonic rocks exposed belong to the anorthosite-mangerite-charnockite-granite (AMCG) suite, which underlies approximately 60 % of

the Adirondack Highlands (Hamilton et al., 2004). The petrogenisis of AMCG suites has been debated for decades, but detailed U-Pb geochronologic work presented in McLelland et al. (2004) and Hamilton et al. (2004) shows that granitoid lithologies (1158 Ma) are statistically older than anorthositic and other mafic members of the suite (1154 Ma), but overlap in age (Figure 5e). These data were interpreted as showing that AMCG suites are "… coeval, but not necessarily comagmatic" (McLelland et al., 2004). Geochemical and isotopic analysis performed by Regan et al. (2011) showed that coronitic metagabbros of the Adirondack Highlands (McLelland and Chiarenzelli, 1988) are permissible as the parental magma for the anorthosite. Quartz-bearing end-members were interpreted to have been derived from partial melting of lower continental crust where anorthosite formed via fractional crystallization of an asthenospherically derived gabbroic magma (McLelland et al., 2004; Bickford et al., 2008; Regan et al., 2011). The largest body of anorthosite is the Marcy Massif, which underlies the high peaks region of the Adirondack Mountains (Buddington, 1939). This suite of rocks has been interpreted as the result of lithospheric- mantle delamination at the waning phases of Shawinigan orogenesis (McLelland et al., 2004). Therefore, the deformation and metamorphism present throughout AMCG rocks has been interpreted as Ottawan in age.

The Lyon Mountain Granite Gneiss (LMG: nomenclature after Postel, 1952) is the youngest igneous rock exposed within the Adirondack highlands (Buddington, 1939; Postel, 1952; McLelland et al., 2001a,b,c; Selleck et al., 2005; Valley et al., 2009; 2010). It is a leucogranite that rims the Adirondack Highlands and is host to low-Ti magnetite deposits interpreted as forming via kiruna-type Fe – oxide, copper, gold (IOGC) mineralization processes (McLelland et al., 2001b,c; Valley et al., 2009). The LMG contains no consistent shape-preferred orientation (except in the East Adirondack shear zone; see *Grover et al., trip B-2*), and very little evidence of regionally significant subsolidus deformation, although the nature of layering is currently being debated (McLelland et al., 2001a). The LMG has been interpreted as accompanying orogenic collapse at the tail end of Ottawan orogenesis (McLelland et al., 2001a; Selleck et al., 2005).

ROCK TYPES

The ELq contains a wide variety of Precambrian rocks, and contains all of the lithologies exposed within the Adirondack region, with the exceptions of ca. 1.3 Ga tonalite gneisses exposed within the southern Adirondack Mountains (Daly and McLelland, 1993). Major rock units exposed within the ELq are described below, from oldest to youngest, with approximate ages given from the literature. It is important to note that the majority of geochronology cited below was performed on similar rocks from outside of the ELq.

>1203 Ma Grenville Supergroup (after Davidson, 1998)

Four basic units are currently subdivided: 1) Amphibolitic to pyroxenic gneiss: this unit is predominately composed of fine to medium grained amphibolite with cm-scale boudined leucosome, locally contains opx porphyroblasts surrounded by tonalitic leucosomes, and coarse diopsidite; 2) Calc- silicate and marble: this unit is very poorly exposed but commonly contain coarse quartz and diopside crystals, pegmatitic clinopyroxene-bearing leucosomes; 3) Garnetiferous quartzofeldspathic migmatitic gneiss (+/- sillimanite +/- graphite; classically khondolite): this unit is thought to have formed via anatexis of a pelitic to psammitic lithology, and it is commonly associated with very minor quartzite layers and a small amount of amphibolite; 4) biotite gneiss +/- leucosome +/- garnet: this unit is commonly platy and typically is interlayered with meter to sub-meter scaled amphibolite layers. The supracrustal lithologies of

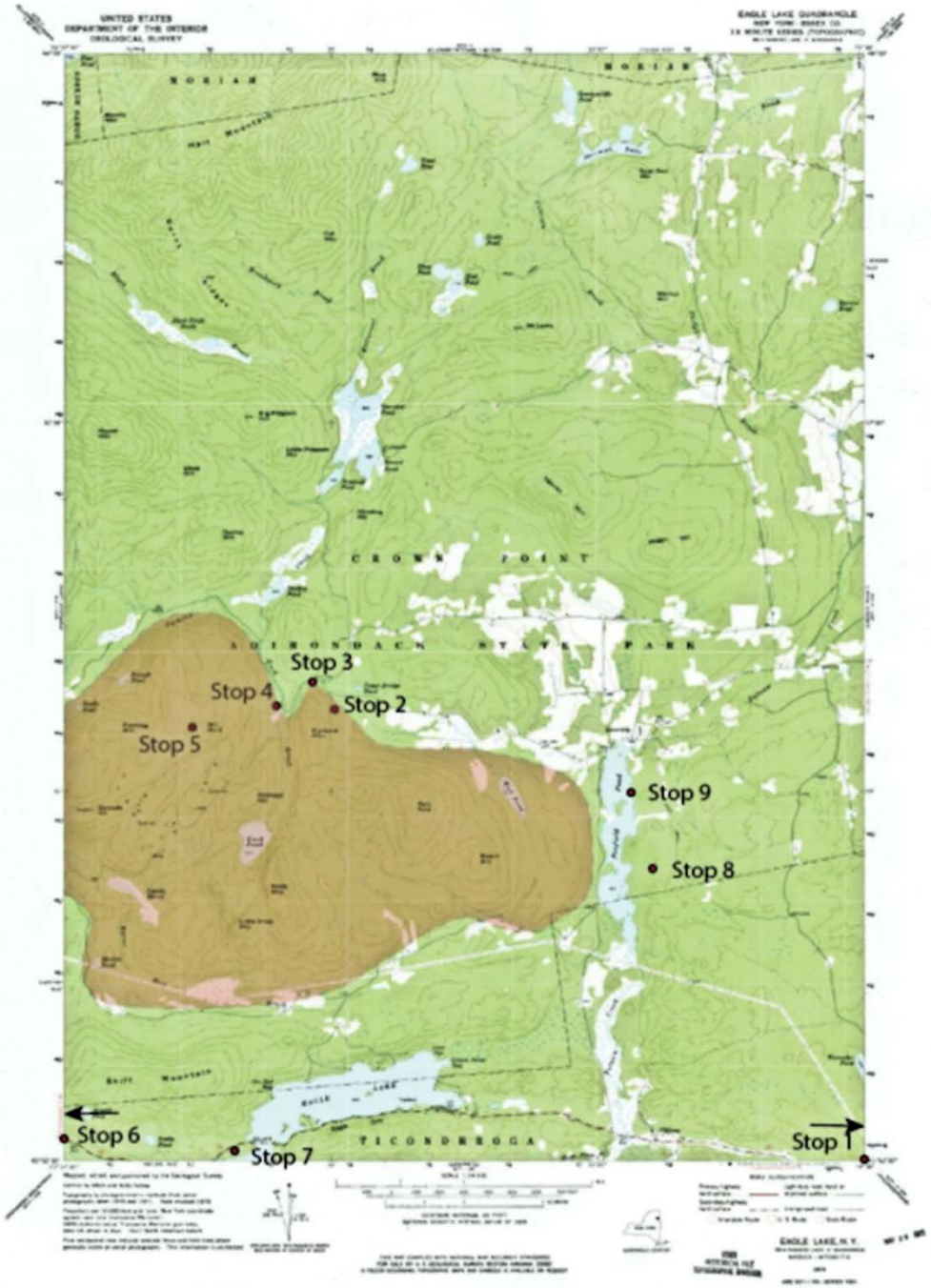

Figure 2: Topographic map of the 7.5 - minute Eagle Lake Quadrangle (ELq) and field trip locations. Shaded region approximates the region mapped at 1:12,000 scale in the area of the historic mining town of Hammondville, NY.

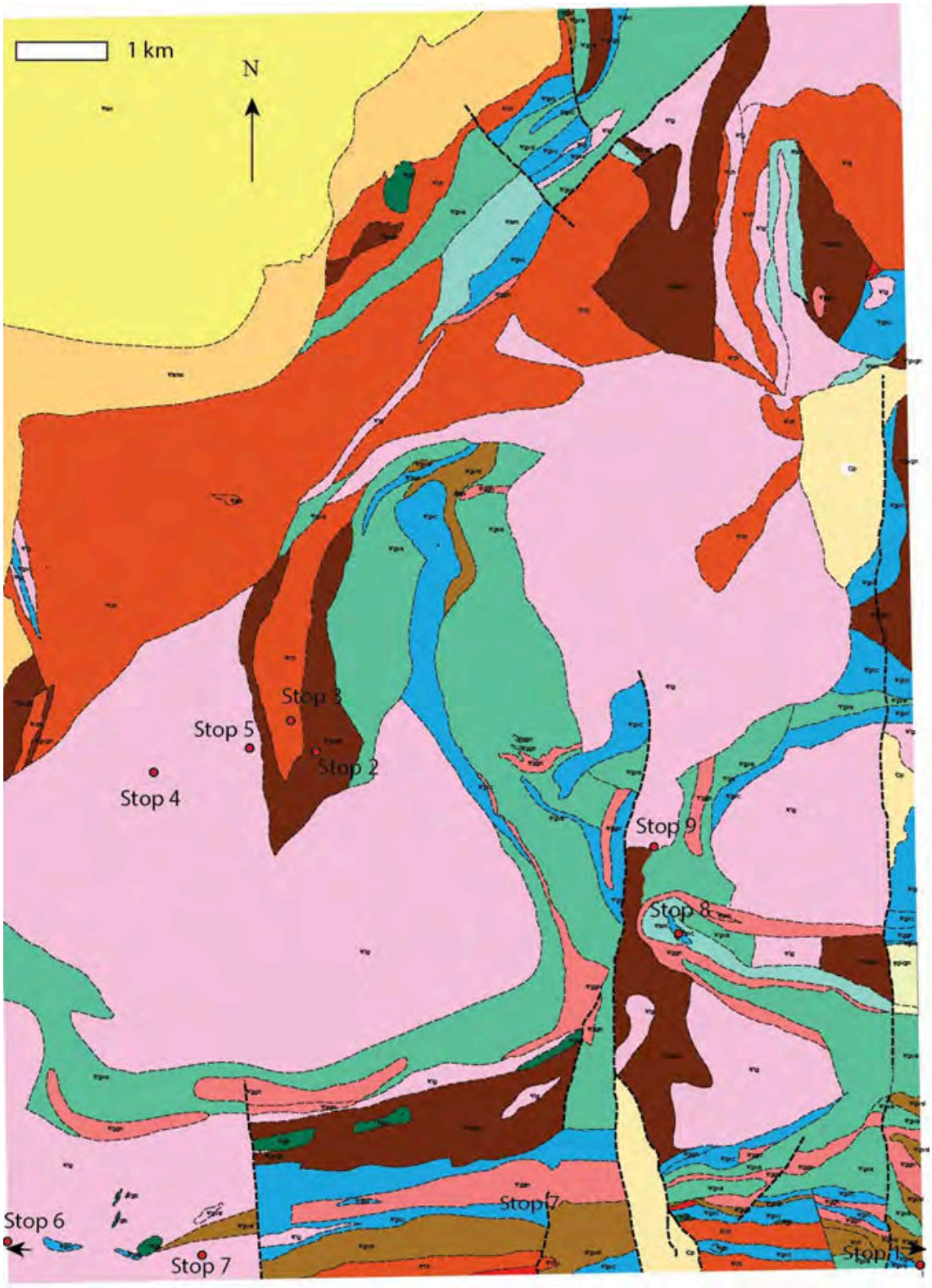

Figure 3a: Preliminary geologic map of the ELq (scaled down from 1:24,000) from March 2015. The map has changed slightly and there will be an updated version on the field trip. See Fig. 3b for the key.

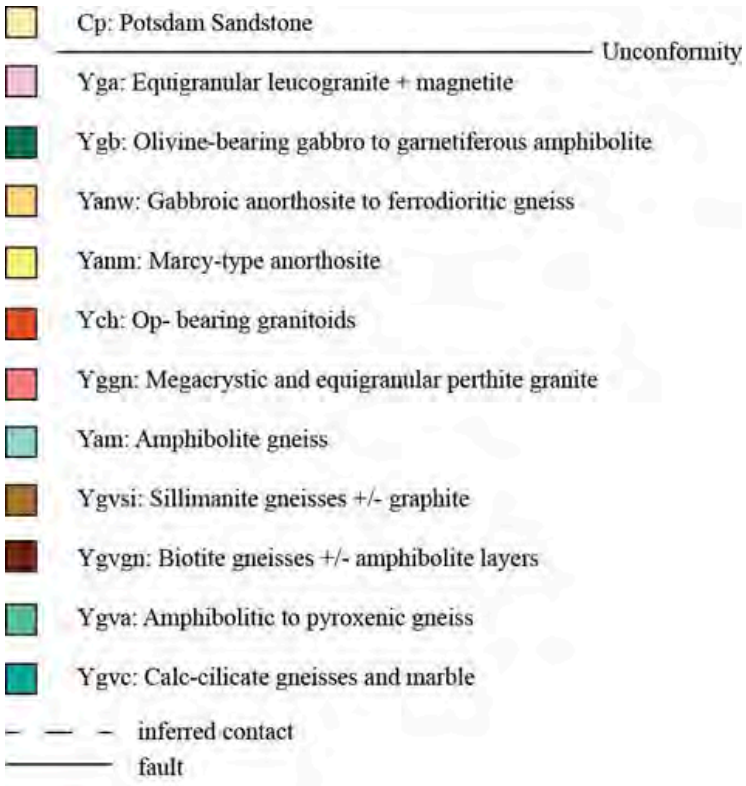

Figure 3b: Description of map units on Fig. 3a.

the ELq are varied and similar to those exposed in the Adirondack Lowlands (Carl et al., 1990; Chiarenzelli al., 2015). These lithologies are interpreted to all have formed during opening and closure of the Trans-Adirondack back arc basin, and based on their potential correlation to the Adirondack Lowlands, and preserved cross-cutting relationships, predate the Antwerp-Rossie suite (ca. 1203 Ma; Chiarenzelli et al., 2012).

Mesoperthite granite gneiss: age unknown

This unit consists of two major components: 1) a biotite –garnet-K-feldspar megacrystic (augen) granitic gneiss and 2) mesoperthite pegmatite. These two components are commonly both present in any one area or exposure of this unit. In places, the transition is exposed where anastomosing strands of variety 1 weave within a larger exposure of variety 2. Effort to obtain a U-Pb crystallization age on this lithology are ongoing. It cross cuts granulite grade fabrics within amphibolite gneisses that are interlayered with calc-silicate gneisses, and are interpreted as members of the Grenville Supergroup. It provides a useful marker layer when tracing out F_2 isoclinal folds (*see below; Figure 7b*). Based on recent mapping it appears to be the same age or older than AMCG lithologies (see below).

Figure 4. Representative field photographs for major units of the Grenville Supergroup. A) Interlayered marble and calc-silicate gneiss exposed along NY 74; B) Quartzofeldspathic gneiss with folded pegmatitic leucosome, suggesting anatexis during D_1 ; C) Amphibolite migmatite gneiss with an orthopyroxene porphyroblast within quartz-rich leucosome; D) highly migmatized and dismembered amphibolite gneiss with coarse garnet crystals.

Ca. 1158 Ma Mangerite-charnockite-granite

Rocks belonging to this suite have been extensively studied, and have fairly well understood petrologic, geochemical, and isotopic systematics (McLelland et al., 2004; Hamilton et al., 2004; Bickford et al., 2010). We will refer to this group as charnockite after Frost and Frost (2008b). The rocks contain (predominately) primary orthopyroxene, plagioclase, K-feldspar, quartz, and ilmenite, with ubiquitous metamorphic hornblende +/- garnet. This unit is strongly deformed throughout the ELq, it is important to note that as you approach the Marcy anorthosite (*see below*), rocks of this suite contain less quartz, and are predominately monzonitic to ferrodioritic. Porphyroclastic and equigranular varieties occur, but mostexposures contain a well-developed stretching lineation. Hornblende and garnet are typically metamorphic phases associated with granulite facies conditions. Some varieties do not contain opx as a primary mafic phase, and are granites. However, given their structural and petrologic similarity, and geochronologic data confirming an equivalent age (McLelland et al., 2004; Hamilton et al., 2004), these granite gneisses are lumped with other charnockitic lithologies.

Figure 5: Representative field photographs of some AMCG-related meta-igneous rock types. A) Biotite-garnet-K-feldspar megacrystic granite (augen), B) Coarse garnet porphyroblast within a mangeritic gneiss, notice the inclusion-rich core, C) Interleaved ferrodioritic gneiss and gabbroic anorthosite indicative of the marginal whiteface facies anorthosite, D) Representative field photograph of Marcy-type anorthosite on Hail Mountain. E) SHRIMP U-Pb geochronology of AMCG rocks from the Adirondack Highlands (McLelland et al., 2004).

Ca. 1154 Ma Anorthosite

Anorthosite underlies the majority of the High Peaks region of the Adirondack Highlands, and underlies the northwestern corner of the ELq. The vast majority of anorthosite is undeformed, or weakly deformed with a weak magmatic to tectonic fabric, but contains strong evidence of a high P-T static metamorphic overprint. This anorthosite is dominated by coarse andesine crystals and distinctive labradorite crystals (Marcy-type). Heterogeneously distributed within, and along the margin of the Marcy

- type anorthosite is what has traditionally been referred to as the Whiteface-type (Walton, 1956). It consists of white gabbroic anorthosite that is finer grained, contains

andesine xenocrysts, and on average more mafics (orthopyroxene + clinopyroxene + garnet) than the Marcy counterpart. Also, the Whiteface

- type generally contains a heterogeneous mixture of ferrodiorite, that also contains andesine xenocrysts (Figure 5c). In contrast to the Marcy-type anorthosite, which contains little evidence for subsolidus deformation, the Whiteface-type contains a very strong and locally mylonitic fabric. The granulite grade assemblage consisting of cpx + opx +/- grt is associated with this fabric. SHRIMP geochronology of this suite suggests that it is coeval, but statistically younger than quartz bearing members of the AMCG suite (McLelland et al., 2004; Hamilton et al., 2004).

Olivine Metagabbro

This suite of rocks occurs throughout the Adirondack Mountains, most notably as satellite plutons exposed along the margin of the Marcy Massif (Buddington , 1939). Forming km – scale plugs, dikes, and lozenges, these bodies are typically cored by olivine metagabbro with little to no penetrative fabric, preserve ophitic to subophitic textures (Whitney and McLelland, 1983), and contain spinel clouded plagioclase laths. This unit contains ubiquitous evidence for a high grade and static metamorphic overprint similar to the Marcy-type anorthosite. The metamorphic assemblage varies, but consistently contains of early biotite-clinopyroxene-hornblende-garnet coronitic textures around primary olivine, spinel clouded plagioclase, and orthopyroxene (Whitney and McLelland, 1973). It is important to note, that this suite of rocks have been dated to be similar in age to the anorthosite-massif (1146 Ma; McLelland and Chiarenzelli, 1988; McLelland et al., 2004), and has been interpreted to be compositionally admissible as the parent magma for the Marcy massif (Regan et al., 2011).

Commonly exposed along the margins of these bodies are ten to 100 meter-thick enveloping garnetiferous amphibolite that parallels the olivine metagabbro margin. A strong tectonic fabric is accompanied by an increase in modal garnet and hornblende (Lagor et al., 2013), and has been shown to be essentially isochemical with respect to their parental olivine metagabbro protolith. Both major and trace elements show marked consistency, and are even identical to a samples of olivine metagabbro analyzed throughout the Adirondack Highlands (Regan et al., 2011).

Ca. 1070 – 1060 Ma Lyon Mountain Granite (Gneiss)(name from Postel, 1952)

The LMG has been studied extensively, partially due to the fact that it hosts the largest Fe-mines in the Adirondack Mountains. Mined throughout the 1800's, the vast majority of mines closed at the turn of the century, with the last mine closing in the 1970s (McLelland et al., 2001b). The LMG itself is an equigranular microperthite granite with both biotite and magnetite as the primary mafic phases, although occasional hornblende is locally present. Aegerine-Augite is also present outside of the ELq, along with acmitic pyroxenes in some of the ores (Lupulescu et al., trip B1). Adjacent to large Fe- deposits and seams, the perthite has been altered to albite by sodic fluids accompanied the mineralization within the region (Mclelland et al., 2001b,c; Valley et al., 2010; Valley et al., 2011a,b). Elsewhere, a potassic metasomatic event has been recognized by Valley et al. (2011a), which is interpreted to occur between igneous crystallization and sodic alteration, but we have yet identify this as a regionally extensive component within the ELq.

There is little evidence of deformation within the unaltered LMG. It contains no stretching lineation (as of yet), and its layering is not metamorphic or due to deformation at the regional scale (Mclelland et la., 2001a). The LMG crosscuts granulite grade fabrics throughout the ELq, and contains numerous xenoliths of S_2 bearing rock types. Contacts with the LMG are typically parallel to subparallel with granulite-grade fabrics within the country-rock, which it locally crosscuts. Geochemically, the lithology is strongly ferroan, alkali to alkali-calcic (after Frost and Frost, 2008), and has been interpreted as syn-kinematic with collapse, but post-kinematic with respect penetrative Ottawan deformation (McLelland et al., 2001a; Selleck et al., 2005). For more description of large Fe-deposits, see Lupulescu et al., trip B1.

STRUCTURAL DATA AND FIELD RELATIONSHIPS

Structural Data

The Eagle Lake quadrangle contains evidence for at least three phases of folding and two phases of penetrative deformation. The oldest fabric within the ELq (S_1, Table 1) is only preserved within rocks of the Grenville Supergroup. It is commonly defined by migmatitic layering (McLelland and Chiarenzelli, 1988; Heumann et al., 2006) within aluminous paragneisses and amphibolite gneisses. Evidence of S_1 is best preserved within hinge regions of F_2 folds, but is otherwise difficult differentiate, due to a strong S_2 overprint. Older gneissosity and folding are currently not well understood or identified, due to transposition during D_2. S_2 is defined by the axial planes of large isoclinal folds (F_2). The axes of these folds is predominantly moderately plunging to the southeast, but the orientation is currently not well constrained. This phase of deformation effected all lithologies except for the LMG. Therefore D_2 had to occur between AMCG magmatism and emplacement of the LMG. S_1 and S_2 are parallel throughout most of the ELq within the Grenville Supergroup lithologies, and can therefore be thought of as a composite fabric within paragneisses.

Table 1: Proposed structural nomenclature for rocks within the ELq.

Fabric generation	Orientation	P-T conditions	Proposed timing	References
S_1	n/a	Greater than sillimanite	1170 Ma	McLelland and Chiarenzelli, 1988 *New data*
$S_2/F_2/M_2$	Shallowly dipping to east (axial surface); isoclinal folds	From 1.0 GPa and 850°C to 0.6 GPa and 600°C	<1160 Ma and >1070 Ma	*New data;* McLelland et al., 2001, 2004; Valley et al., 2010
F_3	Open upright folds plunging shallowly to the southwest	0.5 GPa and 700°C	1060 Ma; extensional collapse	Mclelland et al., 2001; Selleck et al., 2005; Valley et al., 2011a,b; *new data*
D_4	Boudinage, and pegmatite dikes; trending NE		1050-1000 Ma	Valley et al., 2010, *new data*

Associated with S_2 is a fabric that parallels the margin of the Marcy massif. Although not associated with map-scale F_2 isoclinal folds, the similarity between the pronounced lineation within the marginal fabric and the lineation in the interleaved paragneisses suggests that the fabric surrounding the Marcy massif formed synchronously with F_2. The ca. 1150 Ma anorthosite, underlies a large region in the NW corner of the ELq. The Marcy-type grades from an undeformed core, which preserves igneous textures and transitions outward, into highly deformed tectonites of the Whiteface – type anorthosite and other AMCG lithologies. The fabric has a constant stretching lineation orientation within the ELq and is interpreted as parallel to the axes of F_2 folds.

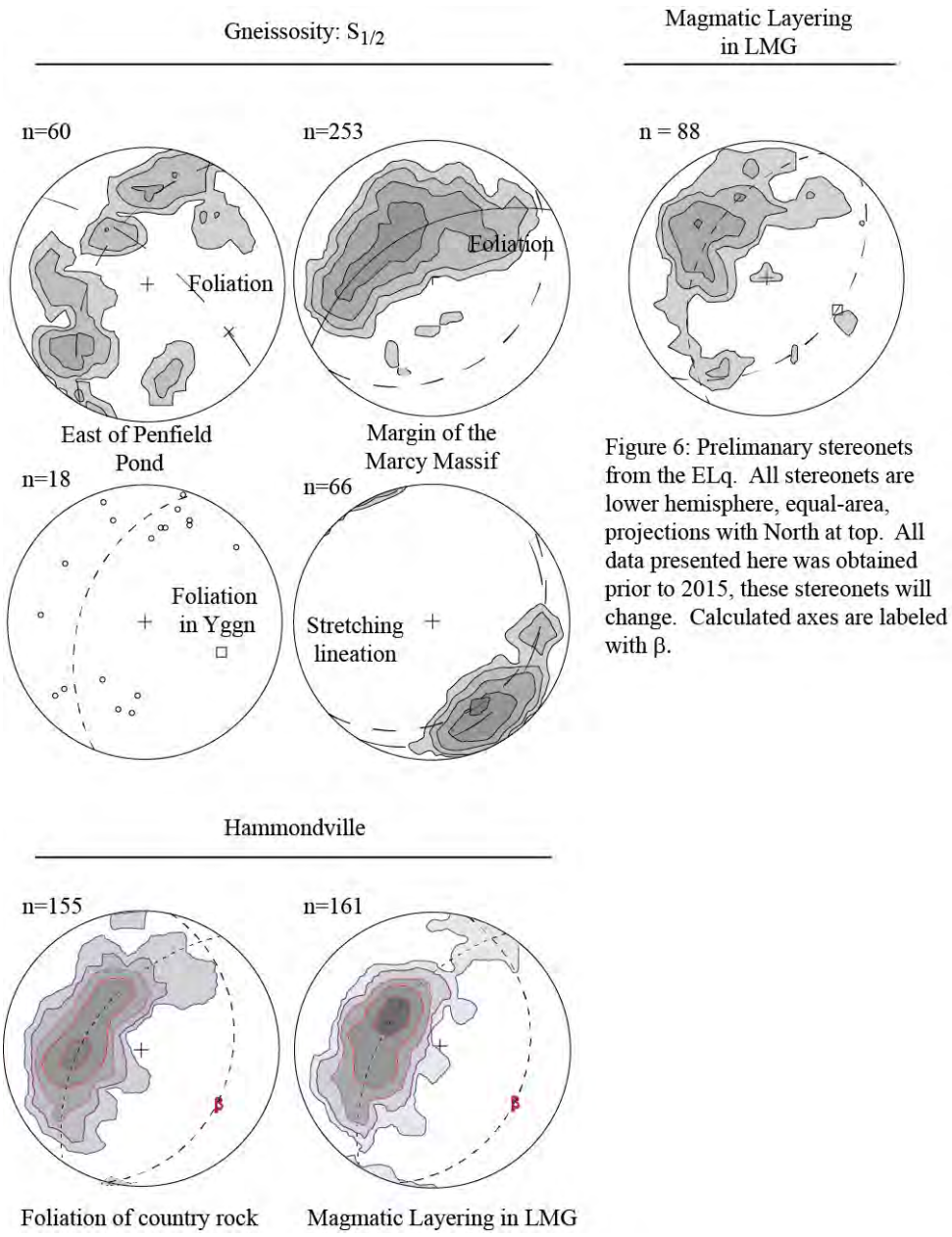

Figure 6: Prelimanary stereonets from the ELq. All stereonets are lower hemisphere, equal-area, projections with North at top. All data presented here was obtained prior to 2015, these stereonets will change. Calculated axes are labeled with β.

The last major phase of deformation, and the major control of the map pattern and stereonet analysis, is large-amplitude, open, upright F_3 folds that plunge 10 – 15° to 110°. These open folds are best developed > 4 km away from the Marcy Massif. All rock types contain evidence of this event, but outcrop-scale D_3 fabrics are not ubiquitous and there remains little evidence for associated widespread D_3 penetrative deformation. A minor phase of D_4 deformation is associated with late, upright, broad amplitude folds and boudinage. Late tabular pegmatite dikes locally follow this fabric and fill boudin necks. Generally, the fabric trends to the NNE, but analysis of this fabric is not yet complete, and may be progressive with respect to D_3.

Field Relationships

There is a large body of work that describes much of the field relationships exposed throughout the Adirondack Mountains (Buddington, 1939; Postel, 1952; *among many others*). More recent descriptions of these relationships are given in several contributions (McLelland and Isachsen, 1986; McLelland et al., 1988a,b).

Table 2: Summary of Grenville-aged rock types and field relationships exposed within the Eagle Lake quadrangle

Rock Type	Relationship	Age	Reference
Lyon Mountain Granite	Cross cuts S_2 and contains xenoliths of rocks with S_2	1070 - 1040 Ma	Buddington, 1939; Postel, 1952; McLelland et al., 2001a,b,c; Valley et al., 2011b
Olivine –bearing metagabbros	Cross cuts S_1; Cross cuts anorthosite; locally contains strong S_2 overprint	1145 Ma	McLelland and Chiarenzelli, 1988; Davidson and Van Breeman, 1988
Anorthosite	Cross cuts and contains xenoliths of Grenville Supergroup	1154 Ma	McLelland et al., 2004
Mangerite, charnockite, granite gneiss	Cross cuts and contains xenoliths of Grenville Supergroup, contains strong S_2 tectonic fabric	1158 Ma	McLelland et al., 2004; Hamilton et al., 2004
Mesoperthite Granite gneiss	Folded by F_2; cross cuts S_1 in Grenville Supergroup	Older than or equal to 1158 Ma	No data
Grenville Supergroup	A minimum of two phases of high grade metamorphism; is cross cut by all igneous rocks; there is currently little to no stratigraphic control in this part of the Adirondack Highlands	Deposition between 1230 and 1203 Ma.	Wasteneys et al., 1998; Chiarenzelli et al., 2010b; 2015

Several field relationships are well demonstrated within the ELq. AMCG lithologies cross cut, contain xenoliths of, and are younger than the Grenville Supergroup. Sillimanite-bearing quartzofeldspathic gneisses are cross cut by gabbroic rocks at Dresdon Station (*see Grover et al., this contribution*), and this is also true for rocks in the ELq. However, there is no question that AMCG rocks contain a granulite facies overprint that is shared with the surrounding supracrustal

sequence. Lastly, the LMG cross cuts all lithologies (localities south of Moose Mountain, eastern margin of Skiff Mountain, summit of Skiff Mountain, Mount Lewis, eastern shore of Penfield Pond, Hammondville, others). The LMG contains open, upright, folds that are sub-meter in scale that are parallel to F_3 and pegmatitic segregations within localized boudin necks (alkali granite or pure quartz in composition). Smaller LMG plutons, east of Penfield Pond appear to have been emplaced within the F_3 folds, and are interpreted as syn-kinematic. This is consistent with the interpretation of Mclelland et al. (2001) and Selleck et al. (2005) that interpreted the LMG to be post kinematic with respect to regional granulite grade deformation and metamorphism.

Forward petrologic modelling of D2

Thermobarometric analysis of assemblages that define the S_2 fabric is currently underway in the ELq with the goal of extending existing P-T data from the Adirondack Highlands (Bohlen et al., 1992; McLelland and Whitney, 1980; Spear and Markussen, 1997; Storm and Spear, 2005). Ferrodioritic gneisses within the marginal anorthosite facies consistently yield estimates of 0.9 GPa and 700°C, similar to results presented in Spear and Markussen (1997). However, there has been little to no forward petrologic modeling done throughout the Adirondack Highlands, despite its routine use in many other metamorphic terranes.

There is one large olivine metagabbro exposed along the margin of the Whiteface-type anorthosite east of Cat Mountain. It is cored by coarse-grained olivine-bearing metagabbro engulfed in garnetiferous amphibolite that contains a strong S_2 fabric. The geometry of the coronite and its relationship to the surrounding tectonites mimics that of the Marcy massif, but on a far smaller scale with an undeformed core, surrounded by tectonites of identical composition (Lagor, 2012). Forward modeling using Theriak-Domino (de Capitani and Petrakakis, 2010) and the Holland and Powell database (updated in 2007) was performed on the coronitic metagabbro to understand the P-T evolution during static metamorphism, and the development of the engulfing garnetiferous amphibolite. Due to variations in αH_2O throughout the rocks history, we have calculated a 3-D pseudosection plotting P, T, and αH_2O. Models were run calculating assemblage, modes of garnet, biotite, amphibole, and plagioclase and garnet composition (Figure 8). Together these result show that a single clockwise decompression path beginning above 1.0 GPa can link all existing quantitative thermobarometric points. Thermobarometry and preliminary forward petrologic models were also calculated for a coronitic metagabbro exposed in Newcomb, NY, in central Essex County for comparison, and yield nearly identical results.

There has been a discrepancy regarding the origin of massif type-anorthosite in that petrologically they appear to form near or at the Moho, and appear to be largely derived from asthenospheric mantle (Buddington, 1939; McLelland et al., 1996, 2004; Hamilton et al., 2004; Regan et al., 2011). However, Valley and O'Neil (1982) performed a systematic stable isotopic analysis of minerals from Grenville Supergroup lithologies exposed within the contact aureole of the Marcy Anorthosite.

Minerals formed during contact metamorphism contain depleted O^{18} (relative to SMOW), requiring interaction of an aqueous meteoric component during contact metamorphism, which has to be relatively shallow in the crust. The decompression P-T path described above may reconcile some of the discrepancies between evidence for both deep and shallow petrogenesis of massif-type anorthosite: it is both. In this model, rocks were largely crystallized at depth, but

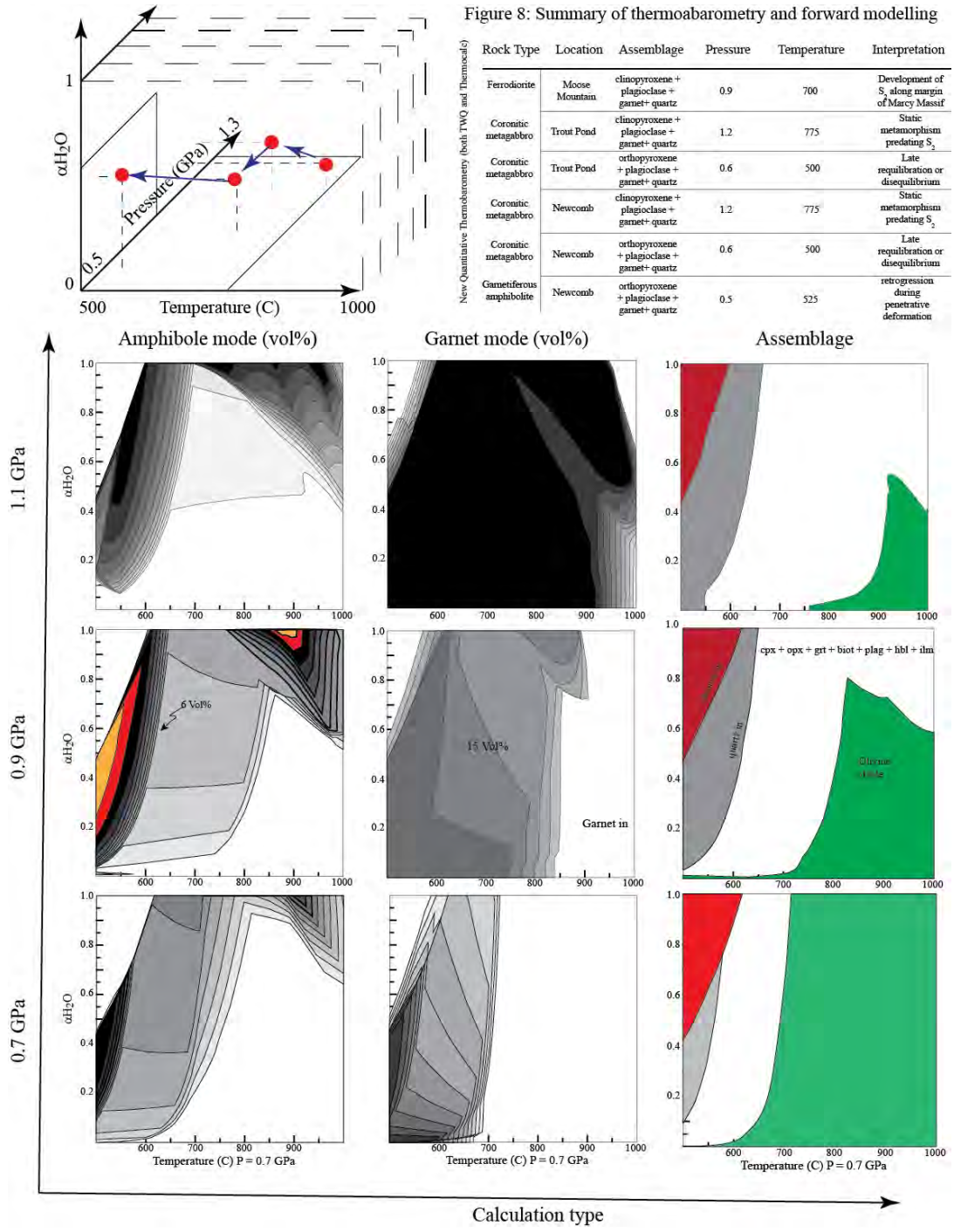

Figure 8: Summary of thermoabarometry and forward modelling

New Quantitative Thermobarometry (both TWQ and Thermocalc)	Rock Type	Location	Assemblage	Pressure	Temperature	Interpretation
	Ferrodiorite	Moose Mountain	clinopyroxene + plagioclase + garnet+ quartz	0.9	700	Development of S_2 along margin of Marcy Massif
	Coronitic metagabbro	Trout Pond	clinopyroxene + plagioclase + garnet+ quartz	1.2	775	Static metamorphism predating S_2
	Coronitic metagabbro	Trout Pond	orthopyroxene + plagioclase + garnet+ quartz	0.6	500	Late requilibration or disequilibrium
	Coronitic metagabbro	Newcomb	clinopyroxene + plagioclase + garnet+ quartz	1.2	775	Static metamorphism predating S_2
	Coronitic metagabbro	Newcomb	orthopyroxene + plagioclase + garnet+ quartz	0.6	500	Late requilibration or disequilibrium
	Garnetiferous amphibolite	Newcomb	orthopyroxene + plagioclase + garnet+ quartz	0.5	525	retrogression during penetrative deformation

Figure 8. Summary of thermobarometry and forward modelling.

the anorthosite bodies, being positively buoyant, were emplaced at mid to upper crustal levels as a crystal mush. Tectonites exposed along the margin of the massif may have formed during its emplacement. The P-T path described above is derived from rocks with structural fabrics that are prime candidates to have accommodated the emplacement of the Marcy Massif, and shows that such a metamorphic history can be modeled.

Structural evolution

The evolution of the area is summarized schematically in figure 10. The earliest recognized phase of penetrative deformation (D_1) is only exposed within the Grenville Supergroup lithologies within the ELq. It is defined by a high grade metamorphic assemblage, and is associated with migmatization in aluminous paragneisses. Recent geochronology (*stop* 1) from just outside the ELq is consistent with geochronology from the southern Adirondack Highlands (Heumann et al., 2006) that suggests anataxis occurred during the Shawinigan phase of deformation. This is consistent with the field relationships that suggest D_1 predates AMCG plutonism. This fabric may have more than one component, but we are unable to differentiate them now. Subsequent deformation (D_2) involved the isoclinal folding of a preexisting gneissosity in the Grenville Supergroup and the Mesoperthite granite gneiss, and the development of a strong axial planar fabric within AMCG lithologies. This phase of deformation is associated with granulite grade deformation within AMCG and older lithologies, but deformed pre-existing leucosome. This fabric has been interpreted as Ottawan in age (ca. 1080 Ma), but there is no direct link between time and structure necessitating this correlation. The LMG cross cuts and contains xenoliths of rocks that contain an S_2 fabric, suggesting the ca. 1070 Ma LMG post dates D_2.

Future work should focus on deciphering the age and kinematics of the structural fabric. Forward modeling presented above suggests that deformation during D_2 may also be explained by AMCG emplacement at the tail end of Shawinigan orogenesis (Regan et al., 2015). The LMG was effected by late open folding (F_3), and based on the map scale pattern, is preliminarily interpreted as syn-kinematic with respect to F_3 folding.

Geochemistry of the LMG

The LMG has been the focus of a number of analytical studies, including detailed U-Th-Pb zircon geochronology (Mclelland et al., 2011; Selleck et al., 2005; Wong et al., 2011; Valley et al., 2011a,b), paired Hf zircon analysis (Valley et al., 2010), and extensive geochemical analsyes of both major and trace element composition (Whitney and Olmstead, 1988; McLelland et al., 2001a,b,c; Valley et al., 2011a,b; Geer et al., 2015). These analyses have been performed on both ore-hosting and non ore-hosting LMG. Geochemically, the LMG is strongly ferroan (Frost and Frost, 2008) with a limited range of SiO_2 content (predominately > 70 %). On modified alkali lime index vs. SiO_2 diagrams (Frost et al., 2001; modified in Frost and Frost, 2008), they plot as alkali to alkali-calcic, forming a cluster at high MALI (figure 9). Trace elements contain systematic depletions in HFSE and enrichments in LILE, except near magnetite ore seams where host rocks show evidence of sodic alteration (Mclelland et al., 2001c; Valley et al., 2010; 2011a,b; Geer et al., 2015). On tectonic discrimination diagrams after Pearce et al. (1984), the LMG plots from a within plate granite to rift field. All of these data strongly suggest an anhydrous crustal source for the LMG. The incompatible element trend is best explained as an inherited subduction signature from preexisting lithologies in the source region (Valley et al., 2011). Furthermore, the lack of lower SiO_2 variants extensive evidence for a relatively high oxygen fugacity (Wones, 1989; McLelland et al., 2001c), and the strongly ferroan major element

composition of the LMG are all consistent with the chemistry of felsic igneous rocks within other extensional settings.

Geochemistry of ore and host rocks within Hammondville and Skiff Mountain

The LMG hosts numerous zones of magnetite mineralization that were mined for iron beginning in the early 19th century. Recently some of these deposits were discovered to contain apatite with elevated levels of REEs (Valley, 2011; Lupelescu, trip B-2). Hammondville was a mining town in the eastern Adirondack Mountains in operation in the 1890s, and was one of the largest producers of iron in the region. Targeted 1:12,000 scale mapping of Hammondville was undertaken to understand the petrogenesis of the LMG and the structural and petrologic relationship of magnetite mineralization and REE distribution. This is part of a larger mapping project in the Eagle Lake quadrangle. Paired ore and host rock samples have been collected for petrologic and geochemical analyses in order to evaluate petrogenetic links between magnetite mineralization and the host granite within the Hammondville region.

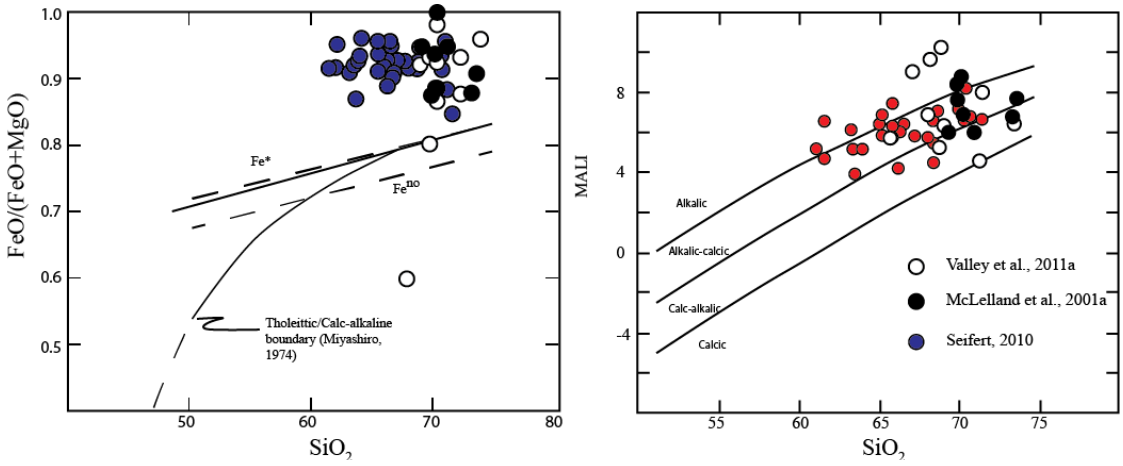

Figure 9. Fe-index and modified alkali-lime index plotted against SiO2 (after Frost et al., 2001; Frost and Frost, 2008; and references therein) for existing geochemistry of the LMG. Also plotted are geochemical data from charnockites sampled throughout the Adirondacks (Seifert, 2010). Please note that the LMG and charnockite gneisses show similar geochemical trends.

The host rock immediately surrounding the magnetite ore in Hammondville is typically a quartz albite rock with amphibole and clinopyroxene. On Harker diagrams there is a clear trend between SiO_2 and Al_2O_3, MgO, $TiO_2Fe_2O_3$ and total alkalis. It is strongly ferroan (Frost and Frost, 2008), similar to past studies (Valley et al., 2011, with a range of SiO_2 from 65% to 75%. They also plot as alkali to alkali-calcic on a modified alkali lime index vs. SiO_2 diagram (Frost et al., 2001; modified in Frost and Frost, 2008). Chondrite normalized REE plots display a slight enrichment in LREE, a pronounced negative Eu anomaly and a depletion in HREE (Sun and McDonough, 1989). The LMG within Hammondville commonly contains a layering interpreted as magmatic in origin because of the lack of strain shown in petrographic thin section, but ongoing discussions surround the role of thermal annealing. Locally, the LMG exhibits strain in areas typically located near major zones of magnetite mineralization.

Ore samples (samples with >34% Fe_2O_3) from Hammondville typically contain magnetite, amphibole, clinopyroxene, quartz and albite. There is a strong Fe_2O_3 trend vs. SiO_2 on a Harker

diagram, however other trends in major element composition are lacking. The ore shares similar REE element trends with the hosts including a pronounced negative Eu anomaly and a depletion in HREE on chondrite normalized diagrams (Sun And McDonough, 1989). However, they exhibit a more level LREE tendency and several samples are much more highly enriched than host rock. Anastomosing seams of magnetite range in thickness from < 1cm to roughly 2 m and commonly branch into multiple seams that can have deformed tendrils extending from the main seam. Petrographic analyses show local deformation in some areas of mineralization that can extend into the surrounding host.

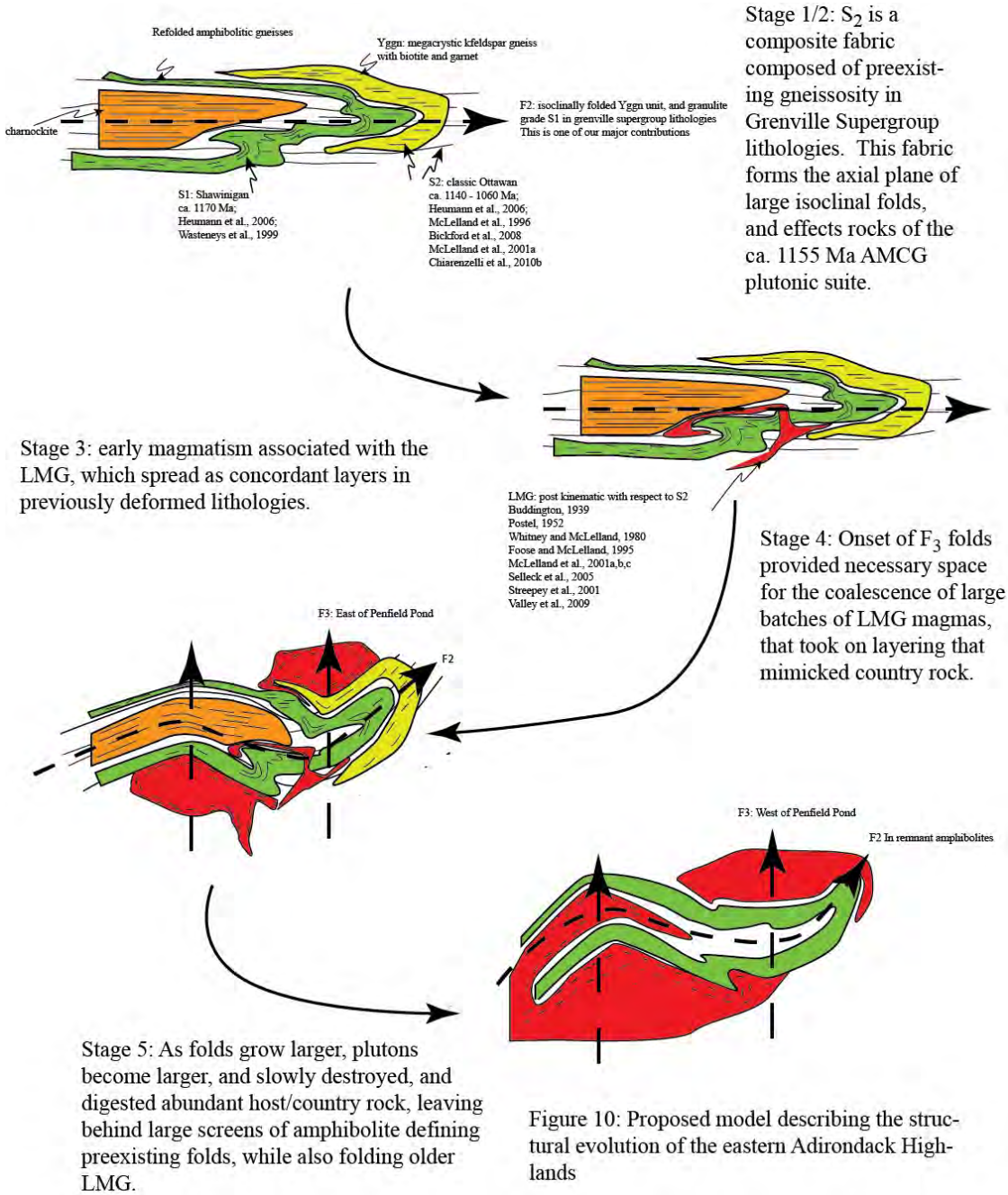

Figure 10: Proposed model describing the structural evolution of the eastern Adirondack Highlands

CONCLUSIONS

The descriptions above provide a basic overview of Grenville Geology of the ELq and beyond. The most important part of this contribution is to put forth a structural nomenclature that is transformative, and represents the major phases of deformation within the ELq and surrounding regions. Good limits exist for the timing of D_1, but little data exists that directly constrains the timing of D_2. Future work should focus on the timing, P-T conditions, and kinematics of this structural fabric.

ACKNOWLEDGEMENTS

First and foremost, we would like to extend a precious thanks to Dr. James McLelland whose rigorous, detailed, and innovative analyses of these rocks has made advances well beyond his predecessors. Secondly, we would like to thank National Cooperative Geological Mapping Fund and the Youth Initiative Fund for providing support to map the Eagle Lake quadrangle. Funding for some of the above geochronology came from a University of Northern Colorado Provost Research and Dissemination grant awarded to Dr. Graham Baird. Paul and Mary-Lloyd Borroughs have been extremely helpful, and beyond nice to the mappers. This project would not be near the place it currently is if it wasn't for their hospitability, friendship, and boathouse. Generous permission from Lyme Adirondack Timberlands (LAT) allowed us to access much of the private land in the quadrangle. Several stops require written permission from LAT to visit these localities; any future visiits must be approved by LAT. The residents of Ticonderoga and Crown Point are acknowledged for their ongoing support. Detailed and thorough reviews were provided by Arthur Merschat and Ryan McAleer, which significantly improved the field trip guide.

ROAD LOG

MEET AT 8:30 AM: Ticonderoga McDonalds Parking Lot (*coordinates in NAD83*)

Location Coordinates: N 43°51.455' W 073°26.258'

0.0 miles: Turn: right out of parking lot and an immediate left onto NY-74

1.0 miles: pull over on right shoulder at long road cut, stop 1.

STOP 1: Roadcut on NY-74, west of Ticonderoga, NY

Location Coordinates: N 43°51.665' W 073°27.495'

The easternmost rock is a poikiloblastic garnet amphibolite that contains garnet-clinopyroxene, plagioclase, and hornblende. Fe-Ti oxides are present as well, though can only be seen in thin section. The garnet crystals can reach upwards of 3 cm in diameter, the best examples are concentrated in the westernmost part of the garnet amphibolite. Schistosity, mostly defined by aligned hornblende and appears to both traverse and wrap around the garnet poikiloblasts, suggesting garnet growth was syn-kinematic.

Further west along the outcrop is a transition zone, marked by a vegetated slope, containing some layers of marble and a rusty weathering paragneiss. West of the transitions zone the vast majority of the outcrop is composed of a garnet-biotite-plagioclase-perthitic microcline-quartz ±

sillimanite migmatitic paragneiss. Leucosome proportion is estimated to be 30-50% and preferentially contains garnet, while biotite is concentrated in the melanosome. Though some texturally late leucosome contains biotite, this can be shown to grade into garnet-bearing leucosome. Both leucosome and melanosome layers are deformed and define a foliation parallel to a schistosity defined by aligned biotite. Quartz and feldspar are granoblastic in both the leucosome and melanosome.

Within the migmatitic paragneiss a number of garnet rich boudins occur, these are possibly deformed and metamorphosed dikes. The boudins indicate stretching in all directions parallel to gneissic layering suggesting a flattening finite strain. Also present within the migmatitic paragneiss are bodies of amphibolite similar to what is present at the east end of the outcrop. Three, 5 to 30 meters wide, unstrained, amoeboid-shaped, pegmatitic granitic plutons also occur in the migmatitic paragneiss.

Mineralogy of the pegmatites includes feldspar, quartz, and biotite. Most feldspar appears to have exsolution lamellae indicating alkali feldspar, but locally plagioclase has been observed. Due to the coarse grain size (upwards of 30 cm for feldspar and quartz and 50 cm. for biotite) the exact lithology has not been constrained, but it is thought to be an alkali-feldspar granite. Locally associated with the pegmatites in the host migmatite are cm. books of graphite.

Fabric orientation is essentially parallel among the garnet amphibolite, the migmatitic paragneiss, and the transitional contact zone between the two. The foliation in the garnet amphibolite and eastern portions of migmatitic paragneiss is approximately 062°, 43° but changes to about 103°, 45° by the westernmost end of the outcrop. Lineation is reasonably parallel to the outcrop face and ranges from a horizontal to 30° plunge, tending 100°. The lineation is defined by aligned hornblende, biotite, or sillimanite, depending on location within the outcrop. Asymmetric tails on garnet poikiloblasts in the garnet amphibolite suggest south side (top) to the west transport.

To constrain timing of geologic events recorded in the outcrop, samples of the migmatitic paragneiss and of pegmatite were processed for U/Pb zircon geochronology. For the paragneiss, given the scale of leucosome and melanosome interlayering, it was not possible to separate the two upon processing, so separated zircon is from both components. Such zircons are euhedral to subhedral, stubby to elongate, yellow to amber to brown in color, and are 100 μm to 500 μm in length.

Cathodoluminescence (CL) of polished grain cross sections show that zircons have a wide variety of internal zoning patterns from oscillatory to irregular zoning (Figure 11 inset). No consistent core-rim zoning pattern (or of any other type) could be generalized for the separated zircon grains. Results of 21 SHRIMP-RG analyses of all types of zircons and all CL zones reveal what it interpreted as a unimodal age distribution. 16 of 21 analyses define a chord with an upper-intercept of 1186 ± 25 Ma, which is interpreted to be the age of migmatization for the paragneiss (Figure 11).

Zircon from one pegmatite body is euhedral to subhedral, equant to stubby, and light pink to purple in color. Zircon size is poorly constrained as most grains are fragments of grains greater than approximately 500 μm. Cathodoluminescence of polished grain cross sections reveal all grains possess oscillatory or sector zoning (Figure 12 inset). No convincing core-rim relationships were found. Fourteen SRHIMP-RG analyses produce what is interpreted as a unimodal distribution of ages. Six if these are nearly concordant and produce a $^{207}Pb/^{206}Pb$ weighted mean age of 1051 ± 25 Ma that is thought to best represent the age of pegmatite formation (Figure 12).

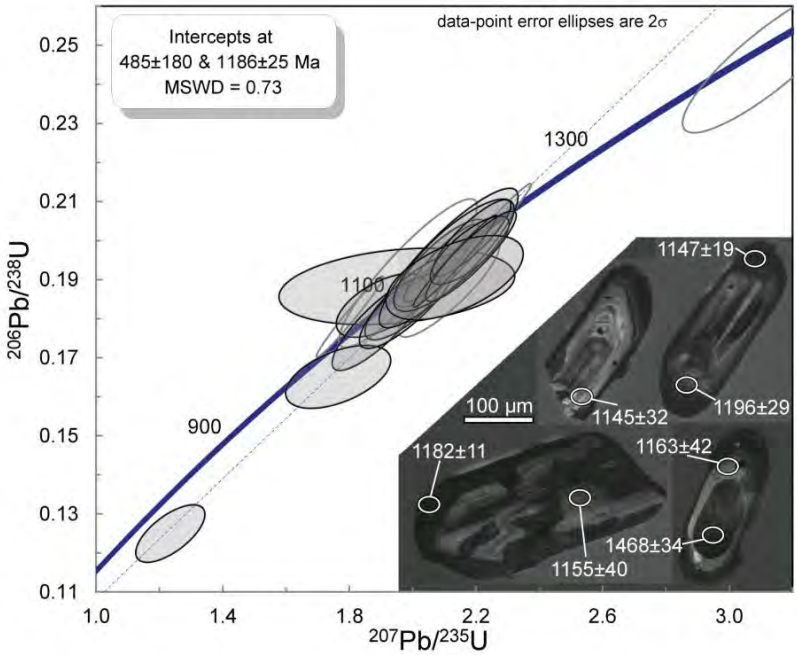

Figure 11. Concordia diagram of U/Pb zircon SHRIMP-RG analysis of the migmatitic paragneiss. Sixteen analyses (shaded) define a chord upper-intercept of 1186 ± 25 Ma (2σ), which is taken as the age of partial melting. One inherited core was analyzed and resulted in a 1468 ± 34 Ma age. Inset shows cathodoluminescence images of representative zircon grains and $^{207}Pb/^{206}Pb$ ages of spot analyses.

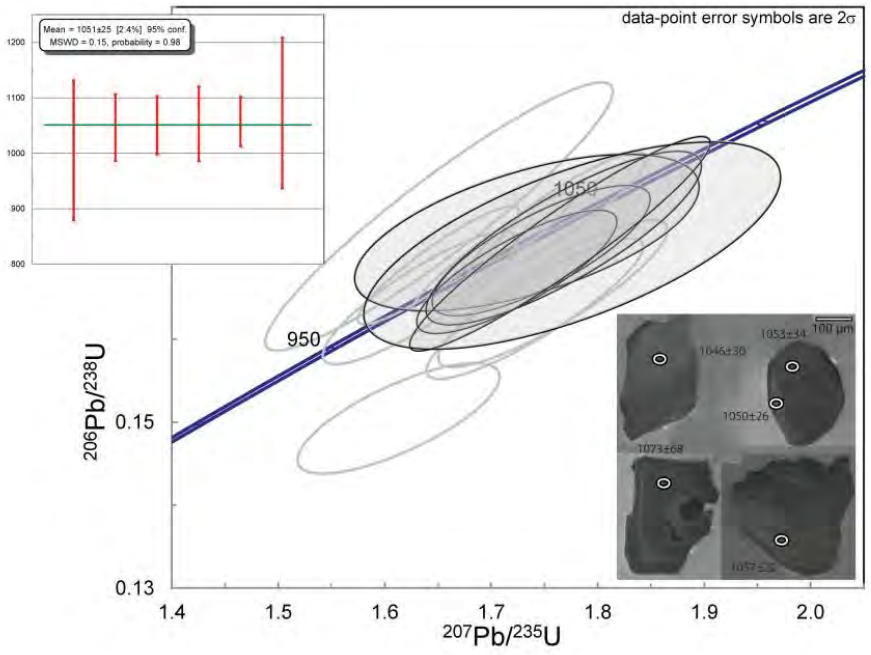

Figure 12. Concordia diagram for 14 U/Pb zircon SHRIMP-RG analyses. Upper-left inset show the $^{206}Pb/^{207}Pb$ weighted mean for the 6 best clustered and concordant analyses (shaded), which produces an age of 1051 ± 25 Ma, thought to be the age of pegmatite. Lower-right inset shows representative grain fragments and spot analyses.

1.0 miles: merge back on NY-74 west (please be careful)

5.4 miles: Turn right onto Corduroy Road (we just drove over a graben, people!)

8.3 miles: Turn left onto Old Furnace Rd

10.9 miles: Pull the car onto the right shoulder (there is really nothing of note here), and walk 235 meters on trail to south, stop 2.

STOP 2: Transposed Grenville Supergroup

Location Coordinates: N 43° 55.548', W 073°34.976'

This is an exposure of metamorphosed and folded meta-siliciclastics of the Grenville Supergroup (Davidson, 1998). Notice the very well layered nature of the rock, the related compositional variability, and the gradational transitions between various layers. Also note several asymmetric folds that are particularly easy to see within leucosome. This suite of rocks saw the following events: 1) deposition, 2) partial melting (M_1), and 3) folding of this migmatitic gneissosity, and the development of axial planar fabric (S_2). These relationships suggest that anatexis and high-grade metamorphism likely accompanied S_1, which is interpreted to be Shawinigan based on the geochronology discussed at stop 1. This suite of rocks is common throughout the ELq, and represents some of the oldest rocks preserved within ELq.

Depart Stop 2, continue on Old Furnace Rd.

11.1 miles: stay left on Old Furnace Rd

11.2 miles: park on right side of road next to mangeritic pavement, stop 3

STOP 3: Contact between mangeritic gneiss and the Grenville Supergroup.

Location Coordinates: N 43°55.753' W 073°35.174'

Several small outcrops are present to the southwest along Old Furnace Road. We will start by the parked cars. In stark contrast to the rocks seen at the previous outcrop, this rock is fairly homogenous. It is a mangeritic gneiss, with hbl +/- grt composing the tails around primary opx (McLelland et al., 1980).

Do you see evidence of more than one phase of deformation within this lithology?

As we move south, we will see a quick transition back into the Grenville Supergroup. This produces an interesting map pattern, a dome structure that is cored by monocyclic mangeritic gneiss, engulfed by meta-siliciclastic rocks of the Grenville Supergroup, with the predominate fabric running parallel to the axial trace of (F2?). However, we know from the previous stop that the predominate fabric we see in the paragneisses is an aggregate of two planar fabrics. The big question is; can we see S1 in the mangeritic gneiss?

Depart Stop 3, continue SW

11.4 miles: turn left onto logging road

12.1 miles: park and walk up old logging road (350 m), stop 4

STOP 4: Hill No. 8

Hill No. 8 is in the northern part of the historic mining town of Hammondville. On the north eastern base is the remains of a great furnace used to melt and separate the ore mined here in the late 19th century (next stop). The remaining slag is the blue stone used on many of the roads in the area that you can see on the drive in and out.

Hill No. 8 was the northern most extent of the mining operations of Hammondville and included two major pits: the Hammond Pit and Number 8 Mine. The number 8 mine is the deepest in Hammondville, reaching depths of up to 1000 ft (Penfield museum, personal correspondence), however the exposure in the Hammond pit is better and more easily accessible.

Magnetite seams in the Hammond pit range from centimeter scale to roughly 2 meters in thickness. The seams display a discrete wavy contact with the host LMG and split into multiple seams in places. They are concordant to the local fabric (038°, 27°) which is much stronger within the vicinity of mineralization. The ore is >70% Fe_2O_3 with slightly elevated REE levels. A thin section of a seam contained beautiful S-C fabrics indicating a reverse sense shear with top to the southeast, Further investigation into the relationship between the timing of deformation and magnetite mineralization is underway. The host LMG immediately surrounding mineralization seems to be very gneissic and contains albite, quartz, amphibole, and pyroxene. It has an Fe_2O_3 content of less than 7%, Na_2O of more that 6.5% and REE levels slightly higher than that of the ore.

A sample of LMG was also collected roughly 100 m from the mine on the western side of Hill # 8 and is elevated in REEs and contains a potassium content an order of magnitude higher than the immediate host. It also records subsolidus deformation, perhaps related to the massive magnetite deposits, however the reverse shear is top to the NW. Again, constraining timing for this is underway.

Turn around and depart Stop 4.

12.9 miles: intersection of logging road with Old Furnace Road, park cars, stop 5

STOP 5: Old Furnace.

Location Coordinates: N 43°55.605’ W 073°35.395’

Old Furnace locality. Depart by turning left onto Old Furnace Road.

18.1 miles: turn left onto Paradox Rd

18.7 miles: turn left onto NY-74 (heading east)

19.8 miles: turn right into parking lot with cannonball, park, walk 350 meters west on NY 74, then go north in the woods, stop 6.

STOP 6: Schofield magnetite mine.

Location Coordinates: N 43.888°, W -73.637°.

WARNING: Route 74 is a busy road with lots of heavy truck traffic.
Walk single file and stay well to the side of the road.

Walk west down the road for approximately a quarter mile until you reach a brown and yellow sign marking the boundary of the Adirondack Park. Proceed into the forest for approximately 75 meters to the base of a cliff.

This stop examines the relationship between magnetite ores and the Lyon Mountain granite (LMG) that hosts the ore. Most of the main ore seam has been mined out and is covered by large blocks of mine waste. However there are places where the relationship between the ore and the host granite can be observed. The main ore seam starts here at the base of the cliff and gradually climbs up the hill to the east parallel to the main foliation in the granite. The host rock on either side of the ore seam is albitized granite and is the result of fluid alteration. The amount of albite in the rock gradually diminishes as distance from the mineralized ore zone increases and perthitic feldspar becomes common. The ore is comprised of magnetite and apatite ± quartz. The apatite is generally reddish in outcrop and is extremely enriched in light rare earth elements and high field strength elements (especially Y, Ce and Nd). The mineralogy of the "granite" varies from perthitic feldspar + quartz + magnetite ± clinopyroxene, biotite, and amphibole in the least altered rocks, to quartz + albite + magnetite ± apatite and chlorite in the most altered zones. The contact between the ore and the granite is generally sharp but a large boulder here at the base of the cliff shows numerous mm-thick layers of magnetite. Zircon grains from the ore have been dated at 1000.9 ± 9.2 (2σ) (Valley et al., 2009).

Proceed uphill along the ore seam approximately 75 meters to the east by following an animal trail and scrambling over boulders. Here the ore is perfectly exposed in a large out of place slab and is where the geochronology sample was collected. Even though a reliable age for the host LMG could not be obtained at Skiff Mountain, the age of the zircon in the ore here is at least 34 my younger than that of the granite. This is based on the age of zircon rims in the LMG that was successfully dated near here at Eagle Lake (see EAGLE LAKE STOP; Figure 13).

Continue following the ore seam uphill to the east. Watch for a small outcrop of hematized breccia. The ore seam will disappear under mine waste rock and forest. At this point head directly uphill until reaching a relatively flat area. You will see what appears to be a ditch, sometimes filled with water, backed by a 3-4 m high outcrop. This is the top of the upper ore seam. Follow this relatively flat area to the west. At 43.886056, 73.637028, the top of the upper ore seam is visible. The ore seam is approximately 0.5 m thick with a second 2-3 cm thick vein just above the main ore. The adjacent granite is typically lacking in disseminated magnetite in the vicinity of the

veins, but disseminated magnetite reappears where veins are lacking and distal to the ore vein. Near the top of this outcrop small lozenge shaped quartz-feldspar-magnetite pegmatites are present (~20-30 cm long). Follow the upper ore seam west for approximately 60 m. Here 1 m below the ore body, there are two amphibolite layers 10 to 20 cm thick. Recent geologic mapping suggests that these are mafic "screens" that were incorporated in the LMG during intrusion. Zircon grains from one of these layers have been dated at 1046 ± 11 Ma (2σ) (Valley et al., 2011) with rare zircon cores that are ~1150 Ma. These layers and the host LMG have been overprinted by Na fluid alteration providing a maximum age for Na fluid alteration. The increase in albitization around the ore suggests Na metasomatism is coeval with zircon growth and ore mineralization. It is probable that the U/Pb age from zircon in the amphibolite layer is the product of metamorphism or possibly a fluid alteration event that is older than the fluids associated with the growth of zircon in the ore at Skiff Mountain.

Depart by turning right out of parking lot, headed east on NY-74.

21.3 miles: enter small pull off on left, walk 75 meters east on NY-74, stop 7.

STOP 7: The Lyon Mountain Granite Gneiss (after Postel, 1956)

From the cars, walk east about 0.3 miles to an outcrop on the right (south) side of the road. At this locality a granitic pegmatite dike crosscuts the fabric of the LMG. The LMG has been altered by K-rich fluid alteration that has been overprinted by minor Na alteration. The crosscutting dike has also experienced minor Na alteration. Both the dike and the granitic hosts have extreme concentrations of potassium for granitic rocks (~8 wt.% for both rocks). It is not clear if the dike is high in potassium because it intruded an already metasomatized rock and thus was enriched in K_2O by a relatively closed system, or if both the dike and the host were altered by potassium bearing fluids together in an open system. Both the dike and the granite experienced subsequent minor sodic alteration. The dike is comprised of coarse microcline, quartz, and biotite, with minor plagioclase, zircon, apatite, and magnetite ± clinopyroxene and muscovite. Plagioclase is secondary and is present interstitially and in "patch" perthite which crosscuts microcline grains.

A sample from the dike was collected for U/Pb zircon geochronology and was dated by Secondary Ion Mass Spectrometry (SIMS). Zircon crystals from this sample are elongate (300-500 µm long), clear with patchy zonation in BSE images, and typically contain large inherited cores of both AMCG (~1150 Ma) and LMG (~1060 Ma) age. The zircon rims from grains with relict cores and grains without cores have a concordant age of 1030.4 ± 1.8 Ma (2σ) (Valley et al. 2011). The aforementioned field relations imply that Na alteration has to be younger than the U-Pb zircon age of the dike. They also suggest that the forces responsible for fabric development within the LMG must have ended by this time.

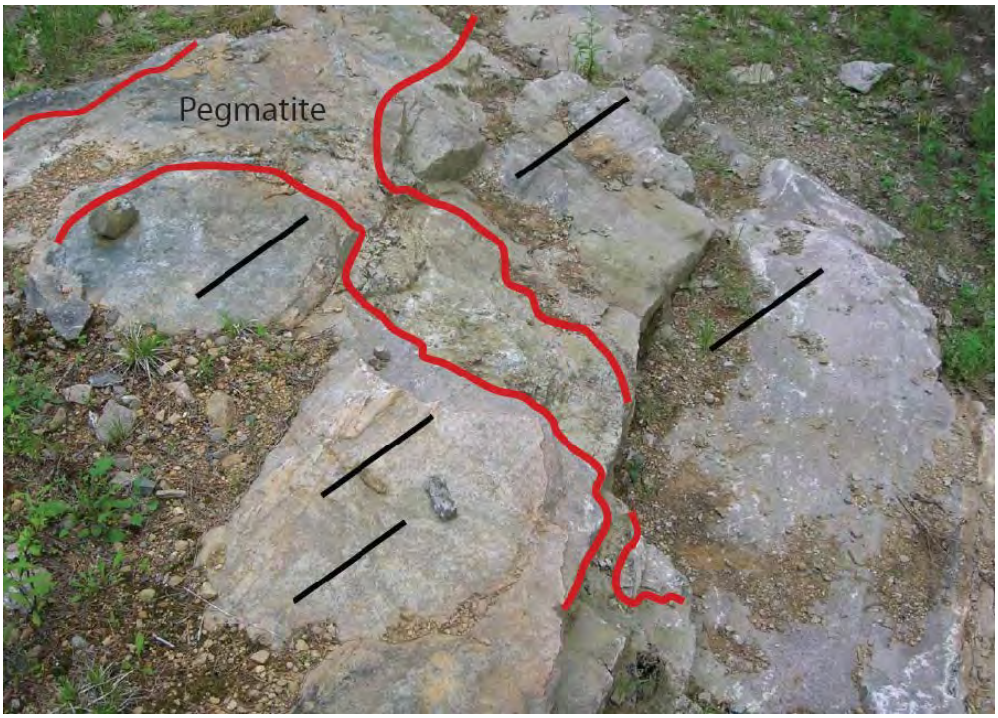

Figure 13: Field photograph showing layering (black lines) in LMG being crosscut by pegmatite dike on 74.

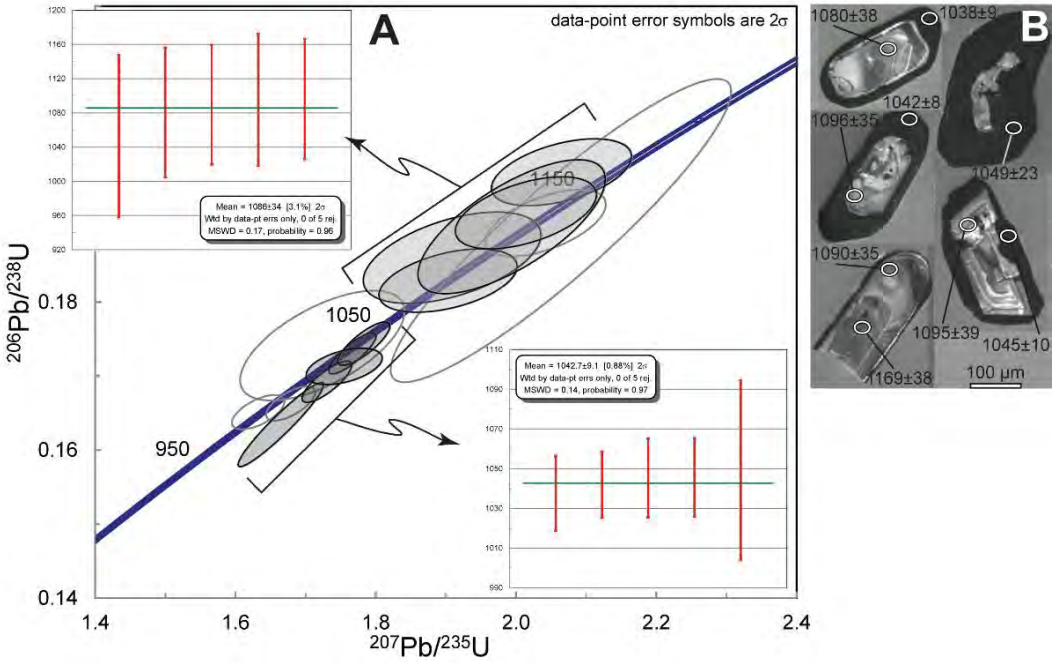

Figure 14: A) Concordia diagram from Skiff Mt. LMG. Shaded ellipses represent analyses used in weighted averages for cores (c. 1086 Ma, upper-left inset) or rims (1043 Ma, lower-right inset). B) Representative zircon cathodoluminescence images and spot analyses. Ages are 2σ $^{207}Pb/^{206}Pb$ ages.

A sample of the host rock was collected within in a few meters of the dike discussed above in order to constrain the timing of Skiff Mt. LMG intrusion. Zircons separated from the sample are euhedral to subhedral, stubby to elongate, typically 200-500 µm long, and are amber to brown in color.

Cathodoluminescence (CL) of polished grain cross sections reveal that most zircons have oscillatory zoned cores and prominent dark rims with subtle and limited oscillatory or patchy zoning (Figure 14). A few grains appear to possess a core, mantle, and rim. In such grains, rim CL is consistent with the rims of other grains, with the mantle and core both having oscillatory zoning. Twenty U/Pb SHRIMP-RG analyses of all zones demonstrate that the cores (or mantle, if three zones are present) are 1086 ± 34 Ma (2σ $^{207}Pb/^{206}Pb$ weighted average, 5 analyses; Figure 14), while rims cluster at 1043 ± 9 Ma (2σ $^{207}Pb/^{206}Pb$ weighted average, 5 analyses, Figure 14). For grains with three zones, only two cores were analyzed and produced 2σ $^{207}Pb/^{206}Pb$ ages of 1169 ± 38 Ma and 1138 ± 28 Ma. These older core ages are interpreted to be inherited, while the c. 1086 Ma age is interpreted to be the magmatic crystallization age of the Skiff Mt. LMG body, with the c. 1043 Ma rim age representing the timing of fluid alteration. Though the timing of fluid alteration age is slightly older than the age of the altered pegmatite dike at the limits of error, we believe that pegmatite dike intrusion and fluid alteration were in close temporal proximity.

Depart and stay east on NY-74

24.7 miles: turn left onto Corduroy Rd

29.5 miles: stay straight

29.7 miles: Turn right onto Towner Hill Road

30.5 miles: stay straight

31.9 miles: Turn right by Gleebus sign

32.9 miles: Take left by amphibolite

33.1 miles: Park at log landing, follow trip leaders into the woods for 30 meters, stop 8.

STOP 8: Highly deformed augen gneiss

Location Coordinates: N 43°54.356' W 073°31.875'

We are in the eastern portion of the quadrangle, which is dominated by large amplitude, upright folds that contain a calculated β-axis of 10 to 112 (Figure 6). There is no identified axial planar fabric associated with this fold generation (F_3). The rock exposed here is a strongly deformed augen granitic gneiss (Yggn on new 7.5' quadrangle map). Any one exposure typically contains both pegmatitic (mesoperthitic) varieties that are weakly deformed as well as biotite-megacrystic varieties that are strongly deformed and contain >5% modal garnet (vol%). The latter unit is isoclinally folded (F_2), and contains a very strong S_2 here. Can we see a lineation? Is there evidence of folding at the outcrop scale (F_1)?

This unit is still undated, but is currently thought to be equivalent or older than ca. 1165 Ma.

Depart Stop 8 by turning around.

33.3 miles: Turn right by amphibolite

34.4 miles: Turn left onto Towner Hill Road

36.6 miles: Turn left onto Corduroy Road

36.8 miles: veer onto Corduroy

38.2 miles: take left onto dirt road, park before bridge, hike west (upstream) on dog trail for 2.0 km, stop 9.

STOP 9: Penfield Pond – granite pegmatite cross cutting amphibolitic gneiss

Location Coordinates: N 43°54.992' W 073°32.189'

We are in the hinge of an F_3 fold. We have walked through the LMG the entire way here. This outcrop contains amphibolitic gneiss, which is locally migmatitic, and a concordant lens of mesoperthite granite. The mesoperthite granite is typically associated with the augen gneiss seen at Stop 8, despite the lack of tectonic fabric within the granite. At one location in the outcrop (Fig. 5a,b), the granite cross cuts the amphibolite gneiss at a low angle. This truncation suggests that migmatization predates the mesoperthite granite, and that migmatitic layering is transposed to be nearly parallel to S_2, but may have occurred during S_1.

REFERENCES CITED

Baird, G. B., and MacDonald, W. D., 2004. Deformation of the Diana Syenite and Carthage-Colton Mylonite Zone: implications for timing of the Adirondack Lowlands deformation. in Tollo, R. P., Corriveau, L., McLelland, J., and Bartholomew, M. J., eds., Proterozoic Tectonic Evolution of the Grenville Orogen in North America: Geological Society of America Memoir, 197: 285-297.

Bickford, M.E., McLelland, J., Selleck, B., Hill, B., and Heumann, M., 2008, Timing of anataxis in the eastern Adirondack highlands: implications for tectonic evolution during the ca. 1050 Ma Ottawan orogenisis: Geological Society of America Bulletin, V. 120, p. 950-961

Bohlen, S.R., Valley, J.W., and Essene, E.J., 1985, Metamorphism in the Adirondacks: Petrology, pressure and temperature: Journal of Petrology, v. 26, p. 971 - 992

Chiarenzelli, J. and McLelland, J., 1993. Granulite facies metamorphism, paleoisotherms, and disturbance of the U-Pb systematics of zircon in anorogenic plutonic rocks from the Adirondack Highlands. Journal of Metamorphic Geology, v. 11, p. 59-70.Chiarenzelli, J., and McLelland, 1991, Age and regional relationships of granitoid rocks of the Adirondack Highlands: Journal of Geology, v. 99, p. 571–590.

Chiarenzelli, J., Hudson, M., Dahl, P., and deLorraine, W. D., 2012. Constraints on deposition in the Trans-Adirondack Basin, Northern New York: Composition and origin of the Popple Hill Gneiss: Precambrian Research, v. 214-215, p. 154-171.

Chiarenzelli, J., Lupulescu, M., Thern, E., and Cousens, B., 2011a, Tectonic Implications of the Discovery of a Shawinigan Ophiolite [Pyrites Complex] in the Adirondack Lowlands: Geosphere, v. 7, p. 333-356

Chiarenzelli, J. R., Valentino, D. W., Thern, E., and Regan. S., 2011b, The Piseco Lake Shear Zone: A Shawinigan Suture [abstract]: Geological Association of Canada, v. 34, p. 40.

Chiarenzelli, J. and Valentino, D., 2008. Igneous protoliths of the Piseco Lake Shear Zone, Southern Adirondacks [abstract]: Geological Association of Canada, v. 33, p. 34.

Chiarenzelli J., Regan, S., Peck, W., Selleck, B., Baird, G. and Shrady, C., 2010a, Shawinigan Magmatism in the Adirondack Lowlands as a Consequence of Closure of the Trans-Adirondack Back-Arc Basin: Geosphere, v. 6, p. 900-916.

Chiarenzelli, J., Lupulescu, M., Cousens, B., Thern, E., Coffin, L., and Regan, S., 2010b, Enriched Grenvillian Lithospheric Mantle as a Consequence of Long-Lived Subduction Beneath Laurentia: Geology, v. 38, p.151-154.

Daly, S. and McLelland, J., 1991, Juvenile Middle Proterozoic crust in the Adirondack Highlands, Grenville Province, northeastern North America: Geology, v. 19, p. 119–122.

Dickin, A., and McNutt, R., 2007, the Central metasedimentary belt (Grenville Province) as a failed back-arc rift zone: Nd isotopic evidence: Earth and Planetary Science Letters, V. 259, p. 97-106

Foose, M. P., and McLelland, J. M., 1995, Proterozoic low – Ti iron – oxide deposits in New York and New Jersey: relation to Fe – oxide (Cu – U – Au – rare element) deposits and tectonic implications, Geology, v. 23, p. 665 – 668.

Frost, B.R., Barnes, C.O., Collins, W.J., Arculus, R.J., Ellis, D.J., and Frost, C.D., 2001, A geochemical classification for granitic rocks: Journal of Petrology, v. 42, p. 2033 – 2048.

Frost, B.R., and Frost, C.D., 2008a, A geochemical classification for feldspathic igneous rocks: Jounral of petrology, v. 49, n. 11, p. 1955 – 1969.

Frost, B.R., and Frost, C.D., 2008b, On charnockites: Gondwana Research, v. 13, p. 30-44.

Hamilton, M.A., McLelland, J.M., and Selleck, B.W., 2004, SHRIMP U/Pb zircon geochronology of the anorthosite-mangerite-charnockite-granite suite, Adirondack Mountains, NY: Ages of emplacement and metamorphism, in Tollo, R.P., Corriveau, L., McLelland, J.M., and Bartholomew, M.J., eds., Proterozoic Tectonic Evolution of the Grenville Orogen in North America: Geological Society of America Memoir 197, p. 337–355.

Hoffman, P.F., 1988, United Plates of America, the birth of a craton: Early Proterozoic assembly and growth of Laurentia: Annual Review of Earth and Planetary Sciences, v. 16, p. 543-603, doi:10.1146/annurev.ca.16.050188.002551.

Heumann, M.J., Bickford, M.E., Hill, B.M., McLelland, J.M., Selleck, B.W., and Jercinovic, M.J., 2006, Timing of anatexis in metapelites from the Adirondack lowlands and southern highlands: A manifestation of the Shawinigan orogeny and subsequent anorthosite-mangerite-charnockite-granite magmatism: Geological Society of America Bulletin, v. 118, p. 1283-1298. doi: 10.1130/B25927.1

Irvine, T.N. and Baragar, W.R.A., 1971. A Guide to the Common Volcanic Rocks. Canadian Journal of Earth Sciences, v. 8, p 523-548.

Isachsen, Y.W., and Fisher, D.W., 1970, Geologic map of New York: Adirondack sheet: New York State Museum, Map and Chart Series 15, scale 1:250000.

Lagor, S., Chiarenzelli, J. R., and Regan, S. P., 2013. Implications of the transition of coronitic metagabbro to garnetiferous amphibolite in the Adirondack Highlands: Geological Society of America Abstracts with Programs,v. 45, p. 800.

Lupulescu, M. V., Chiarenzelli, J. R., Pullen, A. T., and Price, J. D., 2011, Using pegmatite geochronology to constrain temporal events in the Adirondack Mountains. Geosphere, 7, p. 23-29.

McLelland, J.M., Selleck, B.W., and Bickford, M.E., 2010,Review of the Proterozoic evolution of the Grenville Province, its Adirondack outlier, and the Mesoproterozoic inliers of the Appalachians, in Tollo, R.P., Bartholomew, M.J., Hibbard, J.P., and Karabinos, P.M., eds., From Rodinia to Pangea: The Lithotectonic Record of the Appalachian Region: Geological Society of America Memoir 206, p. 1–29.

McLelland, J.M., Bickford, M.E., Hill, B.H., Clechenko, C.C., Valley, J.W., and Hamilton, M.A., 2004, Direct dating of Adirondack massif anorthosite by U-Pb SHRIMP analysis of igneous zircon: Implications for AMCG complexes: Geological Society of America Bulletin, v. 116, p. 1299–1317.

McLelland, J., Hamilton, M., Selleck, B., McLelland, J.M., Walker, D., and Orrell, S., 2001a, Zircon U- Pb geochronology of the Ottawan orogeny, Adirondack Highlands, New York: Regional and tectonic implications: Precambrian Research, v. 109, p. 39–72.

McLelland, J., Daly, S., and McLelland, J.M., 1996, The Grenville orogenic cycle [ca 1350-1000 Ma]: An Adirondack Perspective: Tectonophysics, v. 265, p. 1-28, doi: 10.1016/S0040-1951[96]00144-8.

McLelland, J., Chiarenzelli, J., Whitney, P., and Isachsen, Y., 1988. U-Pb zircon geochronology of the Adirondack Mountains and implications for their geologic evolution. Geology, v. 16, p. 920-924.

Philpotts, A. R., 1967, Origin of certain iron-titanium oxide and apatite rocks, Economic Geology, V. 62, p. 303-315.

McLelland, J., Foose, M.P., and Morrison, J., 2001b, Kiruna-type low Ti, Fe oxide ores and related rocks, Adirondack mountains, New York, High-temperature hydrothermal process, in Slack, J.F., editor, Part I. Proterozoic iron and zinc deposits of the Adirondack Mountains New York and the New Jersey Highlands: Society of Economic Geologists Guidebook Series, v. 35, p. 7-17.

McLelland, J., Morrison, J., Selleck, B., Cunningham, B., Olson, C., and Schmidt, K., 2001c, Hydrothermal alteration of late- to post-tectonic Lyon Mountain gneiss, Adirondack Mountains, New York: Origin of quartz-sillimanite segregations, quartz-albite lithologies, and associated Kiruna-type low Ti Fe-oxide deposits: Journal of Metamorphic Geology, v. 20, p. 175 – 190.

McLelland, J.M. and Whitney, P.R., 1980, A generalized garnet-forming reaction for metaigneous rocks in the Adirondacks: Contributions to Mineralogy and Petrology, v. 72, p. 111-112.

McLelland, J. and Chiarenzelli, J., 1989, Age of xenolith-bearing olivine metagabbro, eastern Adirondack Mountains, New York: Journal of Geology, v. 97, p. 373-376.

Mezger, K., 1992, Temporal evolution of regional granulite terranes: Implication for the formation of lowermost continental crust: Continental Lower Crust, Ed(s): R.M. Fountain et al., p. 447-472.

Mezger, K., van der Pluijm, B., Essene, E., and Halliday, A., 1992, The Carthage-Colten mylonite zone (Adirondack Mountains, New York): The site of a cryptic suture in the Grenville orogeny?: the Journal of Geology, v. 100, p. 630-638.

Peck, W., Selleck, B., Wong, M., Chiarenzelli, J., Harpp, K., Hollocher, K., Lackey, J., Catalano, J., Regan, S., and Stocker, A., 2013. Orogenic to postorogenic [1.20–1.15 Ga] magmatism in the Adirondack Lowlands and Frontenac terrane, southern Grenville Province, USA and Canada: Geosphere.

Postel, A. W., 1952, Geology of Clinton County magnetite district, New York. Geological Survey Professional paper 237.

Regan, S.P., Chiarenzelli, J.R., McLelland, J.M., and Cousens, B.L., 2011, Evidence for an enriched asthenospheric source for coronitic metagabbros in the Adirondack Highlands: Geosphere, v. 7, no. 3, p. 694-709.

Rivers, T. 2008. Assembly and preservation of lower, mid, and upper orogenic crust in the Grenville Province—Implications for the evolution of large, hot, long-duration orogens. Precambrian Research 167:237–59.

Rivers, T., 2011, Upper-crustal orogenic lid and mid-crustal core complexes: signature of a collapsed orogenic plateau in the hinterland of the Grenville Province: Canadian Journal of Earth Science, v. 49, p. 1-42.

Selleck, B., McLelland, J.M., and Bickford, M.E., 2005, Granite emplacement during tectonic exhumation: The Adirondack example: Geology, v. 33, p. 781–784, doi: 10.1130/G21631.1.

Seifert, K.E., Dymek, R., Whitney, P.R., and Haskin, L.A., 2010, Geochemistry of massif anorthosite and associated rocks, Adirondack Mountains, New York: Geosphere, v. 6, p. 855–899.

Spear and Markussen, 1997, Mineral zoning, P-T-X-M phase relations and metamorphic evolution of some Adirondack granulites: Journal of Petrology, v. 38, p. 757-783.

Storm, L., and Spear, F., 2005, Pressure, temperature, and cooling rates of granulite facies migmatitic metapelites from the southern Adirondack highlands, New York: Metamorphic Geology, v. 23, p. 107 – 130.

Sun, S-s.and McDonough, W. F., 1989, Chemical and isotopic systematics of oceanic basalts: Implications for mantle composition and processes, in Saunders, A. D. and Norry, M. J., eds., Magmatism in the ocean basins: Geological Society [London] Special Publication 42, p. 313-345.

Valley, J.W. and O'Neil, J.R. (1982) Oxygen isotope evidence for shallow emplacement of Adirondack anorthosite. Nature, v. 300, p. 497–500.

Valley, P.M., Hanchar, J.M., and Whitehouse, M.J., 2009, Direct dating of Fe oxide-(Cu-Au) mineralization by U/Pb zircon geochronology: Geology, v. 37, p. 223–226, doi: 10.1130/G25439A.1.

Valley, P.M., and Hanchar, J.M., 2008, Timing of fluid alteration and Fe mineralization in the Lyon Mountain Granite: implications for the origin of low-Ti magnetite deposits, in Selleck, B.W., editor, Field Trip Guidebook for the 80th Annual Meeting of the New York State Geological Association, Lake George, NY, P. 135-143

Valley, P. M., 2010, Fluid alteration and magnetite-apatite mineralization of the Lyon Mountain granite: Adirondack Mountains, New York State. PhD thesis, Memorial Univ. of Newfoundland, St.John's, Newfoundland. 282 p.

Valley, P.M., Hanchar, J.M., and Whitehouse, M.J., 2011, New inisghts on the evolution of the Lyon Mountain Granite and associated kiruna-type magnetite-spatite deposits, Adirondack Mountains, New York State: Geosphere, v. 7, n. 2.

Wasteneys, H., McLelland, J., and Lumbers, S., 1999, Precise zircon geochronology in the Adirondack Lowlands and implications for plate tectonic models of the Central metasedimentary belt, Grenville Province, Ontario, and Adirondack Mountains, New York: Canadian Journal of Earth Sciences, v. 36, p. 967–984

Walton, M.S., 1960, Geologic map of the Eagle Lake quadrangle, NY: New York State Geological Survey, Open File Report 1g584, 1:24,000 Series, 1 hand colored sheet.

Wong, M.S., Williams, M.L., McLelland, J.M., Jercinovic, M.J. and Kowalkoski, J., 2011, Late Ottawan extension in the eastern Adirondack Highlands: Evidence from structural studies and zircon and monazite geochronology: GSA bulletin, v. 124, n. 5-6, p. 857 – 869.

Whitney, P. R., and Olmsted, J. F., 1988, Geochemistry and origin of albite gneisses, northeastern Adirondack Mountains, New York, Contributions to Mineralogy and Petrology, v. 99, p. 476–484.

CURRENT RESEARCH IN STRUCTURE, STRATIGRAPHY, AND HYDROGEOLOGY IN THE CHAMPLAIN VALLEY BELT OF WEST- CENTRAL VERMONT

JONATHAN KIM
Vermont Geological Survey, Montpelier, VT 05620

KEITH KLEPEIS
Dept. of Geology, University of Vermont, Burlington, VT 05405

PETER RYAN
Dept. of Geology, Middlebury College, Middlebury, VT 05753

EDWIN ROMANOWICZ
Center for Earth and Environmental Science, SUNY at Plattsburgh, Plattsburgh, NY 12901

INTRODUCTION

Over the past four years, the Vermont Geological Survey and professors and undergraduate students from the University of Vermont, Middlebury College, and SUNY at Plattsburgh geology departments have formed a multidisciplinary fractured bedrock consortium. This consortium integrates varying expertise and resources to comprehensively address applied geologic issues in Vermont, such as groundwater quality (i.e. radionuclides, arsenic, nitrates, fluoride, and manganese), groundwater quantity of domestic and public wells, groundwater-surface water interaction, and shallow geothermal energy. The purpose of this trip is to visit field sites in the Champlain Valley Belt of west-central Vermont that illustrate our group's current research efforts in fractured bedrock hydrogeology. At each site, we will discuss how structural geology, stratigraphy, and hydrogeology (including geophysical well logging) bear on a specific environmental issue. This trip will not only visit classic sites such as the Champlain Thrust at Lone Rock Point and the Hinesburg Thrust at Mechanicsville, where we will discuss refined structural chronologies, but also locations that exhibit a strike-slip fault zone in the Winooski River Spillway (Williston), a well-described wrench fault site in Shelburne, phosphorite layers that explain elevated radioactivity in the bedrock aquifer (Milton), and a site in Hinesburg where field mapping of fractures has been correlated with those in geophysical logs. The following Bedrock Geology of Vermont, Field Area Geology, Structural Geology, Metamorphism, and Geochronology sections are modified from Kim et al. (2011).

BEDROCK GEOLOGY OF VERMONT

Vermont can be divided into several north-northeast trending bedrock belts of generally similar age and tectonic affinity (Figure 1). From west to east the belts are;

1) Champlain Valley: Cambrian – Ordovician carbonate and clastic sedimentary rocks deposited on the eastern (present coordinates) continental margin of Laurentia (e.g., Stanley and Ratcliffe, 1985). This continent was left behind after the Rodinian supercontinent rifted apart during the Late Proterozoic and the intervening Iapetus Ocean formed between it and Gondwana (e.g., van Staal et al., 1998). The margin was deformed and weakly metamorphosed during the Ordovician Taconian Orogeny. It was deformed again during the Devonian Acadian Orogeny.

2) Taconic Allochthons: Late Proterozoic- Ordovician slices of clastic metasedimentary rocks of oceanic and continental margin affinity that were thrust onto the Laurentian margin (Champlain Valley Belt) by arc-continent collision during the Taconian Orogeny (e.g., Stanley and Ratcliffe, 1985).

3) Green Mountain: Late Proterozoic–Cambrian rift- and transitional rift-related metasedimentary and meta-igneous rocks that unconformably overlie Mesoproterozoic basement rocks. These assemblages were deformed and metamorphosed during the Taconian Orogeny (also during the Acadian Orogeny) (e.g., Thompson and Thompson, 2003).

4) Rowe-Hawley: Metamorphosed continental margin, oceanic, and suprasubduction zone rocks of Late Proterozoic-Ordovician age that were assembled in the suture zone of the Taconian Orogeny. These rocks also were deformed and metamorphosed during the Acadian Orogeny. Arc components are part of a Shelburne Falls Arc that collided with the Laurentian margin, causing the Taconian Orogeny (Karabinos et al., 1998). Recent detrital zircon work by McDonald et al. (2014) indicates that the Moretown Formation, the central member of the Rowe-Hawley Belt, had a Gondwanan rather than Laurentian source.

5) Connecticut Valley: Silurian and Devonian metasedimentary and metaigneous rocks deposited in a post-Taconian marginal basin. Tremblay and Pinet (2005) and Rankin et al. (2007) suggested that this basin formed from lithospheric extension associated with post-Taconian collisional delamination processes. These rocks were first deformed and metamorphosed during the Acadian Orogeny.

6) Bronson Hill: Ordovician metaigneous and metasedimentary rocks of magmatic arc affinity and the underlying metasedimentary rocks on which the arc was built (e.g., Stanley and Ratcliffe, 1985). Recent studies show that this is a composite arc terrane with juxtaposed components of Laurentian and Ganderian/ Gondwanan arc affinity (e.g., Aleinikoff and Moench, 2003; Aleinikoff et al., 2007; Dorais et al., 2008; 2011). Accretion of the arc terranes onto the composite Laurentia occurred during the latest stage of the Taconian Orogeny and Silurian Salinian Orogeny (van Staal et al., 2009).

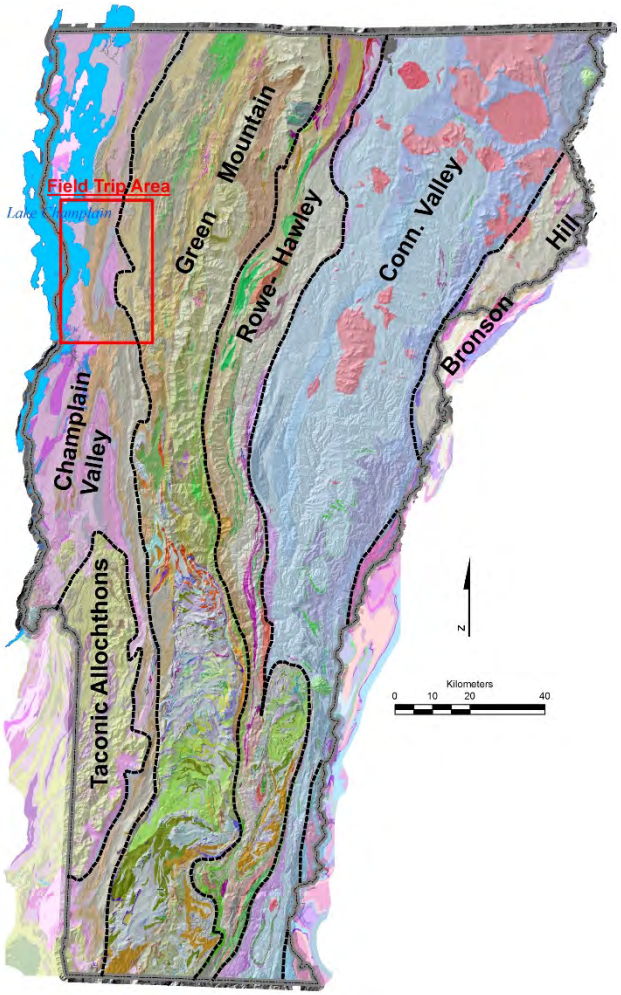

Figure 1. Tectonic belts in Vermont. Modified from Ratcliffe et al. (2011).

FIELD AREA GEOLOGY

The field area for this trip encompasses the western part of the Green Mountain Belt and the Champlain Valley Belt (Figure 1). These belts represent the foreland and western hinterland of the Taconian Orogen of west-central Vermont respectively (e.g., Stanley and Wright, 1997). This region can be divided into three lithotectonic slices which are, from west to east and from structurally lowest to highest: A) the Parauthochthon, B) the Hanging Wall of the Champlain Thrust, and C) the Hanging Wall of the Hinesburg Thrust (Figure 2). The Champlain Thrust forms the tectonic boundary between A and B, whereas the Hinesburg Thrust separates B and C. The Parautochthon is primarily comprised of shales of the Stony Point Formation (note that the Iberville Formation shale is "lumped" with those the Stony Point Formation), representing Taconian flysch, but also contains normal fault- bounded carbonates of the informally-named Charlotte "Block". These lithotectonic divisions are shown on the map in Figure 2 and can be interpreted from the tectonostratigraphic cross section in Figure 3. It is worth noting that the next lithotectonic unit to the west is the autochthon of eastern New York State, where Mesoproterozic metamorphic rocks of the Adirondacks are unconformably overlain by

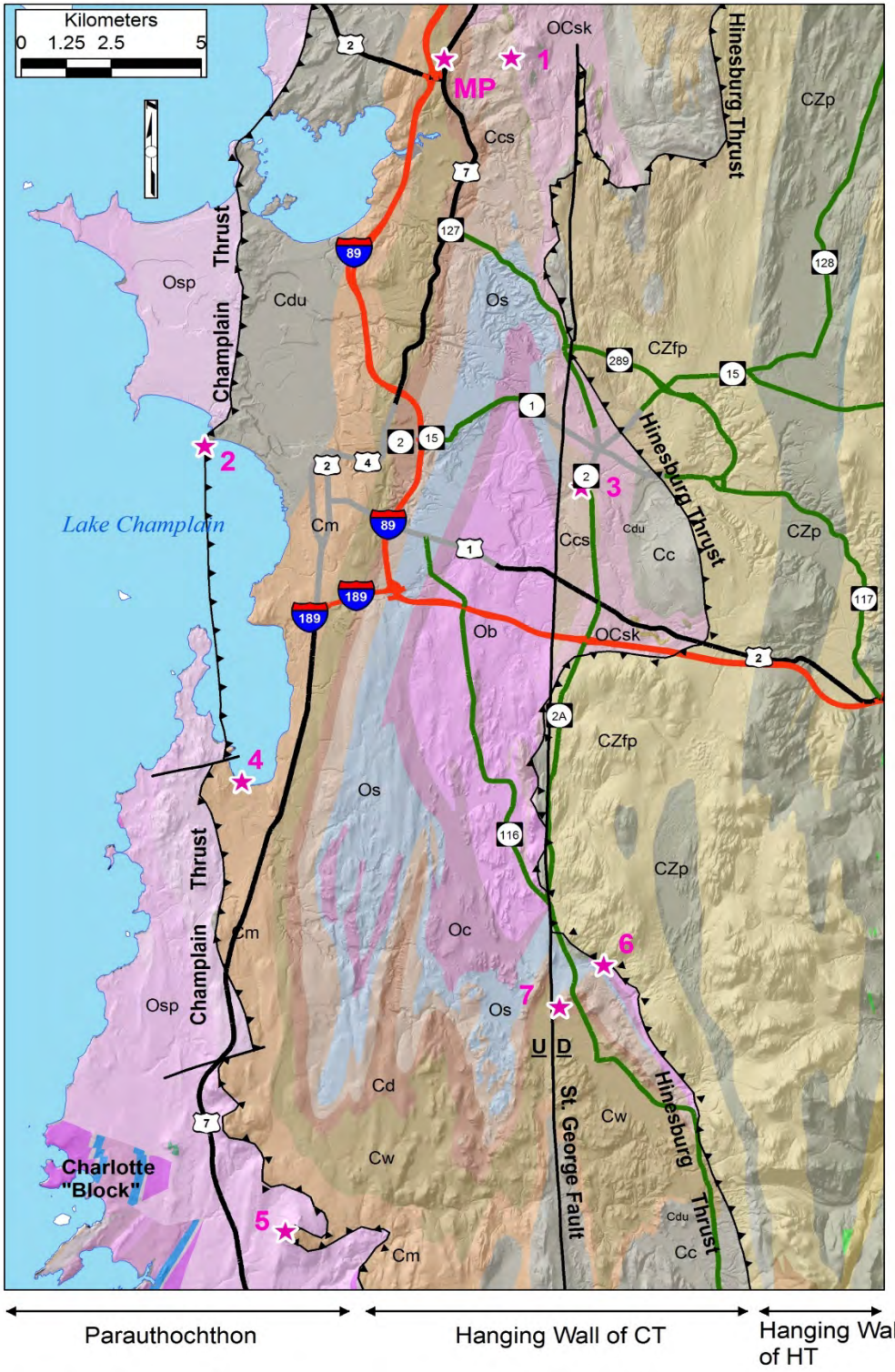

Figure 2A. Bedrock geologic map of the field area showing stop locations. MP = meeting place. Modified from Ratcliffe et al. (2011).

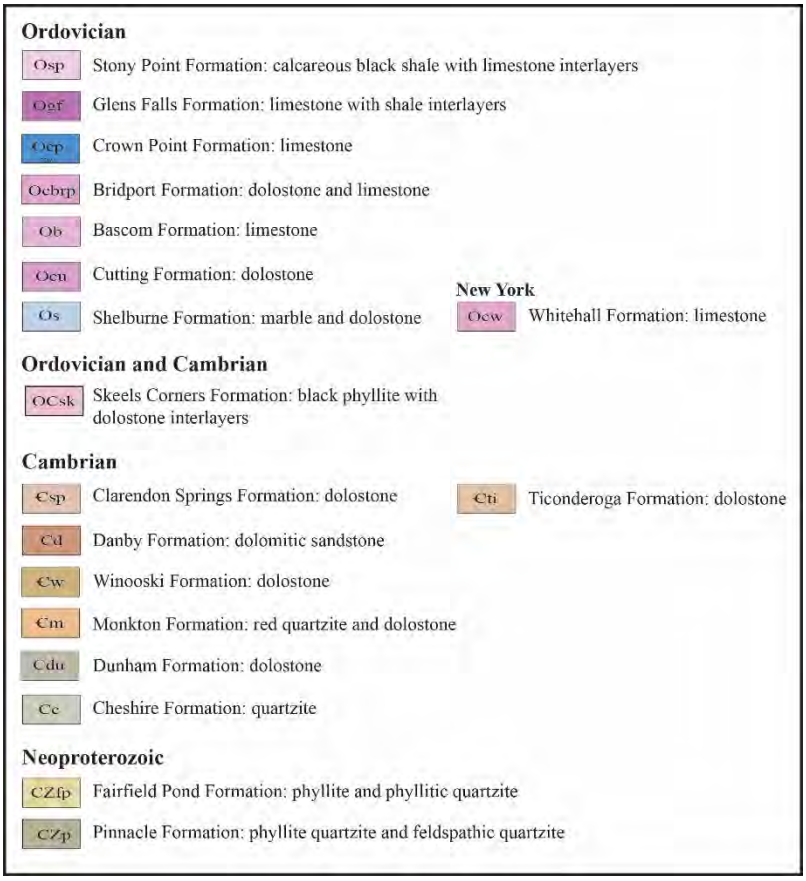

Figure 2B. Lithologic units for the map in Figure 2A.

Lower-Middle Ordovician sedimentary rocks of the Beekmantown Group (Isachsen and Fisher, 1970). There is a major unnamed Ordovician thrust fault in Lake Champlain that separates the Parautochthon from the Autochthon. To the north, Fisher (1968) called this the Cumberland Head Thrust. Although these slices were originally juxtaposed during the Ordovician Taconian Orogeny, subsequent deformation occurred during the Acadian (Devonian) and possibly later orogenies (e.g., Stanley and Sarkisian, 1972; Stanley, 1987).

Stratigraphy of the Lithotectonic Slices

The stratigraphy of the field area has been described in detail by Cady (1945), Doll et al. (1961), Welby (1961), Dorsey et al. (1983), Gilespie (1983), Stanley (1980;1987), Stanley and Sarkisian (1972), Stanley and Ratcliffe (1985), Stanley et al. (1987), Stanley and Wright (1997), Mehrtens (1987; 1997), Landing et al. (2002), Thompson et al. (2003), Landing (2007), Kim et al. (2007; 2011, 2014b), and Gale et al. (2009). The legend in Figure 2B summarizes the lithologies for the map in Figure 2A. More detailed lithologic information is available for each individual stop in the road log. The reader is also encouraged to consult the above references for further information.

Figure 3 shows the tectonostratigraphy of each of the lithotectonic slices in the field area from west (left) to east (right). It is immediately apparent from west to east that each slice cuts into

successively older rocks and, consequently, deeper structural levels. Below are descriptions of the tectonic affinity and lithologies in each slice:

A) Parautochthon

1) Stony Point Formation- Late Ordovician black shales with thin carbonate interlayers that were strongly deformed by the overriding Champlain Thrust. These rocks were interpreted as flysch by Stanley and Ratcliffe (1985) and Rowley (1982).

2) Charlotte "Block"- Late Cambrian – Late Ordovician carbonate sedimentary rocks deposited on the Laurentian continental margin. These rocks were offset by normal faulting, probably during Late Ordovician or later time. The basal dolostone formations in this sequence were assigned using New York State nomenclature to the Ticonderoga/ Whitehall/ Cutting formations by Welby (1961).

B) Hanging Wall of the Champlain Thrust- Early Cambrian – Middle Ordovician carbonate and subordinate clastic sedimentary rocks that were deposited on the Laurentian continental margin. Slivers of Ordovician formations are found between this slice and the Parautochthon.

C) Hanging Wall of the Hinesburg Thrust- Late Proterozoic rift clastic metasedimentary and metaigneous rocks associated with the initial opening of the Iapetus Ocean, including the Pinnacle (CZp) and Fairfield Pond (CZfp) formations. These rocks are overlain by Iapetan drift- stage clastic rocks (argillaceous quartzite and quartzite) of the Cheshire formation (e.g., Stanley, 1980; Stanley and Ratcliffe, 1985). There are smaller lithotectonic packages of rocks that are caught between C and B, represented by the foot wall anticline in Figure 3.

STRUCTURAL GEOLOGY

Thrusts

In the field area, the Champlain Thrust juxtaposes the basal dolomitic member of the Middle Cambrian Monkton Quartzite with the Late Ordovician Stony Point Shale. North of the field area, the Champlain Thrust cuts down section ~2000' into the Lower Cambrian Dunham Dolostone (at Lone Rock Point in Burlington) (Stanley, 1987). Between Burlington and the Quebec border, this thrust generally follows the base of the Dunham Dolostone and then becomes the Rosenburg Thrust in southern Quebec (e.g., Sejourne and Malo, 2007). South of the field area, the Champlain Thrust can be mapped continuously at the base of the Monkton Quartzite to south of Snake Mountain near Middlebury, Vermont (e.g., Stanley and Sarkisian, 1972, Stanley, 1987). South of Snake Mountain, motion on the Champlain Thrust was probably taken up on structurally lower faults such as the Orwell Thrust (M. Gale, personal communication, 2011). Stanley (1987) suggested that total displacement on the Champlain Thrust is 55-100 km. (34-62 miles).

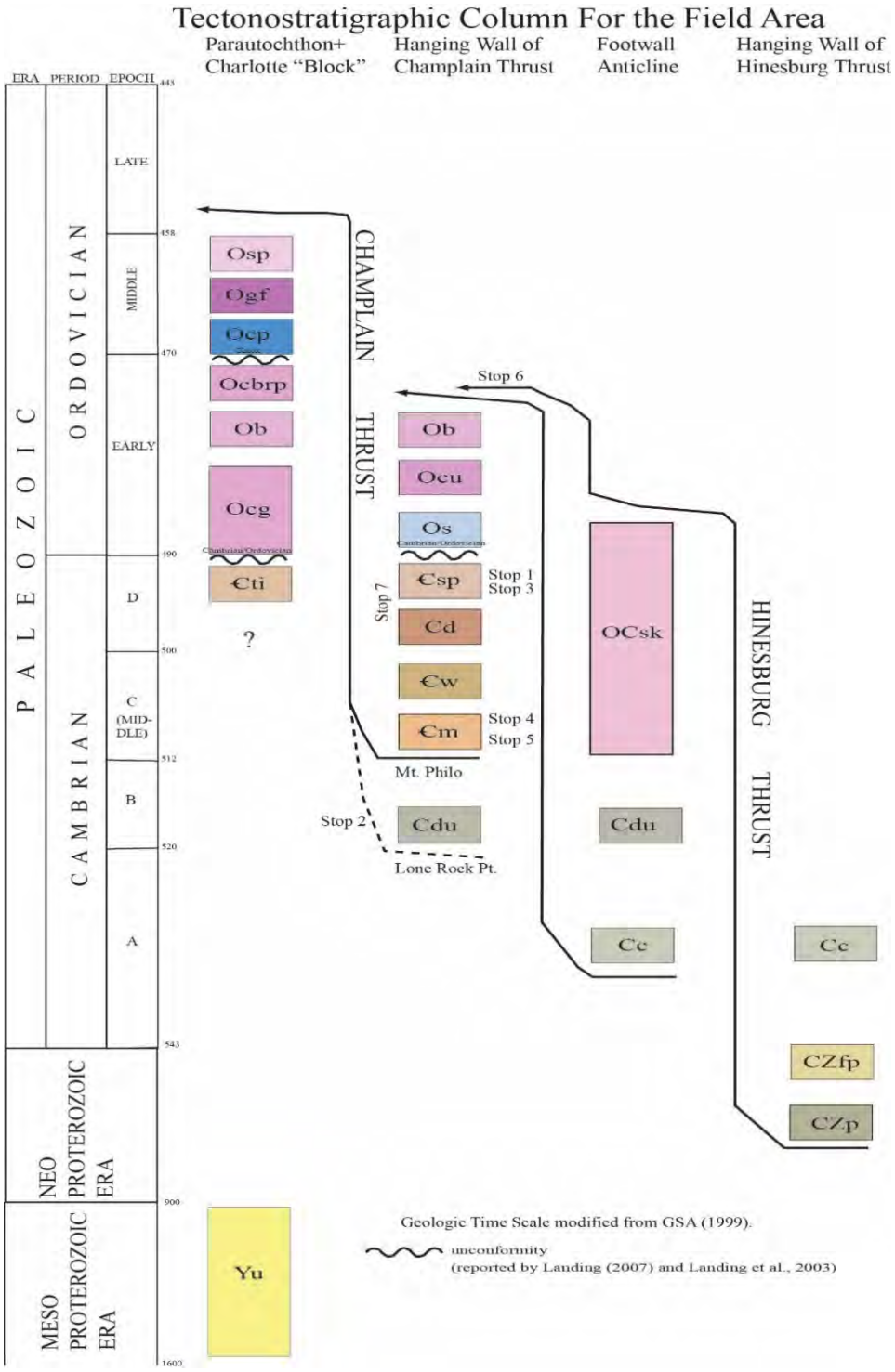

Figure 3. Tectonostratigraphic diagram of each of the lithotectonic slices in the field area from west (left) to east (right). Yu is in New York State.

In the field area, Late Proterozoic- Early Cambrian rift clastic to early drift stage metamorphic rocks of the Hanging Wall of the Hinesburg Thrust were driven westward over weakly metamorphosed sedimentary rocks of the Hanging Wall of the Champlain Thrust along the Ordovician Hinesburg Thrust. Dorsey et al. (1983) proposed that this thrust nucleated in an overturned fold/ nappe that ultimately sheared out along its axial surface. North and south of the field area, the Hinesburg Thrust appears to die out in large fold structures (Ratcliffe et al., 2011). For the southern extension of the Hinesburg Thrust, P. Thompson (personal communication, 2011) suggested that it may actually root in Precambrian basement in the northernmost basement massif. Kim et al. (2013, 2014c), based on mapping in the Bristol and South Mountain quadrangles, extended the Hinesburg Thrust southward into the Ripton Anticline, which is cored by Mesoproterozoic basement. Stanley and Wright (1997) suggested a total displacement of ~6.4 km. (4 miles) on the Hinesburg Thrust.

If the Hines burg and Champlain thrusts represent a typical foreland-propagating (westward in this case) scenario (e.g. Boyer and Elliot, 1984?), then the Hinesburg Thrust should predate the Champlain Thrust. However, because map-scale fold structures (Hinesburg Synclinorium) in the Hanging Wall of the Champlain Thrust were truncated by the Hinesburg Thrust, it is possible that the first motion on the Champlain Thrust predated that on the Hinesburg Thrust (e.g., Doll et al., 1961; Gale et al., 2010). Alternatively, it is plausible that a second episode of motion on the Hinesburg Thrust truncated part of the Hinesburg Synclinorium. Another scenario proposed by Stanley and Sarkisian (1972) and P. Thompson (personal communication, 2011) suggested that the Champlain Thrust moved a second time after formation of the Hinesburg Thrust, partly on the basis of its metamorphic history (described below). The detailed structural history of the Hinesburg Thrust has been discussed by Gillespie (1975), Dorsey et al. (1983), Strehle and Stanley (1986), and is further described in Stop 6 of the Road Log. Descriptions of the deformational history of the Champlain Thrust can be found in Stanley and Sarkisian (1972), Stanley (1987) and in West et al. (2011).

Regional Trends

From the edge of Lake Champlain eastward across the Champlain and Hinesburg thrusts, several regional trends are evident. Nearest the lake, mostly brittle deformation is prevalent and includes blind normal faults (Figure 4a). Farther east, in the hanging wall of the Hinesburg Thrust, mostly ductile deformation, including superposed folds sets, transposed cleavages, and ductile shear bands (Figure 4f) are dominant. The outcrops on this trip exhibit an interesting interplay between ductile and brittle styles of deformation. This interplay has generated a spectacular variety of mesoscopic (outcrop scale) structures. These include many different types of sense of shear indicators that provide a wealth of information on the slip history of two thrusts, as well as the several phases of deformation that predate and postdate thrust faulting.

In addition to changes in the overall style of deformation, the variety of structures preserved along the transect collectively record a first-order increase in finite strain toward the east, with local maxima occurring within a few hundred meters of both the Champlain and Hinesburg thrusts. In the foot wall of the Champlain Thrust/ Parautochthon , F_1 folds of bedding planes (S_0) tighten as their axial planes rotate from steep and moderately east-dipping to shallowly east-dipping (Figures 4b, 4c). The styles and mechanisms of these folds also change from localized fault-bend folds several kilometers below the thrust (Figure 4b), to penetrative fold trains that formed by a combination of interlayer slip and ductile flow near the thrust (Figure 4c). The appearance of two cleavages reflects this increase in finite strain. These include an early

penetrative slaty cleavage (S_1) that formed during F_1 folding and a second localized pressure solution cleavage (S_2) that marks the presence of intraformational thrusts (Figure 4b). A similar increase in strain occurs near the Hinesburg Thrust. In the east-central part of the field area, a faulted anticline lies structurally below the Hinesburg Thrust. Here, isoclinal intrafolial folds of bedding (S_0), stretched pebbles and disarticulated compositional layers reflect a generally high magnitude of finite strain. Where the Hinesburg Thrust is exposed at Mechanicsville, even higher strains are recorded in mylonitic rock of the Cambrian Cheshire Formation.

Another interesting regional trend is the influence of rock type on the style and partitioning of deformation within the section. In general, deformation associated with the emplacement of the two major thrust sheets is expressed differently in competent units than it is in the weaker shales. For example, variations in the thickness and abundance of competent limestone layers have produced distinctive fold styles. In the shales, ductile flow during contraction resulted in recumbent isoclinal folds that became rootless at high strains. In contrast, thick competent limestone layers deformed mostly by interlayer slip, resulting in large inclined folds, preserve numerous *en echelon* vein sets. A similar pattern exists at the regional scale where most of the deformation that accompanied the formation of the Champlain Thrust is partitioned into the weak Stony Point Shales in the footwall. In this latter locality, the deformation is widely distributed. In contrast, deformation in the thick, competent quartzite layers of the Monkton Formation in the hanging wall tends to be more localized and mostly involves interlayer slip (Figure 4d).

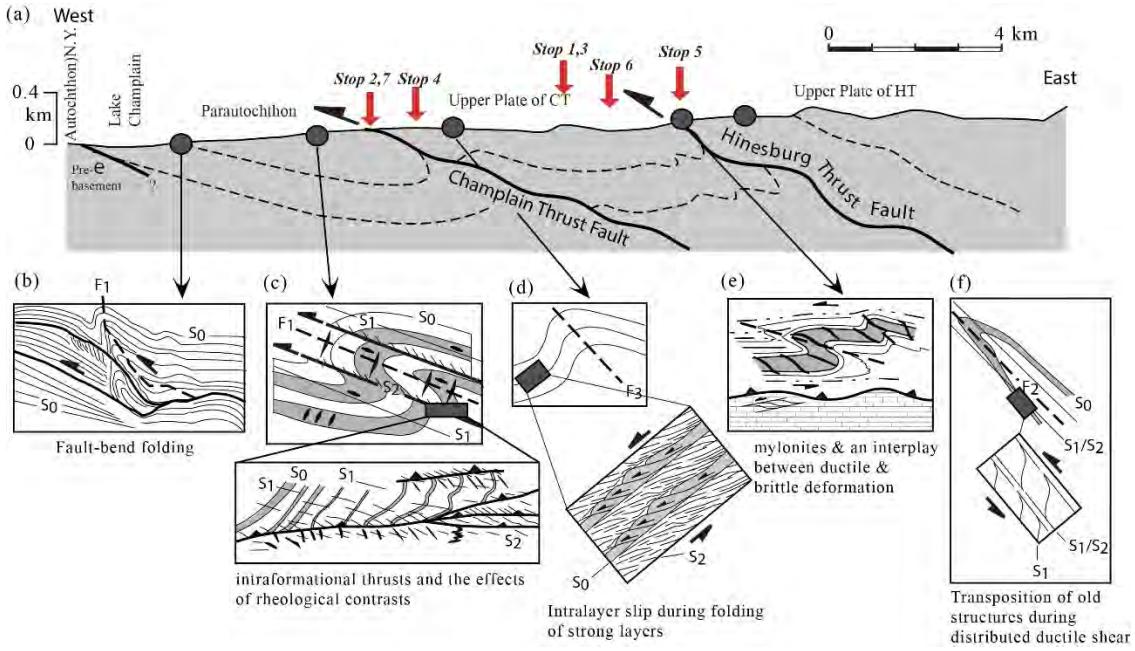

Figure 4. Simplified diagram showing the regional structural trends from west to east.

This influence of lithology and rheological contrasts on structural style also has resulted in many different types of kinematic indicators throughout the section. At Stop 6, competent metapsammite layers located above the Hinesburg Thrust (Figure 4e) preserve asymmetric vein sets and folds that record a top-to-the-northwest sense of shear. In the weaker pelitic layers it is recorded mostly by shear band cleavages. Although these structures generally show similar

top-to-the-west and –northwest senses of motion, the wide variety of types reflect different starting materials. These and many other examples illustrate one of the basic principles of interpreting the great variety of structures observed along this transect: differences in the strength and rheology of the rock units as they deformed can explain much of the great variety of structures observed in the Champlain Valley and in the lithotectonic slices to the east.

Since brittle structures, with the exception of normal faults, are not portrayed on Figure 4, we will give a brief summary of the characteristics of the dominant fracture sets. Fractures that have strikes orthogonal to the dominant planar fabrics (E-W to NE-SW) and steep dips are common throughout the field area. Since Cretaceous dikes intruded along many of these fractures, we know that these fractures are at least Cretaceous in age. Some fracture sets have north-south strikes with moderate-steep dips and can sometimes be associated with fracture cleavages associated with late generation folding (Figure 4C). NW-SE trending steep fractures are also common, but are of uncertain origin. In the field area, detailed fracture data have been acquired in the towns of Williston (Kim et al., 2007), Charlotte (Gale et al., 2009), Bristol (Kim et al., 2013; 2014), and Hinesburg (Thompson et al., 2004); Kim et al., 2014; 2015)

METAMORPHISM

Stanley and Wright (1997) summarized that the Taconian foreland rocks of the Parautochthon and Hanging Wall of the Champlain Thrust are “essentially unmetamorphosed” (p. B1-1) with temperatures of ~200°C and pressures corresponding to depths of ~2.5 km. Stanley and Sarkisian (1972) and Stanley (1974) reported prograde chlorite in fractures in the Monkton Formation in the Upper Plate of the Champlain Thrust, and used this occurrence to suggest that this thrust underwent multiple episodes of motion.

On the basis of field and petrographic observations presented by Strehle and Stanley (1986), Stanley et al. (1987), and this volume (Stop 6), the metamorphic rocks from the westernmost Taconian hinterland (Hanging Wall of the Hinesburg Thrust), reached biotite grade. In the field area, there is a pronounced metamorphic contrast between the rocks above and below the Hinesburg Thrust.

GEOCHRONOLOGY

There are few igneous crystallization or metamorphic ages from the field area. Cretaceous lamprophyre dikes have been reported throughout the field area by (McHone (1978), McHone and McHone (1999), and Ratcliffe et al. (2011) that intruded fractures and foliations. The dikes are likely correlative with the Barber Hill stock in the Town of Charlotte, which has been dated at 111 +/-2 Ma (K/Ar biotite age; Armstrong and Stump, 1971). A whole rock Rb-Sr isochron age of 125 +/- 5 Ma on seven trachyte dikes from the Burlington area was reported by McHone and Corneille (1980), and probably provides an upper limit on the age of these dikes.

Rosenberg et al. (2011) used the K/Ar method to obtain cooling ages of illites from the fault zone of the Champlain Thrust at Lone Rock Point in Burlington. The ages obtained range from Carboniferous (~325 Ma) to Late Jurassic (~153 Ma). These authors speculated that post-Taconian illite growth may reflect fluid flow associated with the Alleghenian Orogeny and the Jurassic-Cretaceous unroofing of the Adirondacks and New England (e.g., Roden-Tice, 2000; Roden-Tice et al., 2009).

The ages of first motion on the Champlain and Hinesburg thrusts in the field area are weakly constrained by the youngest stratigraphic ages of rocks located below these faults. In the case of the Hinesburg Thrust, the age is Middle Ordovician (Bascom Formation, Ob) whereas for the Champlain Thrust it is Late Ordovician (Stony Point Shale).

PREVIEW OF APPLIED GEOLOGIC ISSUES

Stop 1: Elevated naturally-occurring radioactivity levels in groundwater from Clarendon Springs Formation dolostones.

Stop 2: Ductile and brittle structural history of the Champlain Thrust. Effect of structures and lithologies on groundwater flow and chemistry, respectively. High well yields in the hanging wall and lower well yields in the foot wall. Elevated fluoride in some foot wall wells.

Stop 3: A newly-described strike-slip fault zone in the Clarendon Springs Formation and how it fits into the regional brittle structural history of the Champlain Valley Belt.

Stop 4: Using a well-described wrench fault (and fracture site) as context for the regional brittle structural history of the Champlain Valley Belt.

Stop 5: Overview of the Champlain Valley Belt.

Stop 6: Elevated naturally-occurring radioactivity levels in groundwater from wells completed in the hanging wall (Pinnacle, Fairfield Pond, and Cheshire formations) or drilled through the Hinesburg Thrust. High well yields in the foot wall and low yields in the hanging wall.

Stop 7: Integration of bedrock mapping with geophysical logging to understand the hydrogeology of a fractured bedrock well field in the Town of Hinesburg.

FIELD GUIDE AND ROAD LOG

Meeting Point: ***Colchester Park and Ride Lot***- On the east side of Route 7, 0.3 miles north of the intersection of the intersection of Route 7 and Route 2 off Exit 17 (Champlain Islands-Chimney Point) on Interstate 89 in Colchester (at the VTRANS Maintenance Facility).

Meeting Point Coordinates: 44 ^{o} 35.710' N, 73 ^{o} 09.977' W

Meeting Time: 8:30 AM

Cumulative (miles)	Point to Point	Route Description
0.0	0.0	From parking lot, turn left onto Rt. 7 South
0.3	0.3	Continue on Rt. 7 through intersection of Rt. 2
1.3	1.3	Turn left onto Coon Hill Road
1.9	1.9	Turn right onto Galvin Hill Road
2.5	2.5	Turn left onto Tuckaway Pond Lane private drive and continue about 0.25 miles to destination.

Stop 1: Elevated Radioactivity in Groundwater from the Clarendon Springs Formation, Milton, Vermont

Location Coordinates: 44 ^{o} 35.735' N, 73 ^{o} 08.561' W

Introduction

Elevated radionuclide levels were reported in groundwater from ~30% of bedrock wells tested in the Clarendon Springs Formation in the towns of Colcheser Quadrangle.

Lithology

Massive gray dolostone of the Late Cambrian Clarendon Springs Formation.

Structure

The Muddy Brook Thrust (MBT), which is described below, is located in the valley to the east. In this area, the dominant fracture set strikes NE, dips steeply, and is associated with cross faults that offset the MBT and lithologies on both sides (Kim and Thompson, 2001).

Tectonic/Stratigraphic Context

This site is at the north end of the Hinesburg Synclinorium. The shallowly east- dipping MBT carried black phyllites with thin dolostone interlayers over the Clarendon Springs Formation dolostones during the Taconian Orogeny. The MBT is west of and probably synchronous with the Hinesburg Thrust (Kim and Thompson, 2001).

Hydrogeology and Groundwater Geochemistry

Groundwater produced from the Clarendon Springs Formation in Milton and Colchester is known to contain elevated uranium, radium, and alpha radiation. Radioactivity is high enough

that the average alpha radiation from 131 domestic bedrock wells tested in a 12 km^2 area is 32 picocuries per liter (pCi/L), and 22 % of these wells produce concentrations of alpha radiation above the EPA's maximum contaminant level (MCL) of 15 pCi/L; furthermore, the three most contaminated wells, which occur within a kilometer of each other, average 841 pCi/L. Dark grey to black phosphorites (with 7 to 37 % P_2O_5) occur throughout the region that contains elevated radionuclides in well water; in outcrop, these phosphorites occur in two main forms: (1) subangular, pebble-sized clasts in a dolostone matrix, sometimes with imbricated clasts that suggest deposition from a current, and (2) wispy beds of dark grey phosphorite (possibly "hardground"). Breccias are more common than wispy sedimentary layers, and both indicate that the concentrated phosphate is syndepositional in origin. McDonald (2012) cited a model involving upwelling sea water and reducing biochemical conditions as factors responsible for deposition of phosphorite with elevated U.

Rock samples collected from outcrops located upgradient of the most highly contaminated wells exhibited the following: (1) the phosphorites contain 80 to 430 mg/kg uranium while the dolostone matrix contains less than 10 mg/kg U; (2) the phosphorite mineral — as determined by powder XRD — is fluoroapatite, and trace amounts of autunite also occur in some phosphorites; (3) a gamma ray survey of a 160 m deep bedrock well documents the interbedding of U-rich phosphorite beds and dolostone beds throughout the Ccs in Milton-Colchester, perhaps alternating cyclically. U-rich phosphorites produce a gamma ray signal of 500 to 3400 cps whereas U-poor carbonates have a signal < 50 cps gamma radiation; and (4) SEM-EDS element maps (Bachman, 2015) show that phosphorite clasts and layers lacking significant post-depositional deformation contain the highest levels of uranium. SEM-EDS also indicates that U occurs in two broadly-defined mineralogical forms: (1) diffusely distributed U in cryptocrystalline fluoroapatite, and (2) perhaps more importantly, concentrated U in microcrystalline minerals (e.g. autunite, coffinite, brannerite) scattered throughout the phosphorite. This may suggest that uranium was initially substituted for Ca in fluoroapatite — during crystallization on the seafloor (consistent with literature reports)—, but then was incorporated into anhedral secondary minerals when (at least some of the) fluoroapatite dissolved. This could have occurred any time from very early diagenesis to dolomitization. Weathering of pyrite may trigger U release by locally lowering pH — evidence for this is the occurrence of autunite [$Ca(UO_2)_2(PO_4).nH_20$] in rusty Fe hydroxide matrix at the boundary of weathered pyrite and adjacent, unweathered fluorapatite.

Cumulative (miles)	Point to Point	Route Description
2.5	0.0	Turn right onto Galvin Hill Road.
3.1	0.6	Turn left onto Coon Hill Road
3.8	0.7	Turn left onto Rt. 7 South
7.2	3.4	Turn right onto Rt. 127 (Blakely Road)
9.5	7.0	You will pass Colchester Middle School on your right.
9.9	7.4	You will see Mallets Bay on the right.
10.9	8.4	Turn left onto Prim Road (extension of Rt. 127)
12.1	9.6	Continue straight through intersection of Marce Road
13.1	10.6	At the fork in the road, bare left to the stoplight.
15.0	12.5	Take Rt. 127 to exit for North Avenue Beaches on the right.
15.4	12.9	Follow ramp to the T, and turn left onto North Avenue.
15.8	13.3	Turn right onto Institute Road at Burlington High School
16.0	15.5	Turn right into Rock Point into Rock Point Episcopal Center
16.2	15.7	Park in lot on the right.

Stop 2: Champlain Thrust at Lone Rock Point

Location Coordinates: 44 ^{o} 29.441' N, 73 ^{o} 14.931' W

Introduction

This stop description was modified from West et al. (2011). The Champlain thrust fault at Lone Rock Point is arguably the iconic geologic feature in Vermont and perhaps the finest thrust fault exposure in eastern North America. The "older-on-top-of-younger" relationship exposed here is a fundamental indicator of thrust faulting. Hitchcock et al. (1861) was the first to recognize that the contact relationships exposed at Lone Rock Point are the result of major regional faulting.

Lithology

Early Cambrian massive dolostone of the Dunham Formation structurally overlies Late Ordovician Iberville Formation black shales (Figure 5).

Structure

An interesting feature at Lone Rock Point is the interplay between ***brittle deformation and ductile flow*** mechanisms. Brittle deformation involves the breaking of material along discrete surfaces, which can be fractures, veins or, if they accommodate slip, faults. These two styles are not completely independent of one another, and commonly occur together to accommodate shortening. The material type and the conditions under which deformation occurs typically dictates the types of deformation processes. As such, the type of parent lithology (what type of rock was present prior to deformation) is a critical influence on style of deformation. At Lone Rock Point two significantly different rock types are juxtaposed with the strong Dunham dolostone thrust above the weak Iberville shale (Fig. 5A). Deformation is not restricted to slip along the fault plane, and can be dived into two domains as described by Stanley (1987). These are composed of an inner fault-zone including the fault surface at the base of the Dunham dolostone and a proximal region consisting of broken limestone and highly contorted shale. The outer fault-zone occurs in the Iberville Shale and consists of a high concentration of veins,

subordinate faults, and tightly folded compositional layering. By recognizing various features within both the Iberville Shale and the Dunham dolostone we can establish various mechanisms of deformation and compare the way these two units accommodate shortening. For this reason, the exposure of the Champlain Thrust fault at Lone Rock point is an excellent location to teach fault-zone processes and the influence of material properties on deformation.

The following sections briefly describe key features that document deformation styles and the motion history of Lone Rock Point.

Structural Slickenlines. The basal surface of the Dunham Formation is the slip surface on which a significant amount of displacement has occurred. This surface contains corrugations referred to as fault mullions with wavelengths on the order of half a meter. These features, as depicted in Figure 8 can form with crest lines parallel to the motion of the fault and, therefore, can help constrain motion direction. In addition to fault mullions, striations can occur from the scraping and gouging of the fault surface by resistant objects. These also help constrain the motion of the Champlain Thrust fault (Figure 5B).

Original Bedding. Despite the highly deformed nature of the Iberville Formation, compositional layering is visible as resistant quartz rich layers. These layers are frequently folded and faulted into small isolated pods surrounded by soft clay rich rock. Although dolostones of the Dunham Formation are massively bedded, depositional surfaces are intact and relatively undisturbed (Figure 5A).

Veins and Mineral Slickenlines. Veins form from the deposition of material from solutions that fill voids in rocks. The calcite veins at Lone Rock Point display complex geometries, including folding, faulting, and shearing. The shear veins, in particular, can be good indicators of the motion history of deformation and frequently form lineated surfaces known as mineral slickenlines. The formation of mineral slickenlines generally involves the infilling of void space with material created by offsets on the fault surface (Figure 5C).

Cleavage. Cleavage planes are formed from the preferential alignment of mineral grains due to flattening, which is accommodated by dissolution and the removal of soluble material. Cleavage is common in shales of the Iberville Formation, and are generally is oriented at low angles to the fault surface. However, as the distance increases away from the fault, the orientation of cleavage planes tends to steepen. This rotation of cleavage planes can be used to infer the sense of motion on the thrust surface.

Fractures. Unlike the intensely deformed Iberville Formation, massive dolostones of the Dunham Formation are relatively intact and show little evidence of internal deformation (i.e., no visible cleavage). However, fractures (breaking of the rock along discrete planes without differential motion), are common in this more competent unit. New fracture data will be presented for the hanging wall.

Subordinate Faults. Many small scale faults can be observed within the footwall rocks of the Iberville Formation that offset folds, cleavage, and veins. These faults do not continue into structurally overlying dolostones of the Dunham Formation. These small scale faults in the Iberville tend to rotate into the direction of the fault motion with proximity to the fault (Stanley, 1987). Because the Champlain thrust fault at Lone Rock Point contains numerous features that help constrain the transport direction along the fault plane, an exercise can be constructed to identify as many of the features that contain motion information (i.e. fault

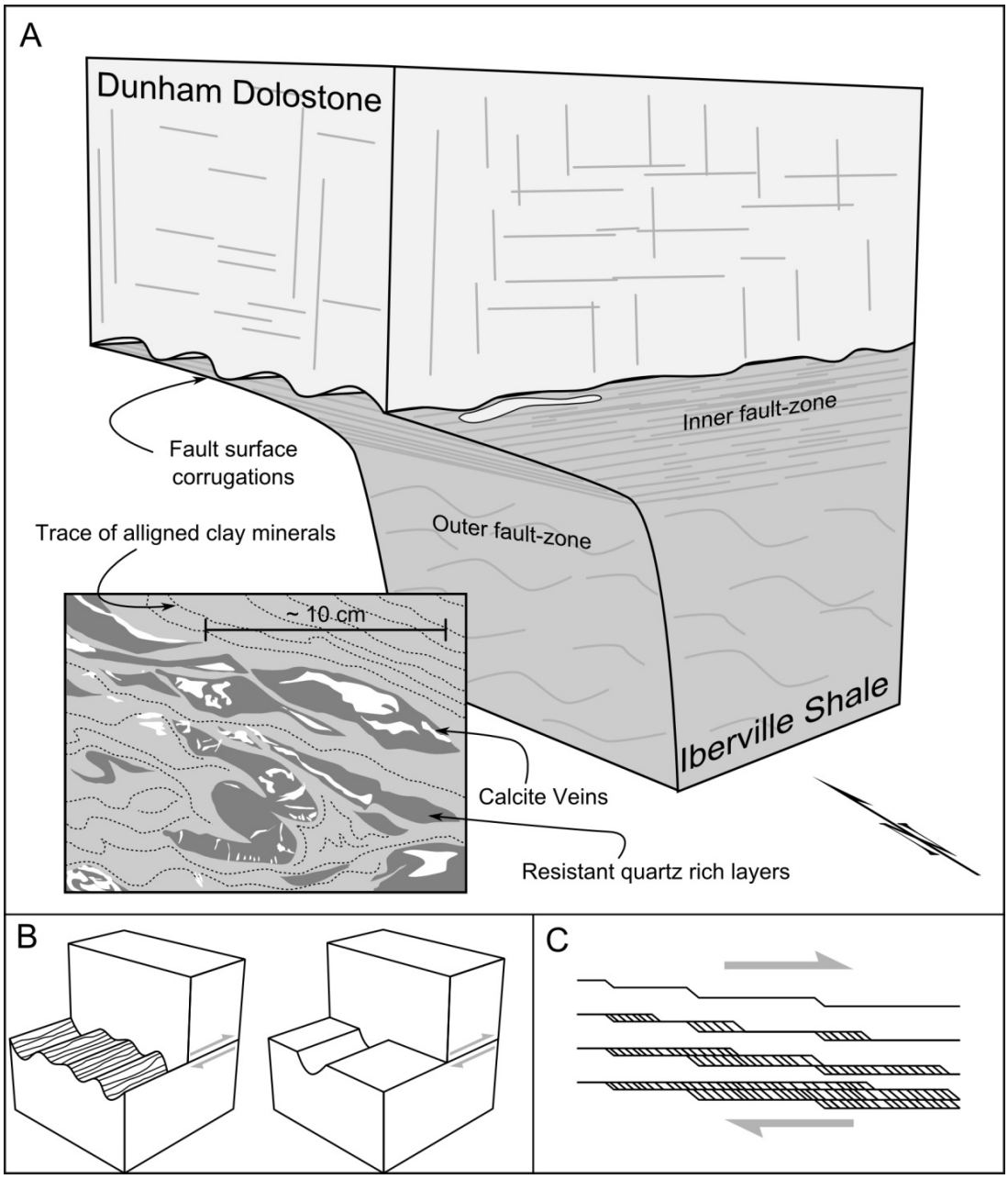

Figure 5. Sketches showing the general geometry of features observed at the Champlain Thrust fault at Lone Rock Point. (A) Block diagram of the Champlain Thrust fault with the resistant Dunham Formation (massive dolostones) above the weak Iberville Formation (calcareous shales). The fault-zone is divided into two domains consisting of the inner fault-zone and the outer fault-zone. The inset sketch depicts the relationships between folded and faulted quartz-rich layers (dark gray), clay rich shale material (light gray), alignment trajectories of clay minerals (dashed lines), and the geometries of calcite veins (white). (B) Block diagrams of two mechanisms of structural slickenline formation (modified from Means, 1987). The left diagram shows the formation of fault corrugations while the right diagram illustrates gouging caused by resistant material within the upper plate. (C) Formation of mineral slickenlines by the infilling of voids caused by steps within the fault surface.

mullions, gouges, and mineral slickenlines). These features generally indicate displacement and tectonic transport in a west-north-west direction. Teaching considerations include the following questions: How does the geometry of folded compositional layering change with proximity to the fault? How does the orientation of the dominant cleavage change with proximity to the fault surface? Is displacement constrained to slip along the fault surface only? What is the general temporal progression of deformational style using cross-cutting relations? What fundamental influence does the type of bedrock have on deformation style? These questions address the fundamental aspects of thrust faulting and the inherent relationship between initial lithology and deformation mechanisms.

New Work on Foot Wall Structures

The following has been modified from Strathearn et al. (2015). Although the Champlain Thrust has been studied previously at Lone Rock Point, the multiple generations of ductile and brittle structure in shales of the footwall have never been systematically defined. We present the following relative chronology of structures:

1) Formation of bedding planes (S_0), characterized by thin layers of carbonate within black shale.

2) Formation of rootless isoclinal folds (F_1) of brittle carbonate layers and the development of an spaced pressure solution cleavage (S_1) that parallels the axial planes of the folds.

3) The S_1 cleavage is deformed into asymmetric S-C shear bands that merge into parallelism with, and are cut by intraformational thrusts. The thrusts form oblate, eye-shaped structures that are stacked on top of one another forming thrust duplexes. A second cleavage (S_2) defines a part of the S-C fabric and is intensified in thrust zones. Calcite slickenlines on fault surfaces plunge to the SE and NW and slip directions fan up to 40 degrees with respect to one another in different thrust horses

4) Formation of sets of upright, north (F_3) and east-striking (F_4) folds of S_2 warping the CT.

5) Formation of conjugate sets of normal faults that record top-down-to-the–north and -south kinematics.

6) Formation of the steeply-dipping fracture sets (N-S and E-W striking) that cut across competent lithologies.

Hydrogeology and Groundwater Geochemistry

In a case study examined on this field trip (Hinesburg Thrust; Kim et al., 2014a), the hanging wall is sometimes responsible for producing groundwater with elevated radionuclides. In the case of the Champlain Thrust, the culprit is the footwall. Of 35 tests for fluoride (note: F can cause bone disease), 37 % (13/35) exceeded the Vermont recommended F level in public water systems (0.7 mg/L). [Relative to the EPA MCL of 4 mg/L, however, only 3/35 wells were above the F threshold]. Sodium is elevated in ~ 45 % of footwall wells (13/29) relative to EPA's 20 mg/L Drinking Water Equivalency Level (guidance level), and the average Na concentration in footwall wells (82 mg/L) is four times greater than the DWEL. Both issues are related to the behavior of illite in this black shale-influenced bedrock aquifer system. Regarding fluoride, diagenetic illites typically contain 0.2 to 0.5 % F in isomorphous substitution for OH (Thomas et al., 1977), so dissolution of illite or exchange of Cl^- or OH^- for F^- are potential F sources in groundwater.

Dissolution of apatite (4 % F) could also be a source, although it is far less abundant and likely less reactive than illite. Other potential F minerals (e.g. fluorite, titanite) are not likely F sources in this system. Regarding elevated Na, we observe a weak but positive correlation of Na and Ca in solution, an occurrence that likely relates to Na-Ca ion exchange. When Ca is released to solution upon weathering of calcite (nearly ubiquitous in these Ordovician black shales), the higher-charge, less-hydrated Ca^{+2} cation is more strongly attracted to cation exchange sites (e.g. on illite) than is Na^{+1}, and the exchange reaction releases Na^{+1} into solution. This also is cited as the cause of high Na in black slate-influenced wells of the Taconics of southwestern Vermont (Ryan et al., 2013). Another element worth noting in footwall wells of the Champlain thrust is arsenic, which exceeds 10 ppm in 3 % of wells tested for As and exceeds 5 ppm in 10 % of wells (3/29); by comparison, in Taconic slates, 22 % of bedrock wells (52/236) exceed 10 ppb and 24 % exceed 5 ppb. Deeper anoxia in the Taconic seaway relative to open-shelf Iberville and Stony Point shale depositional environments is likely the cause of greater amounts of pyrite and arsenic in Taconic black slates.

Cumulative (miles)	Point to point	Route Description
16.2	0.0	Turn left out of the parking lot, then follow Episcopal Center driveway.
16.4	0.2	Turn left onto Institute Road
16.6	0.4	Turn Right on North Avenue heading south. (BHS sports field should be on your right)
17.1	1.5	Turn left onto Sherman Street.
17.2	1.6	Turn right onto Park Street (127 South)
17.5	1.9	Continue straight through the intersection with College Street
17.8	2.2	Turn left onto Maple Street
17.9	2.3	Continue straight through the intersection with Pine Street
18.0	2.4	Turn right onto St. Paul Street.
18.8	3.2	Continue onto Route 7 South.
19.9	4.3	Take the ramp to the right for I-189 East.
21.4	5.8	Take the ramp to the right for I-89 South (Montpelier).
24.6	9.0	Take the ramp to the right for exit 12 (Williston and Essex).
26.8	9.2	Turn left at the light onto Route 2A.
27.1	9.5	Use the middle lane.
27.6	10.0	Continue through the intersection with Route 2
28.6	11.0	Continue straight through the intersection with Industrial Road on your left and Mtn View Road on your right.
29.7	12.1	Turn left into Overlook Park parking lot before the bridge.

Stop 3: Strike Slip Fault Zone in the Winooski River Gorge, Williston/Essex, Vermont

Location Coordinates: 44 º 28.817’ N, 73 º 07.020’ W

Introduction

The Winooski River flows through a bedrock gorge downstream of a hydroelectric dam at the Essex/Williston border. During bedrock mapping in the Town of Williston (Kim et al., 2007), it was observed that most of the bedrock channels were northeast-striking fracture intensification domains (FIDs). Further investigation revealed a more complicated scenario.

Lithology

Massive gray dolostone of the Late Cambrian Clarendon Springs Formation.

Structure

Preliminary mapping and analysis of the brittle structures in the Winooski River Gorge reveals that the river channels are northeast- striking and steeply-dipping fracture intensification domains (FIDs) that are also strike-slip fault zones. Throughout the river gorge, these faults are intersected by steeply-dipping, north-northeast striking Riedel shear zones. Riedel shears usually form at a 10-20 degree angle to the main strike slip fault, in clockwise and counterclockwise directions, respectively, to right lateral and left lateral displacements (e.g Twiss and Moores, 2006). The Riedel shears in this gorge are consistent with left lateral displacement on the main strike-slip faults.

Tectonic/Stratigraphic Context

This body of Clarendon Springs Formation is bounded to the east by the Ordovician Muddy Brook Thrust Fault and to the west by the presumed Mesozoic down-to-the-east St. George normal fault.

Figure 6. Northeast striking, steeply-dipping strike-slip fault zone in the Winooski River gorge.

Hydrogeology and Groundwater Geochemistry

Bedrock geochemical analysis indicates some interesting differences in Ccs composition here compared to the phosphorite-bearing localities in Milton-Colchester and Highgate (McDonald, 2012). P_2O_5 here in the Winooski gorge is < 0.5 % whereas P_2O_5 ranges from to 7.4 to 36.9 % in phosphorite-rich dolostone and phosphorite layers or clasts. Uranium is also low in the Ccs in

the Winooski River gorge (1.3 to 8.3 ppm) relative to Milton-Colchester (where it reaches 432 ppm). No phosphorite clasts or layers are observed in the Winooski River gorge, explaining the low amounts of P and U at this locality. Geochemically-notable are two samples of black wispy clasts coated with Fe hydroxide that contain 120 and 283 ppm As (for comparison, As < 16 ppm at Milton-Colchester outcrops). These black wispy clasts occur in a dolomitic breccia, and yet while this facies appears similar in outcrop to some of the phosphorite occurrences at Milton-Colchester, the black wispy clasts in Winooski gorge contain < 0.5 % P_2O_5 and < 10 ppm U. In terms of major elements, the Winooski gorge Ccs black clasts are dominantly Si, Mg and Ca; otherwise, only elevated iron (5.7 and 10.1 % Fe_2O_3, respectively) and arsenic (120 and 283 ppm, respectively) are anomalous relative to other dolomitic Ccs rocks. One possible interpretation: if the black color is from mature organic matter, these wispy black clasts may represent an organic-rich shallow marine or subaerial layer that was incorporated into a cave breccia. The As-bearing Fe hydroxide is likely remnants of weathered disseminated pyrite.

The municipalities in the vicinity of Winooski gorge are part of the Champlain Water District and their drinking water is supplied from Lake Champlain. We know of no chemical data for bedrock wells in this area, so it is unknown how the composition of this belt of Clarendon Springs Formation may affect groundwater.

Cumulative miles	Point to point	Route Description
29.7	0.0	Turn Right out of parking lot onto Route 2A.
30.7	1.0	Continue straight through the intersection.
32.3	2.6	Take right turn onto ramp for I-89 North
32.5	2.8	Merge onto I-89 North
35.8	6.1	Take exit 13 (Shelburne and Burlington) for I-189
36.1	6.4	Continue onto I-189 West.
37.5	7.8	At the fork in the road, stay to the left.
37.5	7.8	At the stoplight, turn left onto Route 7 South.
40.4	10.7	Make a right turn onto Bay Road
41.4	11.7	Turn right into parking lot for the Shelburne Bay boat access.

Stop 4: Wrench Faults and Fractures at the Shelburne Boat Access, Shelburne, Vermont

Location Coordinates: 44 ^{o} 24.035', 73 ^{o} 14.083'

Introduction

This site was used by Rolfe Stanley of the University of Vermont as a teaching outcrop for his structural geology classes for decades and is currently used by Keith Klepeis. Stanley (1974) wrote a Geological Society of America Bulletin article that details the structural history of this site.

Lithology

Early Cambrian ferruginous quartzite of the Monkton Formation. Stanley (1974) reported that the quartzite at this site is composed of 93% quartz, 5% hematite, 1% microcline, and traces of zircon, plagioclase, detrital staurolite, and dolomite.

Structure

As outlined by Stanley (1974), there are three major structural features at this site, which are:

1) High – Angle Wrench Faults:

   A) *Generation 1* Northeast to west striking, moderately-steeply dipping faults (Figure 7).

   B) *Generation 2* North-northeast to north-northwest striking, steeply dipping faults that offset generation 1 faults (Figure 7).

2) *En Echelon* Fractures: Dextral and sinistral *en echelon* fracture arrays that are filled with quartz. The trend of the *en chelon* arrays corresponds to the strike of a particular fault. These arrays are only associated with the first generation of high angle faults (see fracture arrays on Figure 7).

3) Fractures: The four major fractures sets (contoured maxima) at this field site are: A) East-west striking, steeply north-dipping, B) North-south striking, steeply west-dipping, C) Northwest striking, steeply southwest-dipping, and D) Northeast striking, steeply northwest dipping. Set A is associated with the first generation wrench faults whereas sets B, C, and D overprint set A and are associated with the second generation wrench fault generation.

Tectonic/Stratigraphic Context

Stanley (1974) proposed that the east-west striking and steeply dipping wrench faults were related to the Shelburne Bay cross-fault, which offsets the Champlain Thrust. Both sets of wrench faults were presumed to be related to the Devonian Acadian Orogeny. Kim et al. (2011; 2014) described dome and basin fold patterns in the Champlain Valley Belt that were the result of the superposition of fold sets with steeply dipping ~north-south and ~east-west striking axial surfaces. Could the two sets of wrench faults and their associated fractures be related to these folding events?

Hydrogeology and Groundwater Geochemistry

We are using this study as a detailed context for fracture analysis throughout the Champlain Valley Belt. These brittle structures may influence groundwater flow in the bedrock aquifer.

Cumulative miles	Point to Point	Route Description
41.4	0.0	Turn left onto Bay Road.
42.4	1.0	Turn right onto Route 7 South (Shelburne Road).
49.2	7.8	Continue straight through the intersection with Ferry Road.
51.6	10.2	Turn left onto State Park Road.
52.2	10.8	Continue straight through the intersection into Mt Philo State Park.

Stop 5: Mount Philo State Park in Charlotte, Vermont

Location Coordinates: 44 º 16.804' N, 73 º 13.082' W

Introduction

This stop description, which was modified from Kim et al. (2011), is designed to give an overview of the four major tectonic zones in the Lake Champlain area of west-central Vermont and eastern New York, which are, from west to east, and from structurally lowest to highest: 1) Autochthon, 2) Parautochthon, 3) Hanging Wall of the Champlain Thrust, and 4) Hanging Wall of the Hinesburg Thrust. A major thrust fault separates the Autochthon from the Parautochthon on the west side of Lake Champlain.

Lithology

At the top of Mt. Philo, you are standing on the upper member of the Monkton Formation, which is a ferruginous quartzite. The lower dolomitic sandstone member of the Monkton Formation is exposed near the Champlain Thrust below.

The autochthonous rocks on the west side of Lake Champlain include Mesoproterozoic metamorphic rocks of the Adirondacks (see Yu in Figure 3) that are uncomformably overlain by sedimentary rocks of the Beekmantown Group (Isachsen and Fisher, 1970). The Autochthon is structurally overlain by by: 1) Late Cambrian- Middle Ordovician weakly-metamorphosed sedimentary rocks of the Parautochthon, 2) weakly- metamorphosed sedimentary rocks of the Hanging Wall of the Champlain Thrust; and 3) low grade (chlorite-sericite to biotite) rift clastic metasedimentary rocks of the Hanging Wall of the Hinesburg Thrust.

Structure

At this lookout, the Champlain Thrust is ~160' vertical feet (50 m.) below your feet, where the dolomitic lower member of the Monkton Quartzite is in tectonic contact with the Middle Ordovician Stony Point Shale. From Mt. Philo, one can see the geomorphic expression of this thrust to the south as the slope breaks (steep = Monkton and gentler = Stony Point) on Buck and Snake mountains, and to the north on Pease Mountain.

Tectonic/Stratigraphic Context

At the Lone Rock Point exposure of the Champlain Thrust in Burlington (e.g Stanley, 1987)(Stop 2), this thrust juxtaposes the Lower Cambrian Dunham Dolostone with the Iberville Shale; this suggests the presence of an along-strike ramp that climbs ~2000' (610 m.) up section between Burlington and Mt. Philo. The stratigraphic throw of the Champlain Thrust is ~9000' (2743 m.) at Lone Rock Point and ~6000' (1830 m.) at Mt. Philo (Stanley, 1987). Total displacement along the Champlain Thrust ranges from 34-62 miles (55-100 km.) (Stanley, 1987; Rowley, 1982).

Apatite fission track work by Roden-Tice (2000) indicates that the exhumation of the Adirondacks was complete by the Cretaceous. This uplift may have reactivated faults between the Champlain Valley and Adirondacks.

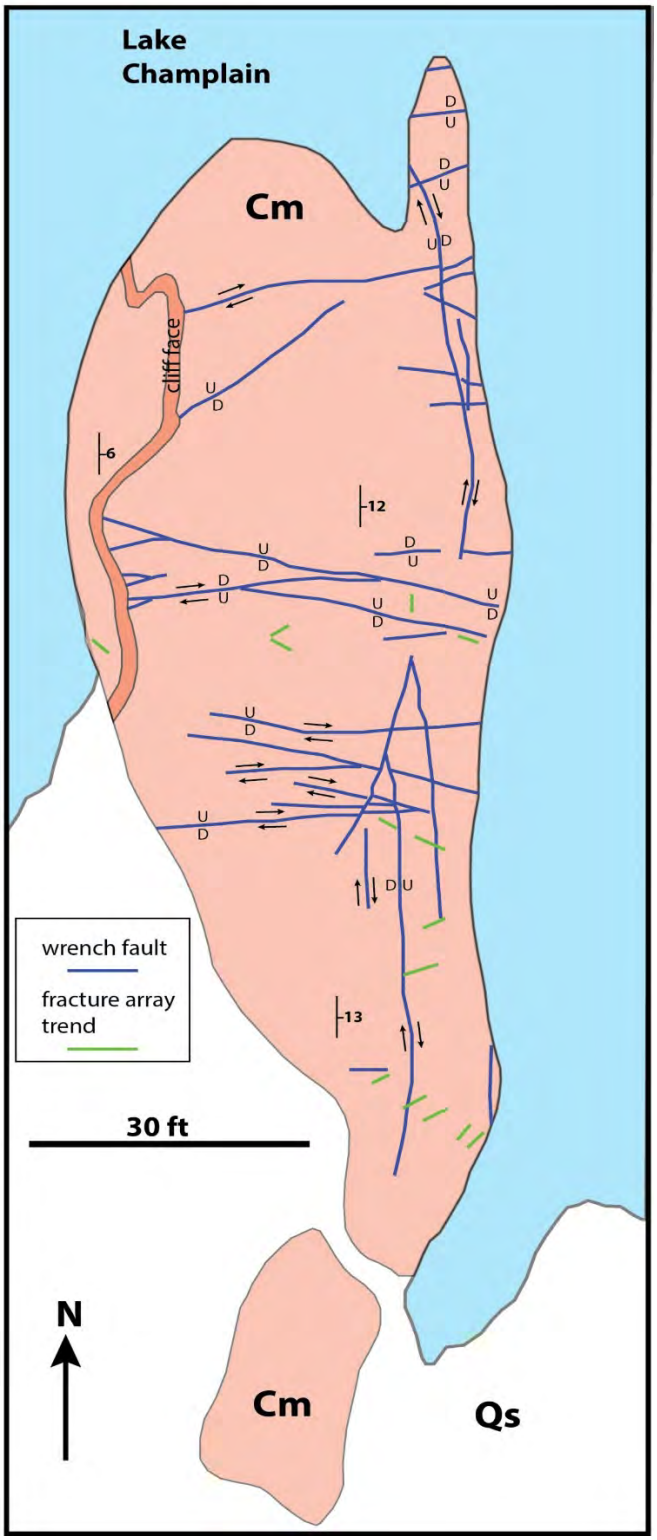

Figure 7. Brittle structure map of the Shelburne boat access. Modified from Stanley (1974). Cm = Monkton Formation quartzite and Qs = Quaternary surficial material.

Hydrogeology and Groundwater Geochemistry

Based on domestic well logs, average yields from the Monkton Formation in the Town of Charlotte are very favorable (Springston et al., 2010). Although we do not know of any bedrock groundwater wells that penetrate through the Monkton Formation into the underlying shales, Charles Welby (pers. Comm., 2009) said that numerous wells do. Such wells are often characterized by unpleasant amounts of hydrogen sulfide (rotten egg smell) gas. A Middlebury College student will be investigating the groundwater chemistry of the hanging and foot wall aquifers of the Champlain Thrust during 2015-2016.

Cumulative miles	Point to Point	Route Description
52.2	0.0	Turn right onto Mt Philo Road
54.7	2.5	Turn right onto Charlotte Road
56.4	4.2	Continue straight through the intersection with Spear Street Extension.
60.6	8.4	Turn left onto Route 116 N
60.8	8.6	Turn right onto Mechanicsville Road
61.7	9.5	Continue straight through intersection with Richmond Road.
62.3	10.1	Turn left onto Place Road East (a small gravel/dirt road)
62.4	10.2	Turn right onto an un-named road
62.5	10.3	Park on the right

Stop 6: Hinesburg Thrust at Mechanicsville, Vermont

Location Coordinates: 44° 21.126', 73 ° 06.472'

Introduction

Elevated radionuclide levels have been reported in groundwater from numerous bedrock wells completed in the Hanging Wall of the Hinesburg Thrust and drilled through this thrust (Kim et al., 2014a). This stop description was modified from Kim et al. (2011).

Lithology

The Hinesburg Thrust at Mechanicsville places overturned light green and gray metapsammitic schists and quartzites of the Early Cambrian Cheshire Quartzite (argillaceous member) on top of a slice of deformed dolomites, limestone and marble of the Ordovician Bascom Formation (Thompson et. al., 2004). The hanging wall rocks display a lower greenschist facies metamorphic mineral assemblage that includes chlorite, quartz, sericite, and biotite. The footwall is dominated by a chloritic and graphitic carbonate mineral assemblage, indicating that the Hinesburg Thrust is marked by an abrupt change in metamorphic grade as well as a change in lithology.

Structure

The thrust fault itself is defined by a narrow zone (<10 cm thick) of cataclastic dolomite at the top of the Bascom Formation (Figure 8). The dolomites below the fault are highly fractured and

sheared. Ductile shear bands (C' type) deform a penetrative phyllitic cleavage (S_1) up to at least a meter beneath the fault. The shear bands are variable in orientation, but most dip gently to the northeast (298 31 NE). Quartz rods define a mineral stretching lineation on C' shear planes. This lineation plunges gently to the east and southeast (093 02). The asymmetry of the shear bands yields a consistent top-to-the-northwest sense of displacement on the Hinesburg Thrust.

Above the Hinesburg Thrust at Stop 6 the metapsammite schists and quartzite layers of the Cheshire Fm are mylonitic (Strehle, 1985; Strehle and Stanley, 1986). The oldest structures preserved include a compositional layering (S_0) defined by alternating bands of micaceous and quartz-rich laminae and >3 cm thick quartzite beds (Figure 8). This layering, which most likely represents sheared, stretched, and recrystallized bedding planes, is deformed into a series of tight-isoclinal, reclined-recumbent folds (F_1). A fine grained mylonitic foliation (S_1) defined by the alignment of graphite, mica, and recrystallized quartz parallels the axial planes of the F_1 folds (Figure 8). On S_1 surfaces, a penetrative mica and quartz mineral lineation (L_1) plunges gently to the east and southeast. Locally, and especially within thin quartzite bands, the L_1-S_1 fabric is deformed by a series of shear bands (C' type) similar to those in the foot wall rocks (339 13 NE). Both sets yield a similar top-to-the-northwest sense of shear parallel to the L_1 mineral lineation (106 12). The S_1 foliation also parallels the surface of the Hinesburg Thrust and is interpreted here to reflect early ductile thrusting at depth prior to the final emplacement of the Cheshire Fm onto the Bascom Fm along the semibrittle Hinesburg thrust fault.

The structural features observed in the mylonitic rocks above the Hinesburg Thrust display an elegant interplay between ductile deformation, in the form of folds and cleavages, and brittle deformation, in the form of veins. Throughout the outcrop the mylonitic S_1 foliation locally is cross cut by a set of quartz veins (V_1) that are tightly folded within the F_1 folds, indicating that they formed during folding, probably as a result of pressure solution and fluid transfer processes. Cross cutting both the S_1 cleavage and the V_1 veins is a second set of asymmetric quartz tension gashes (V_2) that localized within thick (>30 cm) quartzite layers (Figures 8, 9a). The tips of the asymmetric veins penetrate into the mylonitic schist surrounding the quartzite layers. A close inspection of the V_2 veins (both on the outcrop and in thin section) indicates that they are sheared and protomylonitic (look for the milky white, recrystallized appearance and the presence of quartz ribbons). These characteristics contrast with a younger set of quartz tension gashes (V_3) that cross cut the V_2 set in the same quartzite layers (Figure 8). The V_3 vein set is only weakly deformed, less recrystallized than the V_2 veins, and are mostly symmetric to slightly asymmetric. A black, quartz-poor pressure solution selvage surrounds the veined quartzite layers (Figure 9a) strongly suggesting that the vein material was locally derived and that dissolution and fluid migration depleted these zones of silica during progressive deformation. These relationships indicate that crystalplastic deformation alternated with brittle deformation as the superposed sets of tension gashes formed.

Both the V_3 and V_2 vein sets, as well as the F_1 folds, S_1 cleavage, and quartzite layers, are all deformed into a series of northwest-vergent asymmetric folds (F_2) of variable tightness (Figure 18). The fanning of the V_2 vein sets around fold hinges is a good indicator that they are folded (Figure 19c, 19d). The tightest folds are recumbent and tend to occur nearest the Hinesburg Thrust close to the base of the mylonitic section. Farther above the thrust, the F_2 folds tend to be more open and upright to gently inclined. This increase in fold tightness and orientation suggests that the folds record an increase in finite strain downward toward the Hinesburg Thrust.

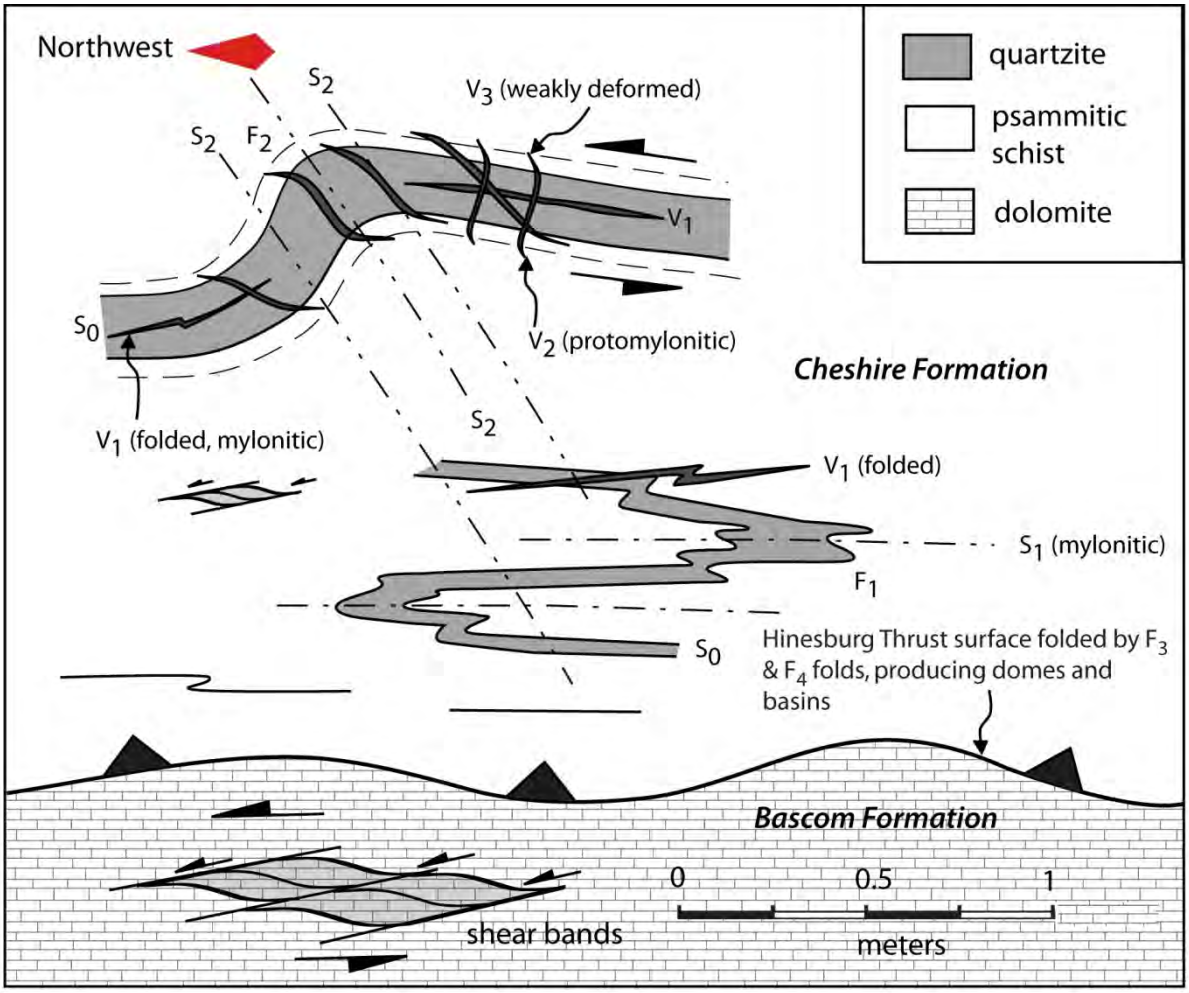

Figure 8. Sketch of structural relationships above and below the Hinesburg Thrust on vertical cliffs at Mechanicsville (Stop 5). Cliff face is oriented parallel to an L_1 quartz-mica mineral lineation.

A spaced crenulation cleavage (S_2) parallels the axial planes of the F_2 folds and also displays variable dips (Figures 8, 9d). In addition to recording a strain gradient, the variability in axial plane and cleavage orientation with increasing fold tightness provides kinematic information. The rotation of fold axial planes and S_2 to the northwest as fold tightness (and finite strain) increases, yields a top-to-the-northwest sense of shear identical to that indicated by the shear bands (Figure 9d). This relationship indicates that the F_2 folds reflect progessive deformation during the same ductile thrusting event that produced the S_1 mylonites and F_1 folds.

The following model, which is based on sketches of features at Mechanicsville, explains the evolution of the veins and the F_2 fold structures. See if you can find features on the outcrop that record each of these stages:

Stage 1 (Figure 9a).

En echelon arrays of quartz veins (V_2) open perpendicular to the direction of maximum stretch (X) of the instantaneous strain ellipse (ISE) in quartzite layers.

Stage 2 (Figure 9b)

After the V_2 veins finish forming, noncoaxial shear zones localized by the rheological contrast between the shale and the quartzite causes the parts of the vein tips that extend into shale to deform and rotate to the left. This process causes the veins to become asymmetric. A new set of veins (V_3) open

perpendicular to X-direction of instantaneous strain ellipse (ISE). A comparison of instantaneous and finite strain ellipses and the asymmetry of the two vein sets yield a top-to-the-NW sense of shear, identical to that recorded by shear bands in the mylonitic matrix. Note that this process differs than that which forms sigmoidal veins in brittle shear zones where the veins continues to open during shearing (Figure 10). In this latter model, a comparison of instantaneous and finite strain ellipses yields a top-to- the-SE (normal) sense of shear. This is because, in this latter case, the tips of V_2 veins are younger than their centers and so the former record instantaneous strains (ISE, Figure 10) and the latter record finite strains (FSE, Figure 10). We ruled out this model because, given the top-to-the-NW sense of shear at Mechanicsville, it would produce V_2 and V_3 vein asymmetries opposite to those observed (Figure 19). In the Mechanicsville model, the vein is required to form quickly and finish opening before ductile shear begins, yielding an asymmetry similar to that of a shear band.

Stage 3 (Figure 9c)

As the rotation of the veins during noncoaxial shear continues, the F_2 folds begin to form along with an axial planar crenulation cleavage (S_2). The F_2 axial planes and S_2 cleavage initially form at 45° to the quartzite layers and then rotate to the northwest toward the shear plane (defined by S_1). The V_3 vein sets also begin to rotate toward the northwest as noncoaxial shear continues.

Stage 4 (Figure 9d)

As noncoaxial shear continues the F_2 folds continue to rotate and tighten, recording a progressive increase in finite strain durign ductile thrusting. The S_2 crenulation cleavage rotates to the northwest along with the folds. The V_2 veins exhibit a characteristic fanning geometry around fold hinges, indicating that they also rotated during folding. The F_1 and S_1 structures are transposed parallel to S_2. The rotation of F_2 axial planes to the left with increasing fold tightness yields a top-to-the-northwest sense of shear, which is the same as that indicated by the asymmetric veins and shear bands.

The Hinesburg Thrust surface, and all other structures above and below it, are corrugated by two orthogonal sets of gentle, upright folds, forming a dome and basin pattern with a wavelength on the order of a few meters (Figure 10). This fold geometry mimics a kilometer scale dome and basin interference pattern formed by north-plunging (F_3) and east and west plunging (F_4) folds across the field trip area. These orthogonal fold sets are among the youngest ductile structures preserved at Stop 6. On the thrust surface itself two orthogonal crenulation lineations (L_3, L_4) mark the presence of the corrugation folds (Figure 11). A regional correlation of similar structures across the field area indicates that the orthogonal fold sets everywhere postdate thrust sheet emplacement and imbrication on the Champlain, Hinesburg and Iroquois thrusts. Earle et al. (2010) suggested that the two folds sets formed together as a result of a constrictional style of deformation during the Acadian orogeny, possible reflecting the reactivation of inherited basement faults or lateral thrust ramps. However, it is also possible that the fold sets formed in sequence as separate events.

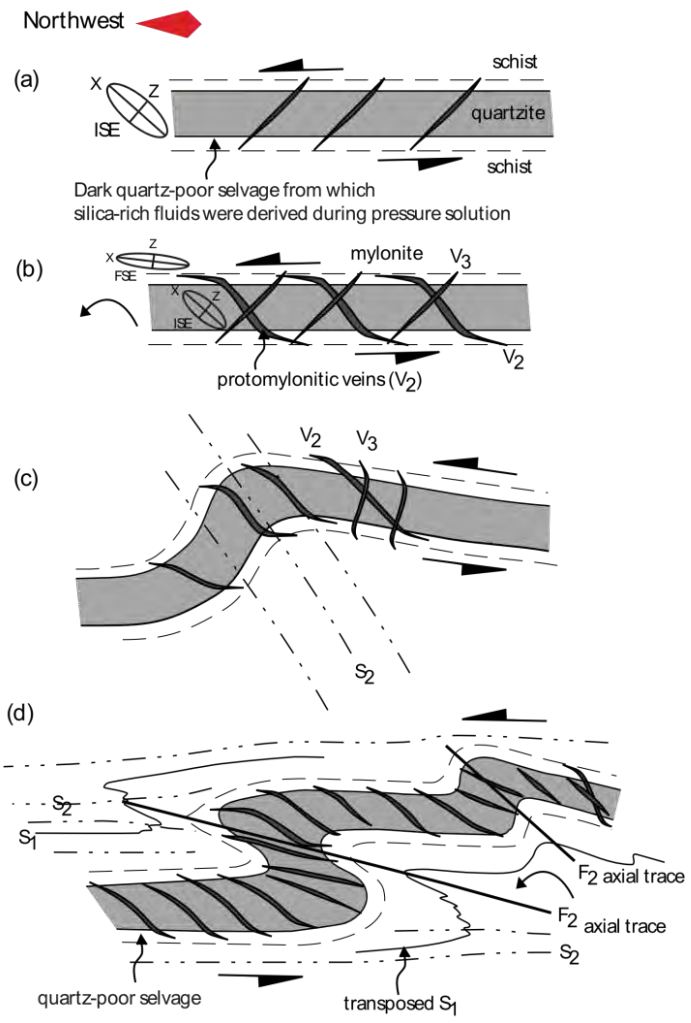

Figure 9. Cartoon showing the preferred model of progressive formation of F_2 fold and veins structures in the mylonitic hanging wall of the Hinesburg Thrust at Mechanicsville. This model requires the veins to finish opening prior to the onset of noncoaxial shear.

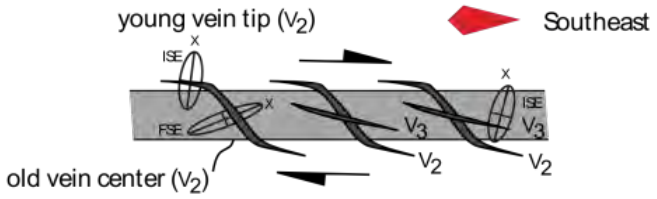

Figure 10. Cartoon showing an alternative model of progressive formation of vein sets during simple shear. This model requires the veins to continue to open during shearing. This model does not predict the correct orientation of V_3 veins or the top-to-the-NW sense of shear observed in the outcrop.

Hydrogeology and Groundwater Geochemistry

Elevated levels of alpha radiation (> 15 pCi/L as gross alpha) were observed in 38 % (12/31) of bedrock wells drilled into the hanging wall, including wells that penetrated the thrust into carbonates below; for comparison, no wells [0/21] in the carbonate-dominated footwall west of the thrust front exceeded 15 pCi/L (the EPA MCL). The source of the elevated radioactivity was evaluated by testing groundwater from hanging wall and footwall bedrock wells and by analyzing compositions of bedrock from local outcrops. The chemical composition of groundwater in hanging wall and footwall aquifers is mainly controlled by whole-rock geochemistry. Hanging wall groundwater is enriched in alpha radiation, K, Cl, Ba, Sr and U, whereas footwall groundwater is enriched in Ca, Mg, and HCO_3. These signatures reflect the distinct compositions of phyllite-dominated bedrock in the hanging wall compared to Ca-Mg-CO3-rich limestones and dolostones of the footwall. Elevated alpha radiation and U in wells that produce from footwall carbonates below the thrust recorded compositions that are intermediate to hanging wall and footwall end-members, indicating that alpha and U are transported in groundwater downward through the thrust via fractures into the footwall below (Kim et al., 2014a).

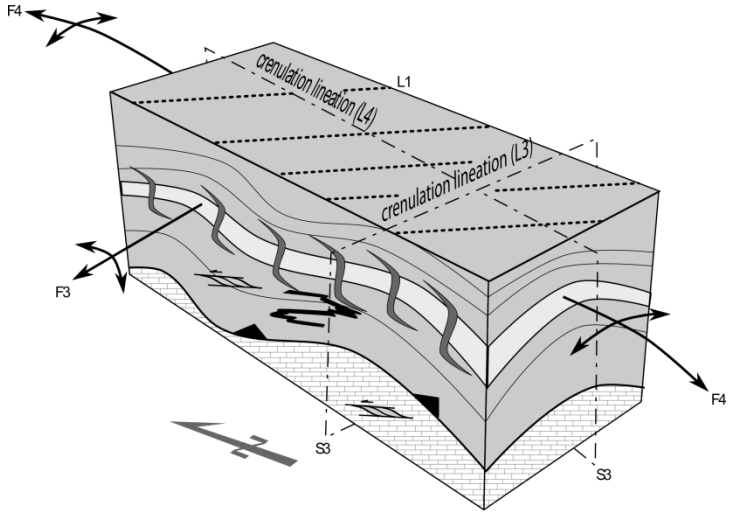

Figure 11. Block diagram showing the relative geometry of orthogonal fold sets that deform the Hinesburg Thrust surface and the mylonites at Mechanicsville, producing a dome and basin pattern. The two fold sets (F_3 and F_4) are associated with two steeply dipping orthogonal cleavages.

Cumulative miles	Point to Point	Route Description
62.5	0.0	Leave on un-named road, left onto Place Road East
62.7	0.2	Turn right onto Mechanicsville Road
63.2	0.7	Turn right onto CVU Road
63.8	1.3	Continue straight through intersection with Route 116 onto Shelburne Falls Road
64.3	1.8	Turn right into Geprags Community Park

Stop 7: Multiple Structural Generations and Hydrogeology at Geprags Park, Hinesburg, Vermont

Location Coordinates: 44 ^{o} 20.448' N, 73 ^{o} 07.389' W

Introduction

The Town of Hinesburg drilled three bedrock wells in Geprags Park in 1996. Although these wells were completed as future public water supplies, surface water contamination in one of these wells precluded them from ever being used. The Vermont Geological Survey and SUNY at Plattsburgh conducted comprehensive geophysical logging of these wells during 2012-2014 using temperature, conductivity, gamma, caliper, and accoustic televiewer tools. During 2014, Hinesburg drilled two new wells at a nearby site, which is also located on Shelburne Falls Road, but closer to the intersection with Route 116. These wells were drilled to increase water production for the town. One of these new wells (#48477) was logged with the previously mentioned tools. One well in Geprags Park (#7797) and another on the Wainer property were logged using a heat pulse flowmeter. Structures and lithologies were also mapped in the field to compare with those in the wells.

Lithology

In order of decreasing age, Early Ordovician Shelburne Formation (marble and dolostone), Late Cambrian Clarendon Springs Formation (dolostone) and Danby Formation (dolomitic sandstone), and Middle Cambrian Winooski Formation (dolostone).

Structure

All lithologies are folded by the north-plunging Hinesburg Synclinorium, which is thought to have formed during the Ordovician Taconian Orogeny. In the western half of Geprags Park, this synclinorium is truncated by the north striking and steeply east-dipping St. George Fault, a down to the east normal fault of presumed Cretaceous age (Figure 2). The dominant fracture set in this area is axial planar to parasitic folds in the Hinesburg Synclinorium (Figure 12). Isolated east-west trending fracture zones also occur (Figure 13). The integrated geophysical logs for Geprags Park well #7797 showed that this well was completed through the St. George Fault.

Tectonic/Stratigraphic Context

This site sits in a similar tectonic context to Stop 3, in the hanging wall of the Champlain Thrust just east of the St. George Fault.

Hydrogeology and Groundwater Geochemistry

Using temperature, conductivity, caliper, and acoustic televiewer logs for the four wells, we were able to delineate water producing zones. A summary cross section for Geprags Park only was drawn by Kim et al. (2014b) In addition, the attitude of structures intersecting each well were calculated from the acoustic televiewer logs. Using structural data from bedding and fractures acquired in the field as a template, we were able to accurately categorize the borehole structures. Finally, we were able to determine which structures were producing groundwater in each well (Kim et al, (2015). All of our data has been presented to the Consulting Hydrogeologist for the Town of Hinesburg.

Cumulative miles	Point to Point	Route Description
64.3	0.0	Turn left onto Shelburne Falls Road
64.8	0.5	Turn left onto Route 116
66.8	2.5	Bear right onto Route 2A
71.7	7.4	Left onto I-89 North
71.9	7.6	Merge onto I-89 North
85.6	21.3	Take exit 17 (Lake Champlain Islands and Milton)
85.8	21.5	Turn left onto Route 2 East
85.9	21.6	Turn left onto Route 7 North
86.3	21.9	Turn right into Colchester Park and Ride
		END OF ROAD LOG

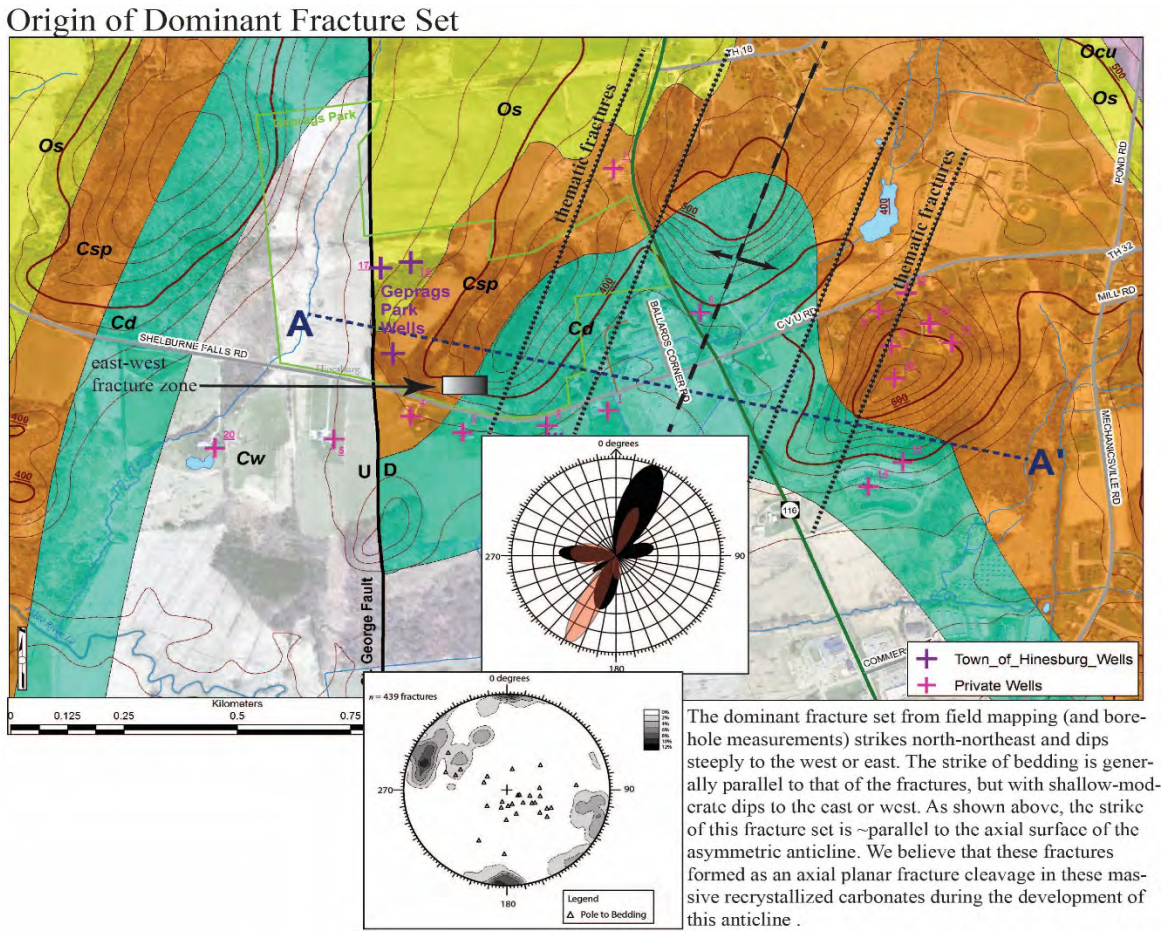

Figure 12. Rose diagram and equal area net for all structural data acquired in the field (black = fractures and red = bedding) (Salvini et al., 1999) overlaid on bedrock geologic map (modified from Kim et al. (2015). Map base modified from Ratcliffe et al. (2011). Note that the dominant fracture peak is axial planar to the fold in the Hinesburg Synclinorium.

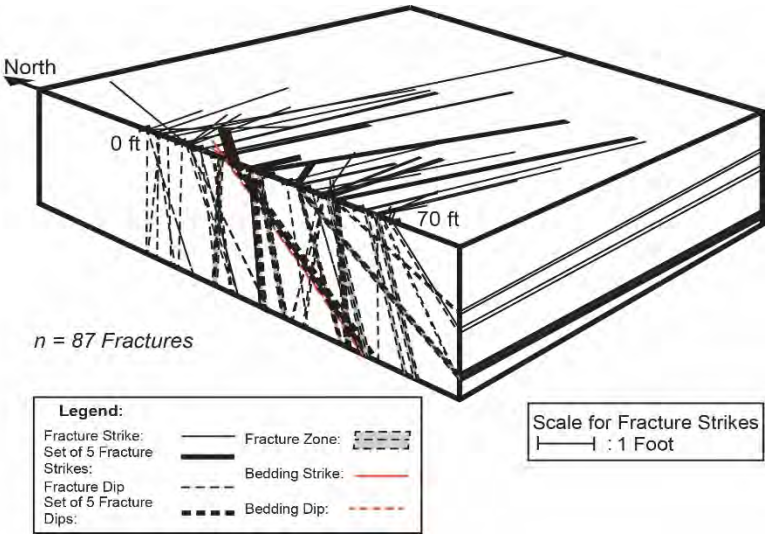

Figure 13. 3-D configuration of fractures at an outcrop in Geprags Park where east-west trending fractures are dominant (Chirigos, pers. comm., 2015)

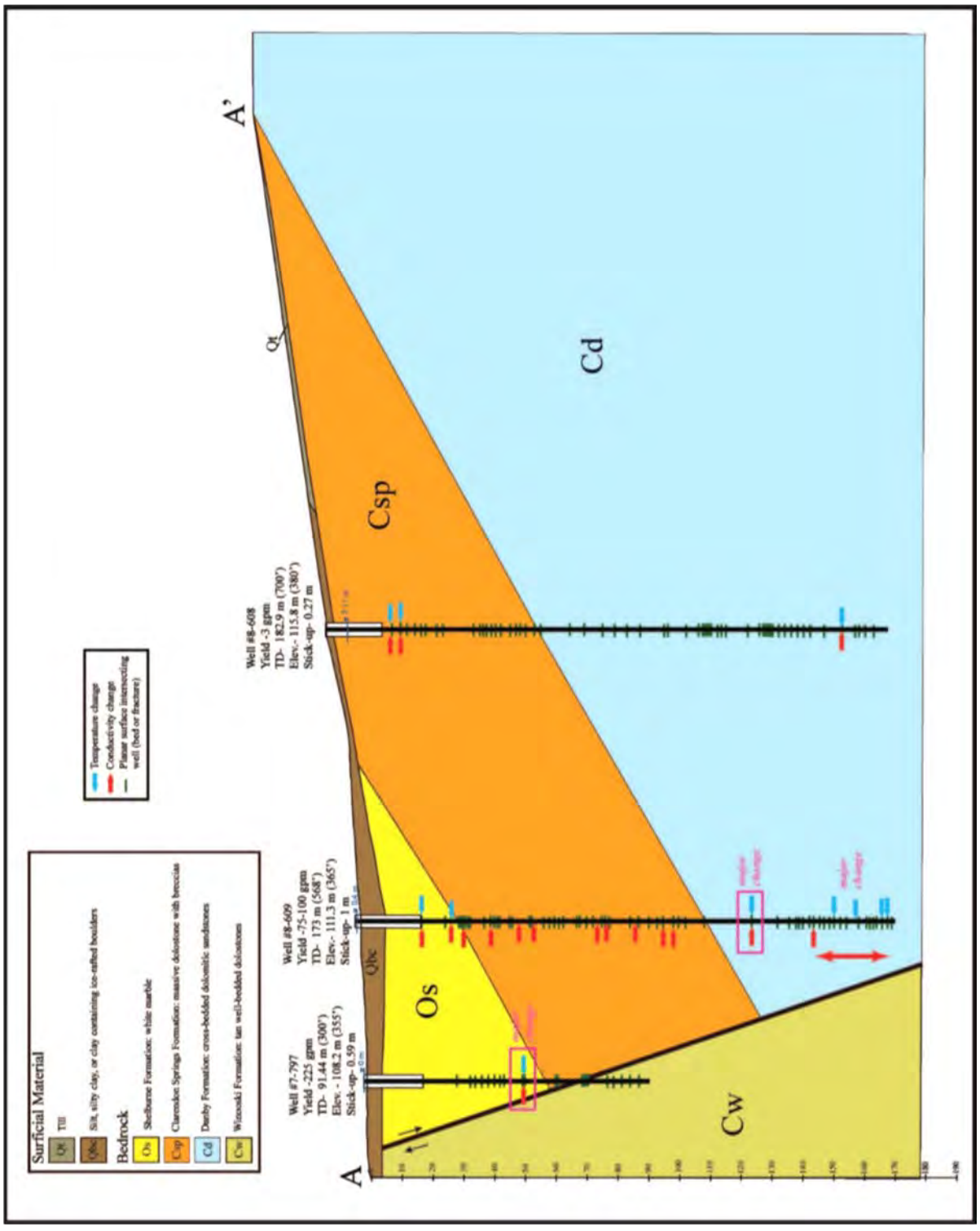

Figure 14. Summary cross section for the well logs in Geprags Park. West =left and right = east. Modified from Kim et al., (2014b).

REFERENCES CITED

Aleinikoff, J., Wintsch, R., Tollo, R., Unruh, D., Fanning, C.M., and Schmitz, M., 2007, Ages and origins of rocks of the Killingworth dome, south-central Connecticut: Implications for the tectonic evolution of New England: American Journal of Science, v. 307, p. 63-118.

Armstrong, R.L., and Stump, E., 1971, Additional K-Ar dates, White Mountain magma series, New England: American Journal of Science, v. 270, p. 331-333.

Bachman, N., 2015. Origin and Speciation of Uranium in the Phosphorite of the Clarendon. Springs Formation Dolostone; Milton and Colchester. Unpub. Bach. Thesis, Middlebury College, VT, 74 p.

Bazilchuk, N., 2000, Tainted Water Persists: Burlington Free Press, p. 1B, June 5, 2000.

Boyer, S.E. and Elliott, 1982, Thrust Systems: American Assoication of Petroleum Geologist Bulletin, v. 66, p. 1196-1230.

Cady, W.M., 1945, Stratigraphy and structure of west-central Vermont: Geological Society of America Bulletin, v.56, p.515–587.

Doll, C.G., Cady, W.M., Thompson, J.B., Jr. and Billings, M.P., 1961. Centennial Geologic Map of Vermont. Vermont Geological Survey, Scale 1:250 000.

Dorais, M.J., Atkinson, M., Kim, J., West, D.P., and Kirby, G.A., 2011, Where is the Iapetus suture in northern New England? A study of the Ammonoosuc Volcanics, Bronson Hill terrance, New Hamphire: Canadian Journal of Earth Science, v.48, p.1209-1225.

Dorais, M, Workman, J., and Aggarwal, J., 2008, The petrogenesis of the Highlandcroft and Oliverian plutonic suites, New Hampshire: Implications for the structure of the Bronson Hill terrane: American Journal of Science, v. 308, p. 73-99.

Dorsey, R.L., Agnew, P.C., Carter, C.M., Rosencrantz, E.J., and Stanley, R.S., 1983, Bedrock geology of the Milton quadrangle, northwestern Vermont: Vermont Geological Survey Special Bull. No. 3, 14 p.

Earle, H., Kim, J., Klepeis, K., 2010, Comparison of Ductile Structures across the Hinesburg and Champlain Thrust Faults in NW Vermont: Geological Society of America *Abstr. with Progr.*, v.42, n.1, p.88.

Gale, M. and Thompson, P., 2010, New bedrock map and cross-sections of Vermont: Structural and stratigraphic constraints for northern Vermont: Geological Society of America *Abstracts with Programs*, v.42, n.1, p.54.

Gale, M., Kim, J., Earle, H., Clark, A., Smith, T., and Petersen, K., 2009, Bedrock Geologic Map of Charlotte, Vermont, 3plates, 1:24,000: Vermont Geology Survey Open File Report VG09-5, 3 plates.

Gillespie, R., 1975, Structure and Stratigraphy along the Hinesburg Thrust, Hinesburg, Vermont: Master's Thesis, University of Vermont Dept. of Geology, 63 p.

Gudmundsson, A., 2011, Rock Fractures in Geologic Processes: Cambridge University Press, Cambridge, 578 p.

Isachsen, Y.W., and Fisher, D.W., 1970, Geologic map of New York, Adirondack sheet: New York State Museum and Science Service Map and Chart Series 15, scale 1:250,000.

Karabinos, P., Samson, S.D., Christopher Hepburn, J., and Stoll, H.M., 1998, Taconian Orogeny in the New England Appalachians: Collision between Laurentia and the Shelburne Falls arc: Geology, v. 26, p. 215-218.

Kim, J. and Thompson, P., 2001, Bedrock Geologic Map of the Colchester Quadrangle, Vermont Geological Survey Open File Maps and Report VG01-1 , scale 1:24,000.

Kim, J., Gale, M., Laird, J., and Stanley, R., 1999, Lamoille River valley bedrock transect #2, *in* Wright, S.F., ed., Guidebook to field trips in Vermont and adjacent regions of New Hampshire and New York: New England Intercollegiate Geological Conference, v. 91, p. 213–250.

Kim, J., Gale, M., Thompson, P. & Derman, K., 2007, Bedrock Geologic Map of the Town of Williston, Vermont, 1:24,000: Vermont Geological Survey Open File Report VG07-4.

Kim, J., Klepeis, K., Ryan, P., Gale, M., McNiff, C., Ruksznis, A., and Webber, J., 2011, A Bedrock Transect Across the Champlain and Hinesburg Thrusts in West-Central Vermont: Integration of Tectonics with Hydrogeology and Groundwater Chemistry: in West, D., editor, New England Intercollegiate Geological Conference: Guidebook for Field Trips in Vermont and adjacent New York, 103rd Annual Meeting, Middlebury, Vermont, Trip B1, p. B1-1 – B1-35.

Kim, J., Weber, E., and Klepeis, K., 2013, Bedrock Geologic Map of the Bristol Quadrangle, Addison County, Vermont: Vermont Geological Survey Open File Map VG13-1, scale 1:24,000, 2 plates.

Kim, J., Ryan, P.C., Klepeis, K., Gleeson, T., North, K., Bean, J., Davis, L., Filoon, J., 2014a. Ordovician thrust fault controls hydrogeology and geochemistry of a bedrock aquifer system in NW Vermont: northeastern Appalachian foreland. Geofluids 14, 266-290. DOI: 10.1111/gfl.12076.

Kim, J., Romanowicz, E., and Dorsey, M., 2014b, The Subsurface Expression of a Faulted and Folded Bedrock Aquifer in the West-Central Vermont Foreland: Geological Society of America, Abstracts with Programs, v. 46, #2, p. 48.

Kim, J., Gale, M., Chu, K., Cincotta, M. and Cuccio, L., 2014c, Bedrock Geologic Map of the northern portion of the South Mountain Quadrangle, Addison County, Vermont: Vermont Geological Survey Open File Report VG14-1, scale 1:24,000, 1 plate.

Kim, J., Romanowicz, E., Dorsey, M., and Strathearn, C., 2015, Hydrogeological Analysis of a Complexly Folded and Faulted Bedrock Aquifer in the Champlain Valley of West-Central Vermont: Geological Society of America, Abstracts with Programs, v. 47, #3, p. 129.

Landing, E. 2007. Ediacaran-Ordovician of East Laurentia-Geologic Setting and Controls on Deposition along the New York Promontory Region. in S.W. Ford Memorial Volume: Ediacaran-Ordovician of East Laurentia. New York State Museum Bulletin 510, edited by E. Landing, pp. 5-24. The University of the State of New York, Albany, New York.

Landing, E., 2002, Early Paleozoic Sea Levels and Climates: New Evidence from the East Laurentian Shelf and Slope: *in* J. McLelland and P. Karabinos, *eds*., New England Intercollegiate Geological Conference, Guidebook for Fieldtrips in New York and Vermont, p. B6-1-B6-22.

Landing, E., Westrop, S.R., van Aller Hernick, L., 2003, Uppermost Cambrian—Lower Ordovician faunas and Laurentian platform sequence stratigraphy, eastern New York and Vermont: Journal of Paleontology, v.77, n.1, p.78-98.

McDonald, E., 2012. A Model for Uranium Occurrence in the Late Cambrian Clarendon Springs Formation: Implications for Groundwater Quality in Northwestern Vermont. Unpub. Bach. Thesis, Middlebury College, Vermont, 127 pp. http://middarchive.middlebury.edu/cdm/ref/collection/scholarship/id/80.

McDonald, F.A., Ryan-Davis, J., Coish, R.A., Crowley, J.L., and Karabinos, P., 2014, A newly identified Gondwanan terrance in the northern Appalachian Mountains: Implications for he Taconic orogeny and closure of the Iapetus Ocean: Geology, doi: 10.1130/G35659.1

McHone, J.G., 1978, Distributions, orientations, and ages of mafic dikes in central New England: Geological Society of America Bulletin, v. 89, p. 1645-1655.

McHone, J.G., and Corneille, E.S., 1980, Alkalic dikes of the Lake Champlain Valley: Vermont Geology, v. 1, p. 16-21.

McHone, J.G., and McHone, N.W., 1999, The New England – Quebec Igneous Province in Western Vermont, *in* Wright, S.F., *editor*, Guidebook to Field Trips in Vermont and Adjacent Regions of New Hampshire and New York, New England Intercollegiate Geological Conference Guidebook, p.341-358.

Mehrtens, C., 1997, Digital compilation bedrock geologic map of the Lake Champlain South one-degree sheet, Vermont: VGS Open-File Report VG97-01A, 2 plates, scale 1:100000.

Mehrtens, C.J., 1987, Stratigraphy of the Cambrian platform in northwestern Vermont: Geological Society of American Centenial Field Guide—Northeastern Section, v.5, p.229-232.

Moench, R. H., and Aleinikoff, J. N., 2003, Stratigraphy, geochronology, and accretionary terrane settings of two Bronson Hill arc sequences, northern New England: Physics and Chemistry of the Earth, Parts A/B/C, v.28, n.1-3, p.113-160.

Ramsey, J.G., 1962, Interference patterns produced by the superposition of folds of similar type: The Journal of Geology, v.70, n.4, p.466-481.

Rankin, D., Coish, R., Tucker, R., Peng, Z., Wilson, S., and Rouff, A., 2007, Silurian extension in the Upper Connecticut Valley, United States and the origin of middle Paleozoic basins in the Quebec embayment: American Journal of Science, v. 307, p. 216-264.

Ratcliffe, N.M., Stanley, R.S, Gale, M.H., Thompson, P.J., and Walsh, G.J., 2011, Bedrock Geologic Map of Vermont: U.S. Geological Survey Scientific Investigations Map 3184, 3 sheets, scale 1:100,000.

Roden-Tice, M.K., Tice, S.J., and Schofield, I.S., 2000, Evidence for differential unroofing in the Adirondack Mountains, New York State, determined from apatitie fission-track thermochronology: The Journal of Geology, v.108, p.155-169.

Roden-Tice, Mary K., West Jr., David P., Potter, Jaime K., Raymond, Sarah M., Winch, Jenny L., 2009, Presence of a Long-Term Lithospheric Thermal Anomaly: Evidence from Apatite Fission-Track Analysis in Northern New England: Journal of Geology, v.117, n.6, p.627-641.

Rosenberg, B., Meyers, E., Ryan, P., Eberl, D.D., 2011, K-Ar dating of Illite-rich rocks in the Champlain Valley, Vermont: An investigation of post-Taconic faulting and fluid flow: The Green Mountain Geologist, v.38, n.2, p.4-5.

Rowley, D.B., 1982, A new method for estimating displacements of large thrust faults affecting Atlantic-type shelf sequences: with an application to the Champlain Thrust, Vermont: Tectonics, v.1, p.369-388.

Ryan, P.C., Kim, J.J., Mango, H., Hattori, K., Thompson, A., 2013. Arsenic in a fractured slate aquifer system, New England (USA): Influence of bedrock geochemistry, groundwater flow paths, redox and ion exchange. Applied Geochemistry 39, 181-192. doi: http://dx.doi.org/10.1016/j.apgeochem.2013.09.010.

Salvini, F., Billi, A., Wise, D.U. , 1999, Strike-slip fault-propagation cleavage in carbonate rocks: the Mattinata fault zone, Southern Apennines, Italy. Journal of Structural Geology. vol. 21, pp. 1731-1749.

Sejourne, Stephan, Malo, Michel, 2007, Pre-, syn-, and post-imbrication deformation of carbonate slices along the southern Quebec Appalachian front— implications for hydrocarbon exploration: Canadian Journal of Earth Sciences, v.44, n.4, p.543-564.

Springston, G., Gale, M., Kim, J., Wright, S., Earle, H., Clark, A. and Smith, T., 2010, Hydrogeology of Charlotte, Vermont, 7 plates, 1:24,000: Vermont Geological Survey Open File Report VG10-1.

Stanley, R.S., 1974, Environment of Deformation, Monkton Quartzite, Shelburne Bay, Western Vermont: Geological Society of America Bulletin, v. 85, p. 233-246.

Stanley, 1980, Mesozoic Faults and Their Environmental Significance in Western Vermont: Vermont Geology, v. 1, pp. 22-32.

Stanley, R. and Wright, S., 1997, The Appalachian foreland as seen in northern Vermont, *in* Grover, T.W., Mango, H.N., and Hasenohr, E.J., eds., Guidebook to field trips in Vermont and adjacent New Hampshire and New York: New England Intercollegiate Geological Conference, v. 89, p. B1, 1-33.

Stanley, R., and Sarkisian, A., 1972, Analysis and chronology of strucures along the Champlain Thrust west of the Hinesburg synclinorium: Guidebook to field trips in Vermont and adjacent New Hampshire and New York: New England Intercollegiate Geological Conference, v.64, B5, p.117-149.

Stanley, R., Dellorusso, V., O'Loughlin, S., Lapp, E., Armstrong, T., Prewitt, J., Kraus, J., and Walsh, G., 1987, A Transect through the Pre-Silurian Rocks of Central Vermont: in D. Westerman, *Editor*, Guidebook for Field Trips in Vermont, New England Intercollegiate Geological Conference, pp. 272-295.

Stanley, R.S., 1987, The Champlain thrust fault, Lone Rock Point, Burlington, Vermont: Geological Society of American Centennial Field Guide- Northeastern Section.

Stanley, R.S., Leonard, K., and Strehle, B., 1987, A transect through the foreland and transitional zone of western Vermont: Guidebook to field trips in Vermont, v.79, A5, p.80-104.

Stanley, Rolfe S., and Ratcliffe, Nicolas M, 1985, Tectonic Synthesis of Taconic Orogeny in western New England: Geologic Society of America Bulletin, v.96, p.1227-1250.

Strathearn, C., Klepeis, K., Kim, J., Gombosi, A., Langworthy, M., Johnson, E., and Schachner, B, 2015, Detailed Analysis of Structures in the Foot Wall of the Champlain Thrust at Lone Rock Point, Burlington, Vermont: Geological Society of America, Abstracts with Programs, v. 47, #3, p. 93.

Strehle, B.A., Stanley, R.S., 1986, A comparison of fault zone fabrics in Northwestern Vermont [4 sites in Milton, Mechanicsville (Hinesburg), South Lincoln (Lincoln), and Jerusalem(Starksboro)]: Vermont Geological Survey Studies in Vermont Geology No. 3, 36 p.

Thomas Jr., J., Glass, H.D., White, W.A., and Trandel, R.M., 1977, Fluoride content of clay minerals and argillaceous earth materials: Clays and Clay Minerals, v. 25, p. 278-284.

Thompson, P.J., and Thompson, T.B., 2003, The Prospect Rock thrust: western limit of the Taconian accretionary prism in the northern Green Mountain anticlinorium, Vermont: Canadian Journal of Earth Sciences, v. 40, p. 269-284.

Thompson, T., Thompson, P., and Doolan, B., 2004, Bedrock Geologic Map of the Hinesburg Quadrangle, Vermont Geological Survey Open File Map VG04-2, scale- 1:24,000.

Tremblay, A. and Pinet, N., 2005, Diachronous supracrustal extension in an intraplate setting and the origin of the Connecticut Valley-Gaspe and Merimack troughs, northern Appalachians: Geological Magazine, v. 142, p. 7-22.

Twiss, R.J. and Moores, E.M., 2006, Structural Geology: W.H. Freeman and Co., 736 p.

van Staal, C. R., Dewey, J. F., Mac Niocaill, C., and McKerrow, W. S., 1998, The Cambrian-Silurian tectonic evolution of the northern Appalachians and British Caledonides: History of a complex, west and southwest Pacific-type segment of Iapetus, in Blundell, D., and Scott, A., Eds, Lyell: The Past is the Key to the Present: London, Geological Society Special Publication 143, p.199–242.

van Staal, C., Whalen, J., Valverde-Vaquero, P., Zagorevski, A., and Rogers, N., 2009, Pre-Carboniferous, episodic accretion-related, orogenesis along the Laurentian margin of the northern Appalachians, *in* Murphy, J., Keppie, J., and Hyndes, A., eds., Ancient Orogens and Modern Analogues: Geological Society, London, Special Publications 327, p.271-316.

Welby, C.W., 1961, Bedrock geology of the central Champlain Valley of Vermont: Vermont Geological Survey Bulletin, v. 14.

West, D., Kim, J., Klepeis, K., and Webber, J., 2011, Classic Bedrock Teaching Localities in the Champlain Valley between Middlebury and Burlington, Vermont: in West, D., editor, New England Intercollegiate Geological Conference: Guidebook for Field Trips in Vermont and adjacent New York, 103rd Annual Meeting, Middlebury, Vermont, Trip B1, p. C5-1 – C5-23

ANATOMY OF AN ORDOVICIAN VOLCANIC ARC AND FOREARC BASIN IN THE SOUTHERN QUÉBEC APPALACHIANS

ALAIN TREMBLAY
Département des Sciences de la Terre et de l'Atmosphère
Université du Québec à Montréal
Montréal, Qc, H3C 3P8

INTRODUCTION

This field trip focuses on the lithological characteristics and structural features of an Ordovician forearc basin sequence, the Magog Group, and adjacent volcanic arc, the Ascot Complex, from the oceanic domain (Dunnage Zone) of the southern Québec Appalachians. A particular emphasis will be put on stratigraphic relations within and between both units, which will serve as a template in order to better understand volcanic and sedimentation processes that has been coeval with the Taconian orogeny. We will visit key outcrops in the Sherbrooke area of southern Québec.

The fieldtrip incorporates numerous discussions with scientists involved in the geology of southern Québec over the last 30 years. I wish to express my gratitude to the late P. St-Julien for introducing me to the area and sharing his knowledge during earlier field seasons, P. Cousineau for his sedimentological expertise on the Magog Group, and to the southern Québec Appalachians team of graduate students (B. Lafrance, S. Castonguay, S. Schroetter, P. Pagé, C. Daoust, S. de Souza, P.-E. Mercier and M. Perrot) for their passion for field geology. It must be remembered, however, that this document represents my own vision of the southern Québec Appalachians, and that other interpretations exist. I hope that this short fieldtrip will be a forum for discussion of volcanic arc and related sedimentary basins genesis along the margins of active collision zones.

THE SOUTHERN QUÉBEC APPALACHIANS

The Appalachian belt is the result of the closure of oceanic basins (Iapetus and Rheic oceans and smaller marginal oceanic domains) and collisions of Laurentia, Baltica and Gondwana-derived continental blocks during the Paleozoic. The Québec Appalachians represent a 1000 km-long segment of that mountain belt, covering approximately 75,000 km^2, which corresponds to ca. 25% of the whole surface area of the Northern Appalachians (Figure 1). The southern Québec Appalachians comprise three lithotectonic assemblages (Figure 2): the Cambrian-Ordovician Humber and Dunnage zones (Williams, 1979), and the Silurian-Devonian successor sequence of the Gaspé Belt (Bourque et al., 2000). The Humber and Dunnage zones are remnants of the Laurentian continental margin and of the adjacent oceanic domain, respectively. The Humber»_dunnage boundary corresponds (on the surface) to a zone of dismembered ophiolites and serpentinite slices known as the Baie Verte-Brompton line (BBL; Williams & St-Julien, 1982). The Dunnage zone is unconformably overlain by Upper Silurian and Devonian rocks of the Gaspé Belt (Figure 2).

The Humber Zone is subdivided into External and Internal zones (Tremblay & Castonguay, 2002). The External Humber Zone consists of very low-grade sedimentary and volcanic rocks deformed into a series of northwest-directed thrust nappes. The Internal Humber Zone is made of

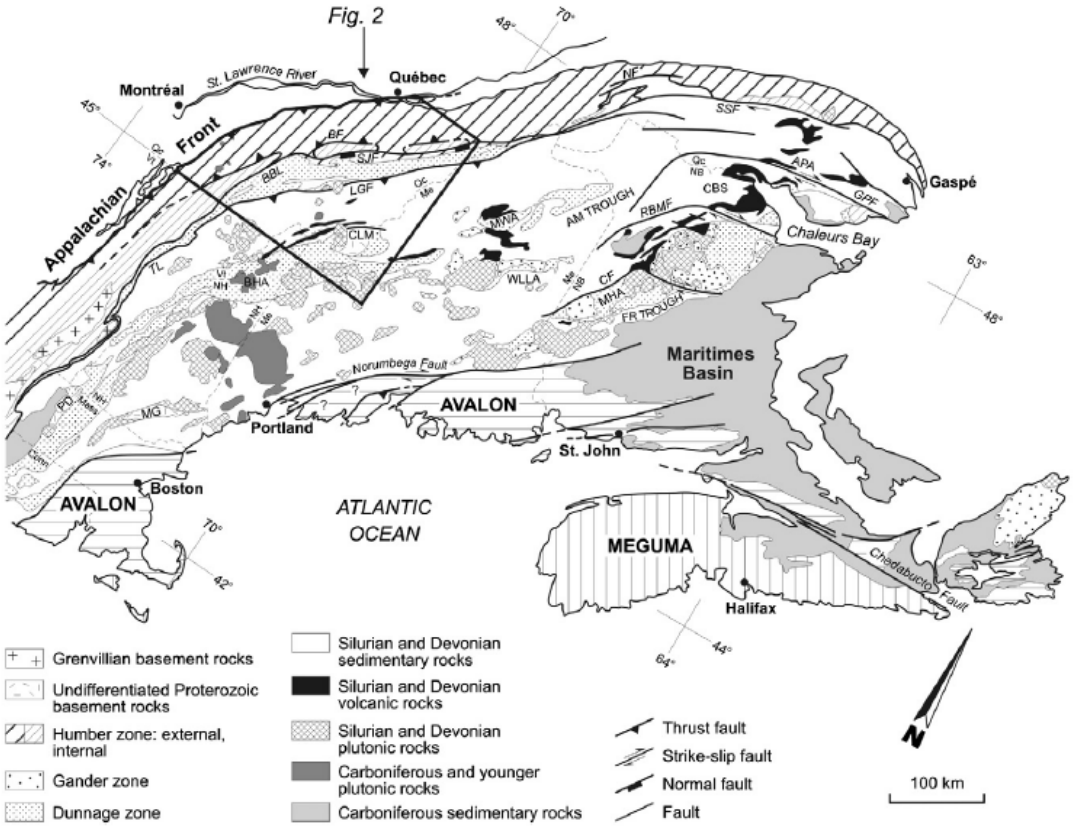

Figure 1. Simplified geological map of the Northern Appalachians of mainland Canada and New England showing the major lithotectonic elements of the region. Modified from Williams (1978). Basement rocks:CLM—Chain LakeMassif;MG—Massabesic Gneiss and PD—PelhamDome.Major anticlinoria and synclinoria:APA—Aroostook–Percé anticlinorium; CBS—Chaleurs Bay synclinorium; BHA—Bronson Hill Anticline;MHA—Miramichi Highlands Anticline;MWA—Munsungun–Winterville Anticline andWLLA—Weeksboro–Lunksoos Lake Anticline. Major faults: BBL—Baie Verte–Brompton Line; BF—Bennett fault; SJF—Saint-Joseph fault; LGF—La Guadeloupe fault; TL—Taconic Line; NF—Neigette fault; SSF—Shickshock-Sud fault; GPF—Grand Pabos fault; RBMF—Rocky Brook–Millstream fault and CF—Catamaran fault. State boundaries: Conn—Connecticut; Mass—Massachussets; Me—Maine; NB—New Brunswick; NH—New Hamshire; Qc—Quebec and Vt—Vermont. Note that the boundary between Medial New England (Gander zone) and Composite Avalon is approximate; see text for discussion. Modified from Tremblay and Pinet (2005).

greenschist- to amphibolite-grade metamorphic rocks that represent distal facies of the External Humber Zone units. The highest-grade metamorphic rocks occur in the core of doubly-plunging dome structures (i.e. the Sutton Mountains and Notre-Dame Mountains anticlinoria; Figure 2). Regional deformation includes a $S_{1\text{-}2}$ schistosity and syn-metamorphic folds and faults, which have been overprinted by a penetrative crenulation cleavage (S_3 of Tremblay & Pinet, 1994) axial-planar to hinterland-verging (southeast) folds and ductile shear zones rooted along the northwestern limb of the Internal Humber Zone (Pinet et al., 1996; Tremblay & Castonguay, 2002; Figure 2).

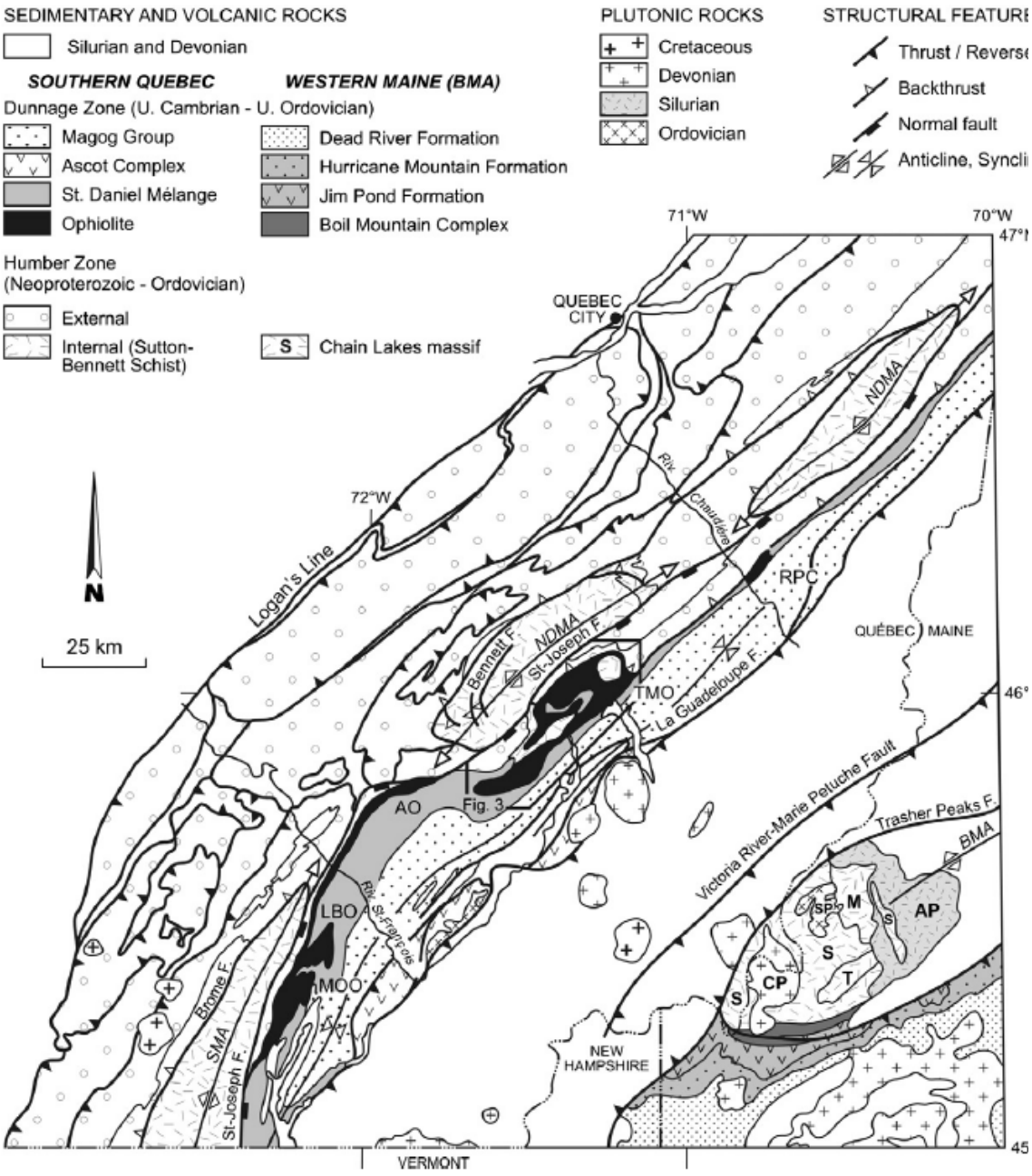

Figure 2. Geological map of the southern Quebec and western Maine Appalachians (modified from de Souza and Tremblay, 2010). BMA—Boundary Mountains anticlinorium; SMA—Sutton Mountains anticlinorium; NDMA—Notre-Dame Mountains anticlinorium; MOO—Mont-Orford ophiolite; LBO—Lac-Brompton ophiolite; AO—Asbestos ophiolite; TMO—Thetford-Mines ophiolite; RPC—Rivière-des-Plante ultramafic Complex; SP—Skinner pluton; AP—Attean pluton; CP—Chain of Ponds pluton; CLM—Chain Lakes massif: S—Sarampus Falls facies; T—Twin Bridges facies; M—McKenney Stream facies. See Fig. 1 for location.

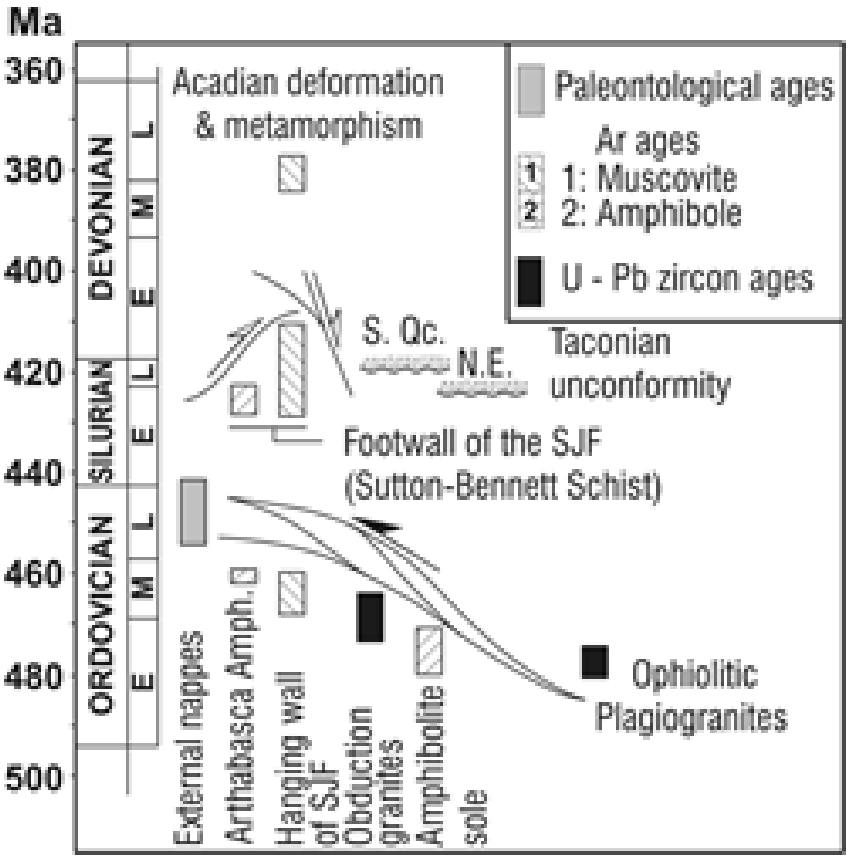

Figure 3. Diagram summarizing age constraints for deformation and metamorphism in the southern Québec Appalachians.

Amphibole and mica $^{40}Ar/^{39}Ar$ ages from the internal Humber Zone vary between 431 and 410 Ma (Figure 3). Ordovician high-temperature step ages (462-460 Ma) suggest that the geochronologic imprint of typical Taconian metamorphism is only locally preserved (Castonguay et al., 2001; 2007; Tremblay & Castonguay, 2002). To the southeast, the Internal Humber Zone is bounded by the Saint-Joseph fault (Pinet et al., 1996) and the BBL, which form a composite east-dipping normal fault system marking a boundary with less metamorphosed rocks in the hanging wall (Figure 2). East of the Saint-Joseph-BBL fault system, continental metamorphic rocks, which yielded Middle Ordovician $^{40}Ar/^{39}Ar$ muscovite ages (469-461 Ma; Whitehead et al., 1995; Castonguay et al., 2001) are locally exposed in the core of antiformal inliers.

THE SOUTHERN QUÉBEC DUNNAGE ZONE

The Dunnage Zone occurs in the hanging wall of the Saint-Joseph-BBL fault system and comprises ophiolites, mélanges, volcanic arc sequences, and marine flysch deposits. In southern Québec it is made up of four lithotectonic assemblages (Figure 2): (1) the Southern Quebec ophiolites, mainly represented by four massifs, the Thetford-Mines, Asbestos, Lac-Brompton and Mont-Orford ophiolites; (2) the Saint-Daniel Mélange; (3) the Magog Group forearc basin; and (4) the Ascot Complex volcanic arc (see Tremblay et al., 1995 for a review).

Ophiolites. The ophiolites of the Thetford-Mines and Asbestos areas are characterized by well-preserved mantle and crustal sections, whereas only the mantle and a dissected part of the oceanic crust are exposed in the Lac-Brompton ophiolite. U/Pb zircon dating from felsic rocks of the Thetford-Mines and the Asbestos ophiolites yielded ages of 479 ± 3 Ma and 478-480 +3/-2 Ma, respectively (Dunning et al., 1986; Whitehead et al., 2000). These three ophiolitic massifs are dominated by magmatic rocks with boninitic affinities (and subordinate tholeiites), a feature which has been attributed to their genesis either in a forearc environment (Laurent & Hébert, 1989; Hébert & Bédard, 2000; de Souza et al., 2008), and/or in a backarc setting (Oshin & Crocket, 1986; Olive et al., 1997). In contrast, only the crustal section is present in the Mont-Orford ophiolite, which contains a greater diversity of magma types, interpreted in terms of arc-backarc (Harnois & Morency, 1989; Laurent & Hébert, 1989; Hébert & Laurent, 1989) or arc-forearc to backarc environments (Huot et al., 2002). The Mont-Orford ophiolite has a maximum age of 504 +/- 3 Ma (David & Marquis, 1994).

Amphibolites from the dynamothermal sole of the Thetford-Mines ophiolite and adjacent continental micaschists yielded $^{40}Ar/^{39}Ar$ ages of 477±5 Ma (Whitehead et al., 1995) and 471-461 Ma (Figure 4; Castonguay et al., 2001; Tremblay et al., 2011), respectively, suggesting that intra-oceanic detachment of the ophiolite (ca. 475-470 Ma) occurred immediately after oceanic crust formation (ca. 480 Ma); with emplacement against continental margin rocks and associated metamorphism occurring afterwards (ca. 470-455 Ma; Tremblay et al., 2011).

Saint-Daniel Mélange. The Saint-Daniel mélange (Figure 2) is a Middle Ordovician (Darriwilian) lithostratigraphic unit that represents the lowermost series of the western (present coordinates) part of a forearc basin that lies on a partly-eroded ophiolite basement and which is mainly represented by the Magog Group (Schroetter et al., 2006). The lower contact of the mélange represents an erosional unconformity marking the base of the forearc basin. The processes that formed the chaotic and breccia units of the mélange were the successive uplift, erosion, and burial by heterogeneous and localized debris flows of different parts of the ophiolite and of the underlying metamorphic rocks during the emplacement of the ophiolite. $^{40}Ar/^{39}Ar$ muscovite ages between 467 and 460 Ma were yielded by metamorphic fragments of basal debris flows of the Saint-Daniel mélange (Schroetter et al., 2006; Tremblay et al., 2011). This is within the age range of regional metamorphism in rock units structurally below the ophiolites and implies that the exhumation of these metamorphic rocks occurred during or shortly after the emplacement of the ophiolite onto the continental Laurentian margin.

Magog Group. The Magog Group (Figure 2; Cousineau & St-Julien, 1994) unconformably overlies both the Saint-Daniel Mélange and the Ascot Complex. It is made up of four units: (i) lithic sandstones and black shales of the Frontière Formation; overlain by (ii) purple-to-red shales, green siliceous siltstones and fine-grained volcaniclastic rocks of the Etchemin Formation; overlain by (iii) pyritous black shales and volcaniclastic rocks of the Beauceville Formation; overlain by (iv) sandstones, siltstones and shales with occurrences of tuff and

conglomerate constituting the Saint-Victor Formation, which makes up over 70% of the thickness of the Magog Group. Graptolites, *Nemagraptus gracilis*, found in the Beauceville and Saint-Victor formations are Late Llandeilian to Early Caradocian (Middle Ordovician). However, the age of the Saint-Victor Formation has been recently put into question by detrital U-Pb zircon ages of 435 to 420 Ma measured in its medial and uppermost strata (de Souza et al., 2014; Perrot et al., 2015; Perrot, in progress).

Ascot Complex. The Ascot Complex (Figure 2) is interpreted as the remnant of a 460 $\pm$ 3 Ma volcanic arc sequence (Tremblay et al., 1989a; Tremblay et al., 2000). It is made up of various metavolcanic rock series, in inferred fault contact with laminated and pebbly phyllites that have been correlated with the Saint-Daniel Mélange (Tremblay & St-Julien, 1990). The Ascot Complex is the sole occurrence of Ordovician peri-Laurentian volcanic arc sequences in the Quebec Appalachians. Correlative volcanic rocks are lacking in Temiscouata and Gaspé Peninsula, either because the inferred arc massif(s) did not developed there or has been buried beneath the Silurian–Devonian cover rocks of the Gaspé belt. Roy (1989) suggested that Middle Ordovician volcanic rocks of the Winterville-Munsungun formations of northeastern Maine correlate with the Ascot Complex but van Staal and Barr (2012) argued that the they rather belong to the Gander margin, a peri-Gondwanan terrane of the Northern Appalachians..

Structure and metamorphism. In the southern Québec Dunnage Zone, regional deformation and metamorphism are related to the Middle Devonian Acadian orogeny (Tremblay 1992a; Cousineau & Tremblay, 1993). Peak metamorphism varies from greenschist grade in the south (i.e., in the vicinity of the Québec-Vermont border), to prehnite-pumpellyite grade in the Chaudière river area (Figure 2). $^{40}Ar/^{39}Ar$ dating of greenschist-grade metamorphic rocks of the Ascot Complex yielded 380-375 Ma (Figure 3; Tremblay et al., 2000). The Magog Group is characterized by tight regional folds, generally overturned to the NW. Folds plunge gently or moderately to the SW or the NE. Evidence for intense Ordovician (Taconian) metamorphism and deformation is absent.

TECTONIC EVOLUTION

In the Northern Appalachians, the Taconian orogeny was historically interpreted as the result of a collision between Laurentia and an island arc terrane that was formed over an east-facing subduction zone (Osberg, 1978; Stanley & Ratcliffe 1985). The Acadian orogeny is viewed as the consequence of the accretion of terrane(s) from the east by either a renewed tectonic convergence (Osberg et al., 1989) or by polarity flip of the Taconian subduction zone (van Staal et al. 1998).

On the basis of age data for arc volcanism and ophiolite genesis in southern Québec, as well as the similar lithological and structural setting of ophiolites of southern Québec and western Maine, Pinet and Tremblay (1995) proposed an alternative hypothesis for the Taconian orogeny. In their model, the Taconian deformation and metamorphism of the Laurentian margin is attributed to the obduction of a large-scale ophiolitic nappe that predates any collisional interaction with the volcanic arc.

The structural evolution of the Laurentian continental margin and adjacent Dunnage Zone of southern Québec has been summarized by Tremblay & Castonguay (2002). The Taconian stage (ca. 480 to 445 Ma) involved the stacking of northwest-directed thrust nappes (Figure 4). That deformation, known as D_{1-2} (Tremblay & Pinet, 1994), progressed from east to west, from

ophiolite emplacement and related metamorphism in the underlying margin in the early stages of crustal thickening, to the piggyback translation of accreted material toward the front (west side) of the accretionary wedge. Obducted oceanic crust remained relatively undeformed except for minor tectonic slicing. Underplating of the overridden margin and the foreland (westward) translation of metamorphic rocks due to frontal

accretion have led to progressive exhumation of deeper crustal levels of the orogeny (Figure 5a), hence preserving Ordovician isotopic ages, parts of which are now preserved below the ophiolite in the downthrown side of the St-Joseph-BBL fault system.

D_3 deformation began in latest Early Silurian time (ca. 430 Ma), and lasted until the Early Devonian (ca. 410 Ma; Figure 4). $^{40}Ar/^{39}Ar$ age data suggest that D_3 first consisted of ductile shear zones defining a major upper plate-lower plate (UP-LP) boundary, i.e. the Bennett-Brome fault, and culminated with normal faulting along the St-Joseph fault and the Baie Verte-Brompton line (Figure 4). The upper plate is made up of a folded stack of D_{1-2} nappes of deformed and metamorphosed rocks of the Taconian accretionary wedge and includes metamorphic rocks that retain Ordovician ages. Low- and high-angle normal faulting was probably activated in Late Silurian-Early Devonian time (Figure 4) and crosscut the UP-LP boundary, which led to the juxtaposition of metamorphic rocks from different crustal levels on both sides of the St-Joseph-BBL fault system. East of the St-Joseph-BBL fault system, the D3 event thus accounts for the presence of external-zone rocks, their juxtaposition with ophiolites or underlying metasedimentary rocks, and the presence of SE-verging recumbent folds (originally interpreted as gravity nappes by St-Julien & Hubert, 1975).

Acadian compression resulted in the folding of D_{1-2} and D_3 structures and in the passive rotation and steepening of high-angle normal faults (Figure 4), which conducted to the current geometry of the belt (Figure 5b). Tectonic inversion of normal faults has probably occurred.

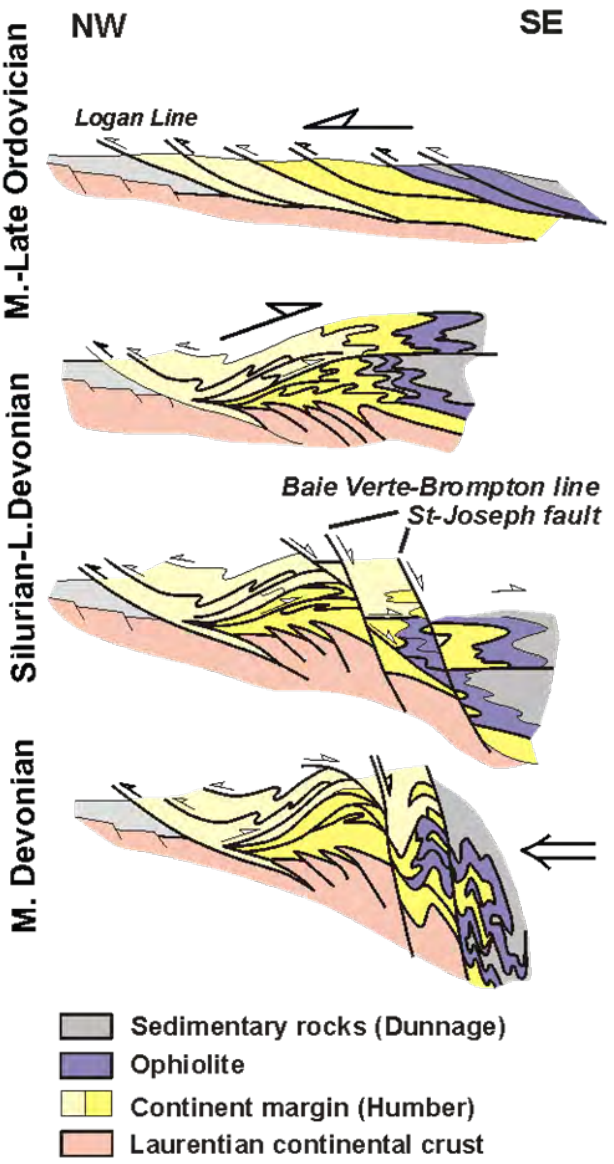

Figure 4. Schematic model for structural evolution of Laurentian margin in southern Quebec. 1- Grenvillian rocks, 2- St. Lawrence Lowlands platform, 3- External Humber Zone, 4- Internal Humber Zone, 5-6- ophiolites and sedimentary rocks of Dunnage Zone, respectively.

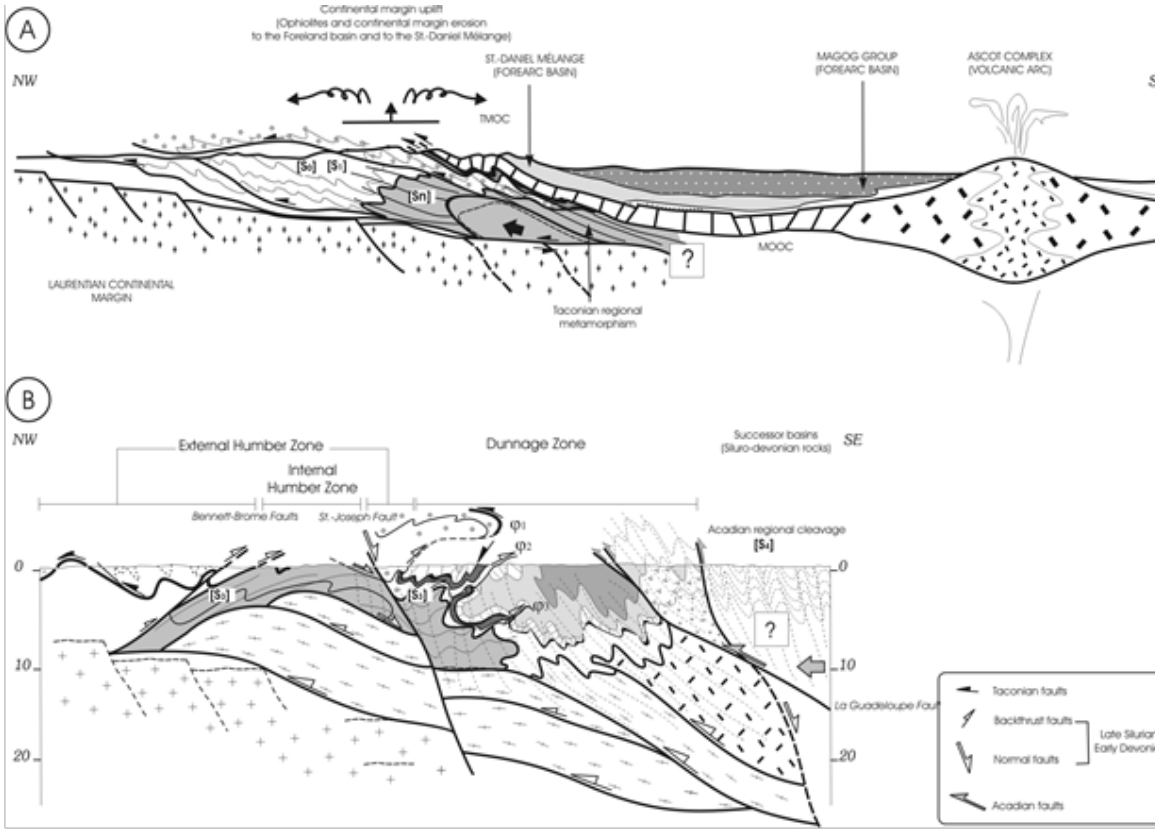

Figure 5. A) Inferred regional tectonic setting of the Southern Québec Appalachians during the Taconian orogeny, and schematic sedimentary and tectonic evolution of the Saint-Daniel Mélange and the Magog Group. B) Schematic composite structural profile across the Laurentian margin and the adjacent oceanic domain. From Schroetter et al. (2005).

GEOLOGY OF THE SHERBROOKE AREA

The Sherbrooke area (Figure 6) exposes three major units of the southern Québec Appalachians, from base to top, the Ascot Complex, the Magog Group and the St. Francis Group, which are briefly described below. During this field trip, we will visit representative outcrops of each unit with, however, a particular emphasis on the Ordovician rocks series.

The Ascot Complex has been divided into three lithotectonic domains separated by mélange-type phyllites, the Sherbrooke, Eustis, and Stoke domains (Tremblay, 1992b; Figure 6). The Sherbrooke domain consists of felsic and mafic volcanic rocks. Felsic rocks are pyroclastic breccias, crystal and aphanitic tuffs, and foliated equivalents. U-Pb zircon dating of a rhyolite from the Sherbrooke domain yielded 441 +7/-12 Ma (David and Marquis, 1994). Mafic rocks are vesicular to amygdaloidal, massive and pillowed basalts, chlorite schists, and a lesser amount of mafic tuffs. The Eustis domain is mainly characterized by quartz-plagioclase-sericite-chlorite schists originating from coarse-grained to conglomeratic volcaniclastic rocks. In the Stoke domain, felsic rocks predominate over mafic volcanic rocks. Felsic rocks are homogeneous, porphyritic to fine-grained pyroclastic rocks of rhyolitic composition. Mafic volcanics are pillowed basalts and chlorite schists. The volcanic rocks are intruded by a granitic massif, the Ascot Complex pluton, interpreted as an equivalent of the extrusive sequence (Tremblay et al.,

1994). The Ascot Complex pluton lacks isotopic dating but $^{40}Ar/^{39}Ar$ high-temperature muscovite ages of 462 Ma has been measured (Tremblay et al., 2000). This is consistent with U/Pb dating of a rhyolite of the Stoke domain, at 460 ± 3 Ma, with a significant proportion (~25%) of inherited zircons of Precambrian and Archean ages (David and Marquis, 1994). The phyllites of the Ascot Complex are laminated argillite and graphitic pebbly mudstone, the latter containing clasts of shale, dolomitic siltstone, and black sandstone. Tectonic slivers of serpentinite occur near major faults such as the La Guadeloupe fault (Tremblay et al., 1989b) and the Massawippi Lake fault zone (Tremblay and Malo, 1991).

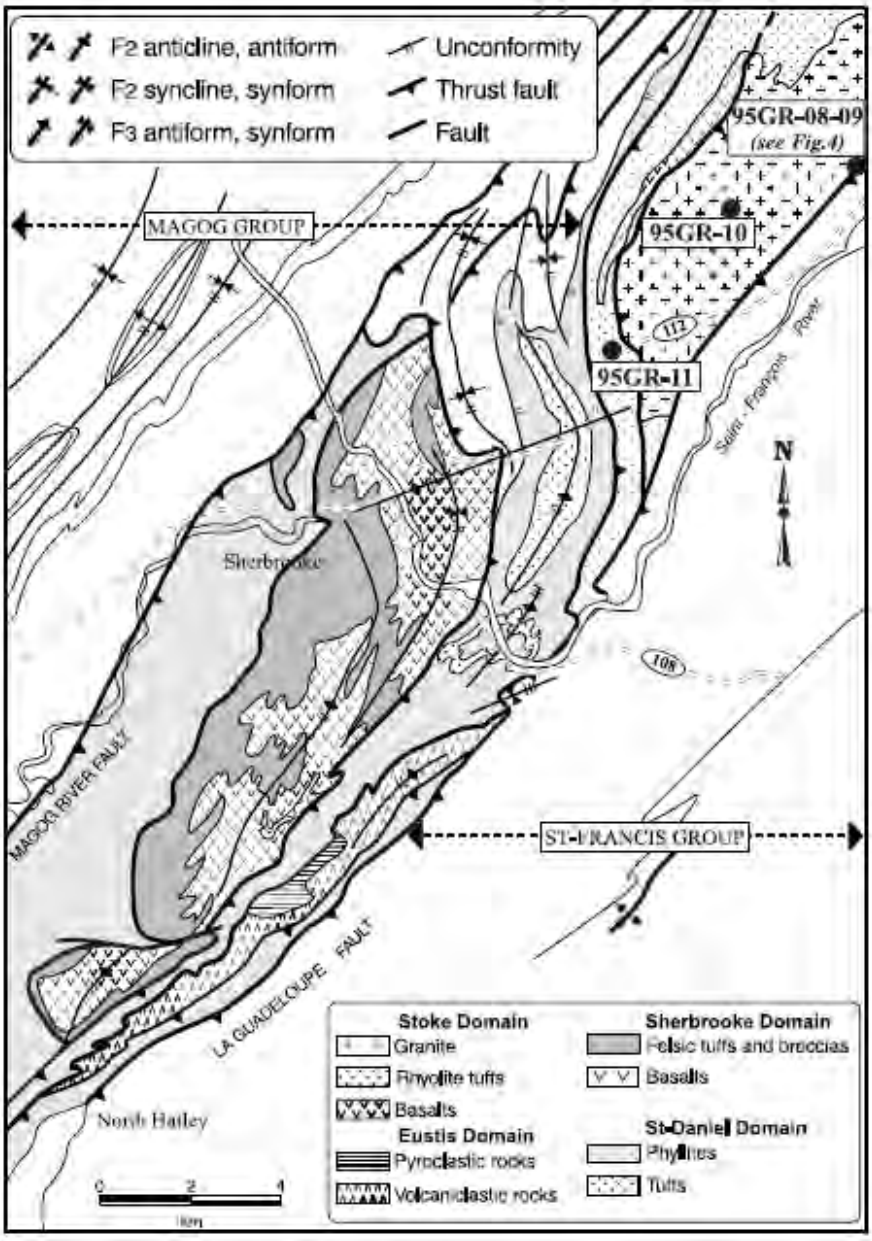

Figure 6. Geology of the Sherbrooke area. From Tremblay et al. (2000).

The Magog Group occupies the core of the St-Victor synclinorium (Figures 2 and 6), which consists of northeast- and southwest-plunging, open to tight folds, commonly overturned to the northwest. In the Sherbrooke area, Tremblay (1992b) subdivided the Magog Group into two units; (i) a lower unit of volcanic conglomerate and feldpathic sandstone with interlayered rusty slates attributed to the Beauceville Formation, and (ii) an upper unit of conglomerate, turbiditic sandstone-shale assemblage and black slates forming the St-Victor Formation. In the Stoke Mountains area, north of Sherbrooke, the lower unit of the Magog Group unconformably overlies the Ascot Complex (Mercier, 2013). U-Pb detrital zircon dating in rocks of this lower unit yielded lower Silurian ages (ca. 435 Ma; Perrot et al., 2015; in progress), which is incompatible with the age of the Beauceville Formation (see above), and suggests that both the lower and upper units belong to the St-Victor Formation. The upper unit is a typical flysch-dominated series, which consists of a lower sandstone-rich and an upper slate-rich turbidite sequences that are separated by a regional stratigraphic marker horizon of channel-facies arkosic sandstone and conglomerate.

The Silurian and Devonian rocks of St. Francis Group crop out east of the Ascot Complex, in the hanging wall of the La Guadeloupe fault (Figure 6), where they occupy the core of the Gaspé-Connecticut Valley trough, a major sedimentary basin that extends from New England to Gaspé Peninsula (Bourque et al., 2000; Tremblay and Pinet, 2005). In the Sherbrooke area, it consists of the Ayer's Cliff and Compton formations. The Ayer's Cliff Formation is a homogeneous sequence of impure limestone and calcareous shale characterized by abundant syn-sedimentary deformation. The contact with the overlying Compton Formation is gradual over several tens of metres. The Compton Formation is a thick sedimentary sequence that has been subdivided into three members (Lebel and Tremblay, 1993), the Milan, Lac-Drolet, and Saint-Ludger members. The Milan member forms a typical turbidite sequence characterized by abundant sedimentary structures. It contains *Chitinozoan* microfauna (van Grootel et al., 1995) and fossil plants (Hueber et al., 1990) suggesting Upper Silurian-Lower Devonian and Lower Devonian ages, respectively, which is consistent with a U-Pb zircon age of 396 ± 5 Ma recently measured in the upper part of the Milan member (de Souza et al., 2014). The Lac-Drolet and Saint-Ludger members are dominated by typical feldspathic wackes and black mudstone, respectively, recording a progressive deepening of the sedimentary basin due to the west-directed progression of the Acadian orogenic front (Bradley et al., 2000).

Structural relationships between Ordovician and post-Ordovician rocks of southern Québec indicate that regional deformation is related to the Acadian orogeny (Cousineau and Tremblay, 1993). From the Québec-Vermont border to east of Québec city (Figure 2), the La Guadeloupe fault has been recognized as a northwest-directed, high-angle reverse fault (Tremblay et al., 1989b; Labbé and St-Julien, 1989; Cousineau and Tremblay, 1993), and is associated with greenschist-grade, quartzofeldspathic and calc-silicates mylonites observed in adjacent units from both sides (Tremblay et al., 1989b; Labbé and St-Julien, 1989; Tremblay et al., 2000). In the Sherbrooke area, regional folds are F_2 folds that trend parallel to down-dip stretching lineations along the La Guadeloupe fault. D_2 folds are locally affected by southeast-verging, F_3 open folds with an axial-planar, northwest-dipping crenulation cleavage (Tremblay and St-Julien, 1990), which clearly postdate the La Guadeloupe fault and associated F_2 folds. These F_3 folds correlate with the «easterly features» of Osberg et al. (1989) in New England, which are refolded by late north-trending folds (Hatch and Stanley, 1988) corresponding to the dome-stage deformation of Armstrong et al. (1992).

FIELD TRIP ROAD LOG

THE MAGOG GROUP AND THE ASCOT COMPLEX

The meeting point for departure is the parking lot of the *Bureau en Gros* store, at the intersection between Jean-Paul-Perrault Street and Portland Blvd (in front of the Portland Mall).

STOP 1.1: The uppermost fine-grained sequence of the Magog Group.

Location: Take Jean-Paul-Perrault Street, and drive to HGW 410N. Follow HGW 410N for approximately 1 km and take the exit to HGW 10W (toward Montreal). Drive for ca. 7 km and take Exit 133 to St-Rock Road. Turn left on St-Rock Road, and then right on the exit back to HGW 10E. Park along the access ramp, the outcrop is the roadcut along both sides of the ramp.

Field description: This outcrop exposes a well-bedded sequence of siltstone and black slate that are typical of the uppermost stata of the St-Victor Formation in southern Québec. Relationships between the bedding and the regional schistosity indicate that this exposure is located along the hinge of a major regional fold that is the St-Victor synclinorium.

The source of the St-Victor Formation is believed to be siliciclastic and fine-grained felsic volcanic rocks (Cousineau, 1990). Detrital chromite and serpentinite indicate an ultramafic component in the source area (St-Julien, 1987). Cousineau (1990) concluded that this deposit originated from two sources: an uplifted accretionary prism (the St-Daniel mélange) to the West, and a volcanic arc (the Ascot Complex) to the East.

Figure 7. Field example of the Magog Group conglomerate showing a boulder-size granitic block.

STOP 1.2: The conglomeratic marker horizon.

Location: Drive back to HGW 10E toward Sherbrooke. Follow the highway for ca. 8 km and take Exit 141 for Monseigneur-Fortier Blvd (next exit after HGW 410S). Turn left on Monseigneur-Fortier Blvd, right on Lionel-Groulx Blvd and then right again on Arnold-Pryce Road. Drive approximately 100 metres and park (there is a private road to the right). The outcrop is a roadcut on your right along the bike path.

Field description: This outcrop is a typical exposure of conglomerate and arkosic sandstone that make a stratigraphic marker horizon in the Sherbrooke area (Figure 6). The conglomeratic facies constitutes ca. 50% of this unit. It contains cm- to dc-sized, subangular to well-rounded clasts and blocks of volcanic, granitic and sedimentary rocks. Some granitic blocs can be up to 1 metre in diameter (Figure 7). Volcanic rocks fragments are predominant. This conglomerate forms a metres-thick lenticular horizon within feldspathic sandstones. The conglomerate and sandstone belong to the former lower Silurian (?)

Sherbrooke Formation which was interpreted as a basal unconformity by St-Julien (1963), but has been since re-interpreted and included into the Magog Group by St-Julien et al. (1972) and St-Julien and Hubert (1975). Preliminary results of a regional U-Pb detrital zircon dating study suggest, however, that it effectively belongs to the Silurian (Perrot et al., 2015; Perrot, in progress).

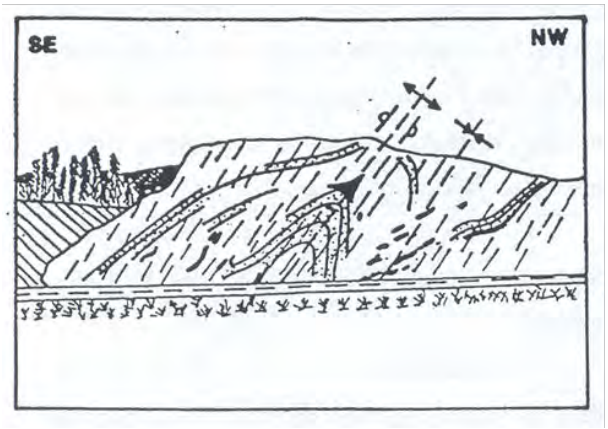

Figure 8. Field sketch of the antiformal structure exposed at Stop 1.3.

STOP 1.3: Typical sandstone-rich turbidites of the Magog Group.

Location: Drive back to HGW 10E (55N) and follow the exit for HGW 610E. Drive ~ 2 km and take Exit 3, right after crossing the river, to St-François Street. Turn left. There is a parking lot at ca. 100 metres, park there. The outcrop is a huge roadcut along the access ramp to HGW 610E.

Field description: This is an exposure of the typical sandstone-rich turbidites of the Magog Group. It comprises interbedded quartzo-feldpathic sandstone, siltstone and mudslate. Sandstone beds are characterized by various primary structures such as graded-bedding, cross-laminations and ripples. Intraformational breccias are locally visible. The outcrop corresponds to the hingeof an overturned anticline (Figure 8). Fold-related faults are found and the presence of bedding-parallel shear zones indicates that flexural-slip folding was dominant.

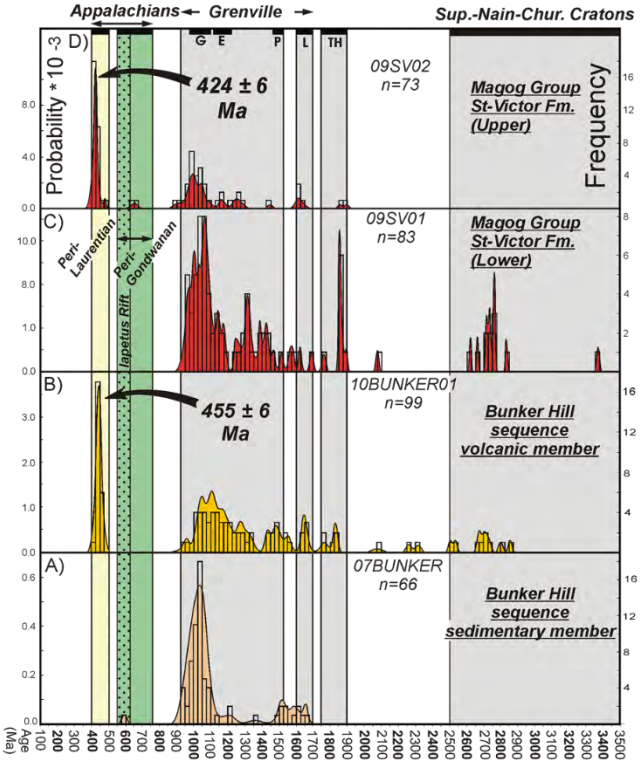

Figure 9. Probability density distribution–frequency diagrams of detrital zircon ages for samples of (A) the Bunker Hill sequence sedimentary member—07BUNKER; (B) volcanic member —10BUNKER01; and Magog Group (C) 09SV01, (D) 09SV02. The age–probability density distribution plots shown in the insets of (B) and (D) are for the youngest age clusters from which were calculated weighted mean ages.

This outcrop is at the same stratigraphic level than the 09SV02 sample of de Souza et al. (2014), which yielded the following age results by U-Pb zircon dating: 41% of the zircons yielded two Ordovician ages (480 ± 12 Ma; 459 ± 23 Ma) and 31% yielded Silurian to Early Devonian ages (Figure 9D). Nine of these analyses yielded Silurian-Early

Devonian concordant ages ca. 90 percent to 105 percent, determining an age cluster from which was calculated a weighted mean $^{238}U/^{206}Pb$ age of 424 $\pm$ 6 Ma (Figure 9D).

STOP 1.4: The lowermost sequence of the Magog Group and the contact with the Ascot Complex phyllites.

Location: Drive back to HGW 610E and follow it until the intersection with Road 112 (approximately 7 km). At the intersection with Road 112, turn around the traffic circle and drive back HGW 610 toward the West. Drive approximately 800 metres and park (there is a service road on your right). The outcrop consists in a series of roadcuts along the highway.

Field description: In the Sherbrooke area, the lower most stratigraphic unit of the Magog Group is made up of volcanic conglomerate and sandstone. On the basis of regional mapping, it was interpreted as unconformably overlying the sedimentary rocks of the Ascot Complex (Tremblay, 1992b). This outcrop is a new roadcut that exposes this contact. We will walk the section from East to West (from the Ascot Complex phyllites toward the contact with the Magog Group).

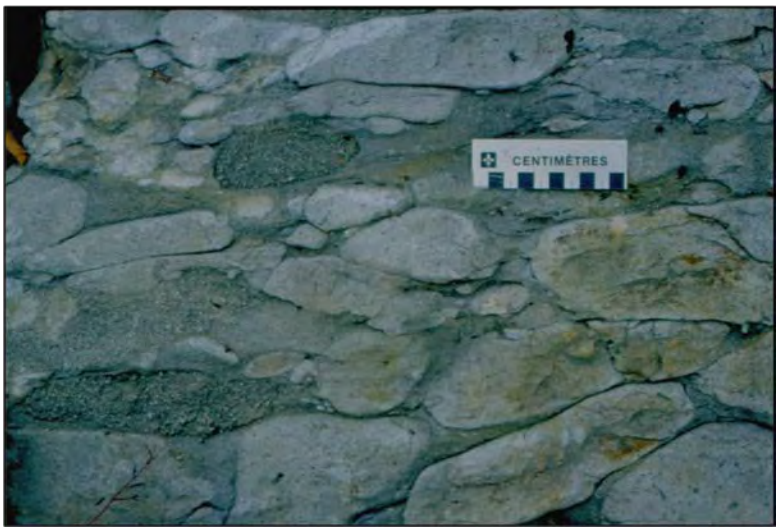

Figure 10. Volcanic conglomerate of the lowermost stratigraphic unit of the Magog Group in the Sherbrooke area.

The phyllites of the Ascot Complex consist here of black and rusty argillite with occasional but typical, cm-sized nodules of pyrite. The deformation of these rocks is complex; three generations of folds and fabrics can be seen. The contact with the Magog Group corresponds to a diffuse zone, approximately 1 metre-wide, in which well-bedded sandstone strata (typical of the Magog Group) progressively appear. The main point to examine here is the deformational contrast between the Ascot phyllites and the Magog Group strata: is there a missing structural fabric in the latter?

Stratigraphically higher (westward) along the section, the outcrop exposes a volcanic, polygenic conglomerate (Figure 10) which constitutes more than 50% of the basal unit of the Magog Group in the Sherbrooke area (Tremblay, 1992b). Cm-scale clasts consist of felsic volcanic and pyroclastic rocks, less commonly of pelite, granite and siltstone. Regionally, this sequence is interlayered with quartz-feldspar sandstone and lithic tuff. In the Stoke Mountains area (approximately 10 km to the northeast), this same sequence unconformably overlies the felsic volcanic rocks of the Stoke domain (Mercier, 2013), and yielded preliminary U-Pb detrital zircon ages of ca. 435 Ma (Perrot, in progress).

STOP 1.5: The Ascot Complex – interlayered felsic and mafic lavas of the Stoke domain.

Location: Continue on HGW 610W and take Exit 7 to 12e Avenue. Turn left onto 12e Avenue and then back onto HGW 610E. Drive the highway until Road 112. Turn right on Road 112, and then left on Gastin Street after 150-200 metres. Turn left on Bibeau Road until the end (ca. 300 metres) and park. The outcrop is an abandoned access ramp, ca. 100 metres to the east of the parking lot.

Field description: This outcrop nicely exposes a series of felsic and mafic volcanic rocks and schists of the Stoke domain (Figure 6). In terms of REE profiles (Figure 11), the felsic volcanics are very homogeneous. They are LREE-enriched and show a typical negative Eu anomaly that is attributed to the fractionation of plagioclase (Tremblay et al., 1989a). The mafic rocks are tholeiitic basalts with a typical MORB-type REE composition (Figure 11).

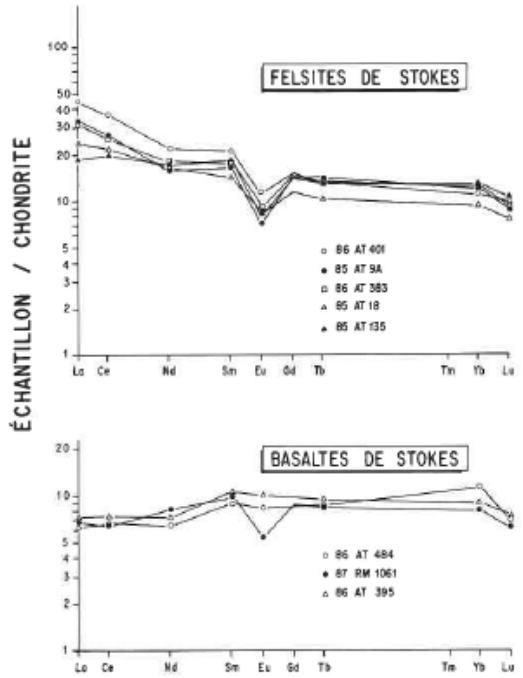

Figure 11. REE patterns for rhyolitic and basaltic lavas of the Stoke domain. From Tremblay et al. (1989a).

On the outcrop, the volcanic rocks are strongly sheared and hydrothermalized. The northern wall of the ramp exposes a ca. 5-10 metres-wide ductile shear zone marked by sericite-rich «paper» schist on the hanging wall, and chlorite-carbonate laminated schist on the footwall. $^{40}Ar/^{39}Ar$ muscovite dating of a felsic schist in the vicinity of this outcrop (along road 122) yielded plateau ages of ca. 379 Ma (Figure 12), which corresponds to the age of regional metamorphism (Tremblay et al., 2000).

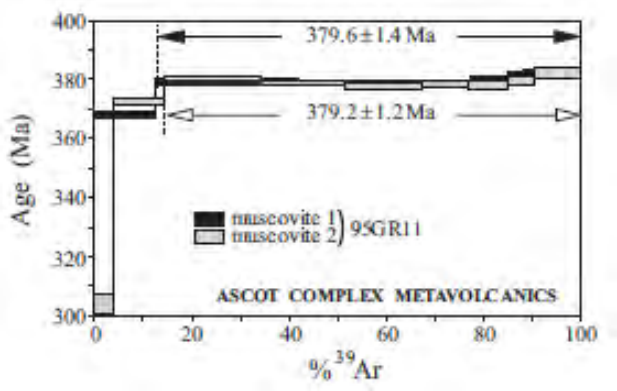

Figure 12. $^{40}Ar/^{39}Ar$ spectra of muscovites from felsic metavolcanic rocks of the Stoke domain; sample 95GR-11. Modified from Tremblay et al. (2000).

STOP 1.6: The Ascot Complex – the granitic synvolcanic intrusion.

Location: Drive back to Road 112 and turn right. Drive for 1.2 km and park on your right.

Field description: The volcanic rocks of the Stoke domain are intruded by a granitic massif, the Ascot Complex pluton, interpreted as a plutonic equivalent of the extrusive sequence (Tremblay et al., 1994). The Ascot Complex pluton is a well-foliated granitic rock showing the same deformational style and fabrics as the adjacent volcanic rocks. It is a coarse-grained rock (4-7 mm in diameter) of deformed crystals of quartz, plagioclase, K-feldspar, chlorite, muscovite and epidote with minor amounts of biotite, sphene, zircon, calcite and pyrite. K-feldspar is only

locally visible. Granophyric texture is common. Chlorite/muscovite ratios are variable and are mostly the product of metamorphic recrystallization and alteration of primary minerals.

In a comparative geochemical study between granitic boulders found in conglomerates (Stop 1.2) of the Magog Group and the Ascot Complex intrusive rocks, Tremblay et al. (1994) have shown that both are quite similar (Figure 13), and that their petrographical and geochemical characteristics suggest that both types of granitoids are peraluminous, anatectic granitic magmatic pulses originating from destructive plate magmatism.

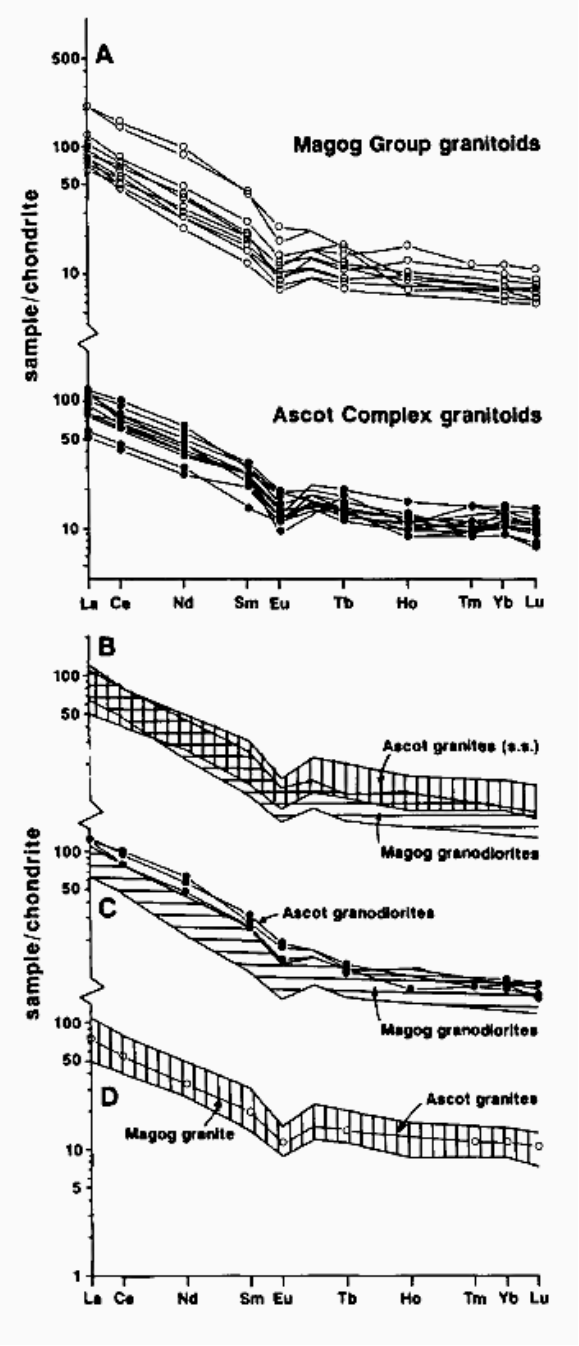

Figure 13. Chondrite-normalized REE data for the Magog Group and Ascot Complex granitoids. From Tremblay et al. (1994).

STOPS 1.7 and 1.8: Hanging wall and footwall of the La Guadeloupe fault–sheared metasedimentary and granitic rocks.

Location: Continue on Road 112 for approximately 2.5 km and turn right on Biron Road. Drive it for 2.5 km and park at the intersection with Provost Street; stop 1.7 is a roadcut at that intersection. For stop 1.8, drive another 800-900 metres along Biron Road and turn right onto Mont-Blanc Street. The outcrop is on your right approximately 100 metres from the intersection with Biron Road.

Field relations: In the Stoke Mountains area, the progressive development of granitic mylonites related to the La Guadeloupe fault is nicely exposed in the Big Hollow brook section (Figure 14; Tremblay et al., 2000), which has been used as a type section for the $^{40}Ar/^{39}Ar$ dating of the regional Acadian metamorphism. Isotopic analyses of sheared rocks of the Big Hollow section clearly demonstrated that Acadian peak metamorphism in the southern Québec Appalachians can be tightly constrained in the 380-375 Ma time range (Figure 15).

These two stops illustrate the intensity of shear deformation that can be observed in metasedimentary (Stop 1.7) and granitic rocks (Stop 1.8) in the hanging wall and footwall, respectively, of the La Guadeloupe fault.

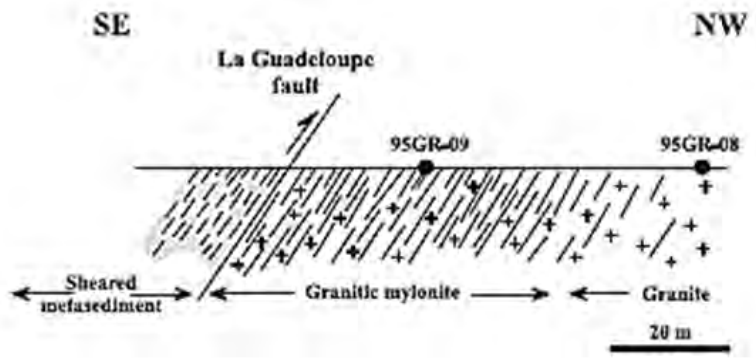

Figure 14. Schematic profile of the La Guadeloupe fault at Big Hollow Brook. From Tremblay et al. (2000).

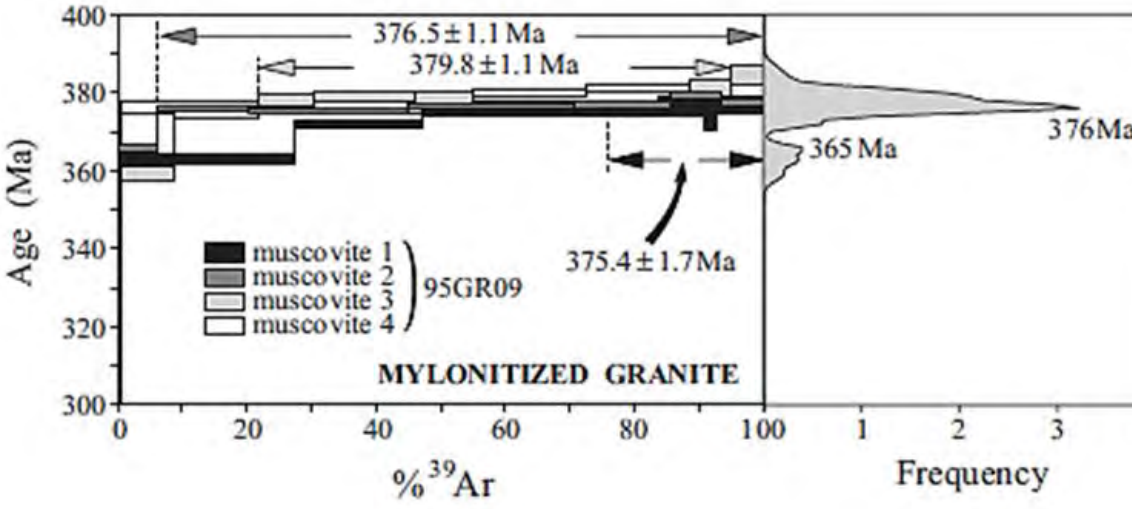

Figure 15. $^{40}Ar/^{39}Ar$ spectra of muscovites from a mylonitized granite of the Big Hollow Brook section (see Figure 14). The apparent age frequency diagram is also shown. From Tremblay et al. (2000).

STOP 1.9: Contact between felsic volcanic rocks of the Eustis domain and black phyllites.

Location: Follow Moulton Hill road until the intersection with College Street (Road 108), just after another bridge over St-François River. Turn right onto College Street and then (downtown) left on Road 143. Drive for approximately 1.5 km and park (there is a small dirt road right after the second traffic circle for safe parking). Walk back to the traffic circle, the outcrop is a huge roadcut on the left.

Field description: This is a new outcrop that exposes the northwestern contact between the volcanic rocks of the Eustis domain and the laminated phyllites of the Ascot Complex. Based on constrasting lithological facies and on geochemical characteristics of the volcanic rocks, the contact between the different domains of the Ascot Complex and the surrounding sedimentary rocks has been originally interpreted as faults (Tremblay, 1992b). However, such a contact is superbly exposed on this outcrop (Figure 16) and, obviously, it does not correspond to a tectonic contact but is rather depositional, and probably represents a disconformity between a «basement» made up of an heterogeneous series of volcanic rocks (i.e. the domains of the Ascot

Complex) and a sequence of manganiferous, fine-grained siltstone grading up into deep-marine mudstone representing an *in situ* seafloor sedimentation. If correct, such an interpretation raises important questions regarding the origin and the accretionary history of the Ascot Complex.

On this outcrop, cm-thick layers of brown-colored siltstone and sandstone, and more rarely, limestone are visible in the phyllites. Locally preserved cross-laminations and gradded-bedding structures indicate that stratigraphy is overturned, and that the phyllites overly the volcanic rocks. Fabrics and structures visible in the phyllites are quite complex and three generations of folding are visible (Figure 17). This structural complexity has been attributed to the proximity of the La Guadeloupe fault (Tremblay and St-Julien, 1990; see next Stop) which is located less than a hundred metres to the SE.

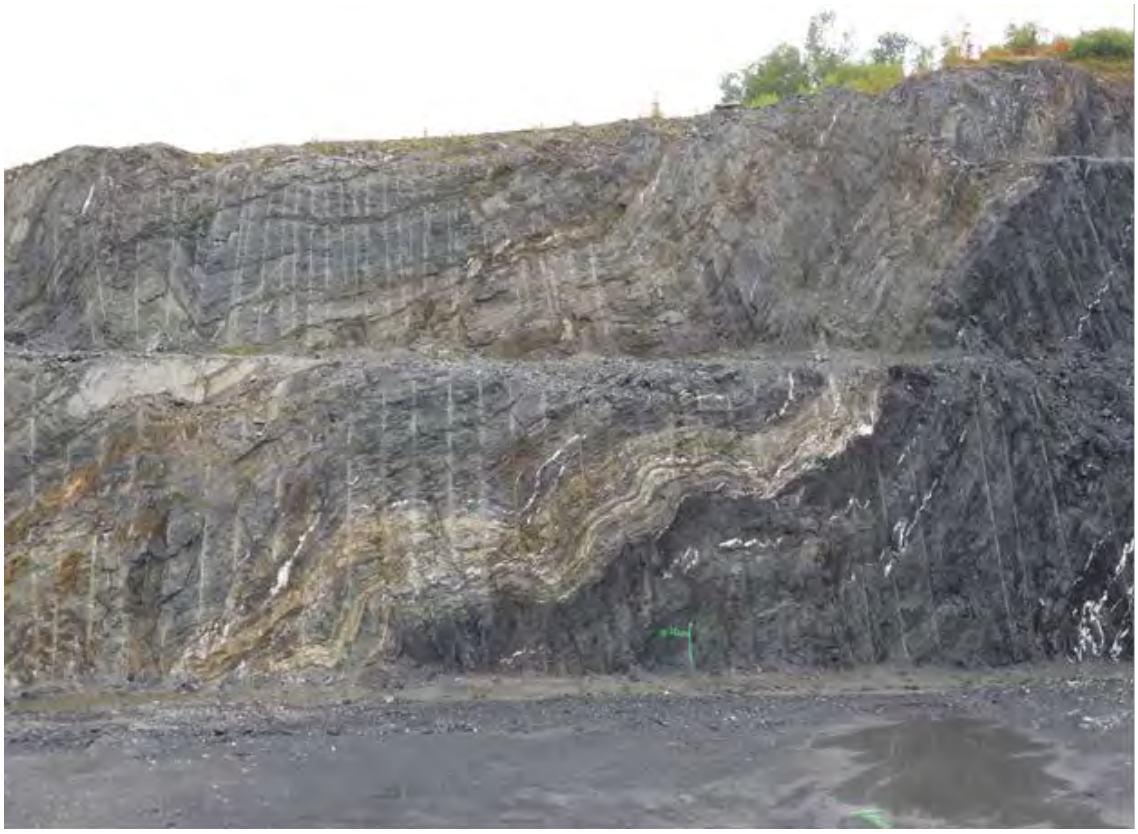

Figure 16. Field photograph of the contact between the felsic rocks of the Eustis domain (pale-colored rocks on the left side) and the black phyllites of the Ascot Complex. Looking south.

Figure 17. Field photograph of the phyllites, showing S_1 (parallel to bedding), S_2 and S_3.

STOP 1.10: Quartz-sericite schist of the Eustis domain.

Location: Continue on Road 143 for approximately 5 km and turn right onto Road 108 (Capelton Road). After ca. 1.5 km, turn right on Du Boisé Street. Drive ca. 100 metres and park.

Field description: The felsic pyroclastic rocks of the Eustis domain are lithologically and chemically similar to those of the Sherbrooke domain, suggesting that both domains are possible lateral equivalents. D_2 deformation is however stronger in the Eustis domain than elsewhere. S_2 is there a mylonitic foliation, axial-planar to F_2 folds which are crosscut by anastamosing ductile genetically related to the La Guadeloupe fault (Tremblay and St-Julien, 1990). This outcrops is structurally located a few tens of metres in the footwall of the La Guadeloupe fault and exposes a typical example of quartz-sericite schist of the Eustis domain. Note the intensity of structural fabric development and the down-dip plunges of the mineral lineation.

End of field trip.

REFERENCES CITED

Armstrong, T. R., Tracy, R. J., and Hames, W. E., 1992. Contrasting styles of Taconian, Eastern Acadian and Western Acadian metamorphism, central and western New England: Journal of Metamorphic Geology, 10: 415–426.

Bourque, P.-A., Malo, M. and Kirkwood, D. 2000. *Paleogeography and tectono-sedimentary history at the margin of Laurentia during Silurian–earliest Devonian time: the Gaspé Belt, Québec*. Geological Society of America Bulletin 112: 4–20.

Bradley, D.C., R.D. Tucker, D. R. Lux, A.G. Harris, and D.C. Mc Gregor. 2000. *Migration of the Acadian orogen and foreland basin across the Northern Appalachians of Maine and Adjacent areas.* United States Geological Survey, Professional Paper 1624, 49 pages.

Castonguay, S., Ruffet, G. and Tremblay, A. 2007. *Dating polyphase deformation across low-grade metamorphic belts: An example based on $^{40}Ar/^{39}Ar$ muscovite age constraints from the southern Québec Appalachians, Canada*. Geological Society of America Bulletin, 119: 978-992.

Castonguay, S., Ruffet, G., Tremblay, A. and Féraud, G., 2001. *Tectonometamorphic evolution of the southern Quebec Appalachians: 40Ar/39Ar evidence for Ordovician crustal thickening and Silurian exhumation of the internal Humber zone.* Geological Society of America Bulletin, 113: 144-160.

Cousineau, P.A. 1990. *Le Groupe de Caldwell et le domaine océanique entre St-Joseph-de-Beauce et Sainte-Sabine.* Ministère des ressources naturelles du Québec, MM 87-02, 165 pages.

Cousineau, P.A., and St-Julien, P. 1992. *The Saint-Daniel Mélange: Evolution of an accretionary complex in the Dunnage terrane of the Québec Appalachians*. Tectonics, 11: 898-909.

Cousineau, P.A., et St-Julien, P. 1994. *Stratigraphie et paléogéographie d'un bassin d'avant-arc ordovicien, Estrie-Beauce, Appalaches du Québec.* Journal Canadien des Sciences de la Terre, 31: 435-446.

Cousineau, P.A. & Tremblay, A. 1993, Acadian deformation in the southwestern Québec Appalachians. Geological Society of America Special Paper 275, pp. 85-99.

David, J. et Marquis, R. 1994. *Géochronologie U-Pb dans les Appalaches du Québec: application aux roches de la zone de Dunnage.* La Revue géologique du Québec, 1: 10-15.

de Souza, S. and Tremblay, A., 2010. *The Rivière-des-Plante ultramafic Complex, southern Québec: Stratigraphy, structure, and implications for the Chain Lakes massif In* Tollo, R.P., Bartholomew, M.J., Hibbard, J.P., and Karabinos, P.M., eds., From Rodinia to Pangea: The Lithotectonic Record of the Appalachian Region: Geological Society of America Memoir 206, pp. 1–17 (doi: 10.1130/2010.1206(07).

de Souza, S., Tremblay, A. and Ruffet. G. 2014. *Taconian orogenesis, sedimentation and magmatism in the southern Quebec-northern Vermont Appalachians: stratigraphic and detrital mineral record of Iapetan suturing*. American Journal of Science, 314: 1065-1103.

de Souza, S., Tremblay, A., Daoust, C. and Gauthier, M. 2008. *Stratigraphy and geochemistry of the Lac-Brompton ophiolite Complex and evolution of SSZ magmatism in the southern Québec Dunnage Zone,* Canada. Canadian Journal of Earth Sciences, 45: 1-16.

Dunning, G.R., Krogh, T.E., and Pederson, R.B., 1986. *U–Pb zircon ages of Appalachian–Caledonian ophiolites*. Terra Cognita, 6, L51.

Harnois, L. and Morency, M. 1989. *Geochemistry of Mont Orford ophiolite complex, Northern Appalachians*, Canada. Chemical Geology, 77: 133–147 (doi:10.1016/0009-2541(89)90138-1).

Hatch, N. L., and Stanley, R. S., 1988. *Post-Taconian structural geology of the Rowe-Hawley zone and the Connecticut Valley belt west of the Mesozoic basins.* U.S. Geological Survey Professional Paper 1366, pp. C1–C36.

Hébert, R. and Laurent, R. 1989. *Mineral chemistry of ultramafic and mafic plutonic rocks of the Appalachian ophiolites, Québec, Canada*. Chemical Geology, 77: 265–285 (doi:10.1016/0009-2541(89)90078-8).

Hébert, R. et Bédard, J.H., 2000. *Les ophiolites d'avant-arc et leur potentiel minéral: exemple des complexes ophiolitiques du sud du Quebec*. Chroniques de la Recherche Minière, 539: 101–117.

Hueber, F. M., Bothner, W. A., Hatch, Jr., N. L., Finney, S. C., and Aleinikoff, J. N., 1990, *Devonian plants from southern Quebec and northern New Hampshire and the age of the Connecticut Valley trough.* American Journal of Science, v. 290, n. 4, p. 360–395, http://dx.doi.org/10.2475/ajs.290.4.360

Huot, F., Hébert, R., and Turcotte, B., 2002. *A multistage magmatic history for the genesis of the Orford ophiolite (Quebec, Canada): a study of the Mt. Chagnon massif*. Canadian Journal of Earth Sciences, 39: 1201–1217.

Labbé, J.-Y. et St-Julien, P. 1989. *Evidences de failles de chevauchement acadienne dans la région de Weedon, Québec*. Journal Canadien des Sciences de la Terre, 26: 2268-2277.

Laurent, R. and Hébert, R., 1989. *The volcanic and intrusive rocks of the Québec Appalachians ophiolites (Canada) and their island-arc setting.* Chemical Geology, 77: 287–302.

Lebel, D. et Tremblay, A. 1993. *Géologie de la région de Lac-Mégantic (Estrie)*. Ministère de l'Énergie et des Ressources du Québec, DV 93-04 (carte géologique).

Mercier, P.-E. 2013. *Analyse stratigraphique et structurale du Groupe de Magog et de la Ceinture de Gaspé, région des Monts Stoke, Appalaches du Québec*. Mémoire de maîtrise, UQAM.

Olive, V., Hébert, R. and Loubet, M., 1997. *Isotopic and trace element constraints on the genesis of a boninitic sequence in the Thetford Mines ophiolitic complex, Québec*, Canada. Canadian Journal of Earth Sciences, 34: 1258-1271.

Osberg, P.H. 1978. *Synthesis of the geology of Northeastern Appalachians, U.S.A. In* Tozer, E.T. and Schenk, P.E. eds., Caledonian-Appalachian orogen of the North-Atlantic region. Geological Survey of Canada Paper 78-13, pp. 137-147.

Osberg, P.H., Tull, J.F., Robinson, P., Hon, R., and Butler, J.R., 1989, *The Acadian orogen In* The Appalachian-Ouachita orogen in the United States (eds R.D.Jr. Hatcher, W.A. Thomas, and G.W. Viele), pp. 179-232, Geological Society of America., Geology of North America, v. F-2.

Oshin, O.I. and Crocket, J.H., 1986. *The geochemistry and petrogenesis of ophiolitic rocks from Lac de l'Est, Thetford Mines complex, Québec, Canada*. Canadian Journal of Earth Sciences, 23: 202-213.

Perrot, M., Tremblay, A. and David, J. 2015. *Syn- to post-Taconian basin formation in the Southern Québec Appalachians, Canada: constraints from detrital zircon U-Pb geochronology*. EUG meeting, Vienne.

Pinet, N. and Tremblay, A., 1995. *Tectonic evolution of the Québec-Maine Appalachians: from oceanic spreading to obduction and collision in the Northern Appalachians*. American Journal of Science, 295: 173-200.

Pinet, N., Tremblay, A., and Sosson, M., 1996, *Extension versus shortening models for hinterland-directed motions in the southern Québec Appalachians.* Tectonophysics, 267: 239-256.

Roy, D.C. 1989. *The Depot Mountain Formation: transition from syn- to post-Taconian basin along the Baie Verte-Brompton Line in northwestern Maine*. Maine Geological Survey, Studies in Maine Geology, vol. 2, pp. 85-99.

Sasseville, C., Tremblay, A., Clauer, N. and Liewig, N. 2008. *K-Ar time constraints on the evolution of polydeformed fold-thrust belts: the case of the Northern Appalachians (southern Quebec).* Journal of Geodynamics, 45: 99-119.

Schroetter, J.-M., Tremblay, A., Bédard, J.H. and Villeneuve, M. 2006. *Syncollisional basin development in the Appalachian orogen: the Saint-Daniel mélange, southern Québec, Canada*. Geological Society of America Bulletin, 118: 109-125.

Stanley, R.S., and Ratcliffe, N.M. 1985. *Tectonic synthesis of the Taconian orogeny in western New England.* Geological Society of America Bulletin, 96: 1227-1250.

St-Julien, P., 1987, *Géologie des régions de Saint-Victor et de Thetford-Mines (moitié Est).* Ministère des ressources naturelles du Québec, MM 86-01, 66 pages.

St-Julien, P. 1963. *Preliminary report on Saint-Élie-d'Orford area, Sherbrooke and Richmond counties.* Department of Natural Resources, Québec, PR #492, 14 pages.

St-Julien, P., and C. Hubert. 1975. *Evolution of the Taconian orogen in the Quebec Appalachians*. American Journal of Science, 275-A: 337-362.

St-Julien, P., Hubert, C., Skidmore, B. and Béland, J. 1972. *Appalachian structure and stratigraphy.* Quebec XXIV: International Geological Congress, Montreal, Guidebook 56, 99 pages.

Tremblay, A. 1992a. *Tectonic and accretionary history of Taconian oceanic rocks of the Québec Appalachians.* American Journal of Science, 292: 229-252.

Tremblay, A. 1992b. *Géologie de la région de Sherbrooke*. Ministère des ressources naturelles du Québec, ET 90-02, 80 pages.

Tremblay, A., and St-Julien, P. 1990. *Structural style and evolution of a segment of the Dunnage zone from the Quebec Appalachians and its tectonic implications*. Geological Society of America Bulletin, 102: 1218-1229.

Tremblay, A. and Castonguay, S. 2002. *The structural evolution of the Laurentian margin revisited (southern Quebec): implications for the Salinian Orogeny and Appalachian successor basins*. Geology, 30: 79-82.

Tremblay, A. and Malo, M. 1991. *Significance of brittle and plastic fabrics within the Massawippi Lake Fault Zone, southern Canadian Appalachians.* Journal of Structural Geology, 13: 1013-1023.

Tremblay, A. and Pinet, N. 2005. *Diachronous supracrustal extension in an intraplate setting and the origin of the Connecticut Valley-Gaspé and Merrimack troughs, Northern Appalachians*. Geological Magazine, 142 (1): 7-22.

Tremblay, A. and Pinet, N., 1994. *Distribution and characteristics of Taconian and Acadian deformation, southern Quebec Appalachians.* Geological Society of America Bulletin, 106: 1172-1181.

Tremblay, A., Hébert, R. et Bergeron, M. 1989a. Le Complexe d'Ascot des Appalaches du sud du Québec: pétrologie et géochimie. Journal Canadien des Sciences de la Terre, 26: 2407-2420.

Tremblay, A., Malo, M. and St-Julien, P. 1995. Dunnage Zone - Québec; Canadian Appalachians Region In Chapter 3 of Geology of the Appalachian/Caledonian Orogen in Canada and Greenland, Harold Williams, (co-ord.); Geological Survey of Canada, Geology of Canada, no. 6, pp. 179-197 (aussi Geological Society of America, The Geology of North America, vol. F-1).

Tremblay, A., Ruffet. G. and Bédard. J.H. 2011. *Obduction of Tethyan-type ophiolites – a case-study from the Thetford-Mines ophiolitic Complex, Québec Appalachians, Canada*. Lithos, 125: 10-26.

Tremblay, A., Ruffet, G. and Castonguay, S. 2000. *Acadian metamorphism in the Dunnage zone of southern Québec, northern Appalachians: 40Ar/39Ar evidence for collision diachronism*. Geological Society of America Bulletin, 112: 136-146.

Tremblay, A., St-Julien, P. et Labbé, J.-Y. 1989b. *Mise à l'évidence et cinématique de la faille de La Guadeloupe, Appalaches du sud du Québec.* Journal Canadien des Sciences de la Terre, 26: 1932-1943.

Tremblay, A., Laflèche, M.R., McNutt, R.H. and Bergeron, M. 1994. *Petrogenesis of Cambro-Ordovician subduction-related granitic magmas of the Québec Appalachians, Canada.* Chemical Geology, 113: 205-220.

van Grootel, G., Tremblay, A., Soufiane, A., Achab, A. et Marquis, R. 1995. *Analyse micropaléontologique du synclinorium de Connecticut Valley-Gaspé dans le sud du Québec: étude préliminaire.* Ministère des Richesses naturelles, Québec, MB 95-26, 32 pages.

van Staal, C.R. and Barr, S.M. 2012. *Lithospheric architecture and tectonic evolution of the Canadian Appalachians and associated Atlantic margin*. Chaper 2 *In* Tectonic styles in Canada: the LITHOPROBE Perspective. Edited by J.A. Percival, F.A. Cook and R.M. Clowes, Geological Association of Canada, Special Paper 49, 55 pages.

van Staal, C.R., Dewey, J.F., Mac Niocail, C., & McKerrow, W.S., 1998. *The Cambrian-Silurian tectonic evolution of the Northern Appalachians and British Caledonides: history of a complex, west and southwest Pacific-type segment of Iapetus*. Geological Society of London Special Publication 143, 199-242.

Whitehead, J., G. R. Dunning and J. G. Spray. 2000. *U-Pb geochronology and origin of granitoid rocks in the Thetford Mines ophiolite, Canadian Appalachians.* Geological Society of America Bulletin, 112: 915-928.

Whitehead, J., Reynolds, P.H. and Spray, J.G. 1995. *The sub-ophiolitc metamorphic rocks of the Québec Appalachians.* Journal of Geodynamics, 19: 325-350.

Williams, H., 1979. *The Appalachian orogen in Canada.* Canadian Journal of Earth Science, 16: 792-807.

Williams, H., and St-Julien, P., 1982. *The Baie Verte-Brompton Line: Early Paleozoic continent ocean interface in the Canadian Appalachians In* Major Structural Zones and Faults of the Northern Appalachians (eds J. Béland, and P. St-Julien), pp. 177-208, Geological Association of Canada Special Paper 24.

SEDIMENTOLOGY AND STRATIGRAPHY OF THE CAMBRIAN-ORDOVICIAN POTSDAM GROUP (ALTONA, AUSABLE AND KEESEVILLE FORMATIONS), NORTHEASTERN NY

DAVE LOWE
Department of Earth Sciences, University of Ottawa, Ottawa, ON, Canada

RYAN BRINK, CHARLOTTE MEHRTENS
Department of Geology, University of Vermont, Burlington 05405

INTRODUCTION

Geological Setting

The Cambrian to Lower Ordovician Potsdam Group is the lowermost unit of the Paleozoic platform succession overlying rocks of the 1 – 1.5 Ga Grenville orogen within the Ottawa Embayment and Quebec Basin, two semi-connected fault-bounded basins that form an inboard salient of the St. Lawrence platform succession in eastern Ontario, northern New York State and western Quebec, over an area of approximately 26,000 km^2 (Figure 1). Potsdam strata was deposited from the Late Early Cambrian until the Early Ordovician at subequatorial latitudes between 10^o – 30^o south approximately 200 – 400 km inboard of the south-facing Laurentian margin, during the late postrift and subsequent passive margin phase associated with the rifting and breakup of Rodinia (Torsvik et al. 1996; McCausland et al. 2007, 2011; Lavoie, 2008; Allen et al., 2009; Figure 2). It is mainly a siliciclastic unit that, in general, exhibits an upwards progression from terrestrial to marine deposits (Sanford and Arnott, 2010; with some exceptions, including the Altona Formation and Riviere Aux Outardes Member, see below). This terrestrial to marine progression is shared by stratal equivalents of the Potsdam Group on the Laurentian margin and in other North American cratonic basins that collectively form at the base of the Sauk Megasequence, a transgressive Megasequence that records eustatic rise across much of Early Paleozoic Laurentia preceding the Taconic Orogeny (Sloss, 1963; Lavoie, 2008).

There is no consensus from the existing Potsdam literature to suggest whether the Ottawa Embayment and Quebec Basin were pre-existing basins that were passively filled during the Early Paleozoic or were active rift or tectonically-reactivated basins. Also poorly understood is the relationship between these basins to structures within the rift margin to the east. However, features of the Potsdam including its highly irregular isopach distributions, presence of internal unconformities, variable provenance, localized soft-sediment structural deformation, in-situ brecciation, and debris flows adjacent to faults all suggest that tectonism played a role in Potsdam sedimentation, probably by the reactivation of inherited zones of tectonic weakness and pre-existing faults that developed in the Proterozoic (e.g. Wiesnet and Clark, 1966; Wolf and Dalrymple, 1984; Landing et al., 2009; Sanford and Arnott, 2010). In fact, the Ottawa Embayment and Quebec Basin lie in an area of prolonged rifting referred to as the Ottawa-Bonnechere Graben, a probable aulocogen that became active in the Neoproterozoic and was reactivated episodically until the Mesozoic and even until more recent times (Kay, 1942; Kumarapeli and Saull 1966; Kamo et al. 1995; Roden-Tice et al. 1999; Aylesworth et al. 2000; Malka et al. 2000; Bleeker et al. 2011); though the exact timing of episodic tectonic events is

poorly constrained. Also poorly understood from existing literature is the approximate configuration of the basins and adjacent highlands during the Cambrian-Ordovician and the original extent of Cambrian-Ordovician strata due to post-Ordovician faulting, Mesozoic hotspot migration and unroofing of the Adirondack Dome (Kay, 1942; Fisher, 1968; Isachsen, 1975; Crough 1981; Roden-Tice et al. 1999).

The Potsdam Group is made up of four formations: the Altona, Ausable, Hannawa Falls and Keeseville Formations (Figure 3), which are described in more detail below. This trip will focus on the Potsdam strata in from the southern Quebec Basin and westward along the axis of the Oka-Beauharnois Arch that separates the Quebec Basin and Ottawa Embayment. In this area the Altona, Ausable and Keeseville Formations are present and exposed (Figure 4).

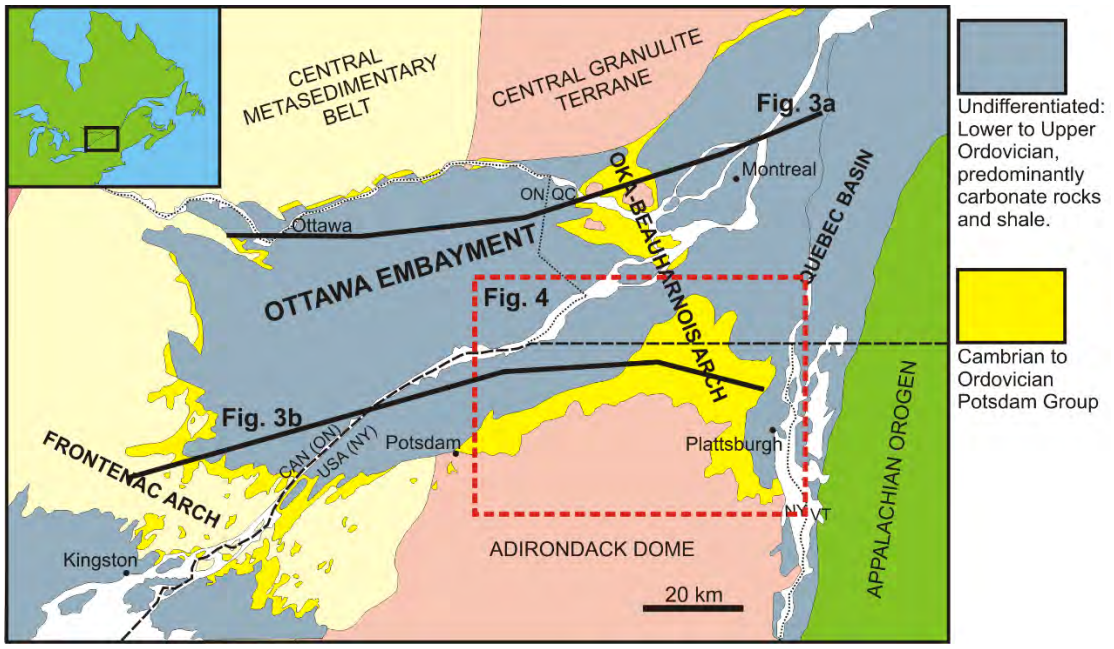

Figure 1: Base map of the Potsdam Group in the Ottawa Embayment and Quebec Basin. The solid black lines represent the ~E-W stratigraphic correlations in Figure 3, and the red square outlines the location of the map in Figure 4.

Previous Investigations of the Cambrian – Early Ordovician Stratigraphy of the Ottawa Embayment and Quebec Basin

The Potsdam Group is one of the oldest named rock units in North America (Emmons, 1838) and for almost 200 years has been studied locally in either New York State, Ontario and Quebec (Emmons, 1838, 1841; Logan, 1863; Alling, 1919; Chadwick, 1920; Wilson, 1946; Clark, 1966; 1972; Otvos, 1966; Fisher, 1968; Greggs and Bond, 1973; Brand and Rust, 1977; Selleck 1978a & b; Wolf and Dalrymple, 1984; Globensky, 1987; Salad Hersi et al. 2002; Dix et al. 2004; Landing et al. 2009; Sanford, 2007; see also Sanford and Arnott, 2010 for detailed discussion). Many of the early studies and a few more recent studies are essentially geological reports that form the basis for the Potsdam lithostratigraphic framework and the existing unit names in New York, Ontario and Quebec (e.g. Emmons, 1838, 1841; Logan, 1863; Alling, 1919; Chadwick, 1920; Wilson, 1946; Clark, 1966, 1972; Fisher, 1968; Wolf and Dalrymple, 1984; Globensky, 1987), while other generally more recent studies have provided depositional age constraints,

interpretations of depositional environments stratigraphic revisions and sequence stratigraphic interpretations (e.g. Greggs and Bond, 1973; Brand and Rust, 1977; Selleck 1978a & b; Wolf and Dalrymple, 1984; Globensky, 1987; Salad Hersi et al. 2002; Dix et al. 2004; Landing et al. 2009; Sanford and Arnott, 2010). Of these studies, only few (Lewis, 1963; Otvos, 1966; Sanford and Arnott 2010) include systematic examination of the Potsdam Group throughout the entire Ottawa Embayment and Quebec Basin, while the rest were generally confined to either New York, Ontario or Quebec. Other recent studies of the Potsdam Group have focused mainly on the paleoecology of Cambrian-Ordovician invertebrate trace makers and their preserved ichnological record, and include evidence of the earliest terrestrial animal life on Earth (Clark and Usher, 1917; Bjerstedt and Erickson 1989; MacNaughton et al. 2002; Hagadorn and Belt 2008; Collette and Hagadorn 2010; Hagadorn et al. 2011).

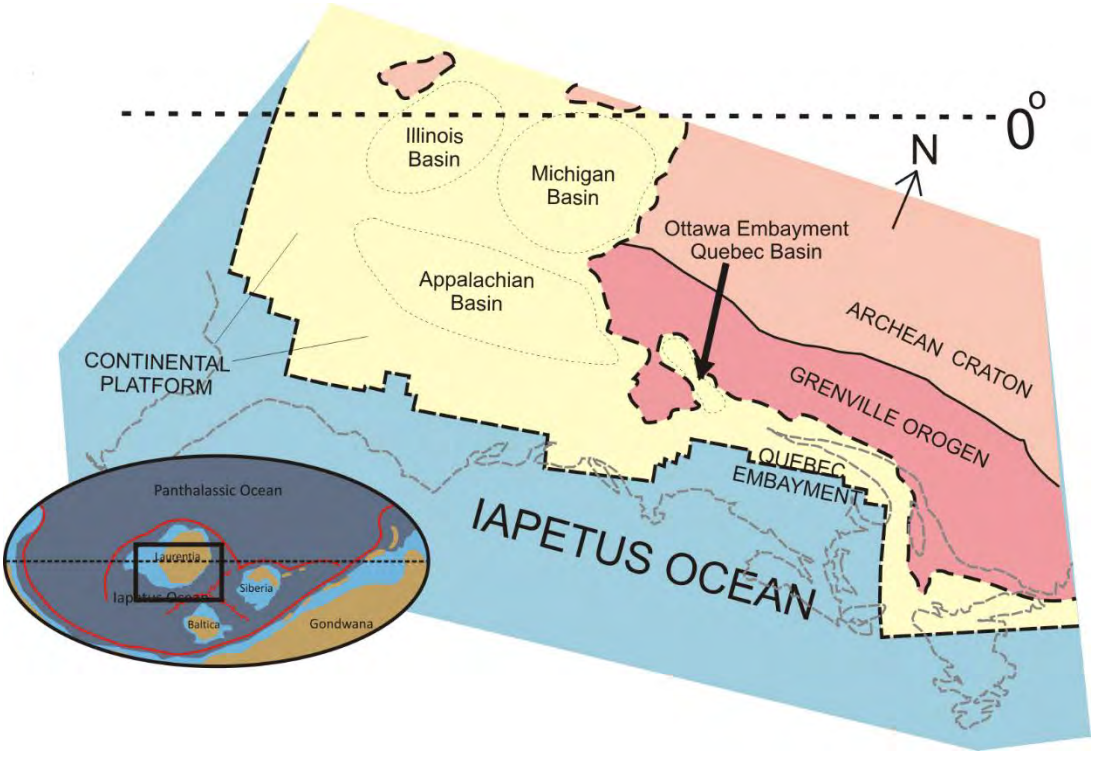

Figure 2: Paleogeographic map showing the location of the Ottawa Embayment and Quebec Basin relative to the global position and orientation of Laurentia in the Late Cambrian.

Recent studies by Landing and coworkers (2009) described the Altona Formation as shallow marine sandstone which onlapped the Laurentian craton. Faunal evidence allowed Landing to establish that this unit is *Olenellus* zone in age, an older age for the basal Potsdam than had previously been known. Brink (2014 and ms in prep.) examined the Altona Formation northwest of Plattsburgh, NY and described details of its stratigraphy (see field trip stop descriptions below). The work of Sanford (2007) and Sanford and Arnott (2010) provide comprehensive descriptions of the Potsdam Group throughout the Ottawa Embayment and Quebec Basin and a basis for ongoing sedimentological and stratigraphic investigations by the first author of this paper.

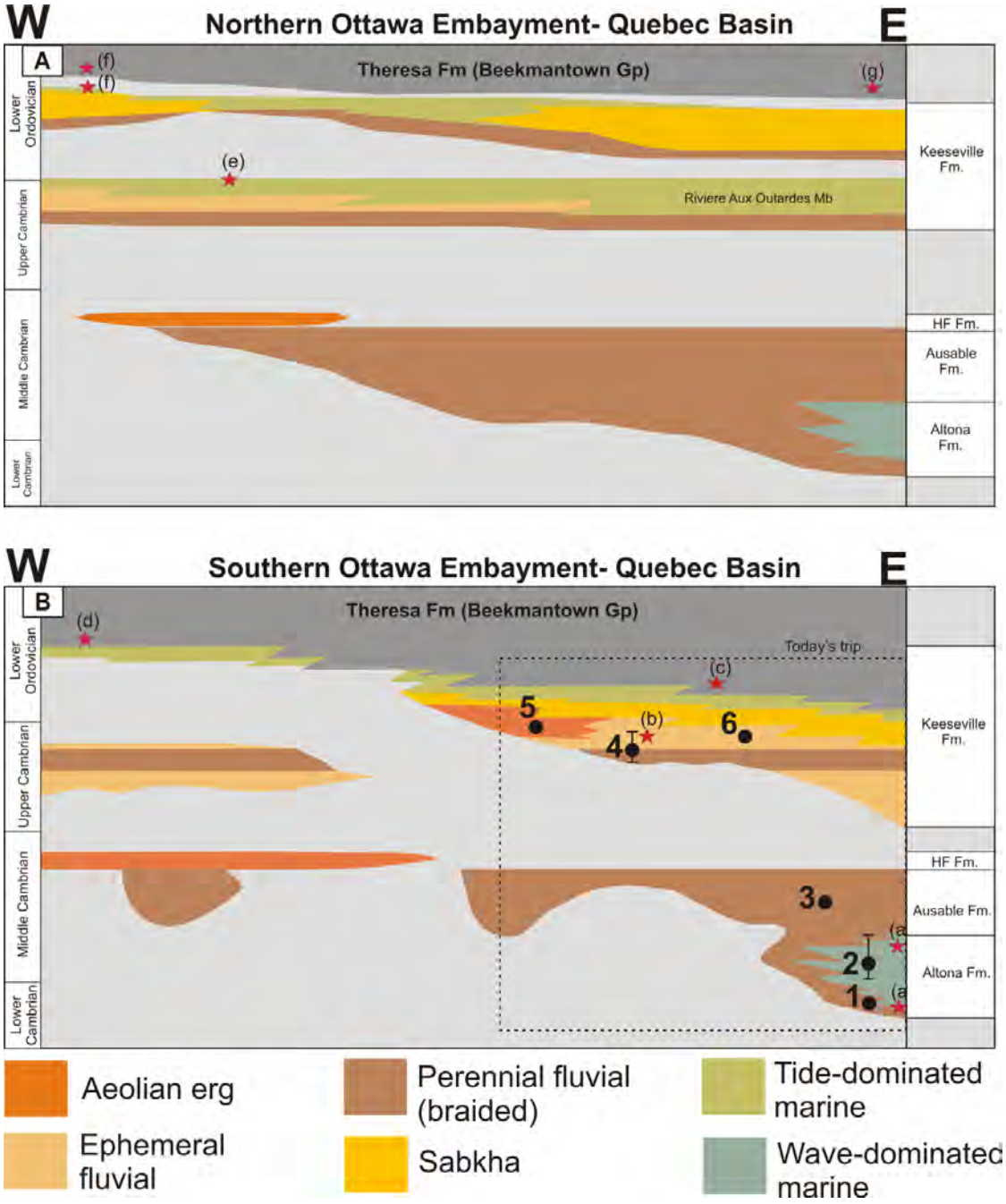

Figure 3 (A, B): Stratigraphic correlation of units of the Potsdam Group in the northern (A) and southern (B) parts of the Ottawa Embayment-Quebec Basin. The approximate stratigraphic locations of today's field trip stops are indicated by numbers 1-6. Biostratigraphic age controls are shown by the red stars: (a) Landing et al., 2009; (b) Fisher, 1968; (c) McCracken, 2014; (d) Greggs and Bond, 1973; (e) Nowlan, 2013; (f) Brand and Rust, 1977; (g) Salad Hersi et al., 2002. HF Fm. = Hannawa Falls Formation.

Potsdam Group Stratigraphy

Altona Formation

The Altona Formation represents the oldest Cambrian unit in northern New York, recording cyclic deposition in shallow marine and fluvial environments under both fair-weather and storm conditions. It occurs in the western Quebec Basin where it thins from the north to the south. In northeastern New York it is ~80 m thick and exposed in fault blocks along the northeastern Adirondacks, whereas in subsurface ~20 km north of downtown Montreal it only reaches a thickness of ~36 m.

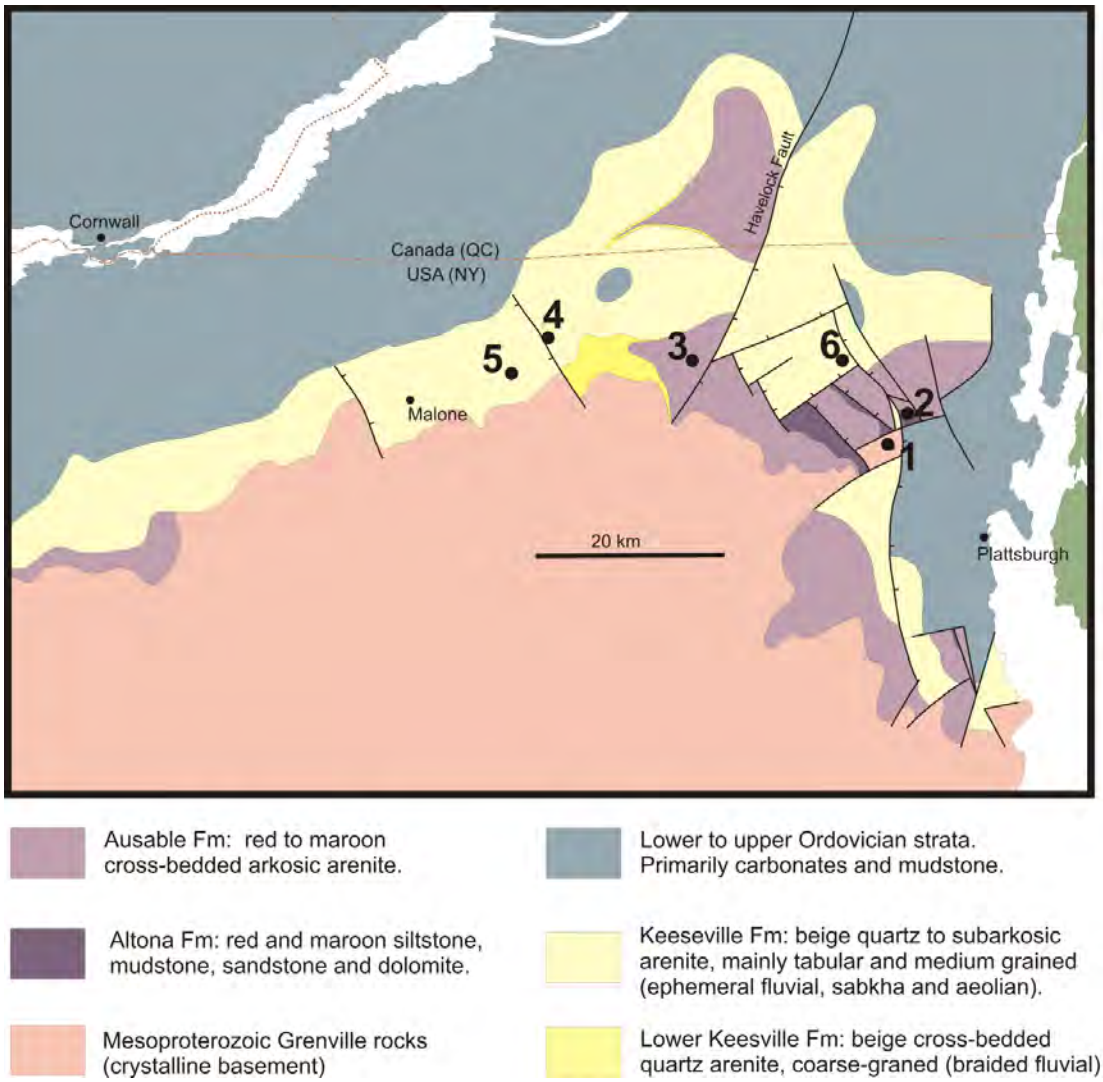

Figure 4: Simplified geologic map of the Northeastern Adirondack margin highlighting the Potsdam Group. Today's field trip stop locations are shown by numbers 1-6.

Lithofacies descriptions, stratigraphic trends and environmental interpretations were developed from detailed measurement and description of five outcrops and one well log through the Altona. Based on the recognition of sedimentary structures such as hummocky cross stratification, oscillatory ripples, graded bedding, trough and tabular cross stratification, and bioturbation, as

well as subtle lithologic changes, six lithofacies representing non-marine, middle to upper shoreface, offshore, and carbonate ramp environments were identified (Table 1). The lowermost horizons of the Altona are found to lie only one meter above Precambrian basement. Although poorly exposed, the basal beds are interpreted to be sheetflood deposits (alluvial) that were reworked on the shoreface. The uppermost Altona, approaching the contact with the overlying non-marine Ausable Formation, is characterized by inter-tonguing marine to non-marine siltstones and cross stratified medium sandstones. Throughout the 84-meter thick section, stratigraphy records a transition from upper/middle shoreface to carbonate ramp deposition and offshore muds before cycling between upper shoreface, carbonate ramp and non-marine deposits before grading into the Ausable Formation. Although conformable and gradational in the southern Quebec Basin (see above) the Altona-Ausable contact in the Northern Quebec Basin is abrupt.

Table 1. Altona Formation lithofacies and environmental interpretations (from Brink, 2014).

Litho-facies	**Description**	**Interpretation**	**Representative Stratigraphy**
1	fine to mdm-grained well sorted ss. Upward-bundling ripples, combined flow ripples, swaley cross bedding. May have erosive bases to trough cross stratification	2D and 3D wave-generated ripples on storm-influenced upper-middle shoreface	base of Atwood Farm
2	heterolithic: dolostone, siltstone and fine-grained ss. Coarse-tail graded bedding and cross stratification may be present. Bioturbation	offshore carbonate ramp influenced by storm-generated seaward transport of sand	Middle of Atwood Farm
3	arenaceous dolostone containing poorly sorted mdm-grained sand exhibiting graded bedding and cross lamination	nearshore carbonate ramp (more proximal than L2); possible eolian deposition of sand	base of Atwood Farm.
4	heterolithic: red and grey mudstone with thin laterally discontinuous beds of sand, silt and dolostone; SS beds are cross laminated with planar bases, HCS present (Jericho locality). Bioturbation	lower shoreface to offshore with periodic tempestite deposition	Atwood Farm, Jericho
5	poorly exposed poorly sorted mdm-grained feldspathic ss, possible graded bedding and cross lamination	nearshore wave(?) reworked tempestite deposits	top of Atwood Farm
6	mdm to coarse-grained poorly sorted	fluvial (sheetflow) to marginal marine	onlap PC basement; top of Atwood Farm

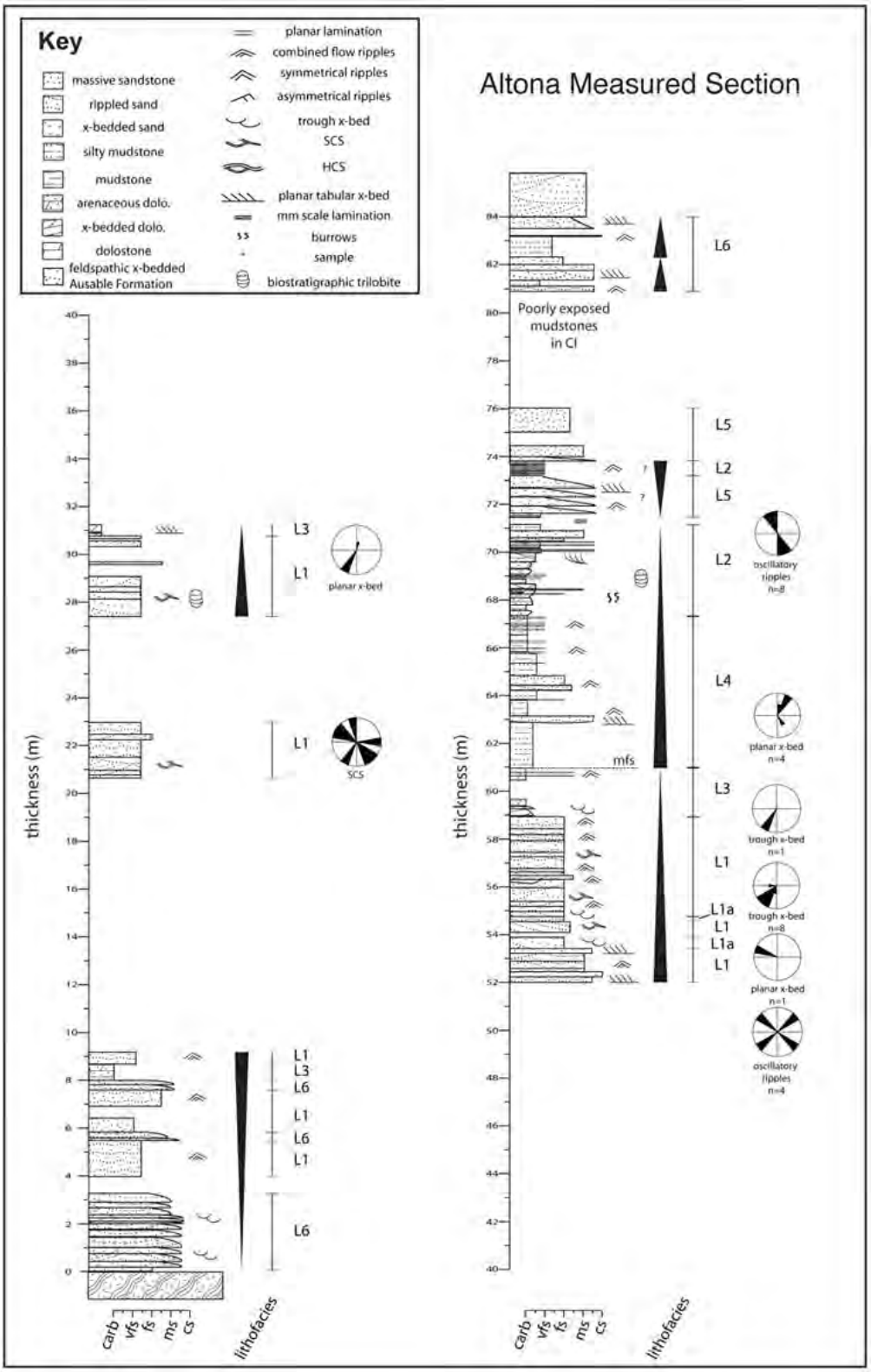

Figure 5. Composite stratigraphic column for the Altona Formation.

The provenance of the Altona sandstones was determined from thin section point counts, XRD and SEM analysis. Sandstones are subarkose to arkose in composition ($Q_{19}F_5 1L_0$ to $Q_{95}F_5L_0$) with an accessory mineral suite including ilmenite, apatite, rutile, and zircon. Integrating the compositional data, particularly the accessory mineral suite, with detrital zircon dates obtained by Chiarenzelli et al. (2010) of 1000- 1300 Ma suggests that Adirondack meta-sediments are a likely source rock.

The Altona Formation stratigraphy includes the transition from a transgressive systems tract to highstand systems tract, an interpretation based on interpretation of depositional environments and the identification of parasequences and associated flooding surfaces. The TST stratigraphy consists of basal onlap with marginal marine and fluvial deposits followed by shallow marine shoreface deposition and culminating in carbonate ramp deposition (HST). Parasequences lower in the Altona exhibit retrogradational stacking characteristic of the transgressive systems tract. Within the middle of the Altona section the first appearance of offshore mudstones marks the maximum flooding surface and the onset of the highstand systems tract. The carbonate-mudstone interval in the Altona stratigraphy represents a highstand condensed section characterized by low sedimentation rates, an interpretation based on the paucity of coarser sediment and the presence of burrows.

Ausable Formation

The Ausable Formation of probable Middle Cambrian age comprises coarse-grained and pebbly arkosic sandstone formerly assigned to the Ausable Member in northeastern New York (e.g. Alling, 1919; Fisher, 1968) and the Covey Hill Formation in Ontario and Quebec (Clark, 1966, 1972; Sanford and Arnott, 2010). The Ausable Formation is braided fluvial in origin (see below) and over most of the Ottawa Embayment – Quebec Basin unconformably overlies Precambrian Grenville basement, representing ~500 Myr of erosion and non-deposition, except where it overlies the Altona Formation in the Quebec Basin. It is conformably overlain by the Hannawa Falls Formation in the southwestern Ottawa Embayment, but elsewhere is overlain unconformably by the Keeseville Formation. Fossils that could provide depositional age constraints are absent in the Ausable Formation as are other features such as ash beds or sources of young detrital zircons that could directly constrain its depositional age. However, in the southern Quebec Basin biostratigraphic age constraints are available from the underlying Altona Formation (Landing et al., 2009) and overlying Keeseville Formation (Walcott, 1891; Fisher, 1955; Flower, 1964) that constrain the depositional age of the Ausable Formation to Middle Cambrian.

The Ausable Formation is thickest at ≥ 450 m in the Valleyfield Trough, approximately ~40 km southwest of the island of Montreal and maintains significant thicknesses (typically ~300 – 400 m thick) south- and northwards along the western Quebec Basin and the axis of the Oka-Beauharnois Arch. In the northern Ottawa Embayment the Ausable thins continuously eastward to ~8 m thick in the hanging wall trough of the Gloucester Fault beneath downtown Ottawa. The Ausable is generally absent throughout the southern Ottawa Embayment except for isolated accumulations, ~0.5 - 25 m thick, along the northern Adirondacks (e.g. along the St. Regis River in Nicholsville NY and near Redwood NY), and immediately east and south of the Big Rideau Lake in Ontario and in a few other locations on the Frontenac Arch. These units are correlated to one another regionally on the basis of stratigraphic position, detrital composition (i.e. arkose) and similarity in detrital zircon populations (see below).

The Ausable Formation consists of a lithofacies assemblage of poorly- to moderately-sorted coarse-grained cross-stratified sandstone with subordinate conglomerate and rare planar stratified sandstone and fine-grained beds and lamina collectively interpreted to have been deposited by sandy and gravelly braided rivers. Dune and unit bar cross-strata commonly build low angle downstream-accreting elements, 0.5 - 5 m thick, interpreted to record the build-up and downstream migration of low relief in-channel and bank-attached compound braid bars (e.g. Lunt and Bridge, 2004; Bridge and Lunt, 2006, see Stop 3: Great Chazy River, North Branch Near Ellenburg). Common thin (≥ 7 cm) laterally-continuous beds consisting of fine-grained muddy sandstone are interpreted as overbank deposits. In many places rip-up clasts of these layers are present, even where the layers have been eroded. Petrographic analysis reveals that these layers contain eluvial clay and silt, amorphous iron oxides, degraded detrital feldspar and swollen detrital biotite, which collectively record subaerial weathering under humid conditions on floodplains. Braided fluvial strata are organized into recurring packages, 1.3 – 7 m thick and bounded by laterally continuous surfaces, that record the deposition of successive channel belts (see Stop 3: Great Chazy River, North Branch Near Ellenburg for more details).

A combination of detrital framework mineralogy, detrital zircons (from the first author and from Chiarenzelli et al., 2010) and regional paleoflow analysis suggests that the fluvial Ausable Formation was sourced mainly from local hinterlands now covered by Paleozoic strata in the southern Ottawa Embayment with some sourcing from farther north in the Laurentian craton (Figure 6). Paleoflow analysis shows that regional fluvial systems formed a roughly radial pattern emanating from what are now the south-central Ottawa Embayment and adjacent Adirondack Lowlands, with eastward paleoflow in the northern Quebec Basin, southeastward paleoflow in the southern Quebec Basin and southwestward paleoflow along the northwestern margin of the Frontenac Arch. Detrital zircon ages all form mono-modal cumulative probability peaks of ~1.17 Ga with a narrow distribution of ages (Figure 7) similar to the age of plutonic rocks common in the Frontenac Terrane of the Central Metasedimentary Belt and northern Adirondacks which extends from the Frontenac Arch/Adirondack Lowlands northeastward beneath Paleozoic cover to the Laurentian Massif bordering the northern Ottawa Embayment (Marcantonio et al., 1990; Chiarenzelli and McLelland, 1991). However, one sample of the Ausable from the northern Quebec Basin just west of Montreal suggests major contributions from the ~1.17 Ga source but with additional cumulative probability peaks of ~1.11 and ~1.44, and ~2.65 Ga (Figure 7). Though the Archean zircons are probably from Grenville cover sequences, the other peaks most likely indicate mixed sourcing from areas farther to the northwest in addition to local sources.

The Ausable Formation is unconformably overlain by the Keeseville Formation along the axis of the southern Oka-Beauharnois Arch that separates the southern Ottawa Embayment and Quebec Basin. The contact is exposed in outcrop along the Riviere Aux Outardes in Franklin, QC; ~3 km north of the U.S.-Canada border, and is also present in several cores in southern Quebec. It is a cryptic and previously unrecognized disconformity that separates arkosic braided fluvial strata of the Ausable and quartz arenite braided fluvial of the Keeseville Formation. The top of the Ausable is characterized by an erosional surface with ~15 – 25 cm of relief and capped by a ~4 – 10 cm thick massive pebble conglomerate. This conglomerate is preferentially cemented by intergranular silica that preserves high intergranular volumes, and over the ~1.5 – 2 m of Ausable section below this conglomerate detrital feldspar grains are preferentially degraded, detrital biotite degraded and swollen and eluviated matrix is present. Collectively these features suggest the development of an initial lag, probably by aeolian deflation, and subsequent development of a silcrete paleosol with an upper duricrust and underlying illuviated horizons.

This disconformity probably represents a gap in time spanning the Middle to Late Cambrian, though biostratigraphic age constraints are not present across the contact.

In the western Ottawa Embayment and along the Frontenac Arch the contact separating the Ausable and Hannawa Falls Formation is conformable and transitional. It is characterized by a ~0.3 – 1.9 m thick section of cobble-pebble conglomerates interbedded with upper medium- to coarse-grained wind-ripple stratified sandstone. Eluviated matrix, degraded feldspar and coarse-very coarse sandstone deflation lags are common in the wind-ripple stratified sandstone beds. An upward loss of feldspar from the avg. ~30% that characterizes the Ausable to ≤8% that characterizes the Hannawa Falls Member also occurs across this interval. Altogether, these transitional beds record deflation of fluvial strata, loss of feldspar through aeolian abrasion, and episodic flash flooding during a climate shift from humid to arid conditions sometime in the Middle Cambrian preceding erg deposition of the Hannawa Falls erg succession (see below).

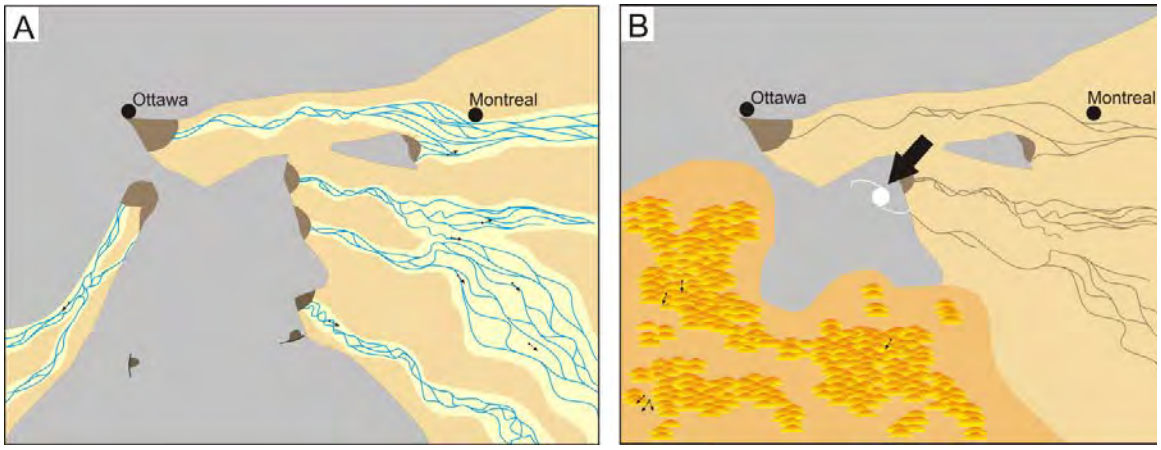

Figure 6: Inferred paleogeographic reconstruction of the Ottawa Embayment and Quebec Basin in the Middle Cambrian during deposition of the Ausable Formation (A) under humid conditions and later deposition of the Hannawa Falls Formation (B) under arid conditions. Panels are constructing using mean paleoflow from key sections (black dots with arrows) in conjunction with detrital zircon ages (see Figure 7 and text for more discussion). Large arrow on B indicates the prevailing wind direction.

Hannawa Falls Formation

The Hannawa Falls Formation is defined by the commonly red but locally buff to white quartz arenites of aeolian and sandy sheetflood-dominated ephemeral fluvial origin (see below). These occur as patchy isolated stratigraphic outliers, ~2 – 22 m thick, at or near the base of the Potsdam succession in the western Ottawa Embayment and throughout the Frontenac Arch/Adirondack Lowlands in eastern Ontario and northern New York (Jefferson and St. Lawrence Counties). The Hannawa Falls Formation is a major part of the unit formerly defined as the Hannawa Falls Member by Sanford and Arnott (2010), including the well-known red bed exposures along the Raquette River south of the town of Potsdam first described by Emmons (1838). Although previously not recognized as a stand along formation, it is considered such herein on the basis of its distribution, distinctive red coloration due to hematite rims on detrital quartz grains (in most places) and characteristic large-scale aeolian cross-stratification. It conformably overlies the Ausable Formation (see above description from the top Ausable Formation) or unconformably overlies Grenville basement where the Ausable is absent. It is

unconformably overlain by the Keeseville Formation (see description below). The Hannawa Falls Formation is undated but is most likely Middle Cambrian and perhaps upper Middle Cambrian based on its conformable relationship with the Middle Cambrian Ausable Member. Most of the Hannawa Falls Formation consists of large-scale cross bedding interpreted to record the migration of aeolian dunes in an arid erg setting, while some strata near the top and base of the Hannawa Falls Formation record ephemeral fluvial sheet flood deposition. Based on its areal distribution and the scale of aeolian dune cross-bedding the Hannawa Falls Formation records the formation of an inland erg succession covering 19,600 km^2 km over the western Ottawa Embayment, with the development of sheetflood-dominated fluvial systems in places during the later phase of the Hannawa Falls sedimentation.

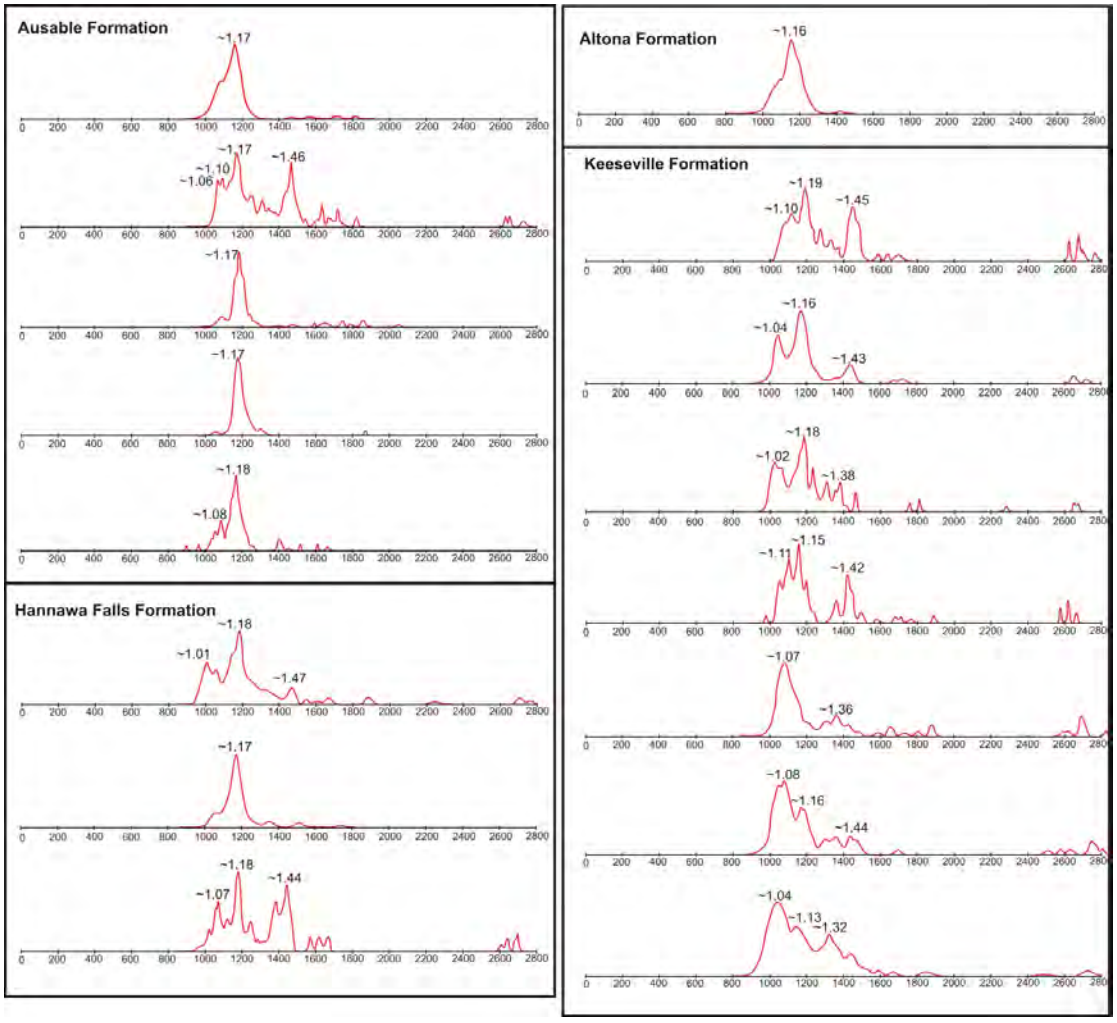

Figure 7: Detrital zircon ages from the Potsdam Group. Data is partly from Chiarenzelli et al. (2010) supplemented by samples from the first author of this paper. See text for discussion of ages. The x axis is in myr and the labelled peaks (i.e. ~1.17) are in Gya.

The change in detrital composition from arkose to quartz arenite along the transitional Ausable – Hannawa Falls contact can be attributed to (a) the mechanical breakdown of feldspar during a change to windblown transport, and/or (b) sedimentary recycling, and/or (c) a change in

regional sediment sources due to a change in regional transport mechanism from local fluvial drainage to regional windblown transport (as shown in Figure 6). Detrital zircons from the Hannawa Falls suggest a combination of all three factors. Similarities to detrital zircon assemblages to those of the Ausable (i.e. with prominent ~1.17 and ~1.44 Ga peaks, Figure 7) suggest sourcing from unconsolidated braided fluvial strata of the Ausable Formation. However, some younger detrital zircon peaks (~1.02 – 1.05 Ga) indicate possible input directly from Grenville basement in the Northern Adirondacks (Chiarenzelli and McLelland, 1991). Paleowind directions also support this interpretation, with mean paleowinds from the modern northwest indicating sand transport towards the west and southwest away from Ausable braided fluvial deposits (Figure 6b). Furthermore, the abundance of early diagenetic iron oxide cements and rims in this unit suggests that either a small amount of Fe-bearing minerals were present as detrital grains or formed a residual iron-oxide dust that coated quartz grains during transport and/or following deposition.

The Hannawa Falls is unconformably overlain by the Keeseville Formation. The contact is an erosional disconformity locally but is more commonly expressed as an angular unconformity in areas where underlying Hannawa Falls strata is locally tilted or folded and truncated by flat-bedded Keeseville strata (e.g. Sanford and Arnott, 2010). Lithified clasts of Hannawa Falls are commonly present in the lower ~1 – 2 m of overlying Keeseville strata and in addition a ~0.3 – 2 m horizon of exceptionally red and relatively poorly-cemented sandstone occurs in Hannawa Falls strata directly beneath the unconformity. Within this horizon intergranular hematite and kaolinite cements preserving high primary intergranular volumes occur at the expense of later pore-filling silica cements common elsewhere. Typically, the concentration of hematite and kaolinite cements increases upwards gradationally towards the unconformity defining a crude zonation. Therefore, this horizon is interpreted as a paleosol, specifically a ferric oxisol (under the classification of Mack et al., 1993), a.k.a. laterite, formed by groundwater leaching and near-surface precipitation of insoluble residual Fe- and Al-rich phases. The time gap represented by this unconformity is not known due to an absence of depositional ages above and beneath the unconformity, but potentially spans the Late Middle Cambrian to the middle Late Cambrian (perhaps 5 - 10 Myr). Based on similarity in stratigraphic position and probable age, this unconformity is correlated to the one that separates Ausable and Keeseville strata farther west.

Keeseville Formation

The Keeseville Formation is defined by buff to white silica-cemented supermature quartz arenite with ≤ 5% detrital feldspar and local quartzite clast cobble-boulder conglomerates with quartz arenite matrix. The term Keeseville Formation (Sanford and Arnott, 2010) replaces Keeseville Member (from Emmons, 1841; Fisher 1968) and also the Nepean Formation in Ontario (from Wilson, 1946) and the Cairnside Formation in Quebec (from Clark, 1966; 1972). The Keeseville unconformably overlies the Ausable or Hannawa Falls Formation or Grenville Basement throughout most of the Ottawa Embayment and Quebec Basin. In spite of its uniform detrital composition across the Ottawa Embayment and Quebec Basin the Keeseville Formation nonetheless records deposition under a number of terrestrial to marine environments, is dissected by at least one internal regional unconformity over much of the study area, has diverse provenance based on detrital zircon analysis and spans a long interval of geologic time from the Latest Middle Cambrian to the Middle Early Ordovician. The contact between the Keeseville Formation and overlying carbonate-cemented Theresa Formation is conformable or unconformable (see descriptions and discussion below). Based on available age constraints and contact relationships the Keeseville Formation and the base of the Theresa Formation are

diachronous and young to the west-northwest in general (also see Fisher, 1968; Sanford and Arnott, 2010).

Six depositional environments are interpreted from detailed lithofacies and architectural analysis of Keeseville lithofacies associations: braided fluvial, sheetflood-dominated ephemeral fluvial, aeolian, lacustrine, sabkha/playa and tide-dominated marine. On this fieldtrip we will visit examples of braided fluvial, sheetflood-dominated ephemeral fluvial and aeolian facies associations (see Stops 4 – 6). Aeolian strata of the Keeseville are described by Hagadorn et al. (2011) (at the Rainbow Quarry, Stop 5) and generally consist of large scale-cross stratified sets made up mainly of inversely-graded aeolian grain flow and wind ripple strata. Braided fluvial strata in the Keeseville are similar to those in the Ausable Formation. Sheetflood-dominated ephemeral fluvial strata, however, are unique to the Keeseville Formation and previous unrecognized (However, Sanford and Arnott 2010 suggest their presence). These are now recognized on the basis of dominant planar-stratified sandstone consisting of mixed aeolian, adhesion and shallow water facies and deflation lags that record aeolian reworked/deflated terminal splay deposits (e.g. Abdullatif, 1989; Hampton and Horton, 2007; Nichols and Fisher, 2008). These are usually interstratified with lesser and coarse-grained scour-based supercritical bedform strata (cross-stratified sets formed by antidunes, chutes-and-pools and cyclic steps) recording high energy sheet flood conditions. Rare channel features filled with dune cross-stratification recording the souring and filling of distributary channels also occur locally. Ephemeral fluvial strata were deposited in an arid or semi-arid fluvial environment where the recurrence interval between geologically-significant floods could be 100s or even 1000s of years (Knighton and Nanson, 1997; Tooth, 2000; see Stops 4 and 6). In places, delicate surface features including enigmatic adhesion warts and wrinkles are common, as are desiccation cracks, collectively indicating windblown adhesion and early surface cementation and/or binding, most likely by a combination of microbial mats and efflorescent salts (e.g. Goodall et al., 2000; Vogel et al. 2009).

The oldest known Keeseville Formation strata occur in the lower parts of the Ausable Chasm near the town of Keeseville, and are assigned to latest Middle Cambrian based on *Crepicephalus* Zone trilobite assemblage (Walcott, 1891; Flower, 1964; Lochman, 1968; Landing et al., 2009), while the upper parts of the ~140 m thick Chasm section are probably Upper Cambrian (Hagadorn and Belt, 2008). The Keeseville Formation here consists of deposits of a supratidal coastal sabkha. Neither the lower contact between the Keeseville and Ausable formations nor the upper contact between the Keeseville and Theresa formations are exposed here.

About ~45 – 60 km north of the Ausable Chasm, over a ~2000 km^2 area straddling the New York Quebec Border north of the Adirondack highlands, the Keeseville Formation is ~65 – 120 m thick and consists of a conformable succession of intercalated ephemeral fluvial and braided fluvial strata with rare aeolian deposits (see Stops 4 - 6), capped by sabkha and finally overlain sharply by tide-dominated marine strata. The intercalated fluvial strata are ~45 – 80 m thick and well-characterized by outcrops in and around the town of Altona and Moores and at the Chateauguay Chasm farther west (Stop 4), as well as at the nearby Ducharme Quarry near Covey Hill and near Franklin in Quebec. Ephemeral – braided fluvial contacts are sharp (as in Chateauguay Chasm, stop 4) and record a change in regional climate from arid/semi-arid to humid (and vice-versa). Sabkha deposits near the top of the Keeseville here are ~10 – 40 m thick and are sharply overlain by ~9 – 17 m thick tide-dominated marine strata. The latter strata grade upward conformably into the Theresa Formation by an increase in the thickness and proportion of dolomite cemented beds, making it difficult to pinpoint the exact Potsdam-Theresa contact.

The Keeseville here is most likely Upper Cambrian, but the highest beds may be lowermost Ordovician. Such an age is supported by: (a) correlation to ephemeral and braided Keeseville strata in the Western Ottawa Embayment that unconformably overlie the late Middle Cambrian Hannawa Falls Formation, (b) trilobite faunas reported by Fisher (1968) from the Chateauguay Chasm, and (c) conodonts from the lower part of the overlying Theresa analyzed as part of this study (McCracken, 2014) that suggest a Lower Ordovician (probably Late Tremadocian) age for the basal Theresa in this area.

In the northern Quebec Basin near Montreal ~40 – 60 km north of the NY-QC border the Keeseville Formation reaches thicknesses of ~180 m. Lithofacies are generally similar here as farther south, however this area an unconformity dissects the Keeseville Formation into two unconformity-bound units (i.e. allounits). At the top of the lower Keeseville allounit is a locally carbonate-bearing tide-dominated marine unit called the Riviere Aux Outardes member, which is overlain by fluvial and marine strata of the upper Keeseville allounit. These two allounits including the Riviere Aux Outardes member extend westward to the northwestern Ottawa Embayment in the Ottawa area where the Keeseville Formation is only ~30 m thick. Here, conodonts from the Riviere Aux Outardes Member provide a lowermost Lower Ordovician age (Nowlan, 2013), supporting a Lower Ordovician age for the upper part of the Keeseville Formation in this area. The presence of the marine Riviere Aux Outardes member and the unconformity that dissects the Keeseville Formation in the northern Ottawa Embayment indicates that a latest Cambrian – earliest Ordovician transgression and regression occurred here, but is not recorded farther south in the northern Champlain Valley. In the northern Ottawa Embayment sabkha or tide-dominated marine strata of upper Keeseville allounit is unconformably overlain by the Theresa Formation (e.g. Salad Hersi et al., 2002; Dix et al., 2004), though new age constraints suggest that this unconformity is of shorter duration that previously thought. Near Montreal the basal Theresa Formation is Tremadocian (Salad Hersi et al., 2002), whereas near Ottawa it is Arenigian (Brand and Rust, 1977) indicating westward transgression.

In the southwestern Ottawa Embayment the Keeseville Formation unconformably overlies the upper Middle Cambrian Hannawa Falls Formation. Although relatively thin (~8 – 26 m) the Keeseville here is subdivided into two allounits by an internal unconformity, much like in the Northern Ottawa Embayment. The lower allounit of probable Upper Cambrian age is ~5 – 18 m thick and consists of ephemeral and braided fluvial strata capped locally by a silcrete horizon (Selleck, 1978). The contact between ephemeral and braided fluvial strata in this area is correlated to the Upper Cambrian ephemeral-braided fluvial contact farther east (Figure 3b). Tide-dominated marine deposits of the upper Keeseville allounit are ~5 – 10 m thick, of probable lowermost Ordovician age and onlap the locally erosional surface of the lower fluvial allounit recording marine tidal ravinement and subsequent deposition. The contact between the upper marine Keeseville and Theresa Formation is sharp. It is unclear whether the Keeseville-Theresa contact is a subtle paraconformity or simply a flooding surface at this location; however, the latter is more likely because of the lack of evidence for erosion or paleosol development in the uppermost Keeseville. The basal Theresa is the same age or slightly younger (uppermost Tremadocian; Greggs and Bond, 1973) than the Theresa Formation ~180 km farther east along the NY-QC border and near Montreal, and is older than the Theresa farther north near Ottawa.

The provenance of the Keeseville Formation is as complex as its stratigraphy and involves a combination of sedimentary recycling and direct souring from previously insignificant source areas of the nearby Grenville Basement. Detrital zircon samples from the generally terrestrial Upper Cambrian Keeseville succession are either identical to that from the Ausable Formation in

the north with prominent ~1.17 and ~1.44 Ga peaks, or form larger peaks of younger ages (~1.02 - 1.1 Ga) but still with prominent ~1.17 and minor ~1.44 Ga peaks common to the underlying Ausable and Hannawa Falls formations. This suggests significant sedimentary recycling from the underlying Ausable and Hannawa Falls formations, but with increasing input probably from the adjacent Northern Adirondacks and along the suture zone between the Frontenac and Elzevir terranes along the western and northwestern margins of the Ottawa Embayment. Up section in the mainly marine Lower Ordovician Keeseville in the western Ottawa Embayment these younger Grenville sources (~1.02 - 1.1 Ga) predominate with very little "Ausable/Hannawa Falls" signal remaining, most likely recording the progressive loss of detritus through sedimentary recycling and/or by dilution by the progressive input of sediment from newer sources.

Definition of the Keeseville – Theresa contact remains elusive in spite of many years of study, and has previously been defined by the base of the lowermost pervasively carbonate-cemented bed (Cushing, 1908; Wilson, 1946; Brand and Rust, 1977; Williams and Wolf, 1982) or the top of the uppermost silica-cemented bed (Salad Hersi and Lavoie, 2000) and is either unconformable (Greggs and Bond, 1973; Salad Hersi et al., 2002; Dix et al., 2004), conformable (Cushing, 1908; Wilson, 1946; Clark, 1972; Brand and Rust, 1977; Selleck, 1984) or both (Sanford and Arnott, 2010). Numerous complications arise from the lithologic criteria used to define the Keeseville-Theresa contact. First of all, the presence of the Riviere Aux Outardes member which is locally dolomitic and occurs well below the top of the Keeseville complicates the use of the "lowermost dolomitic bed" as the base of the Theresa and silica-cemented strata present in the mid to upper Theresa complicate the use of the "uppermost quartz arenite bed" as the top of the Keeseville. In addition, parts of the overlying Theresa Formation are lithologically similar to the uppermost marine unit of the Keeseville Formation (Fisher, 1968; Greggs and Bond, 1973; Selleck, 1984) which further complicates placement of the contact. Finally, where an unconformity is recognized it does not usually coincide with either of the lithologic criteria used to define the base of the Theresa, and therefore this unconformity may actually occur fully within in the upper Keeseville or the lower Theresa, depending on how these units are defined. For now we consider the base of the lowermost carbonate-cemented bed as the best criteria to define the Keeseville – Theresa contact. Based on this criterion the available age constraints suggest the Keeseville –Theresa contact is diachronous, younging from Tremadocian to Arenigian towards the west-northwest. Unconformities developed in the northern Ottawa Embayment and Quebec Basin where the Theresa transgressed terrestrial or shallow marine Potsdam strata deposited on topographic highs (e.g. Salad Hersi et al., 2002; Dix et al., 2004), whereas the contact is gradational in the southern Quebec Basin where accommodation was space was greater (e.g. Clark, 1972). The contact in the southwestern Ottawa Embayment, although sharp, is interpreted as a conformable flooding surface.

Comparison to the Cambrian Stratigraphy of Vermont

The Cambrian section in Vermont was deposited on a thermally subsiding shelf margin of the Iapetus Ocean. The late Precambrian Pinnacle, Fairfield Pond and Tibbit Hill Formations record the formation of Iapetus Ocean crust on the rifted Grenville margin; dates for the Tibbit Hill in Vermont are ~615 Ma (O'Brien & van der Pluijm, 2012). Overlying the rift-related Precambrian units, the poorly age-constrained Cheshire Quartzite. The succeeding Dunham Dolostone contains *Salterella conulata* fossils (Mehrtens and Gregory 1984) which are thought to be correlative to the base of the Olenellus trilobite zone (Yochelson, 1983). While there are general

similarities in the Cambrian stratigraphy along strike in the Appalachians (for example, all units record fluctuating sea level on a shallow marine shelf) the Cambrian stratigraphy of western Vermont is slightly different from that to the north (Newfoundland) and south (Pennsylvania, Tennessee, Virginia). Unlike these other areas, the Vermont Cambrian stratigraphy consists of cyclically alternating siliciclastic and carbonate deposition from the earliest Cambrian into the Lower Ordovician. Goldberg and Mehrtens (1997) suggested that at least in the Lower Cambrian, both local uplifts of Grenville basement contributing siliciclastic material to the Iapetus shelf in the Vermont region occurred in concert with fluctuating sea level.

In addition to the shallow marine shelf sequence, the Cambrian stratigraphy of northwestern Vermont includes an intrashelf basin, termed either the St. Albans Reentrant (Mehrtens and Dorsey 1987) or the Franklin Basin (Shaw, 1958), which existed along strike of the shallow marine units to the south. Cherichetti et al. (1998) suggested that asymmetrical rift geometry controlled facies and thickness variation in the syn-rift stratigraphy and it is possible that these differences in subsidence history influenced deposition of the succeeding Cambrian stratigraphy (Mehrtens and Brink, 2014). Despite being thrust westward approximately 80 km (Stanley, 1999) the stratigraphy within the upper plate of the Champlain Thrust is coherent, and contacts between the shelf and basin sediments along the margin of the St Albans Reentrant/Franklin Basin are preserved. The relationship between the St Albans Reentrant/Franklin Basin and the Ottawa Bonnechere aulacogen on the Laurentian craton to the west is not clear but as early as 1983 Landing suggested that the SAR/Franklin and the Ottawa Bonnechere basins were genetically related.

Because of the revised age of the base of the Potsdam Group (Landing, et al, 2009) the Altona Formation is now interpreted to be at least in part coeval with the Monkton Formation in Vermont The bulk of the Monkton is a heterolithic wave and tidally-influenced unit that records tidal flat progradation basinward, however there is significant paleoenvironmental variation in the Monkton, which records fluvial, tidal and wave-generated sedimentary structures. The "classic" Monkton are those lithofacies exposed in the Burlington area, where the unit is commonly known as the "red rock." This Monkton displays the classic prograding tidal flat shallowing-upward cycles (SUCs). The most complete exposure of the Monkton is found in the Colchester area, where a continuous 286 meter thick section of tidal sand shoals interfinger with tidal flat sediments. A significant covered interval of nearly 100 meters occurs below the lowest exposed overlying Winooski Dolostone. In the Burlington area the Monkton/Winooski contact is exposed in Whitcomb's Quarry in Winooski, and the contact is entirely gradational and defined by the uppermost bed of red silts and sands of the Monkton. Thus, it is presumed that the Colchester covered interval also represents the progressive increase in carbonate matrix within wave-reworked sands of the shelf margin.

Figure 8 presents the proposed sequence stratigraphy correlation of the Monkton and Altona Formations. Two possible interpretations of the correlation are presented, depending on whether the covered interval at the top of the section represents the top of the Monkton (the preferred interpretation) or includes the base of the overlying Winooski (less likely, as this would make this unit significantly thicker here than elsewhere in Vermont). The onset of carbonate sedimentation on the Iapetus margin reflects sea level highstand and resulting decrease in siliciclastic sediment supply into the basin. This sea level stand is represented by the mudstone-dolostone interval in the Altona Formation stratigraphy (68-74 meter interval). The resumption of clastic deposition at the top of the Altona could reflect rejuvenation of a clastic source (uplift) or re-equilibration of sea level and sediment supply. Unfortunately, the poor

quality of exposure of this critical interval in the Altona makes it very difficult to distinguish sedimentary structures that would more definitively distinguish the relative contribution of wave-reworked shoreface processes from fluvial input.

A cartoon of the proposed paleogeographic relationship between the Monkton and Altona Formations is shown in Figure 9. Ongoing efforts to retrieve detrital zircons from the Monkton should further establish age and provenance relationships with the Altona Formation. The Danby Formation, which overlies the Winooski Dolostone, is a mixed siliciclastic-carbonate unit which had traditionally been viewed as the shelfward equivalent of the classic Potsdam Sandstone; the unit was actually called the "Potsdam Sandstone" by earliest workers in Vermont (see Cady, 1945). The Danby extends from near the Vermont-Massachusetts border northward to its pinch out on the margin of the St. Albans Reentrant/Franklin Basin. The unit is more carbonate rich to the south (a dolostone) and becomes more arenaceous to the north. Detailed section measurement, description and petrography by Mehrtens and Butler (1989) led to their recognizing mixed siliclastic-carbonate lithofaces recording peritidal to shallow subtidal environments. Ongoing research to retrieve detrital zircon from the Danby should clarify its relationship to the Potsdam.

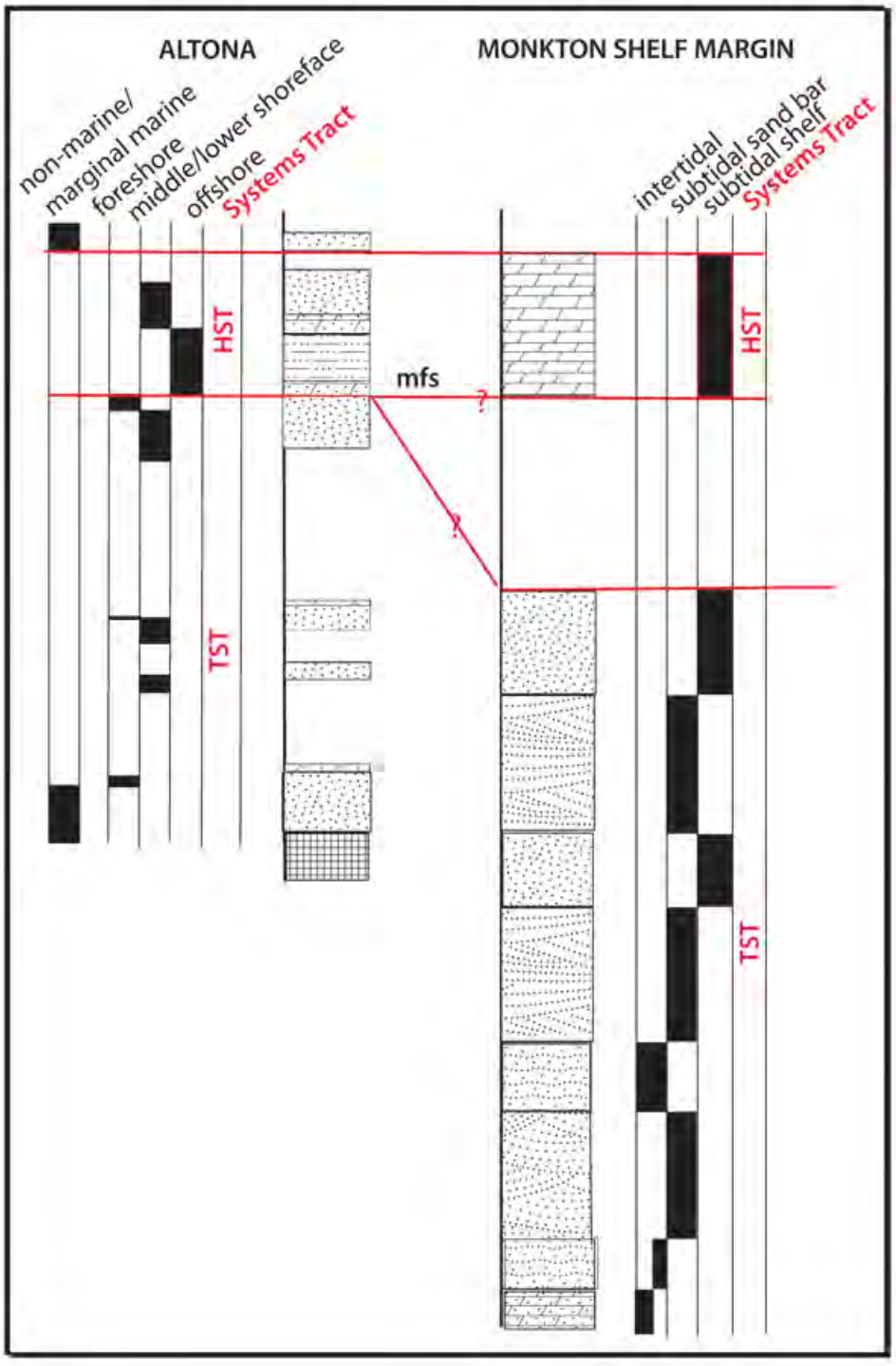

Figure 8. Sequence stratigraphic correlation of the Monkton and Altona Formations.

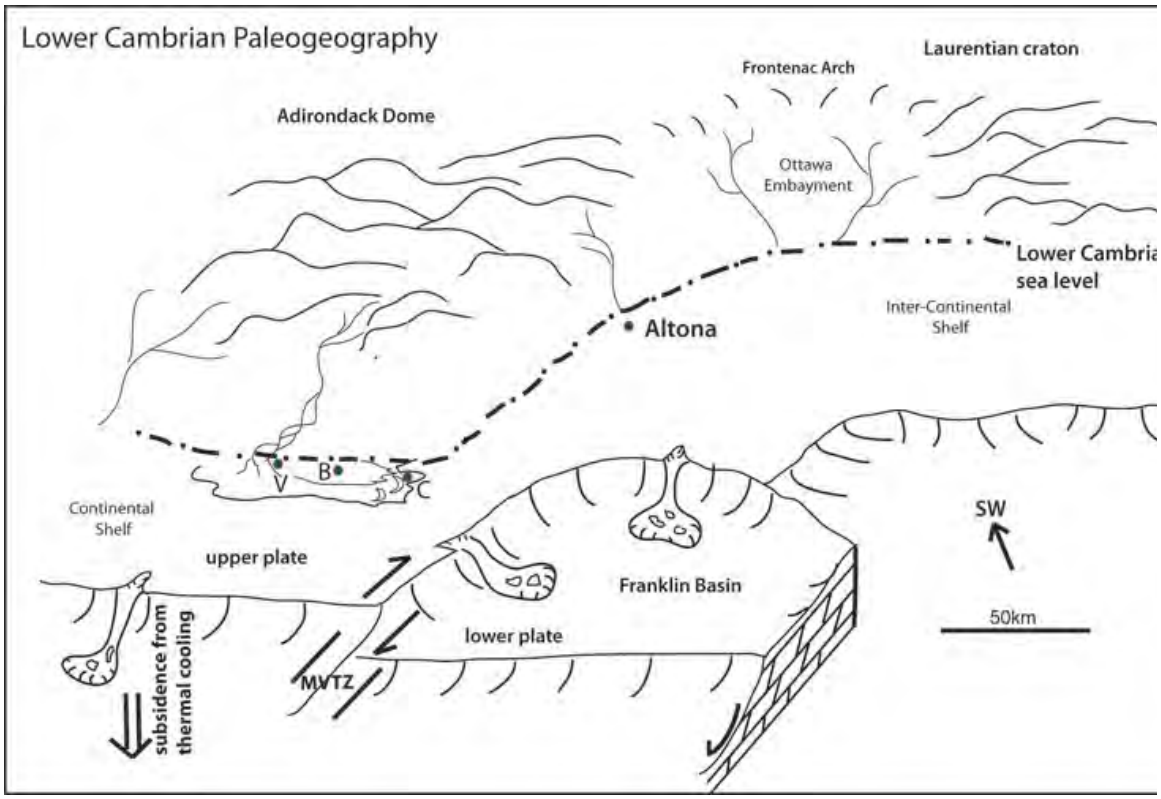

Figure 9. Schematic cartoon illustrating the possible paleogeographic relationship between the Altona (NY) and Monkton (VT) Formations in the late Lower Cambrian (from Brink, 2014). The Monkton is shown lying eastward of the Altona; palinspastically restored the east-west distance between these units ~80 km. Northward (present day coordinates) prograding Monkton tidal flat facies are shown, passing into a sand shoal complex on the margin of the Franklin Basin. The Altona Formation, a wave-dominated deposit, experienced high energy, storm-dominated conditions in a more craton-ward position, thus the cartoon suggests that the Laurentian shelf margin was characterized by headlands and embayments. The cartoon implies that these features might be related to the Franklin Basin/Ottawa-Bonnechere aulacogen, although this relationship is speculative.

FIELD GUIDE AND ROAD LOG

Meeting Point: Southeastern parking lot of Hudson Hall on the SUNY Plattsburgh campus. The lot is located at the corner of Beekman and Broad streets.

Meeting Point Coordinates: 44.696°N, 73.467°W

Meeting Time: 8:30 AM

Distance (miles) Cumulative	Point to Point	Route Description
0.0	0.0	Assemble in the southeastern parking lot of Hudson Hall.
0.3	0.3	Leave parking lot, turn right at the entrance, immediately right again onto Broad Street and proceed northwestward. At the traffic light with Prospect Street, turn right.
1.0	0.7	Junction with the Tom Miller Road. Turn left.
3.5	2.5	Traffic light and unmarked intersection with the Military Turnpike (Rte 190). Turn right.
4.4	0.9	Intersection with Route 274. Continue straight on Military Tpke.
11.1	6.7	Left turn onto unmarked dirt road accessing a portion of the Parker Sugarbush.
11.2	0.2	Proceed up hill to parking area. Park and walk remaining 0.15 mile up to Stop 1.

STOP 1: MURTAGH HILL, NY: The basal Altona Formation

Location Coordinates: (UTM Z18 NAD83 0611739; 4961998)

Walk up the dirt road until power lines are visible ahead and then veer into the woods on the left. BE CAREFUL OF SYRUP PIPING AND SUPPORTING GUIDE WIRES!! Proceed ~25' to the small stream and walk upstream to Stop 1. NO HAMMER OUTCROP (there is plenty of float available to sample).

This outcrop (Figure 10) exposes the stratigraphically lowest horizons of the Altona Formation in the region. The 3.5 meter thick exposure of coarse-grained, poorly sorted arkosic sandstones of Lithofacies 6 can be observed in close proximity to Precambrian basement rocks. Beds have non-planar (erosional?) bases and may exhibit graded bedding. Planar cross bedding can be present.

Based on grain size, graded bedding and the stratigraphic position of this lithofacies above basement and below arenaceous dolostones it is interpreted as recording sheetflood deposition into the marginal marine setting.

Figure 10. The basal Altona Formation at Murtagh Hill.

Distance (miles) Cumu-lative	Point to Point	Route Description
11.2		
11.4	0.2	return to the vehicles and proceed back down the hill to the intersection with the Military Turnpike (Rte 190). southward 0.2 mi to Rte. 9N. Turn Right
12.3	0.9	Proceed east on Rte 190 to Recore Road on the left. Turn left
12.8	0.5	Proceed down Recore Road to the intersection with Harvey Road on the left. Turn left onto Harvey.
14.2	1.4	Continue until T intersection with Atwood Road. Turn Right
14.6	0.4	Pass the Atwood Farms on your left and pull off the road at the farm field access road. STOP 2.

STOP 2: ATWOOD FARM, NY: The Altona Formation

Location Coordinates: (UTM Z18 NAD83 0613785 4964185)

Walk northward across field, following dirt track, until a small stream is reached. Turn right and follow the stream until it joins the branch of the West Chazy River. At the river's edge, turn right and walk downstream approximately 100 feet to the outcrops.

Stop 2A (UTM Z18 NAD83: 0613806 4964506). NO HAMMER!

The first stop exposes Lithofacies 1 of the Altona Formation, between 22 to 24 meters in the Altona composite section (Figure 11). Although covered in moss and lichen, patient viewing will reveal a variety of ripple morphologies that are very characteristic of much of the Altona sandstones. Lithofacies 1 is a very fine to medium grained, moderately well-sorted sandstone containing a variety of sedimentary structures including upward bundling ripple cross laminations, combined flow ripple cross laminations, and swaley cross stratification (Figure 9). Along with these structures, planar cross stratification and dwelling burrows have been identified. Planar cross stratification is up to 1 m thick, pinches out laterally over 10 m, and is generally topped by 2D or 3D weakly asymmetrical ripple cross lamination. Swaley cross stratification up to 2 m thick passes into upward bundling cosets of ripple cross laminations < 0.5 m thick. Individual ripples consist of both form concordant and form discordant morphologies with wavelengths of up to 10 cm and amplitudes < 8 cm. Sandstones are dolomitized, reacting weakly to dilute HCl.

Lithofacies 1 is interpreted to represent sediment that accumulated on a wave-dominated upper to middle shoreface that was periodically inundated by storms. This interpretation is based on the combination of sedimentary structures including upward bundling ripples, swaley cross stratification, combined flow ripple cross lamination and planar cross stratification.

Walk upriver and cross the small access stream before ascending up to the field (while it is possible to walk in the shallow channel and view the stratigraphy, for efficiency with a large group we will ascend up to the field, walk northward and descend to the river at various points. WARNING: old, difficult to see barbed wire is present in the woods. Be careful!).

Stop 2B (UTM Z18 NAD83: 0613688 4964712) Mudstone

This portion of the Altona stratigraphy, between 62-65 meters in the Altona composite section (Figure 12), exposes Lithofacies 4, a heterolithic unit dominated by mudstone but containing sandstone, siltstone, and dolostone. Note the interbedded nature of the sandstones and mudstones as well as the sedimentary structures found within the sandstones. Mudstones are red and grey in color with mm scale laminations. Trace fossils are present but rare. Sandstones are poorly sorted, fine to coarse-grained, and contain planar cross beds and ripple cross lamination. Slightly thicker and finer-grained sandstone beds contain structures resembling hummocky cross stratification (HCS). Planar cross beds have erosional bases, are occasionally graded, and change thickness laterally over ~50 meters from 4 to 30 cm. Ripple cross laminations are present with cosets less than 10 cm thick and are either form concordant or discordant. Siltstones contain 1 cm thick ripple cross lamination and locally there are 1–2 cm thick lenses or nodules of dolostone.

Lithofacies 4 is interpreted to record deposition of offshore muds near the transition from the lower shoreface to offshore zones. The intercalated beds of sand are interpreted as tempestite

deposits; episodically high energy deposition in an overall lower energy, further offshore setting. Transitions between lithologies are abrupt; there are no mud-rich dolostones, sandstones or muddy siltstones that would be expected on a graded shelf. This suggests the possibility that the deposition of mud represents a salinity controlled discharge-related event from hypopycnal flow.

Figure 11. Lithofacies 1 of the Altona Formation at Atwood Farm (Stop 2A).

Figure 12. Lithofacies 4 (mudstone) of the Altona Formation at Atwood Farm (Stop 2B).

Stop 2C: (UTM Z18 NAD83: 0613633 4964839). Dolostone bench

A prominent dolostone bench forms a small waterfall between 67-69 meters in the Altona composite section (Figure 13). Dolostone beds may contain disseminated sand-sized clastic material but the majority of beds are carbonate. Thin section analysis has not revealed fossils, sedimentary structures or fabrics that can be used to interpret paleoenvironments as there is evidence of multiple dolomitization events. The carbonate material may be shallow water (photic zone) algal in origin or it may be a chemical precipitate ("whitings"). The shoreline setting suggested for the clastic lithofacies of the Altona suggests that the near shore clastics may have passed offshore into more clear water carbonate ramp deposits. During sea level highstands, clastic material would be trapped in terrigenous fluvial systems which allowed carbonate deposition to commence. The interbedding of sandstone/mudstone and dolostone would record discharge events rather than sea level fluctuations. Dolostone beds containing clastic material frequently exhibit graded bedding of the sand, which may represent punctuated mixing during storm events. Dolostones containing fine sand disseminated throughout the carbonate may record eolian input of clastics.

Stop 2D: (UTM Z18 NAD83: 0613533 4964930) Poorly exposed uppermost Altona

This portion of the Altona stratigraphy, 81-84 meters in the Altona composite section, is poorly exposed but includes Lithofacies 5, a poorly sorted, feldspathic fine to medium-grained sandstone (Figure 14). 50 cm thick beds appear to be graded with faint ripple cross laminations. Due to its graded nature, stratigraphic position interbedded with dolostones, and stratigraphic position (overlain by Lithofacies 6), this lithofacies is interpreted to have been deposited under

conditions of waning flow velocities associated with discharge events in the adjacent terrestrial fluvial system (Ausable Fm.). This lithofacies is interpreted to represent "event beds": siliciclastic sediment washed onto the carbonate ramp following a runoff event (storm). This lithofacies may represent the nearshore component of the event beds represented by the graded planar cross bedded sandstones of Lithofacies 4.

Figure 13. Dolostone bench in the Altona Formation at Atwood Farm (Stop 2C).

Figure 14. Lithofacies 5 (feldspathic fine to medium-grained sandstone) of the Altona Formation at Atwood Farm (Stop 2D).

Ascend up to the fields and walk south back to the vehicles, which need to turn around to retrace the route back to the Military Turnpike.

Distance (miles)		
Cumu-lative	Point to Point	Route Description
14.6		
14.8	2.0	Atwood Road to intersection with Rt. 190 (Military Turnpike), go right.
28.6	13.8	Near Ellenburg turn left to continue onto Rt. 190 (Military Turnpike)
29.0	0.4	Turn Right onto Rt. 190 (Star Road)
30.4	1.4	Turn R onto Cashman Road
30.5	0.1	Park in the angler's parking or onto shoulder STOP 3

STOP 3: Great Chazy River, North Branch Near Ellenburg: The Ausable Formation

Location Coordinates: (UTM Z18 NAD83: 0589017 4970697)

Park at the angler's parking along Cashman Road. Walk south almost to the intersection of Cashman Road and Rt 190 (Star Road) and work your way down to the river. The section is continuous on the east side of the river from beneath the bridge southwards for some distance upriver. The section at this stop is along a river and waterproof footwear may be needed,

depending on the current water level. **Watch your step, as rocks are strewn across the riverbed and may be slippery.**

This stop showcases the lithofacies and architectures of braided fluvial strata of the Middle Cambrian Ausable Formation, stratigraphically beneath the Keeseville but above the Altona. We are now on the foot wall of the east-dipping normal Havelock fault upon which lower potions of the Potsdam succession are exposed on the axis of the Oka-Beauharnois Arch (Figures 1 and 4), but nevertheless the Altona –Ausable contact is probably several hundred meters in the subsurface at this location. Strata here records deposition of pebbly arkose by braided rivers in a humid climate setting. The braided rivers flowed roughly SE and had nearby hinterlands 70 – 150 km to the NW. These rivers drained into a ~N-S trending sub-basin that covered ca. ~10,000 - 15,000 km^2 in this region, resulting in the deposition of ~300 – 400 m of braided fluvial arkose that occurs from Montreal south to Plattsburgh (Figure 6a).

Most of the section consists of ~5 – 15 cm thick cross-stratified sets of moderately sorted upper medium to very coarse-grained pebbly sandstone formed by 2D or 3D dunes in shallow high energy steady unidirectional currents; although thicker (~15 – 45 cm) planar-tabular sets are interpreted to have been deposited by simple downstream-accreting solitary bars (i.e. unit bars, see Bridge, 2003; Reesink and Bridge, 2011) (Figure 15). Architectural analysis reveals that dunes and unit bars coalesced to form larger-scale accretional elements (bounded by the red lines in Figure 15) where in which sets and cosets bounded by accretion surfaces dip at low angles in the downstream direction. These accretional elements are interpreted as the deposits of low relief compound braid bars in shallow braided rivers, ubiquitous components of modern and ancient braided fluvial environments. Other features include 4 – 10 cm thick pebble conglomerates that record energetic bar-top deposition and ~ 1.5 – 6 cm thick argillaceous fine-grained sandstone beds and associated local rip-up clasts. In thin section the latter beds are shown to contain preferentially degraded feldspars, swollen biotite and eluvial clay and silt (Figure 16) recording preferential weathering (mostly by hydrolysis) and illuviation, and are therefore interpreted as overbank floodplain deposits.

Relatively thick (~1.3 – 2.5 m) repetitive successions usually capped by thin overbank deposits are recognized here and elsewhere (bounded by heavy black lines in Figure 15) and interpreted as channel belt successions. At this outcrop the at least one entire channel belt succession is exposed, over- and underlain by parts of others.

Return to the vehicles, which need to turn around to retrace the route back to the Star Road (Rt. 190).

Distance (miles) Cumu-lative	Point to Point	Route Description
30.5		
30.6	0.1	Turn cars around and proceed south to T junction with Star Rd (Rt. 190), turn right
38.8	8.2	At Brainardsville turn right onto Rt. 374 (Lake Road)
42.8	4.0	Turn left onto Pulp Mill Rd
43.7	0.9	Turn right onto Jerdon Rd
43.9	0.2	Turn right into the High Falls Campground parking, DRIVE SLOWLY. STOP 4A

Figure 15: Outcrop photo, log and interpretation of architectures from Stop 3, just north of the bridge. Numerous orders of bounding surfaces exist (green, red and black) that record deposition of different orders of braided fluvial elements: from dunes/unit bar (UB) cross-strata, to compound braid bar deposits (outlined in red) and finally channel belt deposits (outlined by heavy black line).

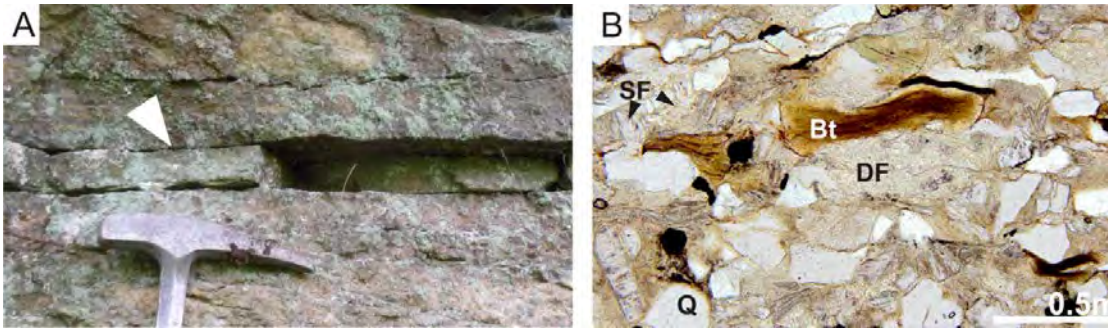

Figure 16: A) an argillaceous fine-grained sandstone bed interpreted as a thin overbank deposit (outlined by bedding planes, indicated by arrow). B) thin section photomicrograph of same bed. Eluviated matrix is common as are skeletal and degraded feldspar grains (SF and DF), hydrated biotite (Bt) and quartz grains (Q).

STOP 4: Chateguay Chasm: the Keeseville Formation

Location Coordinates: (UTM Z18 NAD83: 0571974 4972971)

While entering the High Falls campground parking lot please DRIVE SLOWLY. After parking, proceed to the main building. Access to the lower falls (stop 6A) will cost $2 per person. Leave the building through the back door and proceed along the marked trail and stairs to the High Falls viewpoint. The section is wonderfully exposed all the way down the stairs and also father north along the trail that follows the Chateguay River.

Stop 4A.

This very thick section exposes a sharp but conformable contact between two distinct parts of the Upper Cambrian quartz arenitic Keeseville Formation (Figure 17). The lower part was deposited in a coarse-grained sandy braided fluvial setting and exhibits large-scale cross-stratification formed by large dunes and unit bars with ~westward paleoflow. Although in the past this lower unit has been correlated to the Ausable Formation due to similarity in sedimentary lithofacies, its detrital composition, detrital zircon ages and its westward paleoflow instead suggest that this is a part of the Keeseville Formation. The upper part of the section exhibits a planar-tabular character. Based on lithofacies analysis it is interpreted to have been deposited mostly by unconfined terminal ephemeral sheet floods in an arid or semi-arid terrestrial environment (i.e. ephemeral fluvial). Each sheet flood deposit was largely deflated and reworked by the wind during the long recurrence intervals between flooding, which resulting in a generally tabular architecture with abundant windblown deflation lags. In places, particularly near the top of the section, upstream,-migrating scour-filling features are exposed and interpreted as supercritical chutes-and-pools or cyclic steps. These features, particularly cyclic steps, are better exposed and thus described at stop 6B.

The sharp contact separating the braided and ephemeral fluvial strata records a shift in climate of from humid to semi-arid. This climate shift is correlated to a global Late Cambrian climate fluctuation at around ~494 Ma recorded by numerous isotopic and lithofacies indicators and attributed to orbital forcing (Cherns et al., 2013).

Figure 17: Contact between mostly cross-stratified braided fluvial and planar-stratified ephemeral fluvial sandstones of the Keeseville Formation at the lower part of the Chateauguay Chasm (Stop 4A).

Return to the parking lot, where we will proceed back to Jerdon Road and make our way to the section above the High Falls that exposed the ephemeral fluvial unit.

Distance (miles)		
Cumu-lative	Point to Point	Route Description
43.9	-	Exit High Falls parking, turn right on Jerdon Rd.
44.1	0.2	Turn left on Pulp Mill Rd.
44.2	0.1	Turn right onto La Plant Rd.
44.2	0.02	Park along the shoulder of La Plant Rd.

Stop 4B.

After leaving the High Falls parking lot, turn left (south) on to Jerdon Road. Then turn left (east) on to Pulp Mills Road, cross the bridge and turn right (south) on to La Plant Road. Park along La Plant Road and walk back to Pulp Mill Road and turn left (west). Cross the bridge and then make a right and walk north along a beaten path towards the Chateguay River. The outcrop is continuous along both sides of the river. From this (the east) side the finer detail of the

ephemeral fluvial deposits can be seen, while spectacular large-scale features, including cyclic steps, can be seen by looking across to the other side of the river.

Most of the section along the west side of the river consists of planar-stratified medium to very coarse grained sandstone (Figure 18). Many if not most planar laminations are inversely graded and record deposition by the migration of wind ripples. Many planar layers are capped by coarse- to very coarse-grained deflation lags. Bedding surfaces are either featureless or expose low relief regular or irregular features suggesting adhesion and/or microbial processes. Sand Grains, although coarse, are rounded with common pits and bulbous edges, suggesting aeolian processes. Eluvial silt and clay is common along grain margins, indicating illuviation of fine-grained windblown material. Scours and low angle cross-stratified sets, probably formed by antidunes under energetic sheet floods, are common (as in Figure 18). Altogether this association records episodic deposition by terminal sheet floods (i.e. terminal splays) followed by long periods of aeolian deflation and reworking in an ephemeral fluvial environment. Most of these features can be observed close-up while walking north along the exposed sections. Farther north, pink colored apatite-cemented layers occur in lower parts of the section. These preserve high primary intergranular volumes and prohibit silica overgrowths present elsewhere (Figure 19) and thus are early intergranular cements. The origin of the phosphate is unknown, but was most likely derived from phosphate-bearing brines from underlying basement rocks.

As we walk back along the outcrop to Pulp Mill road, a large scour-filling feature can be seen on the other side of the river. This feature (outlined in Figure 20) is interpreted as a cyclic step deposit. Cyclic steps form under high energy and shallow supercritical flows in which the formation of hydraulic jumps permits the buildup and upstream-migration of cross-stratified sandstone (see Figure 20). This scour records the upstream-migration of the erosional trough of a cyclic step bedform. On the upstream side of the trough the flow accelerated causing erosion, while further downflow the flow expanded under a stable hydraulic jump resulting in stoss-side deposition (e.g. Cartigny et al. 2014). The sets are bounded by erosion surfaces that record natural fluctuations in the quasi-stable hydraulic jump during the same flood event. The final position of the cyclic step trough and its subsequent fill under subcritical flow conditions is recorded by the symmetrical scour immediately upstream of cyclic step sets, which contains downstream-migrating dune cross-stratified sandstone (Figure 20). Thus this features records high energy sheet flood conditions, perhaps during an atypically voluminous high energy flood or a flood closer to the source of overland drainage (such as a nearby isolated storm cell or front). The erosion and filling of cyclic step troughs (the scour) are crucial to the preservation of these features from subsequent aeolian reworking/deflation.

Following some discussion/observation, views of the east side can be made from the Pulp Mill Bridge and by a small beaten path on the other side of the bridge. But USE CAUTION the bank is VERY STEEP and quite high on this side. **DO NOT GET TOO CLOSE TO THE EDGE!** From here we can examine the large-scale stratal architecture of these deposits that previously we examined close-up. Most of the upper section is made up of the planar-stratified aeolian-reworked terminal splay deposits we examined close-up, while some parts below are interpreted as scour-filling antidune cross-strata or cyclic step sets (Figure 21).

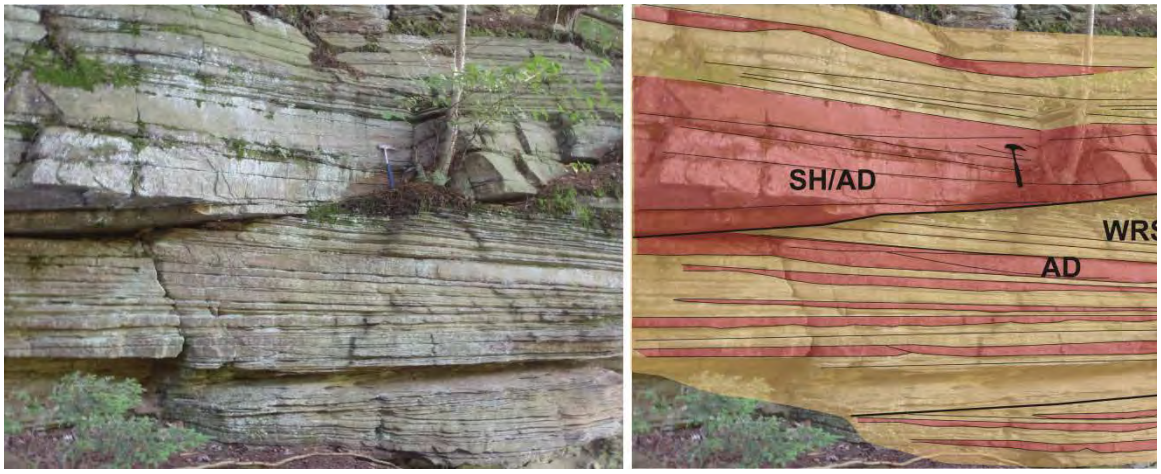

Figure 18: Outcrop photo and lithofacies interpretation of face at Stop 4B (Chateauguay Chasm, upper part). The section consist of interbedded sheetflood (pink) and aeolian (yellow) deposits (AD = antidune cross-strata; SH = massive sheet flood strata; WRS + DF = mainly wind ripple strata with some deflation lags). In this environment, most terminal sheet flood deposits were reworked by wind into aeolian sand sheets. Only the most energetic and therefore thickets sheet flood deposits were preserved. A prominent scour is present at the base of the thickets sheet flood deposit (heavy black line).

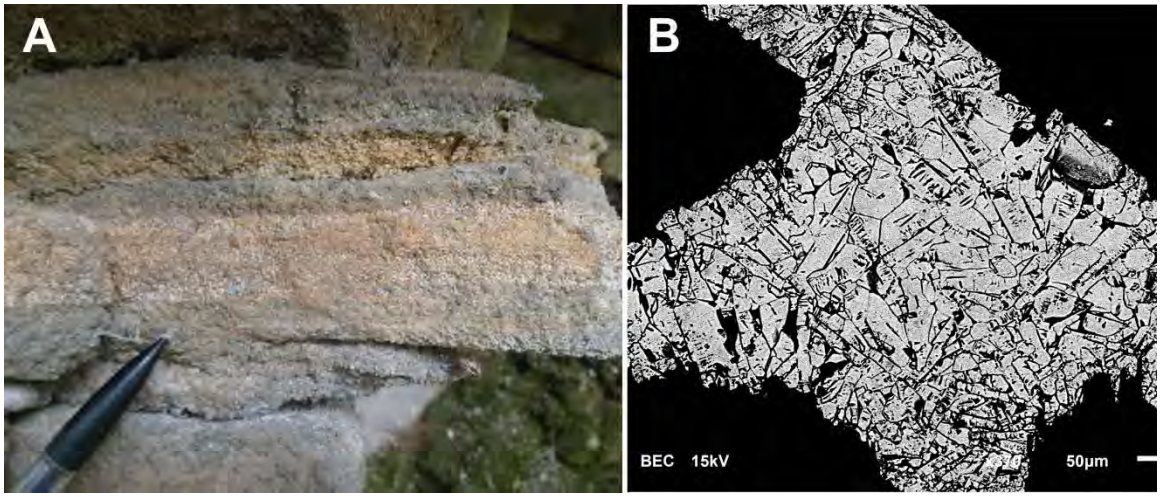

Figure 19: Early apatite cements near the base of the section. A: in outcrop these are identified by pink, roughly planar bands. B: SEM image of intergranular pore space between quartz grains (black) filled with the intergranular apatite cement.

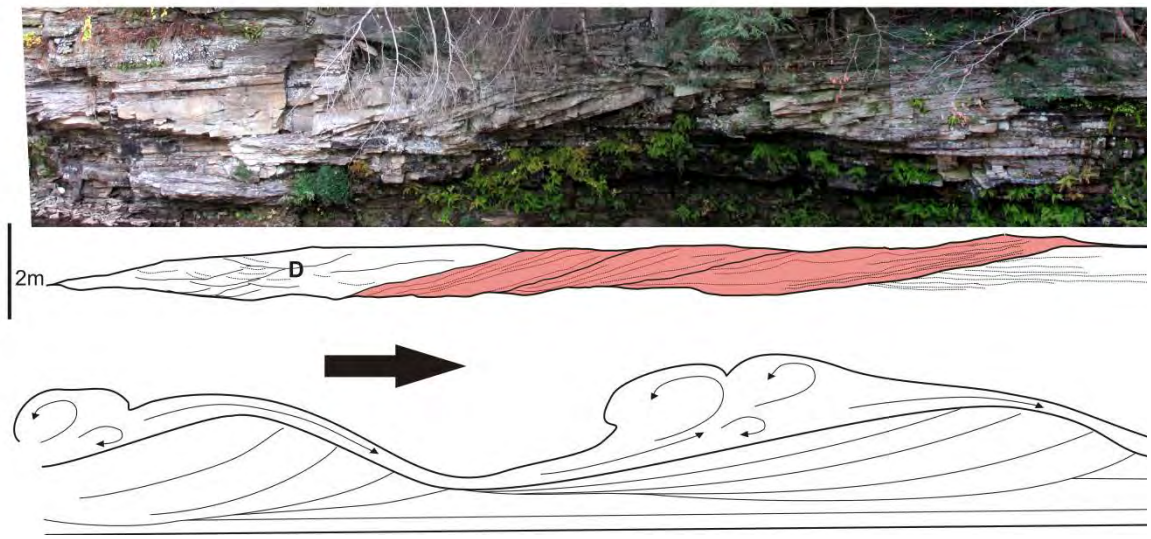

Figure 20: Scour-filling feature interpreted as an upstream-accreted cyclic step deposit that formed under a quasi-stable hydraulic jump in a high energy supercritical flow. Upstream-dipping cyclic step sets (in pink) are separated by erosional contacts caused by fluctuations in the flow/hydraulic jump during the same event. The more symmetrical scour at the upstream end records the final position of the cyclic step through that was subsequently filled by sand dune cross-strata (D) during that later stage of the flood. The line diagram at the bottom is a simplified model for the formation and migration cyclic steps with the arrow indicating the flow direction. Cross-strata only preserved in cyclic step troughs (as in this example).

Ascend the path back to Pulp Mill Rd and return to the vehicles parked on La Plant Road. We must turn the vehicles around and proceed back to the T junction with Pulp Mill Road.

Distance (miles)		
Cumu-lative	Point to Point	Route Description
44.2	0.02	Turn cars around and proceed south to T junction Pulp Mill Rd., turn left
44.3	0.1	Turn left onto Healy Rd.
45.1	0.8	Turn right onto Hartnett/Cook Rd.
48.1	3.0	Turn left onto Quarry Rd.
49.5	1.4	Continue to the end of Quarry Rd. Park just before or just beyond the gate. STOP 5

Figure 21: Annotated composite photo of the section on the west side of the upper Chateauguay Chasm section (Stop 4B). Scale bar is ~12 m.

STOP 5: Rainbow Quarry: The Keeseville Formation

Location Coordinates: (UTM Z18 NAD83: 0567998 4968956)

Park at or just beyond the quarry entrance. The best section is exposed in the southwest corner of the Quarry. Here relatively thick (~4-6 m) sets and cosets of cross-stratified medium grained sandstone are present and are interpreted to have been formed by the migration of large aeolian dunes in a generally dry aeolian erg setting (Figure 22). Close examination of the cross beds reveals inverse graded grain flow deposits in foreset strata and inversely-graded wind ripple laminations in the toe sets. At this location and at a similar quarry ~1.6 km southwest of here the aeolian dune sets are separated by generally planar stratified sandstone underlain by horizontal surfaces erosion that most likely record dry to damp interdune erosion and deposition of interdune sand flats (see Hagadorn et al. 2008 for more details). Aeolian erg strata here are interpreted to be coeval to the ephemeral fluvial strata at the top of the previous stop (Chateauguay Chasm) and most likely accumulated by the deflation and downwind transport of the ephemeral fluvial splay deposits at the Chateauguay Chasm. This correlation is supported by similarities in detrital zircon ages.

Figure 22: Large-scale cross-stratified sets formed by the migration of aeolian dunes in an arid erg setting at Stop 5. Arrow points to book bag for scale.

Turn vehicles around and proceed northward along Quarry Road.

Distance (miles)		
Cumu-lative	Point to Point	Route Description
49.5		
50.8	1.3	Drive to T junction with Cook Rd. Turn left
51.3	0.5	Turn left onto Flynn/Willis Rd (Rte. 36). Continue through sharp turns.
54.7	3.4	At T junction with Brainardsville Rd. (Rte. 24) turn left
60.1	5.4	At Brainardsville continue straight onto Rte. 190 (Star Rd.)
69.8	9.7	At T junction near Ellenburg turn left onto Rte. 190 (Military Turnpike)

70.2	0.4	At T junction near Ellenburg turn right onto Rte. 190 (Military Turnpike)
78.9	8.7	Turn left onto Devils Den Rd.
80.7	1.8	Turn left into Feinberg Park. STOP 6

STOP 6: Lasalle Dam, Altona NY: The Keeseville Formation

Location Coordinates: (UTM Z18 NAD83: 0606129 4970511)

Park at the Feinberg Park and walk south along Devils Den Road across the bridge. The outcrop is along both sides of the river, and the section is continuous upriver to the abandoned McGregor Powerhouse. Following some discussion on the south side of the river, the north side can be accessed directly from Feinberg Park.

This section exposes a part of the Upper Cambrian Keeseville Formation which underlies the surrounding area in Altona north of the Flat Rock State forest (Figure 4). Here the Keeseville consists of a sheetflood-dominated ephemeral fluvial facies association that was deposited on a Late Cambrian coastal plain inboard of the paleo-shoreline located at or somewhere south of the Ausable Chasm section, ca. 40 km to the south, which was mostly a coastal sabkha throughout the Late Cambrian. A good modern approximation for such a setting might be the coastal plain of the Skeleton Coast of Northern Namibia in which ephemeral rivers discharge directly into the Atlantic forming ephemeral fluvial "deltas".

Most of this section consists of beds of slightly inclined (≤ 10°) or horizontal planar-stratified medium grained quartz arenite usually truncated by low angle or horizontal surfaces (Figure 23). Internally these beds consist of finely-interlaminated shallow water (depth-limited orbital ripples, upper plane bed, rare current ripples) and aeolian (wind ripple and adhesion) lithofacies recording alternating wet and dry conditions. Coarse-grained deflation lags are common and desiccation cracks are also present but rare. These beds are interpreted terminal splay lobes in an ephemeral fluvial setting, and were built up over time by the accretion of episodic flood deposits. Flood deposits were largely reworked by the wind between episodic floods, resulting in common aeolian and adhesion features. Features such as oscillation ripple marks, parting lineations and adhesion ripples and warts immediately catch the eye on the bedding planes of these terminal splay lobes but belie the aeolian influence on deposition. Keep an eye out for less obvious features, such as inversely-graded laminations or low relief step-like features on bedding planes attributed to wind ripple stratification, coarse-grained deflation lags, or featureless planar laminations and surfaces most probably recoding the adhesion of windblown sand onto damp surfaces (i.e. adhesion stratification: Hunter, 1980; Kocurek and Fielder, 1982). Infiltrated matrix is also present in these strata and can be seen in thin section, and record the infiltration of clays into the vadose zone by illuviation, probably during rainstorms.

Upper medium to coarse-grained antidune cross-stratification is also present at this section and record high energy, probably more proximal, waning shallow sheet flood conditions. Antidune strata are recognized by low angle symmetrical trough-cross stratified bottom sets and convex-up low angle symmetrical formsets with wavelengths in the order of ~25 cm – 1 m (Figures 23 and 24). It has a very similar structure to HCS, something noted from numerous fluvial deposits (Cotter and Graham, 1991; Rust and Gibling, 1990; Fielding, 2006) and also from experimentally produced antidune cross-stratification (Alexander et al., 2001; Cartigny et al., 2014). However, several features including the small thickness and wavelengths of sets and formsets, its 2D form

on bedding planes, its relatively coarse grain size and lack of association with bioturbated lower shoreface deposits rules out classic HCS.

Also present near the base of the section are erosionally-based and crudely channelized trough cross-stratified sandstone formed by the migration of subaqueous dunes. These strata record the filling of an erosional distributary channel (like an arroyo or wadi) that had previously funneled energetic flood waters to terminal splays, probably during the late stages of lower energy floods leading to the abandonment of this particular distributary channel.

Isolated *Proticnites* trackways formed by arthropods have been observed at this location, but are rare.

Return to vehicles in Feinberg Park and exit right onto Devils Den Rd.

Distance in miles		
Cumu-lative	Point to Point	Route Description
	0.0	Turn right onto Devils Den Rd.
	1.8	Turn left onto Rte. 190 (Military Turnpike)
	13.9	Turn left onto Tom Miller Road.
	2.5	Turn right onto Prospect Rd.
	0.8	Turn left onto Broad Street.
	0.0	Turn left on Beekman street and immediate left into Hudson Hall parking lot.

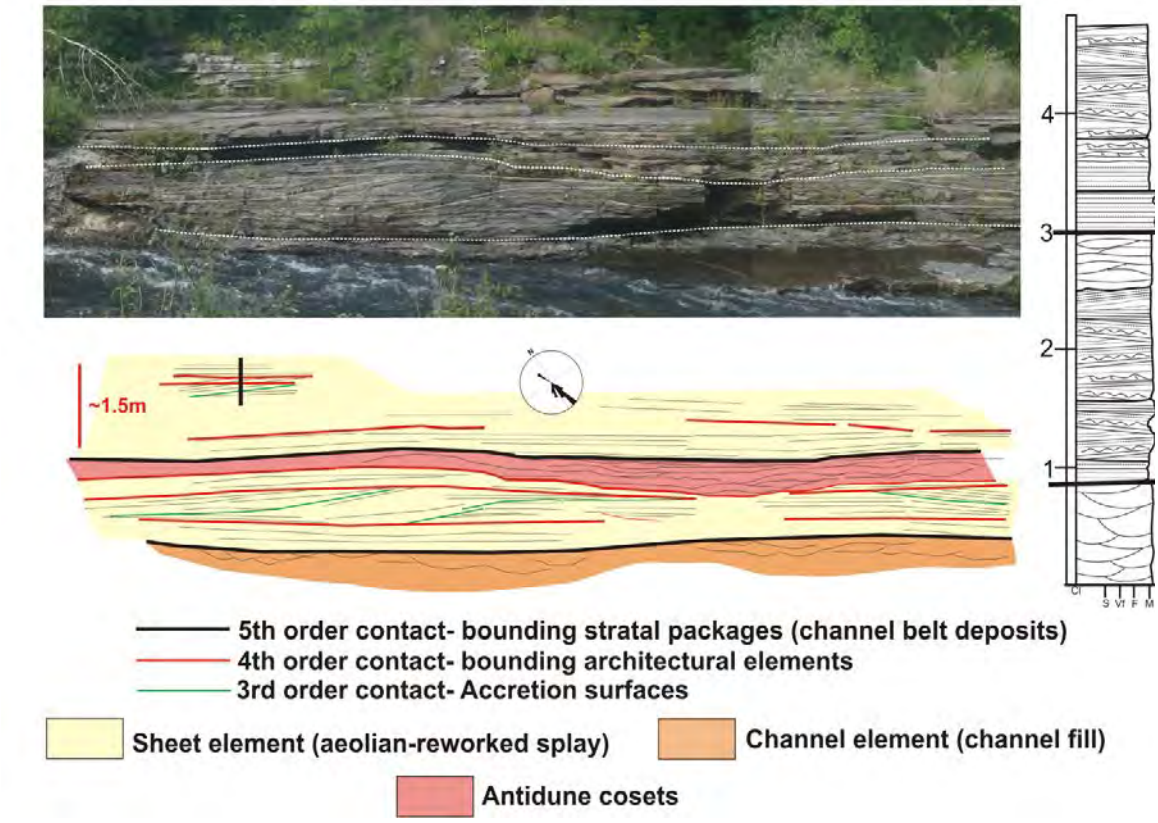

Figure 23: outcrop photo, log and sketch of section at Lasalle Dam (Stop 6). See text for more details.

Figure 24: Hummocky-looking antidune stratification at the Lasalle Dam section (Stop 6).

REFERENCES CITED

Abdullatif, O.M. 1989. Channel-fill and sheet-flood facies sequences in the ephemeral terminal river gash, Kassala, Sudan. Sedimentary Geology, 63: 171-184.

Allen, J.S., Thomas, W.A., and Lavoie, D. 2009. Stratigraphy and structure of the laurentian rifted margin in the northern Appalachians; a low-angle detachment rift system. Geology (Boulder), 37: 335-338.

Alling, H.L. 1919. Geology of the Lake Clear region (parts of Saint Regis and Saranac quadrangles). Bulletin - New York State Museum and Science Service, 207: 111-145.

Alexander, J., Bridge, J.S., Cheel, R.J., and Leclair, S.F. 2001. Bedforms and associated sedimentary structures formed under supercritical water flows over aggrading sand beds. Sedimentology, 48: 133-152.

Aylsworth, J.M., Lawrence, D.E., and Guertin, J. 2000. Did two massive earthquakes in the Holocene induce widespread landsliding and near-surface deformation in part of the Ottawa Valley, Canada? Geology, 28: 903-906.

Bjerstedt, T.W. and Erickson, J.M. 1989. Trace fossils and bioturbation in peritidal facies of the potsdam-theresa formations (cambrian-ordovician), northwest adirondacks. Palaios, 4: 203-224.

Bleeker, W., Dix,. G.R., Davidson, A., LeCheminant. 2011. Tectonic Evolution and Sedimentary Record of the Ottawa-Bonnechere Graben: Examining the Precambrian and Phanerozoic History of Magamatic Activity, Faulting and Sedimentation. Joint Annual GAC/MAC meeting, Ottawa, Guidebook to Field Trip 1A, 98 p.

Brand, U. and Rust, B.R. 1977. The age and upper boundary of the Nepean Formation in its type section near Ottawa, Ontario. Canadian Journal of Earth Sciences = Revue Canadienne des Sciences de la Terre, 14: 2002-2006.

Bridge, J.S. 2003. Rivers and floodplains; forms, processes, and sedimentary record. Blackwell Publishing, Oxford, United Kingdom .

Bridge, J.S. and Lunt, I.A. 2006. Depositional models of braided rivers. Special Publication of the International Association of Sedimentologists, 36: 11-50.

Brink, R., 2014. Sedimentologic Comparision of the latest Lower Cambrian/earliest Middle Cambrian Altona Formation (NY) and the Lower Cambrian Monkton Formation (VT), unpub. M.S. Thesis, Department of Geology, University of Vermont, 135pp.

Cady, W. M. (1945). Stratigraphy and structure of west-central Vermont. *Bulletin of the Geological Society of America, 56*(5), 515-587. doi:http://dx.doi.org/10.1130/0016-7606(1945)56[515:SASOWV]2.0.CO;2

Cartigny, M.J.B., Ventra, D., Postma, G., and van, d.B. 2014. Morphodynamics and sedimentary structures of bedforms under supercritical-flow conditions; new insights from flume experiments. Sedimentology, 61: 712-748.

Chadwick, G.H. 1920. The Paleozoic rocks of the Canton Quadrangle. University of the State of New York, State Department of Education, Albany, NY, United States.

Cherns, L., Wheeley, J.R., Popov, L.E., Ghobadi Pour, M., Owens, R.M., and Hemsley, A.R. 2013. Long-period orbital climate forcing in the early Palaeozoic? Journal of the Geological Society, 170: 707-710.

Chiarenzelli, J.R., and McLelland, J.M. 1991. Age and regional relationships of granitoid rocks of the Adirondack highlands. Journal of Geology, 99: 571-590.

Chiarenzelli J., Aspler, L. B., Donaldson, J. A., Rainbird, R., Mosher, D., & Regan, S. P., Ibanez-Mejia, M., and Franzi, D.A., 2010, Detrital zircons of Cambro-Ordovician sandstone units in eastern Ontario and northern New York. *Abstracts with Programs - Geological Society of America, 42*(1), 118.

Cherichetti, L., B. Doolan, C. Mehrtens, 1998, The Pinnacle Formation: A Late Precambrian Rift Valley Fill with Implications of Iapetus Rift Basin Evolution, Northeastern Geology, vol. 20, p. 175-185.

Clark, T.H. 1966. Châteauguay Area. Québec Department of Natural Resources Geological Report 122.

Clark, T.H. 1972. Montreal Area. Québec Department of Natural Resources Geological Report 152.

Collette, J.H., and Hagadorn, J.W. 2010. Three-dimensionally preserved arthropods from Cambrian Lagerstaetten of Quebec and Wisconsin. Journal of Paleontology, 84: 646-667.

Cotter, E. and Graham, J.R. 1991. Coastal plain sedimentation in the late Devonian of southern Ireland; hummocky cross-stratification in fluvial deposits? Sedimentary Geology, 72: 201-224.

Crough, S.T. 1981. Mesozoic hotspot epeirogeny in eastern North America. Geology (Boulder), 9: 2-6.

Cushing, H.P. 1908. Lower portion of the Paleozoic section in northwestern New York. Bulletin of the Geological Society of America, 19: 155-176.

Dix, G.R., Salad Hersi, O., and Nowlan, G.S. 2004. The Potsdam-Beekmantown Group boundary, Nepean Formation type section (Ottawa, Ontario): A cryptic sequence boundary, not a conformable transition. Canadian Journal of Earth Sciences, 41: 897-902.

Emmons, E. 1838. Report of the second geological district of the state of New York. New York Geological Survey, Annual Report, 2: 185-252.

Emmons, E. 1841. Fifth annual report of the survey of the second geological district of New York]. New York Geological Survey, Annual Report, 5: 113-136.

Fisher, D.W. 1955. Time span of the Theresa and Potsdam formations in the region peripheral to the Adirondack Mountains, New York. Bulletin of the Geological Society of America, 66: 1558-1559.

Fisher, D.W. 1962. Correlation of the Cambrian rocks in New York State. New York State Museum and Science Service, Albany, NY, United States.

Fisher, D.W. 1968. Geology of the Plattsburgh and rouses point, New York-Vermont, quadrangles. New York State Museum and Science Service, Albany, NY, United States.

Flower, R.H. 1964. The nautiloid order Ellesmeroceratida (Cephalopoda). New Mexico Bureau of Mines and Mineral Resources, Memoir 12, Socorro, New Mexico, 234 p.

Globensky, Y. 1987. Geology of the Saint Lawrence Lowlands; Geologie des basses-terres du Saint Laurent. Ministere de l'Energie et des Ressources Centre de Diffusion de la Geoinformation, Quebec, QC, Canada.

Goldberg, J. and C. Mehrtens ,1997. Depositional Environments and Sequence Stratigraphy Interpretation of the Lower Middle Cambrian Monkton Quartzite, Vermont, Northeastern Geology, vol.20, pp.11-27.

Goodall, T.M., North, C.P., and Glennie, K.W. 2000. Surface and subsurface sedimentary structures produced by salt crusts. Sedimentology, 47: 99-118.

Greggs, R.G. and Bond, I.J. 1973. Erratum; A principal reference section proposed for the nepean formation of probable tremadocian age near ottawa, ontario. Canadian Journal of Earth Sciences = Revue Canadienne des Sciences de la Terre, 10: 329.

Hampton, B.A. and Horton, B.K. 2007. Sheetflow fluvial processes in a rapidly subsiding basin, Altiplano Plateau, Bolivia. Sedimentology, 54: 1121-1147.

Hagadorn, J.W., and Belt, E.S. 2008. Stranded in upstate New York; Cambrian scyphomedusae from the Potsdam Sandstone. Palaios, 23: 424-441.

Hagadorn, J.W., Collette, J.H., and Belt, E.S. 2011. Eolian-aquatic deposits and faunas of the middle cambrian potsdam group. Palaios, 26: 314-334.

Hunter, R.E. 1980. Quasi-planar adhesion stratification; an eolian structure formed in wet sand. Journal of Sedimentary Petrology, 50: 263-266.

Isachsen, Y.W. 1975. Contemporary arching along the eastern flank of the Adirondack Dome, and possible implications for tectonics and seismicity. Abstracts with Programs - Geological Society of America, 7: 79.

Kamo, S.L., Krogh, T.E., and Kumarapeli, P.S. 1995. Age of the Grenville dyke swarm, Ontario - Quebec: implications for the timing of Iapetan rifting. Canadian Journal of Earth Sciences, 32: 273-280.

Kay, G.M. 1942. Ottawa-Bonnechere graben and Lake Ontario homocline. Bulletin of the Geological Society of America, 53: 585-646.

Kocurek, G. and Fielder, G. 1982. Adhesion structures. Journal of Sedimentary Petrology, 52: 1229-1241.

Knighton, D., and Nanson, G. 1997. Distinctiveness, diversity and uniqueness in arid zone river systems. In Arid zone geomorphology; process, form and change in drylands, pp. 185-203.

Kumarapeli, P.S., and Saull, V.A. 1966. St. Lawrence valley system -- North American equivalent of east African rift valley system. Canadian Journal of Earth Sciences, 3: 639-658.

Landing, E. (1983). Highgate Gorge; upper Cambrian and Lower Ordovician continental slope deposition and biostratigraphy, northwestern Vermont. *Journal of Paleontology, 57*(6), 1149-1187.

Landing, E., Amati, L., & Franzi, D. A. ,2009, Epeirogenic transgression near a triple junction; the oldest (latest Early-Middle Cambrian) marine onlap of cratonic New York and Quebec. *Geological Magazine, 146*(4), 552-566.

Lavoie, D. 2008. Appalachian foreland basin of canada. In The sedimentary basins of the United States and Canada, Vol. 5, pp. 65-103.

Lewis,T.L. 1963. A paleocurrent study of the Potsdam Sandstone of New York, Quebec, and Ontario. Unpublished PhD thesis, Ohio State Univerity, Akron, Ohio, 148 p.

Lochman, C. 1968. Crepicephalus faunule from the Bonneterre Dolomite (Upper Cambrian) of Missouri. Journal of Paleontology, 42: 1153-1162.

Logan, W.E. 1863. Report on the geology of Canada. Geological Survey of Canada, Ottawa, ON, Canada.

Lunt, I.A. and Bridge, J.S. 2004. Evolution and deposits of a gravelly braid bar, sagavanirktok river, alaska. Sedimentology, 51: 415-432.

Mack, G.H., James, W.C., and Monger, H.C. 1993. Classification of Paleosols. Geological Society of America Bulletin, 105: 129-136.

MacNaughton, R.B., Cole, J.M., Dalrymple, R.W., Braddy, S.J., Briggs, D.E.G. and Lukie, T.D., 2002. First steps on land: Arthropod trackways in Cambrian-Ordovician eolian sandstone, southeastern Ontario, Canada. Geology, v. 30, p. 391–394.

Malka, E., Stevenson, R.K., and David, J. 2000. Sm-Nd geochemistry and U-Pb geochronology of the Mont Rigaud stock, Quebec, Canada: A late magmatic event associated with the formation of the Iapetus Rift. Journal of Geology, 108: 569-583.

Marcantonio, F., McNutt, R.H., Dickin, A.P., and Heaman, L.M. 1990. Isotopic evidence for the crustal evolution of the Frontenac Arch in the Grenville Province of Ontario, Canada. Chemical Geology, 83: 297-314.

McCausland, P.J.A., Van, d.V., and Hall, C.M. 2007. Circum-iapetus paleogeography of the precambrian-cambrian transition with a new paleomagnetic constraint from laurentia. Precambrian Research, 156: 125-152.

McCracken, A.D. 2014. Report on 2 Early Ordovician conodont samples from the Potsdam Group near Saint-Chrysostome, southwestern Quebec submitted by David Lowe and Bill Arnott (University of Ottawa). NTS 031H/04. Con. No. 1791. Geological Survey of Canada, Paleontological Report 2-ADM-2014, 7 p.

Mehrtens, C. and R. Butler, 1987, Sedimentology of the Upper Cambrian Danby Formation, Western Vermont: An Example of Mixed Siliciclastic and Carbonate Sedimentation. Northeastern Geology, vol. 11, pp. 84-97.

Mehrtens, C. and R. Dorsey, 1987, Bedrock Geology and Stratigraphy of a Portion of the St. Albans and Adjacent Highgate Center Quadrangles, Vermont. Vermont Geol. Surv. Sp. Bulletin No. 9.

Mehrtens, C. and G. Gregory, 1984, An Occurrence of *Salterella conulata* in the Dunham Dolomite (Lower Cambrian) of Northwestern Vermont, and its Stratigraphic Significance. Jour. Paleont., v. 58, pp. 1143-1150.

Nichols, G.J. and Fisher, J.A. 2007. Processes, facies and architecture of fluvial distributary system deposits. Sedimentary Geology, 195: 75-90.

Nowlan, G.S., 2013. Report on two samples from Lower Ordovician strata in the vicinity of Rockland in eastern Ontario submitted for conodont analysis by David Lowe and Bill Arnott (University of Ottawa); NTS 031G/11; CON # 1777. Geological Survey of Canada, Paleontological Report 004-GSN-2013, 3 p.

O'Brien, T.,M., & van der Pluijm, B.,A. (2012). Timing of Iapetus Ocean rifting from Ar geochronology of pseudotachylytes in the St. Lawrence rift system of southern Quebec. *Geology (Boulder), 40*(5), 443-446.

Otvos, J., E.G. 1966. Sedimentary structures and depositional environments, Potsdam formation, upper Cambrian. American Association of Petroleum Geologists -- Bulletin, 50: 159-165.

Reesink, A.J.H. and Bridge, J.S. 2011. Evidence of bedform superimposition and flow unsteadiness in unit-bar deposits, South Saskatchewan River, Canada. Journal of Sedimentary Research, 81: 814-840.

Roden-Tice, M., Tice, S.J., and Schofield, I.S. 2000. Evidence for differential unroofing in the Adirondack Mountains, New York State, determined by apatite fission-track thermochronology. Journal of Geology, 108: 155-169.

Rust, B.R. and Gibling, M.R. 1990. Three-dimensional antidunes as HCS mimics in a fluvial sandstone; the Pennsylvanian south bar formation near Sydney, nova scotia. Journal of Sedimentary Petrology, 60: 540-548.

Salad Hersi, O., Lavoie, D., Hilowle Mohamed, A., and Nowlan, G.S. 2002. Subaerial unconformity at the Potsdam–Beekmantown contact in the Quebec reentrant: Regional significance for the Laurentian continental margin history. Bulletin and Canadian Petroleum Geology, 50: 419-440.

Sanford, B.V. 2007. Stratigraphic and structural framework of the Potsdam Group in eastern Ontario; PhD Thesis, University of Ottawa, Ottawa ON.; 222 p.

Sanford, B.V. and Arnott, R.W.C. 2010. Stratigraphic and structural framework of the Potsdam group in eastern Ontario, western Quebec and northern New York State. 597, Geological Survey of Canada, Ottawa, ON.

Selleck, B.W. 1978. Syndepositional brecciation in the Potsdam sandstone of northern New York State. Journal of Sedimentary Petrology, 48: 1177-1184.

Selleck, B.W. 1984. Stratigraphy and sedimentology of the Theresa Formation (Cambro-Ordovician) in northeasten New York State. Northeastern Geology, v. 6, p. 118-129.

Shaw, A., 1958, Stratigraphy and structure of the St. Albans area, northwestern Vermont, Geol. Soc. Am. Bull., vol. 69, pp.s519-568.

Sloss, L.L. 1959. Sequences in the cratonic interior of North America. Bulletin of the Geological Society of America, 70: 1676-1677.

Stanley, R. (1999). The Champlain thrust fault at Lone Rock Point. *Annual Meeting-New England Intercollegiate Geological Conference, 91*, 359-364.

Tooth, S. 2000. Process, form and change in dryland rivers; a review of recent research. Earth-Science Reviews, 51: 67-107.

Torsvik, T.H., Smethurst, M.A., Meert, J.G., and Van, D.V. 1996. Continental break-up and collision in the Neoproterozoic and Paleozoic - A tale of baltica and laurentia. Earth Science Reviews, 40: 229-

Vogel, M.B., Des Marais, D.J., Turk, K.A., Parenteau, M.N., Jahnke, L.L., Kubo, M.D.Y. 2009. The role of biofilms of activley forming gypsum deposits at Guerro Negro, Mexico. Astrobiology. V. 9, 875-893.

Walcott, C.W. 1891. Correlation papers; Cambrian. U. S. Geological Survey, Reston, VA, United States.

Wiesnet, D.R., and Clark, T.H. 1966. The bedrock structure of Covey Hill and vicinity, northern New York and southern Quebec. U.S.Geological Survey Professional Paper, : D35-D38.

Williams, D.A. and Wolf, R.R. 1984. Paleozoic geology of the Westport area, southern Ontario. Ont. Geol. Surv., Toronto, ON, Canada.

Wilson, A. E., 1946. Geology of the Ottawa-St. Lawrence Lowland, Ontario and Quebec. Geological Survey of Canada, Memoir 241, 66p.

Wolf, R.R., and Dalrymple, R.W. 1984. Sedimentology of the Cambro-Ordovician sandstones of eastern Ontario. Ontario Geological Survey Miscellaneous Paper: 240-252.

Yochelson, E. L. (1983). Salterella (early Cambrian; agmata) from the Scottish highlands. *Palaeontology, 26, Part 2*, 253-260.

QUATERNARY DEGLACIATION OF THE CHAMPLAIN VALLEY WITH SPECIFIC EXAMPLES FROM THE AUSABLE RIVER VALLEY

DAVID A. FRANZI
Center for Earth and Environmental Science, SUNY Plattsburgh, Plattsburgh, NY 12901

DAVID J. BARCLAY
Geology Department, SUNY Cortland, Cortland, NY 13045

REBECCA KRANITZ and KELLY GILSON
Center for Earth and Environmental Science, SUNY Plattsburgh, Plattsburgh, NY 12901

INTRODUCTION

Deglacial events and paleoenvironments in northeastern New York were influenced by the high relief of the Adirondack Mountains and predominance of north to northeast-draining river valleys (Figure 1). Landforms and sediments within these valleys record sequences of proglacial lakes that existed between the retreating margin of the Laurentide Ice Sheet (LIS) and drainage divides farther south. In general, these proglacial lakes evolved from small headwater impoundments to lowland lakes as the LIS exposed connecting spillways, and each change in lake level caused concomitant changes in tributary stream channels as river systems adjusted to the drop in local base level. Because of the interdependence of these water bodies and the adjacent LIS margin, the chronology of these lakes forms a key record for constraining the timing and style of deglaciation of this area.

In this trip we will examine the field evidence for these lakes and consider the implications of their chronology. In particular, we will focus on the methods used to reconstruct the sequence of proglacial lakes in the Ausable River valley and the constraints that this lake chronology places on a putative interval of post-LIS alpine glaciation in the Adirondacks. These deglacial events and deposits have influenced the evolution of modern drainage patterns, and we will also consider the geomorphology of Ausable Chasm and the nearby Ausable River delta at the shoreline of Lake Champlain as they relate to late Pleistocene and Holocene landscape evolution.

Background

The principal elements of the regional deglacial chronology have been recognized since the early 20th century and are updated and summarized by Rayburn et al. (2005) and Franzi et al. (2007) (Figure 2). Glacial Lake Vermont formed in the Champlain Valley and expanded northward with the receding ice front. Simultaneous ice retreat in the St. Lawrence Valley allowed Glacial Lake Iroquois in the Ontario basin to expand along the northern flank of the Adirondack upland. Chapman (1937) recognized two levels of Lake Vermont, an earlier and higher Coveville level and a later and lower Fort Ann level. Franzi et al. (2002) suggested that the Coveville stage persisted until the ice front retreated into the northern Champlain Lowland and enabled Glacial Lake Iroquois to breakout across the St. Lawrence-Champlain drainage divide at Covey Hill

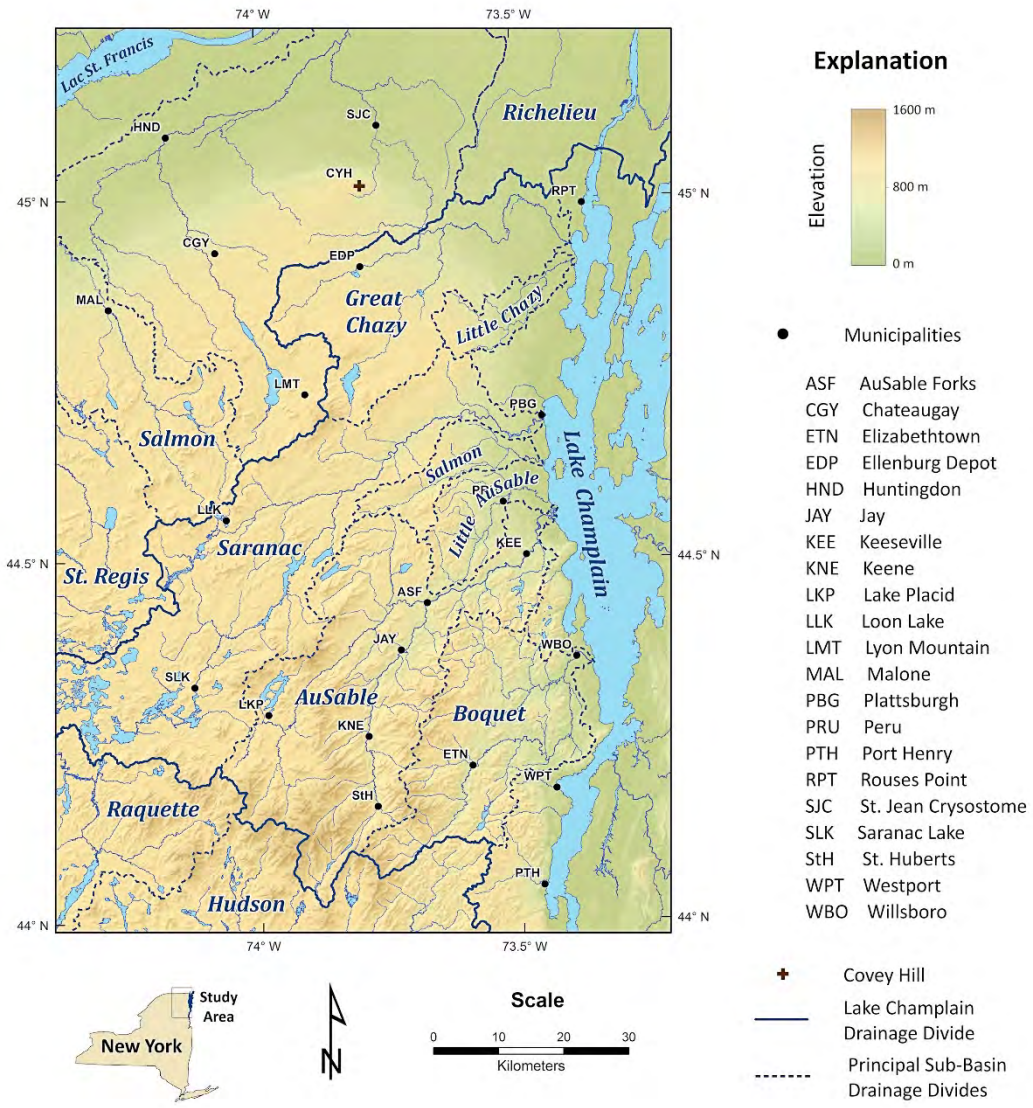

Figure 1. Principal drainage basins in the Adirondack Mountains and Champlain Valley of northeastern New York. The Lake Champlain drainage basin is delimited by a solid blue line.

(Figure 1). This catastrophic outburst released approximately 570 km^3 of water from the Ontario basin (Rayburn et al., 2005) and lowered the water surface in the St. Lawrence Valley to the Frontenac level (Pair et al., 1988). The breakout flood-wave moved south through the Champlain Valley and may have eroded the threshold at the south end of Glacial Lake Vermont, thereby causing the water level drop from the Coveville stage to the Fort Ann stage (Franzi et al. 2002). Ice margin recession from the northern flank of Covey Hill enabled a second breakout flood that released approximately 2500 km^3 of water from the Ontario basin and left proglacial lakes in the St. Lawrence and Champlain valleys fully confluent at the Fort Ann level (Rayburn et al., 2005; Franzi et al., 2007). This freshwater lake remained in the lowlands until ice recession near Quebec opened the St. Lawrence Valley and so allowed free drainage to the Gulf of St. Lawrence. Marine waters intruded into the glacio-isostatically depressed lowlands to

form the Champlain Sea, which then slowly freshened over the subsequent millennia as isostatic rebound gradually raised the region to its modern elevation.

Less is known about the sequence of ice-impounded lakes in the headwaters of the Saranac, Ausable, and Boquet river basins (Figure 1). Landforms and sediments of these high-level water bodies have long been recognized (e.g. Alling, 1916, 1918, 1920; Kemp and Alling, 1925; Denny, 1974; Craft, 1976; Diemer and Franzi, 1988; Gurrieri and Musiker, 1990; Franzi, 1992; Barclay, 1993), but their relationships with each other and the retreating ice sheet margin remain poorly resolved.

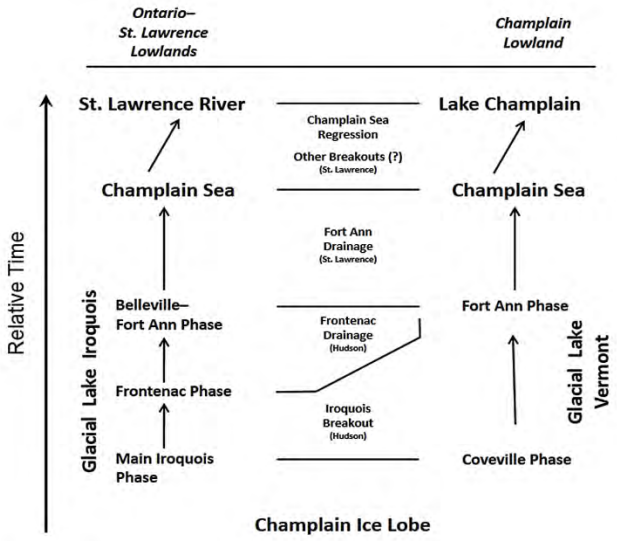

Figure 2. A generalized regional deglacial chronology for the Champlain and St. Lawrence valleys.

A related issue in these headwater valleys is whether or not alpine glaciers developed following retreat of the LIS. Ogilvie (1902), Johnson (1917), and Alling (1918, 1920) all suggested that cirque and/or valley glaciers developed in a few high valleys and deposited moraines that post-dated the regional ice sheet deglaciation. This hypothesis was extended by Craft (1969, 1976, 1979) who interpreted landforms and sediments in multiple valleys as evidence of kilometers-long valley glaciers. However, Fairchild (1913, 1932) considered the evidence for post-LIS alpine glaciers in the Adirondacks to be weak, and Barclay (1993) re-examined landforms and sediments in three valleys and found their interpretation as deposits of local alpine glaciers to be equivocal. The debate over whether or not alpine glaciers existed in the Adirondack High Peaks following LIS retreat from the region mirrors similar debates for and against post-LIS alpine glaciers in other mountain areas of the northeastern United States (e.g. Johnson, 1917; Goldthwait, 1970; Waitt and Davis, 1988; Davis, 1999).

REGIONAL DEGLACIATION

Ice-Margin and Proglacial Lake Correlations

Franzi (1992, unpublished), Franzi et al. (2002), Franzi et al. (2007) and Rayburn et al. (2007) used ice marginal landforms and glacier-profile models (e.g. Shilling and Hollin, 1981; Benn and Hulton, 2010) to map and correlate recessional ice margin positions and their associated proglacial lake phases in the Ausable, Boquet and Saranac valleys. Kranitz et al. (2014) used GIS techniques to extend this analysis into the Chazy, Chateaugay and Salmon basins and proposed correlations to the ice-margin stands of Denny (1974) (Figure 3).

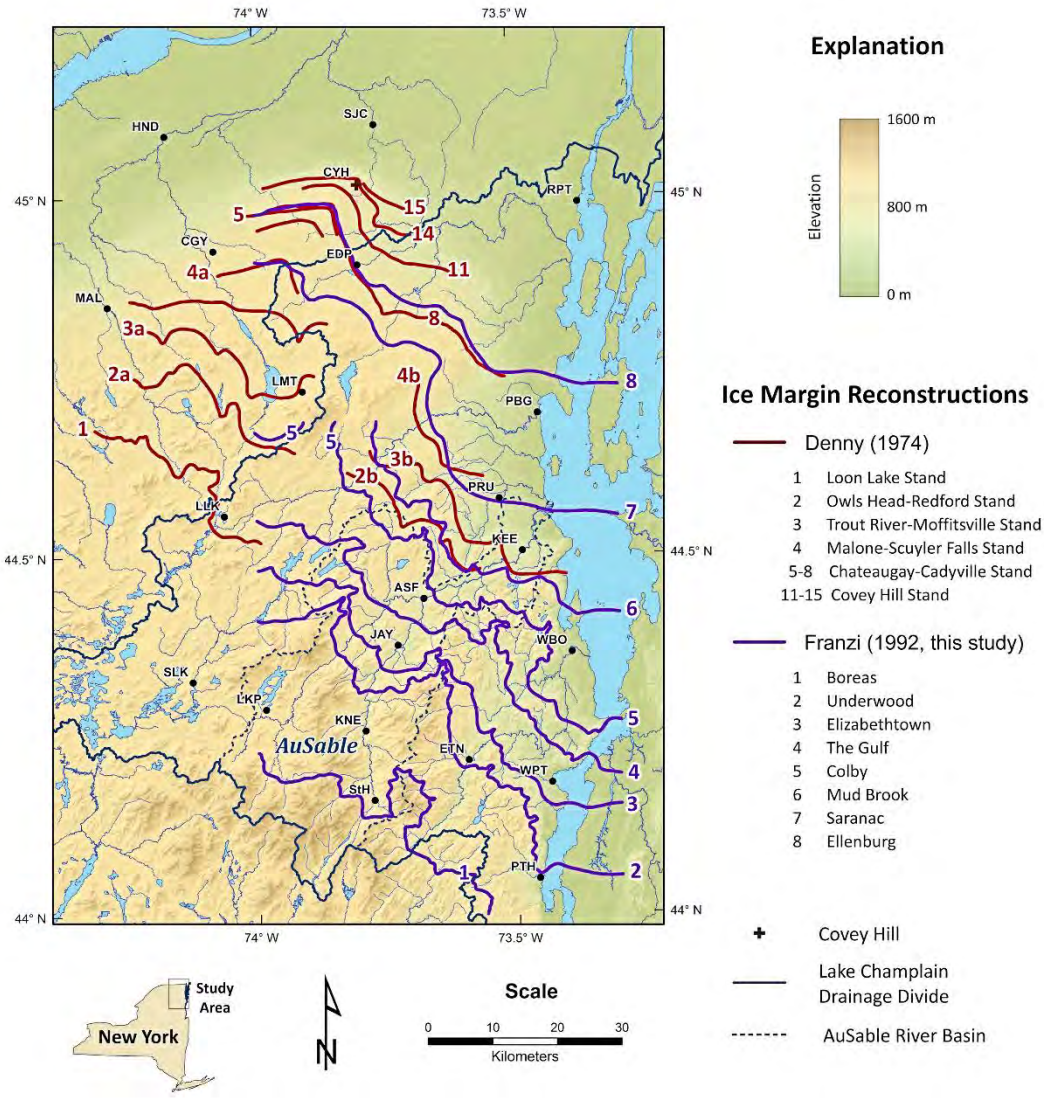

Figure 3. Late Pleistocene ice margin reconstructions from Denny (1974), Franzi (1992, unpublished). Not all of the ice margin stands of Denny (1974) are depicted. Cities and towns are keyed to the explanation in Figure 1.

Shorelines for the regional proglacial lakes Coveville, Fort Ann and Iroquois and the upper marine limit of the Champlain Sea were reconstructed by fitting a topographic trend surface to the surface elevations of shoreline deposits (compiled by Rayburn, 2004) and intersecting those surfaces with a 10-meter digital elevation model (DEM) for northeastern New York region. Adirondack lake shorelines were approximated by projecting a first-order trend surface from the lake outlet elevation at a gradient of 0.8 m/km (Denny, 1974; Franzi, 1992; Rayburn, 2004). The up-valley extent of fluvial-deltaic sandplains in major tributaries to the St. Lawrence and Champlain valleys were determined using an isostatic-rebound-corrected trend surface that projected up-valley at a gradient of 2 to 4 m/km (Boothroyd and Ashley, 1975).

GIS software facilitates regional correlation of glacial deposits and landforms by allowing the user to work easily at different scales and apply simple models to plot shorelines, inwash/outwash and glacier surface profiles. In several instances, the use of ice-surface profile models led to reinterpretation of previously correlated ice-marginal deposits. These techniques generally produce realistic correlations, especially when used in combination with field evidence to correlate well-developed ice-marginal deposits and landforms in adjacent valleys.

Regional Deglacial Chronology

The results correspond well with interpretations presented in previous investigations in the region or provide reasonable alternative explanations. The regional deglacial chronology is summarized in the examples of ice margin and proglacial lake reconstructions presented in Figure 4A-E.

Loon Lake–Elizabethtown (Figure 4A): This ice margin combines the Loon Lake stand of Denny (1974) in the upper Saranac River basin and the Elizabethtown ice margin (Franzi, unpublished; Franzi et al., 2007; Rayburn et al., 2007) in the Ausable, Boquet and Champlain valleys (Figures 3 and 4A). Meltwater outflow in the upper Saranac River basin deposited thick bodies of outwash and drained to the west through the St. Regis River basin (Denny, 1974). Lakes Chapel, Elizabethtown and Hoisington fronted the ice margin in the Ausable and Boquet river basins. These proglacial lakes drained eastward to Lake Coveville (Coveville stage of Lake Vermont) in the Champlain Valley. The ice margin is dated by a musk-ox bone found in prodeltaic mud in Lake Hoisington that yielded a corrected AMS age of 11,280 ± 110 yr. B.P. (AA-4935), which corresponds to 13,438–13,020 calibrated years B.P. (Rayburn et al., 2007).

Malone–Keeseville (Figure 4B): The Malone–Keeseville ice margin roughly follows the Malone–Schuyler Falls stand of Denny (1974) in the St. Lawrence drainage basins between Malone and Lake Chazy and follows ice margin 6 of Franzi (unpublished) in the Saranac, Salmon and Ausable river basins (Figure 3). This interpretation was guided by projecting ice-marginal deposits in the Saranac River valley near Moffitsville into the Chazy Lake valley using the PROFILER ice-surface model (Benn and Houlton, 2010) and if correct means that Malone–Schuyler Falls ice margins 4a and 4b (Figure 3) do not correlate as Denny (1974) suggested.

Ellenburg–Plattsburgh (Figure 4C): This ice margin corresponds with the ice margins 5 and 8 of the Chateaugay–Cadyville stands of Denny (1974) and ice margin 8 of Franzi (unpublished) (Figure 3). Lake Iroquois occupies the St. Lawrence Valley and a smaller proglacial lake occupies the upper North Branch of the Great Chazy River basin at the Ellenburg Moraine. This reconstruction depicts Lake Coveville near its maximum extent in the Champlain Valley. Further ice recession allowed Lake Iroquois to break-out eastward across the St. Lawrence–Champlain drainage divide near Covey Hill, which triggered the transition from the Coveville to the Fort Ann level of glacial Lake Vermont.

Lake Fort Ann (Figure 4D): Lake Fort Ann is depicted at the lower Fort Ann level (Chapman, 1937), at which time the lake had a stable outlet across the Hudson–Champlain drainage divide near Fort Ann.

Champlain Sea (Figure 4E): The Champlain Sea is depicted near the upper marine limit, which occurred shortly after the drainage of Lake Fort Ann.

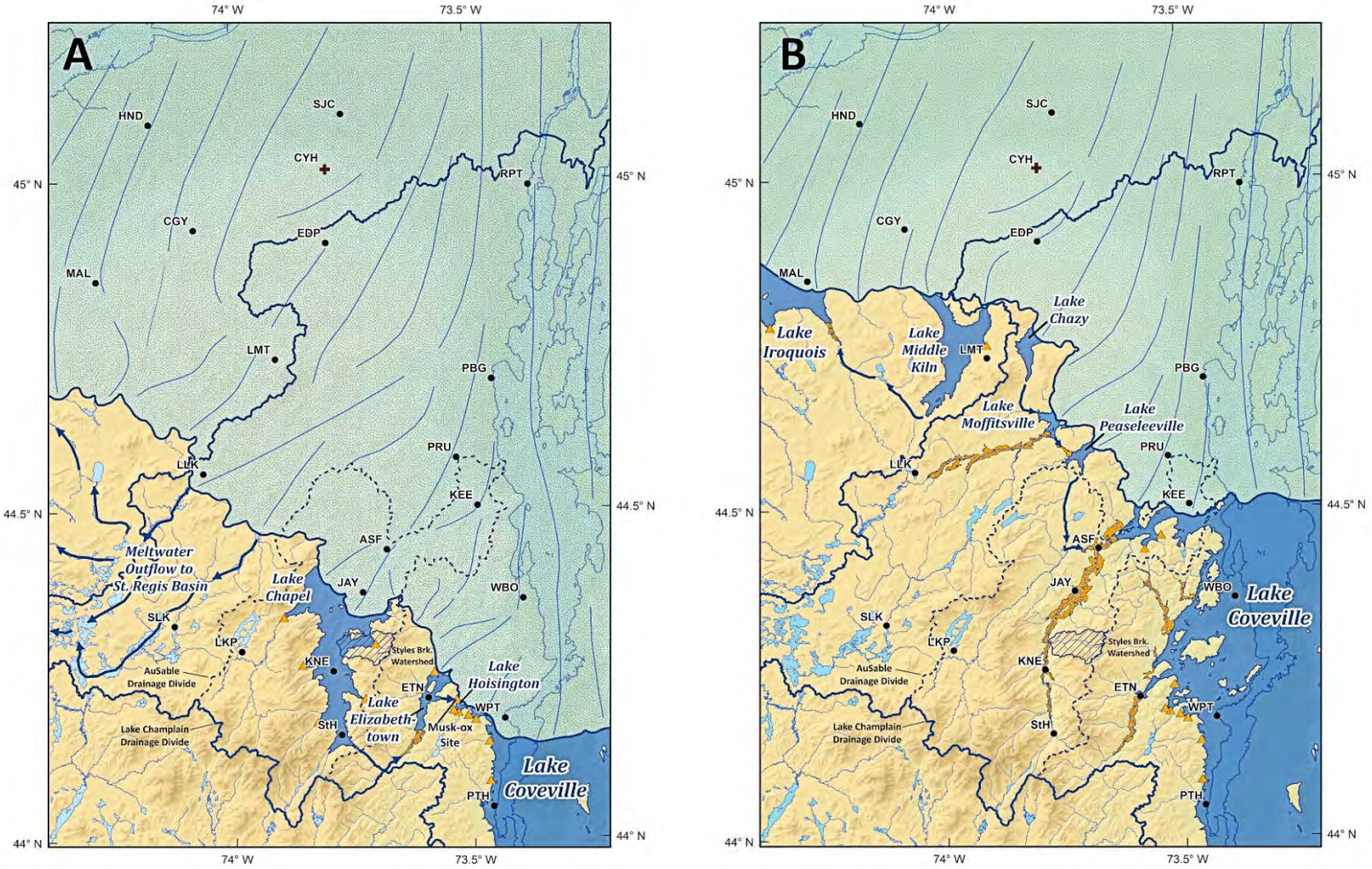

Figure 4. The Loon Lake–Elizabethtown (4A) and Malone–Keeseville (4B) ice margins in the northeastern Adirondack uplands and western Champlain Valley.

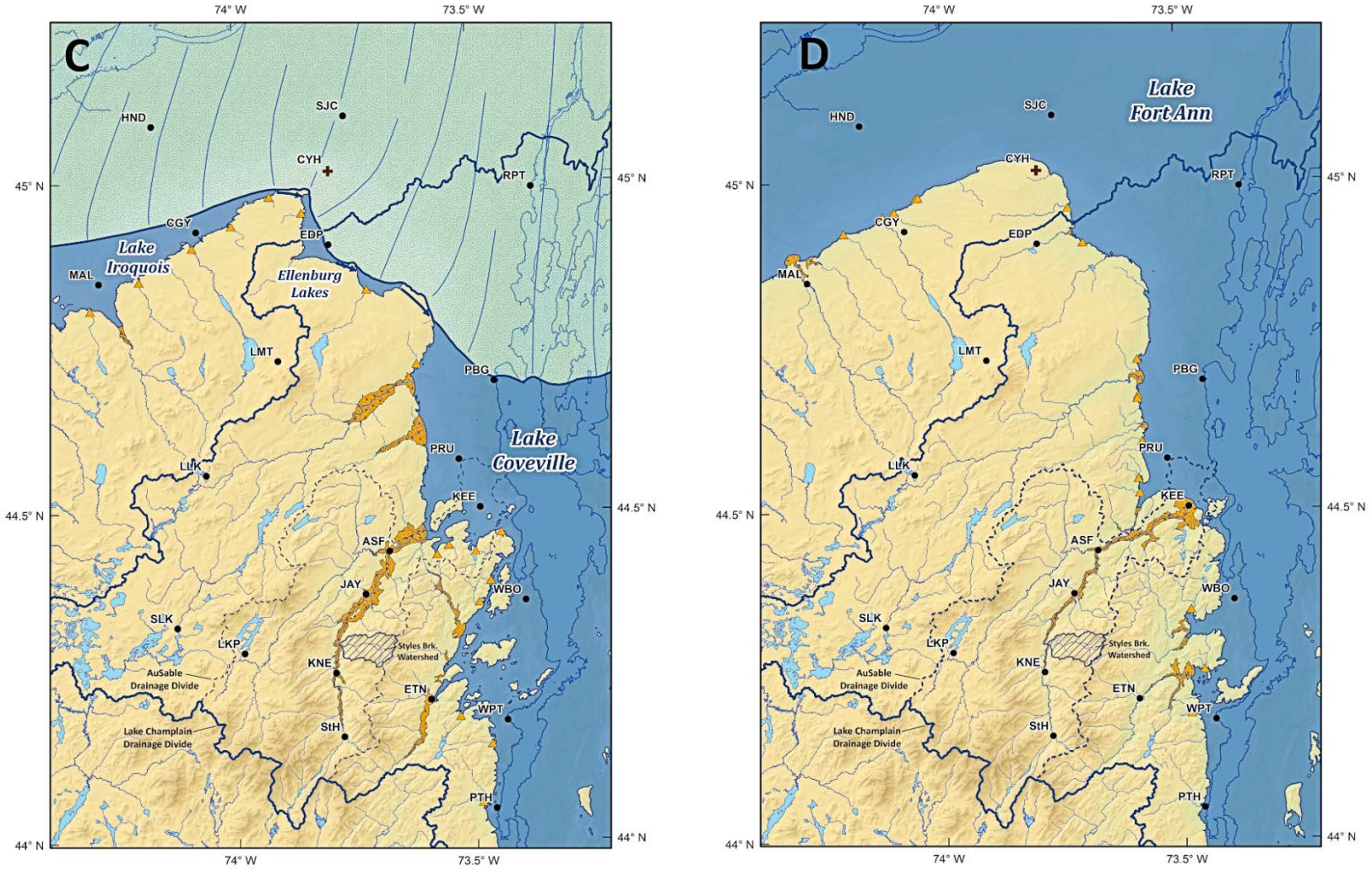

Figure 4 (continued). The Ellenburg–Plattsburgh (4C) ice margin and the lower Fort Ann Phase of proglacial Lake Vermont (4D) in the Champlain and St. Lawrence valleys.

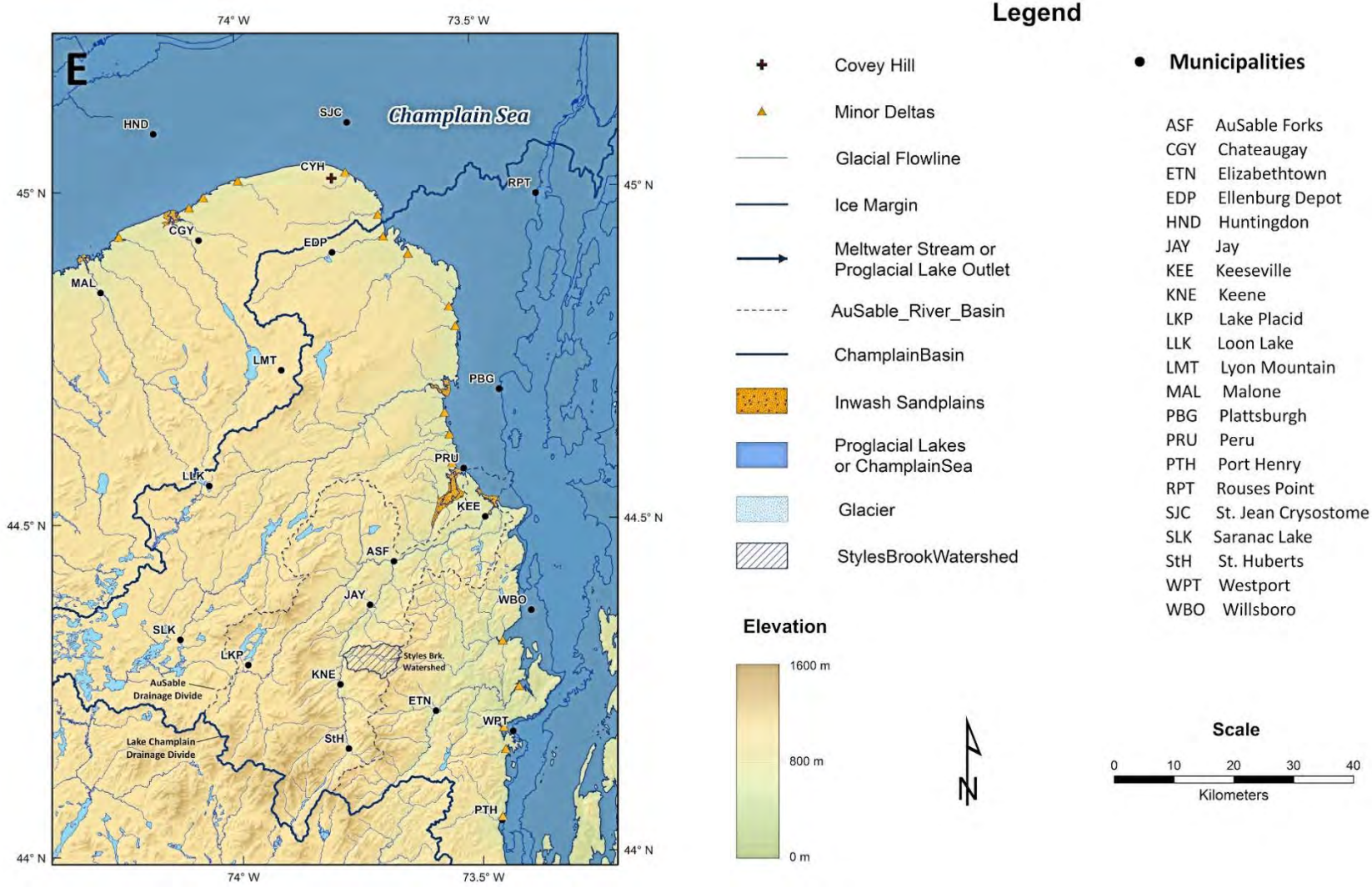

Figure 4 (continued). The Champlain Sea (4E) near the upper-marine limit in the Champlain and St. Lawrence valleys.

Deglaciation in the Ausable Valley

The Ausable River has two principal tributaries, the East and West branches, which originate in the High Peaks south of Lake Placid and Keene Valley (Figure 5). The West Branch Ausable River flows northward from the mountains surrounding South Meadow into the Lake Placid Basin. The river then flows northeastward through Wilmington Notch, where the valley floor drops more than 200 meters in elevation, to its confluence with the East Branch at Au Sable Forks. The East Branch Ausable River is fed by the Ausable Lakes, south of St. Huberts, and flows northward through Keene Valley. Below Au Sable Forks the Ausable River flows northeastward through a broad, gently sloping valley to Keeseville where the river descends approximately 100 meters through Ausable Chasm to its current delta on Lake Champlain.

Deglaciation in the Ausable Valley occurred by the generally synchronous northward recession of active continental ice lobes that blocked local surface drainage and created deep proglacial lakes. These lakes expanded northward with ice recession and drained to lower levels, often by sudden breakout, as lower outlets on the Ausable–Boquet drainage divide were uncovered. The first deglacial chronology for the region was developed by H.L. Alling nearly a century ago (Alling, 1916, 1918, 1920; Kemp and Alling, 1925), although many of the lake stages originally proposed have been abandoned in the light of more recent data or were renamed to reflect the location of their presumed outlets (e.g. Diemer and Franzi, 1988; Franzi, 1992).

Franzi (1992) recognized six proglacial lake stages in the East Branch valley (Figure 6), although this remains a conservative estimate and will likely change as studies in the region continue. The sequence begins with proglacial Lake Boreas in the Ausable Lakes valley south of St. Huberts (Figures 5 and 6), which drained southward across a 615-meter a.s.l. (above sea level) bedrock threshold immediately north of Boreas Pond into the upper Hudson basin (Deimer and Franzi, 1988). Lake Boreas was probably coeval with the proglacial lakes described by Gurrieri and Musiker (1990) near South Meadow in the West Branch Valley. Subsequent lake stages, respectively controlled by cols near Chapel Pond, South Gulf, The Gulf, Colby Mt. and Mud Brook/Trout Pond, occupied portions of both the East Branch and West Branch valleys and drained eastward into the Boquet drainage basin.

The Spruce Hill col (515 meters a.s.l., Figure 5), lies just above the maximum projected shoreline elevation for Lake Chapel, and thus, is not considered to represent an intermediate lake stage between lakes Chapel and South Gulf. Possible westward drainage of proglacial Lake Chapel into the upper West Branch Valley via Wilmington Notch (Alling, 1916; 1918, 1920) is considered unlikely (Diemer and Franzi, 1988). A series of meltwater channels and plunge basins, the latter now occupied by small ponds, on the south side of Wilmington Notch originate above the projected level of Lake Chapel and may record an earlier episode of ice marginal meltwater drainage.

Proglacial lake drainage in the South Meadows area was generally westward (Alling, 1916, 1918, 1920; Gurrieri and Musiker, 1990). However, at least one episode of eastward drainage into Lake Chapel may have occurred via Cascade Lakes col, morphology of which is consistent with that of known outlet channels in the region. This valley originates at a bedrock threshold at 665 meters a.s.l. on the divide between the East and West Branch of the Ausable River, which is nearly the same as the elevation of the Heart Lake threshold which Gurrieri and Musiker (1990) proposed as an outlet for an early South Meadows lake. A deltaic plain immediately south of Owls Head, southwest of Keene (Figure 5), may record outflow from the Cascade Lakes valley when ice in the Keene Valley lay on the north flank of Owls Head. The possible eastward

drainage of proglacial lakes in the South Meadows area to the Keene Valley requires simultaneous retreat of continental ice lobes in the East Branch and West Branch valleys.

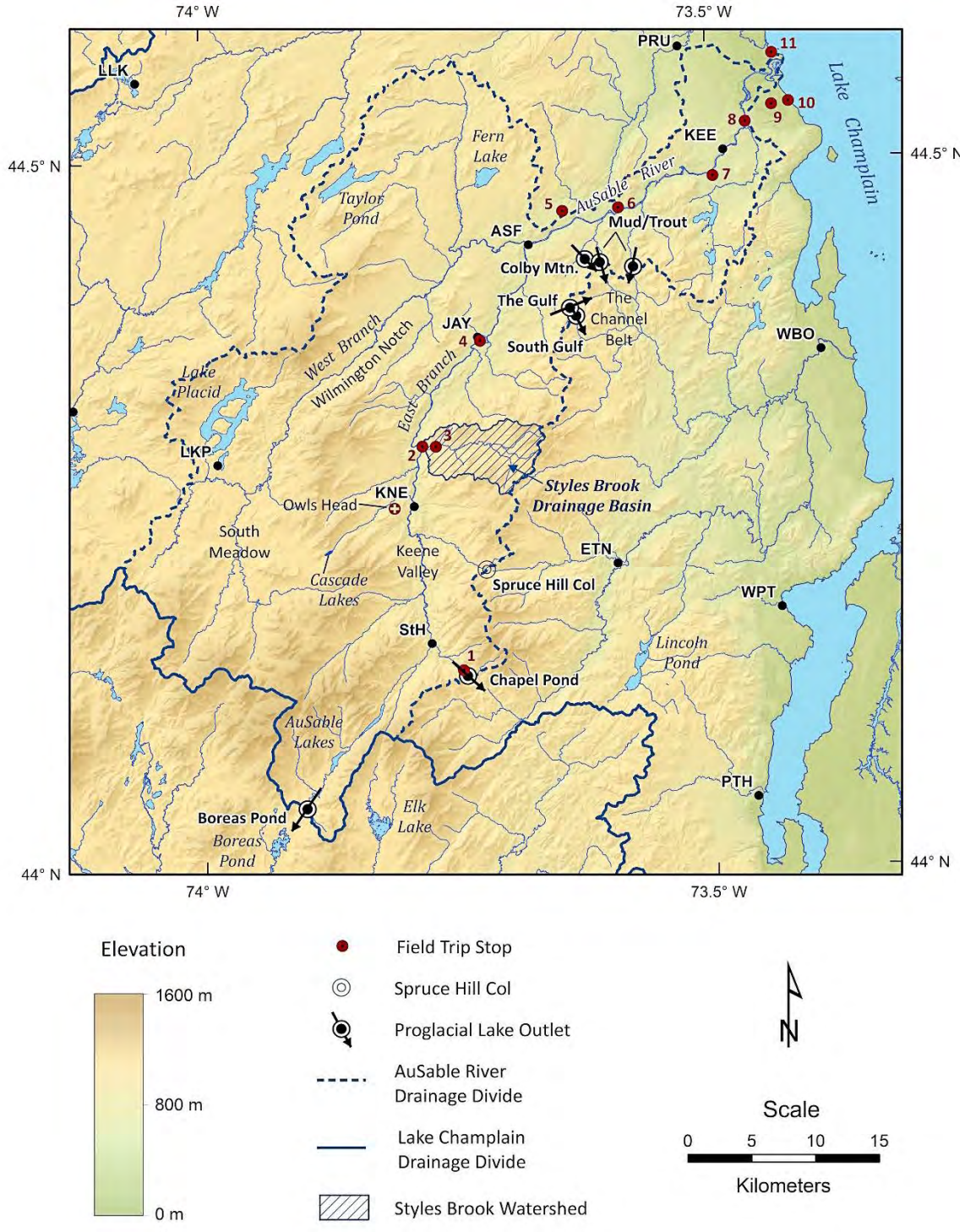

Figure 5. Map of the Ausable River drainage basin, showing the locations of inferred proglacial lake outlets (Franzi, 1992), geographic features and the Styles Brook drainage basin. Cities and towns are keyed to the explanation in Figure 1.

STYLES BROOK VALLEY

Setting and Tropical Storm Irene

Styles Brook is located about 5 km north of Keene and is a major east-bank tributary of the East Branch Ausable River (Figure 5). The basin drains westwards from peaks around 800-1100 meters a.s.l. (Figure 7), which are substantially lower than the highest peaks of the Adirondacks (up to 1629 m) to the south of Keene and Lake Placid. The study area is located along ~2 km of the lower valley where Styles Brook has incised a 20-50 m-deep V-shaped valley during the Holocene into the Pleistocene-age valley fill deposits (Figures 7 and 8). Bedrock is exposed at the downstream end of the study reach and forms a local base level for Holocene fluvial processes in the lower valley.

This area experienced severe flooding during Tropical Storm Irene in 2011. A total of 161 mm of rainfall was recorded near Jay (Figure 5) in a 17-hour period (E. Romanowicz, unpublished data), although anecdotal evidence from local residents who operated manual rain gauges during the event suggests that total precipitation at Styles Brook may have been considerably higher. The U.S. Geological Survey gauge on the East Branch Ausable River at Au Sable Forks recorded a peak stage of 5.64 m, which was 3.51 m above flood stage and 1.01 m above the previous record stage. Debris strand lines and tree scars indicate that lower Styles Brook rose almost 4 m above its low flow level. This extreme flow washed-out NY Route 9N at the mouth of the basin and caused extensive scouring of the streambed and adjacent bluffs in the study reach.

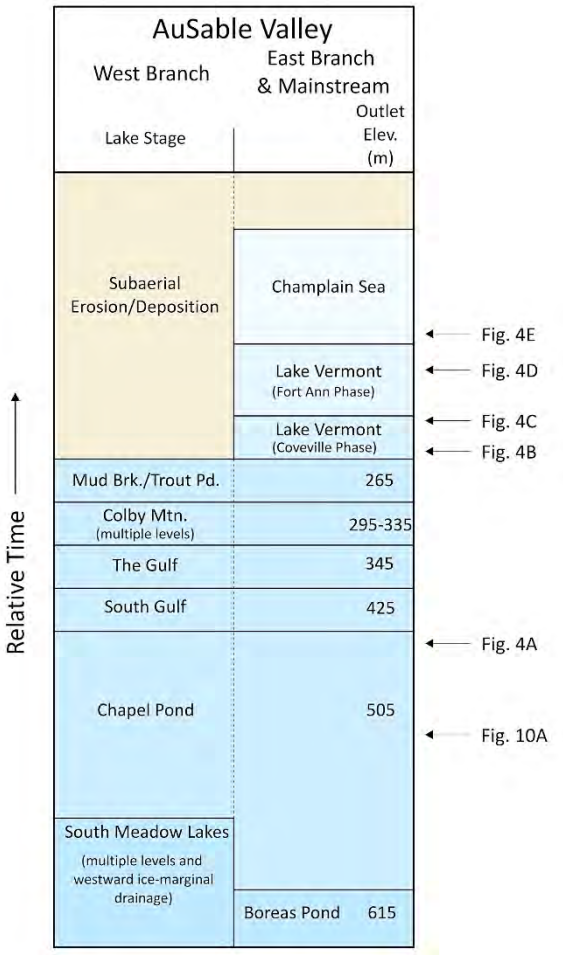

Figure 6. Proglacial lake sequences and outlet elevations in the Ausable Valley (from Franzi, 1992). The approximate time slices for the regional deglacial chronology in figures 4 and 10 are shown to the right of the figure.

Fieldwork was done in the study reach in September and October 2011. *In situ* Pleistocene-age sediments were documented along ~2 km of the lower valley where the recent erosion had created exceptionally fresh exposures of the lower bluffs along the bottom of the stream-incised V-shaped valley.

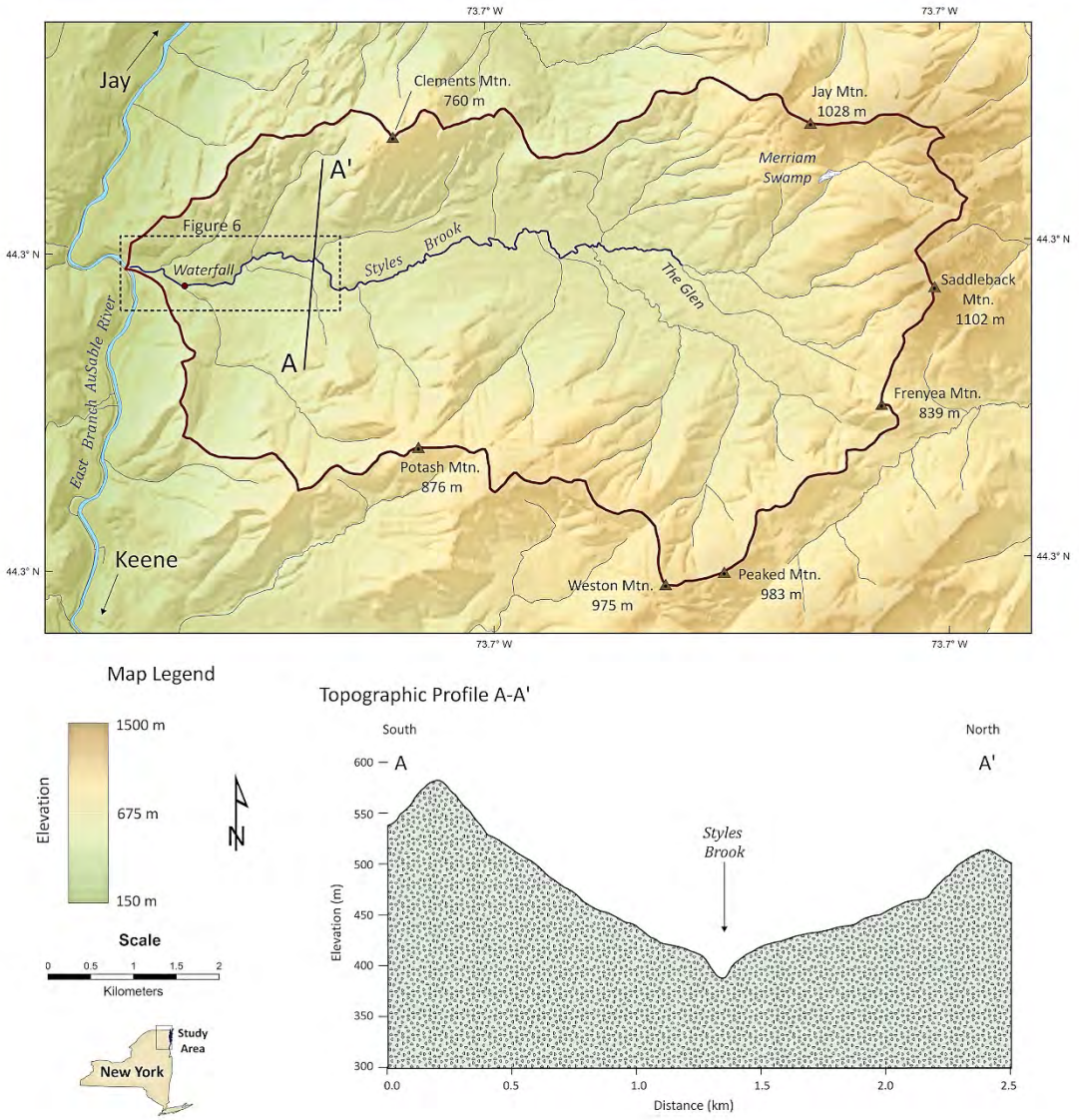

Figure 7. Map of the Styles Brook drainage basin showing the extent of the study area in Figure 8 and a cross sectional topographic profile along line A-A'. Profile has 4 x vertical exaggeration.

Pleistocene Deposits and Ice Margin Reconstruction

Sediments exposed in the study reach included matrix-supported massive diamictons, matrix-supported stratified diamictons, clast-supported diamictons, boulder beds, cobble beds, granule to sandy gravels, ripple cross-bedded and laminated sands and silts, and dropstone-bearing rhythmically bedded sandy silts and clays (Figure 9). Beds were discontinuous along outcrop

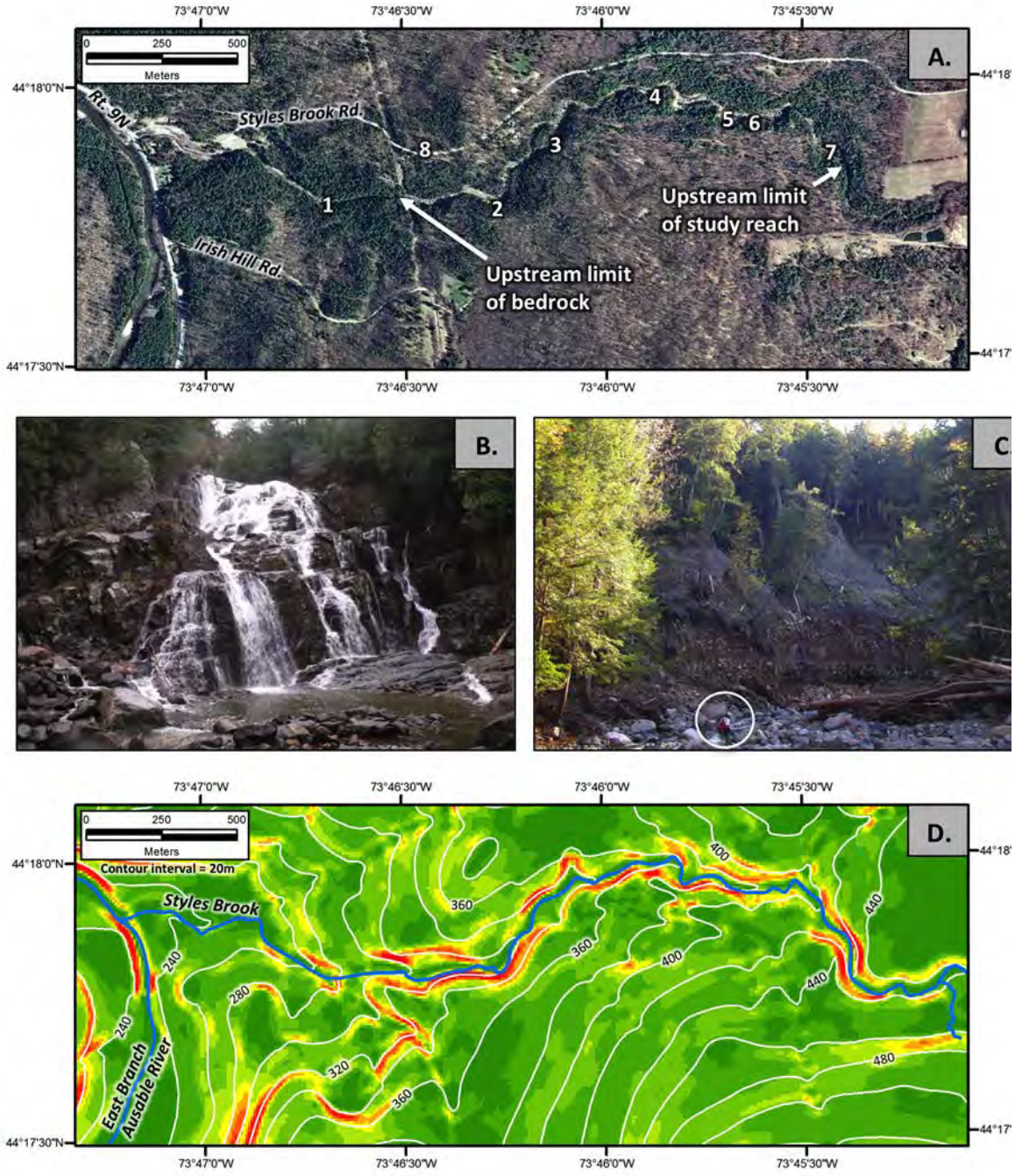

Figure 8. Study area along lower Styles Brook. A) 2013 orthophotograph with site numbers. B) Site 1, waterfall on bedrock. C) Site 2, ~40 m bluff of Pleistocene-age sediments, figure in middle-ground for scale. D) Slope map derived from 10-meter digital elevation model with steepest slopes (35-55°) in red, these steepest slopes adjacent to the channel are the bluffs of Pleistocene-age sediment.

Figure 9. Pleistocene sediments in Styles Brook valley. A) Site 3, laminated silts and sands (Fl) draped over topography of underlying clast-supported boulder bed (Bcm). B) Site 4, clast-supported boulder bed (Bcm) overlain by multiple bedded diamictons (Dms). C) Site 5, deformed clay, silt, and fine sand. D) Site 6, interbedded diamictons (Dms) with 21° dip towards SW. E) Site 6, laminated silts and sands (Fl) overlain by clast-supported boulder bed (Bcm), laminated silts and sands (Fl), and clast-supported diamicton (Dcm). F) Site 6, granule gravel (GRmc) overlain by thinly bedded sands (Sl) and silts (Fl). G) Site 7, silt and clay rhythmites with dropstones.

and generally could be traced laterally for only a few tens of meters. The vertical arrangement of beds was highly variable with fine-grained deposits often interbedded with coarser units (Figure 9E) or draped over the topography of underlying units (Figure 9A). Some fine-grained units were deformed (Figure 9C) and many beds throughout the area showed a dip towards the southwest (Figure 9D). In places, interbedded silts and clays were pervasively sheared and had slickensides at the contact with underlying beds.

We interpret the sediments at sites 2 to 7 (Figure 8A) to have been deposited in a proglacial lake. Finer grained units indicate periods of quiet deposition from the water column while cobble beds and diamictons represent episodic grain flows and subaqueous mass flows along the lake bottom. The deformation of finer units show dewatering and syndepositional movement, and in places this movement was directed towards the southwest down an inferred paleoslope of the lake floor. While some sediment could have originated from an ice-margin to the west or from the headwaters and side slopes of the valley to the east, another source may have been from the low-point on the drainage divide immediately west of Clements Mountain (Figure 7). This saddle on the divide is at the apex of a fan-shaped landform that extends south into the study reach and we infer that the LIS margin stood against the north slope of Clements Mountain and delivered sediment southwards through the saddle while the units at sites 2 to 7 were deposited.

A reconstruction of the LIS margin at the Clements Mountain position is shown in Figure 10. At this time the East Branch Ausable Valley was occupied by proglacial Lake Chapel, which drained southward through the Chapel Pond spillway (505 m) into proglacial Lake Underwood in the Boquet Valley. Clements Mountain was an island in Lake Chapel, which was about 300 meters deep at this time in the area near the modern mouth of Styles Brook valley. This water depth is similar to water depths in front of large lacustrine-calving glaciers in southern Alaska today (e.g. Yakutat Glacier, Trüssel et al., 2013), and so it is likely that the LIS margin in Lake Chapel was similarly calving large tabular icebergs at this time. Clements Mountain and the adjacent ridgeline would have formed a natural pinning point in Lake Chapel for the calving LIS margin, and so it is reasonable to infer that the retreating margin paused at this location during the regional recession.

As the LIS margin subsequently continued to retreat northwards, it uncovered successively lower spillways at South Gulf (425 m) and then The Gulf (345 m). As each spillway opened the lake level in the East Branch Ausable Valley would have dropped in elevation and then stabilized, and lake-marginal streams would have incised through their previous deposits to build new deltas and alluvial plains graded to each new, lower water surface. At Styles Brook the delta for Lake The Gulf is at site 8 (Figure 8A) and has a surface elevation of 346 m. Franzi et al. (2007) suggest retreat rates of about 190 to 440 m/yr for the LIS ice margin in the Champlain Valley during this time; application of these rates to the East Branch Ausable valley gives 45 to 110 years for the ice margin to retreat from the Clements Mountain position to opening of The Gulf spillway (Figure 5).

Implications for a Post-LIS Valley Glacier

Styles Brook is important because it is one of the locations where Craft (1976, 1979) suggested that a local valley glacier formed following retreat of the LIS. Roadwork in 1966 created exposures up to ~10 m high along ~220 m of Styles Brook Road near the junction with Route 9N, and Craft (1976, 1979) interpreted one unit therein as a till. Because this unit was not found on the west side of the East Branch Ausable River, he inferred that the till had been deposited by a

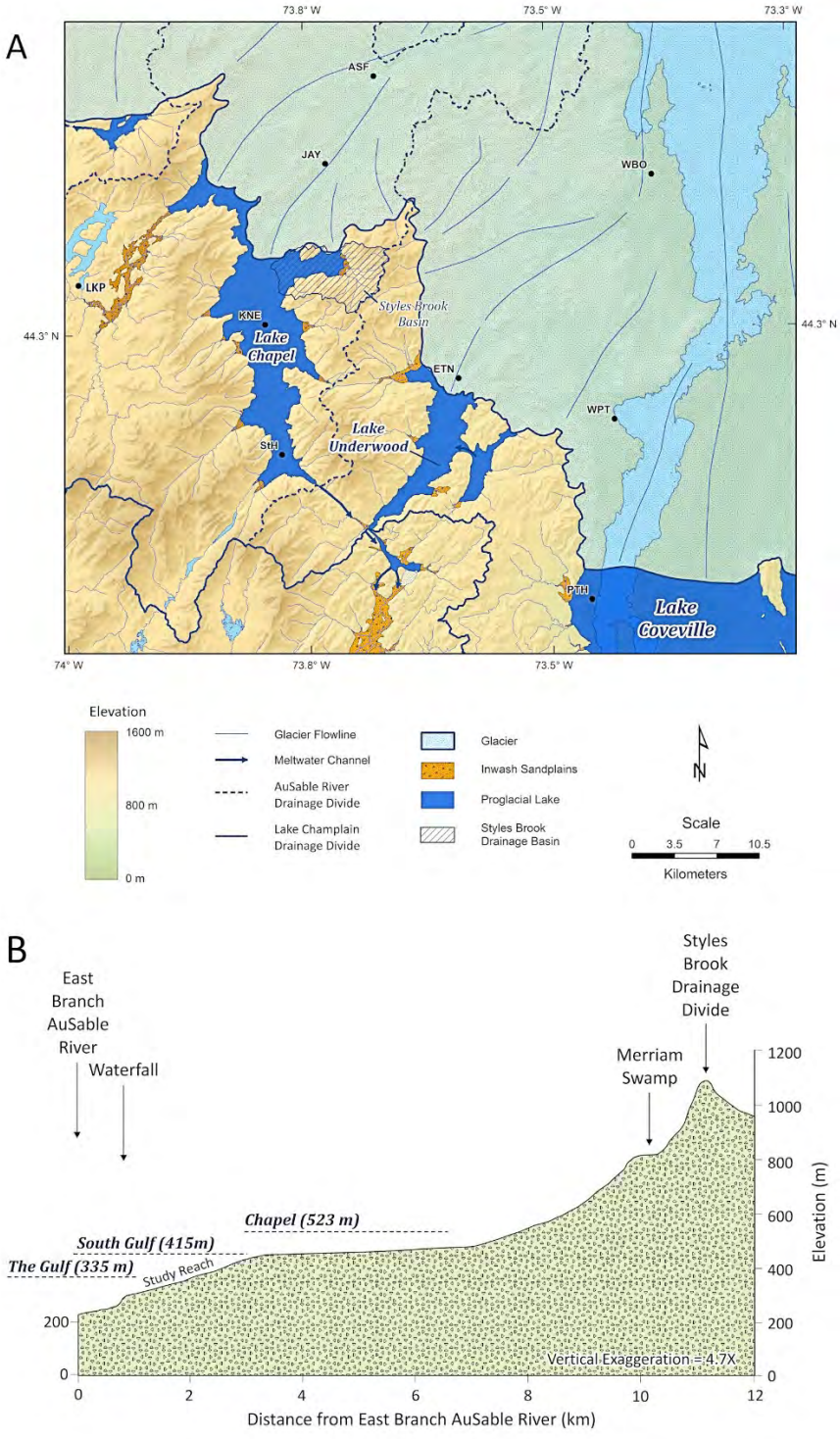

Figure 10. Proglacial lakes at Styles Brook Valley. A) Ice margin reconstruction, Clements Mountain on the north side of Styles Brook Valley is the large island at the ice margin in Glacial Lake Chapel. B) Longitudinal profile of modern Styles Brook valley with projected water levels for lakes in East Branch Ausable River valley.

local valley glacier that extended about 11 km from Jay Mountain and other peaks at the east end of Styles Brook valley (Figure 7).

It is difficult to reconcile this interpretation with our findings. We found proglacial lake deposits in the lowest areas of Styles Brook valley (sites 2 to 7) and these appear to be a conformable sequence up to a proglacial lake delta at the modern land surface (site 8). While arguably there could be a till somewhere within the sediment sequence that we did not observe, the deglacial chronology leaves only decades to perhaps a century for deposition of the proglacial lake sediments and landforms, which is too little time for an 11-km-long valley glacier to form, advance, and retreat in this area. The extant delta at the modern land surface precludes advance of a local valley glacier after drainage of the last proglacial lake. The simplest interpretation is that the sediments and landforms in lower Styles Brook Valley were all deposited close to the LIS margin and in multiple stages of a proglacial lake as the LIS margin retreated, and that no local valley glacier advanced over this site following LIS deglaciation. This conclusion is consistent with the findings of Ackerly (1989), who modeled the putative valley glacier at Styles Brook and found it to be implausible because the ice surface profile projected over the mountains at the head of the valley.

AUSABLE RIVER DELTAS NEAR KEESEVILLE

Evolution of the Champlain Sea Deltas

The principal elements of the following discussion are derived from Denny (1974) who wrote a detailed account of the evolution of the Ausable River delta from the time of the Champlain Sea to its avulsion into its present course.

The Ausable delta at the upper marine limit lies at an elevation of about 107–110 meters a.s.l. and formed a linear delta complex with smaller streams to the northwest (Figure 11A). The Ausable River's upper marine delta lies on top of the Cambrian Potsdam Formation at Ausable Chasm (Field Trip Stop 8), and thus, its construction must predate the cutting of the gorge. Forced regression caused by postglacial isostatic rebound led to incision of the deltaic deposits and underlying bedrock and successive regrading of the delta complex to falling baselevel. The pattern of regrading was interrupted by the exhumation of a bedrock sill (Point A on Figure 11A, see also Figure 28 in Denny (1974)), which inhibited further downcutting and led to the development of a broad floodplain and an elongated meander bend on the Ausable River between the sill and the emerging Ausable Chasm. Incision continued in response to falling baselevel below the sill and the Wickham Marsh basin began to form by vertical and lateral erosion of the deltaic sediments by the Ausable River and its lowermost tributaries. At some point in the process isostatic uplift raised a bedrock sill at St. Jean sur Richelieu in southern Quebec above sea level and the water body in the Champlain Valley transitioned from the saline Champlain Sea to modern freshwater Lake Champlain.

The Ausable River established its present course by channel avulsion near Point B on Figure 11A. Most likely, the avulsion was by a combination of cutbank erosion on the meander near Point A and headward erosion, perhaps enhanced by spring sapping, of gullies in the Dry Mill Valley (Figure 11A). Eventually the low divide composed of older deltaic sediment between the meander bend and Dry Mill valley near Point A was breached, the Ausable River rapidly established its present course and the channel above Wickham Marsh was abandoned (Figure 11B).

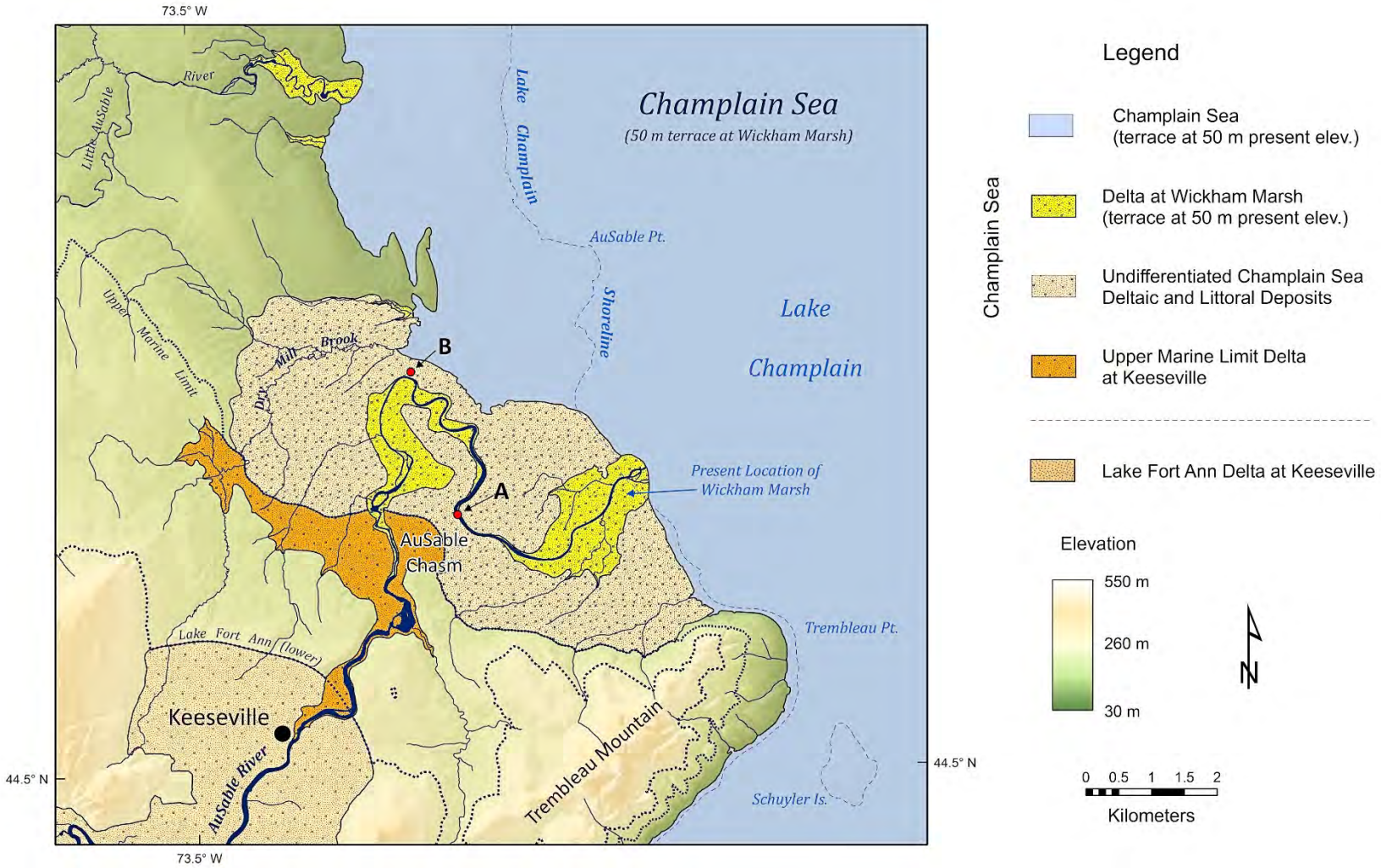

Figure 11A. Map of the Lake Fort Ann and Champlain Sea delta complex at the mouth of the Ausable River near Keeseville (after Denny, 1974). The marine shoreline is drawn at the margin of a deltaic terrace at a present elevation of 50 meters a.s.l. Points A and B are explained in the text.

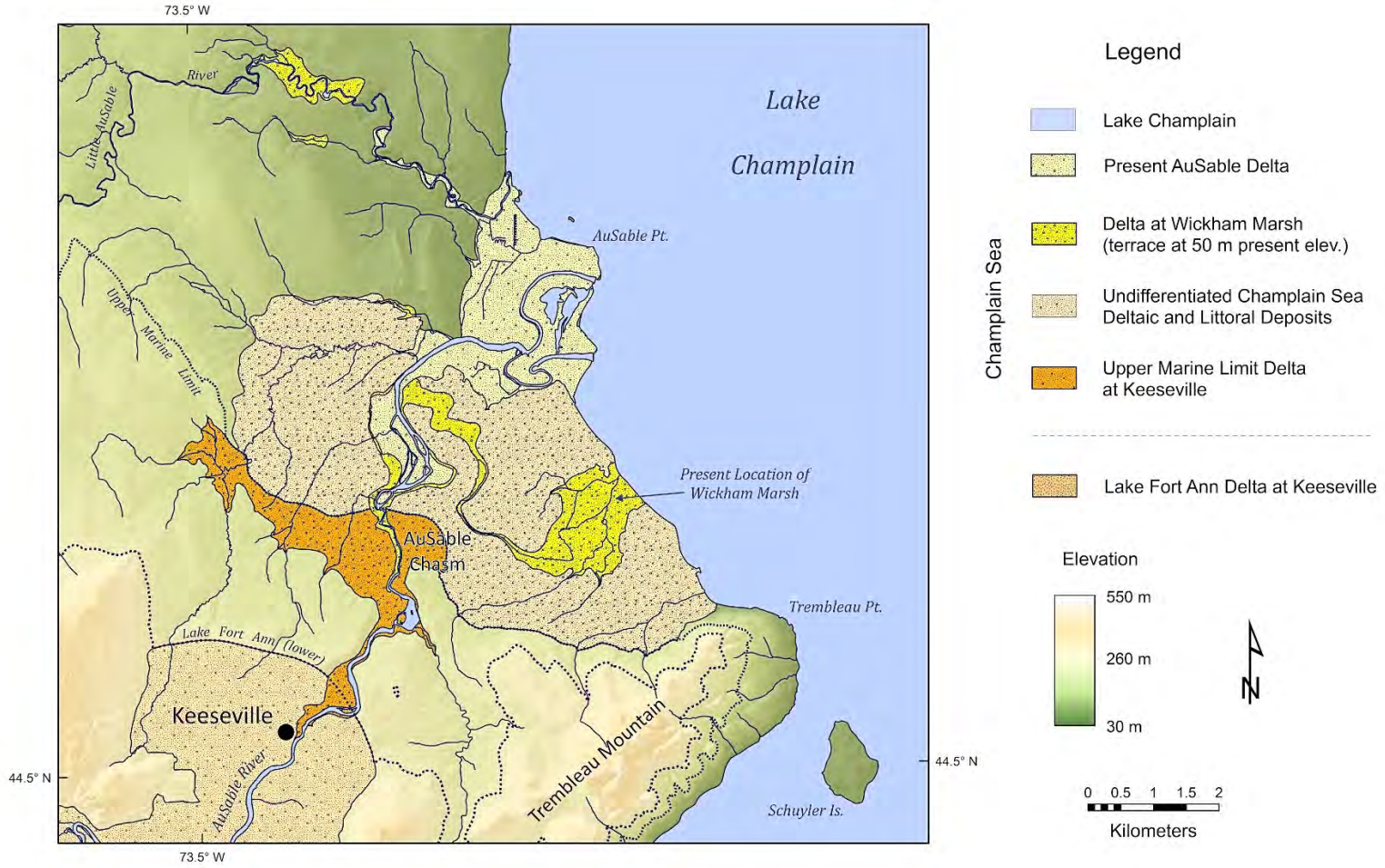

Figure 11B. Map of the modern shoreline of Lake Champlain showing the Lake Fort Ann and Champlain Sea delta complex at the mouth of the Ausable River near Keeseville (after Denny, 1974).

FIELD GUIDE AND ROAD LOG

Meeting Point: Comfort Inn and Suites, 411 West Cornelia Street (NY Route 3).

Alternate Meeting Point: Intersection of US Route 9 and NY Route 73 in New Russia, NY (west of Exit 30 on Interstate 87). Please inform the field trip leaders if you plan to meet the group at this location.

Meeting Point Coordinates: 44.696° N, 73.488° W

Alternative Meeting Point Coordinates: 44.106° N, 73.694° W

Meeting Time: 8:00 AM (approximately 8:45 AM at the alternative meeting point in New Russia)

Distance in miles (km)		
Cumu-lative	Point to Point	Route Description
0.0 (0.0)	0.0 (0.0)	Assemble in the northeastern parking lot of the Comfort Inn and Suites. Leave parking lot, turn left at the entrance and proceed toward Cornelia Street (NY Route 3). Turn left onto Cornelia Street and proceed west for 0.4 miles to the I-87 on-ramp.
0.4 (0.6)	0.4 (0.6)	Intersection I-87 (Northway) and West Cornelia Street; Turn left onto the entrance ramp and follow the signs to I-87 South. Proceed southward on I-87 to Exit 30 in North Hudson, NY (48.5 miles).
48.9 (78.7)	48.5 (78.0)	Intersection I-87 and US 9. Turn right on US Route 9 and proceed west about 2.2 mi (3.5 km) to the intersection with NY Route 73.
51.1 (82.2)	2.2 (3.5)	Intersection of US 9 and NY 73. Bear left onto NY Route 73 and proceed west for approximately 0.2 mi (0.3 km) to arrive at the alternate meeting point, located at a turn-off on the south side of the road.
51.3 (82.5)	0.2 (0.3)	Alternate Meeting Point. Continue west on NY 73 after the group assembles at this stop.
54.9 (88.3)	3.6 (5.8)	Turn left into the Chapel Pond parking area on the south side of NY 73. Stop 1: Chapel Pond.

STOP 1: Chapel Pond, Keene Valley, NY

Location Coordinates: (44.141^{o} N, 73.747^{o} W)

Chapel Pond Pass (elev. 505 meters a.s.l.) served as the outlet for proglacial Lake Chapel. We shall use this scenic spot to present a brief summary of the field trip, regional geography and deglacial lake chronology of the Ausable Valley.

Distance in miles (km)		
Cumu-lative	Point to Point	Route Description
54.9 (88.3)		Return to the vehicles and continue west on NY 73 through the villages of St. Huberts and Keene Valley.
62.2 (100.1)	7.3 (11.7)	Intersection with NY 9N. Continue north on NY 73 and 9N to Keene. The road leading to Norton Cemetery on the right is underlain by reddish brown varved clay that was deposited in proglacial lakes in the East Branch valley.
64.2 (103.3)	2.0 (3.2)	NY Routes 73 and 9N separate in the village of Keene. Follow NY 9N north to Styles Brook.
67.2 (108.1)	3.0 (4.8)	Intersection of NY 9N and Styles Brook Road. Turn right onto Styles Brook Road and proceed east to Stop 2.
67.3 (108.3)	0.1 (0.2)	Stop 2: Styles Brook Mouth, Jay, NY

STOP 2: Styles Brook Mouth, Jay, NY

Location Coordinates: (44.299 º N, 73.785 º W)

We shall stop briefly near the mouth of Styles Brook to discuss Tropical Storm Irene, the damaged it caused, the restoration efforts and natural recovery of the fluvial system. We may also use this opportunity to consolidate vehicles to reduce parking congestion at the next stop.

Distance in miles (km)		
Cumu-lative	Point to Point	Route Description
67.3 (108.3)		Return to the vehicles and continue east on Styles Brook Road for 0.8 mi (1.3 km). Park well off the road for Stop 3.
68.1 (109.6)	0.8 (1.3)	Stop 3: Styles Brook Valley bottom.

STOP 3: Styles Brook Valley Bottom, Jay, NY

Location Coordinates: (44.299 º N, 73.771 º W)

We will access the Styles Brook study area via a trail that crosses private property. Time constraints prevent us from viewing the entire study reach but the flood damage and late Pleistocene sediment exposures at this location are typical.

Distance in miles (km)		
Cumu-lative	Point to Point	Route Description
68.1 (109.6)		Return to the vehicles and return west to NY 9N, approximately 0.9 mi (1.4 km).
69.0 (111.0)	0.9 (1.4)	Intersection of Styles Brook Road and NY 9N. Turn right on NY 9N and travel north for 6.7 mi (10.8 km) to the village of Jay. The town is built on a stream terrace that is graded to the lower Lake Fort Ann delta at Keeseville.
75.7 (121.8)	6.7 (10.8)	Intersection of NY 9N and County Route 82. Turn right onto County Route 82 for 0.6 mi (1.0 km) to Glen Hill/Mill Hill Road.
76.3 (122.8)	0.6 (1.0)	Turn sharply right onto Glen Hill/Mill Hill Road and proceed to the parking lot at the covered bridge in Jay.
76.5 (123.1)	0.2 (0.3)	Stop 4: Jay Covered Bridge, discussions and lunch.

STOP 4: Jay Covered Bridge, Jay, NY; Discussions and Lunch Stop

Location Coordinates: (44.373^{o} N, 73.727^{o} W)

The covered bridge in Jay lies adjacent to a knickpoint formed by a metanorthosite outcrop in the East Branch channel. We shall take advantage of this scenic location to enjoy lunch and discuss our paleogeographic reconstructions and implications of Styles Brook stratigraphy and landforms for alpine glaciation.

Distance in miles (km)		
Cumu-lative	Point to Point	Route Description
76.5 (123.1)		Return to the vehicles and return to NY 9N via Glen Hill/Mill Hill Road and County Route 82 (approximately 0.8 mi (1.3 km)).
77.3 (124.4)	0.8 (1.3)	Intersection of County Route 82 and NY 9N. Turn right on NY 9N and travel northeast 5.9 mi (9.5 km) to the Village of Au Sable Forks.
83.2 (133.9)	5.9 (9.5)	Intersection of NY 9N (Main Street), West Ausable Road, and North Main Street. Continue through the traffic light to North Main Street.
83.4 (134.2)	0.2 (0.3)	Intersection of North Main Street, Silver Lake Road, Palmer Street and Golf Course Road. Continue northeast on Golf Course Road.
85.3 (137.2)	1.9 (3.1)	Intersection of Golf Course Road and Dry Bridge Road. Bear slightly right onto Dry Bridge (no stop in this direction) for 0.2 mi. (0.3 km).
85.5 (137.6)	0.2 (0.3)	Park on the roadside near the intersection of Dry Bridge and Buck Hill roads. Stop 5: Clintonville Pine Barren.

STOP 5: Clintonville Pine Barren, Clintonville, NY

Location Coordinates: (44.464° N, 73.643° W)

The Clintonville pine barren is situated on a large deltaic sandplain built by the Ausable and Little Ausable rivers into an embayment of glacial Lake Coveville in the lower Ausable Valley (Figures 4B and 4C). The Little Ausable River was originally a tributary of the Ausable River but the lowering of glacial Lake Vermont water level to the Fort Ann stage initiated downcutting into the Coveville delta deposits and resulted in its diversion across the Ausable drainage divide to its present course (Figure 4D). The Clintonville pine barren is a fire-dependent ecosystem, consisting primarily of pitch pine with an understory of heath plants that has adapted to the low nutrient and drought-prone soils of the deltaic sandplain.

Distance in miles (km)

Cumu-lative	Point to Point	Route Description
85.5 (137.6)		Return to the vehicles and continue east on Dry Bridge Road for 2.9 mi (4.7 km) to the intersection with Clintonville Road.
88.4 (142.2)	2.9 (4.7)	Intersection of Dry Bridge and Clintonville roads. Take a sharp right onto Clintonville Road and travel south 1.2 mi (1.9 km) to NY 9N.
89.6 (144.2)	1.2 (1.9)	Intersection of Clintonville Road and NY 9N. Carefully turn left at the stop sign and immediately enter a small gravel pit on left, adjacent to NY 9N. Stop 6: Clintonville Stream Terrace Deposits.

STOP 6: Clintonville Stream Terrace Deposits, Clintonville, NY

Location Coordinates: (44.466° N, 73.587° W)

The upper portion of the north face of this small gravel pit exposes about 4m of medium to thickly bedded pebble gravel, sand and minor silt that is part of a stream terrace graded to the lower glacial Lake Fort Ann delta at Keeseville. Individual beds range from about 0.1 to 1.0 meters thick and are traceable for several meters across the exposure. The middle approximately 2–3 meters of the section contains a remarkable set of climbing dunes, the upper and lower bedding surfaces of which dip gently upvalley.

The stream terrace gravel and sand disconformably overlies a discontinuous (0.0–0.7 m thick) layer of reddish brown rhythmically laminated silt and clay (varves). The undisturbed clay section is inaccessible but estimates from photographs indicate that it contains at least 20 silt-clay couplets. The west wall of the pit is oriented perpendicular to the paleocurrent and parallel to the valley slope. The rhythmite section in this exposure is thicker (up to a meter thick) and contains soft sediment deformation and slump structures. The rhythmites are draped over 5–6m of sandy, light brownish gray diamicton. The sandy texture of the diamicton is typical of surface till deposits in the region but is markedly dissimilar to the silty, dark gray diamictons observed in exposures at Styles Brook.

Distance in miles (km)		
Cumu-lative	Point to Point	Route Description
89.6 (144.2)		Return to the vehicles and travel east on NY 9N for 0.2 mi (0.3 km) to the intersection with Lower Road.
89.8 (144.5)	0.2 (0.3)	Turn right onto Lower Road for 0.4 mi (0.6 km) to the bridge across the Ausable River.
90.2 (145.1)	0.4 (0.6)	Turn right onto the bridge and cross the Ausable River (0.1 mi, 0.2 km) to the Dugway Road and Burke Road Intersection.
90.3 (145.3)	0.1 (0.2)	Turn left onto Dugway Road and travel 4.6 mi (7.4 km) east to the intersection with Augur Lake Road.
94.9 (152.7)	4.6 (7.4)	Augur Lake Road Intersection. Turn left onto Augur Lake Road and travel east for 0.2 mi (0.3 km) to Stop 7.
95.1 (153.0)	0.2 (0.3)	Stop 7: Lake Vermont Lacustrine and Deltaic Deposits, Keeseville, NY.

STOP 7: Lake Vermont Lacustrine and Deltaic Deposits, Keeseville, NY.

Location Coordinates: (44.487^{o} N, 73.493^{o} W)

This exposure lies along the south bank of the Ausable River approximately 0.5 mi upstream (south) of the Keeseville Industrial Park (KIP) section that was described by Diemer and Franzi (1988), Franzi et al. (2002) and Franzi et al. (2007) and contains a similar record of lacustrine and deltaic sedimentation. The basal portion of the section consists of approximately 3 meters of dark gray silt and clay rhythmites that probably record pro-deltaic varved clay sedimentation in the Coveville phase of Lake Vermont. Water depth here at this time exceeded 80 meters. Deltaic sedimentation at this site began following the glacial Lake Iroquois breakout when glacial Lake Vermont was lowered to the Fort Ann level. The ice front would have receded about 30 km north to the Cobblestone Hill ice margin over this time interval at an average retreat rate of approximately 0.44 km/yr (Franzi et al., 2007). The locus of deltaic sedimentation shifted nearly 10 km downvalley (eastward) during the breakout (Figures 4C to 4D) from the Coveville-level Clintonville delta at approximately 205 meters a.s.l. to the lower Fort Ann-level delta in Keeseville at approximately 155 meters a.s.l.

The deltaic section at this site exposes approximately 10 meters of lower to middle delta slope foreset and bottomset beds. Excellent examples of ripple-drift cross lamination are commonly exposed.

Distance in miles (km)		
Cumu-lative	Point to Point	Route Description
95.1 (153.0)		Return to the vehicles and continue east on Augur Lake Road for 0.5 mi (0.8 km) over the Adirondack Northway (I-87) to the intersection of US Route 9.
95.6 (153.8)	0.5 (0.8)	Intersection of Augur Lake Road and US 9. Turn left and proceed north for 1.3 mi (2.1 km) through the village of Keeseville to the stoplight at the intersection of US 9 and NY 9N.
96.9 (155.9)	1.3 (2.1)	Intersection of US 9 and NY 9N. Turn right and travel north on US 9 (North Ausable Street) for 1.5 mi (2.4 km) to Stop 8: Ausable Chasm.
98.4 (158.3)	1.5 (2.4)	Stop 8: Ausable Chasm.

STOP 8: Ausable Chasm, Keeseville, NY.

Location Coordinates: (44.525° N, 73.462° W)

Ausable Chasm is a post-glacial gorge cut deeply into the Cambrian-aged Keeseville Member or, to a lesser extent, the Ausable Member of the Potsdam Formation. Landing et al. (2007) note three items of interest in the Cambrian section; 1. the occurrence of scyphomedusae impressions 2. siliciclastic microbial structures and 3. a low-diversity suite of trace fossils. These features are typically restricted to medium to fine grained quartz arenites and rare mudstones in the exposures immediately upstream from the US 9 bridge over the chasm, which are interpreted to represent shallow to emergent littoral sand flat facies (Landing et al., 2007). The scyphomedusae impressions from these outcrops were recently described by Hagadorn and Belt (2008). The outcrops also contain extensive horizontal trackways of *Climactichnites* and *Protichnites* (Landing et al., 2007).

A delta complex built by the Ausable and several smaller streams to the northwest overlie the Potsdam sandstones at this location (Figure 4E) (Denny, 1974; Franzi et al., 2007). Forced regression of the Champlain Sea shoreline accompanied isostatic uplift of the region causing the Ausable River to cut through the unconsolidated deltaic sediments and the underlying Potsdam Formation. Incision through the bedrock was probably accomplished by a combination of gradual incision and knickpoint migration and was influenced by the well-developed joint system in the sandstone, resulting in a rectangular channel pattern through the chasm.

Distance in miles (km)		
Cumu-lative	Point to Point	Route Description
98.4 (158.3)		Return to the vehicles and follow the signage to exit the Ausable Chasm parking lot to NY Route 373.
98.7 (158.8)	0.3 (0.5)	Intersection of exit road and NY 373. Turn left and proceed northwest on NY 373 for 0.2 mi (0.3 km) to the intersection with US 9.
98.9 (159.1)	0.2 (0.3)	Intersection of NY 373 and US 9. Turn right and proceed northeast for 0.8 mi (1.3 km) to the intersection with Giddings Road.
99.7 (160.4)	0.8 (1.3)	Intersection of US 9 and Giddings Road. Turn right and proceed east on Giddings Road for 1.0 mi (1.6 km) to Stop 9.
100.7 (162.0)	1.0 (1.6)	Stop 9: Spring Sapping Channels in Champlain Sea Deltaic Deposits.

STOP 9: Spring Sapping Channels in Champlain Sea Deltaic Deposits.

Location Coordinates: (44.538° N, 73.432° W)

Spring sapping channels like the two at this site are commonplace in the deltaic deposits surrounding Wickham Marsh. In 1985 the heads of these channels were located several tens of meters farther downstream and their headcuts stood 2 meters high with slight to moderate spring flow near their bases. Since then, the channel heads have migrated headward and the height of the headcuts decreased. We shall discuss the significance of spring sapping as a channel-forming process in the Champlain Sea deltaic deposits and its possible role in the channel avulsion that led to the abandonment of the Wickham Marsh delta lobes and the creation of the modern Ausable delta in Lake Champlain (Figures 11A and 11B).

Distance in miles (km)		
Cumu-lative	Point to Point	Route Description
100.7 (162.0)		Return to the vehicles and travel eastward for 0.8 mi (1.3 km) on Giddings Road to Wickham Marsh.
101.5 (163.3)	0.8 (1.3)	Stop 10: Wickham Marsh.

STOP 10: Wickham Marsh.

Location Coordinates: (44.540° N, 73.419° W)

Wickham Marsh is a bayhead wetland on Lake Champlain that is separated from the main waterbody by a barrier beach, although nearly all of the beach is presently buried by a railroad embankment. The marsh's basin was cut as the Ausable River and smaller tributaries adjusted to falling baselevel during the latest stages of the Champlain Sea (Figures 11A and 11B) and possibly early Lake Champlain (Denny, 1974). Spring sapping might have contributed to the development of the tributary stream networks. The lowest deltaic terrace presently lies about 4

meters below the level of Lake Champlain and represents the last deltaic surface formed before the avulsion of the Ausable River to its present course.

Distance in miles (km)		
Cumu-lative	Point to Point	Route Description
101.5 (163.3)		Return to the vehicles and backtrack southwest for 1.8 mi (2.9 km) on Giddings Road to US 9.
103.3 (166.2)	1.8 (2.9)	Intersection of Giddings Road and US 9. Turn right on US 9 and head north for 3.2 mi (5.1 km) to the Ausable Point State Park entrance.
106.5 (171.4)	3.2 (5.1)	Turn right into Ausable Point State Park on Ausable Point Road. Proceed 0.9 mi (1.4 km) to the parking lot at Stop 11: Ausable Delta on Lake Champlain.
107.4 (172.8)	0.9 (1.4)	Stop 11. Ausable Delta on Lake Champlain.

STOP 11: Ausable Delta on Lake Champlain.

Location Coordinates: (44.571° N, 73.429° W)

This scenic spot provides an opportunity to conclude the trip on the modern Ausable delta and summarize the deglacial history of the region.

Distance in miles (km)		
Cumu-lative	Point to Point	Route Description
107.4 (172.8)		Return to the vehicles and backtrack northwest for 0.9 mi (1.4 km) on Ausable Point Road to US 9.
108.3 (174.3)	0.9 (1.4)	Intersection of Ausable Point Road and US 9. Turn left and proceed south on US 9 for 0.5 mi (0.8 km) to Bear Swamp Road.
108.8 (175.1)	0.5 (0.8)	Turn right onto Bear Swamp and head west for 2.8 mi (4.5 km) toward the intersection of Bear Swamp Road and I-87.
111.6 (179.6)	2.8 (4.5)	Intersection of Bear Swamp Road and I-87. Turn right onto the northbound entrance ramp of I-87 and proceed 7.7 mi (12.4 km) to Exit 37.
119.3 (192.0)	7.7 (12.4)	Take Exit 37 and follow the signage to the Comfort Inn and Suites.
		END OF ROAD LOG

REFERENCES CITED

Ackerly, S.C., 1989, Reconstructions of mountain glacier profiles, northeastern United States: Geological Society of America Bulletin, v. 101, p. 561-572.

Alling, H.L., 1916, Glacial lakes and other glacial features of the central Adirondacks: Bulletin of the Geological Society of America, v. 27, p. 645-672.

Alling, H.L., 1918, Pleistocene Geology, in Miller, W.J., Geology of the Lake Placid Quadrangle: New York State Museum Bulletin, no. 211/212, p. 71-95.

Alling, H.L., 1920, Glacial Geology, in Kemp, J.F., Geology of the Mount Marcy Quadrangle, Essex County, New York: New York State Museum Bulletin, no. 229/230, p. 62-84.

Barclay, D.J., 1993, Late Wisconsinian local glaciation in the Adirondack High Peaks region, New York: B.Sc. thesis, University of East Anglia, United Kingdom, 77 p.

Benn, D.I. and Hulton, N.R.J., 2010, An Excel™ spreadsheet program for reconstructing the surface profile of former mountain glaciers and ice caps: Computers and Geosciences, v. 36, p. 605-610.

Boothroyd, J.C. and Ashley, G.M., 1975, Process, bar maprphology, and sedimentary structures on braided outwash fans, northeastern Gulf of Alaska, in Jopling, A.V. and MacDonald, B.C. (Eds.), Glaciofluvial and Glaciolacustrine Sedimentation: SEPM, Special Publication N0. 23, p. 193-222.

Chapman, D.H., 1937, Late-glacial and postglacial history of the Champlain Valley: American Journal of Science, 5th Ser., v. 34, p. 89-124.

Craft, J.L., 1969, Surficial geology and geomorphology of Whiteface Mountain and Keene Valley, in New York State Geological Association 40th Annual Meeting, Field Trip Guidebook: New York State Geological Association, p. 135-137.

Craft, J.L., 1976, Pleistocene local glaciation in the Adirondack Mountains, New York: Ph.D. dissertation, The University of Western Ontario, London, Ontario, Canada, 226 p.

Craft, J.L., 1979, Evidence of local glaciation, Adirondack Mountains, New York: 42nd Reunion of the Northeast Friends of the Pleistocene, 75 p.

Davis, P.T., 1999, Cirques of the Presidential Range, New Hampshire, and surrounding alpine areas in the northeastern United States: Géographie Physique et Quaternaire, v. 53, p. 25-45.

Denny, C.S., 1974, Pleistocene geology of the northeastern Adirondack region, New York: U.S. Geological Survey Professional Paper 786, 50 p.

Diemer, J.A. and Franzi, D.A., 1988, Aspects of the glacial geology of Keene and lower Ausable valleys, northeastern Adirondack Mountains, New York, in Olmsted, J.F. (Ed.), New York State Geological Association Field Trip Guidebook, 60th Annual Meeting, Plattsburgh, NY, p. 1-27.

Fairchild, H.L., 1913, Pleistocene geology of New York I: Science, v.37, p. 237-249.

Fairchild, H.L., 1932, New York moraines: Bulletin of the Geological Society of America, v. 43, p. 627-662.

Franzi, D.A., 1992, Late Wisconsinan lake history in the Ausable and Boquet valleys, eastern Adirondack Mountains, New York: New York State Museum Open File Report 2M-127, p. 54-62.

Franzi, D.A., Rayburn, J.A., Yansa, C.H. and Knuepfer, P.L.K., 2002, Late glacial water bodies in the Champlain and Hudson lowlands, New York, in New York State Geological Association-New England Intercollegiate Geological Conference Joint Annual Meeting Guidebook: p. A5 1–23.

Franzi, D.A., Rayburn, J.A., Knuepfer, P.L.K. and Cronin, T.M., 2007, Late Quaternary history of northeastern New York and adjacent parts of Vermont and Quebec: 70th Reunion of the Northeast Friends of the Pleistocene, Plattsburgh, New York, 73 p.

Goldthwait, R.P., 1970, Mountain glaciers of the Presidential Range in New Hampshire: Arctic and Alpine Research, v. 2, p. 85-102.

Gurrieri, J.T. and Musiker, L.B., 1990, Ice margins in the northern Adirondack Mountains, New York: Northeastern Geology, v.12, p. 185-197.

Hagadorn, J.W. and Belt, E.S., 2008, Stranded in upstate New York: Cambrian Scyphomedusea from the Potsdam Sandstone: Palaios, V.23, p.424-441.

Johnson, D.W., 1917, Date of local glaciation in the White, Adirondack, and Catskill mountains: Bulletin of the Geological Society of America, v. 28, p. 543-552.

Kemp, J.F. and Alling, H.L., 1925, Geology of the Ausable Quadrangle: New York State Museum Bulletin, no. 261, 126 p.

Kranitz, R., Farrow, T., Katz, C. and Franzi, D.A., 2014, Reconstructing late Pleistocene paleogeography and sedimentary environments in northeastern New York using geographic information systems: Geological Society of America, Abstracts with Programs, v. 46, no. 2, p. 47.

Landing, E., Franzi, D.A., Hagadorn, J.W., Westrop, S.R., Kröger, B., and Dawson, J.C., 2007, Cambrian of East Laurentia—Field workshop in eastern New York and Vermont, *in* Landing, E., (ed.), Ediacaran–Ordovician of east Laurentia, S.W. Ford Memorial Volume: New York State Museum Bulletin 510, p.25–71.

Ogilvie, I.H., 1902, Glacial phenomena in the Adirondack and Champlain Valley: Journal of Geology, v. 10, p. 397-412.

Pair, D., Karrow, P.F. and Clark, P.U., 1988, History of the Champlain Sea in the central St. Lawrence Lowland, New York, and its relationship to water levels in the Lake Ontario basin, in Gadd, N.R., (Ed.), The Late Quaternary development of the Champlain Sea basin: Geological Association of Canada, Special Paper 35, p. 107–123.

Rayburn, J.A., 2004, Deglaciation of the Champlain Valley, New York and Vermont, and its possible effects on North Atlantic climate change: unpublished PhD dissertation, Binghamton University, Binghamton, New York, 158 p.

Rayburn, J.A., Knuepfer, P.L.K. and Franzi, D.A., 2005, A series of Late Wisconsinan meltwater floods through the Hudson and Champlain Valleys, New York State, USA: Quaternary Science Reviews, v. 24, p. 2410-2419.

Rayburn, J.A., Franzi, D.A., Knuepfer, P.L.K., 2007, Evidence from the Lake Champlain Valley for a later onset of the Champlain Sea and implications for late glacial meltwater routing to the North Atlantic: Palaeogeography, Palaeoclimatology, Palaeoecology, v. 246, p. 62-74.

Schilling, D.H. and Hollin, J.T., 1981, Numerical reconstructions of valley glaciers and small ice caps, In Denton, G.H. and Hughes, T.J. (Eds.), The Last Great Ice Sheets. Wiley, New York, p. 207–220.

Trüssel, B.L., Motyka, R.J., Truffer, M. and Larsen, C.F., 2013, Rapid thinning of lake-calving Yakutat Glacier and the collapse of the Yakutat Icefield, southeastern Alaska, USA: Journal of Glaciology, v. 59, p. 149-161.

Waitt, R.B. and Davis, P.T., 1988, No evidence for post-ice sheet cirque glaciation in New England: American Journal of Science, v. 288, p. 495-533.

NON-POINT SOURCE POLLUTION IN THE LITTLE CHAZY RIVER OF NEW YORK

ROBERT D. FULLER AND DAVID A. FRANZI
Center for Earth and Environmental Science, State University of New York, Plattsburgh, NY 12901

STEVEN KRAMER AND ERIC YOUNG
Miner Agricultural Research Institute, Chazy, NY 12921

INTRODUCTION

The Little Chazy River watershed (Fig. 1) drains into Lake Champlain, which is an oligotrophic to mesotrophic water body with low to moderate levels of phosphorus and nitrogen, the primary nutrients for primary productivity and principal determinants for associated water quality issues. Major sources of nutrients in Lake Champlain include point sources such as municipal sewage treatment plants and non-point sources including urban runoff and agricultural inputs. Extensive dairy operations in the Lake Champlain basin produce large quantities of manure, which is applied back to soils and can potentially become a major source of nutrients to nearby surface waters (Fig. 2). Consequently, reduction of nutrient inputs to Lake Champlain, which promotes healthy and diverse aquatic ecosystems and provides for sustainable human use and enjoyment of the lake, is a priority.

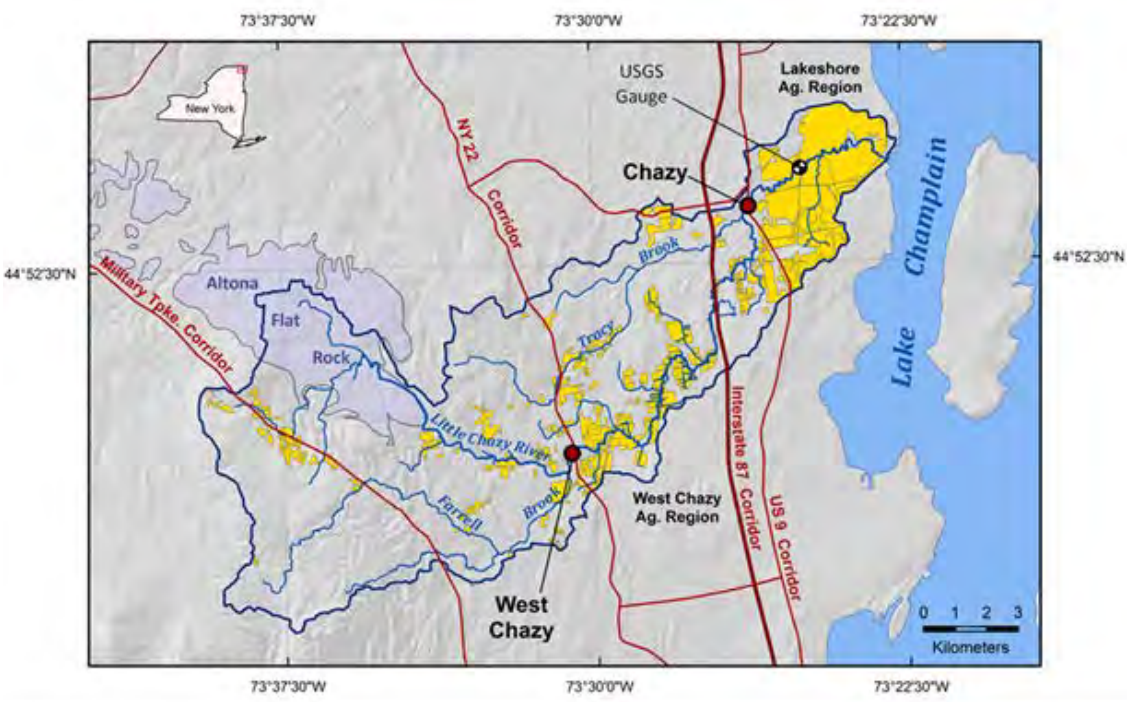

Figure 1. Map of northeastern New York, showing the distributions of agricultural land (yellow shading) and sandstone pavements or "Flat Rocks" (purple shading) in the Little Chazy River watershed. The Flat Rocks extent is from maps by Denny (1974). The figure is from Oetjen et al. (2012).

SUNY Plattsburgh and the William H. Miner Agricultural Research Institute (Miner Institute) used a high-resolution monthly synoptic water-sampling strategy to examine the spatial and downstream distribution of nutrient concentrations (i.e. nitrate-N, total phosphorus and soluble reactive phosphorus) in the Little Chazy River and its principal tributaries for five full years between January 2008 and December 2012 (Fig. 1). The Little Chazy River watershed is typical of medium-sized (basin area = 145 km^2), rural watersheds in the region, possessing a broad range of watershed issues and concerns reflected throughout the Champlain lowlands. Agriculture accounts for approximately 17% of land cover in the watershed, compared to approximately 24% of land cover county-wide, most of which is concentrated near the lake shore east of Chazy village. The watershed was identified on the 1996 Lake Champlain Basin Waterbody Inventory/Priority Waterbodies List Report as a class C river with possible impaired fish survival (NYSDEC, 2001). Karim (1997) cited on-site septic problems, particularly in Chazy and West Chazy, and high levels of livestock and crop agriculture as water pollution concerns in the watershed. The Little Chazy River has the highest median nutrient concentrations and median unit nutrient load (nutrient load per unit area of watershed) of any New York tributary to Lake Champlain that is monitored as part of the Lake Champlain Long-term Water Quality and Biological Monitoring Program (Vermont DEC and New York DEC, 2002).

Figure 2. Agricultural tributary entering the Little Chazy River 23 km from the mouth at Lake Champlain. Many of these tributaries receive inputs from tile-drained fields supporting dairy operations with attendant applications of manure solids and liquids.

Geological Setting: The Little Chazy River originates in upland forests in the northeastern foothills of the Adirondack Mountains and flows eastward through the Champlain lowland to its mouth at Lake Champlain. It has two principal tributaries, Farrell Brook (basin area = 27 km^2)

and Tracy Brook (basin area = 25 km^2). The headwater region is a predominantly forested area of moderate relief (<400 m) that is underlain by thin glacial soils (generally <3m thick), Cambrian clastic sedimentary rocks and high-grade Mesoproterozoic metamorphic rocks. This region (Fig. 1) includes a large area of exposed sandstone bedrock, or sandstone pavement, known locally as Altona Flat Rock (Franzi and Adams, 1993). Mainstream gradient in the headwater region commonly exceeds 10 m/km (Fig. 3).

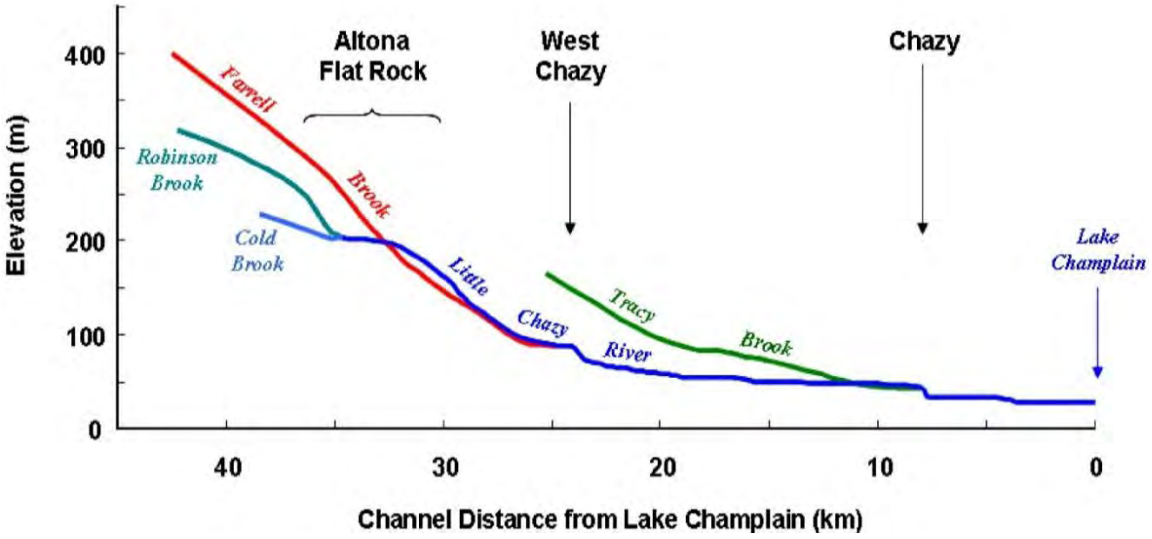

Figure 3. Stream profiles for the Little Chazy River and its principal tributaries.

The river descends steeply through dense headwater woodlands to the Champlain lowland and flows through a patchwork of forested and agricultural lands before emptying into Lake Champlain. The Champlain lowland is underlain by thick glacial, glacial-lacustrine, and glacial-marine sediments, and lower Paleozoic sedimentary rocks. Local relief in the lowland is generally less than 100 m and the mainstream channel gradient averages approximately 1 m/km. Prominent knickpoints (locations where stream gradient increases abruptly) on the Little Chazy River occur in the lowland portion of the watershed at the villages of Chazy and West Chazy (Fig. 2), where the river flows across bedrock obstructions. Dams at Route 9 and the Fiske Road in the village of Chazy create consecutive narrow, nearly sediment-filled impoundments that extend roughly 6 km upstream from Route 9. Other flow-control structures in the watershed include a series of small dams or weirs that extend downstream from Lake Alice on Tracy Brook to the Village of Chazy and abandoned dams, either flood damaged or otherwise compromised, on the Little Chazy River at West Chazy and two large dams at Altona Flat Rock. Most of the flow-control structures in the watershed date to the early 20th century when William H. Miner constructed several hydroelectric projects in the region (Dawson et al., 1981; Landing et al., 2007).

ANALYTICAL METHODS

Stream Hydrology: SUNY Plattsburgh and Miner Institute monitored river height, water temperature and logger temperature at 13 stream gaging stations (Fig. 4); four stations on Tracy Brook (TROSS, LKALI, LKALO and TB87), one station at the mouth of Farrell Brook (DENO) and

eight stations on the main channel of the Little Chazy River below Miner Dam (MDAM, NEPH, GUEST, LANG, CHALIZ, WOOD, LC87 and CHAZY). All SUNY/Miner stations were equipped with Tru-Trac WT-HR water height (stage) dataloggers. Stream discharge records for the U.S. Geological Survey (USGS) gauging station near the river mouth east of Chazy (USGS) were obtained from the USGS website (http://waterdata.usgs.gov/ny/nwis/uv/?site_no=04271815). The USGS stream gage operated through the winter season and records are available from Water Year 1990 to November 2014.

Water Quality Sampling: Synoptic sampling involves the collection of closely spaced water samples in a short time period (generally less than four hours) to provide a snapshot of nutrient concentrations (nitrate-N, total phosphorus and soluble reactive phosphorus) and loadings throughout the watershed (Fig. 4). Sample spacing along the mainstream, tributaries and other inflows varied with accessibility and land use. Channel distance between samples varied from more than 5 km in forested upland regions to a few hundred meters in villages or agricultural lands where anthropogenic inputs such as ditches and drains are more common.

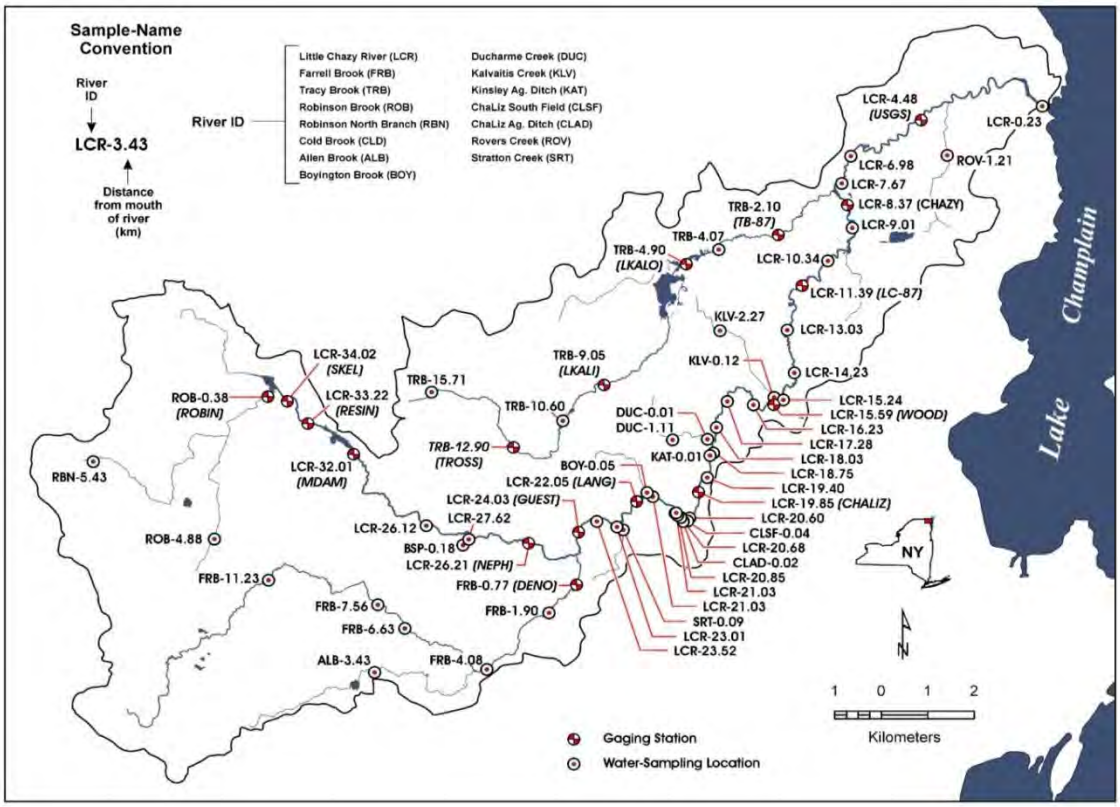

Figure 4. Locations for stream gaging stations and water-quality sampling stations used in this study.

Water Quality Analysis: Water samples were collected in acid-washed, 500 ml polyethylene bottles within a period of approximately four hours to minimize temporal variations in nutrient concentrations. At the end of the collection period, samples were transported to the lab in coolers within a period of one hour and immediately split into two fractions; one which was filtered through a 0.47µ membrane filter to remove particulates and the other left unfiltered. Filtered subsamples were analyzed for nitrate using a Dionex Ion Chromatograph with conductimetric detection and colorimetrically for soluble-reactive phosphorus (primarily

phosphate) using a UV-Vis spectrophotometer with the ascorbic acid method (APHA, 1998). For total phosphorus, unfiltered water samples were digested using potassium persulfate in sulfuric acid on a block digester (APHA, 1998), followed by analysis for soluble-reactive phosphorus.

High-Resolution Temporal Sampling: A high-resolution temporal sampling strategy was used to evaluate the temporal distribution of nutrient concentrations at the USGS gaging station (Fig. 4) through three sequential runoff events in October 2010. Sampling interval varied from 3-4 hours during the initial phases of the rainfall events to >24 hours during periods of prolonged baseflow. In order to relate flow to instantaneous nutrient loading for each event, a system was developed to make each parameter (time, flow and load) dimensionless relative to its maximum value.

Dimensionless time = $t/t_{peak\ flow}$

Dimensionless discharge = Q/Q_{peak}

Dimensionless load = L/L_{peak}

Where t = time, Q = discharge in m^3/sec and L = Load in Kg/day.

RESULTS and DISCUSSION

Spatial Variability in Water Quality

Mainstream Nitrate, Total Phosphorus and Soluble Reactive Phosphorus concentrations in headwater forests were typically low (< 1 mg/L NO_3-N,< 10 µg/L P) and increased substantially upon entering lowland agricultural regions (Figs. 5A and 5B). Occasional abrupt increases in nitrate concentrations (Fig. 5A) within the agricultural areas may be attributed to high concentrations in inputs from agricultural ditches or tiles, but this trend was not consistent due to the low discharges measured in many of these tributaries. Nitrate-N concentrations generally leveled off at 0.4-0.5 mg/L in the agricultural area between West Chazy (Lang) and Chazy and actually decreased in two small, narrow impoundments in the village of Chazy. Decreases in nitrate concentration in the impoundment is most likely due to dilution, conversion to more chemically reduced forms, or sequestration in algae, aquatic macrophytes and sediments, particularly during the growing season. Nutrient concentrations increased substantially in the 7 km-long reach between the village of Chazy and Lake Champlain, where the river traverses a low-relief, intensively managed agricultural area developed on relatively deep glacial-marine soils. The Chazy wastewater treatment facility is also located in this reach, however little change was found in nutrient concentrations above and below its discharge.

Phosphorus (total phosphorus and soluble-reactive phosphorus) (Fig. 5B) concentrations also increased downstream, but with a pattern different from nitrate. Concentrations increased only slowly through the central portion of the watershed, with the largest increases occurring in the bottom reach, as with nitrate. Phosphorus concentrations also exhibited substantially more temporal variability; an effect of variable manure applications, overland transport during storm events or possibly measurement errors associated with relatively low phosphorus concentrations (10-100 µg/L).

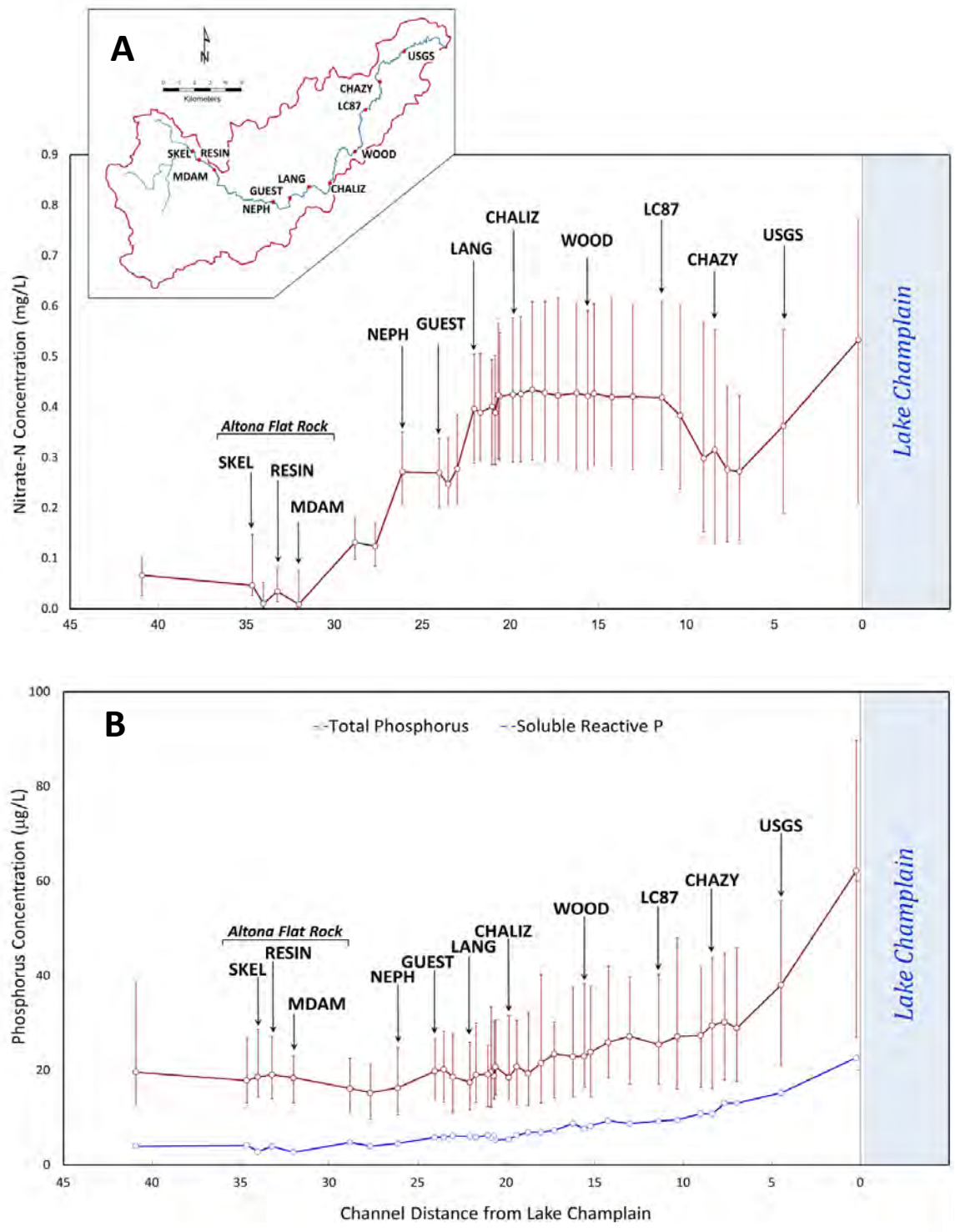

Figure 5. Box plots showing the longitudinal variability of median monthly nitrate-N (A), total P (B) and Soluble Reactive P (B) along the main channel of the Little Chazy River (error bars for nitrate-N and total phosphorus show 25th to 75th percentile range; n=62 for each point, except Altona Flat Rock headwater samples with sporadic flow).

Soluble Reactive P (largely free phosphate) comprised on average 31.4 +/- 6.9% (mean +/- S.D.) of Total Phosphorus concentrations, but increased from roughly 20% in the headwaters, to as high as 45% in the lower reaches (Fig. 6). Indeed, the increases in total P concentrations downstream are largely driven by increases in soluble reactive P, the form most available to aquatic biota. Large increases in nutrient concentrations in the lowermost reaches of the Little Chazy River, especially phosphorus (Fig. 5B), may be related to not only the large areal extent of agriculture in the lower reaches of the watershed (Fig. 1) but also to large areas of surface-drained agricultural fields near the lake that potentially contribute to overland flow from manured fields.

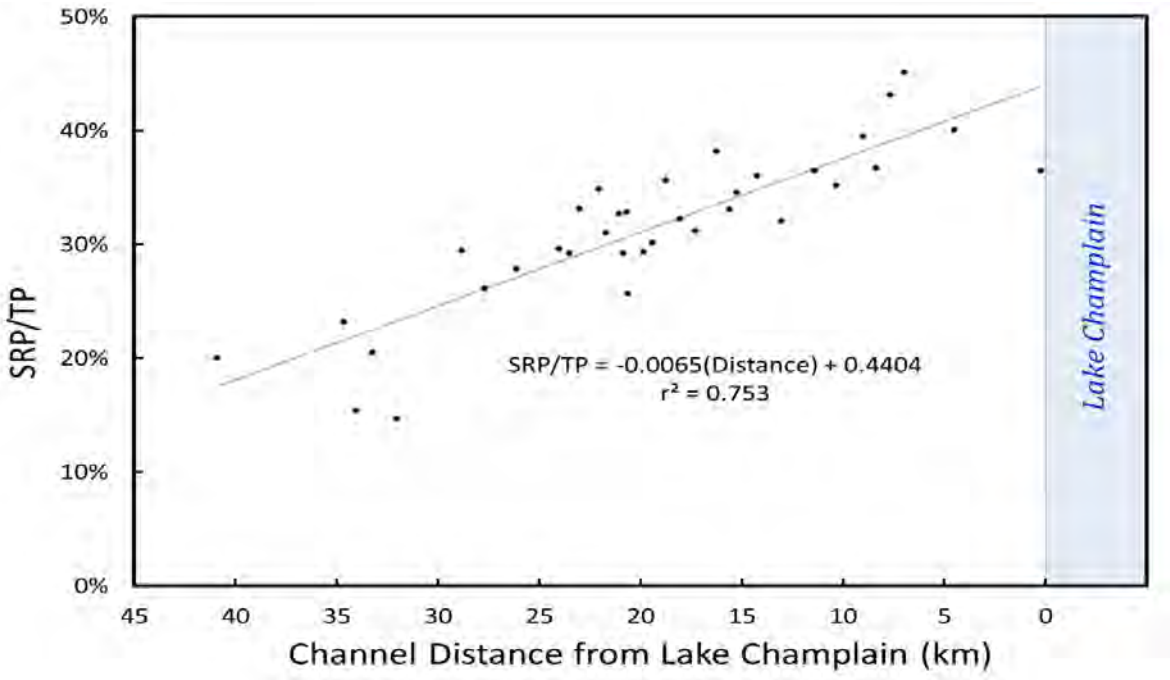

Figure 6. The ratio of soluble reactive P (SRP) to total P (TP) as a function of channel distance from Lake Champlain.

Temporal Variability – Seasonal Scale

Seasonal effects on stream nitrate concentrations (Fig. 7) were pronounced, with winter concentrations (Nov-Apr) being consistently higher than summer concentrations (May–Oct) throughout the watershed. There are many possible explanations for this relationship, but the most likely include extensive plant uptake of nitrogen in the summer growing season, as well as a lack of manure application to fields during much of the growing season, except on hay fields. Extremely low concentrations of nitrate were observed throughout the Altona Flat Rock pine barrens (Fig. 7). This oligotrophic ecosystem occurs on extremely thin soils (< 5cm) overlaying sandstone pavement, and it is possible that its unique vegetation actively scavenges nitrate from soil solutions and surface waters. As streams exit the Pine Barrens they enter a forested zone over deeper glacial tills and nitrate concentrations rise to levels (0.1 – 0.2 mg/L NO_3-N) more generally representative of forested sites. Increases throughout the stretch beginning at station NEPH (Fig. 7) are most likely influenced by the effects of agriculture.

Also apparent is a pronounced decrease in nitrate-N concentrations beginning at the Ratta site (Fig. 7) in the summer months. This site is the beginning of a small river-wide impoundment that is held by a small dam in the village of Chazy. In the summer months, during active transpiration and low flow, the residence time of water in this impoundment increases, and nitrate is lost. The mechanism for this loss is unclear, but may include biological uptake or conversion to more reduced forms.

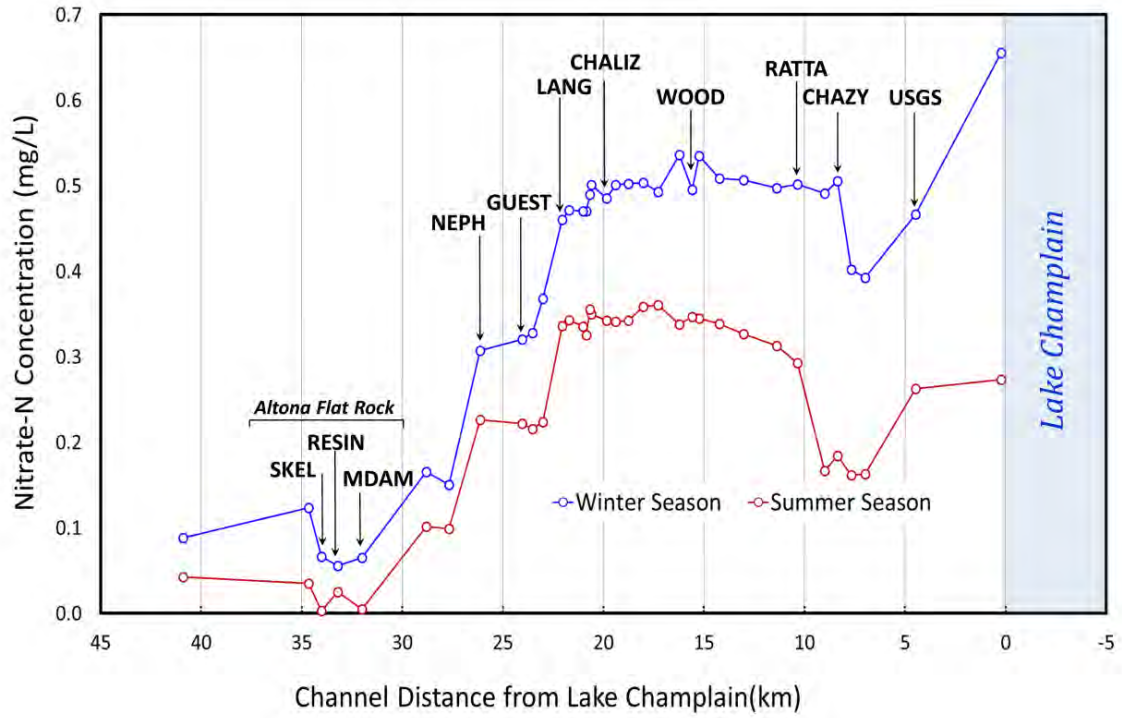

Figure 7. Nitrate-N concentrations as a function of channel distance from Lake Champlain and seasonality. Winter months are an average of November through April while summer months include May through October.

Temporal Variability – Event Scale

Three significant precipitation events occurred in October 2010 (Fig. 8A); 63.0mm (30 Sept. to 2 Oct.), 25.4mm (6-8 Oct.) and 48.8mm (14-17 Oct.). The resulting stormflow volumes were 1.34 hm^3, 1.01 hm^3 and 2.37 hm^3, respectively. Nutrient concentrations rose sharply during the initial rising limb of each major runoff hydrograph but returned to near background level concentrations by the time of peak discharge (Fig. 8A and 8B). Highest concentrations for all analytes corresponded to periods of active rainfall. Nitrate-N concentration for the third rainfall event dropped well below pre-storm background levels after peaking around 2 mg/L. Nitrate-N peak concentrations consistently lagged those for the SRP and total phosphorus peak by 4-11 hours for all three events. Moreover, the highest peak concentrations for total phosphorus and SRP occurred during the third (14-17 Oct.), and largest, runoff event while Nitrate-N reached its highest peak concentration during the first (30 Sep–2 Oct.) runoff event.

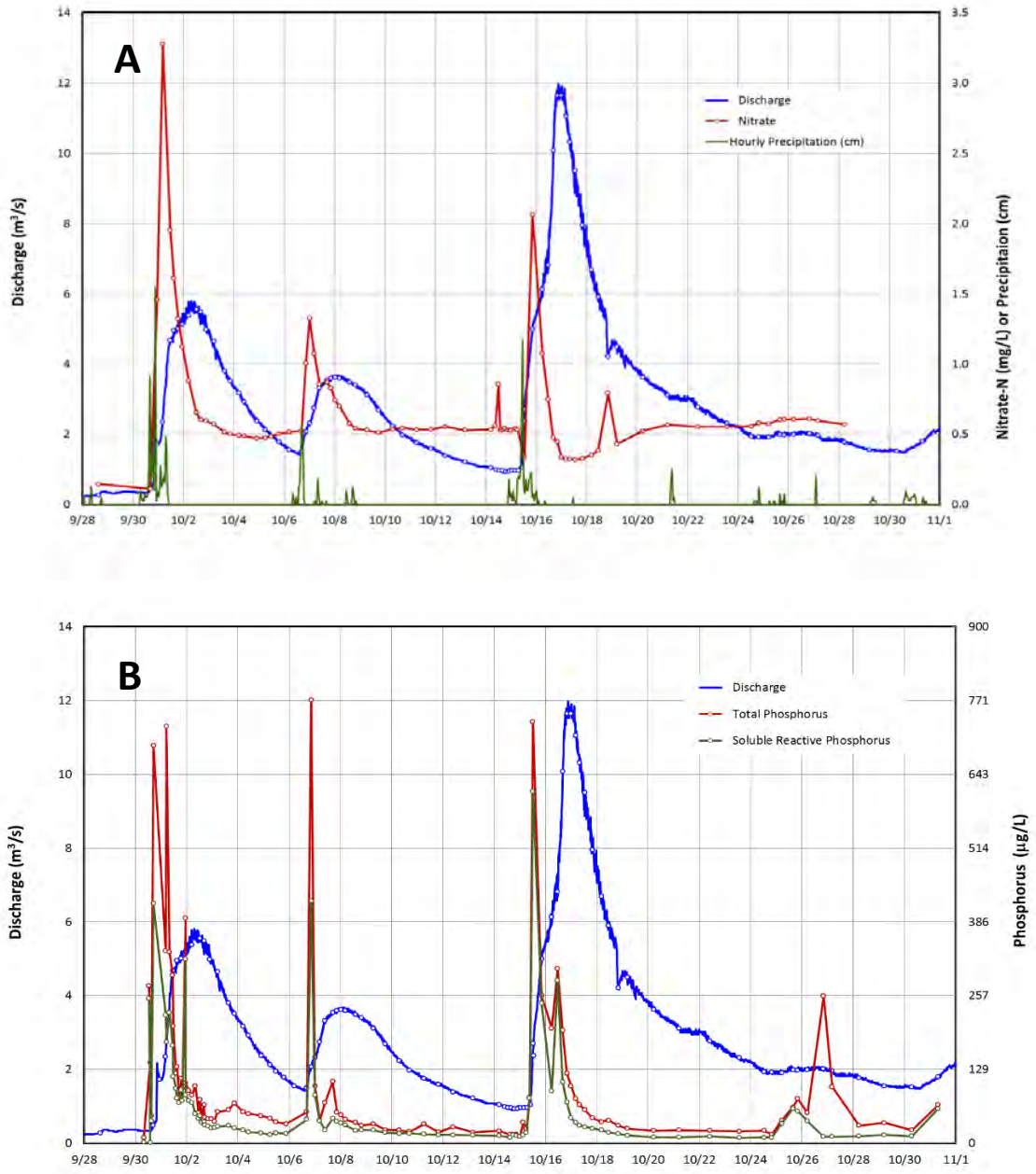

Figure 8. Temporal variability of solute chemistry for the Little Chazy River at the USGS gaging station for three runoff events in October 2010. A) Precipitation, discharge, and nitrate-N concentration. Provisional discharge data are from the USGS. B) Soluble reactive phosphorus, total phosphorus and stream discharge.

Concentrations of nitrate-N, SRP, total P, and TSS peaked on the rising limb of the runoff hydrograph during intense rainfall (Fig. 8). These high concentrations were most likely due to initial surface water runoff (overland flow) during active rainfall, which removed large quantities of particulate and soluble nutrients that had been accumulated or stored on the soil surface between runoff-producing rainfall events. Reapplication of manure to accessible fields was

observed near the USGS gage site between events 1 and 2 but no reapplication was observed prior to the third event, perhaps in part due to the saturated soil conditions. Nutrients present in the soil due to nitrification and mineralization may also have been flushed through shallow subsurface runoff pathways at the beginning of rainfall events.

Nitrate-N concentrations typically fell to background levels between 0.4–0.6 mg/L shortly after the crest of the stream hydrograph, reflecting the concentration of soluble nitrate-N in runoff that followed subsurface pathways during the later portion of the event and between events.

The relatively low nitrate-N peak concentration and the subsequent drop below the background concentrations during event 3 (Fig. 8A) may be explained by depletion of land surface sources between events 2 and 3. Consequently, the initial runoff from this event was relatively depleted in nitrate-N by the cumulative flushing effect of surface nitrate-N by the two preceding events and the initial runoff from the third event. This may also be influenced by the relative high mobility of nitrate, which is not influenced by adsorption and subsequent desorption. Nitrate-N concentrations return to background levels only after stormflow recedes and subsurface runoff pathways dominate the chemical signature.

We observed that for all three events, SRP and Total P peak concentrations precede the nitrate-N peak by several hours (Fig. 8B). We hypothesize that differences in runoff pathways and nutrient mobility may explain this observation. Overland runoff pathways should contain both soluble and particulate nutrients, thus nutrient concentrations generally rise as the first overland flow reaches the stream channel. Preceding events, organic N and P are transformed to nitrate and phosphate by mineralization and/or nitrification at the land surface and shallow subsurface environments. Nitrate is mobile and travels through the soil with percolating ground water. SRP will also leach into the soil but tends to be adsorbed onto soil particulates, particularly oxides. Thus SRP and nitrate concentrations rise together during the initial overland flow segment, but mobile nitrate continues to rise as subsurface flow paths become more prominent later in the event, while SRP concentrations decline during this phase due to adsorption. Additional evidence for this hypothesis can be seen as SRP concentrations toward the middle of the event decline more slowly as desorption replenishes some of the SRP lost to runoff.

The observed dependence of nitrate-N concentration on time- and rainfall-dependent runoff pathways during storm events is shown in the hysteresis of dimensionless nitrate-N load and dimensionless discharge during the three October 2010 runoff events (Figs. 9A and 9B). High loadings were consistently observed in the initial stages of the event, during active precipitation and overland flow due a combination of high concentration combined with moderate flows. Loadings continued at high levels as concentrations declined, but flows increased on the rising limb. As peak flows were reached, loadings declined as concentrations fell precipitously. This hysteresis effect suggests that stream discharge may be a poor surrogate for predicting nutrient loadings in this area.

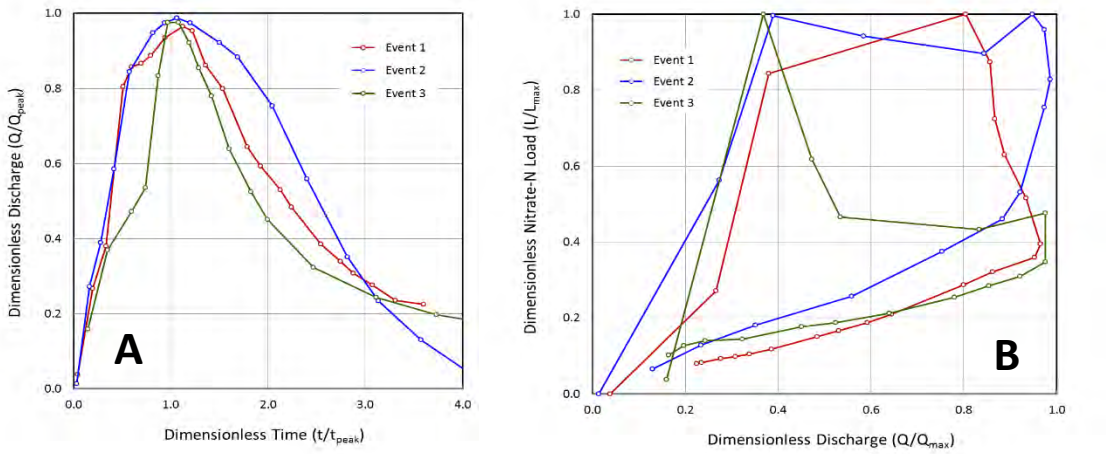

Figure 9. A) Dimensionless hydrographs for three runoff events in October, 2010. B) Plot of Dimensionless nitrate-N Load and Dimensionless Discharge, showing a discharge-dependent hysteresis effect on nitrate-N load.

CONCLUSIONS

The Little Chazy River headwaters rise in typical Northern Hardwood/Mixed forest communities on relatively deep glacial till and outwash soils, as well as unique, oligotrophic Pine Barren ecosystems growing on extremely thin organic soils shallow to bedrock. These headwaters have minimal agricultural influence. Surface water nutrient concentrations, particularly nitrate, tend to be relatively low in these reaches due to a lack of anthropogenic inputs, and biological uptake in these nutrient deficient soils.

Nitrate concentrations rise abruptly as the river leaves the upland forests and enters lowland areas dominated by agriculture with soils developed in till and glacial lacustrine and marine deposits. The more mobile nitrate anion arising from agricultural inputs is soluble and moves through these soils readily. In contrast, phosphorus concentrations do not rise notably in lowland reaches, possibly due to phosphate adsorption to hydrous oxides common in these soils.

Farther downstream (e.g. stations LANG to LC87 in Fig. 5), where the Little Chazy River enters areas dominated by fine-grained lacustrine and marine parent materials, nitrate concentrations remain relatively constant, whereas median total P gradually increases by as much as 45%. Moderate intensity agriculture, in which many fields drain through tile drain systems, may contribute to this increase in total P levels by surface erosion during precipitation events or direct flow through macropores to subsurface tiles. These runoff pathways may allow runoff to bypass sites of potential phosphate adsorption to hydrous oxide clays in subsurface soil horizons.

Small impoundments in the main channel, beginning at the RATTA site (Fig. 7), coincide with a rapid decrease in nitrate concentrations, particularly in the summer months. This reduction in nitrate concentration may be due to uptake of nitrate by biota or conversion to more chemically reduced forms. Nitrate concentration is further reduced by dilution at the lower end of the

impoundment where Tracy Brook, which drains predominantly forested/wetland areas, enters the main channel.

In the lowest reaches of the watershed, both nitrate and phosphorus fractions increase markedly. This reach has the most extensive agriculture in the watershed with large dairy farms and their attendant manure applications. These fields are typically underlain by fine-textured glacial-marine soils, some of which are not tile-drained resulting in a greater proportion of overland flow during snowmelt and precipitation events and contributing to direct washout of surface applied manure. Lack of subsurface drain systems may also promote flooding of these soils during wet periods, and subsequently changes in redox status causing desorption and release of previously adsorbed P to surface waters (Young and Ross, 2001).

Event level sampling during three large events demonstrated that maximal loading of nitrate and P fractions occurred early in the event on the rising limb with low to moderate discharge but high concentrations, during periods of active precipitation and possibly overland flow. Loadings continued at high levels through peak flow, due to a combination of lower concentrations but with high discharge. The relationship between flow and discharge exhibited pronounced hysteresis.

In summary, concentrations of P fractions and nitrate exhibited pronounced changes in concentration and loadings throughout the Little Chazy River watershed on different spatial and temporal scales. Much of this variability can be explained by flow through different ecosystems, effects of land-use practices, differences in soils and their management, as well as in-stream processes. Many of the complex interactions of these processes must be sorted out at edge of field studies.

ACKNOWLEDGEMENTS

We gratefully acknowledge the funding and support we have received from the New York State Department of Environmental Conservation, Nature Conservancy, New England Interstate Water Pollution Control Commission, United States Environmental Protection Agency and the Lake Champlain Basin Program.

FIELD GUIDE AND ROAD LOG

Meeting Point: Southeastern parking lot of Hudson Hall on the SUNY Plattsburgh campus. The lot is located at the corner of Beekman and Broad streets.

Persons using this log in the future should be aware that the field trip stops are located on private property that is owned and patrolled by the William H. Miner Agricultural Institute. A permit must be obtained from the Miner Institute to access this property.

Meeting Point Coordinates: 44.691°N, 73.467°W

Meeting Time: 9:00 AM

Distance in miles (km)

Cumu-lative	Point to Point	Route Description
0.0 (0.0)	0.0 (0.0)	Assemble in the southeastern parking lot of Hudson Hall. Leave parking lot, turn left at the entrance onto Beekman Street and proceed north.
0.9 (1.4)	0.9 (1.4)	Junction of Beekman and Tom Miller Rd., turn left at the traffic light and proceed west.
1.5 (2.4)	0.6(1.0)	Junction of Tom Miller Rd. and Quarry Rd., turn right and proceed north. Proceed straight through next traffic light, as Quarry Rd. becomes State route 22.
6.7 (10.8)	5.2 (8.4)	Junction of route 22 and O'Neill rd., turn left and proceed west. Follow O'Neill Rd. as it curves to the right and continue northward.
10.8 (17.4)	4.1 (6.6)	Intersection of O'Neill rd. and W. Church St., turn left and proceed west.
11.6 (18.7)	0.8 (1.3)	Intersection of W. Church St. and Barnaby Rd., turn right onto Barnaby Rd. and proceed north. Continue on Barnaby Rd. as it becomes a gravel surface and continue proceeding north on Miner Agricultural Research Institute property.
13.8 (21.2)	2.2 (3.5)	Left turn through locked gate, continue west on dirt road for 0.3 miles.
14.1 (21.2)	0.3 (0.5)	Stop at log cabin adjacent to the headwaters of the Little Chazy River immediately below Miner Dam.

STOP 1: Miner Dam, Town of Chazy, NY

Location Coordinates: (44.837°N, 73.571°W)

The Miner Dam was constructed near the headwaters of the Little Chazy River circa 1913 and was abandoned shortly thereafter due to excessive leakage. These headwaters traverse the Altona Flat Rock Pine Barrens, consisting largely of jack pine, pitch pine and lichens growing on a thin mantle of organic soil over sandstone bedrock. The area was scoured by a catastrophic breakout flood at the end of the last ice age, approximately 13,000 years ago. Lacking a substantial mineral soil, these ecosystems are oligotrophic, with extremely low nitrate-N

concentrations (Fig. 4A), particularly during the summer growing season (Fig. 6). Nitrate is probably removed by biological uptake, both in the soil and in the impoundments above the dam. Phosphorus concentrations are also low (Fig 4B), and are largely in an organic or particulate bound form (Fig. 5).

Distance in miles (km)		
Cumu-lative	Point to Point	Route Description
13.2 (21.2)	0.0 (0.0)	Return to the vehicles and proceed eastward on dirt road 0.3 mi to gate
13.5 (21.7)	0.3 (0.5)	At gate, turn right and proceed southward on dirt road. Continue on Barnaby Rd. as it becomes paved to junction of Barnaby Rd. and W. Church St.
15.7 (25.3)	2.2 (3.5)	Turn left at junction of Barnaby Rd. and W. Church St. and proceed eastward on W. Church St., through the flashing light as it becomes E. Church St.
17.7 (28.5)	2.0 (3.2)	Park on south side of road next to agricultural tributary.

STOP 2: Agricultural Tributary Sample site, Town of Chazy, NY

Location Coordinates: (44.822°N, 73.498°W)

This site (StratAgTrib) illustrates the importance of agricultural inputs and their influence on nutrient concentrations in the Little Chazy River (Fig. 2). Immediately upstream from this site, nitrate concentrations rose as the River traversed dairy agricultural operations on well-drained, sandy glacial till and outwash parent materials. Numerous agricultural tributaries and ditches in the Little Chazy River receive inputs from tile-drained fields which receive manure applications, typically 2-3 times per year (Fig. 2). Nutrient concentrations in these tributaries are typically high, but low flows typically cause only minor increases in nutrient concentrations in the Little Chazy River. However, their effects are cumulative.

Distance in miles (km)		
Cumu-lative	Point to Point	Route Description
17.7 (28.5)	0.0 (0.0)	Return to the vehicles and proceed eastward on E. Church St.
18.0 (29.0)	0.3 (0.5)	At junction of E. Church St. and Fiske Rd., turn left and proceed northward.
19.6 (31.5)	1.6 (2.6)	At junction of Fiske Rd. and Slosson Rd., turn right and proceed eastward.
20.9 (33.6)	1.3 (2.1)	Park near wooden bridge over the Little Chazy River.

STOP 3: Wood Sample site along the Little Chazy River, Town of Chazy, NY

Location Coordinates: (44.846°N, 73.456°W)

The Wood sample site is more typical of the lowland reach of the drainage basin, with soil parent materials composed of fine-textured glacial lacustrine sediments. River gradients are typically low, and many of the agricultural fields have subsurface drainage. Evidence of river meanders is common, and during high flows extensive streambank erosion can occur. Throughout this reach, total phosphorus concentrations increase slowly, driven largely by the soluble reactive phosphorus fraction. Nitrate concentrations, however, remain relatively constant throughout this reach, suggesting that the magnitude of different flow paths may vary for the two nutrients. Downstream from this site, the River enters some small impoundments in which nitrate concentrations decline, particularly during low flow, suggesting either conversion to other forms and subsequent loss or biological sequestration.

Distance in miles (km)		
Cumu-lative	Point to Point	Route Description
20.9 (33.6)	0.0 (0.0)	Return to the vehicles and proceed westward on Slosson Rd. Go straight through the intersection with Ashley Rd.
22.2 (35.7)	1.3 (2.1)	At the junction of Slosson Rd. and Fiske Rd. (Old Route 348), turn right.
26.1 (42.0)	3.9 (6.3)	Proceed on Fiske Rd. northeastward, going over the interstate into the village of Chazy. At the junction of Fiske Rd. and Route 9, turn left.
26.2 (42.2)	0.1 (0.2)	At the junction of Route 9 and Old Route 191(Miner Farm Rd.), turn right.
27.2 (43.8)	1.0 (1.6)	At the junction of Miner Farm Rd. and Stetson Rd., turn left and proceed northward.
28.4 (45.7)	1.2 (1.9)	Proceed 1.2 miles on Stetson Rd. to the USGS sample site immediately before the bridge over the Little Chazy River.

STOP 4: USGS Sample site along the Little Chazy River, Town of Chazy, NY

Location Coordinates: (44.902°N, 73.415°W)

The U.S. Geological Survey maintains a discharge monitoring gauge at the USGS sample site, providing continuous flow data. Episodic sampling sampling was conducted at this site during three successive storm events in the fall of 2010. During each of these events, maximum concentrations of both nitrate, total P and soluble reactive P were observed on the rising limb of the hydrograph, while precipitation was still falling. By the time the maximum flow was observed, concentrations had declined to baseline levels. Loadings were near maximum levels at moderate flows on the rising limb due to high concentrations, and during the peak of the event due to high flows. The relationship between discharge and load shows a marked hysteresis.

Immediately upstream from this site is the outflow from the publicly owned treatment works for the village of Chazy. Sampling immediately upstream and downstream of this site showed only

slight increases in concentration of either N or P fractions, suggesting that this source is small relative to other sources, such as those arising from agricultural practices. Immediately downstream, both nitrate and P fractions increase rapidly, as the lower stretch of the drainage basin has extensive agriculture, almost all with subsurface drainage.

Distance in miles (km) Cumulative	Point to Point	Route Description
28.4 (45.7)	0.0 (0.0)	Return to the vehicles and proceed southward on Stetson Rd. to the first stop sign.
28.8 (46.3)	0.4 (0.6)	At the junction of Stetson Rd. and N. Farm Rd., turn left and proceed westward into the village of Chazy to the stop sign.
30.0 (48.3)	1.2 (1.9)	At the junction of N. Farm Rd. and Route 9, turn right and proceed northward.
30.4 (48.9)	0.4 (0.6)	At the junction of Route 9 and Route 191 (Miner Farm Rd.), turn left.
32.0 (51.5)	1.6 (2.6)	Proceed westward on route 191, over the interstate, to the junction of Ridge Rd. and turn right (northward).
32.7 (52.6)	0.7 (1.1)	Continue on Ridge Rd. for 0.7 miles and park near the dirt road leading into the field on the right.

STOP 5: R15 Agricultural Field at Miner Institute, Town of Chazy, NY

Location Coordinates: (44.899°N, 73.467°W)

The R15 agricultural field is operated by the William H. Miner Agricultural Research Institute, a fully functional research dairy farm. Miner Institute conducts research on dairy operations as well as their impacts on the environment. The R15 field has been tile-drained since 1975, and includes extensive shallow groundwater sampling devices, a deep groundwater monitoring well, and a meteorological station. At this site, we will conduct a demonstration of "smoking" a tile line. This demonstrates the connectivity of subsurface tiles (approximately 1 m deep) to the surface through soil macropores which include worm tunnels as well as structural cracks. This provides a potential route for direct and rapid transit of pollutants applied on the surface, such as those through manure application, to tiles and surface waters.

Distance in miles (km) Cumulative	Point to Point	Route Description
32.7 (52.6)	0.0 (0.0)	Return to the vehicles and proceed northward on Ridge Rd. to the first stop sign.
33.8 (54.4)	1.1 (1.8)	At the junction of Ridge Rd. and McBride Rd., turn right to stay on Ridge Rd. and proceed eastward.
35.3 (56.8)	1.5 (2.4)	At the intersection of Ridge Rd. and Lavalley Rd., turn right and proceed eastward.

36.5 (58.7)	1.2 (1.9)	Pass over the Interstate and continue eastward to the junction with Route 9.
37.0 (59.5)	0.5 (0.8)	Turn left and proceed northward and park next to Edge of Field site.
End of Trip		

STOP 6: Edge of Field Study Site, Town of Chazy, NY

Location Coordinates: (44.940°N, 73.440°W)

The USDA-NRCS edge-of-field (EoF) monitoring program is designed to quantify impacts of various nutrient management practices on runoff water quality. Data collection and analysis for EoF projects utilize a small paired watershed approach. Typically, one best management practice is evaluated in comparison to a reference condition. The objective of our project is to quantify water quality impacts associated with the practice of controlled subsurface tile drainage (CD) as compared to the standard practice of freely-drained subsurface tile drainage (FD). The practice of CD uses inline water control structures (AgriDrain, Adair, IA) to artificially raise the drainage outlet elevation during the non-growing season. Studies show that CD can reduce annual drainage flow volumes by as much as 80 % compared to FD. The two crop production fields were selected due to their close proximity, similar soil types, and for their ability to be instrumented properly to capture both surface and subsurface runoff water. The fields are currently in 2nd year production of corn for silage. Subsurface drainage tile (slotted plastic drain tile, 10-cm i.d.) was installed via a tile-plow at an average depth of 1.2 m below the soil surface during November 2014 (10.7 m spacing between tile lines within each field). Subsurface drainage water from each field's lateral lines flows to a main outlet pipe (schedule 40 PVC, 20-cm i.d.) that drains to individual concrete manholes (1.2-m i.d. and 2.4 m deep) where flow is gauged and sampled. Drainage water flows are measured by routing water through a plastic barrel equipped with a v-notch weir and stilling well that houses a pressure transducer-data logger to capture water elevation changes related to flow differences. Drainage flows are gauged by rating curves developed between measured flows and water height inside the barrels. Variation in nutrient and sediment concentrations will be quantified by taking multiple samples over an event using flow-programmable autosamplers. Overland flow is measured from each field by routing surface water to a fiberglass flume (Plasti-Fab, Tualatin, Oregon) using a combination of natural swales, field contouring and an earthen, clay berms. Event-based and seasonal mass loads of total N, nitrate-N, ammonium-N, total P, dissolved (<0.45µm) reactive P (orthophosphate), unreactive P (particulate-organic P), and total suspended solids will be calculated. Baseline monitoring will occur for two years after which CD treatment will be implemented and monitored over four years. Differences in mass nutrient loads between FD and CD will be evaluated using analysis of covariance. Agronomic data is also being tracked (i.e., yields, fertilizer and manure inputs and nutrient uptake) and will be utilized to calculate N and P mass balances each year of the study. A field-scale water quality model (APEX) will also be parameterized and calibrated as part of the project. Results will help quantify tradeoffs between drainage intensity, surface/subsurface hydrology, and nutrient loss dynamics at the field scale.

REFERENCES CITED

APHA, 1998. Standard Methods for the Examination of Water and Wastewater, 20th Edition. American Public Health Association, American Water Works Association, and Water Environment Federation, Washington, D.C.

Dawson, J.C., Heintz, J.F., Friedrichs, C., and West, L., 1981, William H. Miner and hydroelectric power development at Heart's Delight Farm, Chazy, New York, p.3-32, *in* Dawson, J.C., (ed.), Proceedings 1981 Eighth Annual Lake Champlain Basin Environmental Conference, Miner Center, Chazy, New York, June 9,–10, 1981.

Denny, C.S., 1974, Pleistocene geology of the northeastern Adirondack region, New York: United States Geological Survey, Professional Paper 786, 50p.

Franzi, D.A., and Adams, K.B., 1993, The Altona Flat Rock jack pine barrens: A legacy of fire and ice: Vermont Geology, V.7, p.43–61.

Karim, A.M., 1997, Clinton County, New York Priority Area Assessment Report 1997: Clinton County, New York, 11p.

Landing, E., Franzi, D.A., Hagadorn, J.W., Westrop, S.R., Kröger, B., and Dawson, J.C., 2007, Cambrian of East Laurentia—Field workshop in eastern New York and Vermont, p.25-80, *in* Landing, E., (ed.), Ediacaran–Ordovician of east Laurentia, S.W. Ford Memorial Volume: New York State Museum Bulletin 510, p.25–71.

NYSDEC, 2001, The 2000 Lake Champlain Basin Waterbody Inventory and Priority Waterbodies List, Encompassing all or portions of Clinton, Essex, Franklin and Washington Counties: Bureau of Watershed Assessment and Research, Division of Water, NYS Department of Environmental Conservation, 309p.

Oetjen, K., Kranitz, R., Zimmermann, T., Kramer, S., Fuller, R.D., and Franzi, D.A., 2012, Spatial and temporal variability of anion concentrations and suspended solids in the Little Chazy River, northeastern, New York: Geological Society of America, 2011 Abstracts with Programs, Northeastern Section Meeting, Hartford, Connecticut, V.44, No.2, 18-20 March, 2012.

Vermont DEC and New York State DEC, 2002, Lake Champlain Long-Term Water Quality and Biological Monitoring Program–Program Description: Vermont Agency of Natural Resources, Department of Environmental Conservation, New York State Department of Environmental Conservation and the Lake Champlain Basin Program, 11p.

Young, E.O. and Ross, D.S., 2001, Phosphate release from seasonally flooded soils: a laboratory microcosm study: Journal of Environmental Quality; Vol. 30 Issue 1, p91-101.

GEOBOTANY OF GLOBALLY RARE SANDSTONE PAVEMENT PINE BARRENS, CLINTON COUNTY, NY

JACOB N. STRAUB and RACHEL E. SCHULTZ
Center for Earth and Environmental Science, State University of New York at Plattsburgh, Plattsburgh, NY 12901

INTRODUCTION

Geobotany is the study of plant distributions, which often are determined by the interaction of plants with the underlying geology of an area. Historic and contemporary geologic and climatological influences have shaped the sandstone pavement pine barrens botanical community, which is considered rare in New York and the world (Edinger et al., 2014). The pavement barrens of Clinton County, New York were created over 12,000 years ago when glacial Lake Iroquois drained into glacial Lake Coveville (Franzi and Adams 1993). Plants have been able to survive in this harsh, nutrient poor ecosystem due to specialized characteristics and interactions with other organisms. The Altona Flat Rock sandstone pavement pine barren is fire-dependent, and the last stand-replacing fire burned over 1,200 ha in 1957 (Gooley, 1980). Fire acts as an ecological mechanism to restart succession in this type of community. An outstanding quality of this pine barren is its location at the northern extreme of pitch pine and southern extreme of jack pine, and both species depend on fire as a mechanism for reproduction. Another unique community found in the pavement barrens is the perched bog. These acidic peatlands are separated from the water table due to the sandstone bedrock and host unique plant species such as the carnivorous pitcher plant (Edinger et al., 2014). On this field trip we will visit the Altona Flat Rock pine barrens owned by the W.H. Miner Agricultural Research Institute and the Gadway Pine Barrens owned by the Nature Conservancy.

Geological Setting (from Franzi and Adams 1999)

The northeastern New York sandstone pavements (Figure 1) are entirely underlain by nearly flat-lying Potsdam Sandstone (Cambrian) (Fisher, 1968; Lewis, 1971). The lithology of the Potsdam ranges from cross-laminated, orange-pink to pale red, very coarse to medium-grained arkose with quartzitic green shale and conglomeratic interbeds to pinkish gray to very pale orange, well sorted, fine to medium-grained quartz sandstone (Fisher, 1968). The pavement surfaces generally slope north and east from an elevation of more than 300 meters a.s.l. (above sea level) to below 200 meters a.s.l. where they pass beneath surficial deposits in the Champlain Lowland (Denny, 1974). The sloping surfaces are broken into a series of stair-like bedrock treads separated by risers that range from a few decimeters to tens of meters in height. The tread surfaces have little local relief except near stream channels and risers. The eroded edges of truncated trough cross-beds, ripple marks, and solution pits are common minor surface features. Shoreline deposits from the highstand of glacial Lake Vermont (Fort Ann Stage) and morainal deposits (Woodworth, 1905a; Denny, 1970, 1974) lap onto the northern and eastern margins of the pavements.

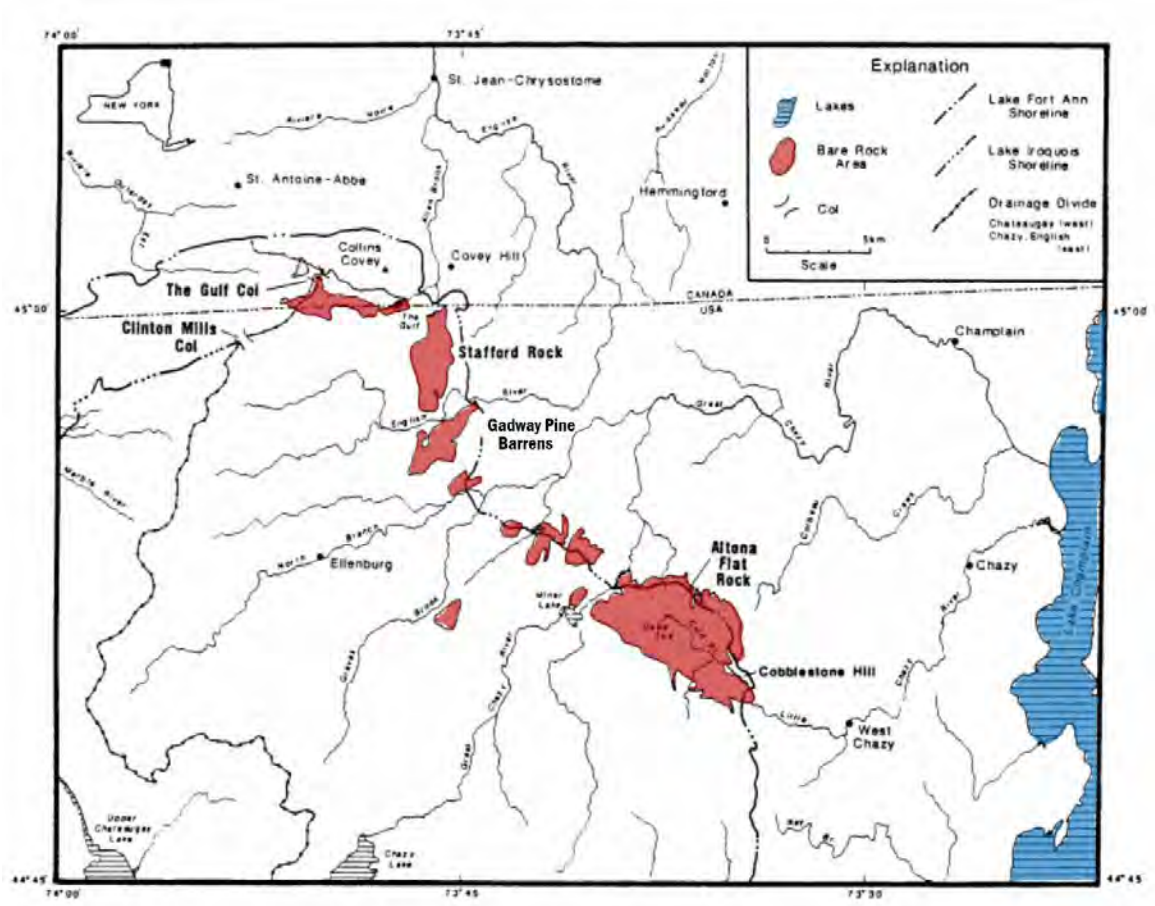

Figure 1. Pavement pine barrens in the upper Champlain Valley in northern New York and Canada formed by the drainage of glacial Lake Iroquois into glacial Lake Coveville including the Altona Flat Rock and Gadway Pine Barrens (from Adams and Franzi 1994).

The sandstone pavements were created more than 12,000 years before present by the erosional effects of ice-marginal streams related to drainage of glacial Lake Iroquois and younger post-Iroquois lakes (Woodworth, 1905a, 1905b; Coleman, 1937; Denny, 1974; Clark and Karrow, 1984; Pair et al., 1988; Pair and Rodrigues, 1993). Lake Iroquois occupied the Ontario Lowland and drained eastward across an outlet threshold near Rome in the western Mohawk Lowland (Coleman, 1937). Lake Iroquois expanded northeastward into the St. Lawrence Lowland during deglaciation between the Adirondack Uplands to the south and the waning Laurentide Ice Sheet margin to the north. The former water level probably stood at a present elevation between 329 and 332 meters a.s.l. near Covey Hill, Quebec (Denny, 1974; Clark and Karrow, 1984; Pair et al., 1988; Pair and Rodrigues, 1993).

Northward recession of the ice front into Chateaugay region diverted glacial meltwater westward along the ice margin and created the well-developed Chateaugay Channels (MacClintock and Stewart, 1965). Drainage through the channels emptied sequentially into the northeastwardly expanding Lake Iroquois as ice recession continued. Westward drainage ended when the ice front in the Champlain Lowland receded from the vicinity of the Ellenburg Moraine. Subsequently, eastward drainage of Lake Iroquois began as lower outlets were exhumed along the drainage divide between the Champlain and St. Lawrence drainage systems

southwest of Covey Hill. The initial drainage may have occurred through a channel approximately 1 km north of Clinton Mills that was controlled by a threshold between 329 and 332 meters a.s.l. (Clark and Karrow, 1984). The falling levels of proglacial lakes in the St. Lawrence and Ontario lowlands temporarily stabilized at the glacial Lake Frontenac level (Clark and Karrow, 1984; Pair et al., 1988; Pair and Rodrigues, 1993) as the ice margin receded northward and the col at The Gulf (308-311 meters a.s.l.) was uncovered. Outflow from these lakes was directed southeastward along the ice margin where it crossed the English, North Branch and Great Chazy watersheds before eventually emptying into Lake Fort Ann which occupied the Champlain Lowland at an elevation between 225 and 228 meters a.s.l. (Denny, 1974). The outflow streams stripped large areas of their surficial cover and cut deep bedrock channels and plunge pools (e.g. The Gulf (MacClintock and Terasme, 1960) and the Dead Sea (Woodworth, 1905a; Denny, 1974)) into the Potsdam Sandstone. The most intense scour (e.g. Stafford Rock, Blackman Rock, and Altona Flat Rock) generally occurred on major watershed divides. The scour of the areas southeast of the St. Lawrence-Champlain divide continued as ice recession caused the drainage of Lake Frontenac around the northern flank of Covey Hill. Denny (1974) suggested that the ice margin may have oscillated in the area around Covey Hill causing the lakes in the eastern St. Lawrence Lowland to refill and empty several times. The lake-drainage episodes ended when the ice front receded from the northern flank of Covey Hill for the last time and the proglacial lake in the St. Lawrence merged with Lake Fort Ann in the Champlain Lowland Lowland (Pair, et. al., 1988; Pair and Rodrigues, 1993). The nature and timing of the outflow floods and their role in the creation of the sandstone pavements has been an issue of considerable debate (e.g. MacClintock and Terasme, 1960; MacClintock and Stewart, 1965; Denny, 1974; Muller and Prest, 1985; Coles, 1990) but it is likely that the erosion occurred in stages, as suggested by Denny (1974) and Coles (1990), rather than as a single massive flood event.

Ecological Setting

The sandstone pavement pine barrens ecosystem, hereafter “barrens”, exists as a discontinuous matrix of unique landforms stretching some 30 km starting at the Gulf unique area and extending as far south as Altona Flat Rock near West Chazy, NY (Figure 1). The barrens are typified by a shallow (5-15 cm), nutrient-poor soil with low water holding capacity, which sharply contrasts with the surrounding landscape of deeper, nutrient-rich soils. As such, plants found here are uniquely adapted to handle these physical and edaphic conditions (Adams and Franzi 1999). Additionally, these harsh living conditions result in low plant diversity relative to the surrounding area, because only plants with adaptations suitable for harsh and frequent disturbance can persist long-term. From north to south the ecological characteristics of the barrens gradually shifts; most notably in structure but less so in species composition. For example, tree height at the Gadway Pine Barrens (near the northern limit) rarely exceeds 7 m, whereas trees at Altona Flat Rock frequently exceed 10 m.

Most of the overstory in the barrens is dominated by a single tree species; jack pine (*Pinus banksiana*), which exists at the southern limit of its present natural range in the Champlain Valley (Burns and Honkala, 1990; Harlow, et al., 1991). This fire-dependent tree competes superiorly in the low nutrient soil and defines the gestalt of the barrens. Jack pine is a relatively short-lived (<150 years), shade-intolerant, boreal species that maintains communities on the sandstone pavements because of its adaptations to the conditions here. At younger ages, jack pines can form dense thickets; however, most the barrens have older trees that are well spaced creating a ‘park like’ visual impression. Near the southern extent of the barrens, pitch pine

(*Pinus rigida*) is present and in some stands is either co-dominant with jack pine or forms pure stands (DellaRocco and Straub 2015). In fact, the jack and pitch pine that co-exist here represents one of the few examples of this relationship in the world. Other overstory trees that exist here include gray birch (*Betula populifolia*), paper birch (*Betula papyrifera*), red oak (*Quercus rubra*), eastern white pine (*Pinus strobus*), red pine (*Pinus resinosa*) red maple (*Acer rubrum*), serviceberries (*Amelanchier* spp.) and quaking aspen (*Populus tremuloides*), however, these species are mostly relegated to the cracks and fissures in the bedrock where deeper soil has accumulated and they are usually short lived (DellaRocco and Straub 2015).

The diversity of understory shrubs is greater than the overstory in the barrens. The understory shrubs are predominantly late lowbush blueberry (*Vaccinium angustifolium*), black huckleberry (*Gaylussacia baccata*), black chokeberry (*Pyrus melanocarpa*), sweetfern (*Comptonia peregrina*), and sheep laurel (*Kalmia angustifolia*). These shrubs belong to the Ericaceae family and are often referred to as 'heaths'. Unlike the well-spaced overstory trees, structurally, these woody shrubs can cover up to 100% of the ground cover making it difficult to travel in some locations (Figure 2). Collectively these shrubs occupy a vertical structure from about 0.25 to 1.50 meters.

Figure 2. Example of the ericaceous shrub species that comprise nearly 100% of the shrub layer at the Altona Flat Rock. Pitch pine dominates the overstory in this photo.

The ground cover of the barrens can be split into two distinct categories; areas that have soil and those where it is absent. In the areas that have soil, species of lichens are common including *Cladonia uncialis*, *C. rangiferina*, and *C. mitis.* Intermixed with the lichen are a diverse group of bryophytes including haircap moss (*Polytrichum commune),* Schreber's big red stem

moss *(Pleurozium schreberi),* two species of broom mosses *(Dicranum polysetum, D. scoparium),* and *Sphagnum* spp.. The lichens and bryophytes are good indicators of shallow or absent soil as these organisms are usually the first to colonize bedrock. Additionally they seem to coexist without a clear dominant species and more information is need to asses if dominance hierarchies exist among this group of organisms at this location. Lichens and bryophytes also serve as suitable substrate for higher vascular plants (see During and Tooren, 1990). There is also a large amount of downed trees that are in various states of decay (Sargis and Adams 2004, DellaRocco and Straub 2015). These logs persist in the understory for many years because of the combination of short growing conditions, low moisture, and strict fire suppression policies (see disturbance regime below). Some portions of the ground cover are absent of soil and here you can directly see the sandstone underlying bedrock. Often these areas are the result of footpaths or game trails but in other spots these barren spots are simply the results of the absence of plant colonization; areas that have yet to accumulate organic matter.

The combined effects of warm summer temperatures, low seasonal water availability with rapid runoff, flammable foliage and buildup of combustible downed wood, create a high-stress environment that is sensitive to natural disturbances, such as wildfires and ice storms. The barrens have a well-documented history of natural and human initiated fires (i.e., Gooley, 1980) which play a large role in the ecology of this site. Importantly the plant communities that dominate the barrens are adapted to survive and/or reproduce following a fire and are often referred to as fire-dependent. Specifically, jack and pitch pine both produce serotinous cones that require fire to melt resin on their cones which complete their ontogeny (Burns and Honkala, 1990). Jack pines as mature trees have thin bark and this trait leads to widespread mortality during a fire. However, the cones from the parent trees, which can also be stored on the branches, open and can successfully germinate after a fire. This sequence created the classic 'even-aged' jack pine stands throughout the barrens. Essentially, one can trace the age of the stand back to the last stand replacing fire. Historically, the fire regime consisted of frequent but low intensity fires that 'restarted' ecological succession; however the last stand replacing fire was probably 1965 at the Altona Flat Rock (Franzi and Adams 1999). Without the return of fire (or a suitable management alternative) the nature and integrity of this rare community type is in jeopardy (Adams and Franzi, 1994; Adams and Franzi 1998; and DellaRocco and Straub 2015).

Scattered sporadically throughout the barrens are perched bogs. The bogs are acidic peatlands that are separated from the groundwater table below due to an impermeable layer such as bedrock (Figures 3 and 4) and most have relatively shallow peat depths of 0.5 to 1.5 m. These nutrient-poor bogs are considered a rare community type in the state of New York and are dominated by sphagnum moss (Edinger et al., 2014). Other plant species found here include shrubs such as leatherleaf (*Chamaedaphne calyculata*) and blueberry species (*Vaccinium* spp.) and herbs including spoon-leaved sundew (*Drosera intermedia*) and northern pitcher plant (*Sarracenia purpurea*) (Edinger et al., 2014). These plants have developed special adaptations to survive in waterlogged and nutrient poor habitats.

Woody species belonging to the heath family (Ericaceae) are prevalent in perched bog communities. These shrubs, including leatherleaf and blueberry, have common characteristics such as tough, waxy leaves that last for 1-4 years (Figure 4) and epicormic branching, the ability to sprout from dormant buds (Eastman 1995). Researchers have determined that these leaf adaptations help the plants conserve nutrients, water, and reduce frost damage (Aerts, 1995; Eckstein et al., 1999; and Wright et al., 2004). Epicormic branching of leatherleaf has been

associated with bog mat development; as old branches are covered in sphagnum moss, new branches radiate out and increase the mat surface (Swan and Gill, 1970).

While carnivory in plants is a rare phenomenon worldwide, we find numerous insectivorous species in northern bogs including sundew and the northern pitcher plant (Figure 5). Both sundew and the northern pitcher plant devote much of their biomass to structures that trap insects including sticky pads and pitchers, respectively. The plants use enzymes to digest the insects to derive nitrogen as opposed to only taking up nutrients from the soil and atmosphere. Therefore, these plants have relatively small and shallow root systems. While both low availability of nutrients and waterlogging stress have been postulated as advantages of carnivory in bog systems, this adaptation is likely due to both stressors (Adamec, 2011).

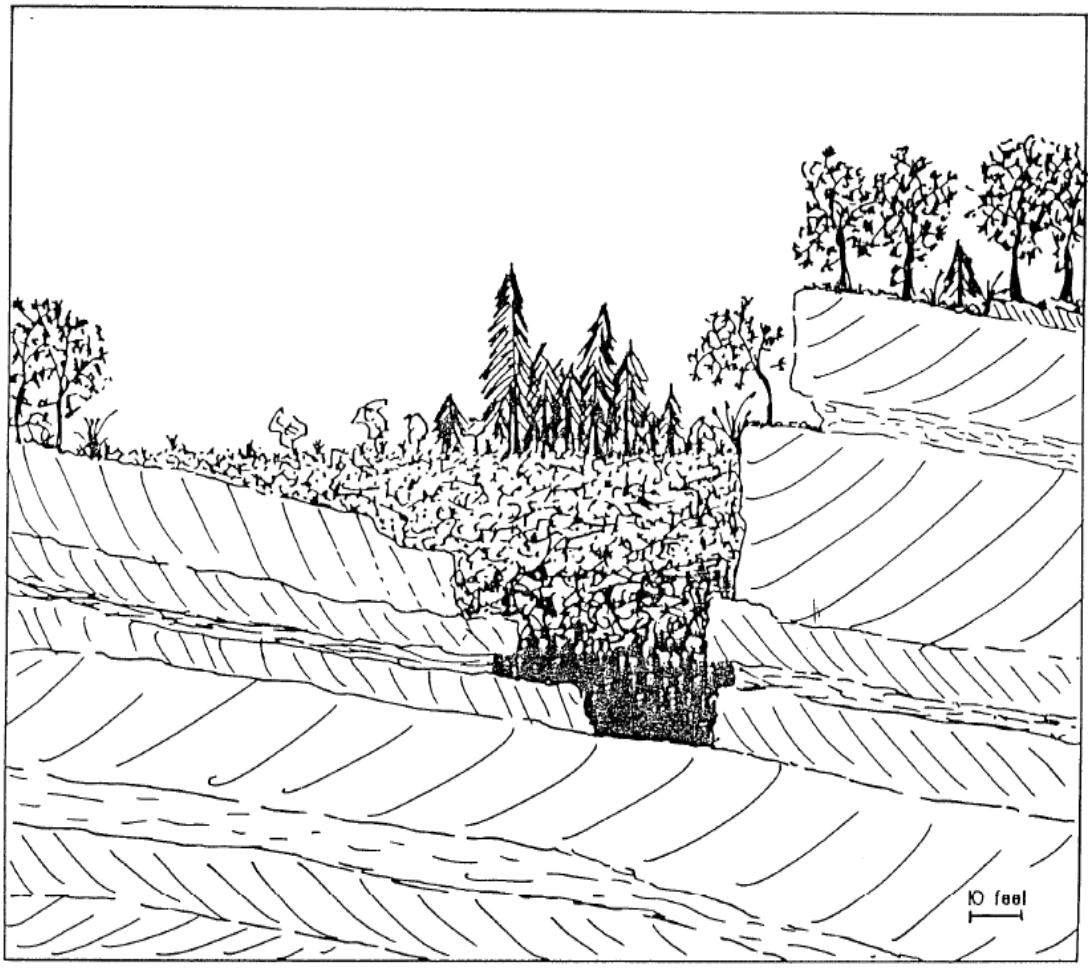

Figure 3. A “ledge” or “perched” bog in cross section. These wetlands are perched above the water table due to water pooling in the space between two ledges of bedrock. Here peat has developed on the bottom and a wetland community is supported on top (from Coles, 1990).

Figure 4. A perched bog at the Altona Flat Rock. This bog is dominated by sphagnum moss and the low-lying shrub, leatherleaf. The edge of the sandstone pine barren is shown in the background.

Figure 4. The waxy, evergreen leaves of the ericaceous shrub, leatherleaf (*Chamaedaphne calyculata*), a dominant plant in perched bogs.

Figure 5. The northern pitcher plant (*Sarracenia purpurea*) is able to trap and derive nutrients from insects and other species that drop into its pitcher. The recurved hairs on the top of the pitcher hinder escape.

Recent Investigations in the Sandstone Pavement Pine Barrens

Year: 2014

Title: Plants as Hydrologic Indicators: A comparative study

Location: Altona Flat Rock

Investigators : Veronica Schmitt (B.S Ecology; 2014) & Jacob Straub (faculty advisor)

Summary: Certain plants tend to grow in areas that have high moisture content in the soil and where the water table is close to the surface. However, these plants vary from region to region. Importantly, scientists have found that these plants can serve as indicators of groundwater hydrology and/or underlying geology. No efforts have been made to determine if plants in the sandstone pavement barrens of Clinton County, NY can serve as indicators of wetland hydrology or geology, although these studies have been conducted elsewhere (Goslee et al. 1997, Lewis 2001). The purpose of this study was collect baseline data on species composition as well as chemical and physical data from a random subset of wetlands from the Altona Flat Rock area.

Eight wetlands were sampled in the spring of 2014 soon after snow melt. Data was collected on acidity, temperature, conductivity, water depth and oxidation reduction potential (Table 1). In addition all plants were identified and compared with Goslee et al. (1997). Goslee et al. (1997) assessed woody and herbaceous plants based on their reliability to predict groundwater, seasonal surface water or permanent surface water. We compiled a list of nine species that serve as hydrology indicators in this area that matched the records from Goslee et al. (1997) (Table 2). However, the degree to which these nine species remain effective and reliable indicators of wetland water source in the barrens remains an important question to be examined. Indeed there are major differences in the physical and chemical attributes most namely the groundwater from the barrens is particularly low in ions (Romanowicz per. communication).

Table 1. Chemical data including pH, specific conductivity (Sp. Cond.; μS / cm), water depth (cm) temperature (°C) and oxidation reduction potential (ORP; millivolts) collected from 5 wetlands at Altona Flat Rock, spring 2014.

Wet-land	pH			Sp. Cond. (μS / cm)			Depth (cm)			Temp. (°C)			ORP (mV)		
	mean	max	min	mean	max	min	mean	max	min	mean	max	min	mean	max	min
1	7.3	7.8	6.6	79.4	105.5	61.0	9.1	15.5	5.0	11.7	14.0	9.3	93	124	79
2	8.0	8.2	7.7	129.2	138.3	121.0	7.8	16.0	0.0	8.9	11.5	6.4	65	86	20
3	5.3	5.8	4.9	24.2	37.3	19.0	19.2	25.0	4.0	9.5	9.7	9.3	241	254	232
4	4.7	4.7	4.6	44.4	51.0	39.0	0.4	2.0	0.0	7.5	8.1	6.6	233	247	218
5	5.2	5.7	5.1	21.0	24.0	19.8	2.0	4.0	0.0	7.1	8.1	6.5	247	257	240

Table 2. Plants that occurred in both the Altona Flat Rock and from Goslee et al. (1999) from central Pennsylvania and used as indicators of wetland water source.

Genus	Species	Common name	Associated hydrology
Glyceria	*striata*	Manna grass	Seasonal and permanent surface water
Juncus	*tenuis*	Path rush	Seasonal surface water
Kalmia	*angustifolia*	Sheep laurel	Groundwater
Mentha	*arvensis*	Mint	Seasonal and permanent surface water
Phalaris	*arundinacea*	Canary grass	Seasonal and permanent surface water
Potamogeton	*pectinatus*	Sago pondweed	Permanent surface water
Thelypteris	*noveboracensis*	New York fern	Groundwater
Thelypteris	*palustris*	Marsh fern	Groundwater
Typha	*latifolia*	Cattail	Permanent surface water

Year: 2015

Title: Fifteen-year Community Type Change in a Sandstone Pavement Barren

Location: Altona Flatrock

Investigators: Thomas DellaRocco (B.S Ecology; 2015) & Jacob Straub (faculty advisor)

Summary: The Altona Flat Rock sandstone pavement barren is a rare fire-dependent ecological community geographically located at the narrow overlap of jack pine and pitch pine species ranges. We studied fifteen year post-ice storm plant community change at the Altona Flat Rock pine barren in Clinton County, New York. Prior research predicted plant community changes in the barren due to fire exclusion. Our study is the first to examine long-term changes in plant species composition of this pine barren community. In the overstory, pitch pine basal area and density remained similar (i.e., < 20% difference) between 1999 and 2014, while density and basal area of red maple increased 67% and 109%, respectively. In contrast, jack pine overstory mortality was 100% between 1999 and 2014. Very few jack pine saplings (12.5 stems/ha) and no pitch pine saplings were present in sample plots. However, a high density of red maple saplings (1,950 stems/ha) existed. Ground cover was dominated by huckleberry, Sphagnum spp., and Schreber's big red stem moss (Figure 6). With absence of fire and the subsequent decreases in jack and pitch pine, this post-ice storm pine barren is developing into a

boreal heath barren dominated by huckleberry with an overstory comprised mostly of red maple. In the absence of fire, or a suitable management alternative, this rare ecological community type may become extirpated from the Northeast. Further research will provide a more complete understanding of the ecological requirements for successful regeneration of pines and associated species in fire-prone ecosystems such as Clinton County's sandstone pavement barrens.

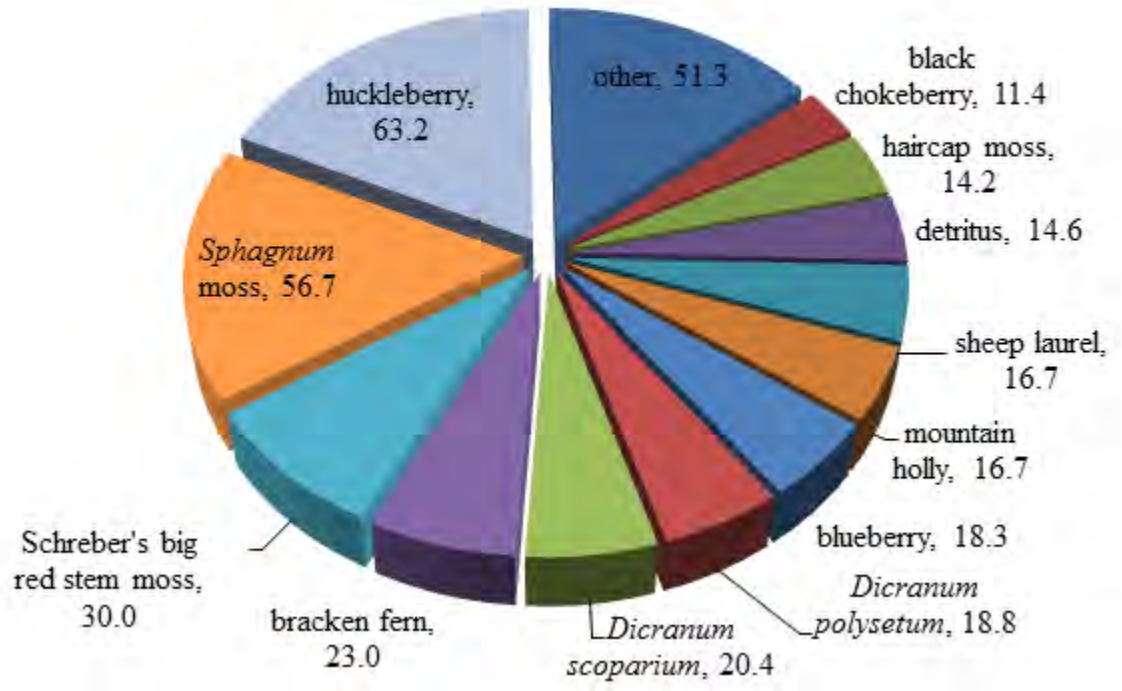

Figure 6. Absolute percent cover by species for ground cover sampled from 1 m^2 plots at Altona Flat Rock pine barren, autumn, 2014.

Year: 2014

Title: Assessment of post-burn jack pine regeneration

Location: Gadway Pine Barren

Investigators : Forest Ecology and Management students at SUNY Plattsburgh

Summary: Since 2011, students in the Forest Ecology and Management course at Plattsburgh State have been monitoring the success of jack pine seedlings, estimating density of live and dead trees, and assessing the characteristics of the ground cover in the burn and adjacent unburned. This fire event has provided a unique opportunity to study succession in this rare community type. In fall 2014 students estimated there were 7,708 jack pine seedlings in the burned area and no seedlings in the unburned area (Figure 7). A great example of the importance of fires to the life cycle of jack pines! In addition, there were large differences in the

number of live and dead standing jack pine trees between the burned and unburned plots (Figure 8). Lastly, exposed bedrock was 30% of the ground cover in burned plots and only 2% in unburned, indicating the fire removed much of the lichen and bryophyte layers.

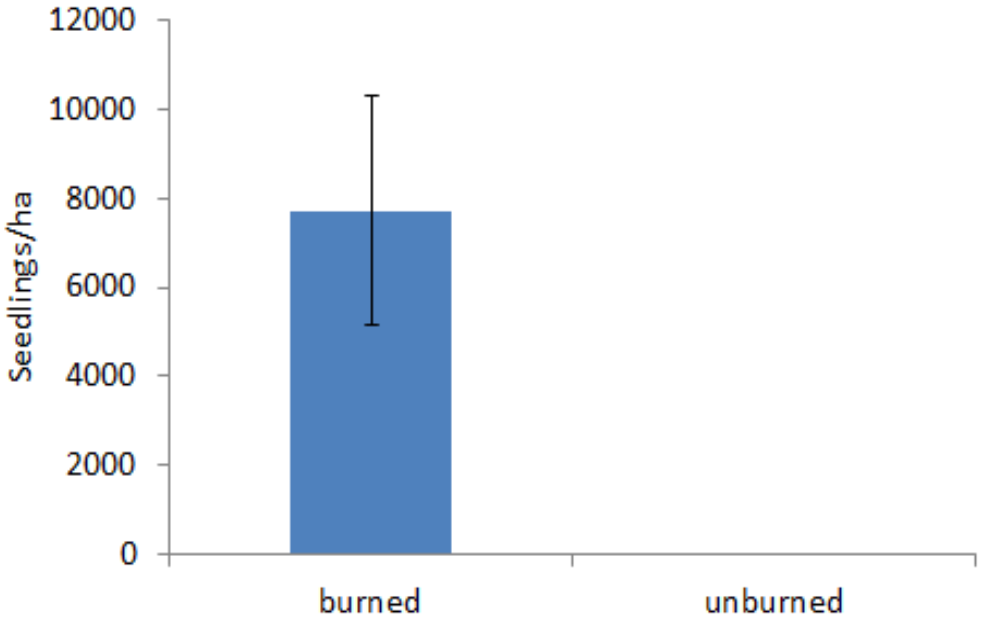

Figure 7. Density of jack pine seedlings at Gadway pine barrens in a burned and unburned area, autumn 2014. The burned area was from a fire in May 2010.

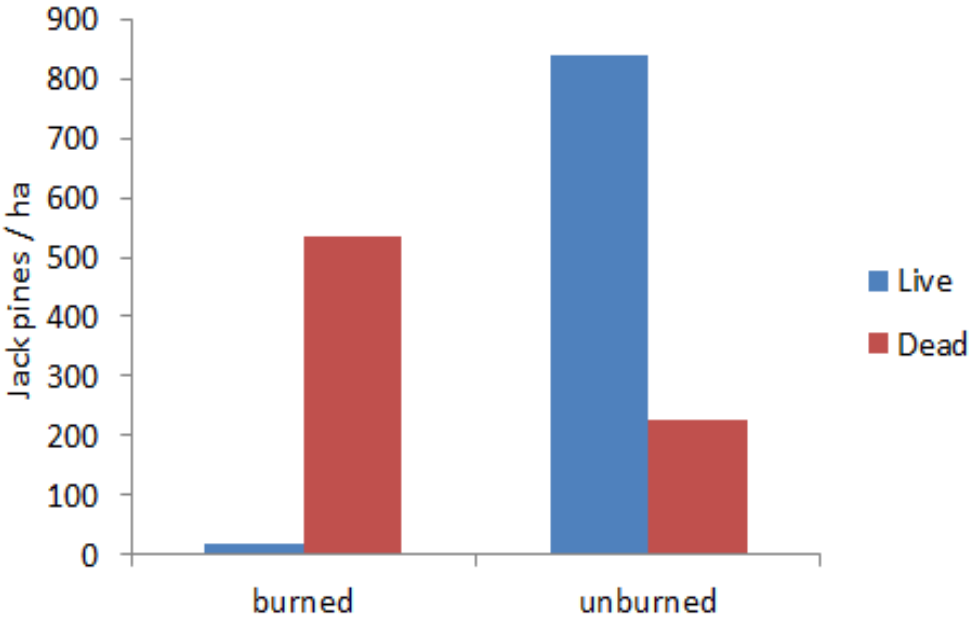

Figure 8. Density of live and dead jack pine trees at the Gadway pine barrens in burned and unburned areas, autumn 2014. The burned area was from a fire in May 2010.

FIELD GUIDE AND ROAD LOG

Meeting Point: Southeastern parking lot of Hudson Hall on the SUNY Plattsburgh campus. The lot is located at the corner of Beekman and Broad streets.

Meeting Point Coordinates: 44.691°N, 73.467°W

Meeting Time: 8:30 AM

Distance in miles (km)		Route Description
Cumulative	Point to Point	
0.9 (1.4)	0.9 (1.4)	Assemble in the southeastern parking lot of Hudson Hall. Leave parking lot, turn left at the entrance, and continue northward on Beekman Ave. to Boynton Ave.
1.4 (2.6)	0.5 (0.8)	Junction of Beekman and Boynton streets. Turn right onto Boynton Ave. 0.5 miles until reaching the turn off for NY-22 N.
10.3 (16.6)	8.9 (14.3)	Turn left onto NY-22 N and follow north for 8.9 miles until reaching W Church St.
11.8 (19.0)	1.5 (2.4)	Turn left onto W Church St. and follow westward until reaching Barnaby Rd.
14.1 (22.7)	2.3 (3.7)	Turn right onto Barnaby Rd. and continue onto Blaine Rd.
14.4 (23.2)	0.2 (0.3)	Stay right to stay on Blaine Rd. for 0.2 miles. You will park at the end of this road.

STOP 1: Altona Flat Rock Pavement Barrens, Chazy, NY

Location Coordinates: (44.837 °N, 73.570 °W)

The Altona Flat Rock pine barren is located in the township of Altona, Clinton County, and is primarily owned by The W. H. Miner Agricultural Research Institute. Altona Flat Rock is the largest of the sandstone pavements in northeastern New York (Figure 1). The central portion of Altona Flat Rock is drained by Cold Brook, a headwater tributary of the Little Chazy River that originates near the Dead Sea.

The Altona Flat Rock was heavily influenced by a large ice storm in 1998 (Irland 1998). An assessment of overstory tree composition at this site in 1999 revealed it was dominated by an admixture of jack pine (*Pinus banksiana*), pitch pine (*P. rigida*), and red maple (*Acer rubrum*). An outstanding quality of this pine barren is its geographic location at the northern limit of pitch pine and southern limit of jack pine (Burns and Honkala 1990). Both species depend on fire for reproduction (Yorks and Adams 2003). This particular sandstone pavement pine barren is fire-dependent and considered a rare ecosystem by the New York Natural Heritage Program

(Edinger et al. 2014). The last stand-replacing fire to affect this pine barren occurred in 1957 and it burned over 1,200 ha. In this type of ecosystem fire acts as an ecological mechanism to set the successional state back to a less developed state (Noble and Slatyer 1980).

Distance in miles (km)		Route Description
Cumulative	Point to Point	
16.9 (27.2)	2.5 (4.0)	Return to the vehicles and backtrack northeast on Blaine Rd. to Barnaby Rd. and continue to Recore Rd.
19.2 (30.9)	2.3 (3.7)	Turn right on Recore Rd. and follow to NY-190.
28.6 (46.0)	9.4 (15.1)	Turn right onto NY-190 W until Alder Bend Rd.
31.6 (50.9)	3.0 (4.8)	Turn right onto Alder Bend Rd.
33.3 (53.6)	1.7 (2.7)	Turn left onto US-11 S and follow to Cannon Corners Rd.
35.8 (57.6)	2.5 (4.0)	Turn right onto Cannon Corners Rd. and follow to Gadway Rd.
36.6 (58.9)	0.8 (1.3)	Turn left onto Gadway Rd. and follow the road to the parking area.

STOP 2: Gadway Pine Barrens, Mooers Forks, NY

Location Coordinates: (44.950410°N, 73.753830°W)

The Gadway Sandstone Pavement Pine Barren is located in Clinton County, near the border with Quebec (Figure 1). The Gadway barren is an outstanding example of a sandstone pavement barren, a globally rare ecological community with fewer than 20 sites in the world and fewer than five sites in New York State. The Gadway barren is approximately 210 ha (520 ac) in size and is dominated by jack pine. With its serotinous cones, jack pine is one of the best examples of a fire-adapted species in New York.

The most recent example of a wildfire in the barrens occurred at Gadway on May 28, 2010. The day prior to the fire, there was lightning area which is believed to have caused this. With winds from a westerly direction, the main fire was a backfire spreading into the barren at a rate of less than 1 m/min. The forest ranger response was rapid and the fire burned only approximately 2 ha (5 ac).

In addition to the exploration of the plant communities at Gadway, we will also visit sites that expose fossils in the Potsdam Sandstone. According to Landing et al. (2007), “arthropod trackways (predominantly *Diplichnites* and *Protichnites*) as well as probable mollusk trackways *Climactichnites* and *Plagiogmus,* are well preserved on some bedding surfaces.”

Distance in miles (km)		Route Description
Cumulative	Point to Point	
37.4 (60.2)	0.8 (1.3)	Return to the vehicles and backtrack northeast on Gadway Rd. to Cannon Corners Rd.
39.9 (64.2)	2.5 (4.0)	Turn right onto Cannon Corners Rd.
41.6 (66.9)	1.7 (2.7)	Turn left onto US-11 N.
44.6 (71.7)	3.0 (4.8)	Turn right onto Alder Bend Rd.
60.8 (97.8)	16.2 (26.1)	Turn left onto NY-190 E
63.3 (101.9)	2.5 (4.0)	Turn left onto Mason St. / Tom Miller Rd.
64.0 (103.0)	0.7 (1.1)	Turn right onto Prospect Ave.
64.3 (103.5)	0.3 (0.5)	Turn left onto Broad St. and left onto Beekman Ave., parking will be on left at Hudson Hall.

REFERENCES CITED

Adamec, L., 2011, Ecophysiological look at plant carnivory, All flesh is grass, Springer, p. 455-489.

Adams, K.B. and Franzi, D.A., 1994, The Clinton County (New York) pine barrens: Glacial catastrophe, historical wildfires, and modern uniquity: Wildflower, v. 10, no. 4, pp. 30-33.

--------, 1998, Fire and Ice: Restoration or requiem for an ecological preserve: Adirondack Research Consortium, Fifth Annual Conference on the Adirondacks.

Aerts, R., 1995, The advantages of being evergreen: Trends in Ecology & Evolution, v. 10, no. 10, p. 402-407.

Burns, R.M., and Honkala, B.H., 1990, Silvics of North America I. Conifers: U.S. Department of Agriculture Forest Service, Agricultural Handbook 654, 675p.

Clark, P.U. and Karrow, P.F., 1984, Late Pleistocene water bodies in the St. Lawrence Lowland, New York, and regional correlations: Geological Society of America Bulletin, v. 95, p. 805-813.

Coleman, A.P., 1937, Lake Iroquois: Ontario Department of Mines 45th Ann. Report, 1936, v. 45, Part 7, p. 1-36.

Coles, J.J., 1990, By fire and by ice: The evolution of an unusual landscape: unpublished M.S. thesis, Department of Botany, University of Vermont, 49p.

DellaRocco, T. and Straub, J.N., 2015, Fifteen-year community type change in a sandstone pavement barren: Scientia Discipulrom (*in review*).

Denny, C.S., 1974, Pleistocene geology of the northeastern Adirondack region, New York: United States Geological Survey, Professional Paper 786, 50p.

During, H. J., and Tooren, B. F. V., 1990, Bryophyte interactions with other plants: Botanical Journal of the Linnean Society, v. 104, no. 1-3, p. 79-98.

Eckstein, R. L., Karlsson, P. S., and Weih, M., 1999, Leaf life span and nutrient resorption as determinants of plant nutrient conservation in temperate-arctic regions: New Phytologist, v. 143, no. 1, p. 177-189.

Edinger, G.J., D.J. Evans, S. Gebauer, T.G. Howard, D.M. Hunt, and A.M. Olivero (editors). 2014. Ecological communities of New York State. Second Edition. A revised and expanded edition of Carol Reschke's ecological communities of New York State. New York Natural Heritage Program, New York State Department of Environmental Conservation, Albany, NY.

Fisher, D.W., 1968, Geology of the Plattsburgh and Rouses Point, New York-Vermont quadrangles: New York State Museum and Science Service, Map and Chart Ser. no. 10, 51p.

Franzi, D.A., and Adams, K.B., 1993, The Altona Flat Rock jack pine barrens: A legacy of fire and ice: Vermont Geology, v. 7, p. 43-61.

Franzi, D.A., and Adams, K.B., and Pair, D.L., 1993, The late glacial origin of the Clinton County Flat Rocks: New York State Geol. Assoc. Field Trip Guidebook, 65th Annual Meeting, p.

Franzi, D.A., and Adams, K.B., 1999, Origin and fate of the sandstone pavement pine barrens in northeastern New York: Guidebook to Field Trips in Vermont and Adjacent Regions of New Hampshire and New York, New England Intercollegiate Geological Conference, 91st Annual Meeting.

Gooley, L., 1980, A history of Altona Flat Rock, located in Clinton County, New York State: Denton Publications, Inc., Elizabethtown, New York, 103p.

Goslee, S.C., Brooks, R.P. and Cole, C.A., 1997, Plants as indicators of wetland water source: Plant Ecology, v. 131, p. 199-206.

Harlow, W.M., Harrar, J.W., Hardin, E.S., and White, F.M., 1991, Textbook of Dendrology, 7th Edition: McGraw-Hill, Inc., New York, 501p.

Irland, L.C. 1998. Ice storm 1998 and the forests of the Northeast: A preliminary assessment. Journal of Forestry, v. 96, no. 9, p.32-40.

Landing, E., Franzi, D.A., Hagadorn, J.W., Westrop, S.R., Kroger, B., and Dawson, J.C. 2007. Cambrian of East Laurentia: Field Workshop in eastern New York and Vermont: in Landing, E. (ed.), Ediacaran-Ordovician of East Laurentia: New York State Museum Bulletin, no. 510, p. 25-80.

Lewis, D.W., 1971, Quantitative petrographic interpretation of Potsdam Sandstone (Cambrian), southwestern Quebec: Canadian Journal of Earth Sciences, v. 8, no. 8, p. 853-882.

Lewis, J., 2012, The application of ecohydrological groundwater indicators to hydrogeological conceptual models: Groundwater, v. 50, no. 5, p. 679-689.

MacClintock, P. and Stewart, D.P., 1965, Pleistocene geology of the St. Lawrence Lowlands: New York State Museum Bulletin, no. 394, 152p.

MacClintock, P. and Terasme, J., 1960, Glacial history of Covey Hill: Journal of Geology, v. 68, no. 2, p. 232-241.

Muller, E.H. and Prest, V.K., 1985, Glacial lakes in the Ontario Basin: in Karrow, P.F. and Calkin, P.E., Quaternary Evolution of the Great Lakes, Geological Association of Canada Special Paper 30, p. 213-229.

Noble, I.R. and Slatyer, R.O., 1980, The use of vital attributes to predict successional changes in plant communities subject to recurrent disturbances: Advances in Vegetation Science, vol. 43 p. 5-21.

Pair, D., Karrow, P.F., and Clark, P.U., 1988, History of the Champlain Sea in the central St. Lawrence Lowland, New York, and its relationship to water levels in the Lake Ontario basin: in Gadd, N. R. (ed.), The Late Quaternary development of the Champlain Sea basin: Geological Association of Canada, Special Paper 35, p. 107-123.

Pair, D.L., and Rodrigues, C.G., 1993, Late Quaternary deglaciation of the southwestern St. Lawrence Lowland, New York and Ontario: Geological Society of America Bulletin, v. 105, p. 1151-1164.

Swan, J. M. A., and Gill, A. M., 1970, The origins, spread, and consolidation of a floating bog in Harvard Pond, Petersham, Massachusetts: Ecology, v. 51, no. 5, p. 829-840.

Sargis, G and K.B., Adams, 2004, Effects of an ice storm on fuel loadings and potential fire behavior in a pine barren of northeastern New York: Scientia Discipulorum v. 1 p. 17-25.

Woodworth, J.B., 1905a, Pleistocene geology of the Mooers Quadrangle: New York State Museum Bulletin, no. 83, 67p.

--------, 1905b, Ancient water levels of the Champlain and Hudson valleys: New York State Museum Bulletin, no. 84, 265p.

Wright, I. J., Reich, P. B., Westoby, M., Ackerly, D. D., Baruch, Z., Bongers, F., Cavender-Bares, J., Chapin, T., Cornelissen, J. H. C., Diemer, M., Flexas, J., Garnier, E., Groom, P. K., Gulias, J., Hikosaka, K., Lamont, B. B., Lee, T., Lee, W., Lusk, C., and Midgley, J. J., 2004, The worldwide leaf economics spectrum: Nature, v. 428, no. 6985, p. 821-827.

Yorks, T.E. and K.B. Adams. 2003. Restoration cutting as a management tool for regenerating Pinus banksiana after ice storm damage. Forest Ecology and Management, v. 177, no.1 p.85–94.

THE MAGNETITE-FLUORAPATITE ORES FROM THE EASTERN ADIRONDACKS, NEW YORK: CHEEVER MINE

MARIAN V. LUPULESCU
Research and Collections, New York State Museum, Albany, NY 12230

JEFFREY R. CHIARENZELLI
Department of Geology, St. Lawrence University, Canton, NY 13617

DAVID G. BAILEY
Geosciences Department, Hamilton College, Clinton, NY 13323

SEAN P. REGAN
Department of Geosciences, University of Massachusetts, Amherst, MA 01003-9297

INTRODUCTION

Iron mining in New York State, a significant supplier of iron ore used in developing the resources and industries of the United States through the first part of the 20th century, has a long and interesting history. Iron ore was mined from Grenville-age metamorphic rocks in the Adirondack Mountains and Hudson Highlands, and from Silurian-age sedimentary rocks in central and western New York (Clinton-type).

Smock (1889) was the first author to present a complete report and the first classification of the iron ores "…which occurs in beds and deposits of workable size in the State of New York". From his report we have brief descriptions, locations, and data on the ore quality, by-products, and output of the major mines operating in the late 19th century. Kemp (1897, 1908), Kemp and Ruedemann (1910), Nason (1922), Alling (1925), Gallagher (1937), Postel (1952), Buddington (1966), Hagner and Collins (1967), Baker and Buddington (1970), Foose and McLelland (1995), Valley et al. (2009), and Valley (2010) all made significant contributions to our understanding of the iron deposits in the Adirondack Mountains, but there is still no agreement as to their origin, and thus Alling's statement from 1925 directed at individuals wanting to understand the "*genesis of these important ore bodies in Northern New York may reach the conclusion that there is a hopeless disagreement among those who have studied these deposits"* is still as valid today as it once was.

On this trip we will visit the Cheever Mine in the eastern Adirondack Mountains. Our goal is to present a brief classification of iron ore deposits in the Adirondacks and to briefly summarize pertinent aspects of the diversity, differences, and similarities between mines and prospects across the Adirondacks and ignite discussion on their origin. According to their mineralogical and geochemical compositions, the principal iron deposits and prospects in the Adirondacks (Figure 1) are 1) low Ti iron oxide – REEs (Mineville, Cheever, Palmer Hill, Rutgers, LaVake, and Arnold Hill mines), 2) low Ti iron oxide (Lyon Mountain and Benson mines), 3) low Ti iron oxide - boron (vonsenite) (Jayville and partially Clifton mines), and 4) Ti – Fe oxides (Tahawus). Based on their general features (Valley et al. 2009; Valley 2010) these ores are considered to belong to the

IOCG (iron oxide – copper – gold) class of iron deposits (e.g., Hitzman et al. 1992) even though copper and gold mineralization is not known at these locations. One possible exception is the Lyon Mountain mines from which Callaverano and Zimmer (2009) reported on associated copper mineralization.

During this field trip we will visit the Cheever mine, Port Henry, Essex County, near Lake Champlain. Due to the elongate, sill-like geometry of the body it was worked at many locations along its length. To avoid confusion we will collectively refer to all the locations as belonging to the Cheever "mine". On this trip we will examine the morphology of the magnetite – fluorapatite ore bodies, the mineralogy of the ore and the host (foot- and hanging-wall), the relation of the ore body to the neighboring coronitic metagabbro, and discuss the igneous origin of the deposit in light of age, major and trace element chemistry, and isotopic composition of the fluorapatites from the ore and host rock.

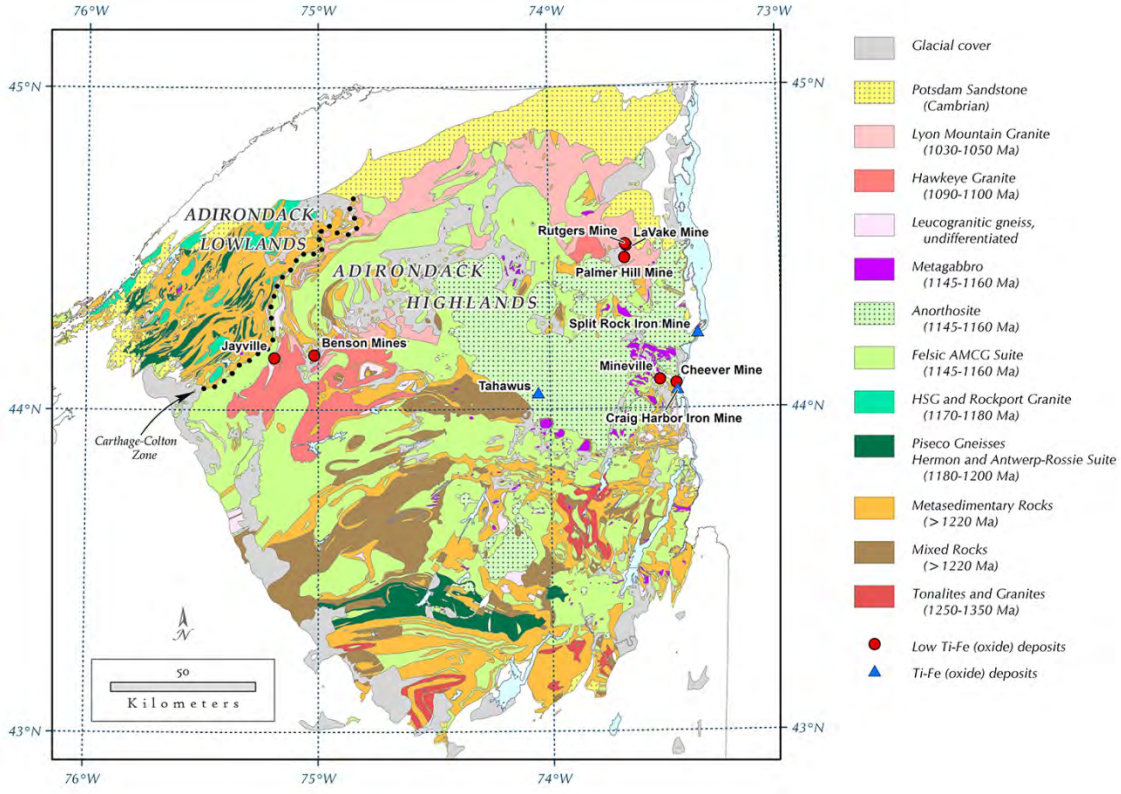

Figure 1. Location of the main iron deposits of the Adirondack Mountains

MINING HISTORY

The discovery of iron ore in the eastern Adirondacks was mentioned in 1749 in the works of the European naturalist named Kalm (Farrell 1996). The Cheever mine, located north of Port Henry, was discovered in 1804 and opened in 1820 (Linney 1943), and was the first important iron mine in the region. Subsequently, Charles Fisher opened the Fisher Hill mine that was worked discontinuously until 1893. The Cheever mine was systematically worked since 1853 and

"owned by the Cheever Ore Bed Company and leased by the New York Mining and Developing Company "(Smock 1889).

In 1824 exploration in nearby Mineville led to the discovery of a magnetite-apatite ore body that was later called the "Old Bed" (Birkinbine 1890). Soon thereafter, new workings northwest of the "Old Bed" produced a magnetite-silicate ore. These works were named the "New Bed". Before 1840, new diggings searched for and found the northern continuation of the "New Bed" and thus, the Barton Hill mines were opened (Farrell 1996). Between 1859 and 1971 when the Mineville works closed for good, the mines were worked intermittently.

The mines from Arnold Hill and Palmer Hill in the Ausable Forks region, Clinton County were small and not significant competitors of the Mineville – Port Henry district. The Arnold Ore Co. operated the Arnold Hill mine for a brief period after 1806 (Postel 1952). Smock (1889) reported some intense renewed activity after 1830. The beginnings of the Palmer Hill mine works are not very clear; it opened in 1825 according to Newland (1908) or 1844 according to Smock (1889). Both mines lasted until 1890 (Newland 1908). The Rutgers and LaVake mines belong to the same mining district, but they were too small and the ore too low-grade to be of any economic importance. The iron ore from the Lyon Mountain region was discovered around 1823 at what is now called the Chateaugay mine (Linney 1943); some prior works were reported in 1798 when the first Catalan forge was operated at Plattsburg (Linney 1943, Cavallerano and Zimmer 2009). In 1803, a new Catalan forge started to process the iron ore from the Pratt vein of what would later be known as the 81 mine (Linney 1943). Large scale operations started in 1867, but did not become significant until 1871. In 1881 the Chateaugay Ore and Iron Co. was organized and operated the mine until 1902 when it became a subsidiary of the Hudson Coal Co., a subsidiary of the Delaware and Hudson Railroad (Gallagher 1937). The mine closed temporarily from 1926 to 1929 because of the recession. Republic Steel Co. leased the mine in 1939. Mining activity in the region stopped for good in 1968 (Cavallerano and Zimmer 2009).

REGIONAL GEOLOGY

The Adirondack Mountains are part of the Grenville Province, formed by a series of orogenies that lasted from 1.3 to 1.0 billion years (Ga) ago. Three distinct orogenies are recognized in the Grenville province (Rivers 2008) including the Adirondacks. These are: (a) Elzevirian (1245 to 1225 Ma); (b) Shawinigan (1190-1140 Ma); and (c) Grenvillian, which included the Ottawan (1090-1020 Ma), and Rigolet (1000-980 Ma) pulses. An important boundary demarked by the Carthage-Colton Shear Zone (Geraghty et al., 1981; Streepey et al., 2001) separates two domains in the Adirondacks, the Central Metasedimentary Belt or Adirondack Lowlands (AL) and the Central Granulite Terrain, or Adirondack Highlands (AH). These two realms differ in terms of their lithologic content, metamorphic grade, and timing of last deformation.

The uplifted region of the Adirondack Highlands has a dome-like shape. The AH contains supracrustal and volumetrically dominant igneous rocks that were metamorphosed at high temperature and medium pressure (granulite facies conditions) during the Shawinigan orogeny. The Ottawan pulse of the Grenville Orogeny (~1050 Ma) in this region has a strong thermal signature with zircon growth, anatexis in the lower crust, and intrusion of igneous rocks of various compositions in an extensional setting (Selleck et al. 2005). The oldest rocks are arc-related tonalities that were emplaced between 1330 and 1307 Ma (McLelland and Chiarenzelli 1990a). This event was followed by a series of younger magmatic events which included

intrusion of the AMCG suite (1165-1155 Ma; McLelland et al. 2004; McLelland and Chiarenzelli 1990b) and intrusion of younger igneous rocks such as the A-type Hawkeye granite (1100-1090 Ma), mangerites from the northern Highlands (1080 Ma), and the A-type Lyon Mountain granite (1070-1040 Ma) (McLelland et al. 1996).

IRON DEPOSITS

The iron deposits from the eastern AH are low-Ti iron oxide ores that belong to the IOCG (iron-oxide-copper-gold) class of iron deposits (Hitzman et al 1992), although the lack of copper and gold also makes them similar to the classic Kiruna-type of iron deposit (Frietsch 1978). Proposed explanations for their origin include: 1) immiscible Fe-rich fluids (Postel 1952), 2) extraction of Fe during the breakdown of the Fe-rich silicates during metamorphism (Hagner and Collins 1967), 3) eruption of Fe-oxide-rich magmas (Whitney and Olmsted 1993), and 4) the interaction of surface-derived saline fluids with mid-crustal rocks in the late stages of the pluton emplacement (Foose and McLelland 1995; McLelland et al. 2002).

In general, the iron ores of the eastern Adirondacks consist of intrusive sheets or dikes that contain abundant low-Ti magnetite associated with fluorapatite, augitic pyroxenes, and trace minerals including zircon, stillwellite-(Ce), monazite-(Ce), and allanite-(Ce). Observations under transmitted light show polygonal and cumulate textures. The ore bodies, each with knife-edge contacts, may be temporally associated with the intrusion of A-type leucogranites (e.g. Foose and McLelland 1995; Valley et al. 2009; 2010; Valley 2010) and granitic gneisses (ca. 1040 Ma). Undeformed pegmatites cross-cutting the ore yield U-Pb zircon ages of ca. 1039 and 1022 Ma, with rims at 949 ±10 Ma (Lupulescu et al. 2011).

Based on the underground geological maps of the Republic Steel Company, McKewon and Klemic (1956) provided a detailed petrography and succession of the host rocks at Mineville. They concluded that the metamorphic sequence stratigraphically began with a basal metagabbro that was the equivalent of Kemp's (1908) "mafic syenite". This was overlain, in turn, by the magnetite-apatite ore of the "Old Bed", granite gneiss, diorite, gabbro, and the magnetite-silicate ore of the Harmony bed. Because the Mineville and Cheever deposits display close mineralogical and petrographic features, descriptions of much of the Cheever mine apply to similar occurrences in the Mineville deposits.

ROAD LOG

The field trip starts at the Port Henry Boat Launch Site. The site is at the intersection of Dock and Velez lanes in Port Henry, Essex County.

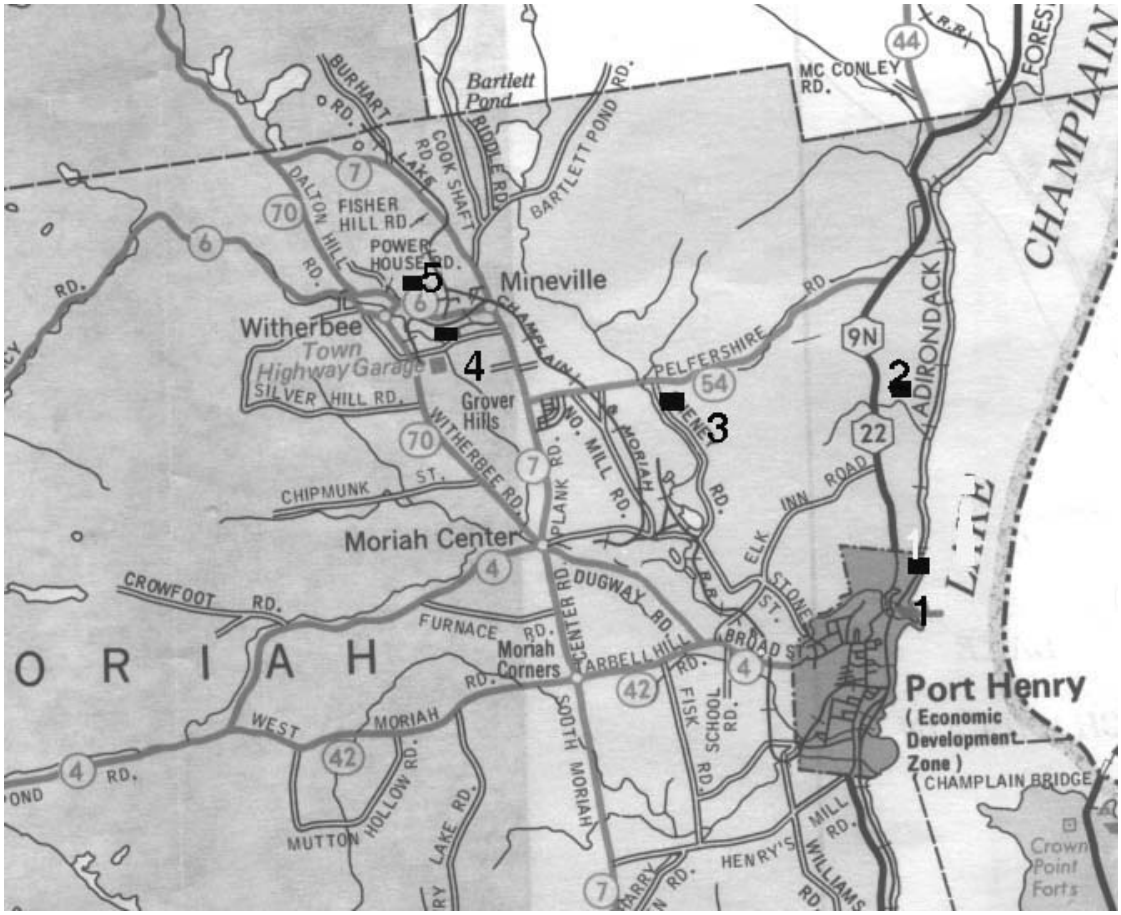

Location map of the Cheever iron deposits and neighboring mines. We will visit only the Cheever mine. (1. Craig Harbor Mine; 2. Cheever Iron Mine; 3. Pelfshire iron Mine; 4. Mineville group of mines; 5. Barton Hill group of mines).

Cumulative mileage	Miles from the last point	Route description
1.5 miles	1.5 miles	Follow Rt22/9N toward north. Stop on the right side of the road in front of the metal gates. Walk around the gates and follow the unpaved Jeep road going north.

Stop 1: Cheever mine

Location coordinates: N 44° 04' 43.5"; W 73° 27' 14.3"

At the Cheever mine, a coronitic metagabbro is spatially associated with the leucocratic rocks containing the magnetite-apatite ore. A similar situation can be seen at the Barton Hill mines in

the Mineville area. The nature of the contact (tectonic vs. intrusive) is not obvious, being obscured by recent alluvium and cover in both cases. The coronitic metagabbro from Cheever mine is sheared toward the contact with the leucocratic rocks which contain quartz, albite, and minor pyroxene, or quartz, albite, microcline, and pyroxene-rich units. Lenses of mafic rocks containing pyroxene, amphibole, fluorapatite, and magnetite can be found in the tailings (the underground works are not accessible).

The coronitic metagabbro occurs in massive or layered form. The massive form contains plagioclase "clouded" with spinels, pyroxenes, garnet and annite (Figure 2). Some pyroxenes display exsolution of tiny elongated lamellae of another pyroxene and ilmenite as the result of the sub-solidus re-equilibration during slow cooling. In some grains, both types of lamellae occur oriented along the two pyroxene cleavages. Rare grains of ilmenite and pyrrhotite pepper the rock. The coronitic metagabbro contains a layered facies with the same composition as the massive one.

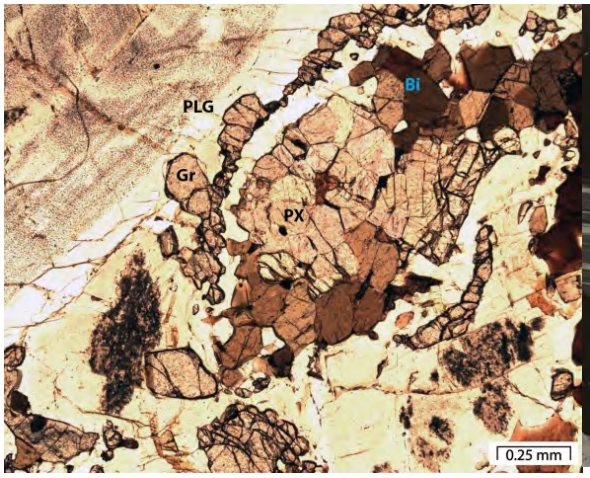

Figure 2. Coronitic metagabbro under the microscope in plane polarized light. Bi – biotite; PLG – plagioclase; Gr – garnet; PX – pyroxene. Plagioclase is clouded with spinels.

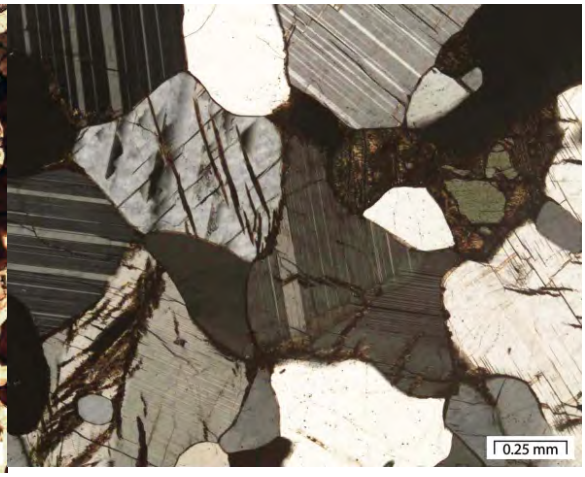

Figure 3. Host granite in cross polarized light. Albite is twinned, quartz is white, and green pyroxene is replaced by chlorite (upper corner).

The footwall rock which hosts the ore is granite that contains predominantly quartz and albite (Figure 3). Minor phases are grains of relict clinopyroxene (replaced by chlorite), zircon (some grains are partially metamict), and magnetite with ilmenite lamellae. The hanging wall rock contains more relict pyroxenes than the footwall, and the magnetite/ilmenite grains are rounded and, in places, associated with pyroxene replaced by chlorite. Further on, the rock displays a gneissic texture with alternating "bands" of quartz and albite, and pyroxene, amphibole, annite, magnetite, and ilmenite and rare grains of apatite and pyrrhotite altered to goethite. Exsolution textures within the pyroxenes are common. This rock grades into a microcline, albite, quartz, pyroxene, amphibole, and ilmenite-rich gneiss. The ore-hosting rocks are undeformed (this observation is sustained also by microscopic study) and contain pyroxene, and rounded, in places droplet-looking, grains of magnetite and or ilmenite.

The rocks have high concentrations of Na_2O (3.48 wt.% in the metagabbro, to 6.31 wt.% in the footwall leucogneiss); K_2O varies from 0.36 % in the footwall rock to 3.63 % in the highest

stratigraphic unit of the hanging wall leucogneiss. All rocks display normative “hypersthene”. The rocks are enriched in REEs, like those from Mineville (Figure 5a, b).

The magnetite-fluorapatite ore at the Cheever Mine forms dikes / sills that have sharp contacts with the host rock. The ore contains abundant magnetite, fluorapatite, and augitic pyroxene. Other mineral phases present include ilmenite, titanite rimming magnetite, zircon, monazite-Ce, stillwellite-Ce, allanite-Ce, and thorite. The amphibole tremolite is very rare, and mostly is the result of the low temperature interraction of clinopyroxene, quartz, and later fluids. A relatively F-rich (1. 19 to 1.58 wt.%) amphibole with blue pleochroism under plane polarized light seems to be the last igneous mineral in the succession. Rare spinel phases were exsolved along the {111} crystallographic planes of the large magnetite grains.

Three samples of Cheever ore and host rock were selected for electron microprobe WDS analysis and in-situ U-Th-total Pb monazite geochronology. WDS compositional mapping was performed on the Cameca SX-50. Quantitative analysis of monazite was performed on the SX-100 ultrachron following procedures outlined in Allaz et al. (2013) at the University of Massachusetts, Amherst. Initially, thin sections were mapped for Mg, Y, Ce, Zr, and Ca or Fe (300 nA, defocused beam; Fig. 8). Close up maps of monazite were done with a fixed stage, using a beam rastering mode for sub-micron resolution, with the current at 200 nA. For large grains, stage mapping was employed due to the sufficient resolution at 2 micron-pixels. Preliminary geochronology will not be presented herein due to extremely low actinide contents

As mentioned above, the ore contains magnetite, apatite, allanite, monazite, stillwellite, and other phases. All thin sections contain sharp boundaries between ore and the host albite-quartz rock with augitic pyroxene crystals. All WDS full section maps show abundant zircon in host rock, but no zircon in the ore. One thin section (Figure 9) contains abundant REE bearing phases interspersed with magnetite. Most notably are medium grained stillwellite (Ca, LREE, Th borosilicate) and coarse symplectic intergrowths of allanite and monazite. Symplectic monazite has very low actinide concentrations, and has been a challenge to date (as noted above). However, the low actinide content suggests a low temperature, post mineralization origin for the symplectite formation. The other two thin sections contain coarse monazite crystals, typically associated with, and sometimes rimming, apatite crystals. Recent grain mapping has revealed several high Th grains, which should yield robust and reliable counting statistics, and thus an acceptable age determination. This work is ongoing.

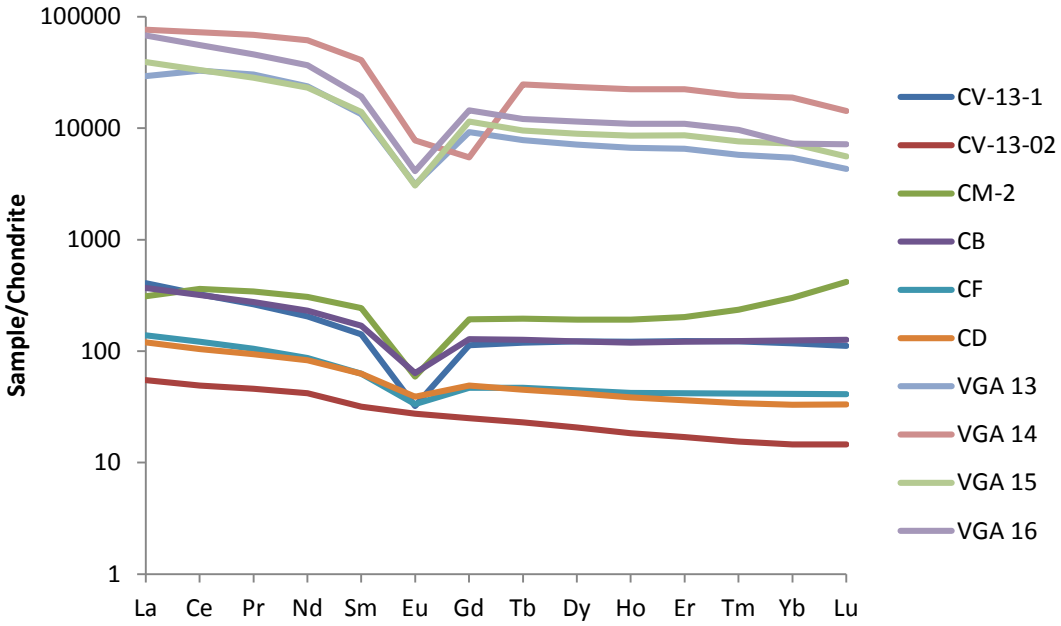

Figure 5a. Apatite/chondrite (VGA 13, 14, 15, 16 –upper group on diagram) and rock/chondrite (CV-13-1, CV-13-2, CM-2, CB, CF, CD-lower group) REE diagram for samples from the Cheever mine.

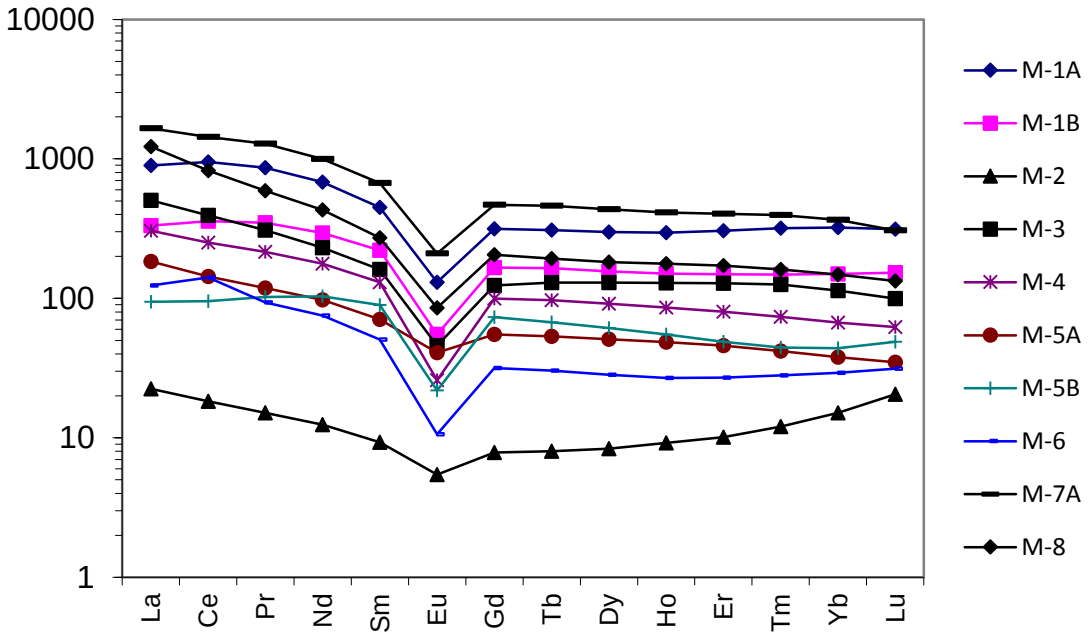

Figure 5b. Rock/chondrite REE diagram for rocks from the Mineville deposit.

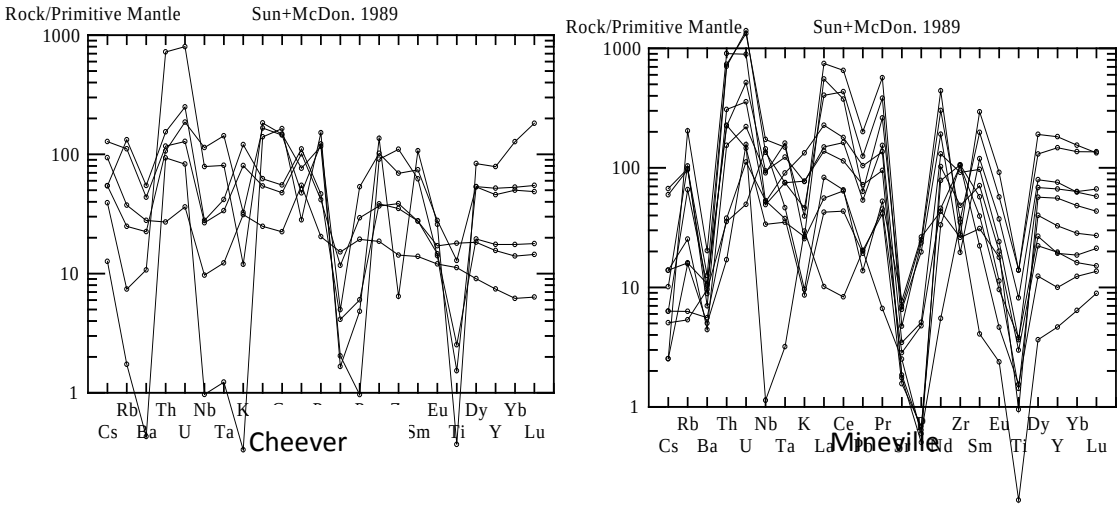

Figure 6. Rock/primitive mantle element abundance diagrams for the Cheever and Mineville rocks.

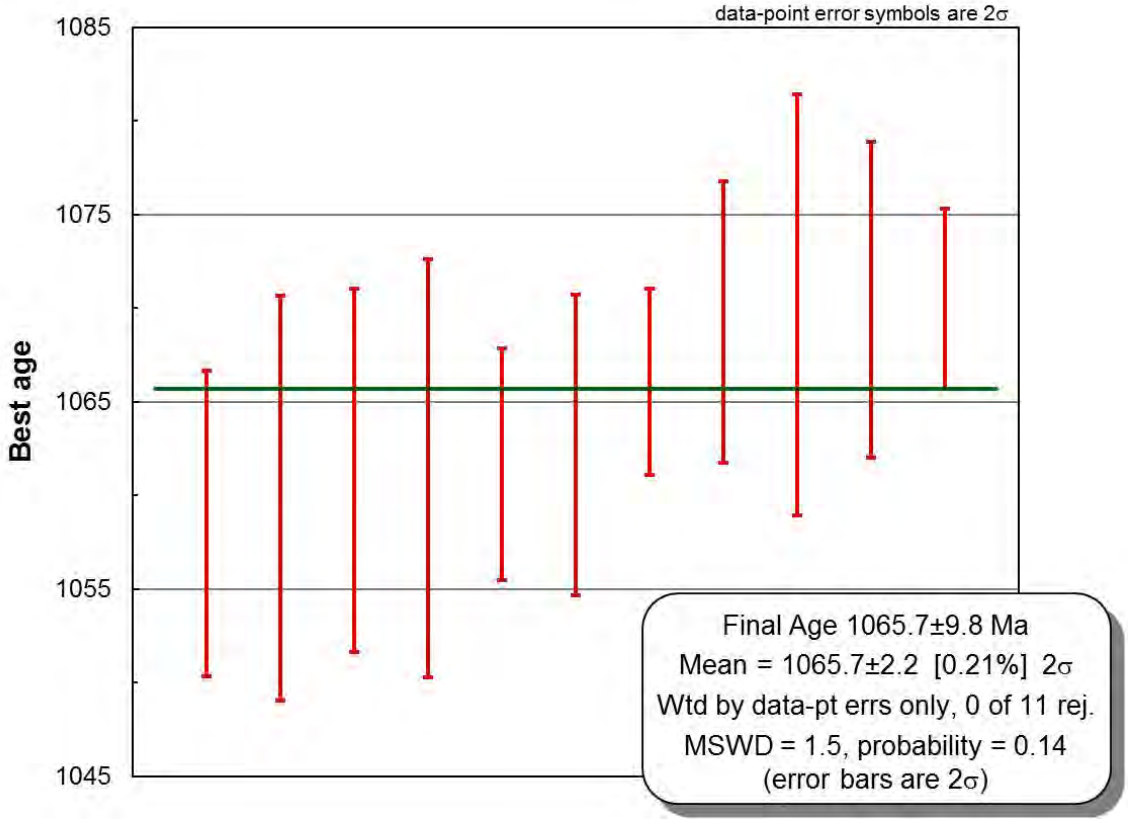

Figure 7. Zircon crystals separated from the ore-hosting rock were dated by LA-MC-IC-MS and yielded an age of 1065.7 ± 9.8 Ma.

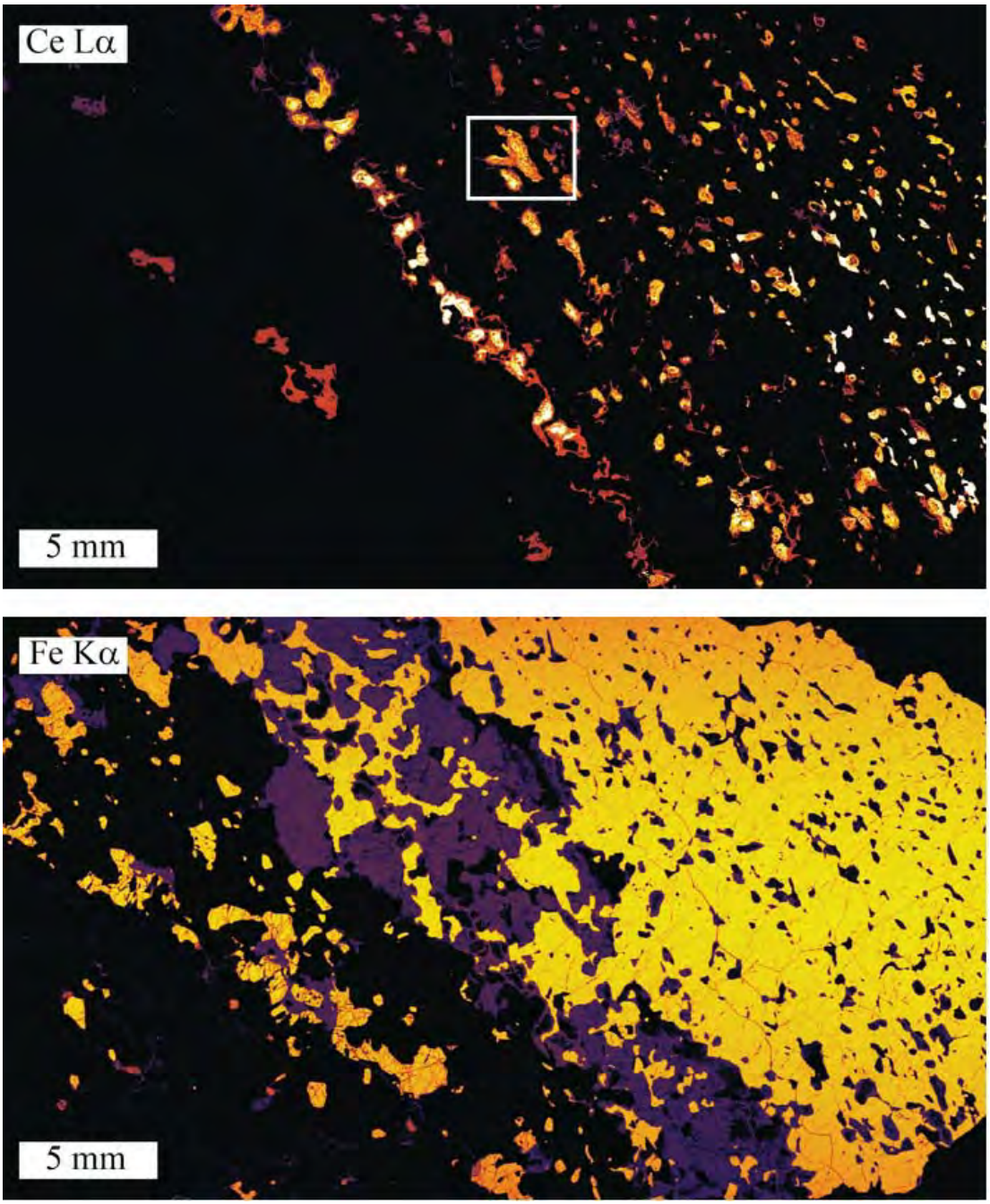

Figure 8. WDS full section maps for the Cheever mine ore. Note the abundance of Ce (proxy for monazite and other REE bearing phases) within the Fe-ore.

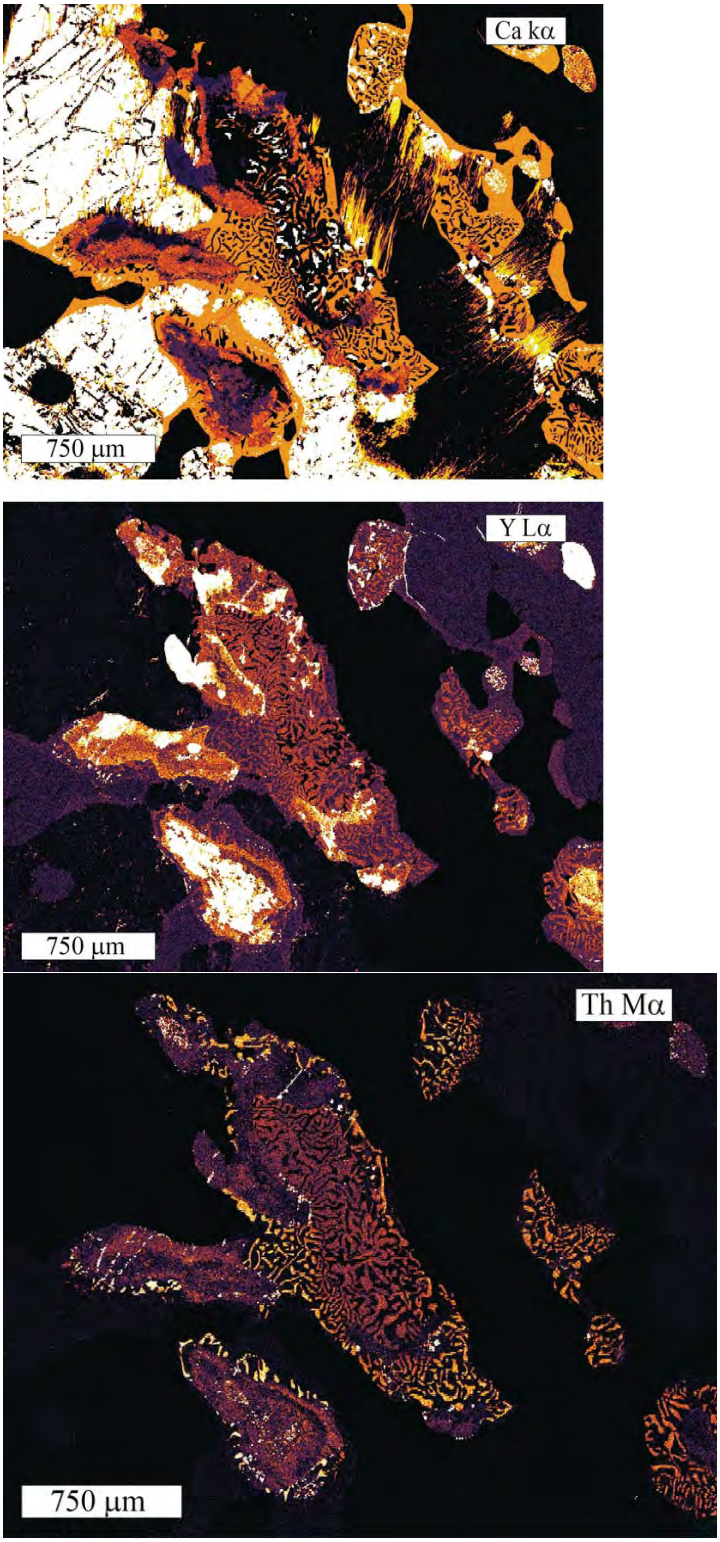

Figure 9. WDS compositional maps for monazite-(Ce) – allanite-(Ce) symplectite in Cheever mine. Within this thin section, all of the monazite contains very low total actinide compositions, consistent with low-temperature formation or dissolution-reprecipitation reactions.

REFERENCES CITED

Allaz, J., Selleck, B., Williams, M.L., and Jercinovic, M.J., 2013, Microprobe analysis and dating of monazite from the Potsdam formation, NY: A progressive record of chemical reactions and fluid interaction: American Mineralogist, v. 98, n. 7, p. 1106 - 1119.

Alling, H. L., 1925, Genesis of the Adirondack magnetites. Economic Geology, v. 20, p. 335 - 363.

Baker, D. R., and Buddington, A. F., 1970, Geology and magnetite deposits of the Franklin quadrangle and part of the Hamburg quadrangle, New Jersey, U. S. Geological Survey Professional Paper 638, 73 p.

Birkinbine, J., 1890, Crystalline magnetite in the Port Henry, New York mines, Transactions of the American Institute of Mining Engineering, v. 18, p. 747 – 762.

Buddington, A. F., 1966, The Precambrian magnetite deposits of New York and New Jersey, Economic Geology, v. 61, p. 484 – 510.

Cavallerano, E. J. and Zimmer, P. W., 2008, History and geology of the Chateaugay mine, Lyon Mountain, New York, with a discussion of previously unreported minerals. Rocks & Minerals, v. 84, p. 446 – 453.

Farrell, P., 1996, Through the Light Hole, North Country Books, Utica, N. Y., 245 p.

Foose, M. P., and McLelland, J. M., 1995, Proterozoic low – Ti iron – oxide deposits in New York and New Jersey: relation to Fe – oxide (Cu – U – Au – rare element) deposits and tectonic implications, Geology, v. 23, p. 665 –668.

Frietsch, R., 1978, On the magmatic origin of the iron ores of the Kiruna type. Economic Geology, v. 73, p. 478-485.

Gallagher, D., 1937, Origin of the magnetite deposits at Lyon Mountain, N.Y. New York State Museum Bulletin 311.

Geraghty, E. P., Isachsen, Y. W., and Wright, S. F., 1981, Extent and character of the Carthage-Colton Mylonite Zone, Northwest Adirondacks, New York: New York State Geological Survey report to the U.S. Nuclear Regulatory Commission, 83p.

Hagner, A. F. and Collins, L. G., 1967, Magnetite ore formed during regional metamorphism, Ausable magnetite district, New York. Economic Geology, 62, p. 1034-1071.

Hitzman, M.W., Oreskes, N., and Einaudi, M.T. (1992) Geological characteristics and tectonic setting of Proterozoic iron oxide (Cu-U-Au-REE) deposits. Precambrian Research, 58, 241–287.

Kemp, J. F., 1897, The geology of the magnetites near Port Henry, N. Y. and especially those of Mineville, Transactions of the American Institute of Mining Engineers, v. 27, p. 147-203.

Kemp, J. F., and Ruedemann, R., 1910, Geology of the Elizabethtown and Port Henry quadrangles, New York State Museum Bulletin 138, 173 p.

Linney, R. J., 1943, A century and a half of development behind the Adirondack iron mining industry, Mining and Metallurgy, v. 24, p. 480-87.

Lupulescu, M. V., Chiarenzelli, J. R., Pullen, A. T., and Price, J. D., 2011, Using pegmatite geochronology to constrain temporal events in the Adirondack Mountains. Geosphere, 7, p. 23-29.

McKeown, F. A., and Klemic, H., 1956, Rare – earth – bearing apatite at Mineville, Essex County, New York, U. S. Geological Survey Bulletin 1046 – B, 23 p.

McLelland, J. and Chiarenzelli, J., 1990a. Geochronology and geochemistry of 1.3 Ga tonalitic gneisses of the Adirondack Highlands and their implications for the tectonic evolution of the Grenville Province: In Middle Proterozoic Crustal Evolution of the North American and Baltic Shields, Geological Association of Canada Special Paper 38, p. 175-196.

McLelland, J. M. and Chiarenzelli, J. R., 1990b. Geochronological studies of the Adirondack Mountains, and the implications of a Middle Proterozoic tonalite suite, in Gower, C., Rivers, T., and Ryan, C., eds., Mid-Proterozoic Laurentia-Baltica: Geological Association of Canada Special Paper 38, p. 175-194.

McLelland, J. M., Daly, J. S., and McLelland, J. M., 1996. The Grenville Orogenic Cycle (ca. 1350-1000 Ma): an Adirondack perspective. Tectonophysics, v. 265, p. 1-28.

McLelland, J.M., Bickford,M. E., Hill, B. M., Clechenko, C. C., Valley, J. W., and Hamilton, M. A., 2004, Direct dating of Adirondack massif anorthosite by U-Pb SHRIMP analysis of igneous zircon: Implications for AMCG complexes. Geological Society of America Bulletin 116: 1299–1317.

Nason, F. L., 1922, The sedimentary phases of the Adirondack magnetic iron ores, Economic Geology, v.17, p.633-654.

Newland, D. H., 1908, Geology of the Adirondack magnetic iron ores with a report on the Mineville-Port Henry group. New York State Museum Bulletin 119.

Philpotts, A. R., 1967, Origin of certain iron-titanium oxide and apatite rocks, Economic Geology, V. 62, p. 303-315.

Postel, A. W., 1952, Geology of Clinton County magnetite district, New York. Geological Survey Professional paper 237.

Rivers, T. 2008. Assembly and preservation of lower, mid, and upper orogenic crust in the Grenville Province—Implications for the evolution of large, hot, long-duration orogens. Precambrian Research 167:237–59.

Selleck, B., McLelland, J.M., and Bickford, M.E., 2005, Granite emplacement during tectonic exhumation: The Adirondack example: Geology, v. 33, p. 781–784, doi: 10.1130/G21631.1.

Smock, J. C., 1889, First report on the iron mines and iron-ore districts in the State of New York, Bulletin of the New York State Museum of Natural History, No. 7, 70 p.

Streeply, M. M., Johnson, E. L., Mexger, K. and Van Der Pluum, B. A., 2001, Early history of the Carthage-Coltom shear zone, Grenville Province, northwest Adirondacks, New York, (USA). Journal of Geology, 109, p. 479-492.

Valley, P.M., Hanchar, J.M., and Whitehouse, M.J., 2009, Direct dating of Fe oxide-(Cu-Au) mineralization by U/Pb zircon geochronology: Geology, v. 37, p. 223–226, doi: 10.1130/G25439A.1.

Valley, P. M., 2010, Fluid alteration and magnetite-apatite mineralization of the Lyon Mountain granite: Adirondack Mountains, New York State. PhD thesis, Memorial University of Newfoundland, St. John's, Newfoundland. 282 p.

Whitney, P. R., and Olmsted, J. F., 1988, Geochemistry and origin of albite gneisses, northeastern Adirondack Mountains, New York, Contributions to Mineralogy and Petrology, v. 99, p. 476–484.

DECIPHERING THE GEOLOGIC EVOLUTION OF THE EASTERN ADIRONDACKS: NEW FIELD, PETROLOGIC AND GEOCHRONOLOGIC DATA

TIMOTHY W. GROVER
Department of Natural Sciences, Castleton University, Castleton, VT 05735

MICHAEL L. WILLIAMS
Department of Geosciences, University of Massachusetts, Amherst, MA 01003

JAMES M. MCLELLAND
Department of Geology, Colgate University, Hamilton, NY 13346

SEAN P. REGAN
Department of Geosciences, University of Massachusetts, Amherst, MA 01003

GRAHAM B. BAIRD
Department of Earth and Atmospheric Sciences, University of Northern Colorado, Greeley, CO 80639

KIMBERLEE A. FRENCH
Department of Natural Sciences, Castleton University, Castleton, VT 05735

CLAIRE R. PLESS
Department of Geosciences, University of Massachusetts, Amherst, MA 01003

INTRODUCTION

Models for the tectonic evolution of the Adirondack Mountains have advanced significantly over the past ten to fifteen years. Prior to this, most workers would suggest that the (ca. 1.06 Ga) Ottawan Orogeny was the dominant deformation-metamorphic event in the Adirondacks. Recently published results from geochronological studies based on high resolution, single grain, U-Pb zircon SHRIMP data (McLelland et al., 2001; Hamilton et al., 2004; Heumann et al., 2006; Bickford et al., 2008), along with geochemical and field based studies in the Adirondack Lowlands (Chiarenzelli et al., 2010; Baird and Shrady, 2011), and recognition of an ophiolite suite in the Lowlands (Chiarenzelli et al., 2011) has resulted in significant revision of models of the tectonic evolution of the Adirondacks. These data reveal a major mountain-building event, the Shawinigan Orogeny (~1.2-1.16 Ga) - previously unrecognized in the Adirondack Highlands, resulted in widespread deformation and high grade metamorphism with accompanying partial melting. After the Shawinigan Orogeny, extensive anorthosite-mangerite-charnockite-granite (AMCG) magmatism (1.16. to 1.14 Ga) is interpreted to reflect a period of lithospheric delamination that resulted in asthenospheric upwelling and decompression melting in the mantle (McLelland et al., 2010) that yielded gabbroic magmas parental to the anorthosites. Thermal effects of the gabbroic magmas provided heat to partially melt portions of the lower crust and produce the felsic magmas of the AMCG suite.

In addition, Selleck et al. (2005) proposed that the Lyon Mountain granite was emplaced at the end of the Ottawan Orogeny (ca 1.05 Ga) and that it accompanied extensional collapse following peak-Ottawan compression. Wong et al (2012) support this model with evidence for an extensional shear zone in the eastern Adirondacks and show, using in situ EMP monazite data that the latest, normal-sense motion along the shear zone occurred from approximately 1.05 to 1.0 Ga.

In summary, important developments include: (1) the recognition that the 1200-1160 Ma Shawinigan Orogeny played a major role in a multiphase orogenic history; (2) the extensive AMCG magmatic suite, previously considered to be anorogenic, is now thought to have occurred during post-Shawinigan lithospheric delamination; (3) the 1090-1050 Ma Ottawan Orogeny may overprint but does not obliterate the earlier Shawinigan features; (4) significant shear zones exist on the western and eastern sides of the Adirondack Highlands that record the early stages of collapse and exhumation of the Grenville orogen.

Distinguishing between Shawinigan, AMCG, Ottawan, and extensional stages in the deformation and metamorphic history is essential for P-T-D-t models and for constraining the Adirondack tectonic history in general. Our work in the eastern Adirondacks will delineate the *nature* and *spatial extent* of both the Shawinigan and Ottawan Orogenies. By nature we mean metamorphic grade, style of deformation, composition of igneous rocks, and importantly, age constraints on each of these processes.

The East Adirondack shear zone is an intriguing feature in the Adirondack Highlands, possibly correlative in timing and history with the Carthage-Colton shear zone on the west side of the Adirondacks. However, many questions remain before this late-stage deformation can be wholly integrated into the tectonic history of the Adirondacks. Our on-going research aims to address the following questions:

1) What is the width, length, and intensity of the East Adirondack shear zone?
2) What is the style of the shear zone, is it constructed of many narrow discrete zones (<10 m) or is it distributed more uniformly over a wide zone (> 100m)?
3) Is this an extensional or a compressional shear zone, or does it have a complex, multiphase, diachronous history similar to the Carthage-Colton shear zone?
4) What was the P-T path during shearing, did the latest extensional phase of shearing recorded by these rocks occur at different crustal levels and therefore different metamorphic grades?
5) How does the shear zone link to other high-strain zones in the Eastern Adirondacks and more broadly to the Carthage-Colton shear zone?
6) What is the timing of shearing and is there an inheritance relationship with deformation in the Shawinigan?

Our approach to answering these questions is multifaceted and includes field work, macro- and microscale structural analysis, petrologic analysis and modeling, and geochronology. Field observations are foundational for all the research that follows. Contacts and map scale structures are mapped; kinematic indicators such as deformed porphyroblasts or porphyroclasts and strong lineations are documented. Oriented polished thin sections are used for microscopic kinematic and textural studies. Extensive compositional mapping and elemental analysis provides the data for forward petrologic modeling using Theriak-Domino software (de Capitani and Petrakakis, 2010) in order to determine not only the P-T conditions of metamorphism but also the sequence of metamorphic reactions. In situ electron microprobe dating of monazite is

used to constrain the timing of metamorphism and deformation (Williams and Jercinovic, 2012). Application of this technique is discussed elsewhere in the paper.

The stops on this trip are designed to illustrate the wide range of rock types present in the eastern Adirondacks including but not limited to metagabbos, deformed anothositic rocks, charnockites, and garnet-sillimanite gneisses. The geologic context of each stop will be discussed and new data, when available, will be presented. Lively discussion is encouraged. Of course this trip is not the first to visit many of these stops and additional information can be obtained from previous NYSGA and NEIGC field trips including McLelland et al. (2011) and Whitney et al. (2002).

OVERVIEW OF ADIRONDACK GEOLOGY

The Grenville Province of Eastern North America is a Proterozoic orogenic belt that represents the culminating continental collision(s) during assembly of the supercontinent of Rodinia (Rivers, 2008). The Grenville Province extends from northeastern Canada through the eastern and southern portion of the U.S. into Texas with proposed correlations in Australia, Antarctica, Baltica and others (Karlstrom et al. 1999). In eastern Canada, the Grenville Province forms a northeast trending belt approximately 2000 km long and 400-500 km wide. The Adirondack Mountains, located in northeastern New York, are a domical uplift of Mesoproterozoic rocks that are part of the Grenville Province (Fig. 1). The Green Mountain and Berkshire massifs represent outliers of the Grenville Province and lie to the east and southeast of the Adirondacks respectively.

The Adirondack Mountains are underlain by complexly folded, faulted and sheared metasedimentary and metaigneous rocks of wide ranging composition and varying in age from approximately 1.4 to 1.0 Ga (Fig. 1). The Adirondacks are subdivided into the Adirondack Highlands and the Adirondack Lowlands. The Carthage-Colton shear zone defines the boundary between the two (Baird and MacDonald, 2004, Baird, 2008, Johnson et al., 2004, Streepey et al., 2001). While both orthogneiss and paragneiss are found in each region, the Adirondack Highlands are dominated by metaigneous rocks, including several large bodies of anorthosite, and granulite facies metamorphic rocks. The Adirondack Lowlands are underlain by predominantly upper amphibolite facies metasedimentary rocks.

Figure 2 is from McLelland et al. (2013). We will use this model for the tectonic evolution of the Adirondacks throughout the remainder of this field trip guide as a tectonic framework for discussion purposes.

The oldest igneous rocks in the Adirondack Highlands are the tonalitic to granitic rocks of the Royal Mountain suite that outcrop in the southern and eastern Adirondacks (Fig. 1). These ~1.3 Ga gneisses are thought to have formed above a NW-dipping subduction zone along the SE margin of Laurentia. Although we will drive by the ca. 1.3 Ga Blue Goose tonalite, these rocks are currently not part of our research and we are not planning on examining them on this field trip.

In McLelland's model, the Shawinigan Orogeny is initially generated by the subduction of the trans-Adirondack Basin (Chiarenzelli et al., 2010) forming an Andean style margin with the Adirondack Lowlands on the leading edge of the overriding plate (Fig. 2). Upon closure of this basin the Adirondack Highlands-Green Mountain block collided with the Adirondack Lowlands-Central Metasedimentary block resulting in nappe style folds and granulite facies

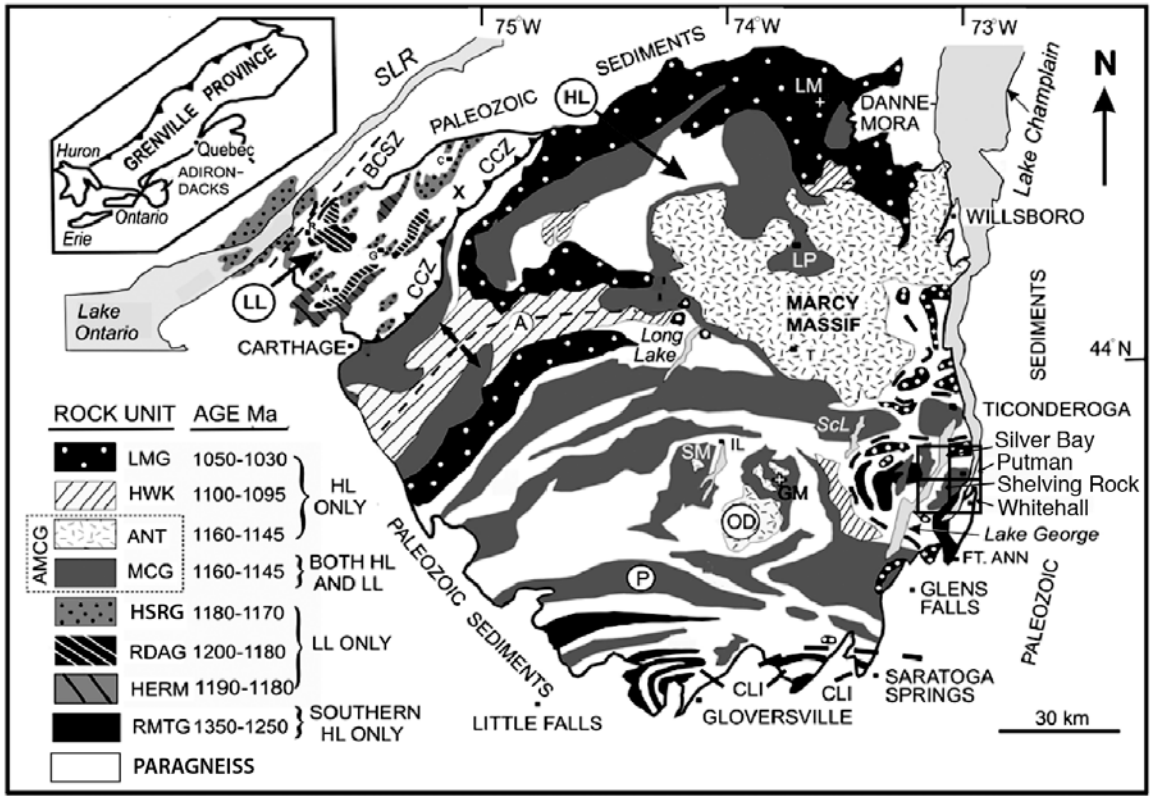

Figure 1. General geologic map of the Adirondacks (after McLelland et al., 2010). Units are as follows: LMG=Lyon Mountain granite, HWK=Hawkeye granite, ANT=anorthosite, MCG=mangerite, charnockite, granite, HSRG=Hyde School – Rockport granite, RDAG=Rossie diorite – Antwerp granodiorite, HERM=Herman granite, RMTG=Royal Mountain tonalite – granite. Silver Bay, Putnam, Shelving Rock, and Whitehall are 1:24,000 quadrangles. CCZ = Carthage Colton Shear Zone, BCSZ = Black Creek Shear Zone, OD = Oregon Dome, A = Arab Mountain Anticline, P = Piseco Anticline, CLI = Canada Lake Isocline, A = Antwerp, C = Canton, G = Gouverneur, SM = Snowy Mountain, IL = Indian Lake, LM = Lyon Mountain, HL = Highlands, LL = Lowlands, LP = Lake Placid.

metamorphism (Heumann et al., 2006; McLelland et al., 2013) (Fig. 2). In this model, this continental lithospheric collision also generated the initial movement along the Carthage-Colton shear zone when the Lowlands block was thrust on top of the Highlands block thus forming an orogenic lid.

McLelland et al. (2010) propose that either towards the waning stages of the compressional deformation associated with the Shawinigan, or shortly after, the overthickened lithosphere began to delaminate. This resulted in upwelling of the asthenosphere and decompression melting in the mantle. Mafic magmas ponded near the base of the crust and begin to fractionate. Plagioclase crystals, being less dense than the parental mafic melt accumulated at the top of the magma. These plagioclase-rich crystal mushes ascended through the crust and crystalized forming the large bodies of anorthosite in the Adirondack Highlands. In addition, heat from the upwelling asthenosphere and ponding magmas generated partial melting in the lower crust. These magmas intruded into the crust and crystalized to form the mangerite-charnockite-granite component of the AMCG suite (McLelland et al., 2010).

The next major compressional event was the Ottawan Orogeny (McLelland et al., 2013), also known as the Ottawan phase of the Grenvillian Orogeny (Rivers, 2008). This orogenic event is proposed to be the result of the collision of Amazonia with the Adirondack Highlands-Lowlands block, which at that time was the eastern edge of Laurentia. Research to date suggests that the Ottawan Orogeny, like the Shawinigan, resulted in nappe-style folding and granulite facies metamorphism (Bickford et al., 2008; McLelland et al., 2013). Ottawan-age deformation and metamorphism has not been recognized in the Adirondack Lowlands (Baird and Shrady, 2011). The Ottawan Orogeny culminated with the assembly of the supercontinent of Rodinia.

A period of orogenic collapse followed the culmination of Ottawan compression. Wong et al. (2012) documented normal-sense, east-directed shear in rocks south Whitehall, NY. In situ EMP monazite data are consistent with this shearing taking place between 1050-1000 Ma. Selleck et al. (2005) suggest that the Lyon Mountain granite was emplaced during extensional collapse. McLelland and Selleck (2011) also suggest that the large, megacrystic garnets are Gore Mountain formed at this time.

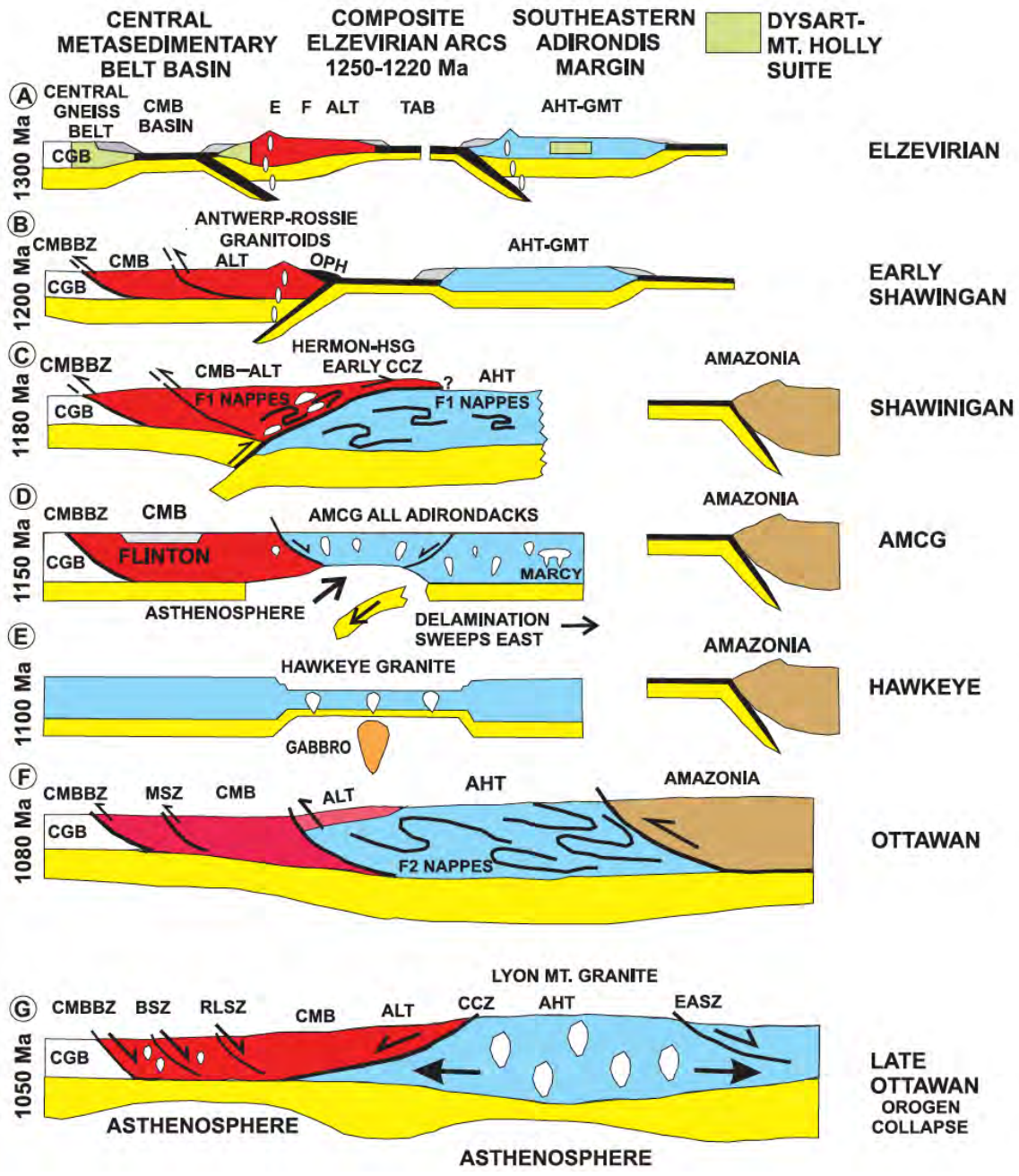

Figure 2. Model of the tectonic evolution of the Adirondack Mountains from McLelland et al. (2013). Abbreviations: AHT =Adirondack Highlands Terrane, AHT-GMT = Adirondack Highlands-Green Mountains Terrane, ALT = Adirondack Lowlands Terrane, AMCG = anorthosite-monzonite-charnockite-granite suite, BSZ = Bancroft shear zone, CCZ = Carthage-Colton Shear Zone, CGB = Central Gneiss Belt, CMB = Central Metasedimentary Belt, E = Elzevir Terrane, EASZ = Eastern Adirondack shear zone, F = Frontenac Terrane, HSG = Hyde School Gneiss , MSZ = Maberly Shear Zone, OPH = Pyrite Ophiolite Complex, RLSZ = Robertson Lake Shear Zone, TAB = Trans-Adirondack basin.

FIELD GUIDE AND ROAD LOG

Meeting Point: Hwy 22 south of Ticonderoga in a parking area on the west side of the road immediately after entering the town of Putnam. If you are driving south from Ticonderoga there is a "Welcome to Putnam" sign just before the entrance to the parking area. The meeting point is about a 90 minute drive from Plattsburgh.

Meeting Point Coordinates: UTM (628044 E, 4851165 N) (See Figure 3)

Meeting Time: 9:00 AM

Distance (miles)		
Cumu--lative	Point to Point	Route Description
0.0	0.0	Assemble in the parking area on the west side of Hwy 22 south of Ticonderoga in the town of Putnam. Depart parking area heading south.
3.1	3.1	Exposures of the "Great Unconformity" with the Cambrian Potsdam sandstone sitting unconformably on nearly vertically dipping Mesoproterozoic gneisses.
3.6	0.5	Pull over as far to the right as possible and park.

STOP 1. Isoclinal folds, Lyon Mountain granite, and AMCG rocks (60 minutes)

Location Coordinates: UTM Z18 NAD83 (628912 E, 4845232 N)

Examine the granitic gneiss in the northern outcrops on the west side of the road. Note the numerous tight to isoclinal similar folds (Fig. 4). The fold axis trends almost due east and has a gentle eastward plunge. If you look closely at the nose of the fold you can see a new axial planar foliation has developed. If we call the folded foliation S_1 then the new axial planar foliation would be S_2. The foliation on the limbs of the axial planar folds would be a composite S_1/S_2 foliation. Our working hypothesis is that S_1 developed during the Shawinigan Orogeny and S_2 developed during the Ottawan Orogeny. However, this may be problematic if these granitic gneiss are part of the AMCG suite. We have collected oriented samples in this region to see if we can use monazite age data to constrain the timing of foliation development.

Further to the north along this outcrop is a reverse fault that is cut by a pegmatite. Where the pegmatite cuts the granitic gneisses it appears as if fluids from the pegmatite interacted with the gneiss and resulted in potassic alteration of the gneiss.

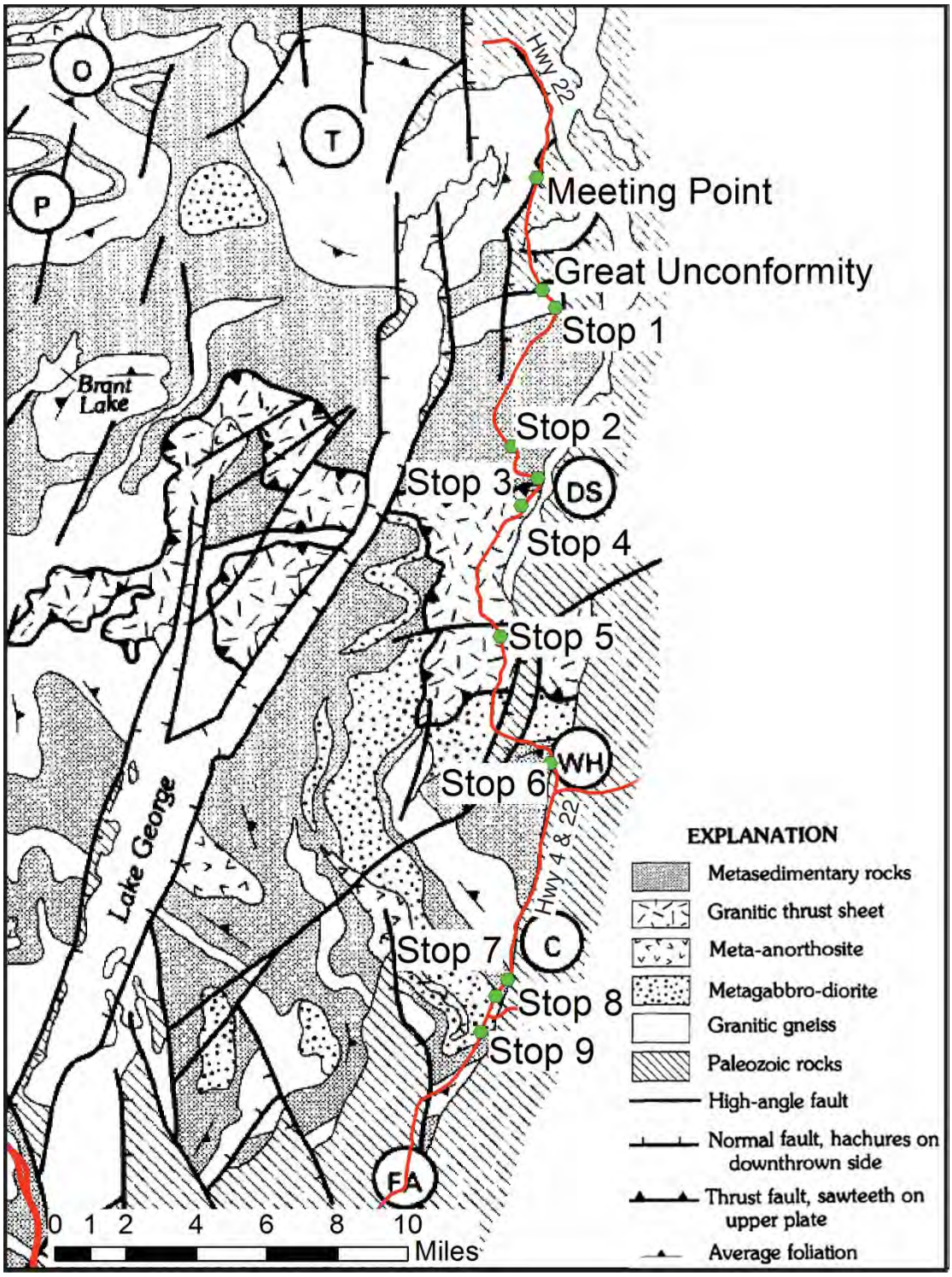

Figure 3. Generalized geologic map of the eastern Adirondacks after McLelland (1990). Also shown are the locations of the stops on this field trip (circles with letters inside): P=Pharoah Mountain, O=Owl's Head Mountain, T=Ticonderoga dome, DS=Dresden Station, WH=Whitehall, C=Comstock, FA=Fort Ann

Proceed south, past a gap in outcrops to the next exposure. Here various phases granites, along with amphibolite that exhibits flow folding are intermixed. The white to gray granitic rock appears locally to be undeformed except for shear zones and is interpreted to be the Lyon Mountain Granite with its typically low (< 0.3 wt.%) MgO composition. The pink granitic rock contains few amphibolite enclaves and is thought to be an AMCG granite. McLelland et al. (2011) refer to this roadcut as an intrusion breccia involving white Lyon Mountain granite that engulfed, disrupted, and flow folded amphibolites. Portions of the Lyon Mountain granite have undergone various phases of alteration by sodic and potassic fluids resulting in elevated concentrations of those elements (Valley et al., 2011).

Figure 4. Tight to isoclinal similar folds in granitic gneiss at Stop 1. Sharpie in fold hinge for scale.

Distance (miles)		
Cumu--lative	Point to Point	Route Description
4.5	0.9	Return to vehicles and head south, outcrops of Potsdam sandstone.
8.1	3.6	Pull over as far to the right as possible and park.

STOP 2 Lineated K-feldspar megacrystic gneiss and migmatitic paragneiss (30 minutes)

Location Coordinates: UTM Z18 NAD83 (626892 E, 4838882 N)

This rock is a biotite-bearing, K-feldspar megacrystic rock with a pervasive linear fabric. Most of the K-feldspar crystals are strung out and completely recrystallized into finer grained mosaics (Fig. 5), however some large crystals are still present. The dominant lineation is gently plunging to the east.

Graham Baird recently analyzed zircons from this sample using the SHRIMP-RG at Stanford University. Zircon in the unit is euhedral to subhedral, elongate, amber colored, and ranges in length approximately 200-400 µm. Cathodoluminescence of polished grain cross sections reveal that all grains possess oscillatory zoning with no conclusive sign of metamorphic rims or common inherited cores (Fig. 6). Fourteen SHRIMP-RG analyses produce what is interpreted as a unimodal distribution of ages with one

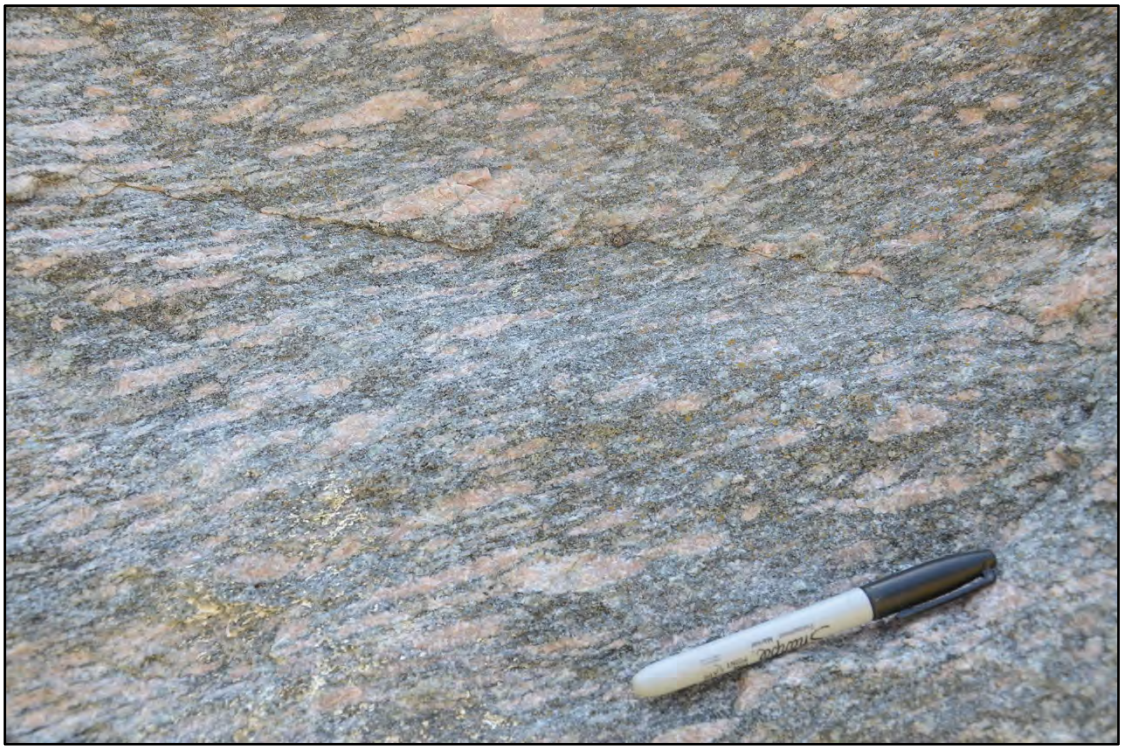

Figure 5. Lineated Bt-bearing, K-feldspar megacrystic gneiss at Stop 2.

inherited core (1497 ± 78 Ma) and 3 anomalously young ages. Seven concordant and near concordant, well clustered analyses produce a 2σ $^{207}Pb/^{206}Pb$ weighted mean age of 1155 ± 15 Ma, interpreted to best represent the age of pluton crystallization (Fig. 6).

The 1155 Ma age is consistent with this granitoid being part of the AMCG suite. The strong, penetrative fabric suggests a phase of deformation after this time.

Further north along the outcrop the K-feldspar megacrystic granitic rocks are intermingled with migmatitic, biotite-bearing gneisses. The contact relationships between these two units are not clear cut. We have sampled both units in order to collect more geochonologic data using EMP analyses of monazite.

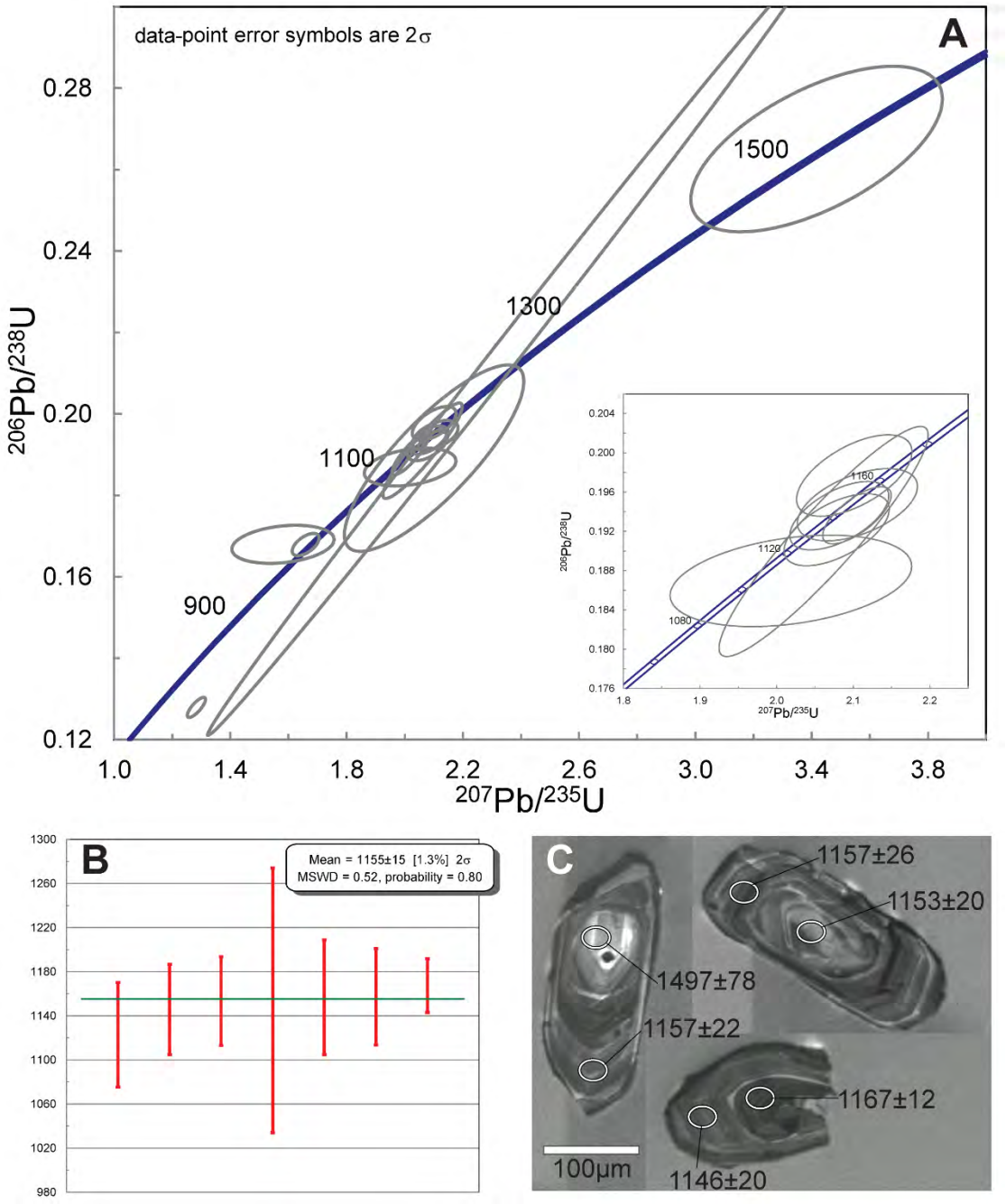

Figure 6. A) Concordia diagram for 14 U/Pb zircon SHRIMP-RG analyses. Inset show the 7 best clustered data used in the $^{206}Pb/^{207}Pb$ weighted mean (B). B) $^{206}Pb/^{207}Pb$ weighted mean of the best data produces an age of 1155 ± 15 Ma (2σ). C) Representative grains and 2σ $^{206}Pb/^{207}Pb$ spot analyses.

Distance (miles)		
Cumu--lative	Point to Point	Route Description
8.3	0.2	Return to vehicles and head south, mafic boudins in metasedimentary rocks.
8.8	0.5	Pull out with folded granitic rocks near southern end. Also a spring with potable water.
9.4	0.5	Turn left on Belden Road, make a U-turn and park near the intersection of Belden Road and Hwy 22.

STOP 3. Garnet-sillimanite gneisses and coronitic metagabbro (60 minutes)

Location Coordinates: UTM Z18 NAD83 (628107 E, 4837420 N)

Many field trips have stopped at this location over the years. McLelland et al. (1988a) cite evidence from this outcrop to show that there were multiple phases of metamorphism recorded by the rocks in the Adirondacks. A sharp contact between garnet-sillimanite gneiss and a coronitic metagabbro is well-exposed in this outcrop (Fig. 7). The gneiss is a garnet-sillimanite-plagioclase-K-feldspar-quartz gneiss with a small amount of biotite. The garnet-sillimanite gneisses here are often referred to as khondalites. This name originated in India and refers to quartz-garnet-sillimanite gneisses with little to no biotite. Khondalites are often associated with quartzites and calc-silicate rocks and that is the case here. This mineral assemblage is consistent with upper amphibolite to lower granulite facies metamorphic conditions. The garnet-sillimanite gneiss is penetratively deformed with a well-developed foliation and a lineation that plunges gently to the east. Much of the metagabbro is undeformed and a coarsely crystalline texture is preserved throughout much of the unit. There are places within the gabbro however that are deformed and foliated. The gabbro is finely crystalline right at the contact with the gneiss (Fig 7c) and appears to get more coarsely crystalline towards the interior of the body suggesting a chilled margin formed at the contact between the gabbro and the gneiss. The contact between the gneiss and the gabbro is, in places, at a high angle to the foliation in the gneiss. These field relationships suggest that the gneiss was deformed and metamorphosed prior to the intrusion of the gabbro (McLelland et al., 1988).

Coronitic metagabbros are found throughout the Adirondacks (Whitney and McLelland, 1973; Whitney and McLelland, 1983; Regan et al., 2011). Figure 8 illustrates the typical corona texture with an olivine core, surrounded by a rim of orthopyroxene, which in turn is rimmed by symplectic intergrowths of garnet and clinopyroxene. The clouding in the plagioclase is due to numerous microscopic spinel inclusions. Another feature of these rocks that ilmenite is rimmed by Ti-rich hornblende. This mineral assemblage and texture developed via subsolidus recrystallization from a rock that was originally an olivine-clinopyroxene-plagioclase gabbro. Preliminary P-T estimates suggest this mineral assemblage developed at approximately 9 kb and 750 °C. The growth of amphibole also requires an influx of an H_2O-bearing fluid.

To the south and west of this outcrop of gabbroic rocks, ferrogabbroic rocks and anorthosites, all thought to be associated with the coronitic metagabbro seen here, have a very strong penetrative fabric and in many locations are mylonites. These rocks contain the mineral

assemblage garnet-clinopyroxene-plagioclase±orthopyroxene which is similar to the mineral assemblage found in the coronitic metagabbros. Kinematic indicators in these rocks suggest a west-directed thrust sense of motion. These observations suggest this period of deformation and metamorphism must postdate the emplacement of the AMCG rocks.

Figure 7. Contact between garnet-sillimanite gneiss and coronitic metagabbro. Figure 7a shows that locally the foliation in the gneiss is parallel to the contact and locally it is at a high angle to the contact. Figure 7b illustrates the sharp nature of the contact. Figure 7c shows that the metagabbro is finely crystalline in the immediate vicinity of the contact.

McLelland et al. (1988b) report a U-Pb zircon, multigrain age of 1144 ± 7 Ma for the metagabbro. This is interpreted as an igneous crystallization age and is consistent with the gabbro belonging to the AMCG suite. However, Aleinikoff (pers. comm.) has reported a preliminary SHRIMP age of ca. 1107 Ma. We dated monazite from the garnet-sillimanite gneisses following the techniques outlined in Williams et al. (2006), Williams et al. (2007) and applied in Williams and Jercinovic (2012). The technique involves locating all the monazite crystals in the thin section through full section mapping with the microprobe followed by detailed mapping of up to 30 monazite crystals in a thin section to identify different

compositional domains within each monazite. Then the microprobe is used for complete spot analyses of different compositional domains in the monazite and ages are calculated from these data. We analyzed monazite from two thin sections of the garnet-sillimanite gneisses. The results are presented in figure 9.

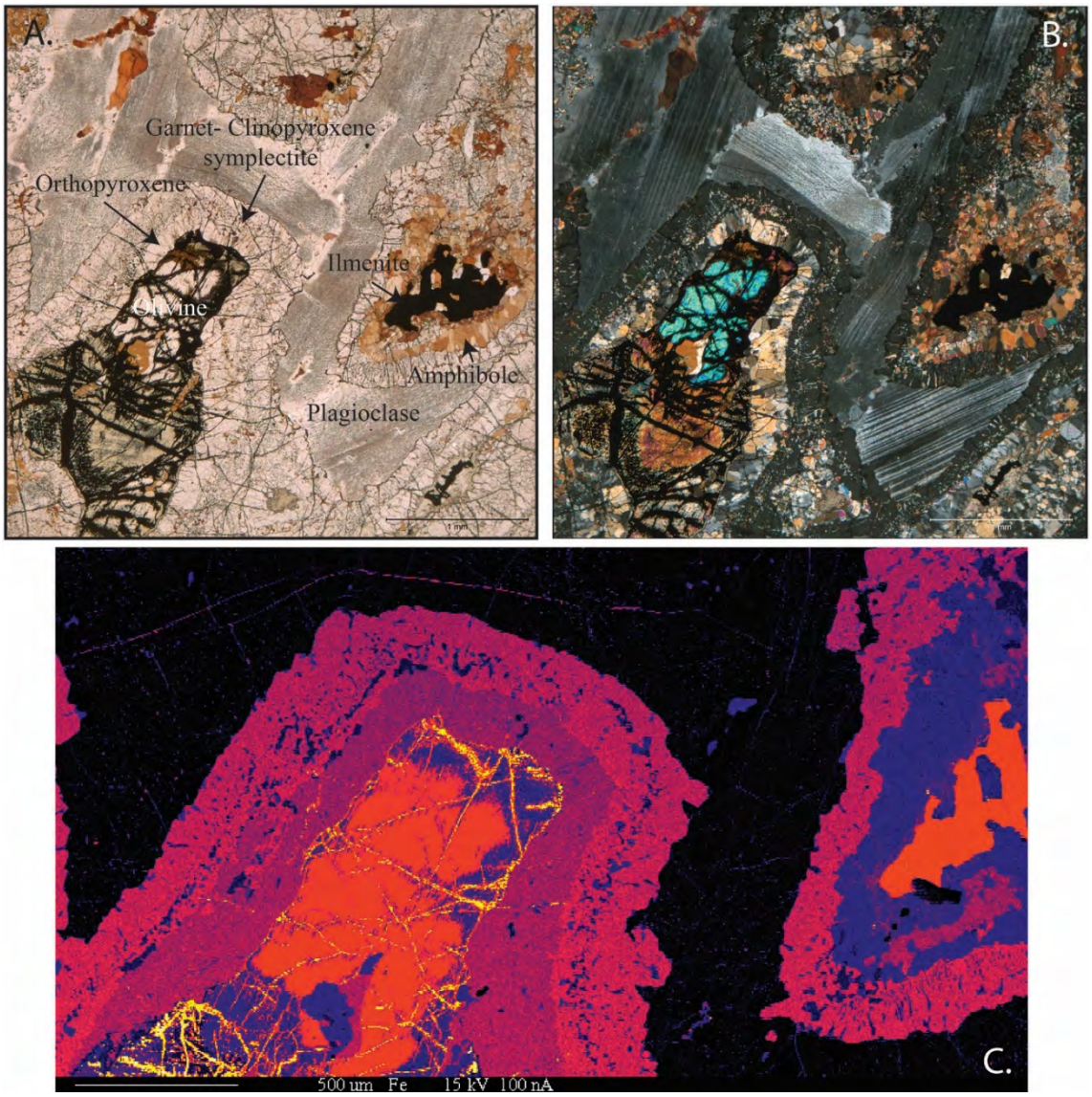

Figure 8. Photomicrographs and Fe-xray map of coronitic metagabbo. Figure 8a and 8b are photomicrographs under plane and cross polarized light respectively. Orthopyroxene surrounds olivine, and is in turn surrounded by garnet-clinopyroxene symplectite. Figure 8c is a Fe-xray map of a portion of the thin section shown in 8a and 8b.

The data broadly suggest three distinct periods of monazite growth. The oldest is set of ages yields a mean age of 1179 $\pm$ 9 Ma. We suggest that this age represents the timing of granulite facies metamorphism and fabric development in the garnet sillimanite gneisses. This age is

consistent with metamorphism and deformation occurring during the Shawinigan Orogeny. The next population of analyses yields ages that cluster around 1151 Ma. We hypothesize that this represents a period of monazite growth driven by a thermal perturbation resulting from the intrusion of the gabbroic rocks. This age correlates well with the reported age of the gabbro. With the exception of one analysis yielding an age of approximately 1050 Ma, most of the remaining monazite ages are 1020 Ma or less. These ages are too young to correlate with the proposed timing of the peak of the Ottawan Orogeny (~1090-1050 Ma). One possibility is that monazite grew during the period of post-Ottawan decompression and uplift.

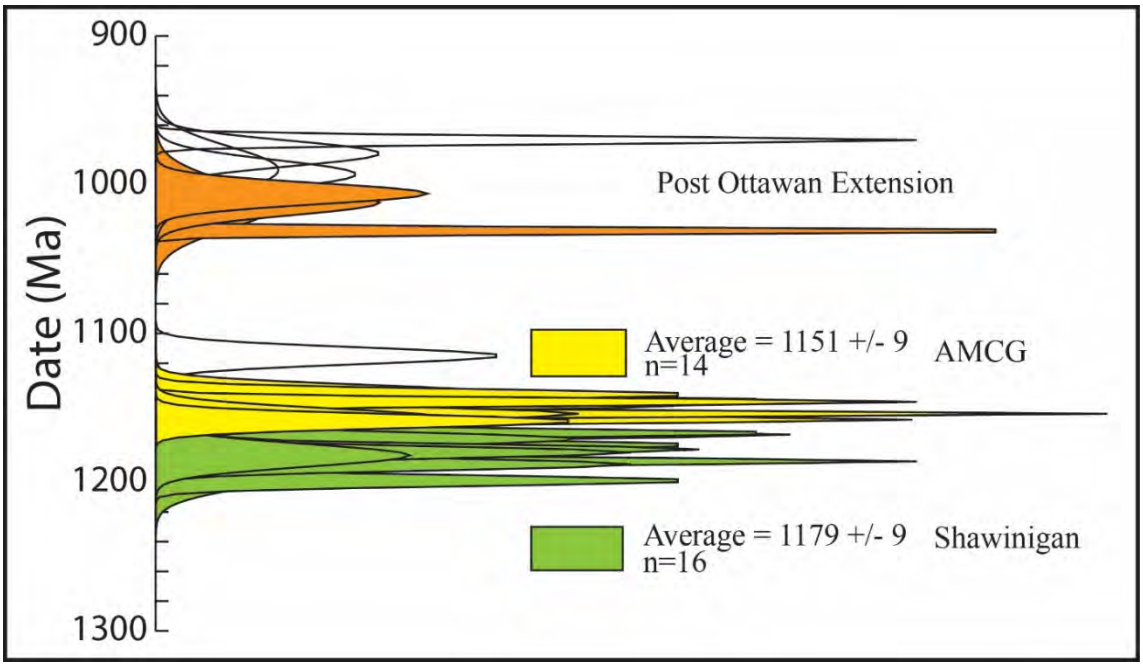

Figure 9. Histogram showing the distribution of ages calculated from spot analyses compositionally and texturally distinct domains in monazite using the Ultrachron at the University of Massachusetts.

The following model is consistent with the field observations and data from this outcrop. The mineral assemblage and the fabric in the garnet-sillimanite gneisses formed during the Shawinigan Orogeny. The gabbro was emplaced at approximately 1150 Ma, after the prominent fabric developed in the gneisses. This time frame is consistent with both the monazite ages from the gneisses and the multigrain age from the gabbro. Following the emplacement of the gabbro there was another period of deformation and metamorphism. This is when the nearby AMCG rocks were deformed and metamorphosed. This is also when the coronitic fabric developed in the metagabbro. This requires in influx of an H_2O–bearing fluid. Unlike the nearby rocks, the coronitic metagabbro was not pervasively deformed at this time nor did any new monazite grow in the garnet-sillimanite gneiss. Perhaps strain was partitioned around this outcrop and the lack of strain resulted in little recrystallization in the largely anhydrous garnet-sillimanite gneisses. The 1020 Ma and younger monazite ages in the garnet-sillimanite gneisses record monazite growth during post Ottawan extensional collapse. We will discuss this further at Stop 8.

Distance (miles)		
Cumu--lative	Point to Point	Route Description
9.5	0.1	Return to vehicles and turn left heading south on Hwy 22.
10.6	1.1	Turn left on LeClaire Road, make a U-turn and park on the shoulder. The stop is in a quarry on the west side of the highway.

STOP 4 Mylonitic gabbroic anorthosite in a gravel pit (30 minutes)

Location Coordinates UTM Z18 NAD 83: (627320 E, 4836160 N)

Since leaving stop 3, we have been passing through a unit of deformed and metamorphosed mafic rocks ranging in composition from gabbroic to anorthositic. Most of the rocks have a well developed foliation. Many contain porphyroclasts of plagioclase that have been variably deformed (Fig. 10). As mentioned earlier, shear sense indicators in these rocks suggest a west-directed, thrust sense of shear. The mineral assemblage in these rocks is typically garnet-augite-hornblende-plagioclase with little to no orthopyroxene or quartz. The presence of hornblende, a hydrous mineral, requires an H_2O-bearing fluid, possibly introduced during deformation. Although we continue to search we have yet to find any monazite in these rocks.

Distance (miles)		
Cumu--lative	Point to Point	Route Description
11.4	0.8	Return to vehicles and turn left heading south on Hwy 22. There is a large outcrop of metagabbro with a white marble xenoltth.
12.4	1.0	Good exposures of dark green charnockite.
14.8	2.4	Pull over on the right side of the road and park. The outcrop is on the east side of the highway, please be careful crossing the road.

STOP 5 Pegmatite, charnockite, and mafic gneiss (20 minutes)

Location Coordinates UTM Z18 NAD83: (626394 E, 4830166 N)

This outcrop contains a beautiful exposure of a post-Ottawan pegmatite dike. The hanging wall of the dike is a mafic gneiss. Xenoliths of the mafic gneiss are in the upper third of the dike and show evidence of reacting with the magma (Fig. 11). If you look across the street you can see the continuation of the dike to the north. Most of the outcrop here is granitic gneiss and maroon-brownish charnockite. These rocks are thought to belong to the AMCG suite. If this is correct foliation in these rocks must have developed from a deformational event after ~ 1155 Ma. Towards the south end of the outcrop there are cm-scale pyroxene crystals. This rocks

Figure 10. Porphyroclastic gabbroic anorthosite from Stop 4. Note the asymmetric plagioclase porphyroclasts.

Figure 11. Pegmatite dike cross cutting charnockitic rocks and mafic gneiss. The black spots in the upper part of the dike are xenoliths of the mafic gneiss in the hanging wall. There is a hammer on the right side of the picture for scale.

contains the high grade mineral assemblage garnet-augite-hornblende-plagioclase-quartz±orthopyroxene, indicating that these are upper amphibolite to lower granulite facies metamorphic rocks.

Distance (miles)		
Cumu--lative	Point to Point	Route Description
16.4-17.0	1.6-2.2	Return to vehicles and continue south on Hwy 22. Outcrops of ca. 1.3 Ga tonalitic rocks (McLelland and Chiarenzelli, 1990).
17.8	0.8	Bridge across Lake Champlain.
19.4	1.6	Pull over on the right side of the road and park. Watch out for poison ivy and unstable rock.

STOP 6. Garnet-sillimanite gneiss (20 minutes)

Location Coordinates UTM Z18 NAD 83: (628669 E, 4824379 N)

The entire road cut consists of well foliated and lineated garnet-sillimanite-K-feldspar-plagioclase-quartz±biotite gneiss. This is another example of khondalite. The sillimanite in this rock forms a prominent lineation of ~10/100. This is similar to all other lineations noted so far on this trip. The mineral assemblage is again consistent with upper amphibolite to lower granulite facies metamorphism.

Distance (miles)		
Cumu--lative	Point to Point	Route Description
20.3	0.9	Return to vehicles and continue south on Hwy 22. Intersection of Rt. 4 and Hwy 22. Continue straight heading south.
20.9	0.6	McDonalds on west side of the road.
25.5	4.6	Pull over on the right side of the road and park.

STOP 7. Long outcrop of many different lithologies found in the Adirondacks (40 minutes)

Location Coordinates UTM Z18 NAD83: (626719 E, 4832092 N)

The rocks in this outcrop include many of the lithologies found throughout the Adirondack Highlands that have probably been tectonically juxtaposed. The foliation is dominantly NE striking and gently dipping to the southeast. As we move southward we will moving structurally down section. The north end of this outcrop is an impure marble that contains coarsely crystalline graphite, diopside, and quartz. The marble also contains numerous inclusions of a variety of different rock types. Observations such as these led Ebenezer Emmons in his 1842 New York State Monograph “Geology of the State of New York: Survey of the Second Geological District” to state “Of Adirondack rocks we know little of their origin except for the marbles

which surely are igneous" (McLelland, pers. comm.). Climb on top of the outcrop for a clear view of a unmetamorphosed, Mesozoic age mafic dike (Fig. 12). There is a millimeter scale chilled margin on the dike. To the south the marble is in contact with a biotite-garnet-quartz-plagioclase±sillimanite gneiss with quartzofeldspathic leucosomes.

As you proceed south from the marble and paragneiss you will encounter a number of different rock types including, garnet-bearing, quartzofeldspathic gneiss, charnockitic gneiss, numerous marbles, calcsilicate rocks with orange grossular garnet and wollastonite, and hornblende-pyroxene plagioclase gneiss.

At the southern end of the outcrop (UTM NAD83: 626522 E, 4832092 N) are biotite-garnet-sillimanite-K-feldspar-plagioclase-quartz gneisses. On some foliation surfaces these rocks contain beautiful matchstick-sized sillimanite. The sillimanite crystals are aligned forming a strong lineation trending approximately 15/135. We are in the process of mapping thin sections from this exposure to look for monazite. We do have monazite data from similar rocks just to the south that we will discuss at the next stop.

Figure 12. Mafic dike intruding marble at Stop 7. Note the rock hammer for scale.

Distance (miles)		
Cumu--lative	Point to Point	Route Description
26.1	0.6	Return to vehicles and continue south on Rt. 4. Turn left into parking area

STOP 8. Lineated sillimanite gneisses, mylonitic granitic rocks, and the East Adirondack Shear Zone (60 minutes)

Location Coordinates: UTM Z18 NAD83 (626163 E, 4813714 N)

There is an outcrop paragneiss immediately to the south of the parking area on the east side of the road. This outcrop contains interlayered garnet-biotite-sillimanite gneisses with greenish calcsilicate lithologies. The well exposed foliation surfaces of the sillimanite-bearing gneisses commonly have well-lineated, coarsely crystalline sillimanite. The lineation is gently plunging to the southeast, similar to that in the last outcrop.

Follow the outcrop to the south remaining on the east side of Hwy 22 for the time being.

Note the interlayer folds in the upper part of the roadcut on the east. This exposure illustrates an older foliation that was transposed into a new foliation (Fig 13). Perhaps this is an example of a Shawinigan S_1 transposed into a younger S_2.

Figure 13. Interlayer folds in paragneiss along Hwy22 at Stop 8. Red line traces some folds. Note hammer for scale.

Across the highway is an asymmetric mafic boudin (Fig. 14) with a long tail that continues to the south in the upper part of the roadcut. Although it is clear the boudin was involved in a period of ductile deformation, the roadcut is oriented almost at right angles to the lineation direction so it is difficult to use the boudin for kinematic analysis.

Figure 14. Photomosaic of a mafic boudin enveloped by mylonitic, granitic gneiss at stop 8. The mylonitic rocks pictured in figure 15 are located approximately in the center of this picture.

The granitic rocks to the left of the mafic boudin in the picture above are mylonitic, LS-tectonites with megacrystic K-feldspar porphyroclasts (Fig 15). The prominent lineation plunges gently to the southeast. Data from this outcrop was cited by Wong et al. (2012) as evidence for the East Adirondack Shear Zone. They report a U-Pb ziron age obtained using the SHRIMP-RG at Stanford, of the granite in figure 15 of ca. 1140 Ma. This date suggests that it is part of the AMCG suite and was emplaced towards the end or after the Shawinigan Orogeny. Following this reasoning they suggest that most of the strain in the rock is therefore related to Ottawan compression or post

Figure 15. Strongly lineated granitic rock in the East Adirondack Shear zone.

Ottawan extension. They examined the asymmetric K-feldspar porphyroclasts as kinematic indicators to document shear sense motion. Although they found some porphyroclasts that suggested top to the west, thrust sense motion more suggest top to the east, normal-sense motion. From this they concluded that this rock experienced both compressive stresses and extensional stresses but the extension event was younger and overprinted the effects of the compressional event.

Wong et al (2012) also report U-Th-Pb electron microprobe ages from in situ monazite crystals. The data are shown in figure 16. Note the two groupings of peaks in the 1100-1000 Ma age range. The older peaks, shown in blue, cluster between 1080-1050 Ma. These data are from analyses of the outer cores of monazite crystals. They are interpreted to represent monazite growth during Ottawan compression and metamorphism. The younger peaks in red are less than 1050 Ma. These ages come from analyses of the tips of monazite crystals that are elongated in the extensional direction. Wong et al (2012) interpret this as monazite growth during extensional collapse following peak Ottawan compression. This period of extension is synchronous with the extension along the Carthage-Colton shear zone (McLelland et al., 2001; Streepey et al., 2001; Johnson et al., 2004).

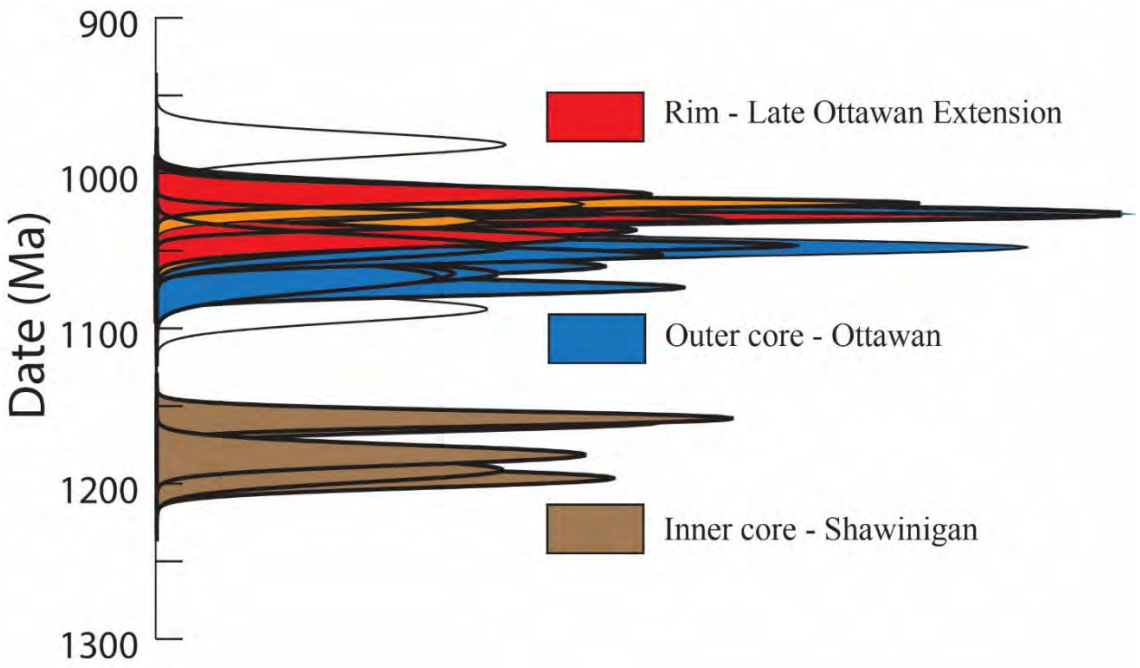

Figure 16. U-Th-Pb electron microprobe ages from in situ monazite from both a mylonitic, K-feldspar megacrystic granite and a garnet-sillimanite paragneiss.

It is interesting to compare this data with that from stop 3. The monazite data from the stop 3 rocks had a strong Shawinigan, AMCG, and post Ottawan signature but virtually no peak Ottawan monazite growth. The monazite data from this outcrop have a strong Shawinigan, peak-Ottawan, and post-Ottawan signature and limited evidence for monazite growth during AMCG times despite AMCG rocks being found in the outcrop.

Distance (miles)		
Cumu--lative	Point to Point	Route Description
27.1	1.9	Return to vehicles and continue south on Rt.4. Turn right on Kelsdy Pond Road. Park on the side of the road. Carefully corss the highway tot the outcrop on the east side.

STOP 9. Mylonitic, migmatitic gneiss

Location Coordinates UTM Z18 NAD83: (625497 E, 4812086 N)

This is a beautiful exposure of a garnet-biotite-plagioclase-K-feldspar-quartz ± sillimanite gneiss (Fig 17). Most of the white layers are interpreted as leucosomes that formed during anatectic melting via a biotite dehydration reaction such as:

$$\text{Biotite} + \text{plagioclase} + \text{sillimanite} + \text{quartz} \rightarrow \text{K-feldspar} + \text{garnet} + \text{melt}.$$

Much of garnet in the leucosomes was probably produced via this reaction.

Figure 17. Photograph of a portion of the outcrop at stop 9. Garnet is visible in the white leucosome, particularly to the right of the hammer. A softball sized feldspar crystal, which is part of a dismembered pegmatite, is in the lower left portion of the picture.

The strongly attenuated nature of the leucosomes, along with also remnants of pegmatite dikes that are now sheared out in the foliation plane (Fig. 17) attest to the significant strain recorded by these rocks. The rocks have the same strong southeast-trending, gently plunging lineation that we have seen in the last two stops. We suggest that some of the strain in these rocks may be the result of post-Ottawan extension collapse in the EASZ.

This outcrop was part of a study by Bickford et al. (2008). They concluded that these rocks underwent partial melting at approximately 1050 Ma at the tail end of the Ottawan Orogeny. They suggest anatexis was facilitated by an influx of H_2O-bearing fluids and decompression as a result of extensional collapse.

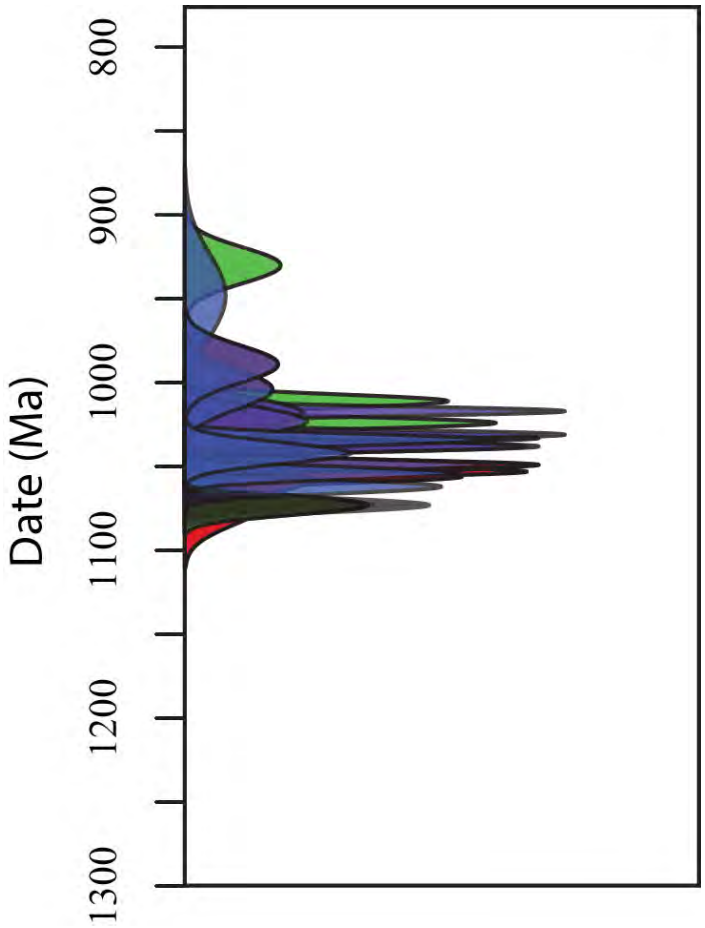

Figure 18. Histogram showing monazite ages from 9 monazite crystals from a single thin section from Stop 9.

Figure 18 shows our preliminary U-Th-Pb electron microprobe monazite data from this outcrop. The data shown in figure 18 are from 9 monazite crystals in a single thin section. Our data show monazite growth from approximately 1080 Ma through 1000 Ma. The data are consistent with recrystallization during the Ottawan and post Ottawan extension and in good agreement with the results of Bickford et al. (2008). It is interesting to note the lack of any Shawinigan or AMCG ages when the rocks approximately one mile to the north have a strong Shawinigan signature. We are in the process of collecting more data in order to further explore the effects of the Shawinigan and Ottawan Orogenies and post Ottawan orogenic collapse on these rocks.

End of Trip.

REFERENCES CITED

Baird, G.B., 2008, Tectonic Significance of Mylonite Kinematic Indicators within the Carthage-Colton Mylonite Zone, Northwest Adirondacks, New York: Abstracts with Programs - Geological Society of America, v. 40, no. 6, p. 235.

Baird, G.B., and MacDonald, W.D., 2004, Deformation of the Diana syenite and Carthage-Colton mylonite zone: Implications for timing of Adirondack Lowlands deformation, in Geological Society of America Memiors 197, Geological Society of America, p. 285–297.

Baird, G. B., and Shrady, C. H., 2011. Timing and kinematics of deformation in the northwest Adirondack Lowlands, New York State: Implications for terrane relationships in the southern Grenville Province. Geosphere, 7 (6): 1303-1323.

Baird, G.B., and Shrady, C.H., 2011, Timing and kinematics of deformation in the northwest Adirondack Lowlands, New York State: Implications for terrane relationships in the southern Grenville Province: Geosphere, v. 7, no. 6, p. 1303-1323.

Bickford, M.E., McLelland, J.M., Selleck, B.W., Hill, B.M., and Heumann, M.J., 2008, Timing of anatexis in the eastern Adirondack Highlands: Implications for tectonic evolution during ca. 1050 Ma Ottawan orogenesis: Geological Society of America Bulletin, v. 120, no. 7-8, p. 950–961.

Chiarenzelli, J., Lupulescu, M., Thern, E., and Cousens, B., 2011, Tectonic implications of the discovery of a Shawinigan ophiolite (Pyrites Complex) in the Adirondack Lowlands: Geosphere, v. 7, no. 2, p. 333–356, doi: 10.1130/GES00608.1.

Chiarenzelli, J., Regan, S., Peck, W.H., Selleck, B.W., Cousens, B., Baird, G.B., and Shrady, C.H., 2010, Shawinigan arc magmatism in the Adirondack Lowlands as a consequence of closure of the Trans-Adirondack backarc basin: Geosphere, v. 6, no. 6, p. 900–916, doi: 10.1130/GES00576.1.

de Capitani, C., and Petrakakis, K., 2010, The computation of equilibrium assemblage diagrams with Theriak/Domino software: American Mineralogist, v. 95, no. 7, p. 1006–1016, doi: 10.2138/am.2010.3354.

Hamilton, M.A., McLelland, J., and Selleck, B., 2004, SHRIMP U-Pb zircon geochronology of the anorthosite-mangerite-charnockite-granite suite, Adirondack Mountains, New York: Ages of emplacement and metamorphism: Geological Society of America Memoir 197,, p. 337–356.

Heumann, M., Bickford, M., Hill, B., McLelland, J., Selleck, B., and Jercinovic, M., 2006, Timing of anatexis in metapelites from the Adirondack lowlands and southern highlands: A manifestation of the Shawinigan Orogeny and subsequent anorthosite-mangerite-charnockite-granite magmatism: Bulletin of the Geological Society of America, v. 118, no. 11-12, p. 1283.

Johnson, E.L., Goergen, E.T., and Fruchey, B.L., 2004, Right lateral oblique slip movements followed by post-Ottawan (1050–1020 Ma) orogenic collapse along the Carthage-Colton shear zone: Data from the Dana Hill metagabbro body, Adirondack Mountains, New York, in Geological Society of America Memior 197, p. 357–378.

Karlstrom, K.E., Harlan, S.S., Williams, M.L., McLelland, J., Geissman, J.W., and Ahall, K.I., 1999, Refining Rodinia: Geologic evidence for the Australia–western US connection in the Proterozoic: GSA Today, v. 9, no. 10, p. 1–7.

McLelland, J., Hamilton, M., Selleck, B., Walker, D., and Orrell, S., 2001, Zircon U-Pb geochronology of the Ottawan Orogeny, Adirondack Highlands, New York: regional and tectonic implications: Precambrian Research, v. 109, no. 1, p. 39–72.

McLelland, J., Lochhead, A., and Vyhnal, C., 1988, Evidence for multiple metamorphic events in the Adirondack Mountains, NY: The Journal of Geology,, doi: 10.2307/30068728.

McLelland, J., Selleck, B., Hamilton, M., and Bickford, M., 2010, Late-to post-tectonic setting of some major Proterozoic anorthosite–mangerite–charnockite–granite (AMCG) suites: The Canadian Mineralogist, v. 48, p. 1025-1046.

McLelland, J.M., Selleck, B.W., and Bickford, M.E., 2013, Tectonic Evolution of the Adirondack Mountains and Grenville Orogen Inliers within the USA: Geoscience Canada, v. 40, no. 4, p. 318, doi: 10.12789/geocanj.2013.40.022.

McLelland, J.M., Wong, M.S., Grover, T.W., Williams, M.L., and Jercinovic, M.J., 2011, Geology and Geochronology of the Eastern Adirondacks (D.P. West, ed.) New England Intercollegiate Geological Conference and Guidebook, p. B2-1 - B2-19.

Regan, S.P., Chiarenzelli, J.R., and McLelland, J.M., 2011, Evidence for an enriched asthenospheric source for coronitic metagabbros in the Adirondack Highlands: doi: 10.1130/GES00629.1.

Rivers, T., 2008, Assembly and preservation of lower, mid, and upper orogenic crust in the Grenville Province--Implications for the evolution of large hot long-duration orogens: Precambrian Research, v. 167, no. 3-4, p. 237–259.

Streepey, M.M., Johnson, E.L., and Mezger, K., 2001, Early History of the Carthage-Colton Shear Zone, Grenville Province, Northwest Adirondacks, New York (USA): The Journal of Geology v. 109, no. 4, p. 479–492, doi: 10.1086/320792.

Valley, P.M., Hanchar, J.M., and Whitehouse, M.J., 2011, New insights on the evolution of the Lyon Mountain Granite and associated Kiruna-type magnetite-apatite deposits, Adirondack Mountains, New York State: Geosphere, v. 7, no. 2, p. 357–389, doi: 10.1130/GES00624.1.

Whitney, P.R., and McLelland, J.M., 1983, Origin of biotite-hornblende-garnet coronas between oxides and plagioclase in olivine metagabbros, Adirondack region, New York: Contributions to Mineralogy and Petrology, v. 82, no. 1, p. 34–41, doi: 10.1007/BF00371173.

Whitney, P.R., and McLelland, J.M., 1973, Origin of coronas in metagabbros of the Adirondack mts., N. Y.: Contributions to Mineralogy and Petrology, v. 39, no. 1, p. 81–98, doi: 10.1007/BF00374247.

Whitney, P.R., Stracher, G.B., and Grover, T.W., 2002, Precambrian Geology of the Whitehall Area, Southeastern Adirondacks (J. McLelland & P. Karabinos, Eds.): New England Intercollegiate Geological Conference and the New York State Geological Association Guidebook for Fieldtrips in New York and Vermont,, p. C2–1–10.

Williams, M.L., and Jercinovic, M.J., 2002, Microprobe monazite geochronology: putting absolute time into microstructural analysis: Journal of Structural Geology, v. 24, no. 6-7, p. 1013–1028.

Williams, M.L., and Jercinovic, M.J., 2012, Tectonic interpretation of metamorphic tectonites: integrating compositional mapping, microstructural analysis and in situ monazite dating: Journal of Metamorphic Geology, v. 30, no. 7, p. 739–752, doi: 10.1111/j.1525-1314.2012.00995.x.

Williams, M.L., Jercinovic, M.J., and Hetherington, C.J., 2007, Microprobe Monazite Geochronology: Understanding Geologic Processes by Integrating Composition and Chronology: Annual Review of Earth and Planetary Sciences, v. 35, no. 1, p. 137–175, doi: 10.1146/annurev.earth.35.031306.140228.

Williams, M.L., Jercinovic, M.J., Goncalves, P., and Mahan, K., 2006, Format and philosophy for collecting, compiling, and reporting microprobe monazite ages: Chemical Geology, v. 225, no. 1-2, p. 1–15, doi: 10.1016/j.chemgeo.2005.07.024.

GEOLOGY AND PETROLOGY OF THE MONT ROYAL PLUTON, MONTREAL

NELSON EBY
Environmental, Earth and Atmospheric Sciences, University of Massachusetts, Lowell, MA 01854

INTRODUCTION

The Cretaceous Monteregian Hills (MH) petrographic province consists of a group of small alkaline plutons, and associated dikes, extending along a linear trend from approximately 30 km west of Montreal, Canada, to approximately 60 km east of Montreal (Fig. 1). Mont Megantic, located approximately 150 km east of Montreal has been included in the MH province (because of its geographic location), but geologically Mont Megantic belongs to the Younger White Mountain petrographic province of New Hampshire, Maine and Vermont. The MH plutons are largely composed of silica-undersaturated alkaline rocks: carbonatite and other strongly silica-undersaturated lithologies occur at Oka, and nepheline normative gabbros and pyroxenites, nepheline-bearing diorites, and feldspathoidal-bearing syenites and monzonites occur at the other MH plutons. Slightly silica-saturated quartz-bearing syenites are found at Monts Brome and Shefford. Philpotts (1974) and Eby (1987) have summarized the geology and petrology of the MH province.

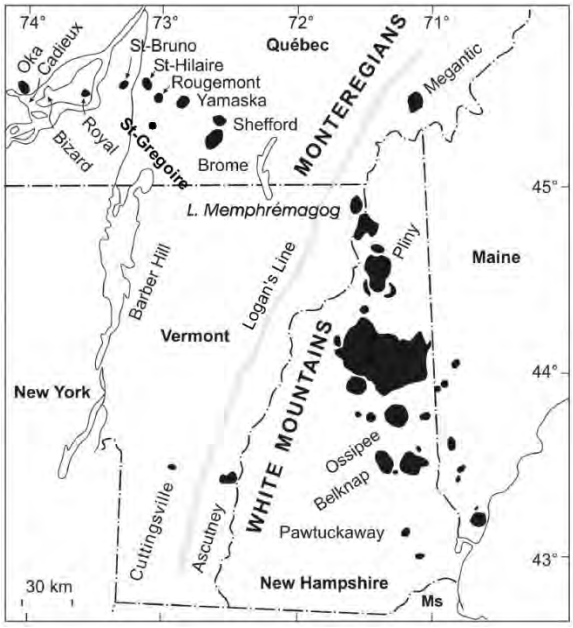

Figure 1. Location and geological setting of the Monteregian Hills and White Mountain igenous provinces (modified from Lentz et al., 2006).

The White Mountain (WM) petrographic province (Fig. 1) consists of two groups of plutons (Eby, 1987), one group (Older WM) intruded during the Jurassic and the other (Younger WM) during the Cretaceous. In contrast with the MH province, all the Younger WM plutons, with the exception of Cuttingsville, are silica-saturated to silica-over-saturated and the dominant lithologies are gabbro, diorite, syenite, quartz syenite, and granite. Rhyolite and basalt are found at Ossipee, a classic ring complex. Of note is that the silica-under-saturated lithologies occur to the west of Logan's Line (which represents the boundary between the Precambrian Grenville terrane and the folded Appalachians) while only silica-saturated lithologies are found to the east. The older WM plutons are dominantly composed of syenite, quartz syenite, and granite. Mafic rocks are generally sparse and are only abundant in the Pliny Range and Belknap Mountain complex (both contain diorite and monzodiorite). Silica-under-saturated rocks, nepheline syenite, occur at Red Hill and Rattlesnake Mountain, ME.

Geology and Petrology of the MH Plutons

The location and shape of the various plutons are shown in Figure 2. With the exception of Oka, which consists of two ring-like structures, the plutons are relatively small and more or less circular in shape. Because the plutons are more resistant to erosion than the surrounding sedimentary rocks they form prominent topographic features in the St. Lawrence Lowlands. On a clear day most of the MH plutons can be seen from the Chalet du Mont-Royal in the Parc du Mont-Royal. This park encompasses much of the top of Mont Royal and is also of interest because it was designed by the well-known landscape architect, Frederick Law Olmsted (who

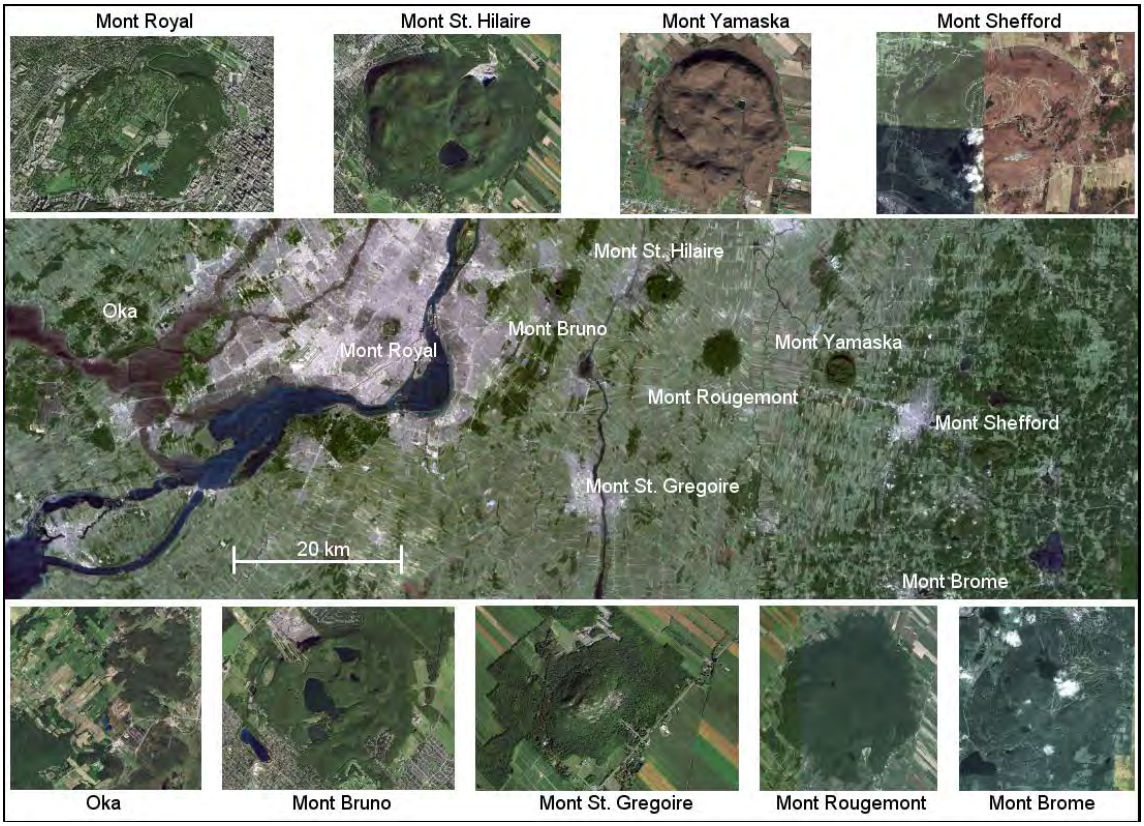

Figure 2. Terrain map (center) showing the location of the Monteregian Hills plutons. Top and bottom images show the terrain for each of the plutons. Because the rocks of the plutons are more resistant to erosion (except at Oka) the individual plutons occur as hills within the St. Lawrence Lowlands. Images are from Google Maps.

also designed the Emerald Necklace in Boston and Central Park in New York City).

The Oka carbonatite complex occurs at the western end of the MH province. It consists of a carbonatite core and a number of strongly-silica-undersaturated lithologies (okaite, melteigite, ijolite, and urtite). Alnoitic rocks are confined to the Oka area. Field oriented descriptions of the Oka complex can be found in Gold et al. (1986) and Lentz et al. (2006).

Monts Royal, Bruno, Rougemont, and Yamaska largely consist of mafic silica-undersaturated lithologies. The common rock types are pyroxenite and gabbro. These largely cumulate sequences frequently show primary igneous foliation. Nepheline is rarely found in the mafic

rocks and the silica-undersaturated character is essentially due to the presence of abundant kaersutite (a Ti-rich amphibole). At Monts Royal and Yamaska, nepheline-bearing gabbros, diorites, monzonites, and syenites intrude the earlier mafic sequences. For further details see Eby (1984, Royal and Bruno) and Eby (1989, Yamaska).

Mont St. Gregoire (formerly known as Mount Johnson) consists of a fine-grained nepheline diorite (essexite) core surrounded by coarser-grained nepheline diorite and nepheline syenite. Various petrogenetic models have been proposed for this pluton, including silicate-silicate liquid immiscibilty (Eby, 1984).

Mont St. Hilaire has been a mecca for mineral collectors for decades. Over 300 minerals, of which at least 30 are new species, have been identified, most from the Poudrette quarry (because of a change in ownership it is now called the Carrière Mont Saint-Hilaire and no mineral collecting is allowed). The eastern half of the pluton consists of nepheline-sodalite syenite while the western half consists of two mafic sequences comprised of pyroxenite, gabbro, nepheline-bearing gabbro and diorite, and monzonite (Currie et al., 1986).

The eastern most plutons, Monts Bome and Shefford, largely consist of gabbros, diroites and a variety of felsic rocks. With the exception of late-stage nepheline-bearing diorites and syenites, the rocks are silica-saturated to slightly silica over-saturated (Eby, 1985a).

Mafic and felsic dikes are widely distributed throughout the MH province and intrude both the plutons and the country rock. The dikes tend to lie along a NW-SE trend. The mafic dikes are classified as lamprophyre (alnoite, monchiquite, camptonite), alkali olivine basalt, and basanite. The felsic dykes are classified as bostonite, solvsbergite, nepheline syenite, and tinguaite. The strongly-silica-under-saturated dikes are concentrated towards the western end of the province. Further details can be found in Bedard et al. (1988) and Eby (1985b), among others.

Geochronology, Geochemistry, and Petrogenesis of the MH Plutons

$^{39}Ar/^{40}Ar$ dating of biotite and amphibole (Foland et al., 1986, 1989; Gilbert and Foland, 1986) indicates that the intrusions had a short emplacement history centered around 124 Ma. Heaman and LeCheminant (2001), using U-Pb dating of perovskite and apatite, determined an emplacement age of 140 Ma for the Île Bizard breccia pipe. The apatite fission-track age for Île Bizard is 121 Ma (reported in Lentz et al., 2006). For the Oka carbonatite complex, fission-track apatite ages range from 116 to 130 Ma (reported in Lentz et al., 2006). U-Pb apatite ages for Oka range from 107 to 132 Ma with two age clusters - 113 to 117 Ma and 125 to 127 Ma (Chen and Simonetti, 2013). These age data indicate an extended period of magmatic activity (~113 to 140 Ma) at the western end of the MH province, which is in marked contrast to the very restricted range of ages determined for the other MH plutons using $^{39}Ar/^{40}Ar$ dating of biotite and amphibole.

For the younger WM intrusions K-Ar ages vary from 108 to 125 Ma (Foland and Faul, 1977). High precision $^{39}Ar/^{40}Ar$ ages have been determined for Green Mountain (120 Ma) and Merrymeeting (121 Ma) (Foland and Allen, 1991). A Rb-Sr isochron age of 122 has been determined for Ascutney (Foland et al., 1985) and Eby (unpublished data) has obtained SHRIMP U-Pb zircon ages of 122 Ma for Ossipee. Thus the high precision geochronology indicates emplacement of the younger WM plutons in a very narrow age range at 122 Ma. These ages are within error identical to those determined for most of the MH plutons. The one exception is Cuttingsville, for which the mean age (based on K-Ar and fission-track titanite dating) is 100 ± 2 Ma (Eby and

McHone, 1997). Taken in total, the existing geochronology of the MH and younger WM does not support a hot-spot trace. The spatial distribution (Fig. 1) of the plutons, however, does suggest that they may represent a failed aulacogen (note the approximately 120° angle between the MH and younger WM plutons).

The rocks of the Monteregian Hills, with the exception of some cumulates, plot in the alkali field on a total alkalis versus silica diagram. Most of the rocks are nepheline normative, although the nepheline normative character of the cumulate rocks is due to the presence of abundant amphibole, rather than the occurrence of nepheline. In the strongly silica-under-saturated sequences there is a well-developed trend of alkali enrichment with increasing silica and this is reflected in the increase in modal nepheline. Rare earth (REE) abundance patterns show moderate to strong enrichment in the LREE with respect to the HREE, with the strongly silica-under-saturated rocks showing the greatest enrichment. Sr, Nd, and Pb isotopic studies by Eby (1985c), Grunenfelder et al. (1985), Wen et al. (1987), and Chen et al. (1994) have led to the conclusion that the source of the MH magmas was a depleted subcontinental lithosphere. During their ascent and emplacement, the magmas interacted to various degrees with the surrounding country rock which could be of Grenville or Lower Paleozoic age. Coupled with the trace element data it was suggested (Eby, 1987) that the subcontinental mantle was metasomatized shortly before or during melting. Recent studies of N, Ar, and Pb isotopic co-variations (Roulleau et al., 2012) and Nd-Sr-Hf-Pb isotopes (Roulleau and Stevenson, 2013) support this model. The authors of the recent studies also concluded that the subcontinental lithospheric mantle was metasomatized by a convecting asthenspheric plume.

In summary, the chemical and isotopic data indicate that the MH magmas were derived from a depleted mantle source (similar to the source that gives rise to ocean island basalts). This source was metasomatized shortly before or during melting. The source was most likely a garnet lherzolite mantle, although in some cases a spinel lherzolite mantle provides a better fit to the data. During ascent the magmas interacted to various degrees with the crust and AFC models involving relatively minor contamination can reproduce the observed chemical trends.

MONT ROYAL

Geological Setting

Mont Royal is elliptical in shape and has a surface area of approximately 4 km^2 (Fig. 3). At the present level of erosion, the intrusion is in contact with Ordovician shales (Utica formation) and limestones (Trenton formation) that have been metamorphosed to the pyroxene hornfels facies. The bulk of the intrusion consists of a hetero-geneous gabbro-pyroxenite body.

A plagioclase-rich leucocratic gabbro can be mapped as a separate unit. The gabbro-pyroxenite body is intruded by a nepheline-bearing diorite and widely distributed leucrocratic dikes which include feldspathoidal monzonites, feldspathoidal syenites, and quartz-bearing syenites. The felspathoidal monzonites are cut by both the feldspathoidal syenite and the quartz-bearing syenites, but cross-cutting relationships have not been observed between the latter two lithologies. Mafic dikes were intruded at the same time.

Petrography

Medium- to coarse-grained gabbro – pyroxenite: In the field changes in lithology are gradational over a few millimeters to centimeters and largely reflect changes in the modal abundances of the constituent minerals (Table 1). The more mafic members (Fig. 4) show a number of features typical of cumulate rocks including adcumulus overgrowths and intercumulus crystals. The more plagioclase-rich gabbros (Fig. 5) do not generally show cumulate textures, but some do show flow banding. The major minerals are titanaugite, kaersutite, opaque minerals (ilmenite and magnetite), occasional olivine, biotite, and plagioclase. The pink titanaugites are often rimmed by green aegirine-augite, and in most samples the pyroxenes have been slightly to extensively altered to red-brown kaersutite. Kaersutite also occurs as separate grains apparently of primary origin, and is locally abundant. Olivine occurs both as isolated grains and within pyroxene. The opaque mineral associated with kaersutite is generally ilmenite, while the rest of the opaque mineral suite is dominated by magnetite. In the more mafic rocks the plagioclase occurs as an intercumulus phase, and it is moderately to strongly zoned. Apatite is an important accessory, ranging from 0.5 to 2%. Feldspathoidal minerals were not observed in any of the specimens.

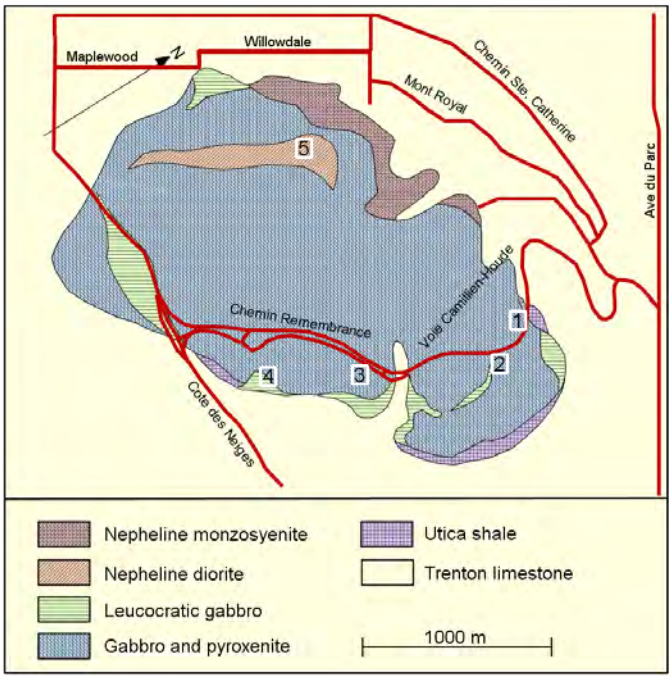

Figure 3. Geologic map of Mont Royal. Modified from Woussen (1969).

Leucogabbro: This unit is characterized by a greater abundance of plagioclase and a lesser abundance of amphibole and pyroxene (Table 1) which gives rise to its lighter color (Fig. 6). Olivine occurs in some samples. Red-brown biotite, apatite, opaque minerals, and titanite are accessories. Feldspathoids are absent.

Nepheline-bearing diorite: This unit (Fig. 7) is similar in appearance to the leucogabbro but it is distinguished from the leucogabbro by the presence of nepheline and orthoclase (Table 1). Kaersutite is more abundant than titanaugite and both minerals are often rimmed by green Na-rich amphiboles. Accessory minerals are biotite, apatite and opaque minerals. Flow banding is commonly observed.

Mafic dikes: The mafic and leucocratic dikes were emplaced simultaneously. The mafic dikes are very fine-grained to fine-grained. The major minerals are amphibole (hastingsite and/or kaersutite), calcic plagioclase, and augite (Fig. 8). Biotite occurs as an accessory mineral. Some varieties consist solely of calcic plagioclase and kaersutite and have been described as camptonite (Woussen, 1969). In some of the samples fine-grained calcic plagioclase - kaersutite enclaves are found in a somewhat coarser-grained matrix composed of pyroxene, amphibole, and plagioclase, which suggests multiple phases of intrusion.

Leucocratic dikes: The *feldspathoidal monzonites* (Fig. 9) consist of variable amounts of plagioclase, alkali feldspar (often perthitic), kaersutite zoned to hastingsite, titanaugite rimmed with pale green pyroxene (usually subordinate to kaersutite), sodalite, and nepheline. The opaque minerals (mostly magnetite) occur as accessories, and a few samples contain accessory red-brown garnet. Titanite, apatite, and zircon occur in trace amounts. The *felspathoidal syenites* (Fig. 10) consist essentially of perthitic alkali feldspar, up to 10% nepheline, minor plagioclase, aegirine-augite, hastingsite, and trace titanite, opaque minerals, and zircon. The *quartz-bearing syenites* (Fig. 11) largely consist of perthitic alkali feldspar and plagioclase. The mafic minerals are light green pyroxene and kaersutite, rimmed with hastingsite. Quartz occurs interstitially and constitutes less than 2% of the rock. Magnetite occurs as an accessory and there are trace amounts of apatite.

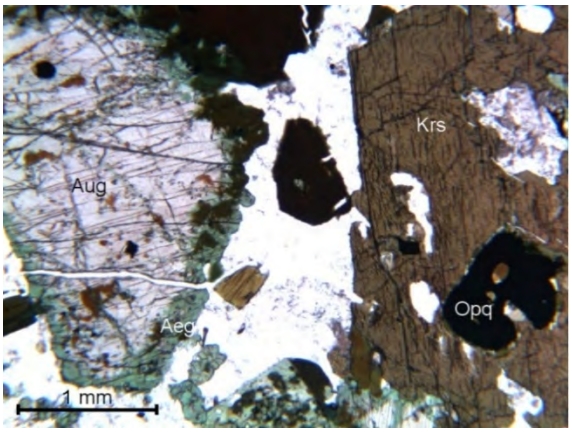

Figure 4a. RY 8 -Pyroxenite (PL)

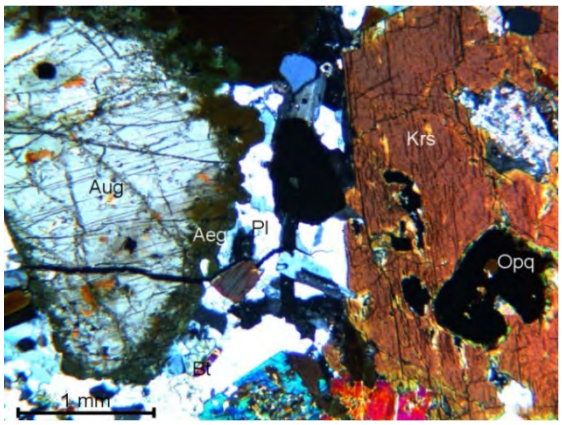

Figure 4b. RY8 - Pyroxenite (XP)

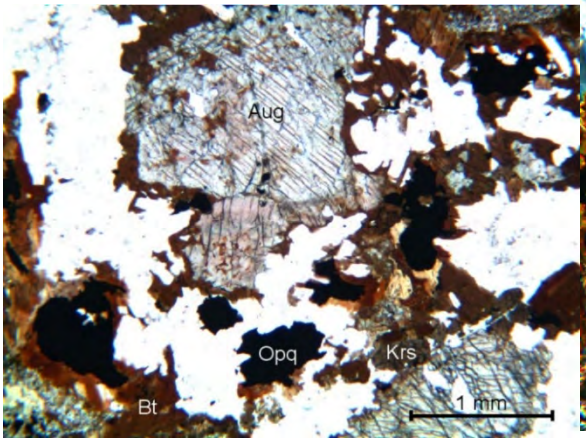

Figure 5a. RY11 - Gabbro (PL)

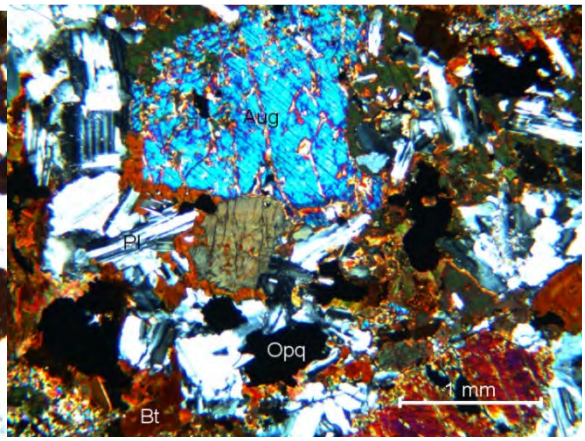

Figure 5b. RY11 - Gabbro (XP)

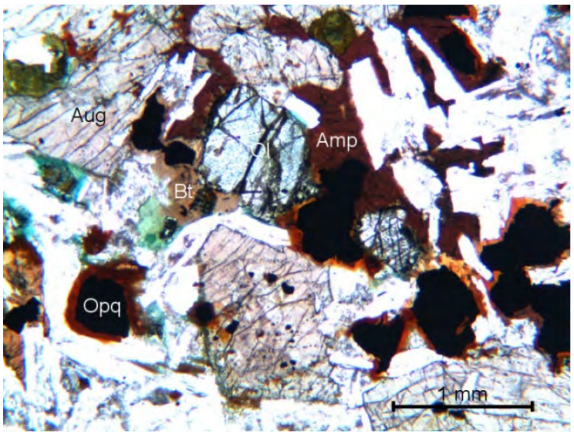

Figure 6a. RY22 - Leucogabbro (PL)

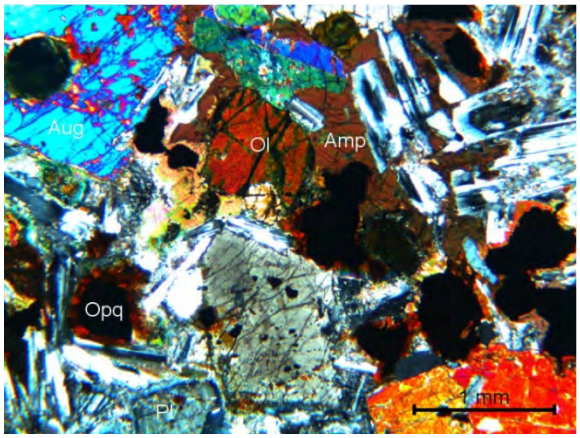

Figure 6b. RY22 - Leucogabbro (XP)

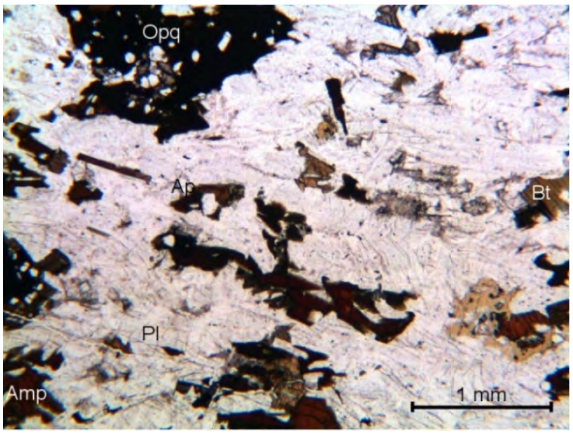

Figure 7a. RY3 - Nepheline-bearing diorite (PL)

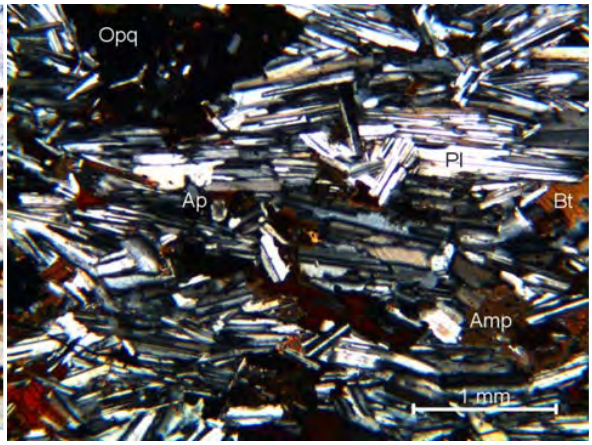

Figure 7b. RY3 - Nepheline-bearing diorite (XP)

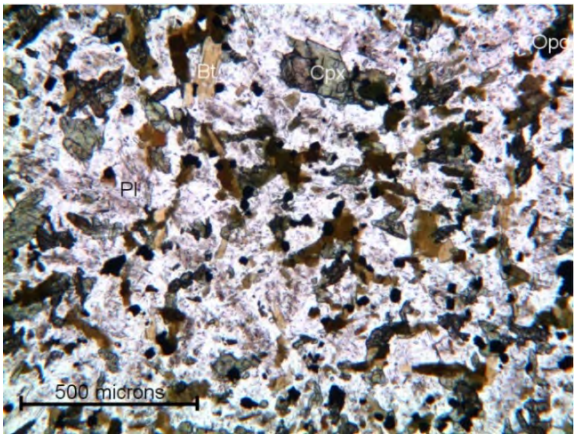

Figure 8a. RY33 - Mafic dike (PL)

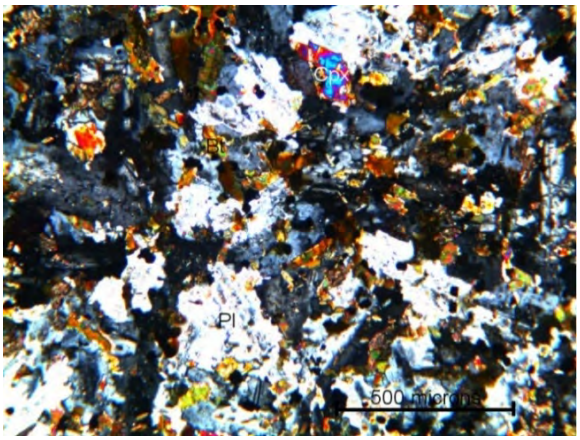

Figure 8b. RY33 - Mafic dike (XP)

Table 1. Mont Royal – modes for mafic igneous rocks

Lithology	Sample	Ol	Cpx	Amp	Pl	Kfs	Nph	Bi	Ap	Opq	Other
Pyroxenite	RY8	-	45.2	36.5	9.6	-	-	2.4	1.1	3.4	1.8
	RY10	-	39.3	42.2	3.9	-	-	0.9	1.0	10.7	2.0
	RY16	-	32.5	46.3	4.2	-	-	0.2	-	16.3	0.4
Gabbro	RY1	-	35.3	23.6	27.1	-	-	5.7	0.3	5.8	2.2
	RY11	0.9	34.1	12.0	38.7	-	-	6.2	0.1	7.9	0.1
	RY23	-	40.4	17.2	27.1	-	-	4.2	0.2	10.5	0.4
	RY29	-	36.0	8.6	31.6	-	-	14.5	1.5	5.5	2.4
Leucogabbro	RY12	-	24.5	4.1	54.1	-	-	7.7	0.9	8.7	-
	RY22	11.1	29.6	4.0	44.1	-	-	5.0	0.5	4.8	0.9
	RY34	0.4	7.4	6.9	79.4	-	-	1.3	0.1	4.1	0.3
Nph diorite	RY3	-	1.1	17.4	60.1	8.8	3.6	5.0	1.9	8.8	-
	RY5	-	11.0	19.2	32.9	11.4	12.9	1.7	3.0	7.9	-

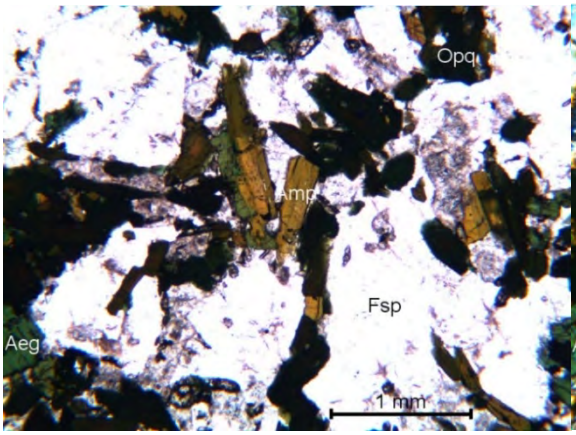

Figure 9a. RY9 – Feldspathoidal monzonites (PL)

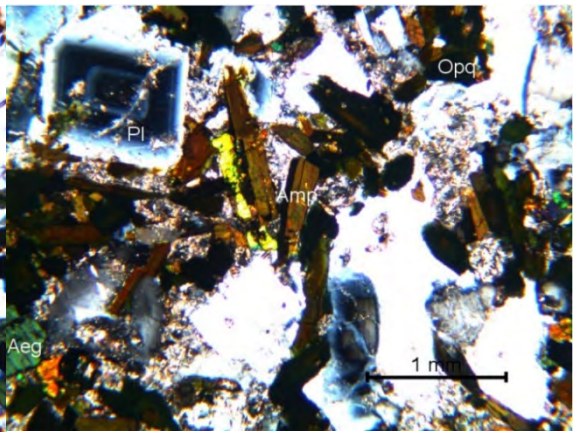

Figure 9b. RY9 – Feldspathoidal monzonites (XP)

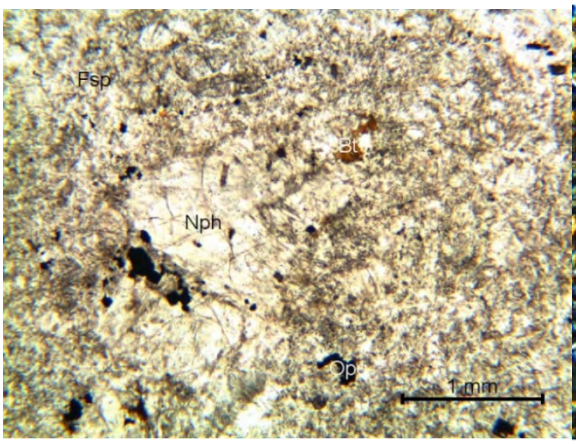

Figure 10a. RY28 – Feldspathoidal syenite (PL)

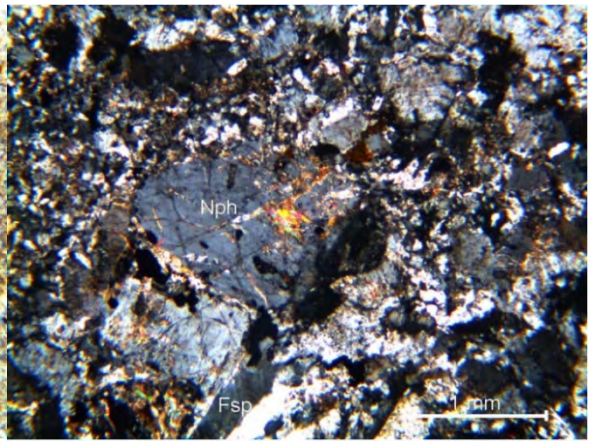

Figure 10b. RY28 - Feldspathoidal syenite (XP)

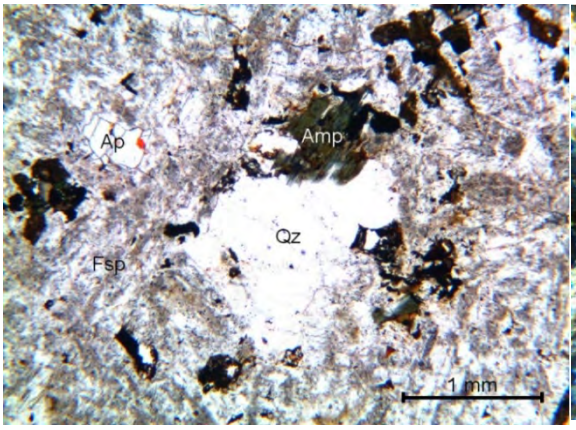

Figure 11a. RY20 – Quartz syenite (PL)

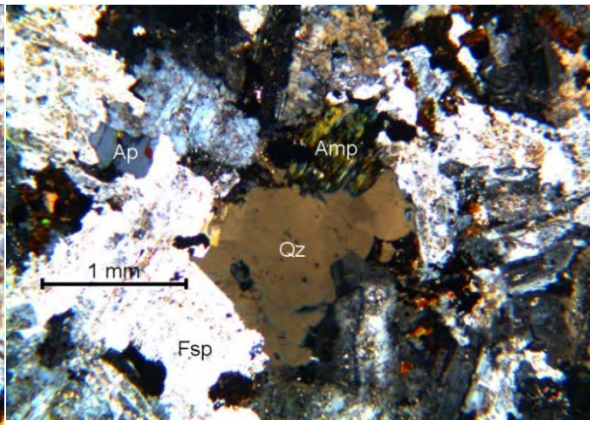

Figure 11b. RY20 - Quartz syenite (XP)

Mineral Chemistry

At Mont Royal the major rock-forming minerals are clinopyroxene, amphibole, and plagioclase. Biotite is locally abundant. Olivine is found in some gabbro and leucogabbro specimens. The olivines show a restricted range of compositions (Fig. 12) centered around Fo_{70}. The clinopyroxenes in the mafic rocks are augite while aegirine-augite occurs in the more felsic rocks and in the pyroxenites and gabbros as rims on augite (Fig. 12). The plagioclases vary from labradorite and bytownite in the mafic rocks to oligoclase in the felsic rocks. K-feldspar occurs in some of the felsic rocks (Fig. 12). The biotites are Mg-rich with the exception of biotites from the nepheline-bearing diorite which are Fe-rich (Fig. 12).

Because of the complexity of the amphibole group, the currently accepted classification scheme (Leake et al., 1997) is based on amphibole chemistry. According to this classification scheme the Mont Royal amphiboles are predominantly kaersutite and hastingsite (Fig. 13). Kaersutite is the common amphibole in the pyroxenites, gabbros, and nepheline-bearing diorites and hastingsite is the common amphibole in the feldspathoidal monzonites and syenites.

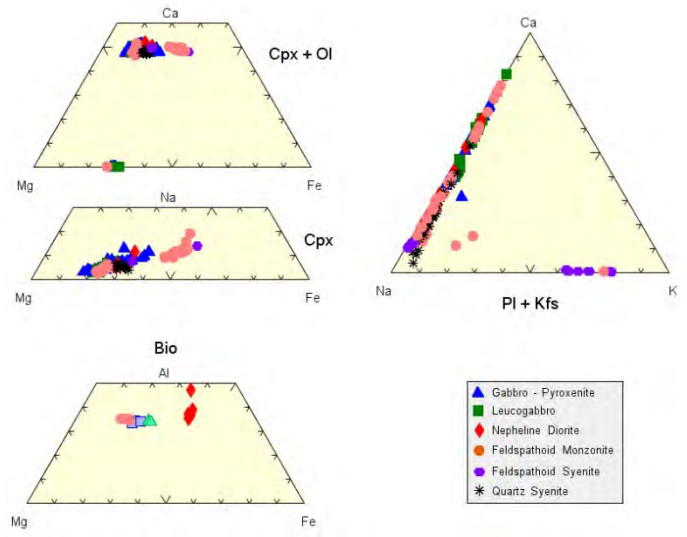

Figure 12. Range of chemical compositions for olivine, pyroxene, biotite and plagioclase.

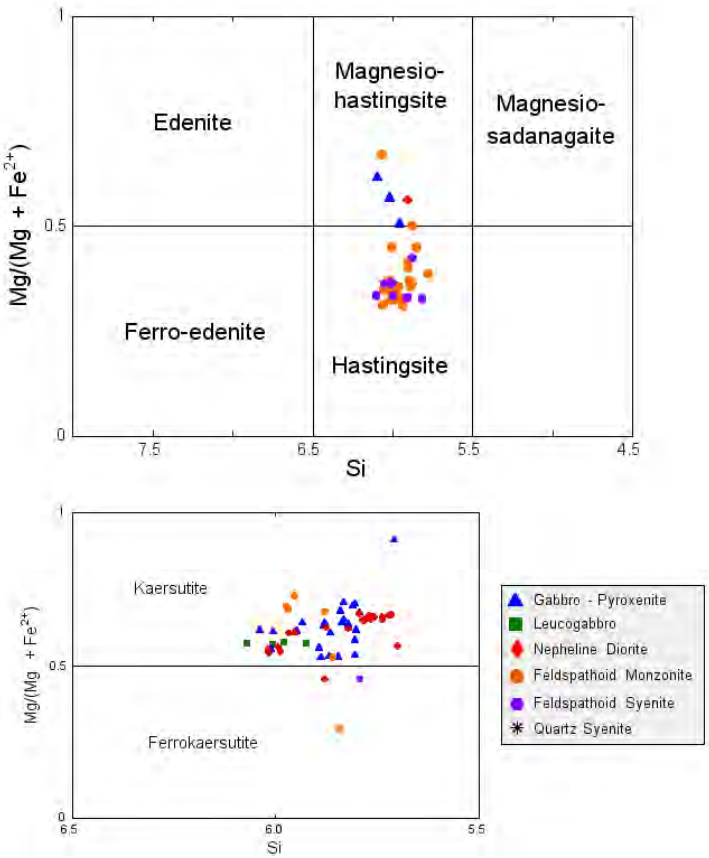

Figure 13. Classification of Mont Royal amphiboles.

Geochemistry

With the exception of the quartz-bearing syenites, all the Mont Royal rocks are nepheline-normative and alkaline (Fig. 14). A well-defined trend (which falls on the Tholeiitic – Calc-Alkaline boundary) towards alkali enrichment is shown in an AFM diagram. The exception is some of the gabbro and pyroxenite samples that plot to the right of the trend, a reflection of their cumulate character. On a TAS diagram (Fig. 14) the Mont Royal rocks plot in both silica-under-saturated and silica-saturated fields. The very low silica samples are cumulates.

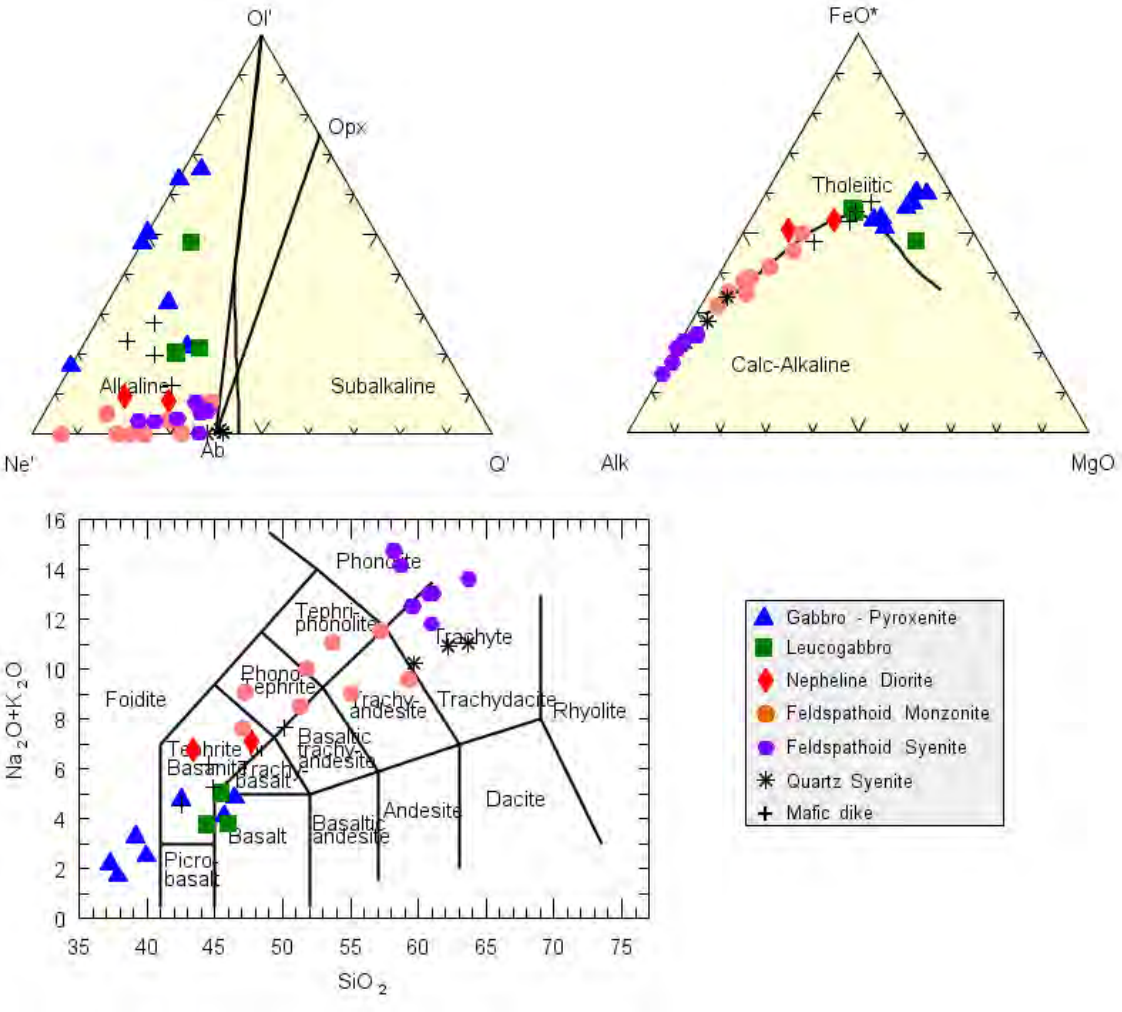

Figure 14. Summary diagrams for Mont Royal whole-rock geochemistry.

REE and primitive-mantle-normalized elemental plots (Fig. 15) and Sr and Pb isotope plots (Fig. 16) are found on the next page. Based on time and interest we will talk about the significance of the data during the field trip.

Geochronology

$^{39}Ar/^{40}Ar$ biotite and amphibole ages for the MH plutons cluster around 124 Ma (Foland et al., 1986, 1989; Gilbert and Foland, 1986). However, none of these studies determined a radiometric age for Mont Royal. Apatite (population method) and titanite (external detector

method) fission-track ages have been determined for Mont Royal. A description of the analytical protocol used in our laboratory can be found in Eby et al. (1995). Apatite and titanite ages are statistically indistinguishable and yield a mean age of 122 Ma. This is a slightly younger age than that determined for the other MH plutons using $^{39}Ar/^{40}Ar$ dating. Of interest are the blocking (or annealing) temperatures for the various systems: ~350°C for $^{39}Ar/^{40}Ar$ biotite, ~250°C for titanite, and ~60°C for complete track retention in apatite. From these data one can infer that the rocks cooled from magmatic to ambient temperatures in several million years which leads to the conclusion that the depth of emplacement was very shallow, no more than ~1 km.

Table 2. Titanite and apatite fission-track ages

Sample	Lithology	Number crystals	Spontaneous Rs	(Ns)	Induced Ri	(Ni)	Dosimeter Rd	(Nd)	Age (Ma)
				Titanite Ages					
RY5	Neph Diorite	7	6.79	114	5.36	90	5.96	1811	118.5 ± 45.5
RY12	Leucogabbro	15	26.6	959	15.4	554	4.67	2879	126.5 ± 22.1
RY17	Mafic dike	8	3.23	62	2.29	44	5.37	1635	118.8 ± 10.3
RY29	Gabbro	4	2.15	206	1.66	159	5.92	1811	120.3 ± 35.4
RY33	Mafic dike	4	5.94	57	4.06	39	5.35	1635	122.8 ± 53.8
							Mean Age:		**121.4 ± 3.3**
				Apatite Ages					
RY10	Pyroxenite	60/60	3.01	433	3.9	561	5.27	1635	126.3 ± 3.1
RY12	Leucogabbro	50/50	9.4	1130	13.8	1654	5.85	1811	123.7 ± 2.9
RY16	Pyroxenite	60/60	4.1	590	5.66	815	5.27	1635	118.6 ± 2.9
RY23	Gabbro	60/60	3.65	525	4.99	719	5.25	1635	119.3 ± 2.9
							Mean Age:		**122.0 ± 3.7**

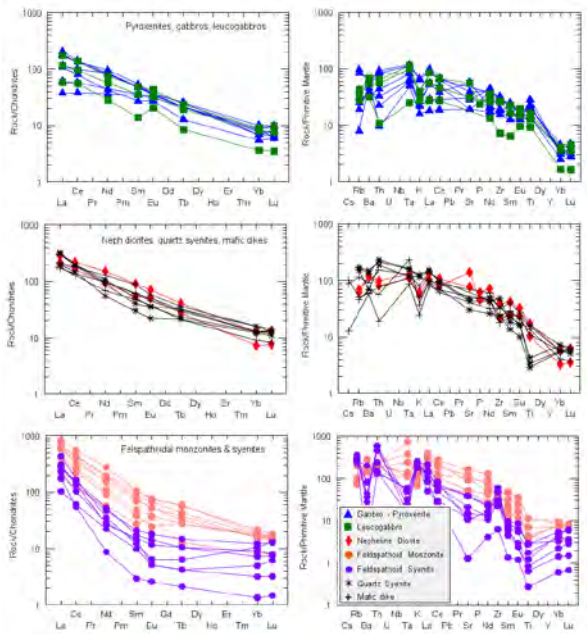

Figure 15. Chondrite normalized REE plots and primitive mantle normalized elemental plots for the various Mont Royal lithologies.

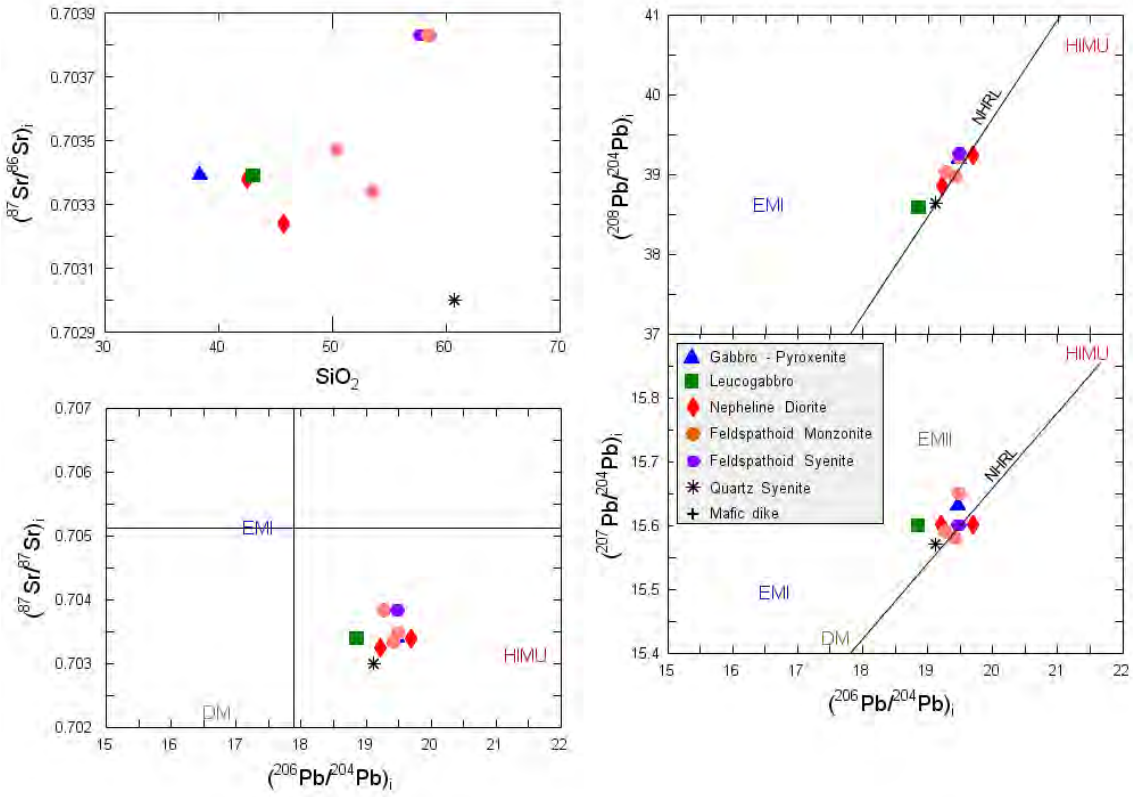

Figure 16. Sr and Pb isotope diagrams for the various Mont Royal lithologies and comparisons with potential mantle sources.

FIELD GUIDE AND ROAD LOG

Meeting Point: Southeastern parking lot of Hudson Hall on the SUNY Plattsburgh campus. The lot is located at the corner of Beekman and Broad streets.

Meeting Point Coordinates: 44.696°N, 73.467°W

Departure Time: 7:30 AM

Distance in miles (km)

Cumu-lative	Point to Point	Route Description
0.0 (0.0)	0.0 (0.0)	Starting in the parking lot for Hudson Hall, SUNY Plattsburgh, corner of Beekman and Broad St., Plattsburgh, NY. Turn left out of parking lot (north) on Beekman St. toward Cornelia St.
0.7 (1.1)	0.7 (1.1)	Turn right onto Boynton Ave.
1.2 (1.9)	0.5 (0.8)	Turn left onto NY-22 N
1.4 (2.2)	0.2 (0.3)	Take the Interstate 87 N ramp.
1.9 (3.0)	0.5 (0.8)	Merge onto I-87 N.
21.6 (34.7)	19.7 (31.7)	Take Exit 42 to Champlain and continue right at end of exit ramp. Merge onto Rt. 11 E.
23.7 (38.1)	2.1 (3.4)	Take a left at the traffic light on Rt.276 N to Lacolle, QC border crossing.
26.0 (41.8)	2.3 (3.7)	Quebec border crossing – Passport or Enhanced License Needed! Continue north on Quebec Rt. 221.
29.7 (47.8)	3.7 (6.0)	Left on Quebec Rt. 202 W to Autoroute 15 N to Montreal.
33.4 (53.8)	3.7 (6.0)	Turn right onto onramp for Autoroute 15 N to Montreal.
62.6 (100.8)	~29.2 (47.0)	Take exit 53 to Pont Champlain. Merge onto Boulevard Marie Victorin/Autoroute 15 N toward Montreal/Quebec/Autoroute 20 /Autoroute 10/Sherbrooke.
63.1 (101.6)	0.5 (0.8)	Take the Autoroute 10/Autoroute 15 N/Autoroute 20/Pont Champlain ramp to the Pont Champlain (Champlain Bridge) to Montreal across the St. Lawrence River.
63.7 (102.6)	0.6 (1.0)	Merge onto Autoroute 10/Autoroute 15 N/Autoroute 20.Continue to follow Autoroute 15 N/Autoroute 20.
67.8 (109.2)	4.1 (6.6)	Take Av Atwater Ave. exit toward Rue Saint-Patrick St.
68.0 (109.5)	0.2 (0.3)	Merge onto Atwater Ave.
68.4 (110.1)	0.4 (0.6)	Turn left to stay on Atwater Ave.
69.7 (112.2)	1.3 (2.1)	Turn right onto Dr. Penfield Ave.
69.8 (112.3)	0.09 (0.1)	Turn left onto Côte-des-Neiges Rd.
69.8 (112.3)	0.04 (0.06)	Keep left to stay on Côte-des-Neiges Rd.
70.3 (113.6)	0.8 (1.3)	Turn right onto Chemin Remembrance.

70.7 (114.2)	0.4 (0.6)	Destination: Mont Royal Park. Turn right into Maison Smith parking area. Parking area is metered. Purchase a ticket from one of the kiosks (Use Canadian cash or credit card). Assemble at the base of the stairs leading into Maison Smith. The field trip will start at 9 AM. We will walk (easy walking) to stops 1 through 4.

Figure 17. Google Map image showing the location of the field trip stops on Mont Royal. Meeting point (Maison Smith) is labeled on the image. Heavy white lines show the walking traverses. The dashed heavy white line shows the driving route from the Maison Smith parking area to Stop 5.

STOP 1: Voie Camillien-Houde traverse. Contact with country rock, pyroxenite and gabbro outcrops

Location Coordinates: (45°30.632'N, 73°35.608'W)

Start the traverse across from lower entrance to the parking lot. The contact between the plutonic rocks and the Utica shale is exposed at this location. Also at this location the underlying Trenton limestone is in faulted contact with the shale. The shale has been metamorphosed to a hornfels and the limestone is slightly metamorphosed. Locally the limestone is intruded by camptonite dikes surrounded by narrow thermal aureoles. Return to the parking lot (look both ways before crossing) and proceed to the upper end of the parking lot and up the steps. Note the large xenolith of Utica Shale halfway up on the right side of the steps. A short walk beyond the steps leads to good exposures of gabbro with steeply dipping layering. Return to the parking lot and walk up the road. In places you will need to walk on the edge of the road. Be careful!

There is an almost continuous exposure of the gabbro-pyroxenite sequence which is cut by multiple felsic dikes. At the end of the traverse, opposite the entrance to the Cimetière Mont-Royal, part of the limestone screen is exposed. The intensely deformed metamorphosed limestone consists of a mixture of calcite marble and a greenish skarn of eipidote, tremolite, zoisite, and diopside.

STOP 2: Belvedere traverse. Pyroxenite and gabbro cut by various mafic and felsic dikes

Location Coordinates: (45°30.167'N, 73°35.500'W)

This traverse is along the road leading to the Belvedere. The pyroxenites and gabbro are intruded by a variety of mafic and felsic dikes. The feldspathoidal monzonite and feldspathoidal syenite dikes are light gray in color, medium-grained, and vary in width from a few millimeters to a few tenths of a meter. The lithologies are distinguished on the basis of the alkali feldspar/plagioclase ratio, a distinction which is not apparent at the outcrop scale. Late stage medium- to coarse-grained quartz-bearing syenites, which weather to a distinctive salmon pink color, cut the feldspathoidal monzonites and feldspathoidal syenites. This traverse ends at the Belvedere. On a clear day there is a superb view of the Monteregian Hills plutons from this location.

STOP 3: Gabbro and pyroxenite

Location Coordinates: (45°30.065'N, 73°35.788'W)

Large outcrops of gabbro in wooded area across from RCMP station.

STOP 4: Foliated leucogabbro

Location Coordinates: (45°29.846'N, 73°35.870'W)

Foliated leucogabbro. Foliation is essentially vertical and the outcrop is cut by a felsic dike. The leucogabbro is distinguished on the basis of a lighter color index due to a greater amount of feldspar. Olivine is found in some specimens. Amphibole is much less abundant relative to the more mafic units.

Distance in miles (km)		
Cumu-lative	Point to Point	Route Description
70.7 (114.2)	0.0 (0.0)	Return to the vehicles. Exit parking area and turn left onto Chemin Remembrance. Our next stop is in the Notre-Dame-des-Neiges Cemetery. The entrance from Chemin Remembrance (which is closest to the outcrops) is closed on Saturday and Sunday. This road log will take you in the main entrance off Chemin de la Côte-des-Neiges.
71.5 (115.4)	0.8 (1.2)	Bear right onto Chemin de la Côte-des-Neiges.
71.6 (115.6)	0.1 (0.2)	Turn right into Notre-Dame-des-Neiges Cemetery.
71.8 (115.9)	0.2 (0.3)	Bear left and after a short distance (<0.05 mi) bear left onto east-west road that passes cemetery office buildings on the right.

72.1 (116.4)	0.3 (0.5)	Proceed to edge of cemetery and turn right. Continue on road that runs along the cemetery boundary.
72.5 (117.1)	0.4 (0.7)	Destination. Park by side of road.

STOP 5: Nepheline-bearing diorite

Location Coordinates: (45°30.318'N, 73°36.567'W)

Nepheline-bearing diorite outcrops are found in the woods next to the grave site. The outcrops extend outside of the cemetery and at the time this field trip guide was written could be accessed through a break in the fence. Sample RY3 and RY5 (Table 1) were collected from this location. RY3 (Fig. 7) is medium-grained and shows a subparallel alignment of plagioclase which is interpreted as a flow texture. RY5 is similar, but coarser-grained.

Distance (miles) Cumu-lative	Point to Point	Route Description
72.5 (117.1)	0.0 (0.0)	Reverse direction and return to cemetery entrance.
73.4 (118.6)	0.9 (1.5)	Turn right onto Chemin de la Côte-des-Neiges.
73.7 (118.9)	0.3 (0.5)	Bear right onto Avenue Decelles.
74.3 (119.9)	0.6 (1.0)	Turn right onto Chemin de la Côte-Sainte-Catherine.
76.2 (122.9)	1.9 (3.0)	Turn left onto Boulevard Saint Joseph.
76.8 (125.4)	1.6 (2.5)	Turn right onto Avenue Papineau.
79.2 (129.3)	2.4 (3.9)	Proceed to Île Ste. Hélène via Pont Jacques Cartier. Turn right off bridge onto Île Ste. Hélène. This exit has a very short slip ramp. Pay close attention to tailgaters and give plenty of warning.
79.3 (129.4)	0.1 (0.15)	At bottom of ramp bear to the left. From this point on bear or turn left (see Fig. 18).
79.5 (129.7)	0.2 (0.3)	Turn left into parking lot. This is the location for Stop 6 and also marks the end of the field trip. To return to Plattsburgh continue east (away from Montreal) on the Pont Jacques Cartier. Turn right (south) onto 132 which eventually becomes 15. Continue to Canada/USA border. On the USA side of the border 15 becomes I-87. Continue on I-87 to Plattsburgh.

STOP 6: Île Ste. Hélène diatreme breccia

Location Coordinates: (45°31.199'N, 73°32.118'W)

The large hill on Île Ste. Hélène is composed of diatreme polymictic breccia (Figs. 19, 20). Many of the buildings (Fig. 21) on the island were built using the breccia and provide some of the best exposures (not to be sampled). The field trip stop is an abandoned quarry which was the source for some of the building material.

Figure 18. Location of Stop 6, an abandoned quarry that is now a parking area. Dashed line shows driving route. Image is from Google Maps.

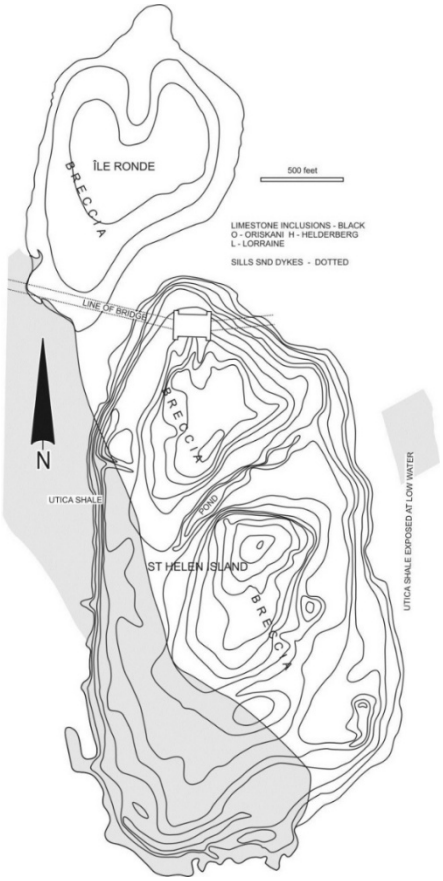

Figure 19. Geological map of the distribution of breccia and Utica shale on Île Ste. Hélène (From Lentz et al., 2006).

Figure 20. Google Earth image of Île Ste. Hélène

Figure 21. Tour Lévis, which occupies the summit of the higher hill, was constructed using the diatreme breccia.

A large variety of clasts can be found in the breccia. These include fossiliferous shale and limestone clasts which contain Devonian brachiopods. The youngest exposed sediments in the St. Lawrence Lowland are lower Silurian in age and thus these clasts represent some of the missing overlying sedimentary column. Other clasts include Trenton limestone, Utica shale, and metamorphic basement clasts. The breccias exposed on Île Ste. Hélène do not contain an igneous matrix. However, the comminuted material does have an elevated Ti content and the presence of analcime, perovskite, and apatite suggest there is an igneous component. Hydrothermal activity subsequent to emplacement resulted in veins carrying calcite, analcime, apatite, and rare Ti-minerals.

REFERENCES CITED

Bedard, J. H. J., Francis, D. M., and Ludden, J., 1988, Petrology and pyroxene chemistry of Monteregian dykes: the origin of concentric zoning and green cores in clinopyroxenes from alkali basalts and lamprophyres, Canadian Journal of Earth Sciences, v. 25, p. 2041-2058.

Chen, J., Henderson, C. M. B., and Foland, K. A., 1984, Open-system, sub-volcanic magmatic evolution: constraints on the petrogenesis of the Mount Brome alkaline complex, Canada, Journal of Petrology, v. 35, p. 1127-1153.

Chen, W., and Simonetti, A., 2013, In-situ determination of major and trace elements in calcite and apatite, and U-Pb ages of apatite from the Oka carbonatite complex: insights into a complex crystallization history, Chemical Geology, v. 353, p. 151-172.

Currie, K. L., Eby, G. N., and Gittins, J., 1986, The petrology of the Mont Saint Hilaire pluton, southern Quebec: an alkaline gabbro – peralkaline syenite association, Lithos, v. 19, p. 65-81.

Eby, G. N., 1984, Monteregian Hills I. Petrography, major and trace element geochemistry, and strontium isotopic chemistry of the western intrusions: Mounts Royal, St. Bruno, and Johnson, Journal of Petrology, v. 235, p. 421-452.

Eby, G. N., 1985a, Monteregian Hills II. Petrography, major and trace element geochemistry, and strontium isotopic chemistry of the eastern intrusions: Mounts Shefford, Brome, and Megantic, Journal of Petrology, v. 26, p. 418-448.

Eby, G. N., 1985b, Age relations, chemistry, and petrogenesis of mafic alkaline dikes from the Monteregian Hills and younger White Mountain igneous provinces, Canadian Journal of Earth Sciences, v. 22, p. 1103-1111.

Eby, G. N., 1985c, Sr and Pb isotopes, U and Th chemistry of the alkaline Monteregian and White Mountain provinces, eastern North America, Geochimica et Cosmochimica Acta, v. 49, p. 1143-1154.

Eby, G. N., 1987, The Monteregian Hills and White Mountain alkaline igneous provinces, eastern North America, *in* Fitton, J. G., and Upton, B. G. J. (Eds.), Geological Society Special Publication No. 30. London, Geological Society, p. 433-447.

Eby, G. N., 1989, Petrology and geochemistry of Mount Yamaska, Quebec, Canada: a mafic representative of the Monteregian Hills petrographic province, *in* Leelanandam, C. (Ed.), Alkaline Rocks, Geological Society of India Memoir 15. Bangalore, India, B. B. D. Power Press, p. 63-82.

Eby, G. N., Roden-Tice, M., Krueger, H. L., Ewing, W., Faxon, E. H., and Woolley, A. R., 1995, Geochronology and cooling history of the northern part of the Chilwa alkaline province, Malawi, Journal of African Earth Sciences, v. 20, p. 275-288.

Eby, G. N., and McHone, J. G., 1997, Plutonic and hypabyssal intrusions of the Early Cretaceous Cuttingsville Complex, Vermont, *in* Grover, T.W., Mango, H. N., and Hasenohr, E. J. (Eds.), Guidebook to Field Trips in Vermont and Adjacent New Hampshire and New York, New England Intercollegiate Geological Conference, Castleton, VT, p. B2-1-B2-17.

Foland, K. A., and Faul, H., 1977, Age of the White Mountain intrusives – New Hampshire, Vermont, and Maine, USA, American Journal of Science, v. 277, p. 888-904.

Foland, K. A., Henderson, C. M. B., and Gleason, J., 1985, Petrogenesis of the magmatic complex at Mount Ascutney, Vermont, USA, Contributions to Mineralogy and Petrology, v. 90, p. 331-345.

Foland, K. A., Gilbert, L. A., Sebring, C. A., and Jiang-Feng, C., 1986, Ar-40/Ar-39 ages for plutons of the Monteregian Hills, Quebec: evidence for a single episode of Cretaceous magmatism, Geological Society of America Bulletin, v. 97, p. 966–974.

Foland, K. A., Chen, J.-F., Linder, J. S., Henderson, C. M. B., and Williams, I. M., 1989, High resolution $^{40}Ar/^{39}Ar$ chronology of multiple intrusion igneous complexes: application to the Cretaceous Mount Brome complex, Quebec, Canada, Contributions to Mineralogy and Petrology, v. 102, p. 127–137.

Foland, K. A., and Allen, J. C., 1991, Magma sources for Mesozoic anorogenic granites of the White Mountain magma series, New England, USA, Contributions to Mineralogy and Petrology, v. 109, p. 195-211.

Gold, D. P., Eby, G. N., Bell, K., and Vallee, M., 1986, Carbonatites, diatremes, and ultra-alkaline rocks in the Oka are, Quebec: Geological Association of Canada, Mineralogical Association of Canada, Canadian Geophysical Union, Joint Annual Meeting, Ottawa '86, Field Trip 21 Guidebook, 51 p.

Grunenfelder, M. H., Tilton, G. R., Bell, K., and Blenkinsop, J., 1985, Lead and strontium isotope relationships in the Oka carbonatite complex, Geochimica et Cosmochimica Acta, v. 50, p. 461-468.

Heaman, L. M., and LeCheminant, A. N., 2001, Anomalous U-Pb systematics in mantle-derived baddeleyite from Île Bizard: evidence of high temperature radon diffusion?, Chemical Geology, v. 172, p. 77-93.

Leake, B. E., Woolley, A. R., Arps, C. E. S., and a cast of thousands, 1997, Nomenclature of amphiboles: report of the subcommittee on amphiboles of the International Mineralogical Association Commission on New Minerals and Minerals Names, Canadian Mineralogist, v. 35, p. 219-246.

Lentz, D., Eby, N. Lavoie, S., and Park, A., 2006, Diatremes, dykes, and diapirs: revisiting the ultra-alkaline to carbonatitic magmatism of the Monteregian Hills: GAC/MAC Joint Annual Meeting, Montreal, Quebec, Field Trip B4, 48 p.

Philpotts, A. R., 1974. The Monteregian Province, *in* Sorenson, H. (Ed.), The Alkaline Rocks. New York, John Wiley, p. 293-310.

Roulleau, E., Pinti, D. L., Stevenson, R. K., Takahata, N., Sano, Y., and Pitre, F., 2012, N, Ar and Pb isotopic co-variations in magmatic minerals: discriminating fractionation processes from magmatic sources in Monteregian Hills, Québec, Canada, Chemical Geology, v. 326-327, p. 123-131.

Roulleau, E., and Stevenson, R., 2013, Geochemical and isotopic (Nd-Sr-Hf-Pb) evidence for a lithospheric mantle source in the formation of the alkaline Monteregian Province (Quebec), Canadian Journal of Earth Sciences, v. 50, p. 650-666.

Wen, J., Bell, K., and Blenkinsop, J., 1987, Nd and Sr isotope systematics of the Oka complex, Quebec, and their bearing on the evolution of the sub-continental upper mantle, Contributions to Mineralogy and Petrology, v. 97, p. 433-437.

Woussen, G., 1969, Notes on the geology of Mont Royal, *in* Pouliot, G. (Ed.), Guidebook for the Geology of Monteregian Hills, The Geological Association of Canda/The Mineralogical Association of Canada, Montreal, Canada, p. 63-73.

THE MIDDLE ORDOVICIAN SECTION AT CROWN POINT PENINSULA, NEW YORK

BRUCE SELLECK
Department of Geology, Colgate University, Hamilton, NY 13346
bselleck@mail.colgate.edu

CHARLOTTE MEHRTENS
Department of Geology, University of Vermont, Burlington, VT 05405
charlotte.mehrtens@uvm.edu

INTRODUCTION

The Chazy, Black River and Trenton Groups are a well studied sequence of fossiliferous limestones, dolostones and sandstones in the Champlain Valley of New York, Vermont and southern Quebec. These rocks record shallow water cyclic sedimentation in the foreland basin of Laurentia prior to and during the initial stages of the Taconic Orogeny. This field trip reviews the stratigraphy of these units, as well as the evidence for reconstructing depositional environments and cyclic sea level changes.

THE CROWN POINT HISTORICAL SITE

This field trip takes place at the scenic Crown Point Historical Site (Figure 1), a *no-hammer, no-collecting locality*. Approximately 120 meters of section is exposed in a combination of excavations, ridges and shoreline exposures that dip ~8° northwest. The overall stratigraphy (Figures 2, 3) from the Crown Point Formation (Chazy Group) to the Glens Falls Formation (Trenton Group) records the Middle Ordovician transgression seen throughout the Appalachians. Correlation of this stratigraphy exposed at Crown Point to the type Trenton in central New York State is provided by *Prasopora spp.* (Mehrtens and Barnett, 1979). Conodonts collected from strata to the north and east (Harris, pers. comm. and Harris, *et al*., 1995; Roscoe, 1973) provide additional age control. Detailed sedimentologic studies of these units have been published by Bechtel and Mehrtens (1995), Mehrtens and Cuffey (2003) and MacLean (1986) and Selleck (1988).

TECTONIC SETTING

The Upper Ordovician stratigraphic sequence of westernmost Vermont and northeasternmost New York consists of several rock units (Chazy, Black River and Trenton Groups) which record sedimentation in a progressively deepening foreland basin located to the west of the accretionary prism-volcanic arc terrain of the Taconic Orogeny. To the west of this foreland basin lay the Grenville Province metamorphic basement and overlying Cambrian sandstones of the Adirondack Mountains and Champlain Valley. To the east lay uplifting Taconian lands along the deforming Iapetus margin. To the west of this foreland basin lay the Grenville Province metamorphic basement and overlying Cambrian sandstones of the Adirondack Mountains and Champlain Valley. To the east lay uplifting Taconian lands along the deforming Iapetus margin. As described by Rowley and Kidd (1981) and Stanley and Ratcliff (1985) the eastern margin of

Laurentia was an eastward dipping continental margin beneath the Iapetus Ocean and associated island arc terrain. The transgressive sequence recorded by the Middle-Upper Ordovician stratigraphy in Vermont, New York and southern Quebec is interpreted to be the result of a combination of factors related to the Taconic arc-continent collision, including foundering produced by passage of the peripheral bulge through the foreland basin (Jacobi, 1981), thrust loading, or a combination of the two processes (Bradley and Kusky, 1986). The global Ordovician eustatic sea level rise (Mussman and Read, 1986) was also a factor in producing the transgressive sequence along the Iapetus margin.

The sequence stratigraphic patterns for the Upper Ordovician strata of eastern Laurentia, resulting from that the interplay of regional tectonism and global eustatic change, have been nicely summarized by Brett, et al 2004, and Cornell, 2008. As illustrated in Figure 2, following the nomenclature of Brett, et al 2004, the sequences of interest at the Crown Point site include the M1B (lowermost Upper Ordovician) comprising the Chazy Group, the M4A, M4B, and M5A, comprising the Black River Group, and the M5A, M5B and M5C, making up the Trenton Group. The M2 and M3 (upper Chazy Group, lower Black River Group) are absent at the Crown Point site, represented by the disconformable contact between the Black River and Chazy Groups.

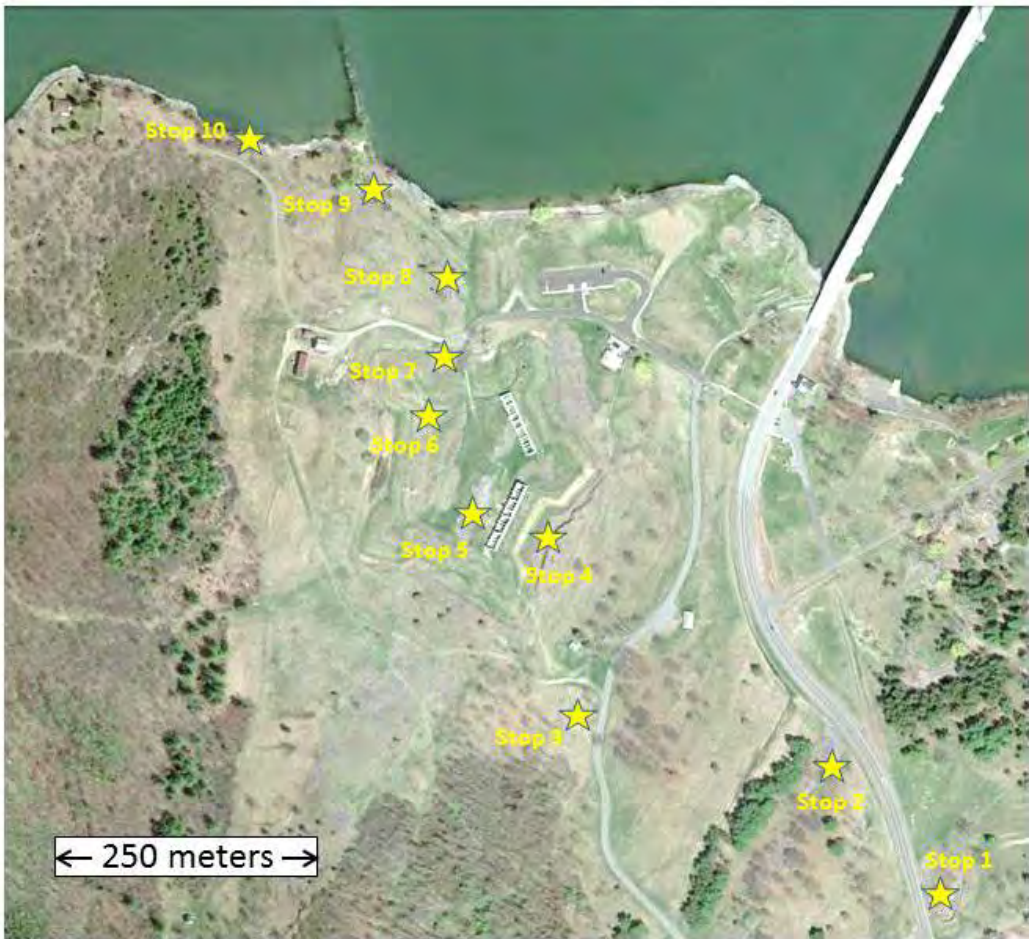

Figure 1. Locality map for the Crown Point Reservation field trip site. Base map from Google Earth.

Important to our understanding of the Upper Ordovician stratigraphy in the Champlain Valley region is the role of syn-depositional block faulting in controlling facies and thickness patterns in the sedimentary sequence. Evidence for active fault movement during deposition of the Middle Ordovician units, a phenomenon described for the Ordovician of central New York by Cisne *et al.* (1982), and southern Quebec (Mehrtens, 1988), includes karstified limestone horizons within the Black River Group (Bechtel and Mehrtens, 1995), clast composition evolution within fault breccias such as the Lacolle Formation (Mehrtens and Gleason, 1988), and condensed stratigraphic sequences, for example, Lower (?)-Middle Ordovician Providence Island Dolostone overlain by the Black River Group, with no intervening Chazy (Bechtel and Mehrtens, 1995). There is also biostratigraphic evidence for an unconformity between the Lower Ordovician part of the Beekmantown Group (Providence Island Dolostone) and basal Chazy (Speyer and Selleck, 1986). The Champlain Valley contains excellent exposures of the Cambro-Ordovician stratigraphic sequence (Welby, 1982) that include autochthonous Ordovician limestones, dolostones sandstones and shales which have been overridden by a series of major thrust faults. The Champlain Thrust, for example, has emplaced siliciclastic and carbonate rocks approximately 80 km westward onto authochthonous black shales (Stanley, 1987).

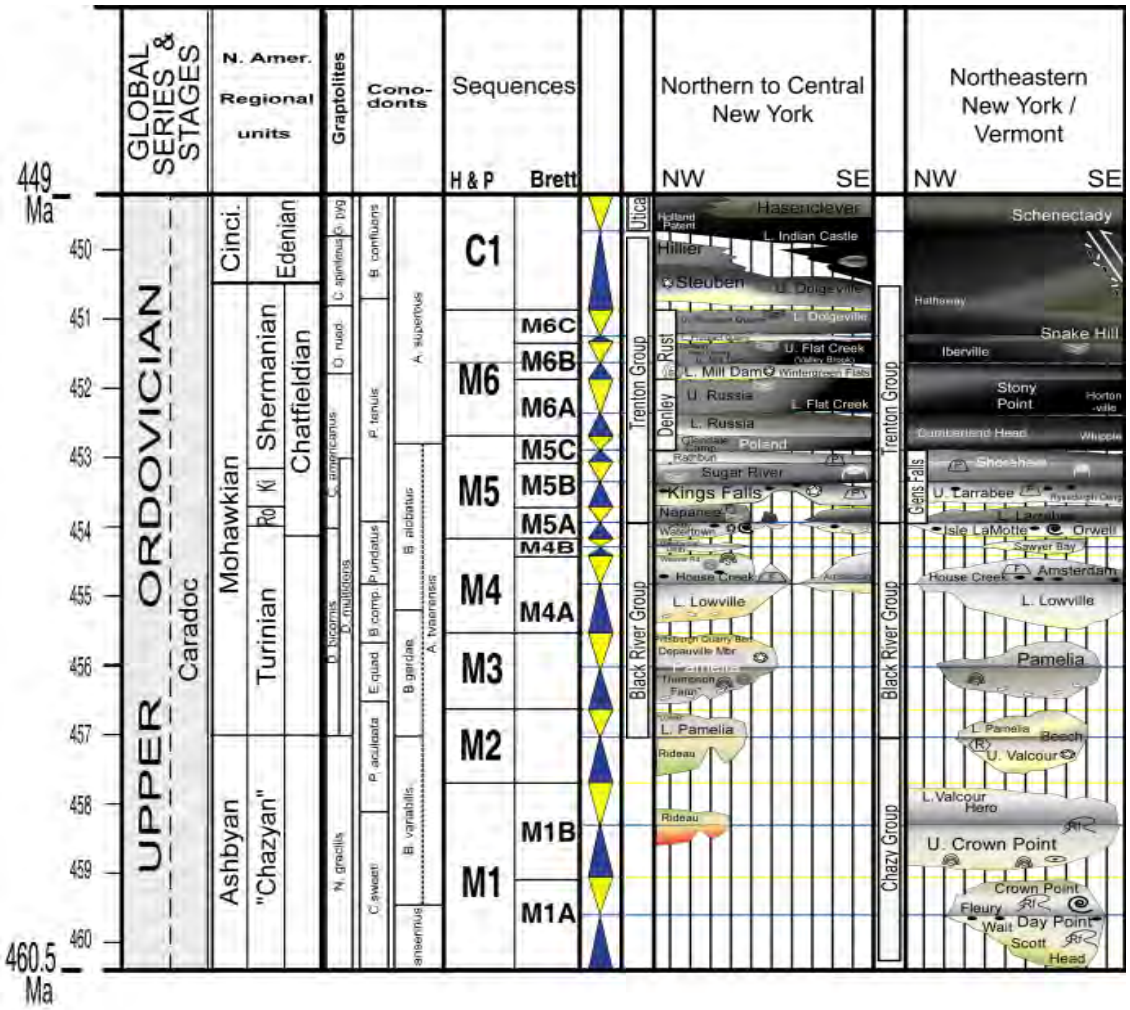

Figure 2. Regional sequence stratigraphy of the Upper Ordovician, northern New York State (from Cornell, 2008).

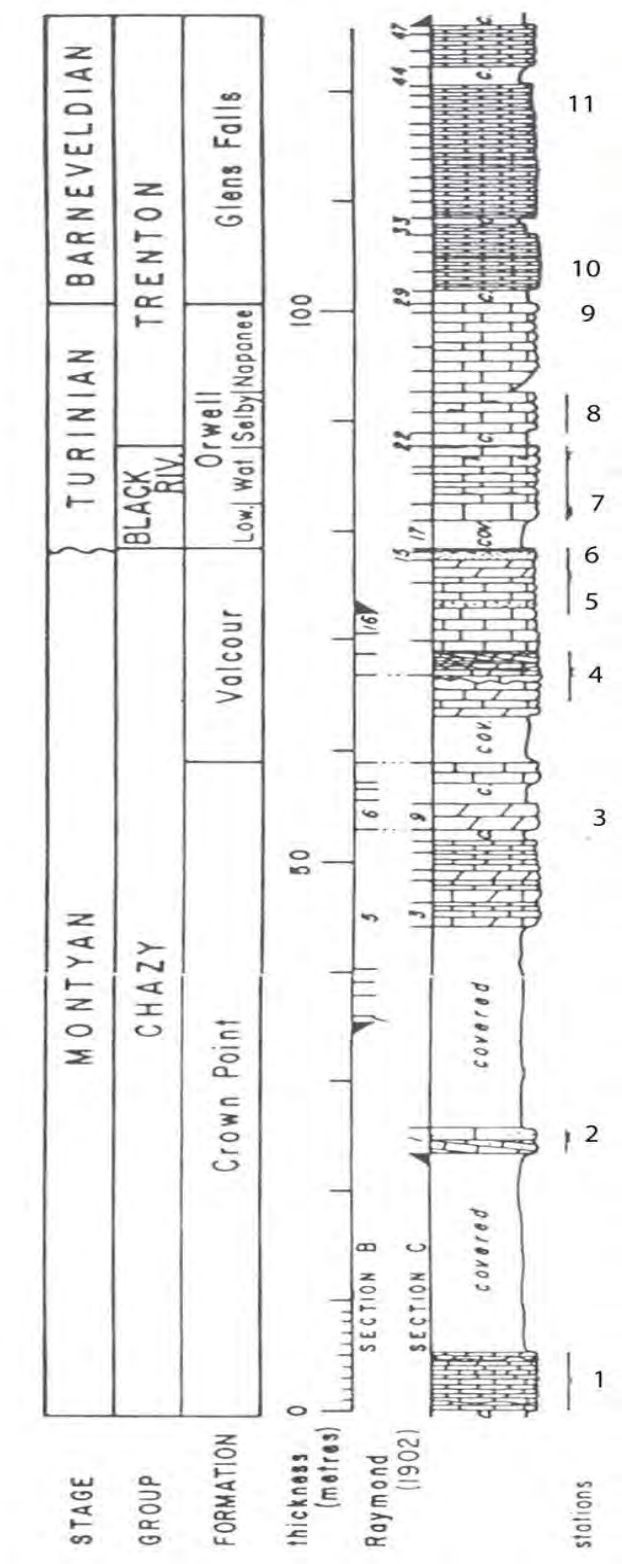

Figure 3. Stratigraphic column for the units visited during this field trip. Numbers refer to field trip stops. Modified from Baldwin and Harding (1993).

CHAZY GROUP

The stratigraphy of the Chazy Group in eastern New York and adjacent Vermont was described by Oxley and Kay (1959) and is summarized in Fisher (1968). Welby (1962) includes a summary of stratigraphic relationships between exposures in New York and Vermont and Hoffman (1963) presents the stratigraphy for the Middle Ordovician units in southern Quebec. Speyer and Selleck (1986), present regional correlations within the Chazy Group in the Champlain Valley.

The Chazy Group is Upper Ordovician (Chazyan Stage) in age (Figure 2). Based on conodonts (Harris, *et al*., 1995) the Chazy spans the upper half of the *Phragmodus polonicus* through *Ca. sweeti* zones (North Atlantic lower latitude province) or the base of the *Pygodus serra* through *Pygodus ans* Zones (North American cosmopolitan province). In terms of graptolites, the unit extends from the base of the *Diplograptus decoratus* to mid-*Nemagraptus. gracilis* zones.

The Chazy Group varies in thickness within the Champlain Valley from 250 meters in the north (Isle la Motte region) to 90 meters at Crown Point, to less than 15 meters at Ticonderoga and to zero at Whitehall (Oxley and Kay, 1959). In the type area in the northern Champlain Valley, the Chazy can be divided into three formations (Figure 2) as well as several members. Organic buildups (called variously biostromes, mounds, and reefs) occur in all three units, however the composition of the framebuilders varies stratigraphically; Pitcher (1964) summarizes the stratigraphic trends in faunal composition. Organic buildups are absent here at Crown Point, although they can be found across the lake and to the north, in Vermont. The nature of the basal contact of the Chazy Group with the underlying Lower Ordovician Beekmantown Group also varies within the Champlain Valley. In the south, basal Chazy horizons are in unconformable contact with tilted, eroded Beekmantown Group strata. In the northern Champlain Valley, basal Chazy horizons (the Scott Member of the Day Point Fm.) are in apparent conformable contact with the Providence Island dolostone of the Beekmantown Group (Speyer, 1982). The nature of the upper contact of the Chazy Group with the overlying Black River Group is lithologically abrupt, but evidence for significant erosion is generally absent (Bechtel and Mehrtens, 1995). This contact is covered at the Crown Point Historical Site.

The basal Chazy unit, the Day Point Formation, is not exposed at Crown Point and will not be seen on this field trip. Mehrtens and Cuffy (2003) described the depositional environments and reef succession in this unit. They documented the growth of bryo-mounds that typically attained one meter in height and which grew seaward of cross-bedded sand shoals. The mounds frequently exhibit internal zonation; early colonizing *Champlainopora chazyensis* often grows on brachiopod shells and are in turn encrusted by *Batostoma chazyensis*. Cycles of sea level are documented by recurring sand shoals as well as variation in upward and outward growth of the bryo-mounds.

The Crown Point and Valcour Formations will be examined on this field trip; in general both units consist of fossiliferous bioclastic wackestones, packstones and grainstones, with varying degrees of fabric-selective dolomitization. Shaley, nodular limestones are present in the stratigraphy, but are rarely exposed at the surface. Environments of deposition vary from subtidal, storm-dominated shelf settings to more nearshore sand shoals and tidal flats. Intervals of penecontemporaneous cementation and karstic erosion may mark intervals of subaerial exposure.

Cements within the Chazy Group at Crown Point typically consist of an early equant to prismatic low-Mg calcite followed by later coarse calcite spar. Dissolution and chert replacement of aragonite bioclasts is common. Dolomitization in the Crown Point limestones is widespread, and

is highly fabric selective in some facies. Variations in primary mineralogy (low-Mg calcite vs. aragonite) appears to have controlled the dolomitization of some bioclastic materials; grain size, sorting, porosity, intensity of borrowing and distribution of early cements (and thus permeability of materials during burial diagenesis) seem to best explain the highly variable patterns of dolomitization (Selleck, 1988).

BLACK RIVER GROUP

The Black River Group in the Champlain Valley is a relatively thin unit (25-30 meters) that consists of massively-bedded wackestones to packstones which represent deposition in lagoonal to shallow subtidal environments. The gradual deepening that characterizes this unit (and which continues into the overlying Trenton Group) is punctuated by cyclic sea level changes that occur on the macroscopic (meter) as well as microscopic (centimeter) scales, the latter visible only in thin section. The lithologic variation within this unit over its outcrop area of New York, Ontario, Quebec and Vermont has contributed to the proliferation of stratigraphic names, however the Pamelia, Lowville (House Creek and Sawyer Bay Members) and Chaumont Formations can be recognized in the Champlain Valley. Bechtel (1993) summarizes the evolution of nomenclature applied to this unit. Based on conodonts (Harris, *et al*., 1995), the Black River Group is Upper Ordovician (Mohawkian Series, Blackriverian Stage).

The lower contact of the Black River with the underlying Valcour Formation of the Chazy Group is covered at Crown Point, however the basal beds of coarse-grained subarkosic sandstones are exposed and will be visited on this field trip. This sandstone represents the accumulation of coarse siliciclastics that were derived from uplifted Proterozoic basement fault blocks, likely exposed in the nearby Adirondack Massif. Coarse, angular quartz and feldspar grains are common in the coarse facies of the upper Chazy Group and lower Black River group in the southern Champlain Valley. The upper contact of the Black River Group with the overlying Trenton Group at the Crown Point site is also within a covered interval.

Cement Stratigraphy of the Black River Group

There are multiple types of cements present within the Black River limestones which record a complex diagenetic history. The general cement stratigraphy pattern records early nonluminescent cement associated with precipitation in oxidizing waters of the shallow meteoric phreatic zone. With increasing reducing conditions, bright and dull luminescent cements represent precipitation under shallow burial conditions. Ferroan calcite with dull to nonluminescence represents precipitation in a late burial situation from high temperature burial fluids. Early marine Black River Group micritic cement is ferroan and very dull luminescence, representing deposition in a reducing, lagoonal environment. Subsequent cementation took place in the shallow meteoric phreatic zone, with nonluminscent cements with bright rims representing oxidizing conditions becoming slightly more reducing with burial. These observations are consistent with those of Mussman, *et al*. (1988) who interpreted such patterns to be related to a cratonward-dipping meteoric water lens beneath tidal flats. Tectonic uplift would lead to stagnation of the aquifer and increasingly reducing conditions. Within this general pattern, however, there are many variations in the Black River limestones which record frequent base level changes associated with sea level fluctuations and block fault movements in the Taconic foreland basin. These base level changes have produced numerous firmgrounds (at

all Black River localities in the Champlain Valley) as well as beachrock (at Arnold Bay, VT) and paleo-karst (at Arnold Bay, Chippen Point and Sawyer Bay, VT localities).

Fractures are common throughout the Black River and their cements also record evolving burial conditions. The cement stratigraphy of the fractures indicates that their formation occurred throughout the diagenetic history of the Black River Group, from early syndepositional events associated with karst and beachrock formation, through to deep burial under reducing conditions. Figures 4 and 5 illustrate some of the observed patterns. In the first thin section (Figure 4, following page) two cement events are visible in the fracture. The first consists of nonferroan scalenohedral crystals extending outward from the fracture wall. These are interpreted to have been precipitated in the meteoric phreatic zone. The later, large ferroan equant blocky crystals in the center of the fracture represent a late burial cement precipitated under reducing conditions.

In Figure 5 (following page), a photograph taken under cathodoluminescence, the zoning of rhombohedral crystals infilling a fracture can be seen. The very symmetrical zoned patterns starts (from the interior outward) with a nonluminescent nonferroan core, a dull rim, a bright orange rim, another dull rim, to another bright rim, and fading to nonluminescent outer rims. The nonferroan to ferroan zonation is indicative of increasing reducing conditions during cementation. The cement stratigraphy of the fractures indicates that their formation occurred throughout the diagenetic history of the Black River Group, from early syndepositional events associated with karst and beachrock formation, through to deep burial.

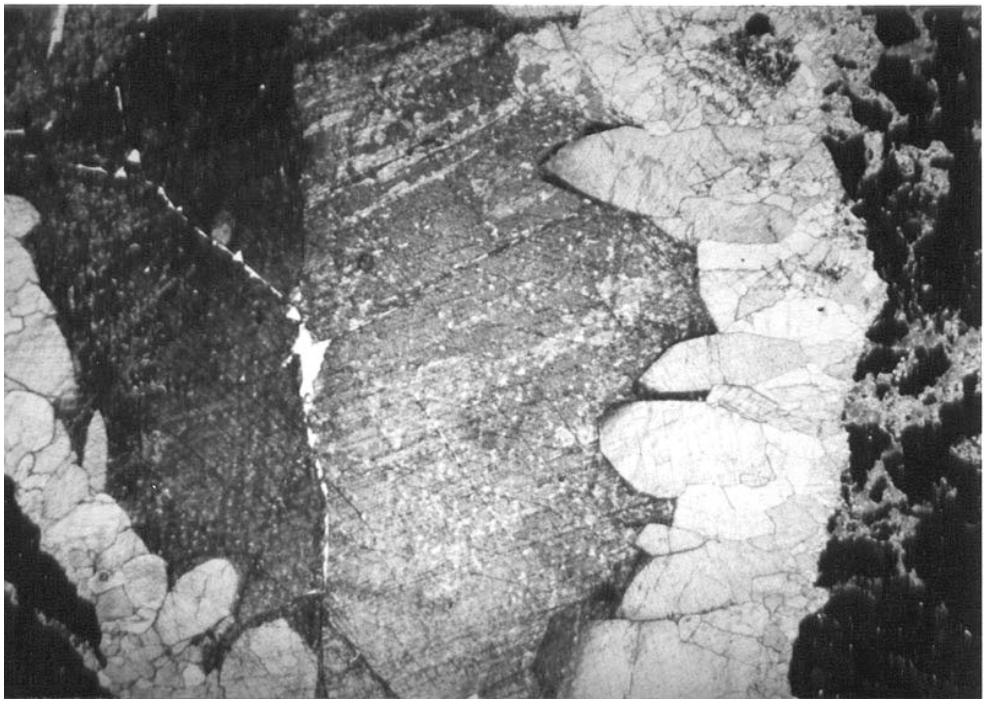

Figure 4. Two generations of fracture cement; field of view is 1.8cm

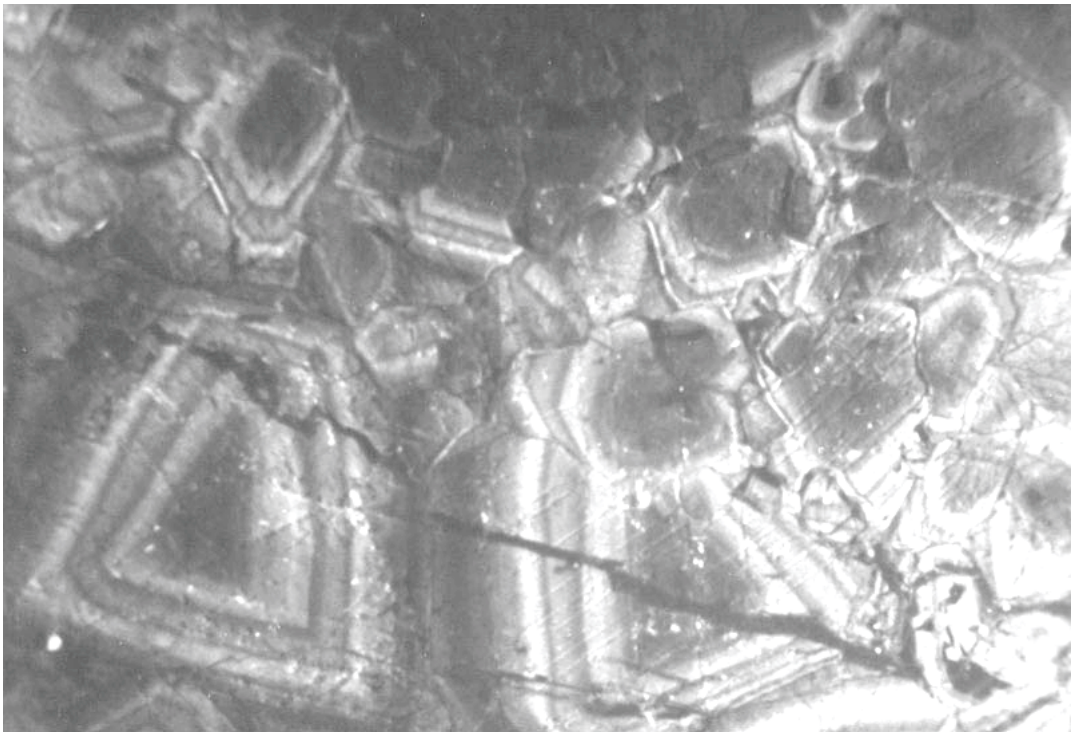

Figure 5. Cathodoluminescent photograph of fracture cements (field of view 0.5mm)

TRENTON GROUP

The contact between the Glens Falls Limestone (Trenton Group) and the Black River Group is covered at most localities in the Champlain Valley, including here at the Crown Point Historical Site. At Arnold Bay, to the northeast of the Crown Point site, the contact is exposed and is interpreted to be a disconformity; the dark gray colored, massively bedded Black River is in sharp contact with the nodular-bedded, laterally discontinuous beds of the Trenton. MacLean (1987) measured the Trenton Group around the Champlain Valley and found that here at Crown Point only 9 meters are exposed (but more may be covered by lakeshore muds) whereas a few miles to the north, at Button Bay it is more than 15 meters thick. The Button Bay exposure is significant because it is the only place where both the lower upper and contacts, with the Black River and Cumberland Head Argillite, respectively, are seen. Bechtel (1993) summarizes the variable nature of the Black River/Trenton contact around the Champlain Valley, New York and Ontario, and he notes that the regional variation in the nature of this contact, as well as the thickness variation along strike, would be expected in a foreland basin actively undergoing syndepositional block faulting.

MacLean (1986) identified seven lithofacies in the Glens Falls Formation, recognized by variations in lithology, bedding style, sedimentary structures and biota. The shallowest bathymetry is represented by a lithofacies consisting of grainstones composed of peloids and oncoids exhibiting pinch and swell bedding, graded bedding and cross laminations, which suggest wave reworking within fair-weather wave base (Figure 5, following page; arrow points to hummocky cross laminae in the grainstone). At the other bathymetric extreme are bioturbated (*Teichinchnus* and *Chondrites*) mudstones interbedded with shale and distal

tempestites/turbidites composed of wackstone/packstone to mudstone couplets (Figure 6, following page). MacLean also recognized a bryozoan-rich wackstone/packstone lithofacies (his Facies F) that is characterized by abundant *Stictopora* and *Eridotrypa* that form dense thickets or lens-shaped patches on the muddy sea floor. In addition to these ramose bryozoa, this lithofaces contains trilobite, gastropod and brachiopod remains; algae are notable absent. These bryozoan thickets are interpreted to have accumulated on the shelf near fair-weather wave base. Although the absence of algae suggests bathymetry below the photic zone, the abundance of interbedded shale suggests that turbidity may have reduced sunlight infiltration.

Using occurrences of *Cryptolithus* and *Prasopora* for correlation, MacLean documented that the Glens Falls stratigraphy in the northern Champlain Valley differed from that in the south; the transition from shallow water (inner ramp) to deep water (outer ramp) is abrupt in the Champlain Islands whereas in the south (including Crown Point) bathymetric change is hard to discern and more cyclic.

The Glens Falls stratigraphy visible at Crown Point is very representative of the bulk of this unit in the southern Champlain Valley, dominated by grainstone to wackestone/mudstone couplets in laterally discontinuous beds (MacLean's Facies C). Grainstone beds are commonly laminated and exhibit fine-tail grading (Figure 7). Thin shale seams separate beds. *Chondrites* and *Helminthropsis* are the dominant ichnofauna. Rare bedding planes exhibit a bedding plane fauna of bryozoa (*Prasopora*, *Stictopora*) and trilobite fragments. Moving up section at Crown Point the hummocky bedding style of the base of the section is replaced by more laterally continuous grainstone beds with sharp, planar bases that grade upwards into bioturbated wackestones/mudstones (MacLean's Facies E). These horizons are interpreted to be bioclastic turbidites.

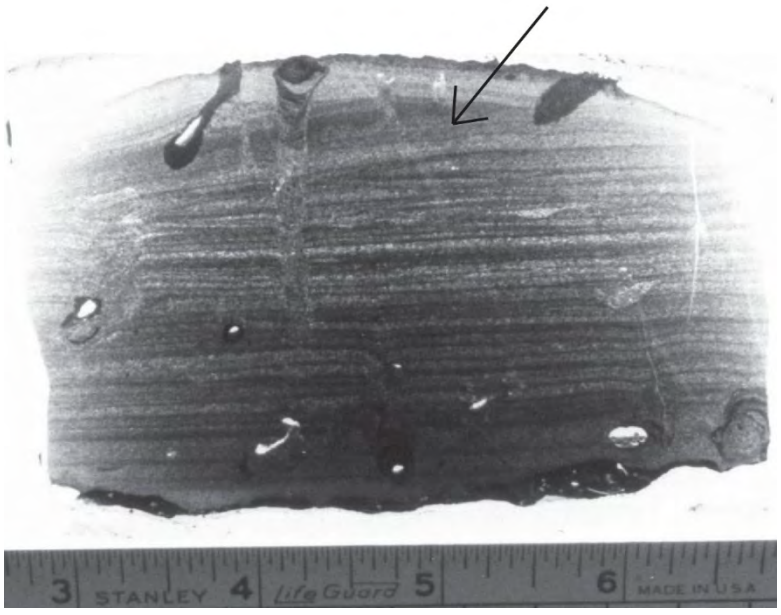

Figure 6. Large thin section (tape for scale) of cross lamination in a Glens Falls Fm. grainstone.

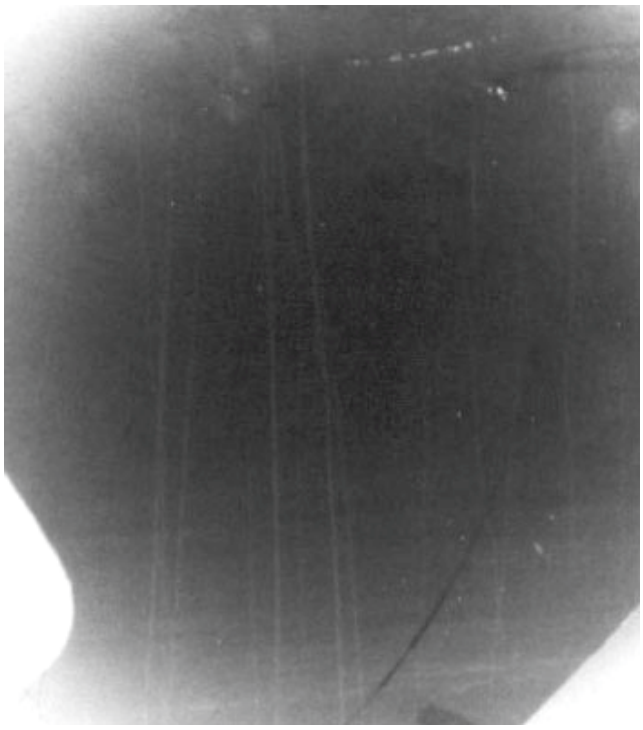

Figure 7. Large thin section (12 cm long) of the outer ramp lithofacies of the Glens Falls Fm.

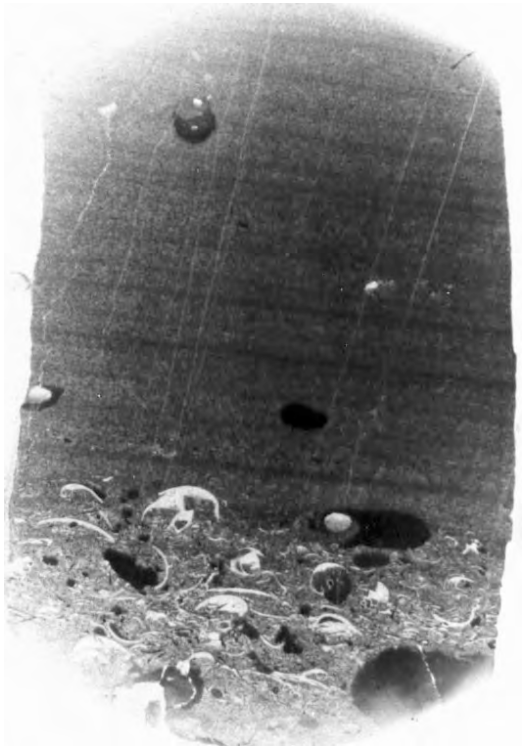

Figure 8. Large thin section (18 cm in length) of graded bed in the Glens Falls Fm.

FIELD TRIP LOG

All the stops for this field trip are within the Crown Point Reservation Historical Site. From the west, take NY Route 22 north from Ticonderoga, continuing north through the village of Crown Point. Turn east onto Route 185 approximately five miles north of the village, following signs to the "Bridge to Vermont." From the north, proceed south on Route 9N through the village of Port Henry. Turn east onto Route 185. The Crown Point site is immediately before the bridge crossing. From the east, take VT Route 22A north from Fairhaven, or south from Burlington, and follow signs to "Bridge to New York." The Crown Point site is immediately over the bridge crossing. Parking is available on the roadside approximately 100 meters south of stop 1. Alternatively, vehicles may be parked within the state historic site, at the picnic pavilion. The

Stop locations are keyed to Figures 1 and 3.

The Crown Point Reservation Historical Site is a no hammer, no collecting outcrop.

Stop 1 – the Redoubt

Approximately 6 meters of burrowed, slightly dolomitic, thin to medium bedded bioclastic packstone and grainstone is exposed at this stop. Some beds are relatively well-sorted grainstones with sharp bases which are interpreted as tempestites. The same interpretation is made for the grainstone intraclast-rich bed visible in the low ledge at the southeast corner of the ditch. Approximately 3 meters above the base of the section abundant *Girvanella* algal oncolites are common allochems. Nuclei of fossil fragments are visible within some oncolites. In other beds fossils are relative abundant, and are best seen on slightly weathered bedding surfaces. Trilobite fragments, brachiopods, bryozoans, pelmatozoan fragments, nautiloids and large *Maclurites magnus* are present (exterior shells and opercula). Dolomite occurs in along shaley seams and in burrow fill.

The relatively high faunal diversity, general bioturbation, and storm-related sedimentation all point to a low energy shallow subtidal environment at depths slightly below fair-weather wave base. The abundant algal oncolites and discrete calcareous algal fossils (e.g., *Hedstromia spp*.) suggest depths well within the photic zone. A possible modern analogue is found in the mixed mud and sand shelf to the west of the emergent tidal flats of Andros Island, Bahamas, as described by Purdy (1963).

We interpret the wavy, irregular dolomite laminae as the result of dolomitization of lime mud, followed by compaction and pressure solution of calcite that produced irregular clay and dolomite-rich stylocumulate seams. Preferential dolomitization of burrows is due to contrasts in permeability of burrow-fill versus burrow-matrix sediment. The burrow-fill material retained permeability longer during diagenesis and allowed more pervasive dolomitization. In similar facies exposed on Bullwagga Bay (the west shore of the Crown Point Peninsula), modular limestone with shaley dolostone seams and stringers are present. The limestone nodules appear to have been cemented prior to significant burial compaction, whereas the shaley dolostone material was compacted around the cemented limestone. The early-cement limestones were resistant to dolomitization. This sort of fabric selective dolomitization is common in the Chazy and Black River Groups throughout the Champlain Valley.

Figure 9. Bioclastic, oncolitic packstone with shaley, dolomitic stylocumulate laminae, Crown Point Formation, in the Redoubt section (Stop 1).

Stop 2 – Ridge of outcrop running NE from entrance gate to highway

WARNING: poison ivy is common along this ledge

Cross-stratified coarse bioclastic grainstones are well-exposed near the main gate along the entrance road and adjacent ridge. Nearly three meters of section form a prominent belt parallel to strike, extending from the entrance road to the main highway. Foreset cross-strata show bipolar dip directions. Angular quartz and feldspar grains are concentrated in some laminae, and along stylolites (Figure 10). The carbonate particles are dominantly sub-rounded abraded pelmatozoan plates with gastropod and brachiopod fragments. Large *Maclurites* fragments and grainstone intraclasts are present on the upper bedding surfaces of these ledges.

We propose that the environment of deposition of this facies was a shallow subtidal wave and current reworked bioclastic sand shoal. Active transport of abraded grains may have been accomplished by tidal currents (as suggested by the bi-directional cross-strata) or by storm-generated currents that produced complex, anastomosing patterns of cross-strata and intervening reactivation surfaces. The lack of burrowing and well-preserved whole-shell body fossils may be due to the inhospitable shifting sand substrate. A modern analogue for this environment would be the unstable sand shoals of the Bahamas Platform (Ball, 1967), as the

scale and style of cross stratification are similar. Oxley and Kay (1959) report that similar strata in the northern Lake Champlain Valley are oolitic.

Figure 10. Coarse bioclastic grainstone with quartz and feldspar sand.

Stop 3 – low ledges adjacent to the entrance road (Picnic Pavilion ridge), approximately 50 meters north of Stop 2

Brown-weathering, slightly shaley dolostone exposed here contains lenses and stringers of fossiliferous lime packstone and wackestone. The fauna is similar to that at Stop 1, with trilobites, small brachiopods and *Maclurites* common. The environment of deposition is assumed to be similar to that of Stop 1, however lacking evidence of storm activity. Note that some of the fossils are almost entirely encased in dolomite, which is assumed to be of replacement origin here.

Stop 4 – SE moat of Fort Crown Point

Approximately 3 meters of thickly laminated limestone and dolostone of the Valcour Formation are exposed in the southeast moat of the British Fort. The dominant facies here is alternating 0.5-2.0 cm thick laminae of limestone and dolostone, we term “ribbon rock.” The limestone ribbons are very fine-grained peloid grainstones or “calcisiltites” and appear blue-grey color on slightly weathered surfaces, and as indentations on more deeply weathered surfaces. The

dolostone ribbons weather tan-brown in color, and consist of an interlocking mosaic of 20-300 micron dolomite crystals of replacement origin. Quartz silt grains are present in the dolostone ribbons, versus medium to fine-grained quartz sand in the limestone ribbons, suggesting the limestone horizons were slightly coarser-grained than the dolostone when deposited.

An erosional surface with 10 to 20 cm of relief is exposed near the base of the south wall of the moat (Figure 11). Similar erosional surfaces occur within this facies in other Chazy exposures in the Champlain Valley. We interpret these to represent micro-karstic solution surfaces on a tidal rock platform that developed during subaerial exposure of cemented limestone. Typically, the rock below the surface is mostly calcite limestone, suggesting that cementation and diagenetic stabilization of the limestone occurred prior to development of the erosional surfaces. Overlying rock horizons contain more dolomite. *Maclurites* shell hash can be found in pockets on the erosional surface. Dolomitized burrows cut across the limestone ribbons in some parts of the outcrop. Trough cross-strata filling low scour surfaces are also visible.

Figure 11. South wall of moat, with multiple sharp erosional surfaces in differentially-weathering "ribbon rock." Rod is ~1 meter.

On the less weathered prominence on the SE corner of the moat, shallow scours containing brachiopod and gastropod debris can be seen. Intraclasts or pseudoclasts of limestone in dolostone are also present. Some "clasts" appear to be cored by dolomitized burrows.

We interpret the stratigraphy seen at this stop as representing a tidal flat to shallow subtidal facies. The alternating limestone/dolostone ribbon rock represents rhythms of slightly coarser-grained (limestone) and finer-grained (dolostone) sediment deposited on the lower reaches of a

tidal flat, similar to the rhythmic bedding described by Reineck and Singh (1980) from the mud/sand tidal flats of the North Sea. These coarse-fine alternations might also reflect storm-related, ebb-surge deposition (Nelson, 1980). Early cementation of the slightly coarser-grained limestone ribbons made this lithology less susceptible to dolomitization, which affected the finer-grained muddy ribbons that became dolomitized. Variations in the intensity of burrowing is interpreted to reflect subtle differences in duration of subaerial exposure of the tidal flat and/or the extent of reworking by tidal currents. Limited *in situ* faunal diversity is to be expected in the tidal flat setting, where organisms are stressed by salinity fluctuations. The absence of mudcracks or evidence of evaporite minerals may indicate that only the lower portion of a humid climate tidal flat system is preserved here.

Stop 5- Parade Grounds near barracks:

As we enter the parade ground from the southwest corner of the moat, note the array of carbonate rocks used in construction of the barracks walls. Chazy, Black River and (rarely) Trenton lithologies can be identified. Restoration of the barracks began in 1916 and in 1976 the New York State Division for Historic Preservation undertook protection and stabilization of the ruins.

The low rock pavement just north of the barracks is within the upper part of the "ribbon rock" unit seen at Stop 4. Immediately up-section, cross-stratified grainstone beds are exposed. Coarse-grained quartz and feldspar sand is easily seen on weathered surfaces. Trough cross-strata and herringbone co-sets of planar-tabular cross-strata are visible on the vertical surfaces. Large, angular clasts of slightly dolomitic grainstone and *Maclurites* are present on bedding surfaces. We interpret this facies as representing a current-dominated sand shoal environment, similar to that seen at Stop 2.

Stop 6- West Parade Grounds

Bechtel and Mehrtens (1993) suggested that the sandstone unit in the westernmost parade ground is the basal sandstone of the Black River Group, an interpretation which differs from that of Speyer and Selleck (1988), who suggested that this unit was part of the underlying Chazy Group. In thin section this sandstone is a quartz-rich sandstone, very poorly sorted, and containing fewer lithic fragments and phosphatic fragments than stratigraphically lower Chazy sandstones. Visible at the very easternmost portion of this ridge is a buff-colored dolostone bed containing pockets of quartz sand (burrow infills?). These basal sandstone and dolostone lithologies are very similar to those described by Walker (1972) in his description of the Pamelia Formation at its type locality in north-central New York. Alternatively, placement of the sandstone unit within the Chazy Group is consistent with the common presence of coarse-grained quartz and feldspar sand within the Chazy at the Crown Point Preserve, whereas the siliciclastic material in the Black River Group at Crown Point is mainly silt and clay. Whatever the stratigraphic placement of the sandstones and dolostones here, it marks an interval when sands were transported from a nearby source area to this possible peri-tidal setting. This interval was followed by marine reworking of the sand and deposition of fine-grained limestone of the basal Black River Group.

Stop 7 – Northeastern moat

WARNING: poison ivy is common along the base of this exposure

There is approximately one meter of covered interval between Stop 6 in the parade grounds and Stop 7 in the northeastern moat. Along this wall are exposed several meters of the lower Black River Group (Lowville Formation, House Creek Member) which in Vermont is termed the Orwell Limestone. At the base of this exposure a series of stylolitized gastropod-bearing (*Liospira*) wackestone beds are overlain by thicker beds of *Phytopsis*-burrowed aphanitic mudstones. This sequence can be interpreted as a shallowing-up cycle (SUC) consisting of subtidal overlain by peritidal lagoonal muds. Examine the sharp contact of the aphanitic mudstone with the overlying wackestones, a contact which in thin section appears to be a firmground (Bechtel, 1993). These SUCs also comprise the base of the Black River Group at other localities in the Champlain Valley. There are three motifs of repetitious bedding that occur in the Black River Group and the cycles seen here at the base are the the thickest, occurring at a macroscopic scale, interpreted to represent 4th order (10,000 to 100,000 years) or smaller cycles. Examination of *Phytopsis* burrows in thin section (Figure 12) reveals that many are filled with graded (fining-up) geopedal silt, evidence of cementation in the meteoric vadose zone.

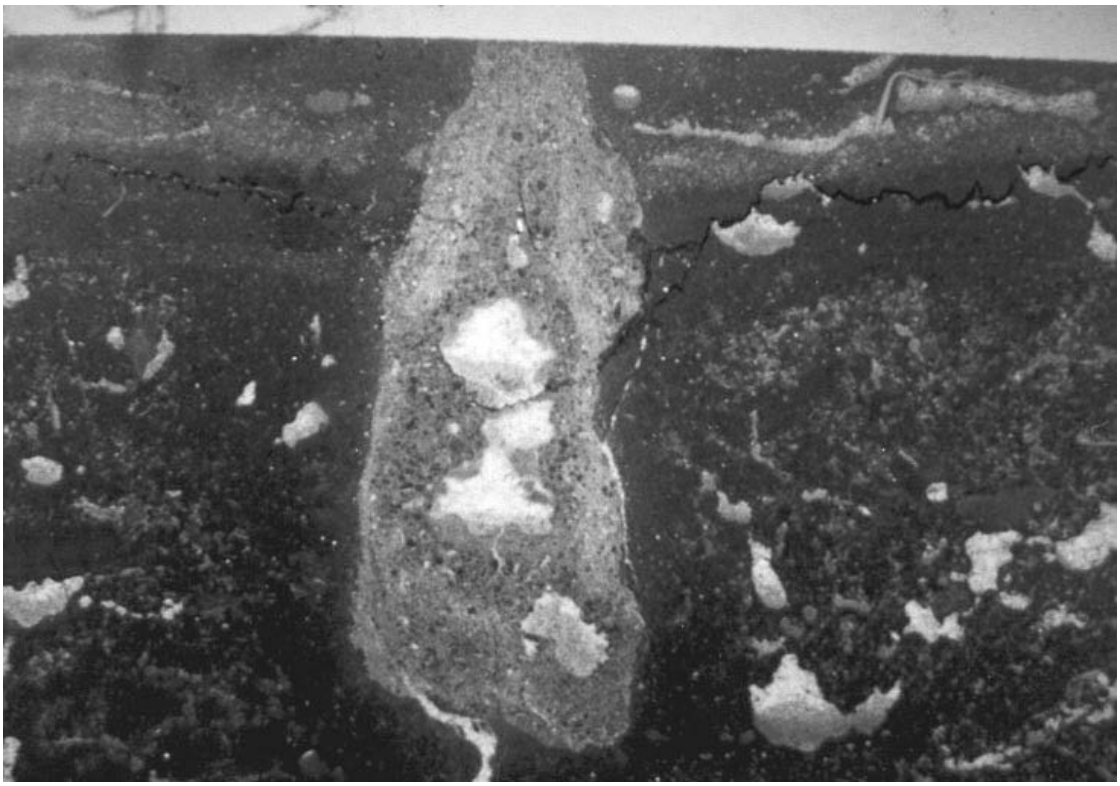

Figure 12. Thin section photomicrograph of burrow fill. Field of view 2.4cm

Continuing up section, several thick packstone beds are exposed. More detailed examination of these beds reveals that they consist of alternating one to six centimeter thick intraclast and oncolite-rich packstone horizons interpreted as tempestites, interbedded with fossiliferous wackestone/packstone horizons. The tempestites consist of graded and crudely imbricated

intraclasts and skeletal fragments. Note the nature of the upper and lower contacts of these horizons. The second common bedding motif in the Black River Group are these tempestite horizons interbedded with *in situ* fossiliferous muds.

The uppermost third of the outcrop appears to be a massive bed of limestone, however closer examination also reveals small scale cycles of alternating wackestone/packstone and grainstone, the third motif of bedding in the Black River strata. These cycles are characterized by a base of thinly laminated or cross laminated grainstone horizons 0.5 to 1 cm thick, overlain by fossiliferous wackestones and packstones. In thin section the bases of the grainstones can be identified as firmgrounds, recognizable by the truncations of allochems and cements present in the underlying mud (Figure 13).

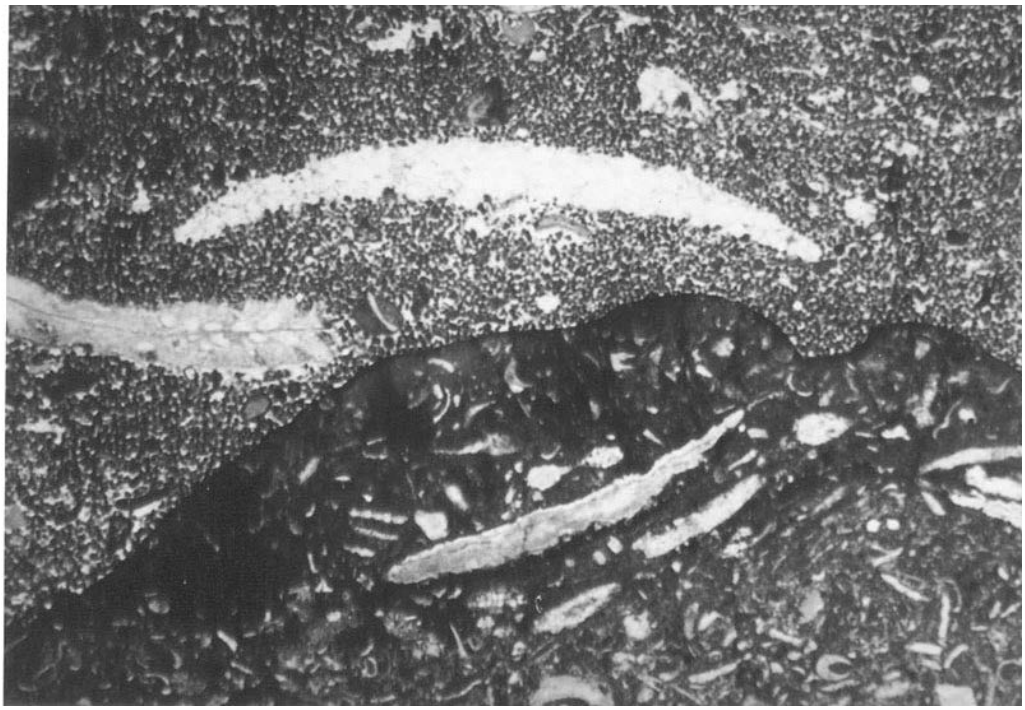

Figure 13. Thin section photomicrograph of a firmground; field of view is 1.5cm

The very top of this exposure (best seen at the next stop) exhibits a burrow mottled fabric with selected dolomitization of many burrows. *Tetradium* occurs in life position in these horizons.

Stop 8 – east-west ridge across the service road

A black chert layer near the top of Stop 7 provides the correlation to Stop 8, the outcrop across the service road. The limestone beds on this ridge commonly consist of alternating wackestone/packstone and planar to cross laminated grainstone beds, as seen at Stop 7, however bedding plane exposures permit identification of many fossils in these, the most faunally diverse beds in the Black River Group. Specimens of gastropods (*Liospira*, *Lophospira, Hormotoma*), *Lambeophyllum, Tetradium*, stromatoporoids, the bivalve *Cyrtodonta*, the brachiopod *Stromphomena sp*. and cephalopods are recognizable. This ridge exposure is most notable for its bedding plane exposures of *Tetradium* and *Lambeophyllum.* It is interpreted as

representing a wave baffle margin lithofacies similar to that described by Walker (1972) at the Black River type section.

A prominent reentrant in the exposure along the path to the north marks a volcanic ash horizon, or K-bentonite (Figure 14). This interval is currently under study, but likely represents the "M/H" bentonite (Brett and Cornell, 2000) that falls within the M4A (upper Lowville Formation) sequence. This prominent ash layer is traceable from the Roaring Brook section in the Black River Valley through outcrop and core in the Mohawk Valley and normal-fault bounded Wells outlier within the south-central Adirondack Massif.

A third cycle motif present in this interval, laminated grainstone overlain by bioturbated wackestone, is interpreted to represent smaller scale 4th order cycles, which could be the result of facies mosaicing and/or small scale base level changes.

There are at least two distinct types of chert occurrences in the Black River Group. One, the infilling of horizontal burrows, is fabric selective. Chert also occurs less frequently as broad bedding plane parallel sheets. The uppermost chert horizon on this ridge, traceable down to the shoreline, is of this latter variety. Clearly, there was a significant source of silica available for chert formation, perhaps a combination of silica derived from sponges (*Tetradium*?) and bentonite alteration. In thin section the chert cross cuts all previous cements, including late fracture-filling calcite, and it is therefore the youngest form of diagenesis present in these rocks.

Figure 14. K-bentonite forms reentrant in Lowville Formation at Stop 8. Rod is 1.5 meters.

Stop 9 – Quarry to the north

WARNING: be extremely careful around the quarry as the thick algal scum in the quarry water obscures where the grass ends and the quarry wall drops off.

The older weathered south walls of the quarry show, by color differentiation, two cycles. There are 3 to 4 cm thick beds of planar laminated skeletal and peloidal hash overlain by burrowed wackestones overlain by intraclast-rich horizons. These cycles represent our third motif of Black River bedding. Interbedded with these cycles are tempestite couplets of mudstone/wackestone and fossil hash layers in which brachiopod-rich layers are abundant. The abundant quarried blocks lying about provide the opportunity to look for cycles, and from these, topping directions.

Stop 10 – shoreline of eastern Bulwaga Bay

The uppermost horizons in the quarry can be traced down to the shoreline to the north where the uppermost Black River strata can be seen (Chaumont Formation). Shoreline bedding planes exhibit horizontal traces of *Chondrites* and opercula of *Maclurites.* There is a thin covered interval of approximately one meter to the basal beds of the Glens Falls Limestone of the Trenton Group. The Glens Falls is characterized by thin beds of nodular to wavy bedded wackestones, mudstones and rare grainstones. Bedding planes along the shoreline contain mostly *Chondrites* and *Helmenthopsis* burrows, however as one moves up section, recognizable fragments of *Cryptolithus*, *Isotelus*, orthid brachiopods, *Stictopora*, and *Prasopora simulatrix* can be found; the latter is important because it permits the correlation of the lower Glens Falls here in the Champlain Valley to the lower Denley Limestone at the Trenton type section in central New York (Mehrtens and Barnett, 1979).

MacLean (1986) interpreted the lithofacies of the basal Glens Falls visible here to represent sedimentation in a shallow subtidal environment periodically influenced by storm activity. In thin section the nodular and wavy bedded wackestones appear thoroughly bioturbated, a process which would influence and enhance subsequent differential compaction. Grainstone beds exhibit more planar bases with basal skeletal fragment lags or finely crushed debris of brachiopod, trilobite and crinoidal material and capped by carbonate mud. MacLean interpreted these as tempestite deposits. Moving further up section (in horizons not seen at Crown Point) the Glens Falls records progressively deepening conditions from the subtidal, storm influenced conditions seen here to bioclastic turbidites separated by authochthonous shale horizons. For those familiar with the lower Trenton Group localities in central New York State (ex., Rathbun Brook, City Brook, Inghams Mills), the paucity of fossiliferous bedding planes here at Crown Point is noteworthy. The overall fine grain size and ichnofauna suggest that bathymetry increased significantly and rapidly from the Black River into the Glens Falls, a transition that might reflect not only rising sea level but base level changes as well. The sedimentologic and faunal transitions from the Glens Falls to the overlying Cumberland Head Argillite and the Stony Point Shale are much more gradational than that of the Black River/Glens Falls contact.

REFERENCES CITED

Baldwin, B. and L. Harding, 1993, Depositional environments in the Mid-Ordovician section at Crown Point, New York. Vermont Geol. Soc. Field Trip vol. 7, pp.29-42.

Ball, M.M., 1967, Carbonate sand bodies of Florida and the Bahamas. Jour. Sed. Pet. vol. 37, pp 556-591.

Bechtel, S.C., 1993, Stratigraphy, sedimentology and cement diagenesis of the Black River Group in the Champlain Basin, Vermont. unpubl. M.S. Thesis, University of Vermont, 230pp.

Bechtel, S.C. and C.J. Mehrtens, 1995, Stratigraphy and sedimentology of the Black River Group, NY & VT. Northeastern Geology, vol. 17, pp. 95-111.

Bradley, D. C, and T.M. Kusky, 1986, Geologic evidence for rate of plate convergence during the Taconic arc-continent collision. Jour. Geology, vol.94, no.5, pp.667-681

Brett, C.E., McLaughlin, P.I., Cornell, S.R., & Baird, G.C., 2004, Comparative sequence stratigraphy of two classic Upper Ordovician successions, Trenton Shelf (New York–Ontario) and Lexington Platform (Kentucky–Ohio): implications for eustasy and local tectonism in eastern Laurentia, Palaeogeography, Palaeoclimatology, Palaeoecology, vol. 210, pp. 295-329.

Cisne, J. L.,D.E. Karig,B.D. Rabe, B.J. Hay, 1982, Topography and tectonics of the Taconic outer trench slope as revealed through gradient analysis of fossil assemblages. Lethaia, vol.15, no.3, pp.229-246.

Cornell, S.R., 2005, Stratigraphy of the Upper Ordovician Black River and Trenton Group Boundary Interval in the Mohawk and Black River Valleys, Geological Society of American Northeast Section Field Trip Guidebook, Saratoga Springs, New York, pp. C1-C23.

Cornell, S. R., 2008, The Last Stand of the Great American Carbonate Bank: Tectonic Activation of the Upper Ordovician Passive Margin in Eastern North America; unpub. PHD Thesis, University of Cincinnati, Cincinnati, OH

Cornell, S. R. and Brett, C.E., 2000, K-Bentonite and Sequence Correlations of Upper Black River and Lower Trenton Limestones from Lake Simcoe, Southern Ontario Canada to Watertown, Northern New York State; Eastern Section AAPG Meeting, London, Ontario, Canada

Fisher, D., 1968, Geology of the Plattsburgh and Rouses Point, New York-Vermont Quadrangles, NY State Mus. and Science Serv. Map and Chart Series no. 10, 51pp.

Harris, A., J. Dumoulin, J. Repetski, and C. Carter, 1995, Correlation of Ordovician rocks on Northern Alaska, *in*, Ordovician Odyssey [International Symposium on the Ordovician system, 7th, Las Vegas] (Pacific Section SEPM/Society for Sedimentary Geology, Book/Publication 77), p. 21-26

Hoffman, H., 1963, Ordovician Chazy Group in southern Quebec. Am. Assoc. Petrol Geol. Bull. vol. 47, pp 270-301.

Jacobi, R.D., 1981, Peripheral bulge; a causal mechanism for the Lower/Middle Ordovician unconformity along the western margin of the Northern Appalachians. Earth and Planetary Sci. Letters, vol.56, pp.245-251

MacLean, D., (1986) Depositional Environments and Stratigraphic Relationships of the Glens Falls Limestone, Champlain Valley, Vermont and New York, unpub M.S. Thesis, University of Vermont, 169pp.

Mehrtens, C.J., 1988, Comparison of foreland basin sequences: the Trenton group in southern Quebec and central New York, *in* Keith, B., ed. The Trenton Group (Upper Ordovician Series) of Eastern North America. Deposition, Diagenesis and Petroleum. Am. Assoc. Petrol. Geol. Studies in Geol no. 29, pp. 139-159

Mehrtens, C.J. and S.G. Barnett, 1979, Evolutionary change in the Bryozoan genus Prasopora as a tool for correlating within the Trenton Group (Mid. Ord.), Geol. Soc.Am. Abstr. With Prog., vol. 11, pp.44

Mehrtens, C.J. and R. Cuffey, 2003, Paleoecology of the Day Point Formation (Lower Chazy Group, Middle-Upper Ordovician) and its bryozoan reef mounds, Northwest Vermont and Adjacent New York. Northeastern Geology, vol. 25, p. 313-329.

Mehrtens, C.J. and A. Gleason, 1988, The Lacolle Formation (Middle Ordovician): evidence of syn-depositional block faulting in the Taconic foreland basin. Northeastern Geol. vol. 10, pp. 259-270

Musman, W., I. Monanez, and J.F. Read, 1988, Ordovician Knox paleokarst unconformity, Appalachians, *in*, Paleokarst, N. James, editor, Springer-Verlag, NY, pp 211-228.

Nelson, C. H., 1982, Modern shallow-water graded sand layers from storm surges, Bering Shelf: A mimic of Bouma sequences and turbidite systems. Jour. Sed Pet.,vol. 52, pp 537-545.

Oxley, P. and G.M. Kay, 1959, Ordovician Chazyan Series of the Champlain Valley, New York and Vermont, Am. Assoc. Petrol. Geol. Bull. vol. 43, pp 817-853

Pitcher, M., 1964, Evolution of Chazyan (Ordovician) reefs of eastern United States and Canada. Can. Bull. Petrol. Geol., vol. 12, pp. 632-691.

Purdy, E. 1963, Recent calcium carbonate facies of the Great Bahamas Bank II-Sedimentary Facies. Jour. Geology, vol. 71, pp. 472-497.

Reineck, H. and I. Singh, 1980, Depositional Sedimentary Environments, Springer-Verlag, N.Y. 561pp.

Roscoe, M.S., 1973, Conodont biostratigraphy and facies relationships of the Lower Middle Ordovician strata in the Upper Lake Champlain Valley. Master's thesis, Ohio State University, 125pp.

Rowley, D.B. and W.S. Kidd, 1981, Stratigraphic relationships and detrital composition of the medial Ordovician flysch of western New England; implications for the tectonic evolution of the Taconic Orogeny. Jour. Geol., vol.89, no.2, pp.199-218

Ryan, P.C., R. Coish, and J., Kristiaan (2007), Ordovician K-Bentonites in western Vermont: mineralogic, stratigraphic and geochemical evidence for their occurrence and tectonic significance, Geological Society of America Abstracts with Programs, v. 39, n. 1, p. 50.

Selleck, B., 1988. Limestone/dolostone fabrics in the Chazy Group (early medial Ordovician) of New York and Vermont, Geol. Soc. Am. Abst. with Prog., vol. 20, no. 1, p.69

Speyer, S., 1982, Paleoenvironmental history of the Lower Ordovician-Middle Ordovician boundary in the Lake Champlain Basin, Vermont and New York, Geol. Soc. Am. Abstr. with Progr. Vol. 14, no. 1, p. 54.

Speyer, S. and B. Selleck, 1986, Stratigraphy and sedimentology of the Chazy Group (Middle Ordovician), Lake Champlain Valley, New York State Mus. Bull. no. 462, pp. 135-147.

Stanley, R.S., 1987, The Champlain Thrust Fault, Lone Rock Point, Burlington, Vermont. Geol. Soc. Am. Centennial Field Guide, Northeastern Section, vol. 5, pp.225-228.

Stanley, R. and N.M. Ratcliff, 1985, Tectonic synthesis of the Taconic orogeny in western New England. Geol. Soc. Am. Bull. vol. 96, pp/1227-1250.

Walker, K., 1972, community ecology of the Middle Ordovician Black River Group of New York State. Geol. Soc. America. Bull, vol. 83, pp.2499-2524.

Welby, C., 1962, Paleontology of the Champlain Basin in Vermont, Vermont Geol. Surv. Special Publ., 88pp.

AN OVERVIEW OF THE EARLY PALEOZOIC STRATIGRAPHY OF THE CHAMPLAIN VALLEY OF NEW YORK STATE

JAMES C. DAWSON

Earth & Environmental Science, State University of New York, Plattsburgh, NY, 12901

TRIP ABSTRACT

This, Sunday only, trip provides participants with an opportunity to visit some of the well-exposed, classic Early/Medial Cambrian to Medial Ordovician clastic and carbonate shelf sequences and the Medial Ordovician foreland basin carbonates and calcareous shales. Stops include the Potsdam Group (Lower/Middle and Upper Cambrian), the Theresa Formation and the Beekmantown Group (Lower Ordovician), the Chazy Group (Middle Ordovician) and the Trenton Group (Middle Ordovician). The trip essentially repeats the author's 2002 Joint New England Intercollegiate Geological Conference/New York Geological Association trip (Dawson, 2002) and is ideal for high school teachers and undergraduates seeking an introduction to these rocks.

INTRODUCTION

The field trip begins at the Comfort Inn, near Exit 37, I-87 'the Northway', Plattsburgh, NY at 8:30 AM and will end about 4:00 PM at the Comfort Inn, Plattsburgh, NY. This trip visits many of the localities that are commonly visited in the undergraduate classes at SUNY Plattsburgh. The field trip description is largely based on the work of Fisher (1968) and Isachsen, et al. (2000) and is not based on any significant research by this author.

TECTONIC SETTING

The Paleozoic rocks of the Lake Champlain Valley of northeastern New York State consist of a sequence that began in the Early/Medial Cambrian (520 Ma) and continued through the Early Ordovician (480 Ma) as a typical quartz sandstone and carbonate, passive shelf margin sequence, that transitions to the initiation of the Taconic foreland basin in Medial Ordovician (460 Ma) time (Isachsen, et al., 2000). The shelf sequence was deposited on the passive margin that formed in the Neoproterozoic (640 Ma) on, what is today, the eastern edge of Proto North America (called Laurentia by Hoffman, 1988 and others), as the continental landmasses, that were later to form Gondwanaland, rifted eastward to form the Iapetus Ocean (Isachsen, 2000).

Isachsen, et. al., (2000) suggest that the Iapetus Ocean began to open approximately 640 Ma; however the earliest of the shelf depositional units are not found in northeastern New York until 120 Ma or so later, when the Lower to Middle Cambrian Potsdam Sandstone, which lies directly on Precambrian meta-anorthosites and metagabbros, is deposited. Overlying, probably unconformably, the Potsdam Sandstone (Figure 1), at approximately the Cambro-Ordovician boundary, is the Theresa Dolostone/Sandstone which is followed unconformably by the dolostones of the Lower Ordovician Beekmantown Group. The shallow shelf carbonates, and the well-known known patch reef bioherms of the Chazy Group unconformably overlie the Beekmantown Group. The Chazy Group is followed by the relatively thin, eastern representation of the Black River Group that is not well exposed in the area (Fisher, 1968).

Toward the end of the Early Ordovician, approximately 480 Ma, an eastward dipping Taconic subduction zone, with an adjacent Taconic Island Arc lying immediately east of the subduction zone, were rafted westward to close a portion of the western Iapetus Ocean. The collision of this Taconic subduction zone and its adjacent Taconic Island Arc with Proto North America created the Taconic Orogeny during medial Ordovician time, approximately 460 Ma (Isachsen, et. al., 2000). The beginnings of this Taconic Orogeny are represented in northeastern New York by the lower portion of the Trenton Group.

As the Taconic Orogeny collision progressed, the eastern edge of Proto North America was uplifted while the region to the west of the uplift, that is now northeastern New York, was down warped into a foreland basin that is associated with steep angle strike slip faulting (Stone, 1957). The beginnings of a part of the northern portion of this downwarp are represented by the Cumberland Head Argillite of the Trenton Group with younger portions of the formation being deposited as flysch in progressively deeper water (Hawley, 1957). As the collision progressed, Lower Cambrian quartz sandstone and carbonate shelf deposits were thrust westward, possibly as gravity driven slides, as thick allochthonous sheets. These thrust faults over-rode the eastern portions of the Cumberland Head Argillite creating significant folding and shearing within the eastern portions of the Cumberland Head Argillite. Portions of the Middle Ordovician Cumberland Head Argillite also form allochthonous strata that appear to have overridden portions of the Lower Ordovician Beekmantown Group. Allochthonous Chazy Group strata are not found in northeastern New York, although they have been described further south near Granville, NY (Selleck and Bosworth, 1985).

The next portion of the tectonic setting is represented by the many mafic dikes (Kemp and Marsters, 1893; Hudson and Cushing, 1931) that cross cut the Paleozoic sequence. These have been interpreted (Fisher, 1968) as being of Late Jurassic/Early Cretaceous age and may be related to the ultrabasic intrusives of the Monteregian Hills of southern Quebec that have been dated at 110 Ma.

STRATIGRAPHIC SUMMARY

Saratoga Springs Group

The Potsdam Sandstone (Figure 1) was described by Emmons, (1843), and named after Potsdam, NY, as being the base of the 'Transition System' in quarries near Potsdam, NY. Three lithologic facies are generally recognized including an Altona Member, the Ausable Member and the Keeseville Member. Early literature refers to the Altona Member (Landing, 2007) as the ‘basal’ member. The Altona Member consists of a maroon, hematitic, feldspathic, micaceous, quartzose dolostone with many maroon shale interbeds (Stop 15). Portions of this basal unit may be early to medial Cambrian (Landing, 2007; Landing et. al., 2009 and Landing et. al., 2013)) and recently Mehrtens (2015) has proposed a partial age equivalency for the Altona Member with the Monkton Formation of northwestern Vermont on the basis of a shared *Olenellus* age fauna and sequence stratigraphy analysis. The Ausable Arkose is a cross laminated, feldspar rich, dolomitic sandstone that occurs irregularly throughout the main Potsdam section. The Keeseville Member (Stops 11, 13, and 14) is a fine to coarse quartz sandstone. Detailed lithologic descriptions of the three units can be found in Lewis (1971) and Wiesnet (1961). Most

Figure 1. Rock Section (after Fisher, 1968).

Age	Lithology/Formation	Thickness	Field Trip Location
Late Jurassic/ Early Cretaceous	Lamprophyre Dikes		Stops 1 and 16
'uncertain'	LaColle Melange		Stops 8 and 9
Ordovician	Trenton Group		
	Iberville and Stony Point Shales	1000'+	
	Cumberland Head Argillite	200'+	Stops 2 and 4
	Glens Falls Limestone		
	Montreal Member	150-200'	Stop 1
	Larrabee Member	30'	
Ordovician	Black River Group		
	Isle LaMotte Limestone	30'	
	Lowville Limestone	12'	
	Pamelia Dolostone	5-40'	
Ordovician	Chazy Group		
	Valcour Limestone		
	upper argillaceous	80-125'	
	lower reefs/calcarentite	40-55'	Stops 6 and 10
	Crown Point Limestone	50-250'	Stops 7 and 16
Ordovician	Beekmantown Group		
	Providence Island Dolostone	150-200'	Stop 3
	Fort Cassin Limestone/Dolostone	150'+	
	Spellman Limestone	100'+	
	Cutting Dolostone	200'+	
	concealed dolostone	75-275'	
Cambrian	Saratoga Springs Group		
	Theresa Dolostone/Sandstone	50'	Stop 12
	Potsdam Sandstone		
	Keeseville Sandstone	455'+	Stops 11, 13 & 14
	Ausable Arkose	250'+	
	Altona Dolostone/Shale	230'+	Stop 15
Precambrian	Meta-anorthosite and Metagabbro pierced by Diabase Dikes (Grenville).		

authors have interpreted the Potsdam Sandstone as being deposited in a complex arrangement of fluvial and aeolian to intertidal and barrier beach environments (Fisher, 1968). This field trip guide follows Fisher's (1968) stratigraphy and includes the Theresa Dolostone/Sandstone (Stop 12) in the Saratoga Springs Group although some authors have included it in the overlying

Beekmantown Group. Much has written about the Potsdam Group through Beekmantown Group boundary in the Ottawa Embayment of eastern Ontario (Dix et. al., 2004) and the Theresa may be a short-lived transgression bounded unconformably above and below. The Theresa is a thick bedded, quartzose dolostone that occupies the stratigraphic position between the quartz sandstones of the Potsdam below and the dolostones of the Beekmantown above.

Beekmantown Group

The Beekmantown Group (Figure 1) was erected (Clarke and Schuchert, 1899) as a new name for the Calciferous Sandrock (Formation) of Emmons (1843) and others and was named for Beekmantown, NY. Unfortunately, the section at Beekmantown, NY is not well exposed and the two main sections described by Brainerd and Seely (1890) as five units (Divisions A through E), north of Shoreham, VT and at West Cornwall, VT, are generally accepted as the type section. Fisher (1968) made a determined effort to carry the Brainerd and Seely (1890) units to northeastern New York and in ascending order he has mapped the Cutting Dolostone, Spellman Formation, Fort Cassin Formation and Providence Island Dolostone. The prevalent unit is the Providence Island Dolostone (Stop 3), a supratidal dolostone.

Chazy Group

The Chazy Group (Figure 1) comprises what is arguably the best known unit of northeastern New York and adjacent Vermont. The Group was originally defined by Emmons (1843); but, many researchers (Brainerd, 1891; Brainerd and Seely, 1888 and 1896; Oxley and Kay, 1959; Pitcher, 1964a and 1964b) have contributed to our understanding of the Group. The Chazy Group consists of three well defined limestone formations that unconformably (Knox Unconformity) overly the Beekmantown Group. The Day Point Formation (Stop 5) consists of gray, cross bedded, calcarenite in northeastern New York with small bioherms of bryozoans, corals and sponges near the top that we will not see on this trip. Above the Day Point lies the Crown Point Limestone (Stops 7 and 16) an argillaceous, medium textured, calcisiltite, calcilutite to argillicalcilutite (Fisher, 1968). The characteristic, large, planispiral gastropod, *Maclurites magnus* Le Sueur (1818) (Stop 7) is common and small stromatoporoid reefs can be found. The Valcour Limestone is the youngest unit of the Chazy Group. The lower part of the Valcour (Stops 6 and 10) contains extensive bioherms of bryozoans, sponges, algae and stromatoporoids and reef flank calcarenites. The upper portion becomes more argillaceous and grades into the Pamelia Dolostone of the Black River Group.

Black River Group

In northeastern New York the exposures of the Black River Group (Figure 1) are limited. Fisher (1968) has mapped, in ascending order, the Pamelia Dolostone, Lowville Limestone and Isle La Motte Limestone as a single Black River group unit with limited success. The Black River group in northeastern New York is relatively thin and consists of thick bedded dolostone, and some argillacous dolostone, of the Pamelia just above the Valcour Formation, and massive, light gray limestones, that are interbedded as the Lowville and Isle La Motte. The best exposures occur in two quarries, one of which has largely been mined out (International Lime and Stone Quarry southeast of Chazy) and one of which is full of water (a shallow quarry southwest of Rouses Point, NY). We will not attempt to visit the Black River Group on this field trip.

Trenton Group

In northeastern New York the Trenton Group (Figure 1) consists of the lower Glens Falls Limestone and the upper Cumberland Head Argillite (Stops 2 and 4). The Glens Falls Limestone in turn is subdivided into a lower Larrabee Member (Kay, 1937), a thick bedded medium gray limestone that we will not see on this field trip and an upper Montreal Limestone, the Shoreham Limestone of Kay (1937) (Stop 1). The transition from the continental shelf deposits of the main portion of the Chazy Group to the more argillaceous grayish black limestone of the Montreal represents a transition from pre-Taconic shelf deposits to the incipient formation of the Taconic Orogeny foreland basin. The Cumberland Head Argillite is a regionally restricted unit that formed as a flysch, turbidity current deposit in a portion of the early foreland basin of the Taconic Orogeny. Above the Cumberland Head Argillite very limited exposures of the Stony Point Shale, can be found in northeastern New York. The non-calcareous Iberville Shale is only found in Vermont and Quebec (Hawley, 1957).

LaColle Melange

Initially the La Colle (Conglomerate) Melange (Figure1) was described as a sedimentary formation (Clark and McGerrigle, 1936; Kay, 1937); but, Stone (1957) and Fisher (1968) have interpreted the unit as a Taconic Orogeny tectonic rock formed by the Tracy Brook (normal) Fault (Stops 8 and 9) and by thrust faults where it is found in Vermont.

ROAD LOG AND STOP DESCRIPTIONS

Meeting Point: The trip begins in the parking lot of the Comfort Inn and Suites/Perkins Restaurant, 411 Route 3, Plattsburgh, NY.

To reach the Comfort Inn, leave I-87 'the Northway' at Exit 37, which is the main Plattsburgh, NY exit. This is a trumpet exit that brings one to Route 3. Turn right (0 miles/0 km) on to Route 3 heading east. Continue through the traffic lights at LaBarre Street (0.1 miles/0.2 km) and Smithfield Boulevard (0.2 miles/0.3 km). Cross under the I-87 bridge and turn right at the traffic light for Consumer Square (0.4 miles/0.6 km). The Comfort Inn will be on your right.

Meeting Point Coordinates: 44.696^{o} N, 73.4881^{o} W

Meeting Time: 8:30 AM, Sunday, September 13th, 2015.

Distance in miles (km)		
Cumu-lative	Point to Point	Route Description
0.0 (0.0)		Assemble in the parking lot of the Comfort Inn. Exit the parking lot and drive to the Consumer Square/ Route 3 traffic light. Turn right/east on Route 3.
0.1 (0.2)	0.1 (0.2)	Continue through a traffic light at Healy Avenue.
0.3 (0.5)	0.2 (0.3)	Continue through a traffic light at Cogan Avenue.
0.6 (1.0)	0.3 (0.5)	Bear right at the Y-intersection. There will be a Walgreens Pharmacy set back on the right and a Liberty Tax service in the crotch of the Y.
0.7 (1.2)	0.1 (0.2)	Continue through a traffic light a Prospect Avenue.

0.9 (1.4)	0.2 (0.3)	Continue through a traffic light at Draper Avenue. There is a large stone SUNY Plattsburgh sign on the left. You will see a concrete pedestrian overpass ahead. The overpass connects to the Hudson Hall and Hudson Hall Annex on your left. The Hudson buildings are named after Professor George H. Hudson (Hudson, 1905; Hudson, 1907; Hudson and Cushing, 1931) who taught science and music at SUNY Plattsburgh for many years. His portrait hangs in the foyer of Hudson Hall.
1.0 (1.6)	0.1 (0.2)	Continue through a traffic light at Beekman Street.
1.1 (1.8)	0.1 (0.2)	At a traffic light, at a Y-intersection, Rugar Street enters on the right.
1.4 (2.3)	0.3 (0.5)	Turn right/south at the traffic light at South Catherine Street.
1.8 (2.9)	0.4 (0.6)	Continue through a traffic light at River Street.
1.9 (3.1)	0.1 (0.2)	Cross the Saranac River and immediately turn left/east on South Platt Street.
2.3 (3.7)	0.4 (0.6)	At a traffic light at Route 9 make a slow right/south on to U. S. Avenue. Do not make the hard right on to Peru Street.
2.7 (4.3)	0.4 (0.6)	Enter the rotary and take the third exit on to New York Road heading east. Do not take the first New York Road exit out of the rotary.
2.9 (4.6)	0.2 (0.3)	At the stop sign turn right/south on to Ohio Avenue. On your right you will note three stone buildings constructed by the U. S. Army before the area became Plattsburgh Air Force Base (PAFB). The oldest building, the Old Stone Barracks, is the one furthest from the road. Construction on this started in 1839, but due to construction and funding issues, the building was not occupied until 1843. The two younger replica barracks date from the 1930s. All three buildings are constructed of local Keeseville Sandstone.
3.1 (4.9)	0.2 (0.3)	Turn left on Marina Drive toward Lake Champlain. You will cross the Canadian Pacific mainline railroad tracks on a very narrow bridge (sound your horn). Wind your way down to a small parking area (Stop 1).

STOP 1: Montreal Member of the Glens Falls Limestone of the Trenton Group and Lamprophyre (Monchiquite) Dike at the former PAFB Marina.

From the parking area walk down the obvious roadway to the lake shore where the former PAFB marina and warf can be seen on Marina Point. To reach the outcrop, hike, approximately 700 or so paces north along the cobble beach shore of Lake Champlain. The Pleistocene sediments forming the bluff between the railroad track and Lake Champlain along the way include a contact between earlier Lake Vermont varved and later Champlain Sea sediments. The Montreal Member and a cross cutting Lampophyre Dike are exposed to varying degrees depending on the water level of Lake Champlain. The Montreal Member is a medium-bedded limestone with some shale partings that weather to medium dark gray. Thin laminations within the medium-thickness beds have been interpreted as turbidity current deposits. Crab Island (the smaller island that can be seen in Lake Champlain two miles/3.2 km southeast of this stop) takes its name from the trilobite, *Isotelus*, that is commonly found in exposures of the Montreal

Member on the island. Fisher (1968) mapped the Lamprophyre Dike as a monchiquite dike, containing phenocrysts of titanaugite with some biotite and barkevikite (a monoclinic amphibole), phenocrysts of olivine and titanomagnetite. After visiting the outcrop return to the vehicles.

ALTERNATIVE STOP 1.

If the Lake Champlain water levels are much over 95 feet above sea level most of the Stop 1 outcrops will be under water. There is an Alternative Stop 1 where the Montreal Limestone (but not the Lamprophyre Dike) can be seen.

To reach the Alternative Stop 1 return to Ohio Avenue and turn right/north (0 miles/0 km). Continue north to the New York Road stop sign (0.2 miles/0.3 km) and go straight ahead. Turn right on to U. S. Oval (0.3 miles/0.48 km). Continue north on the east side of the oval. The former U. S. Army and PAFB parade ground, constructed in 1893, is on your left. On your right you will pass four large, red brick former military buildings including the 22 U. S. Oval agency building, the 34 U. S. Oval apartments, the 52 U.S. Oval Plattsburgh City Recreation Center and the 64-70 apartments. Turn right, just past the last apartment building (0.6 miles/0.96) and continue to the parking area behind the apartment building and park.

After parking, walk north along the paved pedestrian walkway for 0.3 miles/0.5 km to a pedestrian bridge on your right/east. Cross over the Canadian Pacific mainline railroad tracks on the pedestrian bridge and follow the path down to the lake shore. This will bring you to Sailor's Point, the former PAFB beach and picnic area. The Montreal Limestone is exposed at the south end of the cobble beach. From the outcrop you can see Crab Island to the southeast and Marina Point to the south.

Distance in miles (km)		
Cumu-lative	Point to Point	Route Description
3.1 (5.0)		From Stop 1 follow Marina Drive back across the Canadian Pacific mainline railroad track to Ohio Avenue and turn right/north.
3.3 (5.3)	0.2 (0.3)	At the New York Road stop sign turn left/west.
3.5 (5.6)	0.2 (0.3)	Enter the rotary and take the first exit on to Route 9/United States Avenue heading north.
3.7 (5.9)	0.2 (0.3)	At the South Platt Street traffic light bear right and continue north on Route 9.
3.9 (6.2)	0.2 (0.3)	You will pass the Fort Brown historic markers and the remains of the defenses on your left/west. Fort Brown was the left/west flank of the American defense during the land portion of the Battle of Plattsburgh on September 6 – 11, 1814.
		Continue north on Route 9 past the traffic light at the Pike Street intersection.
4.4 (7.0)	0.5 (0.8)	Turn left/west at the T-intersection traffic light on to Bridge Street. Route 9 continues on Bridge Street.
4.6 (7.4)	0.2 (0.3)	At the four-way stop turn right/north on to City Hall Place. Route 9 continues as City Hall Place. Continue north on City Hall Place past the

		Plattsburgh City Hall on your left and the Macdonough (American naval commander during the Battle of Plattsburgh) Monument on your right.
4.8 (7.7)	0.2 (0.3)	Just past the City Hall turn left/west and immediately turn right/north on to Miller Street. Route 9 continues on Miller Street.
5.1 (8.2)	0.3 (0.5)	On Miller Street you will pass the Plattsburgh Post Office on your right and cross the Canadian Pacific mainline railroad tracks on a level crossing.
5.4 (8.6)	0.3 (0.5)	At a traffic light make a slow right turn/north on to Margaret Street. Route 9 continues on Margaret Street.
5.5 (8.8)	0.1 (0.2)	At a traffic light you will cross the Cumberland Head Avenue/Boynton Avenue intersection where the Georgia-Pacific paper mill is located.
6.3 (10.1)	0.8 (1.3)	Cross Scomotion Creek.
6.8 (10.9)	0.5 (0.8)	Continue north on Route 9 past the traffic light for Route 314 (Exit 39, I-87 'the Northway') intersection.
7.5 (12.0)	0.7 (1.1)	Pass Cumberland 12 theatres on your left and cross under the transmission lines that carry St. Lawrence Seaway energy across Woodruff Pond and Lake Champlain on your right to Vermont.
8.4 (13.4)	1.4 (2.2)	Pass the Plattsburgh Rod and Gun Club on your right.
9.8 (15.7)	1.4 (2.2)	Pull over to the right/east side of Route 9 and park near a low road cut, Stop 2.

STOP 2: Cumberland Head Argillite of the Trenton Group on Route 9.

The Cumberland Head Argillite is exposed in this road cut on east of Route 9. At one time the exposures were better on the left/west side. The road cut (Fisher, 1968 - Figure 27) is typical of the Cumberland Head Argillite. The thin bedding (it looks like varves) of fairly distal turbidite deposition can clearly be seen as more calcarous layers alternate with the thinner, pale buff-colored quartz-silt bearing layers being slightly more resistant to erosion. Fresh surfaces of the rock are uniformly black; however, the thin layers can still be distinguished. The rocks in the vicinity are folded; but, the strike is generally N35E with a dip of 23 degrees N. Be sure to look north along Route 9 and see the slight dip that the highway makes north of the road cut. Stop 3 is just beyond the dip.

Distance in miles (km)		
Cumu-lative	Point to Point	Route Description
9.8 (15.7)		Return to the vehicles and continue north on Route 9.
10.3 (17.0)	0.5 (0.8)	Pull over to the right/east side of Route 9 at the next low road cut, Stop 3.

STOP 3: Providence Island Dolostone of the Beekmantown Group on Route 9.

The Providence Island Dolostone is exposed in this road cut on both sides of Route 9, although the exposures are better on the right/east side (Fisher, 1968 - Figure 17). Before examining the outcrop, be sure to look south along Route 9 and recognize that you can see Stop 2. The Rocks at Stop 3 are nearly horizontal, compared to the steeper dips at Stop 2 and the entire Chazy Group and lower portion of the Trenton Group (some 400' or more of rock section) are missing. Fisher (1968) has mapped the edge of the Cumberland Head Allochthon, a Taconic thrust fault, as passing between these two trip stops on the basis of missing section at both the surface and in a 200' deep water well on Cumberland Head.

The Providence Island Dolostone is a thick bedded, massive unit that weathers to the buff color characteristic of dolostones. With careful examination, horizons that display significant soft sediment rip ups and other features characteristic of supratidal environments can be observed. The dolostone is sometimes vuggy and fracture zones that have been filled with secondary crystalline calcite are common.

Distance in miles (km)		
Cumu-lative	Point to Point	Route Description
10.3 (17.0)		Return to the vehicles and continue north on Route 9.
10.6 (17.0)	0.3 (0.5)	Turn right/east on to the Point au Roche Road.
12.2 (19.5)	1.6 (2.6)	At the entrance to Point au Roche State Park turn right/south and enter the park. You are entering the western park entrance that leads to the beach. Follow the park road south past the entrance gate to the beach parking lot.
12.7 (20.3)	0.5 (0.8)	At the beach parking lot head to the far right/southwest corner of the parking lot and park, Stop 4.

STOP 4: Cumberland Head Argillite of the Trenton Group at Point au Roche State Park.

Walk the short distance from the parking lot to Lake Champlain and examine the large outcrop of Cumberland Head Argillite along the shore. The folding and jointing associated with the Taconic thrusting is very obvious. The rock is essentially the same as that seen at Stop 2 and again the thinning bedding of the fairly distal turbidite deposition can be seen as the more calcareous layers alternate with the thinner, pale buff-colored, quartz silt bearing layers being more resistant to erosion.

Distance in miles (km)		
Cumu-lative	Point to Point	Route Description
12.7 (20.3)		Return to the vehicles and retrace your route back to the park entrance.
13.2 (21.1)	0.5 (0.8)	Turn left/west on to Point au Roche Road.
14.8 (23.7)	1.6 (2.6)	Turn right/north on Route 9.

15.8 (25.3)	1.0 (1.6)	A hump in the road will indicate that you are crossing the Ingraham Esker (Denny, 1972).
16.2 (25.9)	0.4 (0.6)	A series of sand pits can be seen to the right/east after you first cross the esker.
16.6 (26.6)	0.4 (0.6)	Route 9 crosses the Ingraham Esker again, just before the hamlet of Ingraham on the left/west.
19.2 (30.7)	2.6 (4.2)	Pass the Giroux Poultry farm on the left/west.
19.5 (31.2)	0.3 (0.5)	Pass Trombley Lane (formerly Slosson Road).
19.6 (31.4)	0.1 (0.2)	Pull over and park on the right/east side of Route 9 in front of a low Road cut that is located on the left/west side of Route 9 in front of a blue house, Stop 5.

STOP 5: Day Point Limestone of the Chazy Group on Route 9.

THIS IS NOT A HAMMER STOP

This road cut is part of the upper part of The Day Point Limestone, probably the Fleury Member of Oxley and Kay (1959). It is a medium gray calcarenite that is both cross bedded and regular bedded in this small exposure. Fisher (1968) mentions this outcrop as containing pelmatozoan debris. Note the nicely developed stylolites.

Distance in miles (km)		
Cumu-lative	Point to Point	Route Description
19.6 (31.4)		Return to the vehicles and continue north on Route 9.
20.7 (33.1)	1.1 (1.8)	As Route 9 makes a bend to the left turn right/east on to Sheldon Lane.
21.1 (33.8)	0.4 (0.64)	On the left/north you will see a quarry with a large white house at its eastern end. Pull over and park at the western end of the quarry, Stop 6.

STOP 6: Valcour Limestone of the Chazy Group at the Sheldon Lane Quarry.

THIS IS NOT A HAMMER STOP

This is the first of two opportunities that we will have to see the bioherms in the Valcour Limestone.
See the Stop 10 description for the details of what to see at this stop.

Distance in miles (km)		
Cumu-lative	Point to Point	Route Description
21.1 (33.8)		Return to the vehicles and turn around. There is a place to do a Y-turn on the left/north side of Sheldon Lane at an orchard access just east of the stop. Return to the intersection with Route 9.
21.5 (34.4)	1.2 (1.9)	Turn right/north on Route 9.
22.2 (35.5)	0.7 (1.1)	Just past a faded red barn on the right/east there is an amateurish 'stonehenge' and an unpaved road. The road leads to the abandoned International Lime and Stone quarry where the Pamelia Dolostone, the Lowville Limestone and the Isle La Motte Limestone formations of the Black River Group (Fisher, 1968 – Figure 25) were once exposed. A few years ago much of the remainder of this outcrop and the quarry floor today consists of Valcour Limestone. Some of the Black River Group remains on the north side of the quarry on private property; but, this exposure is only accessible when the water in the quarry is frozen.
23.1 (37.0)	0.9 (1.4)	At the Fiske Road in Chazy, NY turn hard left/southwest toward West Chazy. Continue southwest on the Fiske Road as it bends to the right/west.
24.3 (38.9)	1.2 (1.9)	Pull over to the right and park as the Fiske Road approaches the bridge over I-87, the Northway, Stop 7.

STOP 7: Crown Point Limestone of the Chazy Group at the Northway in Chazy, NY: *Maclurites magnus* Le Sueur, Death Assemblage.

THIS IS NOT A HAMMER STOP

To reach the outcrop cross the open area to the north and enter the woods on a vague trail behind and to the right of the obvious transmission pole. The vague trail heads north a few yards in a white cedar forest and then bends left/west toward the Northway. The outcrop is close to the Northway, a short distance north of the Fiske Road Bridge and is illustrated in Fisher, 1968 (Figure 20). The Crown Point Limestone is mainly a medium to dark gray calcilutite. This locality exhibits an unusually large assemblage of the planispiral gastropod *Maclurites magnus* along with trilobite and brachiopod fragments. Be sure to note the insipient karst development.

Distance in miles (km)		
Cumu-lative	Point to Point	Route Description
24.3 (38.9)		Return to the vehicles and turn around. Head back east and northeast on the Fiske Road.
24.6 (39.4)	0.3 (0.5)	Turn left/north on Route 9.
24.9 (39.9)	0.3 (0.5)	Cross the Little Chazy River.
25.1 (40.2)	0.2 (0.3)	Pass under the Canadian Pacific mainline railroad bridge.
25.2 (40.3)	0.1 (0.2)	Immediately after passing under the railroad bridge turn left on to the Miner Farm Road. As you turn left watch for an opportunity to continue with your left turn on to a short dead end street that enters the intersection and park on the apron, Stop 8.

Stop 8: Lacolle Melange at the Chazy Railroad Bridge.

The road cut is located along the west side of Route 9 as you walk south along Route 9 toward the railroad bridge and is figured in Fisher, 1968 (Figure 30). Fisher, 1968 maps this locality and the Stop 9 locality as part of the Tracy Brook (normal) Fault. The wide range of clasts are composed of mostly angular sandstone fragments in a sandstone matrix, presumably a tectonically crushed portion of the Keeseville Sandstone.

Distance in miles (km)		
Cumu-lative	Point to Point	Route Description
25.2 (40.3)		Return to the vehicles and carefully return to Route 9 heading north.
26.4 (42.2)	1.2 (1.9)	Cross Corbeau Creek. Corbeau Creek was studied, as a monitored watershed by Professor John Malanchuck and a succession of SUNY Plattsburgh students in the 1970s and 1980s. In recent years SUNY Plattsburgh students have been engaged in watershed studies on the Altona Flat Rock lands owned by the William H. Miner Agricultural Institute.
27.9 (44.6)	1.5 (2.4)	Turn right on Route 9B.
29.5 (47.2)	1.6 (2.6)	Cross the Great Chazy River in Cooperstown, NY.
29.9 (47.8)	0.4 (0.6)	Cross the bridge over the Canadian Pacific mainline railroad tracks.
30.1 (48.2)	0.2 (0.3)	Just past the Hayford Road pull over to the right and park in front of very small outcrop, Stop 9.

STOP 9: Lacolle Melange at Coopersville, NY.

The small outcrop is located adjacent to the south side of Route 9B and is figured in Fisher, 1968 (Figure 29). The breccia clasts include a wide range of sizes and the lithology of the clasts is predominately carbonate fragments, likely of Black River Group and Trenton Group origin. Also refer to the Stop 8 description.

Distance in miles (km)		
Cumu-lative	Point to Point	Route Description
30.1 (48.2)		Return to the vehicles and continue east on Route 9B.
30.4 (48.7)	0.3 (0.5)	Pass the Dumont Road on the right and follow Route 9B around a big bend to the left. Lake Champlain will appear on the right/east.
30.7 (49.2)	0.3 (0.5)	After passing a brown log cottage, # 862, on the left/west turn into a driveway that leads to an open pasture, Stop 10.

STOP 10: Valcour Limestone of the Chazy Group at the Bechard Quarry, near Kings Bay.

To reach the quarry walk across the open pasture to the higher vegetated area that is visible to the west. Once you reach the top of the vegetated mound the quarry can be seen as illustrated in Fisher, 1968 (Figure 22). The bioherms consist of intertidal stromatolites (algae), stromatoporoids, and bryozoans with the various colonies being completely compatible (Pitcher, 1964b) and building their colonies on top of one another. Nautiloid cephalopods have been found.

Distance in miles (km)		
Cumu-lative	Point to Point	Route Description
30.7 (49.2)		Return to the vehicles and turn around. Head south and west on Route 9B.
34.0 (54.5)	3.3 (5.3)	Turn right/north on Route 9.
37.9 (60.7)	3.9 (6.2)	Turn left into the northernmost of the two entrances to the (former) Clinton Farm Supply property (no sign), Stop 11.

STOP 11: Keeseville Sandstone Member of the Potsdam Sandstone Group at the Clinton Farm Supply, Champlain, NY.

The outcrop is exposed along the north side of the northernmost of the two driveways and in the flat area behind the Farm Supply building. In a series of articles (Erickson, 1993a. Erickson, 1993b. Erickson and Bjerstdt, 1993. Erickson, Connett and Fetterman, 1993) the stratigraphy and trace fossils of the Keeseville Sandstone and Theresa Dolostone/Sandstone have been described. Stop 11 (Erickson, 1993a, and Erickson, Connett and Fetterman, 1993) consists of medium bedded, cream colored Keeseville Sandstone. At this locality large scale ripple marks, and an unusual abundance of trace fossils can be seen.

Distance in miles (km)		
Cumu-lative	Point to Point	Route Description
37.9 (60.7)		Return to the vehicles and continue north/left on Route 9.
39.2 (62.7)	1.3 (2.0)	Turn right at the traffic light at Route 11.
39.8 (63.7)	0.6 (1.0)	Cross the Great Chazy River.
40.8 (65.3)	1.0 (1.6)	Turn left at the traffic light on to Route 276.
41.4 (66.3)	0.6 (1.0)	Pass the Northeastern Central School on the left/west.
41.6 (66.6)	0.2 (0.3)	Turn left into the Prospect Hill Quarry, Stop 12.

STOP 12: Theresa Dolostone/Sandstone at Champlain, NY.

The Theresa Dolostone/Sandstone consists of an interlayed, medium and thick bedded, quartzose dolostone. Bjerstedt and Erickson (1989) and Erickson and Bjerstedt (1993) have described the trace fossils of the Theresa in detail and *Skolithos* has been found on the south wall of this quarry.

Distance in miles (km)		
Cumu-lative	Point to Point	Route Description
41.6 (66.6)		Return to the vehicles and retrace your route south on Route 276.
42.4 (67.9)	0.8 (1.3)	Turn right at the traffic light on to Route 11.
44.5 (71.3)	2.1 (3.4)	Follow Route 11 to I-87 the Northway at Exit 41. Anyone needing to leave the trip early can conveniently do this here. Continue west on Route 11 across I-87.
47.5 (76.1)	3.0 (4.8)	Cross the Great Chazy River.
50.2 (80.4)	2.7 (4.3)	Enter Mooers, NY. Route 11 turns right and Route 22 enters on the left. Stay on Route 11 heading west.
52.7 (84.7)	2.7 (4.3)	Make a slow right turn/west off Route 11 on to the Davison Road.

57.9 (93.0)	5.2 (8.3)	The Davison Road comes to a stop sign at a T-intersection with the Cannon Corners Road in Cannon Corners, NY. Turn left/south on the Cannon Corners Road and immediately cross the English River.
58.5 (94.0)	0.6 (1.0)	Turn right/west on to the unpaved Gadway Road at the Adirondack Nature Conservancy 'Gadway Sandstone Pavement Barrens' sign, Stop 13. The 2.2 mile/3.5 km round trip on the Gadway Road is not suitable for vehicles with low clearance and drivers should consolidate riders into high clearance vehicles.

STOP 13: Keeseville Sandstone of Potsdam Sandstone Group at the Gadway Preserve.

Stop 13 consists of three short stops (13a, 13b and 13c) within the stop.

Distance in miles (km)		
Cumu-lative	Point to Point	Route Description
58.5 (94.0)		Stop on the Gadway Road and park (**Stop 13a**) at a bare rock wash. Carefully cross over a barbed wire fence to examine a pavement of large scale ripples in the Keeseville Sandstone.
58.6 (94.2)	0.1 (0.2)	Continue west on the Gadway Road and park (**Stop 13b**) at the next significant open area on the right/north. At the north end of the open area near a red posted sign there is a 4 meter long (10 cm wide) *Protichnites* track. Yochelson and Fedonkin (1993) illustrate several similar examples of this trace fossil in the Keeseville Sandstone of northern New York. Additional trace fossils can be seen near the Adirondack Nature Conservancy sign. Recent literature suggests that the trace fossil *Protichnites* may be the track of a eurypterid-like stem arthropod (Seilacher, 2007; Hagadorn and Seilacher, 2009) or by euthycarcinoid arthropods travelling in pairs (Collette and Hagadorn, 2010; Collette, et. al, 2012). Continue west on the Gadway Road. Follow the arrow to the left track at the Y-intersection. At this point the road becomes solid rock. Continue to the marked turn-around loop.
59.3 (95.3)	0.7 (1.1)	Park (**Stop 13c**) at the turn around loop. Walk about 100 paces beyond the turn-around loop and pass an arrow sign. On the left/south side of the road you can locate additional *Protichnites* tracks. One track is 1.4 meters long (11 cm wide) and some partial tracks cross over one another. Return to the vehicles and return to the intersection of the Gadway Road.
60.4 (97.1)	1.1 (1.8)	Turn right/south on the Cannon Corners Road.
62.9 (101.1)	2.5 (4.0)	Turn left/east on to Route 11.
64.6 (103.8)	1.7 (2.7)	Turn right/south on to the Alder Bend Road toward Irona.
65.8 (105.7)	1.2 (1.9)	At the four-way stop sign turn left/east on to the Irona Road.
68.4 (109.9)	2.6 (4.2)	At the T-intersection stop sign turn right/south on to the Devils Den Road.

68.9 (110.7)	0.5 (0.8)	Continue south past the Miner Farm Road on the left/east.
69.5 (111.7)	0.6 (1.0)	Continue south on the Devil Den Road as it crosses the Great Chazy River. Just upstream from the bridge to the right/west is the McGregor Powerhouse, in Spanish architectural style, and the LaSalle Dam that were constructed by William H. Miner in 1923. Excellent exposures of the Keeseville Sandstone can be found on both sides of the river between the road bridge and the powerhouse.
69.7 (112.0)	0.2 (0.3)	As the Devils Den road bends to the right/southwest turn left and continue going south on the unpaved Rock Road.
70.7 (115.2)	0.6 (1.0)	There is a wide flat rock area of Keeseville Sandstone.
71.5 (115.5)	0.2 (0.3)	There is a second wide flat rock area of Keeseville Sandstone, Stop 14.

STOP 14: Trough Cross Stratification in the Keeseville Sandstone of the Potsdam Sandstone Group on the Rock Road, Altona, NY.

The trough cross stratification is located on the east side of the road, within what goes for a right of way. It is an outcrop of well exposed cross stratification in the Keeseville Sandstone.

Distance in miles (km)		
Cumu-lative	Point to Point	Route Description
71.5 (115.5)		Return to the vehicles and continue south on the Rock Road.
72.3 (116.8)	0.8 (1.3)	Turn left/south at the stop sign intersection with Route 190, 'the Military Turnpike'. You will soon see one of the local wind farms set back on both sides of the road. These units feed their power to the nearby Power Authority of New York's Duley, Altona, NY, substation.
73.9 (119.4)	1.6 (2.6)	On the left/east side of the road you pass the overgrown ruins of Lewis Sage Robinson's Tavern, erected in 1837. The opposite/west side of the road is the site of the Original Log Tavern erected in 1810. This 1810 tavern was visited by President James Madison in 1817.
75.8 (122.4)	1.9 (3.0)	Pass the Blue Chip Way on the right/west.
75.9 (122.6)	0.1 (0.2)	'Truck ½ Mile' sign, warning trucks about the hill ahead. There is no shoulder on the right/west side of Route 190; but, it is possible to park on the left/east side of Route 190, Stop 15.

STOP 15: Altona Dolostone/Shale of the Potsdam Sandstone Group on the Military Turnpike.

Cross to the ditch on the west side of Route 190.Military Turnpike. Examples of the Altona Member of the Potsdam Sandstone can be found in and along the ditch from near the 'Truck ½ Mile' sign south to the near the bottom of the hill. The best exposures are toward the top of the hill. Grenville meta-anorthosite can be found just across the small drainage at the bottom of the hill.

The prominent hard reddish rock is a hematitic, micaceous quartzose dolostone. When highway crews clear the ditch it is also possible to see interbedded red shales; but, these tend to get grassed over in between ditch clearings.

About 2 miles/3.2 km east of here, SUNY Plattsburgh has a series of research hydrology wells on the William H. Miner Agricultural Research Institute's Altona Flat Rock. One of these wells penetrated 235 feet of Altona Dolostone/Shale before entering the underlying Grenville meta-anorthosites and basalt dikes.

Distance in miles (km)		
Cumu-lative	Point to Point	Route Description
75.9 (122.6)		Return to the vehicles and carefully return to Route 190 and continue south.
76.7 (123.9)	0.8 (1.3)	Pass the Murtagh Hill Road on the right/west. Just south of the Murtagh Hill Road on both sides of Route 190 there are good exposures of Grenville meta-anorthosites that have been intruded by a series of diabase dikes, also of Grenville age, and locally known as the Rand Hill Dikes.
77.3 (124.9)	0.6 (1.0)	Pass the Recore Road on the left/east.
83.0 (134.0)	5.7 (9.1)	Turn left/east at the traffic light intersection with Route 374, 'the Cadyville Expressway'.
86.1 (139.0)	3.1 (5.0)	Pass the Wallace Hill Road on the left/north. Route 374 is broadened to four lanes in this vicinity.
86.2 (139.2)	0.1 (0.2)	Pull over to the right and park, Stop 16.

STOP 16: Crown Point Limestone of the Chazy Group with Lamprophyre Dikes on Route 374.

This extensive road cut along both sides of Route 374/Cadyville expressway contains two Late Jurassic/Early Cretaceous lamprophyre dikes on the south side of the road that intrude the Crown point Limestone with a strike of N70W and a dip 85 degrees N. Only the easternmost of the two dikes appears on the north side of the road. Interesting features, including baked zones, zenoliths and partial zenoliths, can be seen associated with the intrusions. The Crown Point Limestone is mainly a medium to dark gray calcilutite. Some of the large planispiral gastropod, *Maculurites magnus* Le Sueur are present along with trilobite and brachiopod fragments.

Distance in miles (km)		
Cumu-lative	Point to Point	Route Description
86.2 (139.2)		Return to the vehicles. Stop 16 is the last stop and from here we will return to the Comfort Inn and Suites. Continue straight ahead.
86.3 (139.4)	0.1 (0.2)	Traffic light intersection with Quarry Road on the right/south and Route 22 on the left/north. Continue straight ahead and immediately access I-87 southbound, 'the Northway', using the Exit 38 entrance ramp on the right. Exit 38, I-87 is a convenient place for those who do not need to return to the Comfort Inn to leave the trip.
88.4 (142.8)	2.1 (3.4)	Leave I-87, the Northway, at Exit 37.
89.0 (143.8)	0.6 (1.0)	Turn right/east on Route 3. Continue east through two sets of traffic lights at LaBarre Street and Smithfield Boulevard.
89.3 (144.3)	0.3 (0.5)	Cross under the I-87 Northway bridge.
89.4 (144.5)	0.1 (0.2)	Turn right into Consumer Square. The Comfort Inn and Suites/Perkins Restaurant will on your right/west.

REFERENCES CITED

Bjerstedt, T. W. and J. M. Erickson. Trace Fossils and Bioturbation in Peritdal Facies of the Potsdam Theresa Formations (Cambrian-Ordovician), Northwest Adirondacks. Palaios, 4: 203-224. 1989.

Brainerd, E. The Chazy Formation in the Champlain Valley. Geological Society of America Bulletin, 2: (3): 293 - 300. 1891.

Brainerd, E. and H.M. Seely. The Original Chazy Rocks. American Geologist, 2: 323 - 330. 1888.

Brainerd, E. and H.M. Seely. The Calciferous Formation in the Champlain Valley. American Museum of Natural History Bulletin 3: 1-23. 1890.

Brainerd, E. and H.M. Seely. The Chazy of Lake Champlain. American Museum of Natural History Bulletin, 8: 305 - 315. 1896.

Clark, T. H. and H. W. McGerrigle. LaColle Conglomerate: A New Ordovician Formation in Southern Quebec. Geological Society of America Bulletin, 47: (5): 665 - 674. 1936.

Clarke, J.M. and C. Schuchert. The Nomenclature of the New York Series of Geological Formations. Science, New Series 10: 874-878. 1899.

Collette, J. H. and J. W. Hagadorn. Three-dimensionally preserved arthropods from Cambrian Lagerstatten of Quebec and Wisconsin. Journal of Palaeontology, 84:646-667. 2010.

Collette, J. H., K. C. Gass and J. W. Hagadorn. *Protichnites Eremita* Unshelled? Experimental Model-Based Neoichnology and New Evidence for a Euthycarcinoid Affinity for this Ichnospecies. Journal of Paleontology 86:(3):442-454. 2012.

Dawson, J. C. Early Paleozoic Continental Shelf to Basin Transition Rocks: Selected Classic Localities in the Lake Champlain Valley of New York State. New England Intercollegiate Geological Conference/New York State Geological Association Joint Field Conference – 2002. Field Trip A-3. Pages A3-1 to A3-13. 2002.

Denny, C.S. The Ingraham Esker, Chazy, New York. Pages B35 - B41 *in* Geological Survey Research 1972. United States Geological Survey Professional Paper 800-B. 1972.

Dix, G. R., O. S. Hersi and G. S. Nowlan. The Potsdam-Beekmantown Group Boundary, Nepean Formation type section (Ottawa, Ontario): a cryptic sequence boundary, not a conformable transition. Canadian Journal of Earth Science 41:897-902. 2004.

Emmons, E. Geology of New-York. Part II. Comprising the Survey of the Second District. Natural History Survey of New York. 437 pages. 1843.

Erickson, J.M. Cambro-Ordovician Stratigraphy, Sedimentation, and Ichnobiology of the St. Lawrence Lowlands-Frontenac Arch to the Champlain Valley of New York. Trip A-3(1). New York Geological Association Field Trip Guidebook, pages 68 - 95. 1993a.

Erickson, J. M. A Preliminary Evaluation of Dubiofossils from the Potsdam Sandstone. New York State Geological Association Field Trip Guidebook. Trip A-3(3), pages 121 - 130. 1993b.

Erickson, J. M. and T. W. Bjerstedt. Traces Fossils and Stratigraphy in the Potsdam and Theresa Formations of the St. Lawrence Lowland, New York. Trip A-3(2). New York State Geological Association Field Trip Guidebook, pages 97 - 119. 1993.

Erickson, J. M., P. Connett, and A. R. Fetterman. Distribution of Trace Fossils Preserved in High Energy Deposits of the Potsdam Sandstone, Champlain, New York. Trip A-3(4). New York State Geological Association Field Trip Guidebook, pages 131 - 143. 1993.

Fisher, D. W. Geology of the Plattsburgh and Rouses Point, New York-Vermont, Quadrangles. New York State Museum and Chart Series Number 10. 51 pages. 1968.

Hagadorn, J. W. and A. Seilacher. Hermit arthropods 500 million years ago? Geology 37:169-170. 009

Hawley, D. Ordovician Shales and Submarine Slide Breccias of Northern Champlain Valley in Vermont. Geological Society of America Bulletin 68: 55-94. 1957.

Hoffman, P. F. United Plates of America, the birth of a Craton: Early proteroxoic Assembly and Growth of Laurentia. Annual Review of Earth and Planetary Sciences 16: 543-603. 1988.

Hudson, G.H. Contributions to the Fauna of the Chazy Limestone on Valcour Island, Lake Champlain. New York State Museum Bulletin 80: 270-295. 1905.

Hudson, G.H. On Some Pelmatozoa from the Chazy Limestones of New York. New York State Museum Bulletin 107: 97-152. 1907.

Hudson, G. H. The Fault Systems of the Northern Champlain Valley, New York. New York State Museum Bulletin 286: 5 - 80. 1931.

Hudson, G. H. and H. P. Cushing. The Dike Invasions of the Champlain Valley, New York. New York State Museum Bulletin 286: 81 - 112. 1931.

Isachsen, Y. W., E. Landing, J. M. Lauber, L. V. Rickard and W. B. Rogers, Editors. Geology of New York: A Simplified Account. New York State Museum Educational Leaflet Number 28. 294 pages. 2000.

Kay, M. Stratigraphy of the Trenton Group. Geological Society of America Bulletin, 48: 233 - 302. 1937.

Kemp, J.F. and V.F. Marsters. The Trap Dikes of the Lake Champlain Region. United States Geological Survey Bulletin 107. Pages 11-62. 1893.

Landing, E. Ediacaran – Ordovician of East Laurentia – Geologic Setting and Controls on Deposition along the New York Promontory Region pages 5-24 in Ed Landing. Editor. Ediacaran – Ordovician of East Laurentia – S. W. Ford Memorial Volume: 12th International Conference of the Cambrian Chronostratigraphic Working Group. New York State Museum Bulletin 510. The University of the State of New York, State Education Department. 94 pages. 2007.

Landing, E., L. Amati and D. Franzi. Epeirogenic transgression near a triple junction : the oldest (latest early-middle Cambrian) marine overlap of cratonic New York and Quebec. Geological Magazine 146:(4):552-566. 2009.

E. Landing, G. Geyer, M. D. Brasier and S. A. Bowring. Cambrian Evolutionary Radiation : Context, correlation, and chronostratigraphy – Overcoming deficiencies of the first appearance datum (FAD) concept. Earth-Science Reviews 123 :133-172. Elsevier. 2013.

Le Sueur, C.A. Observations on a New Genus of Fossil Shells. Journal of the Academy of Natural Science, Philadelphia 1: 310-313. 1818.

Lewis, D. W. Qualitative Petrographic Interpretation of Potsdam Sandstone (Cambrian), Southwestern Quebec. Canadian Journal of Earth Sciences, 8: (8): 853 - 882. 1971.

Mehrtens, C. Comparison of the Monkton and Altona Formations (latest Early-Middle Cambrian): Insights on the paleogeography of the Iapetus shelf. 2015 GSA Northeastern Section Meeting. Geological Society of America Abstracts with Programs 47:(3):101-102. 2015.

Oxley, P. and M. Kay. Ordovician Chazyan Series of Champlain Valley, New York and Vermont, and Its Reefs. American Association of Petroleum Geologists Bulletin, 43: (4): 817 - 853. 1959.

Pitcher, M. G. Evolution of Chazyan (Ordovician) Reefs of Eastern United States and Canada. Ph.D. Dissertation. Columbia University, New York, NY. University Microfilms, Inc. Ann Arbor, MI. #68-8612. 105 pages. 1964a.

Pitcher, M. G. Evolution of Chazyan (Ordovician) Reefs of Eastern United States and Canada. Canadian Petroleum Geology Bulletin, 12: (3): 632 - 691. 1964b.

Selleck, B. and W. Bosworth. Allochthonous Chazy (Early Medial Ordovician) Limestones in Eastern New York: Tectonic and Paleoenvironmental Interpretation. American Journal of Science, 285: (1): 1 - 15. 1985.

Seilacher, A. Trace Fossil Analysis. Springer. New York, New York. 226 pages. 2007

Stone, D.S. Origin and Significance of Breccias along Northwestern Side of Lake Champlain. Journal of Geology 65: 85-96. 1957.

Wieset, D.R. Composition, Grain Size, Roundness, and Sphericity of the Potsdam Sandstone (Cambrian) in Northeastern New York. Journal of Sedimentary Petrology 31: 5-14. 1961.

Yochelson, E. L. and M. A. Fedonkin. Paleobiology of Climactichnites, an Enimatic Late Cambrian Fossil. Smithsonian Contributions to Paleobiology Number 74. Smithsonian Institution Press. Washington, D.C. 74 pages. 1993.

ICE RETREAT AND READVANCE ACROSS THE GREEN MOUNTAIN FOOTHILLS: BOLTON AND JERICHO, VERMONT

STEPHEN F. WRIGHT
Department of Geology, University of Vermont, Burlington, Vermont 05405, swright@uvm.edu

GEORGE E. SPRINGSTON
Department of Earth and Environmental Sciences, Norwich University, Northfield, Vermont 05663

JOHN G. VAN HOESEN
Department of Environmental Studies, Green Mountain College, Poultney, Vermont 05764

INTRODUCTION

This field trip visits several key sites in the towns of Bolton and Jericho Vermont that shed light on the glacial, ice-contact, and lacustrine environments that existed during a relatively short period of time during the retreat of the Laurentide ice sheet across this area. This area lies on the western slope of the Green Mountains, an area dominated by steep slopes and narrow stream valleys that are cut by the broad, low-gradient Winooski River valley (Fig. 1). Stop 1 is a section displaying evidence of at least one cycle of glacial retreat followed by readvance and eventual retreat. Stop 2 visits a working gravel pit where the internal structures of a large delta formed where glacial meltwater flowing south from Bolton Notch entered Glacial Lake Mansfield which occupied the Winooski River valley. Farther north in Bolton Notch Stop 3 visits a series of nested meltwater channels and other ice-contact landforms. The trip finishes at a large landslide section along the Lee River (Stop 4) which

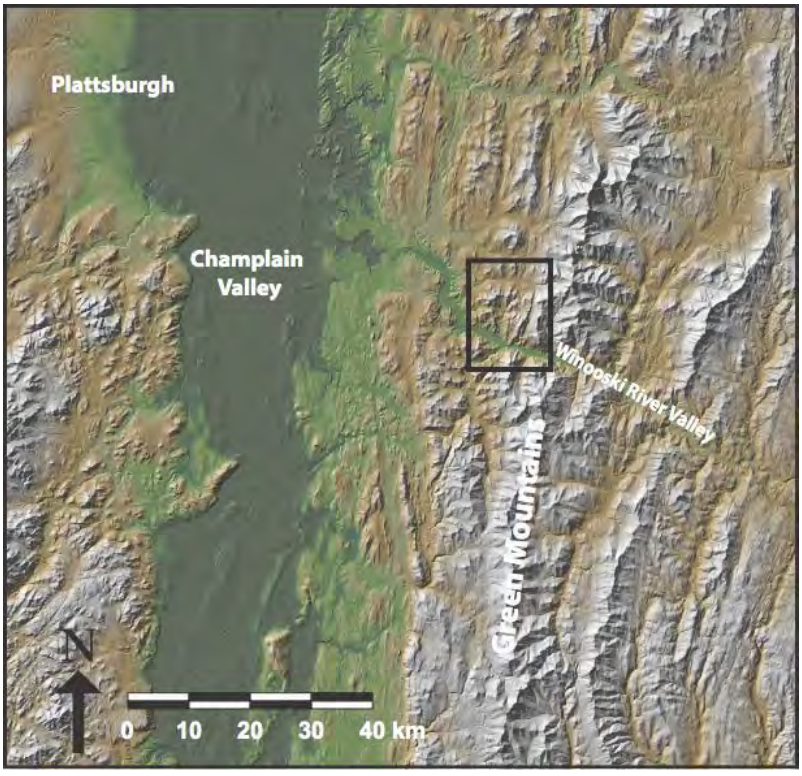

Figure 1: The field trip area is outlined with a box. See Fig. 2 for detailed map.

exposes the full transition from quiet water lake sediments through deltaic sediments where the Lee River delta prograded into the Coveville Stage of Glacial Lake Vermont. The location of all the field trip stops are shown in Figure 2 and more detailed maps accompany the road log. Many of the field stops described in this guide are located on private land. Permission from landowners, noted in the following guide, must be secured before visiting these sites.

Figure 2: A topographic map showing a portion of the Green Mountain foothills cut by the Winooski River which flows WNW towards Lake Champlain. Stop locations are shown as open circles and are labeled on the map. Contours and spot elevations are in meters. Distance measurements in the road log are from the park in the village of Richmond.

GEOLOGIC SETTING

Bedrock Geology

The northern Green Mountains are composed of metamorphic rocks that were (1) originally deposited as sediments in the Iapetus Ocean along the margin of Laurentia, (2) intruded as basaltic dikes and sills through those sediments, or (3) are the now serpentinized tectonic slices of ultramafic rocks derived from Iapetus ocean mantle. The Vermont Bedrock Geologic Map published in 1961 (Doll et al., 1961) interpreted the rocks in the Green Mountains as a largely coherent, yet folded, stratigraphic section. Mapping undertaken during the last 30 years has shown that these rocks are cut by numerous thrust faults occurring on a variety of scales and active during both the Taconic and Acadian orogenies (Stanley and Ratcliffe, 1985; Thompson et al., 1999; Kim et al., 2009). In other words, most geologic contacts within the mountains have been reinterpreted to be tectonic as opposed to stratigraphic contacts. The new Vermont Bedrock Geologic Map and cross-sections (Ratcliffe et al., 2011) clearly display the results of this recent mapping and the reinterpretation of geologic structures.

Small-scale faults, isoclinal folds, and a well-developed foliation associated with the Taconic orogeny are frequently visible in good outcrops. Open upright folds and a spaced cleavage associated with the Acadian Orogeny are also easily visible in many outcrops. The hinge line of the largest of these late Acadian folds, the Green Mountain Anticlinorium, roughly follows the spine of the Green Mountains. This field trip takes place on the west side of the anticlinorium. Good summaries of recent mapping and interpretations in northern Vermont are presented in Thompson et al. (2011) and Kim et al. (2011).

West-northwest-directed thrust faults, active during both the Taconic and Acadian orogenies, and Acadian folding, have produced a mountain range with large-scale structures that generally strike NNE–SSW. These structures, in association with over 350 million years of uplift, differential weathering and erosion, have produced mountain ranges and intervening valleys that are aligned generally NNE—SSW (Fig. 1). Stops 1–3 lie in valleys with this orientation. Rocks in the Green Mountains are also cut by a well-developed joint set oriented ~WNW–ESE. The Lamoille and Winooski rivers both cut across the mountains following ~WSW–ESE courses and many smaller streams, e.g. Mill Brook and the Lee River, follow this course as well (Fig. 1).

Glacial Geology

Current dating of ice sheet retreat across the region indicates that Vermont was deglaciated from southeast to northwest between ~15,500 and ~13,200 calibrated (U-Th) years B.P. (Ridge et al., 2012). The large-scale map pattern of surficial materials in the Green Mountains consists of till-covered mountain slopes adjacent to stream valleys partially filled with variable combinations of ice-contact and/or lacustrine sediments overlain by Holocene alluvium. This pattern is readily visible on the Vermont Surficial Geologic Map (Stewart and MacClintock, 1970) where the drainage networks across the mountains are highlighted by the colors used to denote materials other than till.

The area encompassed by this field trip lies within the NW quadrant of the Camels Hump 15-minute quadrangle mapped by Stewart (1956–1966). Reconnaissance work by Wagner (1972) and detailed mapping of surficial deposits in the town of Jericho by Ladue (1982) both outline a more complex series of surficial units and a correspondingly more complex glacial history than that presented by Stewart's mapping.

Glacial striations measured across the Green Mountains indicate that the regional ice flow was generally from northwest to southeast, obliquely up and over the spine of the Green Mountains (Fig. 3, Wright, 2013). Younger cross-cutting striations in northern Vermont are restricted to the lower elevations and are parallel to the valleys they occur in (e.g. the Champlain Valley, the Lamoille and Winooski river valleys) indicating that late-stage ice-flow was guided by the orientation of the region's valleys as the ice sheet thinned (Fig. 3).

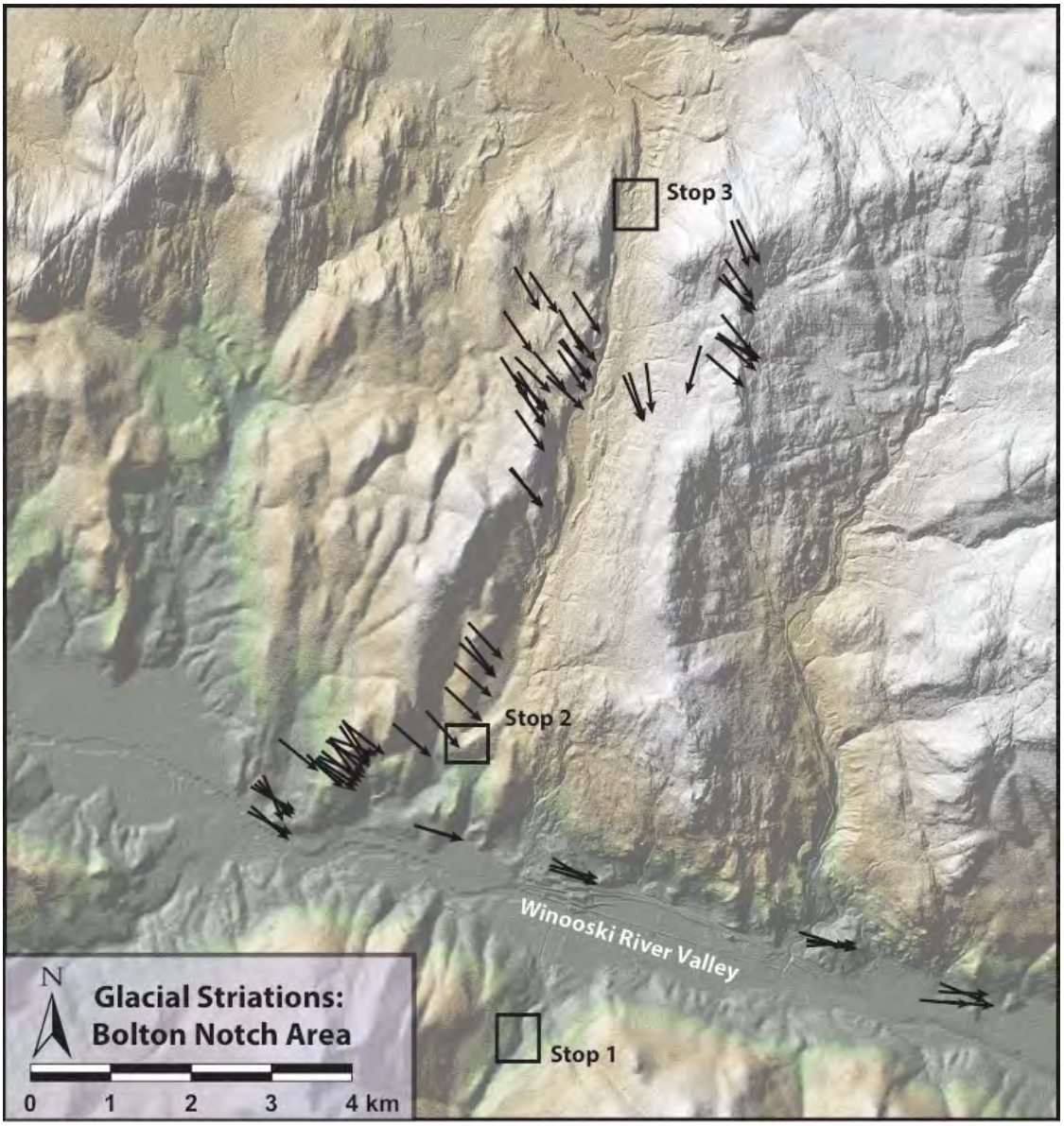

Figure 3: A shaded relief map of the Bolton Notch area showing the orientation of glacial striations. High-elevation striations are uniformly NW to SE and formed when the ice sheet was thick enough to flow obliquely across the mountains. The few striations measured within the notch show some deflection of ice flow to the south, parallel to the orientation of the notch. Striations in the Winooski River valley parallel the valley. Boxes outline the locations of Stops 1–3.

The large rivers in northern Vermont (the Winooski, Lamoille, and Missisquoi) flow generally WNW, across the mountains, and drain into Lake Champlain. As the ice sheet thinned and retreated northward and westward across the mountains, these rivers were dammed producing a series of glacial lakes that inundated these drainage basins (Larsen, 1972, 1987). The largest regional lake was Glacial Lake Winooski that occupied, at its maximum extent, much of the Winooski and Lamoille river drainage basins (Fig. 4). The outlet of this lake was at the drainage divide between the north-flowing Steven's Branch of the Winooski river and the south-flowing Second Branch of the White river, ~13 km south of Barre, at an elevation of 279 m, (915 ft). The isostatically tilted surface of Glacial Lake Winooski rises to the NNW. Based on varve counts from exposures along Muzzy Brook, the Wrightsville Reservoir, and the Waterbury Reservoir, Glacial Lake Winooski existed for no more than ~300 years (Larsen et al., 2001, Larsen et al., 2003) from ~14,090 to 13,790 yr BP,) based on current dating of the North American Varve Chronology (Ridge et al., 2012).

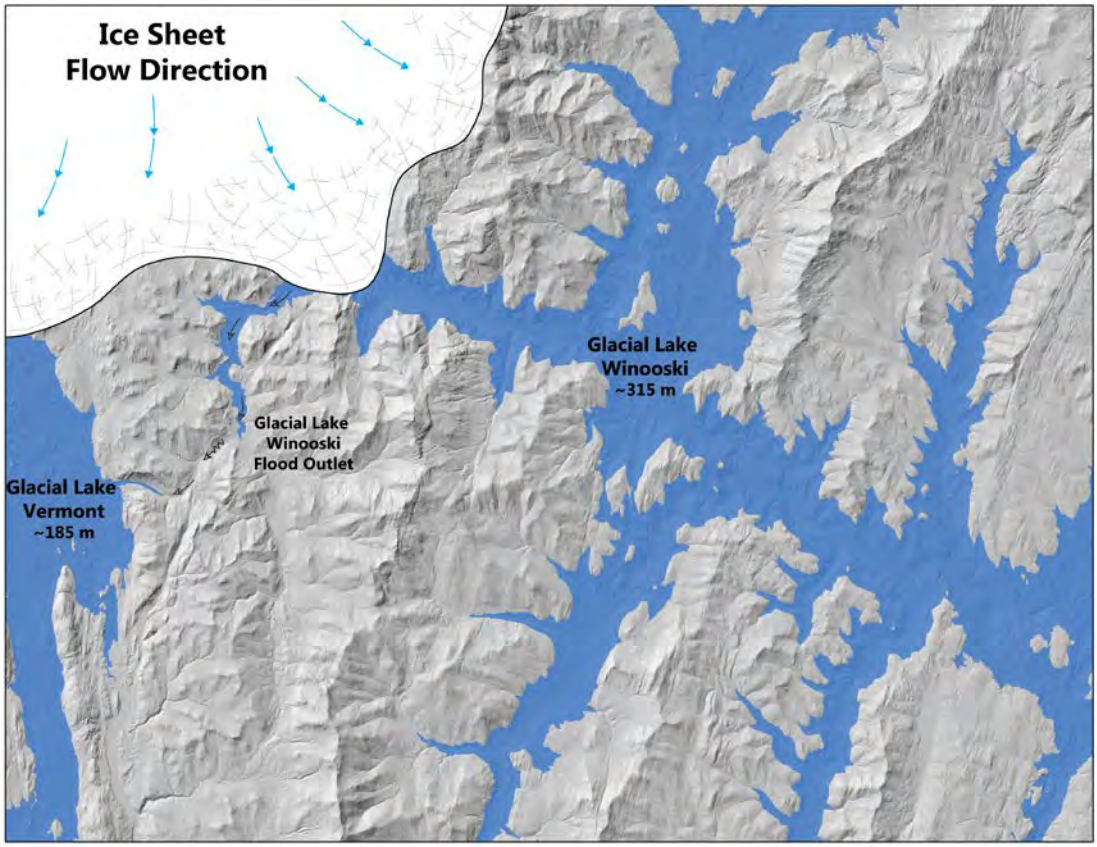

Figure 4: A shaded relief map of north-central Vermont showing the approximate configuration of the Laurentide ice sheet when it dammed the Winooski River valley flooding the drainage basin with Glacial Lake Winooski. A portion of Glacial Lake Vermont occupying the Champlain Valley is also shown. A short additional retreat of the ice sheet from the position shown on the map uncovered two successively lower outlets (the lowest Hollow Brook Outlet is shown as an arrow on the map) which allowed Glacial Lake Winooski to partially drain forming Glacial Lake Mansfield. Labeled lake level elevations are valid for the northwest portion of the map.

Glacial Lake Winooski partially drained when the ice sheet retreated down the Winooski River valley to Jonesville where the impounded water could flow into the Champlain Valley (occupied by Glacial Lake Vermont, Coveville stage) across two successively lower outlets, Gillette Pond and Honey Hollow (Larsen, 1972, 1987, Fig. 4). The ensuing lake (Glacial Lake Mansfield) also occupied much of the Winooski River basin. Continued retreat of the Laurentide ice sheet down the Winooski River valley eventually allowed Glacial Lake Mansfield to drain into the Champlain Valley which was occupied by Glacial Lake Vermont south of the retreating ice sheet. The Winooski river valley was subsequently occupied by an arm of Glacial Lake Vermont.

ACKNOWLEDGEMENTS

We wish to extend our sincere gratitude to the owners of some of the properties visited on this field trip. Specifically these include the owners of the West Bolton Golf course who have granted permission to survey parts of the Golf Course as well as the gravel pit at the north end of Bolton Notch, Sue and Dave Beckman, owners of the active gravel pit at the south end of Bolton Notch, and the McLoughlin family who has allowed this field trip and many UVM students access to the Lee River landslide site.

FIELD GUIDE AND ROAD LOG

New York Meeting Point:

Southeastern parking lot of Hudson Hall (corner of Beekman and Broad Streets), SUNY Plattsburgh campus.

Meeting Point Coordinates: 44.691°N, 73.467°W

Meeting Time: 8:00 AM

Distance				
Cumulative		Point to Point		
miles	km	miles	km	Route Description
0.0	0.0			Turn left out of the parking lot and head north on Beekman Street until reaching Cornelia St.
0.2	0.3	0.2	0.3	Turn right (east) on Cornelia St (NY Rt 3)
0.7	1.1	0.5	0.8	Turn left (north) on Oak St (NY Rt 22N)
1.6	2.6	0.9	1.4	Turn right to merge onto I-87 N
3.0	4.8	1.4	2.3	Take Exit 39 onto NY 314 E toward Cumberland Head. Follow NY 314 to the Plattsburgh-Grand Isle Ferry
7.5	12.1	4.5	7.2	Plattsburgh-Grand Isle Ferry
7.7	12.4	0.2	0.3	After leaving the ferry turn right (south) on West Shore Road (Vt Rt 314)
9.9	15.9	2.2	3.5	Follow West Shore until it intersects Rt 2. Turn right (south). After crossing the causeway, the road traverses part of the modern Lamoille River delta. Old distributary channels are marked by lines of trees growing on the overbank deposits adjacent to the abandoned channels.

20.1	32.3	10.2	16.4	At intersection with I-89, turn right to merge with I-89 S.
39.7	63.9	19.6	31.5	Take Exit 11 and turn right at stoplight (east) on Rt 2 heading towards Richmond.
41.5	66.8	1.8	2.9	At stoplight in the middle of Richmond, turn right (south) on Bridge Street.
41.8	67.3	0.3	0.5	Pull into village parking lot on right just before bridge. The road log that follows will begin and end here. Participants wishing to car pool may leave their cars here.

Vermont Meeting Point

Richmond Village Park, Bridge Street, Richmond Vermont

Meeting Point Coordinates: 44.413 º N, 73.001 º W

Meeting Time: 9:15 AM

Distance				
Cumulative		Point to Point		
miles	km	miles	km	Route Description
0.0	0.0			Turn left out of the parking lot and head north on Bridge Street until reaching the stoplight at the intersection of Route 2.
0.3	0.5	0.3	0.5	Turn right and follow Route 2 East, up the Winooski River valley to the village of Jonesville.
2.9	4.7	2.6	4.2	Abandoned oxbow of the Winooski River on right.
3.8	6.1	0.9	1.4	Jonesville. Turn right at intersection with Cochran Road crossing first the railroad tracks and then the bridge over the Winooski River.
3.9	6.3	0.1	0.2	Turn left (east) at first intersection past bridge onto Duxbury Road and continue up the Winooski River valley, now on the south side of the river.
4.8	7.7	0.9	1.4	Roche Moutonnée on right, immediately adjacent to road. Grooves and striations on the smooth, abraded top and west sides of the roche moutonnée are oriented ~095, parallel to the river valley and the east side has been quarried, indicating ice was flowing ESE, up the river valley.
5.7	9.2	0.9	1.4	Honey Hollow Road intersection: Low-water access to Stop 1 is 0.5 miles up this road.
6.1	9.8	0.4	0.6	Catamount Trail Parking Lot (“P” in Fig. 3). High-water access to Stop 1 is by hiking ~1 km up (south) along the Catamount Trail that leaves from the parking lot. Several large rouche moutonnée are visible across the valley to the north on the south side of Stimson Mountain. All have an asymmetry similar to the one exposed along the road (smooth side facing WNW, quarried side facing ESE).

STOP 1: Preston Brook Landslide

Location Coordinates: 44.371° N, 72.900 ° W

Stop 1 is a large landslide along the east side of Preston Brook in Honey Hollow, a steep, narrow N–S valley typical of the Green Mountains (Fig. 5). There are two ways of accessing this field site. If the water level in Preston Brook is low enough, the bottom of the slide can be accessed by driving 0.5 mile up Honey Hollow road (see above road log) and parking at a small pull-off where a red iron gate blocks an overgrown logging road. The base of the slide is approximately 200 m SE of the iron gate. There is no trail. When Preston Brook is too high to cross, the top of the slide can be accessed by hiking ~1 km up the Catamount Trail to where a gently sloping alluvial terrace separates the trail from the top of the landslide.

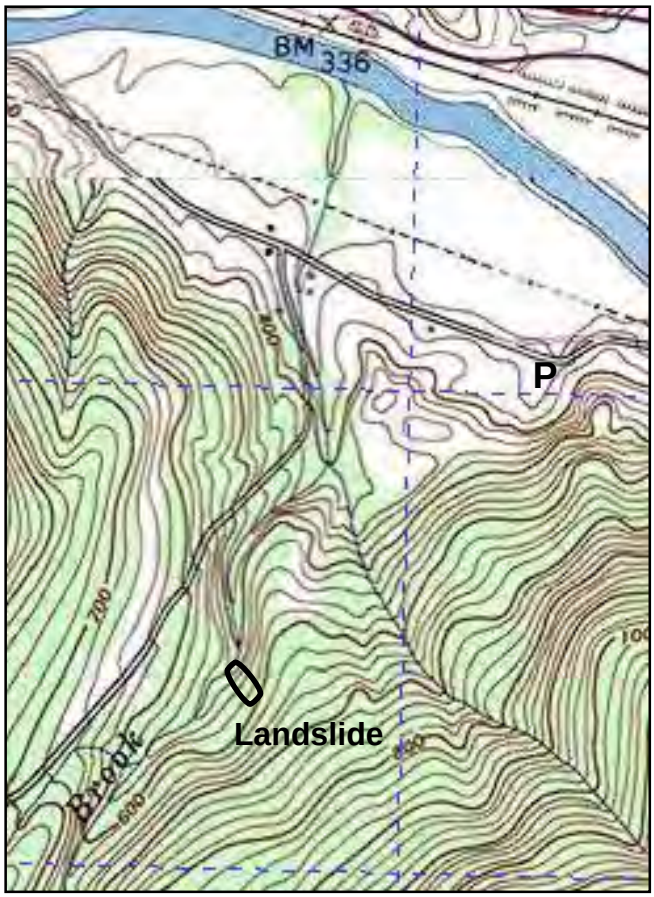

Figure 5: Topographic map showing the location of the landslide (Stop 1) above Preston Brook and the Catamount Trail parking area ("P"). The Winooski River crosses the northern half of the map.

Wright first observed this section in 2008 and as of this writing the exposures are still quite good. Please anticipate that they may not remain so in the future. Continuing slope movements change which parts of the section are visible at different times. Parts of the section are very steep and quite wet. Caution and sturdy/waterproof footwear are recommended.

The landslide exposes an approximately 30 m high section containing lacustrine sediments at three stratigraphic levels separated by both diamict and coarser-grained ice-proximal sediments (Fig. 6). The description that follows divides the section into "Lower,""Middle," and "Upper" parts which are separated by covered intervals. Lacustrine sediments exposed in the "Lower" and "Middle" parts of the section are deformed. One objective of this stop is to ascertain whether structures in these deformed sediments formed by (1) a readvance of the ice sheet or (2) whether they formed during one or more landslides (debris flows) in this narrow, steep-sided mountain valley.

Lower Section

The lowest part of the section (stream-level) consists of fine-grained lacustrine sediments that are folded, faulted, and over-consolidated (Fig. 6). These deformed sediments are overlain by a boulder/cobble/pebble-rich diamict(?). This in turn is overlain by a boulder/cobble gravel that

generally fines upwards into a sequence of sediments consisting largely of silt and very fine sand, with irregular lenses of coarser sand, pebbles, and cobbles (Fig. 6). Bedding is sometimes coherent, but also occurs as a slumgullion of lenses and irregular blebs or isolated fragments of silt/clay or rocks surrounded by finer grained sediments. The finer sediments are very compact and appear to be over-consolidated. Near the top of the lower section an approximately 10 cm thick bed of laminated silt and very fine sand has been both folded and apparently injected (dike-like) into the overlying sediments (Fig. 7). To the right (south) of the fold hinge bedding is continuous at least a short ways down section. To the left (north) of the fold hinge bedding has been pealed/delaminated away from the underlying sediment and highly deformed sediment occupies the space above the now overturned limb of the fold.

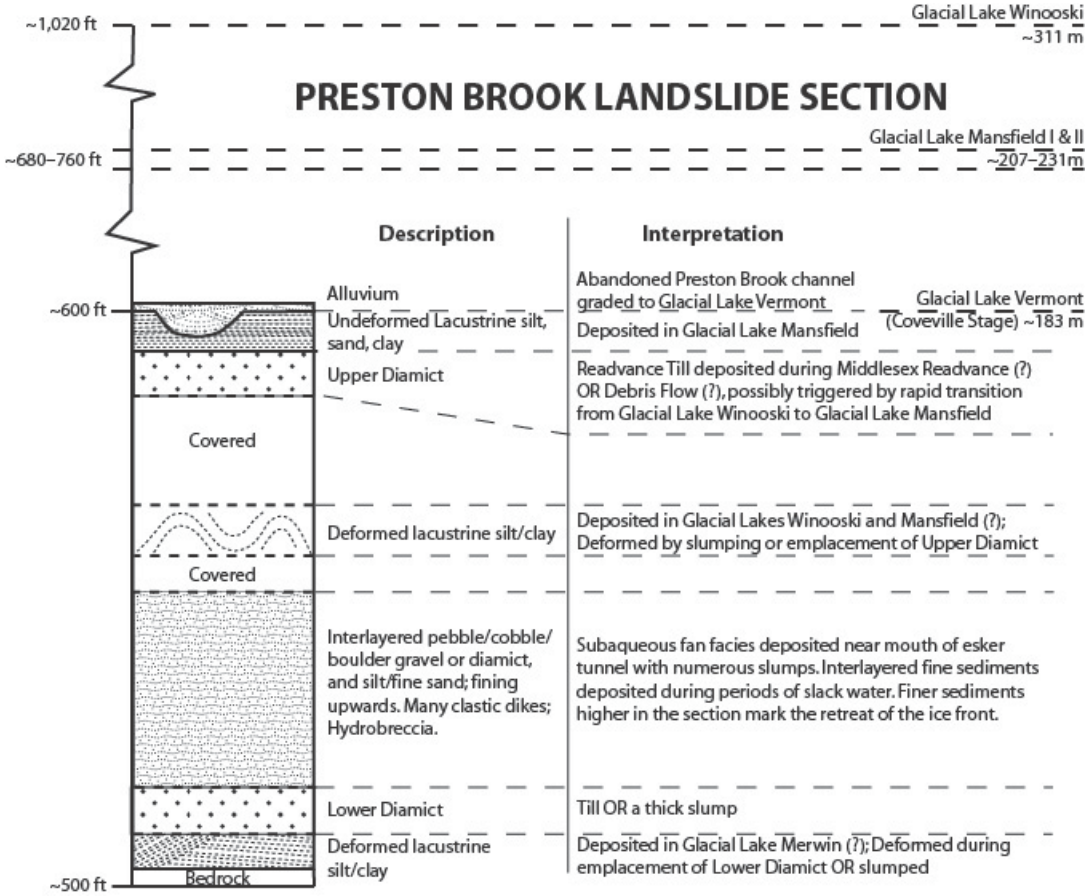

Figure 6: Description and interpretation of the Preston Brook landslide section that extends upwards from the brook to an abandoned fluvial terrace (see Fig. 3 for location). The section exposes three separate units of lacustrine sediments separated by both diamict and glaciofluvial sediments. The lower two units are deformed as a consequence of emplacement of the diamict as till during a glacial readvance or as till remobilized during an underwater landslide. The uppermost part of the section consists of alluvium deposited when Preston Brook flowed across the sediment-filled valley into Glacial Lake Vermont.

Middle Section

The middle part of the section is largely covered and water-saturated, but small exposures consist of silt and clay layers (varves) that have been deformed into meter-scale folds (Fig. 6). The present limited exposure makes it impossible to know whether (1) the entire section is

deformed or (2) whether the deformation is intraformational (i.e. the folds occur only within one stratigraphic horizon and are overlain by undeformed sediments).

Upper Section

The upper part of the section consists of diamict (till?/landslide debris?) overlain by rhythmically bedded (varved) very fine sand, silt, and clay (Fig. 6). While some layers contain intraformational slumps, particularly at the base, this section is undeformed. The lacustrine sediments are overlain by a thin veneer of alluvium which extends across a gently north-sloping terrace (between the landslide headwall and the Catamount trail) and marks the top of the section. An old alluvium-filled stream channel cuts across the uppermost section of lacustrine sediments (Fig. 6).

Figure 7: An exposure of folded and now overturned layer of laminated fine sand and silt that has been "pealed/delaminated" from the underlying beds. Irregular lenses and blebs of medium/fine sand, coarse sand, pebbles and cobbles occur to the left of the fold hinge in the space where the folded layer used to be.

Interpretation

The Preston Brook valley (Honey Hollow), similar to other valleys in the Winooski River basin, was partially flooded by Glacial Lakes Winooski, Mansfield, and Vermont (upper Coveville stage) as the ice sheet retreated NNW (down) the Winooski River valley (Fig. 4). The top of the landslide scarp is at an elevation of ~600 feet (~185 m) which is at or below the elevation of all these lakes (Fig. 6). It is unclear which of the lacustrine sediment units exposed in this section

were deposited in which of these lakes or within a lake that may have preceded the formation of Glacial Lake Winooski. In the interpretation that follows, we have suggested a sequence of events that is consistent with the sediments exposed in this section and our understanding of the glacial history in the Winooski River valley, but other interpretations are also possible.

The fine-grained lacustrine sediments at the bottom of the section indicate that at the time these sediments were deposited, the ice sheet had retreated down the Winooski River valley west of the mouth of Preston Brook in order to flood the valley with lake water. We suggest that this lake formed in the Winooski River valley before the Middlesex Readvance that Larsen (1999) referred to as Glacial Lake Merwin. The tilted, faulted, folded, and over-consolidated nature of these sediments, in conjunction with the overlying diamict, suggest that they were overridden during a readvance of the ice sheet into the Preston Brook valley, the Middlesex Readvance. This readvance occurred during an approximately 100-year long cold period between 13,900 and 14,000 yr b2k and is coeval with the Littleton Readvance in northwestern New Hampshire (Ridge et al., 2012, Thompson, 1999). During this readvance the ice sheet reclaimed most of the Winooski River drainage basin as evidenced by sections of deformed sediments in many of the river's tributary valleys (Larsen 1999, 2001; Larsen et al. 2003; Wright 1999, 2002, 2015).

Glacial Lake Winooski began to form at the end of the readvance when the ice once again began retreating WNW down the river valley. The coarse boulder/cobble gravels that overlie the lower diamict suggest they were deposited near the mouth of an esker tunnel as the ice sheet retreated across this area. The fining up sequence of fluvial sediments that overlie the coarse gravels were most likely deposited in a subaqueous fan that became progressively finer grained as the ice sheet retreated west of the Preston Brook valley. Continued retreat of the ice established a quiet-water arm of Glacial Lake Winooski in the valley when the varved silt/clay sediments in the middle section were deposited. However, by the time the ice retreated far enough down the Winooski River valley to expose the Preston Brook valley only 2 km of additional ice retreat allowed Glacial Lake Winooski to catastrophically drain through the Huntington River and Hollow Brook valleys across two different thresholds to form Glacial Lake Mansfield (Fig. 4). Elsewhere in the Winooski River valley this initial lake elevation drop of ~80 m is stratigraphically instantaneous and clearly recorded by an abrupt increase in grain size (Larsen et al., 2003). Very little of the middle part of the section is exposed, but we suspect that these fine grained, ice-distal, lacustrine sediments were deposited in both Glacial Lakes Winooski and Mansfield and, if better exposed, would show the transition between the two lakes.

The large folded layers of silt/clay visible in the exposed part of the Middle Section may have formed by slumping or they may have formed from shear stresses imparted when the upper diamict was emplaced. One interpretation is that the diamict formed from a debris flow (consisting of remobilized till mixed with lacustrine sediments) originating on the steep valley side that flowed into the lake-flooded valley. After entering the lake the debris flow triggered further slumping/deformation in the already-deposited sediments now exposed in the lower and middle parts of the section (Fig. 7). This slumping may have been triggered by the catastrophic drainage event associated with the transition from Glacial Lake Winooski to Glacial Lake Mansfield.

If the upper diamict is interpreted as a debris flow deposit, then the lacustrine sediments deposited on top of the diamict are most likely Glacial Lake Mansfield sediments as they were deposited in relatively quiet water and the elevation of Glacial Lake Vermont (Coveville Stage) in the valley is only slightly higher than the elevation of these sediments (i.e. when Glacial Lake Vermont occupied the valley this area would have been close to its shoreline).

Another interpretation is that the diamict is a readvance till and deformation in the underlying section was produced by movement of the overlying ice sheet. If this diamict was produced during the Middlesex Readvance, then all the underlying sediments are older than Glacial Lake Winooski and the thin section of lacustrine sediments lying above the diamict were deposited in Glacial Lake Winooski. It is also possible that this diamict records a more recent readvance of the ice sheet, although there isn't any indication in the ice core records of another cold period capable of producing a readvance during the waning stage of Glacial Lake Winooski (~13,700 yr b2k). Unlike the lower diamict, the upper diamict is overlain by sediments deposited in quiet water. If this upper diamict is a till deposited during a readvance, subglacial conduits did not funnel high-energy sediments in the valley as the ice was retreating.

The uppermost lacustrine sediments are cut by a large channel filled with a poorly sorted pebble/cobble/boulder gravel and are overlain by a thin layer of similar sediments interpreted to be historical Preston Brook alluvium. The abandoned stream terrace at the top of the section grades to the elevation of the Coveville stage of Glacial Lake Vermont (Fig. 6). This indicates that the valley was locally filled with at least 100 feet (30 m) of sediment when Preston Brook began incising its present channel when the elevation of Glacial Lake Vermont dropped from the Coveville to Fort Ann stage.

Distance				
Cumulative		Point to Point		
miles	km	miles	km	Route Description
6.1	9.8			Catamount Trail Parking Lot ("P" in Fig. 3).
8.3	13.4	2.2	3.5	Retrace route back west along the Duxbury Road and turn right (north) at Cochran Road recrossing both the Winooski River and the RR tracks.
8.4	13.5	0.1	0.2	Jonesville. Turn right on Rt 2 heading east along the north side of the Winooski River.
9.5	15.3	1.1	1.8	Turn left heading north on the Bolton Notch Road. Road pitches up very steeply as it ascends the face of the Bolton Notch Delta and the entrance to a large gravel pit excavated in that delta.
10.3	16.6	0.8	1.3	Bolton Notch Delta terrace on left. Park at pull-off on left (west) side of road. Pit is owned by Sue and Dave Beckman. Please request permission before visiting.

STOP 2: Bolton Notch Delta

Location Coordinates: 44.391° N, 72.910° W

The active gravel pit on the west side of the road is excavating deltaic sediments deposited by a north-flowing stream originating in Bolton Notch. This is a large delta and many of the foreset and topset beds are composed of very coarse gravels with some very large (m-scale) lag(?) boulders (Fig. 8). The size of the drainage basin is small which suggests that the high-energy stream that built the delta was fed directly by melting ice retreating up the notch and/or by drainage out a glacial lake that formed on the north side of the notch (Fig. 9). No deltas occur (or are not preserved) in other stream valleys farther east suggesting that the Bolton Notch delta formed quickly during a time span too short for significant non-glacial deltas to form in adjacent stream valleys.

Figure 8: Coarse topset beds at the Bolton Notch delta consist of poorly sorted boulder, cobble, pebble, and coarse sand gravels and indicate that a very high-energy stream fed this delta. Large boulder at top-left of photo exceeds 1 m in diameter. Similar large boulders also occur in the underlying forset beds and appear as strong hyperbolic reflectors in GPR profiles.

Well-developed foreset and topset beds are usually exposed in the pit. These are overlain by a thin (~2 m) sheet of medium to fine sand. Duck Brook has eroded a deep channel through this delta isolating an erosional remnant of this deltaic terrace on the west side of the brook. The elevation of the topset/foreset contact, measured using a Trimble GPS, is ~233 m (+/- 1 m). With ~4 m of isostatic uplift[1], this corresponds with the higher 229 m Gillette Pond outlet of Glacial Lake Mansfield (Larsen, 1987, Fig. 7).

The geometry of the ice margin at this time suggests that the Gillette Pond outlet was tenuous at best (Fig. 9).The medium to fine sand overlying the coarse topset beds of the delta was most likely deposited when the lake deepened for a short period of time, drowning the delta (i.e. the delta moved farther up the Bolton Notch valley and only fine-grained bottomset sediments here). A minor readvance of the ice sheet could easily have closed the Gillette Pond outlet allowing the lake elevation to rise for a limited period of time (Fig. 9). Similarly, a relatively small 1–2 km retreat of the ice margin uncovered a lower elevation outlet (Hollow Brook) which allowed the lake elevation to drop ~25 m.

[1] Based on an almost due north uplift slope of 0.7 m/km (Rayburn, 2004)

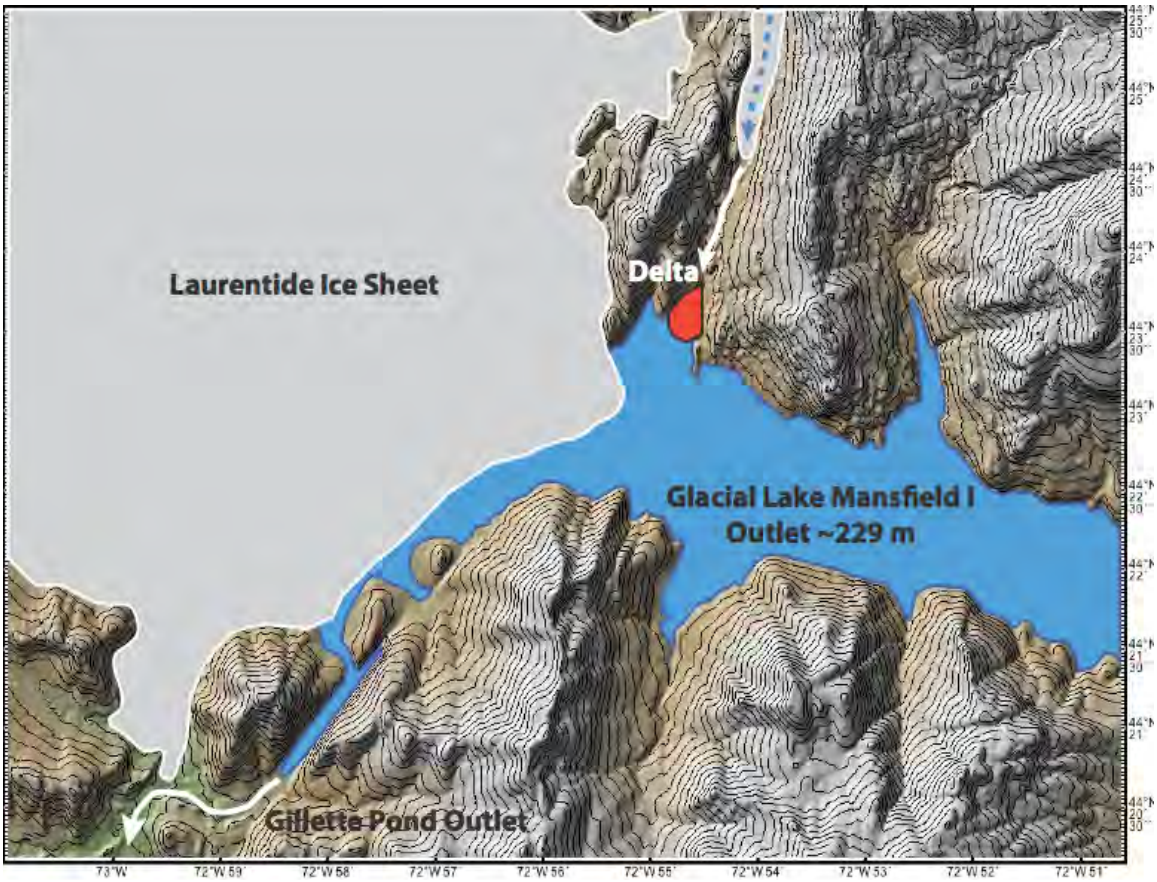

Figure 9: Map depicts the position of the ice sheet when it dammed Glacial Lake Mansfield in the Winooski River valley during the time when the lake utilized the Gillette Pond outlet. The delta at the south end of the Bolton Notch valley (Stop 2) was rapidly built from coarse sediments transported by a high-energy stream emanating from a tongue of the ice sheet in the notch.

Distance				
Cumulative		Point to Point		
miles	km	miles	km	Route Description
10.3	16.6			Stop 2: Bolton Notch Delta. Continue driving north on the Bolton Notch Road.
12.3	19.8	2.0	3.2	Long Trail crosses road. Note: During the summer of 2015 the Long Trail will be rerouted east of here on Stimson Mountain and the trail that crosses here will become an access trail to the Long Trail.
13.4	21.6	1.1	1.8	Continue driving north on the Bolton Notch Road until the road crosses from the east to the west side of the valley. Park on the right side of road just before the gate to an abandoned gravel pit.

STOP 3: Bolton Notch

Location Coordinates: 44.433 N, 72.896 W

Bolton Notch is a north-south U-shaped valley bounded by near vertical bedrock cliffs on either side of a valley floor filled with an unknown thickness of talus, lacustrine, and fluvial sediments. A poorly drained part of the valley floor marks the drainage divide at an elevation of 1180–1200 ft (~365 m) asl (Fig. 10). The objective of this stop is to observe and offer interpretations of (1) a series of terraces and channels that likely formed during ice retreat, (2) a group of kettles occurring immediately south of the gravel pit, and (3) ice-contact and lacustrine sediments exposed in the gravel pit. All of these features occur at or immediately north of the drainage divide. A detailed map of many of the small-scale landforms occurring near the drainage divide of the notch was made at an original scale of 1:4,000 using a hand-held GPS device (Fig. 11).

Striation Data

Striation measurements in the area surrounding the notch indicate a very consistent NW to SE direction of ice flow (Figs. 3, 10). Few measurements have been made on the steep valley sides; however some striations on the lower slopes show deflection to a NNW to SSE direction suggesting that ice flow rotated parallel to the valley as the ice sheet thinned, although the length of time the ice flowed in this direction was probably relatively short. Therefore, despite the distinctive "U" shape of the valley, this form may be more strongly linked to differential weathering and erosion of a relatively weak lithology underlying the valley rather than erosion by moving ice.

Terraces

A nested group of terraces occur along the eastern side of Bolton Notch, near the drainage divide. They are all aligned NE–SW, oblique to the N–S orientation of the valley, and all slope gently to the southwest (Fig. 11). The southernmost terraces are the highest and they progressively step down to lower elevations farther north. The lower-elevation terraces cross-cut adjacent higher-elevation terraces. The elevation difference between adjacent terraces typically ranges between 2–5 m. The most northerly of the terraces leads into a distinctive channel (now flooded) that occupies most of the area at the drainage divide. Farther south this pond drains and forms the modern stream channel that cross-cuts all of the higher terraces (Fig. 11). Most of these terraces are floored with till, but some also contain poorly rounded cobbles and boulders, particularly notable where these materials have been incorporated into stone walls.

These nested terraces are interpreted to be abandoned glacial meltwater channels that formed from water discharging from a tunnel beneath the glacier. This water flowed between the retreating ice front and the steep valley side or older, higher terraces. From south to north, these different terraces, at successively lower elevations, mark the position of the retreating glacier, perhaps at yearly intervals (Fig. 11). It was this glacial meltwater, flowing south through the notch and towards the Winooski River valley, that supplied most of the sediment that accumulated in the Bolton delta (see Stop 2).

Kettles

Several kettles occur in the bottom of the valley south of the gravel pit and two of the larger ones are shown on the detailed map (Fig. 11). Several of the abandoned meltwater channels abruptly drop into the pond suggesting that the pond too is a kettle or network of kettles and streams emanating from the glacier flowed directly across stagnant ice. The implication is that as the retreating ice thinned across the drainage

divide, it thinned enough so it could no longer flow and became stagnant and disconnected from the thicker, still active ice front north of the divide.

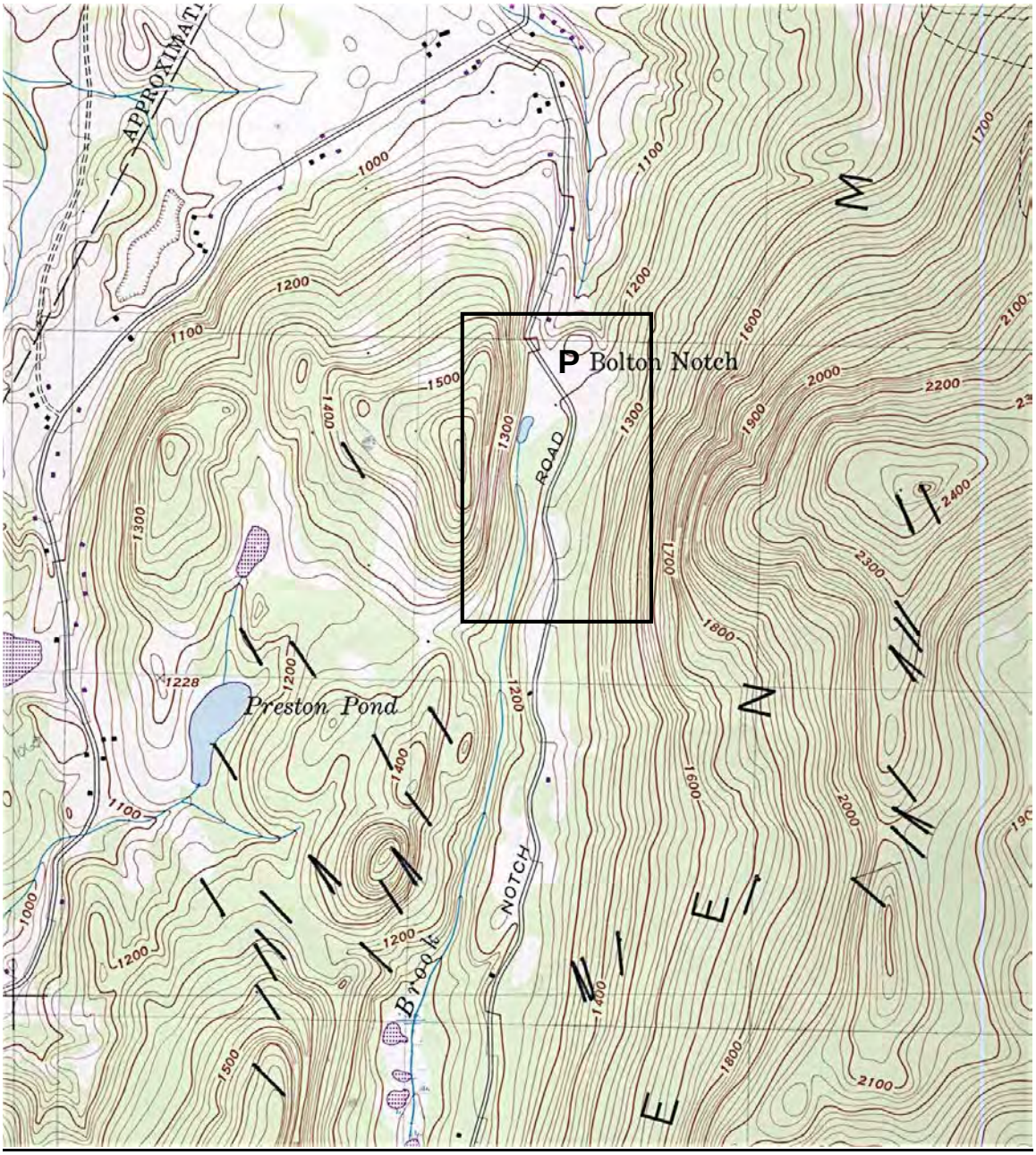

Figure 10: A topographic map of Bolton Notch and surrounding areas. Black lines represent the orientation of glacial striations. In all cases the measurement location is at the northwestern end of the line. "P" denotes the location of the abandoned gravel pit. Box outlines boundary of more detailed map (Fig. 11). Boxes are 1 km square and outline the NAD27 UTM grid. North is to the top of the page.

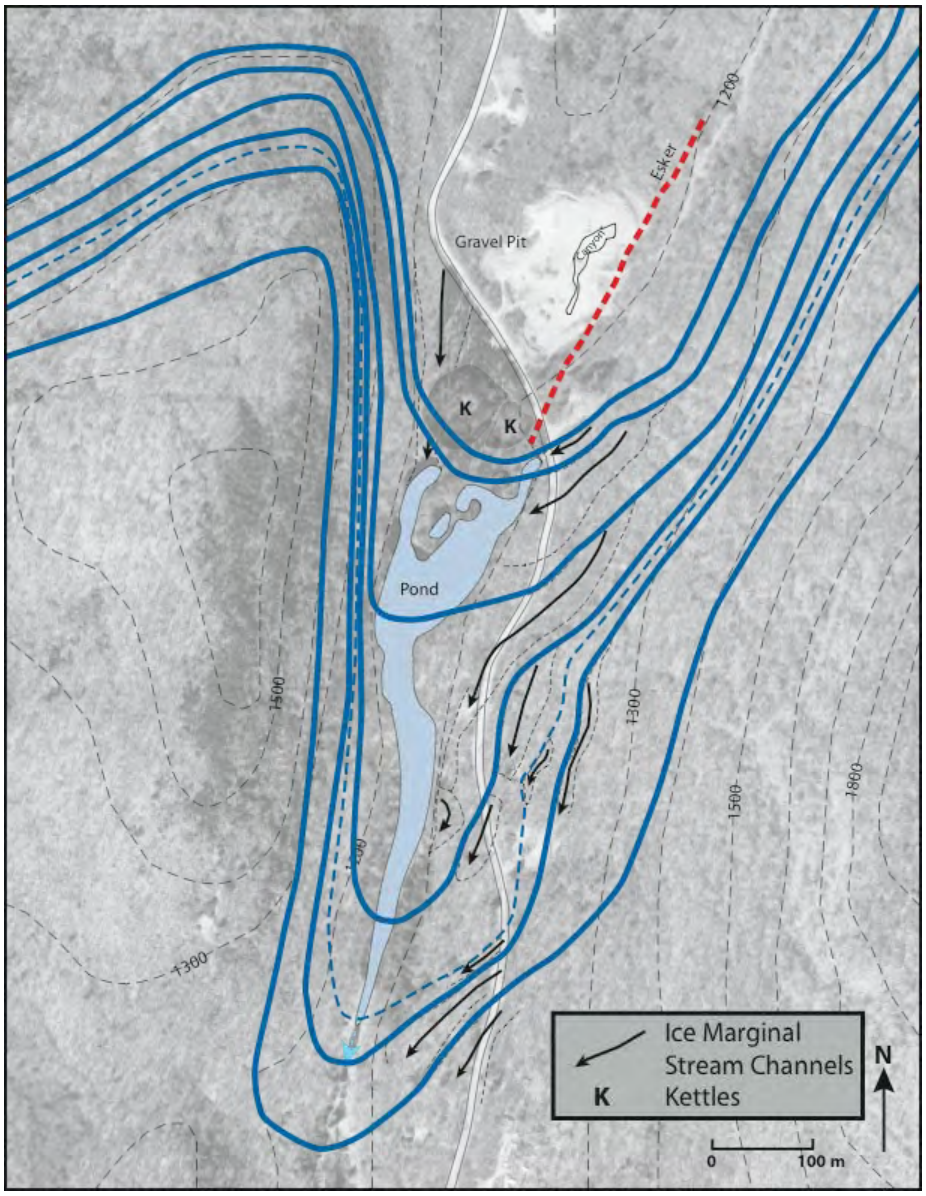

Figure 11: A detailed map of the northern end of the Bolton Notch valley. The pond marks the drainage divide. Arrows show the direction of stream flow along nested fluvial terraces. The highest (and oldest) terraces are to the south and east and progressively step down in elevation to the north and west. These are interpreted as meltwater stream terraces that formed adjacent to the retreating ice sheet as it progressively thinned and retreated to the north. Blue lines mark six different positions of the ice margin are shown and may mark annual retreat positions. Several kettles "K" occur north of the pond. Several of the channels abruptly drop into the pond suggesting that the pond too is a kettle or network of kettles and streams emanating from the glacier flowed directly across stagnant ice. A dashed line along the eastern side of the gravel pit shows the location of an esker. The esker is mantled by lacustrine sediments that accumulated in a small lake that formed when the ice sheet retreated north of the drainage divide. Contours are in feet. Vertical GPS control in this narrow valley was insufficiently precise to accurately contour this map.

Gravel Pit Geology

An old gravel pit lies along the north side of the road, at the northern end of Bolton Notch (Figs. 10, 11). The pit exposes sediments deposited in both an esker and a small glacial lake that formed as soon as the ice front retreated north of the drainage divide. The trace of the esker is shown on Figure 11. While many of the pit faces are slumped, an amazing vertical walled "canyon" has formed between two levels of the pit and offers excellent exposures of sedimentary structures (Fig. 12). Material eroded from this canyon has formed a large alluvial fan immediately below the northern end of the canyon.

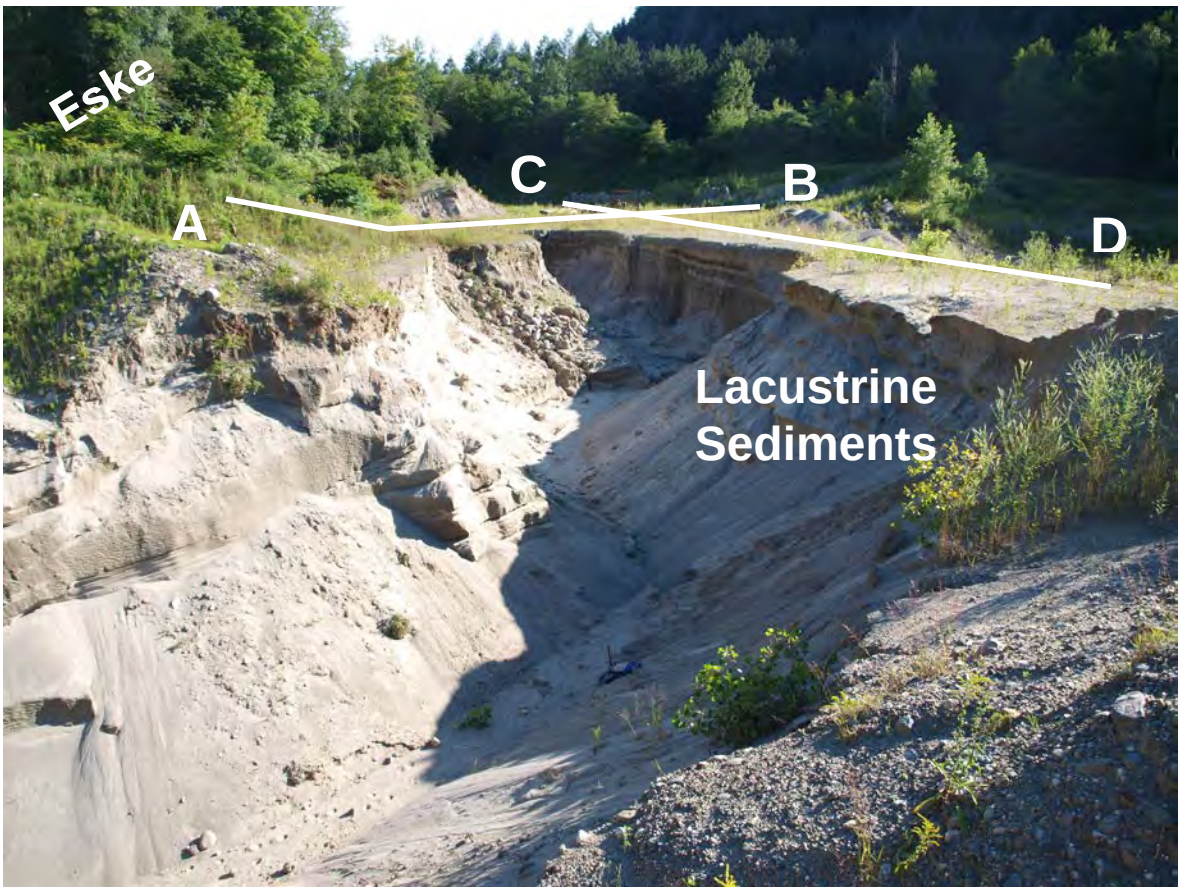

Figure 12: A view within abandoned sand/gravel pit looking south into the upper reach of a deep "canyon" eroded by ephemeral drainage into the bottom of the pit. An esker lies along the wooded left side of the photograph whereas the lacustrine sediments exposed in the canyon were deposited in a small lake whose outlet was a short distance south of the woods in top-center of the photo. White lines show the approximate location of the GPR survey transects shown in Figures 14 and 15.

Much of the esker has been quarried away, but many large rounded boulders occur on the floor of the pit at its southern end and very coarse sediment with additional boulders occurs along the pit's slumped face immediately below and northeast of the road. Many of the boulders deposited in the esker tunnel are high-grade metamorphic rocks (Grenville-age gneisses) that are distinctly erratic to northwestern Vermont and were transported here from the northern Adirondack Mountains or the Laurentian Mountains north of Montréal.

The bulk of the material currently exposed in the pit consists of medium to very fine sand and silt with occasional, relatively thin beds of coarse sand and pebble gravel. Dropstones are common. Cross-bedding and climbing ripples, frequently in beds >1 m in thickness, occur in many beds and all indicate that currents were dominantly flowing to the south, towards the notch. Structureless beds of medium to fine sand imply that these beds are slumped. Coherent blocks of bedded sediment have also slid off the steep side of the esker into deeper water (Fig. 13). There is a general fining-up pattern where the thickest beds of coarse sediment occur in the deepest parts of the pit and the finest interlayered fine sand/silt horizons occur at the uppermost part of the pit. Soft sediment deformation by slumping and/or differential loading is

extensive in some beds.

Figure 13: View of faulted lacustrine sediments (fine sand) exposed in the middle of the "canyon." A coherent block of sediment (bedding parallel to fault plane), slid from its original position higher on the flank of the esker into deeper water along the fault plane during an underwater landslide.

The fine lacustrine sediments exposed here indicate that a small glacial lake existed here once the ice sheet retreated north of the drainage divide (Figs. 10, 11). The lowest elevation channel, leading to and through the pond, marks the final outlet to this lake at an elevation of ~1,190 ft/363 m (Fig 11). This lake was likely small and short-lived as less than 1 km of further ice retreat to the northwest would have uncovered a much lower outlet to the Winooski River valley via the Indian Brook drainage (outlet elevation 920 ft/280 m).

A ground penetrating radar (GPR) survey shows that in the central part of the pit an esker is buried by a sequence of lacustrine sediments that outcrop in most of the pit (Fig. 14). Another GPR survey line emphasizes the continuity of these beds (Fig. 15). The 100 GHz antenna shows coherent reflectors to a "depth" of 300 ns (Fig. 14) whereas penetration with the 200 GHz antenna does not extend much below 150 ns (Fig. 15). However, the 200 GHz antenna shows sedimentary structures in much more detail.

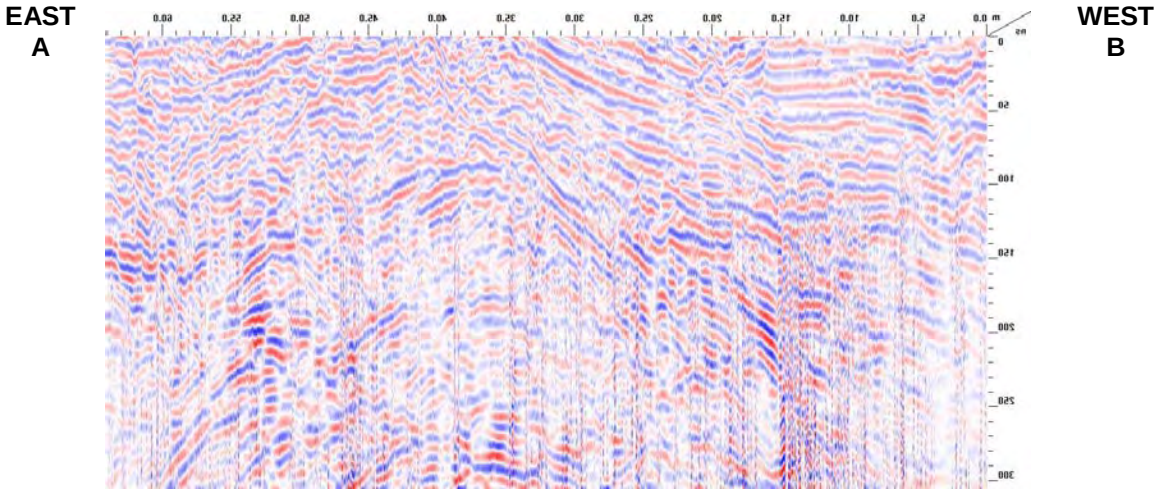

Figure 14: An East–West GPR profile across the floor of the Bolton Notch gravel pit showing the convex-up beds of an esker buried by on lapping lacustrine sediments that show an apparent dip to the west, steeply over the side of the esker and more gently in the basin to the west. 100 MHz antenna. Note that the profile was rotated about a vertical axis to correspond with the orientation of the photograph (Fig. 12) showing the location of the survey.

The large volumes of sand, frequently deposited as meter-thick beds of climbing ripples from south-flowing currents, implies that sediments in this glacial lake originated from a subglacial drainage system, i.e. meltwater and sediments discharging through a tunnel, which formed a subaqueous fan that fined upwards as the ice front receded to the north. Given the small size of the lake basin and the high sedimentation rates at the mouth of subglacial tunnel, the lake probably rapidly filled with sediment. At the northern end of the canyon a large (>15 m wide) channel filled with coarse sand and pebble/cobble gravel cuts across the finer lacustrine sand. This is interpreted to be a stream channel extending from the receding glacier to the drainage divide that was eroded through the recently deposited lacustrine sediment that largely filled the lake basin.

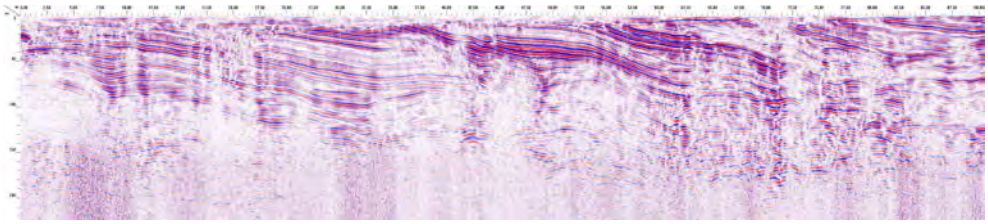

Figure 15: Gently north-dipping continuous beds of lacustrine sand (an apparent dip; real dips are to the NW) are well-imaged in this South–North GPR profile using a 200 MHz antenna (see Fig. 12 for location of survey line). Bedding is truncated by the floor of the pit. These beds were deposited on the western flank of an esker in a small ice-dammed lake when the ice margin was a short distance to the north.

Distance				
Cumulative		Point to Point		
miles	km	miles	km	Route Description
13.4	21.6			Stop 3: Bolton Notch
14.1	22.7	0.7	1.1	Continue driving north on the Bolton Notch Road until reaching a T-intersection with Stage Road. Turn right (north) on Stage Road passing along the boundary of the West Bolton Golf Course.
14.4	23.2	0.3	0.5	West Bolton. Turn left (west) at the 4-way intersection onto Nashville Road.
15.5	24.9	1.1	1.8	West Bolton Flats
18.3	29.5	2.8	4.5	Intersection with Browns Trace Road. Kame deposits with numerous kettles occur both south and west of the road intersection and were described by Wagner (1972) on an earlier NEIGC field trip. Note the many rounded cobbles and boulders in the stone walls. Turn right (north) and drive through the village of Jericho Center.
19.5	31.4	1.2	1.9	Jericho Village
19.9	32.0	0.4	0.6	Turn left (west) on Plains Road.
21.0	33.8	1.1	1.8	Follow Plains Road until its intersection with Schillhammer Road and carefully park along the side of the road so as to not block traffic. *This stop lies on private property and permission must be gained before trying to access the site.*

STOP 4: Lee River Delta (2 hours)

Location Coordinates: 44.485° N, 72.985 W

A large landslide has been recurrently active along an outside meander bend of the Lee River for at least the last 15 years revealing an almost 100 ft (30 m) high section (Fig. 16). From year to year exposures vary, but key parts of the section can be excavated where slumped. The section offers the opportunity to see the almost complete transition between relatively deep water lacustrine sediments upwards through a classic Gilbert-style delta which was deposited in the higher, Coveville stage, of Glacial Lake Vermont. This site lies on private property. Please contact the McLoughlin family (Plains Road, Jericho) for permission to visit the site.

The lowest part of the section is frequently slumped, but consists of rhythmically bedded silt and clay (varves) with occasional dropstones. Bedding is approximately horizontal. Farther up the section the summer silt layers frequently contain beds of medium to fine sand, some of which contain well-preserved asymmetric ripples. Ripples and cross-beds here and farther up the section consistently indicate current flow was to the northwest at the time these sediments were deposited, parallel to the modern course of the Lee River.

The proportion of sand in the section rapidly increases upsection. Winter clay layers are usually present and indicate that the annual accumulation of sand often exceeded 1 m/year. Asymmetric ripples, climbing ripples, and graded beds are common in these still horizontally

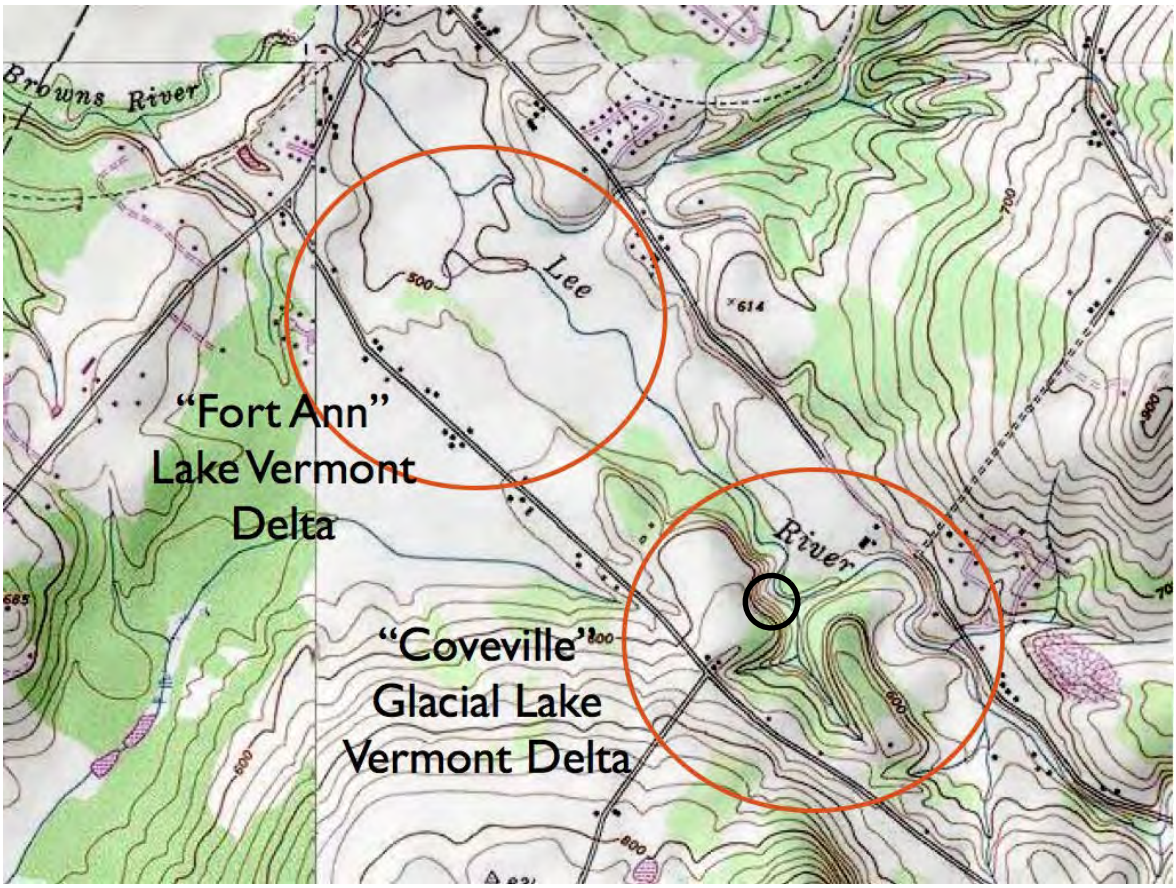

Figure 16: A topographic map of a portion of the Lee River valley. The location of the landslide (Stop 3) is shown with a small circle. Access to the site from the road is via the small stream. The upper Lee River delta marking the Coveville Stage of Glacial Lake Vermont and the lower Lee River delta marking the lower Fort Ann Stage of Glacial Lake Vermont are both circled.

bedded sediments (Fig. 17). Soft sediment deformation resulting from differential loading has produced folds and flame structures in some layers. Calcite-cemented concretions are also common. These are the bottomset beds of a delta encroaching from the east, fed by the Lee River.

Higher in the section the first beds containing coarse sand and pebble gravel appear bedding is inclined to the west northwest. The average grain size continues to increase in these foreset beds. The very top of the section consists of horizontal beds of coarse pebble/cobble gravel, the

topset beds of the delta. Poor exposure usually makes it difficult to ascertain whether the transition between the foreset and topset beds is smooth or truncated. The topset/foreset contact lies ~2 m below the terrace at the top of the landslide. The elevation of that terrace has not been surveyed, but lies between 620–640 ft (189–195 m) asl based on the topographic map and pins the elevation of the Coveville Stage of Glacial Lake Vermont in this part of Vermont (Fig. 18).

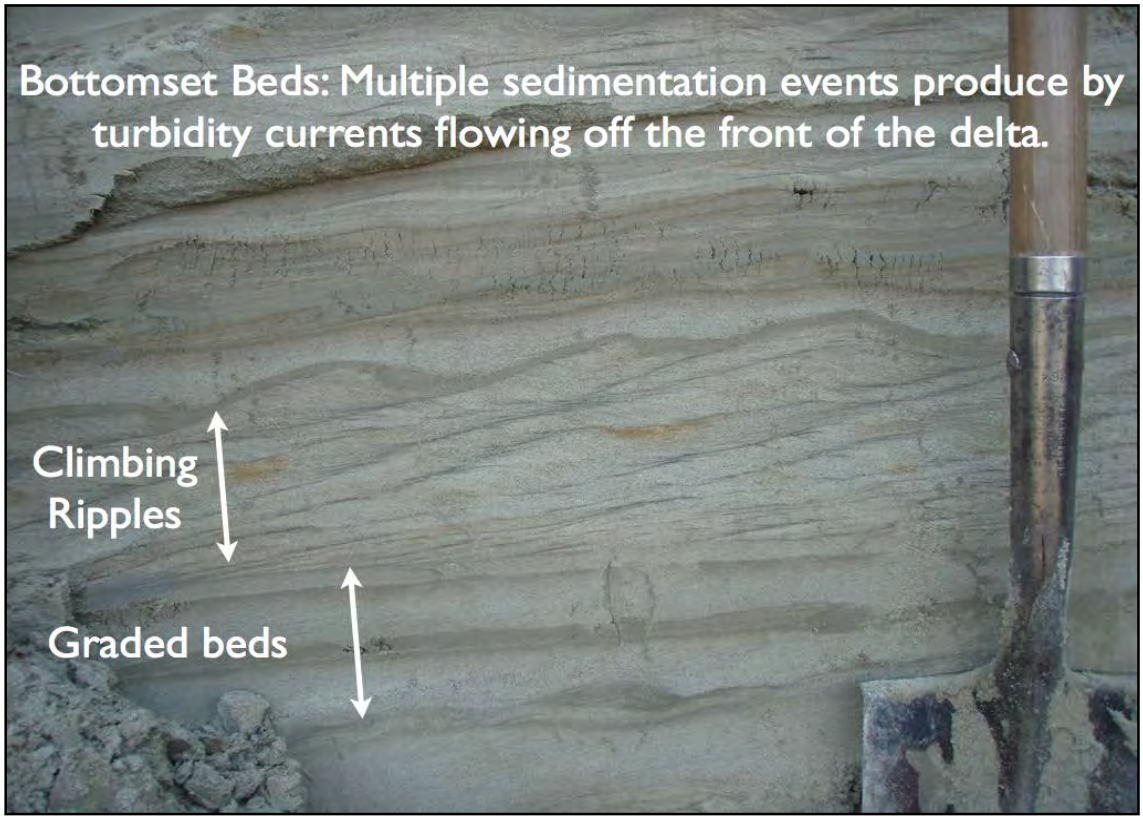

Figure 17: Bottomset beds of the Lee River delta exposed approximately midway up the section. Horizontal beds of graded sand and silt are overlain by climbing ripples capped by silt. Current flow was from left to right, from ESE to WNW

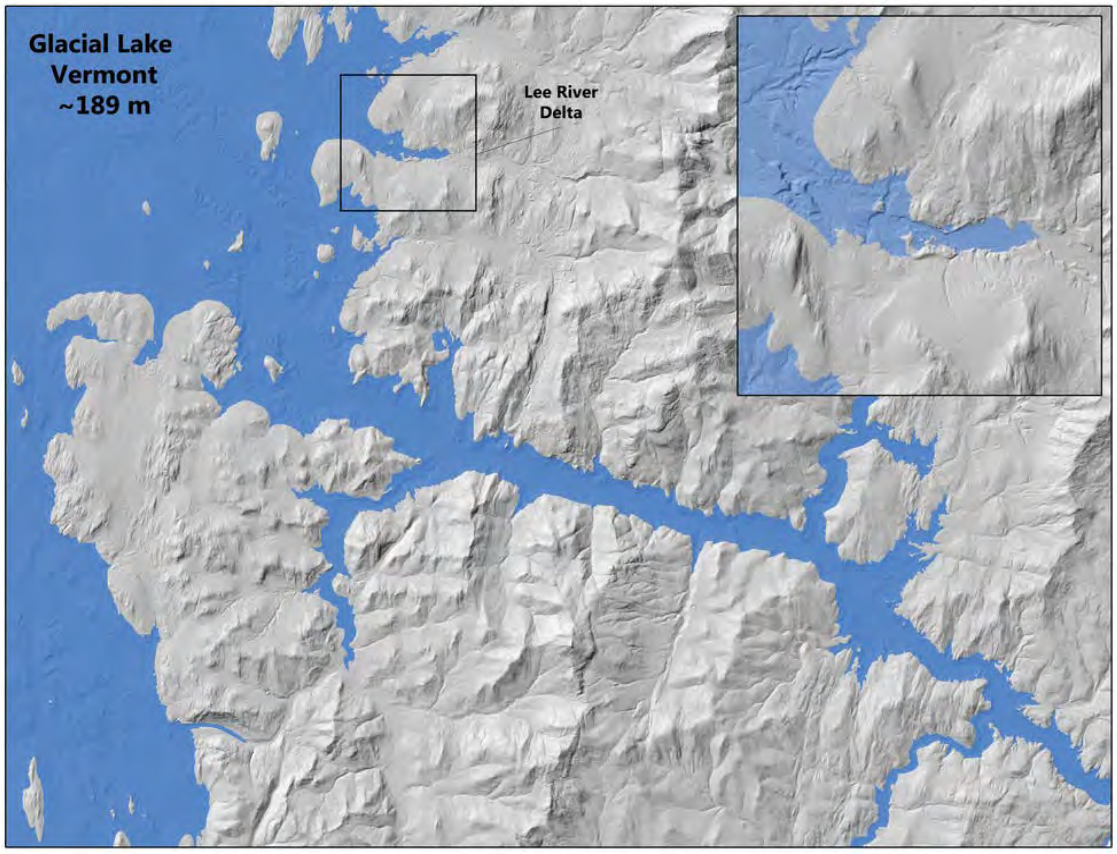

Figure 18: A shaded relief map of the lower Winooski River valley and adjacent Champlain valley shown flooded to the elevation of the Lee River delta (see detailed inset map), the Coveville Stage of Glacial Lake Vermont.

Distance				
Cumulative		Point to Point		
miles	km	miles	km	Route Description
21.0	33.8			Stop 4: Lee River Delta
22.1	35.6	1.1	1.8	Reverse direction and return east on Plains Road until its intersection with Browns Trace Road. Turn right (south) and follow Browns Trace Road to Richmond Village.
24.4	39.3	2.3	3.7	Mill Brook crosses road.
27.7	44.6	3.3	5.3	Intersection with Route 2 in Richmond Village (stoplight). Turn right (west) to return to the Interstate or continue straight through this intersection to return to the town park/bakery parking lot.
28.0	45.1	0.3	0.5	Town Park/Bakery parking lot. End of trip.

REFERENCES CITED

Doll, C.G., Cady, W.M., Thompson, J.B., Jr., and Billings, M.P., 1961, Centennial geologic map of Vermont: Vermont Geological Survey, 1:250,000.

Kim, J., Gale, M., Coish, R., and Walsh, G., 2009, Road to the Kingdom: A bedrock transect across the pre-Silurian Rowe-Hawley belt in central Vermont; in Westerman, D.S. and Lathrop, A.S., eds., Guidebook for field trips in the Northeast Kingdom of Vermont and Adjacent Regions, New England Intercollegiate Geological Conference Guidebook, pp. 95–120.

Kim, J., Klepeis, K., Ryan, P., Gale, M., McNiff, C., Ruksznis, A., and Webber, J., 2011, A bedrock transect across the Champlain and Hinesburg Thrusts in west-central Vermont: Integration of tectonics with hydrogeology, and groundwater chemistry; New England Intercollegiate Geological Conference Guidebook, pp. B1: 1–35.

Ladue, W.H., 1982, The glacial history and environmental geology of Jericho, Vermont; University of Vermont MS thesis, 176 p.

Larsen, F.D., 1972, Glacial history of central Vermont; in Doolan, B.L., ed., NEIGC Guidebook Number 64, pp. 296–316.

Larsen, F.D., 1987, History of glacial lakes in the Dog River valley, central Vermont, in Westerman, D.S., ed. NEIGC Guidebook Number 79, pp. 213–236.

Larsen, F.D., 1999, Glacial history of the Montpelier, Vermont, 7.5-minute Quadrangle, in Wright, S.F., ed., NEIGC Guidebook Number 91, pp. 286–300.

Larsen, F.D., 2001, The Middlesex readvance of the Late-Wisconsinan ice sheet in central Vermont at 11,900 ^{14}C years BP, Geol. Soc. Am. Abstr. w. Programs.

Larsen, F.D., Ridge, J.C., and Wright, S.F., 2001, Correlation of varves of Glacial Lake Winooski, north central Vermont, Geol. Soc. Am. Abstr. w. Programs.

Larsen, F.D., Wright, S.F., Springston, G.E., Dunn, R.K., 2003, Glacial, late-glacial, and post-glacial history of central Vermont; Guidebook for the 66th Annual Meeting of the Northeast Friends of the Pleistocene, 62 p.

Ratcliffe, N.M., Stanley, R.S, Gale, M.H., Thompson, P.J., and Walsh, G.J., 2011, Bedrock Geologic Map of Vermont: U.S. Geological Survey Scientific Investigations Map 3184, 3 sheets, scale 1:100,000.

Rayburn, J.A., 2004, Deglaciation of the Champlain Valley, New York and Vermont and its possible effects on North Atlantic climate change; Unpublished Ph.D. dissertation, Binghamton University, Binghamton, New York, 158 pp.

Ridge, J.C., Balco, G., Bayless, R.L., Beck, C.C., Carter, L.B., Dean, J.L., Voytek, E.B., and Wei, J.H., 2012, The new North American Varve Chronology: A precise record of southeastern Laurentide Ice Sheet deglaciation and climate, 18.2–12.5 KYR BP, and correlations with Greenland Ice Core records; American Journal of Science 312: 685–722.

Stewart, D.P., 1956–1966, Surficial Geologic Maps of the Camels Hump 15' Quadrangle, Unpublished maps (no reports), Vermont Geological Survey.

Stewart, D.P. and MacClintock, P., 1970, Surficial Geologic Map of Vermont, 1:250,000, Vermont Geological Survey.

Stanley, R.S. and Ratcliffe, N.M., 1985, Tectonic synthesis of the Taconic orogeny in western New England; Geol. Soc. Am. Bull. 96: 1227–1250.

Thompson, P.J., Thompson, T.B., and Doolan, B.L., 1999, Lithotectonic packages and tectonic boundaries across the Lamoille River transect in northern Vermont; in Wright, S.F., ed., NEIGC Guidebook Number 91, pp. 51–94.

Thompson, P.J., Gale, M., Laird, J., and Honsberger, I., 2011, Transect across the north-central Green Mountains from the carbonate shelf to ultramafic slivers in the Taconian subduction zone; New England Intercollegiate Geological Conference Guidebook, pp. A1: 1–27.

Thompson, W.B., 1999, History of research on glaciation in the White Mountains, New Hampshire (U.S.A.); Géographie physique et Quaternaire, 53: 7–24.

Wagner, W.P., 1972, Ice merging and water levels in Northwestern Vermont; in Doolan, B. and Stanley, R.S., eds. Guidebook for field trips in Vermont, New England Intercollegiate Geological Conference Guidebook, pp. 317–342.

Wright, S.F., 1999, Deglaciation history of the Stevens Branch Valley, Williamstown to Barre, Vermont; in Wright, S.F., ed., NEIGC Guidebook Number 91, pp. 179–199.

Wright, S.F., 2013, Laurentide Ice Sheet flow across the central Green Mountains, Vermont; Geol. Soc. of Am. Abstr. w. Prog., Vol. 45 p. 105.

Wright, S.F., 2015, Extent of the Middlesex Readvance in the Winooski River Basin, northern Vermont; Geol. Soc. of Am. Abstr. w. Prog., Vol. 47 p. 83.

BOREHOLE GEOPHYSICAL DEMONSTRATION AT ALTONA FLAT ROCK

EDWIN A. ROMANOWICZ

Center for Earth and Environmental Science, SUNY Plattsburgh, Plattsburgh, NY 12901

INTRODUCTION

Geologic Setting

Altona Flat Rock (Flat Rock) is a 2,800 hectare field site located near Altona, New York. It is one of several sandstone pavements in the region that make up a discontinuous belt extending southeast into the Champlain valley from Covey Hill (at the New York and Québec border). The sandstone pavements were created by the denudation of overlying material during a catastrophic breakout of Lake Iroquois. Cambrian Potsdam Sandstone is exposed at the site. An exposed normal fault cuts through the site. Cold Spring Brook flows along the fault trace. The fault scarp is exposed clearly between the reservoir and Chasm Lake (Map 1 and Map 2). The downthrown block is to the north east of the fault.

The lack of surficial deposits makes the site an ideal location for studying fracture-flow hydrogeology. More than 25 bedrock wells from 12 to 140 meters depth have been installed at the site. Elevations and UTM coordinates for each well were measured using a survey-grade GPS. The wells are cased about one meter into bedrock. Below the casing, the wells are open to bedrock.

Potsdam Sandstone has two members; Keeseville and underlying Ausable. The Keeseville is a cream color, thinly bedded quartzitic sandstone (Williams et al 2010). The Ausable is a pink to gray coarse to medium arkosic sandstone (Williams *et al* 2010). The Altona Formation underlies the Ausable member of the Potsdam (Landing *et al* 2007). The Altona is argillaceous with hematite, arkosic sandstone, shale and dolomite (Landing *et al* 2007, Williams *et al* 2010).

Well 102

Well 102 is the deepest well at the site (Map 3). It is 140 m deep, fully penetrating the Cambrian units and extending into the Precambrian basement metamorphic and igneous rock. It has been used extensively for class demonstrations and undergraduate research. Several fractures in well 102 have been identified. Many of these fractures intersect wells nearby (Wells 500A, 500B and 103). Over the past several years, we have studied changes in chemistry of water in well 102 (Klein *et al*., 2013; Dorsey *et al*., 2014 and Mesuda *et al*., 2015). These changes in water chemistry occur due to changes in the relative contribution of groundwater from different sources flowing through different fractures. Well 102 is dominated by an upward flow of water originating in the Altona. Superimposed on this upward flow is a shallow flow system that is sensitive to surface events (precipitation and snow melt). In a 10 meter length of the borehole these two flow systems merge, resulting in rapid changes of water chemistry as conditions change.

Wells 500A and B are each 40 m deep and well 103 is 24 m deep. Despite sharing common fractures with well 102, the changes in borehole water chemistry have not been observed in the other wells. This suggests that an important driving mechanism for the changes observed in

well 102 is the occurrence of upward flow from deeper in the well. The other wells are too shallow to intersect the upward flow system.

Borehole Geophysics Demonstration

This field trip will consist of a demonstration of borehole geophysical techniques at well 102. During the demonstrations we will log gamma, caliper, fluid temperature and resistivity and create an acoustical image of the borehole. We will also measure the vertical velocity of water flow within the borehole using a heat-pulse flow meter. An example of the well log is shown in figure 1.

We will use a Mt. Sopris® Borehole Geophysical system. The system includes a 500-m electric winch with a Matrix® computer interface. Every probe will be zero-referenced to the top of the well. Thus, the top of the well is 0 m depth. The depth of the probe is measured from its bottom. The processing software takes into account the actual location of the sensor(s), so the depths reported in the data are those of the sensor. As the probe is lowered (4-5 $m \cdot min^{-1}$), the probe will automatically take measurements at a pre-programmed depth intervals.

The fluid temperature and resistivity probe measures the temperature and electrical resistance of the fluid in the well casing. Abrupt changes in fluid temperature or resistivity may indicate fractures or lithological units that are contributing water to the well. In deeper wells (>150 m) it is possible to observe the thermal gradient of the crust in the well.

The gamma probe counts gamma rays emitted naturally from the bedrock as a part of gamma decay. This probe is particularly useful in separating shales and carbonates from other sedimentary rocks. The major sources of gamma particles in rocks are potassium, thorium, uranium and radium. The energies associated with these different gamma sources differ. Some probes are able to differentiate between the sources. The probe we are using is not able to differentiate. The gamma probe uses a scintillation crystal. The crystal lights up when exposed to gamma rays. A photomultiplier counts the number of times the scintillation crystal lights up. This number is converted to counts per second (cps).

Gamma logs are not a quantitative tool. The number of counts is not as important as the differences in counts at different depths in the borehole. Shales are often high emitters of gamma particles. The source of the gamma particles is K in clays. Carbonates are typically low gamma emitters. Quartz-rich sandstone would have a very low gamma count, while arkosic sandstone will be high.

Caliper log shows the diameter of the borehole. Three prongs are extended from the caliper probe at the bottom of the well. The probe is then raised to the surface, allowing the prongs to drag along the walls of the borehole. The probe is sensitive enough to detect fractures intersecting the borehole.

The acoustical borehole imager scans the interior of the borehole using RADAR. The return time and reflected energy are recorded. The probe is also equipped with an accelerometer and magnetometer so that one can determine its orientation in three-dimension space. The resulting image from the probe is the wall of the borehole splayed open. Magnetic south is referenced along the center axis of the image. Magnetic north is referenced along the two edges. Fractures, foliations or changes in lithology often result in changes in return energy and travel times. The changes will appear in the image as changes colors. Planar features that intersect the well at perpendicular angles will be shown as bands of alternating colors perpendicular to the long axis of the figure. Features intersecting the borehole at other angles

will appear as a sine wave, with a distinct peak and trough. Since the orientation of the probe is known, it is possible to determine the orientation of the strike and dip of planar features intersecting the borehole. By comparing the acoustical borehole image to the caliper log, one can distinguish between filled fractures, open fractures or foliation.

The heat-pulse flow meter measures vertical fluid flow in the borehole. Two thermistors, one above and one below a heating element monitor ambient fluid temperatures. Baffles direct water flow through the probe, past the sensors and heating element. From the surface, we trigger the heating element to heat for an instant. If there is vertical flow, one of the two thermistors will indicate an increase in ambient temperature. The time between firing the heating element and observing the peak increase in ambient temperature is used to calculate the water velocity or discharge.

FIELD GUIDE AND ROAD LOG

Meeting Point: Southeastern parking lot of Hudson Hall on the SUNY Plattsburgh campus. The lot is located at the corner of Beekman and Broad Streets at the northwest corner of the intersection.

Meeting Point Coordinates: 44.696°N, 73.467°W

Meeting Time: 8:30 AM (The demonstration will continue during the entire morning at the well. You are free to arrive and leave the demonstration at your convenience. If you wish to arrive later than 8:30, please travel directly to the well location.)

Distance in miles (km)		Route Description
Cumulative	Point to Point	
0.0 (0.0)	0.0 (0.0)	Meet at the parking lot south of Hudson Hall on the campus of SUNY Plattsburgh at the corner of Broad and Beekman streets. Proceed from the parking lot, turn left on to Beekman St.
0.9 (1.4)	0.9 (1.4)	Continue to the end of Beekman St., turn left on to Boynton Ave. Boynton Ave. will change to Tom Miller Rd.
1.4 (2.2)	0.5 (0.8)	Turn right on to Quarry Road. Continue north on Quarry Rd. After you cross the intersection with state route 374, Quarry Rd. becomes HW 22. Continue north on 22.
6.7 (10.7)	5.3 (9.9)	Turn left onto O'Neil Rd and proceed west and follow the road as it turns north.
10.8 (17.3)	4.1 (7.4)	Turn left onto West Church and proceed west.
11.6 (18.6)	0.8 (1.3)	Turn right onto Barnaby Rd. There isn't a street sign for Barnaby. The turn is also identified by a sign pointing to Parker's Maple House. Continue north on Barnaby

Distance in miles (km)		Route Description
Cumulative	Point to Point	
12.7 (20.3)	1.1 (1.7)	Barnaby Rd. becomes a seasonal gravel road, continue on Barnaby.
13.8 (22.1)	1.1 (1.8)	Barnaby Rd. turns sharply to the right before an orange gate. Continue through the gate on the gravel road.
14.1 (22.6)	0.3 (0.5)	The gravel road passes in front of a cabin. You may park at the cabin if you wish. If your car has low clearance, it will be best for you to park near the cabin. It is just a brief 300 m walk to the well continuing on the road.
14.3 (22.9)	0.2 (0.3)	Continue on the road past the cabin (either driving or walking). After you cross the bridge on the Little Chazy River you will be on the Potsdam Sandstone. At 14.3 miles or 22.9 km from the starting point you will be at the well. If you drive, please proceed past the well, the road passes through a clearing where there will be plenty of room to park. (44.836°N, 73.574°W)

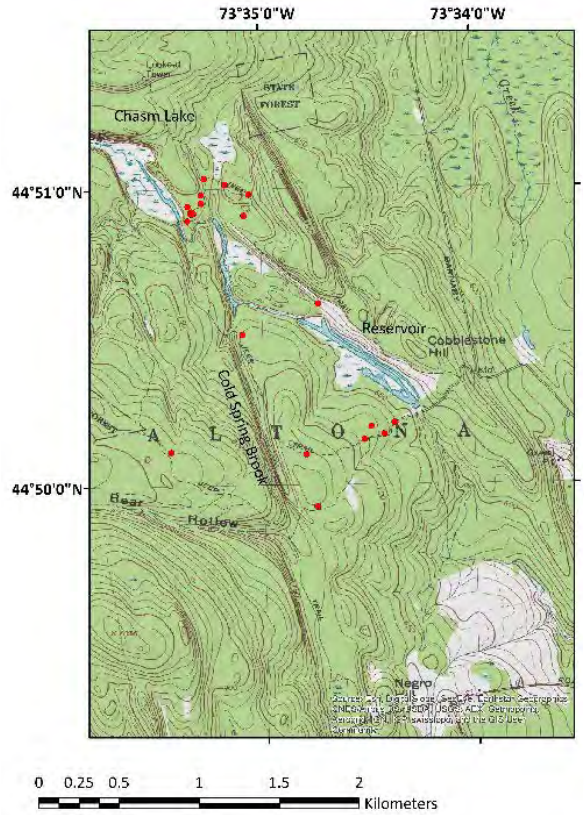

Map 1: This topographic map shows well locations at Altona Flat Rock. The topographic expression of the normal fault is clearly visible along Cold Spring Brook.

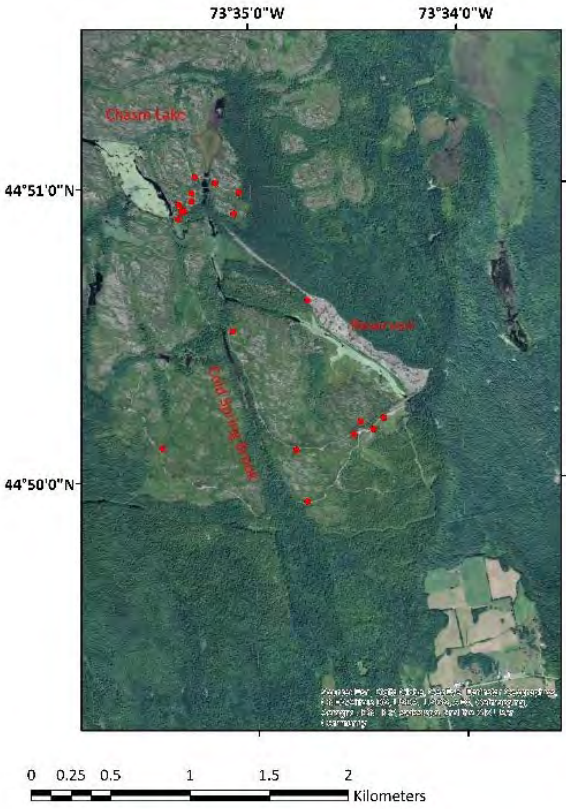

Map 2: Orthophotograph of Altona Flat Rock showing well locations.

Map 3: Detail orthophotograph map of wells located near Well 102.

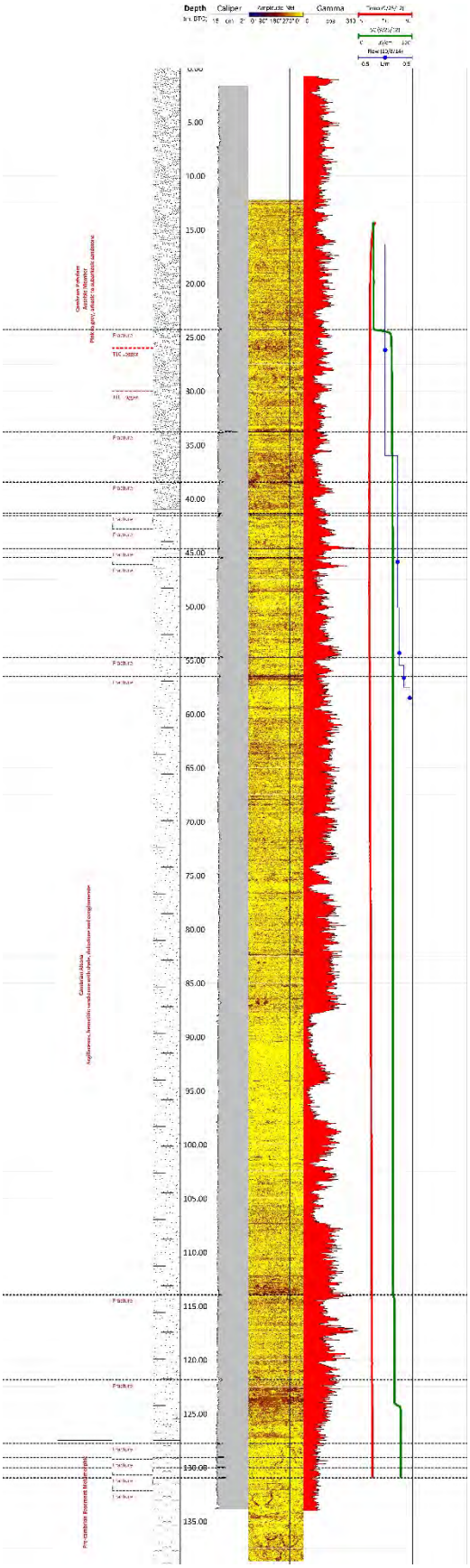

Figure 1: This is a typical well log from well 102. Known lithology is indicated on the left. Fractures are identified by dashed lines extending across the logs. Depths are measured in meters relative to the top of the well casing. The amplitude log has been filtered for better clarity. The gamma log shows decreases in counts per second (cps) as the borehole passes through dolomitic layers in the Altona. At the same depths the acoustical log shows high energy reflectance, which is consistent with carbonates. Fluid temperature shows little variation, however, the fluid resistivity log (measure as specific conductivity) shows a sudden change corresponding with one the fractures. The velocity log shows and upward velocity from deep in the well (+). This velocity decreases to below detection limit between the two shallow fractures suggests that water is removed from the borehole through these fractures.

REFERENCES

Dorsey, M., Drutjons, M., Gilson, K., Keating, S. and Romanowicz, E.A., 2014, A dynamic specific conductivity front caused by changes in relative groundwater inputs from fractures, Northeast Geological Society of America Meeting, Lancaster, PA.

Klein A., Altwerger M., Hinchman C.J., Sullivan, S., Drutjons M. and Romanowicz E.A., 2013, Temporal Variations in a Fracture Controlled Specific Conductivity Front in a Bedrock Well, Altona Flatrock Field Site (Chazy, NY), Northeast Geological Society of America Meeting, Bretton Woods, NH.

Landing E., Franzi D.A., Hagadorn, J.W., Westrop, S.R., Kröger, B., Dawson, J.S., 2007, Cambrian East of Laurentia: A Field workshop in Eastern New York and Vermont, in *Ediacaran-Ordovician of East Laurentia: 12th International Conference of the Cambrian Chronostratigraphy Working Group,* Landing E, (editor), New York State Museum Bulletin 510, S.W. Ford Memorial Volume, New York State Museum: Albany, p 25-72.

Mesuda, J., Dorsey, M., Scott, M., Henrichs, M., and Romanowicz, E.A., 2015, Vertical advective and diffusive transport in borehole, Altona Flat Rock (Chazy, New York), Northeast Geological Society of America Meeting, Bretton Woods, NH.

Williams, J.S., Reynolds, R.J., Franzi, D.A., Romanowicz, E.A. and Paillet, F.L., 2010, Hydrogeology of the Potsdam Sandstone in Northern New York, Canadian Water Resources Journal, 35:4, 399-416.